

Università degli Studi di Napoli Federico II

Dottorato di Ricerca in
Ingegneria Strutturale, Geotecnica e Rischio Sismico

THESIS FOR THE DEGREE OF DOCTOR OF PHILOSOPHY

Multi-scale characterization of existing timber structures for seismic vulnerability and durability assessment

by
DANTE MARRANZINI

Advisor: Prof. Beatrice Faggiano

SCUOLA POLITECNICA E DELLE SCIENZE DI BASE
DIPARTIMENTO D STRUTTURE PER L'INGEGNERIA E L'ARCHITETTURA

Dedicated

to

My Family

FRIDERICVS DEI GRA IMPERATOR ROMANORVM SEMP AVGVST

Multi-scale characterization of existing timber structures for seismic vulnerability and durability assessment

Ph.D. Thesis presented

for the fulfillment of the Degree of Doctor of Philosophy

in Ingegneria Strutturale, Geotecnica e Rischio Sismico

by

DANTE MARRANZINI

October 2023

Approved as to style and content by

Prof. Beatrice Faggiano, Advisor

Università degli Studi di Napoli Federico II

Ph.D. Program in Ingegneria Strutturale, Geotecnica e Rischio Sismico

XXXVI cycle - Chairman: Prof. Iunio Iervolino

www.dist.unina.it/dottorati-di-ricerca/dottorati

Candidate's declaration

I hereby declare that this thesis submitted to obtain the academic degree of Philosophiæ Doctor (Ph.D.) in Ingegneria Strutturale, Geotecnica e Rischio Sismico is my own unaided work, that have not used other than the sources indicated, and that all direct and indirect sources are acknowledged as references.

Parts of this dissertation have been published in international journals and/or conference proceedings (see list of the author's publications at the end of the thesis).

Napoli, October 31, 2023

Dante Marranzini

Abstract

Italy is one of the European countries most exposed to seismic risk, due to the frequency and intensity of earthquakes affecting its territory, as well as the high vulnerability of the built environment. For this reason, seismic prevention and risk mitigation policies assume great importance in national territorial planning.

However, without an adequate vulnerability assessment of the built environment, it is not possible to accurately identify the areas and structures most exposed at risk or design effective mitigation measures. Seismic vulnerability assessment methods vary according to the scale of analysis, as the objectives and level of detail are different. In addition, the multi-scale approach is critical for providing useful information at various decision-making levels and for implementing appropriate mitigation measures. While organization devoted to territorial planning need quick tools for the identification of most urban areas at-risk, the professional community required practical and operational tools to support the knowledge and diagnosis of structures, aimed at vulnerability analysis at the scale of the individual building.

However, it is important to stress that at any scale of analysis, the structural health assessment is a fundamental prerequisite for assessing structural vulnerability. Unlike other building materials, wood is particularly susceptible to degradation phenomena, which can significantly affect its structural performance and thus greatly reduce the service life of timber structures.

In this context, the main focus of the thesis is the characterization of existing timber structures, aimed at the assessment of structural vulnerability, using methodologies at different scales. At the territorial scale, a quick method (Global Durability Factor Method -GDFM) is proposed for estimating the state of preservation of timber structures, considering the environmental and technological aspects of the building, using the support of specially designed survey forms. This methodology is integrated with the semi-quantitative Indicator-Based Approach (IBA) of seismic vulnerability indicators, which is widely applied in large-scale vulnerability analysis. In this thesis, the IBA method is applied to the specific case of large span timber buildings, thus identifying seismic vulnerability criteria among building characteristics such as

geometric and technological aspects. Again, the applied methodology is supported by a survey form, the CARTIS GL form whose 3D section update contribution is shown (Reluis Project WP2 Task 2.3.4)

Subsequently, the explained methods (GDFM and IBA) are applied to a set of case studies, in order to evaluate their efficiency and identify possible critical issues, as well as to test the effectiveness of the illustrated survey forms. Thus from a set of 10 large span timber buildings, those most vulnerable to seismic action are identified, while the service life is determined for a set of 4 timber buildings, recognizing those in the worst state of preservation.

At the detailed scale, contributions and useful tools for the survey, diagnosis and mechanical identification of timber are provided. First, a form for the survey and diagnosis of historical timber trusses is proposed. It is the result of the scientific collaboration activity with the ICOMOS IIWC (Italian International Wood Committee). In the end two experimental campaigns aimed at the mechanical characterization of Acacia dealbata Link logs and ancient wood members in Larch Pine and Chestnut are shown. Several investigation techniques have been applied, showing the procedure and test results. From the performance of non-destructive test and destructive bending tests, correlation models useful for *in situ* mechanical identification have been developed. In addition, innovative surveying techniques (photogrammetry and laser scanner surveying) have been applied on the ancient timber members with the aim to define digital models useful for estimating geometric properties and conducting remote visual strength grading analysis. The applied procedures and devices are extensively described, showing pros and cons of the two methods. In addition, long-term bending tests have been carried out on a small number of ancient timber specimens, evaluating the wood creep behaviour comparing the main findings with what is prescribed by the standards. In the end, the results obtained from the statistical analysis of bending test data have been compared with the performance profiles provided by the standards for visual strength grading, and a comparative evaluation has been carried out.

Keywords: Timber structures; structural vulnerability assessment; seismic vulnerability; wood durability; in situ assessment; mechanical characterization.

Sintesi in lingua italiana

L'Italia è uno dei paesi europei maggiormente esposto a rischio sismico, a causa della frequenza e dell'intensità dei terremoti che interessano il suo territorio, così come per l'elevata vulnerabilità del costruito. Per tale motivo le politiche di prevenzione sismica e di mitigazione del rischio assumono grande importanza nell'ambito della pianificazione territoriale nazionale.

Tuttavia, senza un'adeguata analisi di vulnerabilità del costruito non è possibile identificare in modo accurato le aree e le strutture più a rischio, né progettare misure di mitigazione efficaci. Le metodologie di valutazione della vulnerabilità sismica variano in base alla scala di analisi, poiché gli obiettivi e il livello di dettaglio sono differenti. Inoltre, l'approccio multi scalare è fondamentale per fornire informazioni utili a vari livelli decisionali e per l'attuazione di misure di mitigazione adeguate. Se da una parte gli enti responsabili della pianificazione territoriale necessitano di strumenti speditivi per l'individuazione delle aree territoriali più a rischio, la comunità dei professionisti deve disporre di strumenti pratici ed operativi di supporto alla conoscenza e diagnosi delle strutture, finalizzata all'analisi della vulnerabilità alla scala del singolo edificio.

Tuttavia, è importante sottolineare che a qualunque scala di analisi la conoscenza dello stato di conservazione della struttura è un prerequisito fondamentale per la valutazione della sua vulnerabilità. A differenza degli altri materiali da costruzione, il legno è particolarmente suscettibile a fenomeni di degrado, che ne possono influenzare significativamente le performance strutturali e quindi ridurre notevolmente la vita di servizio delle strutture lignee.

In questo contesto, il tema principale della tesi di dottorato è la caratterizzazione delle strutture in legno esistenti, finalizzata alla valutazione della vulnerabilità strutturale, utilizzando metodologie a diversa scala. Alla scala territoriale si propone un metodo speditivo *(Global Durability Factor Method - GDFM)* per la stima dello stato di conservazione delle strutture lignee, considerando gli aspetti ambientali e tecnologici dell'edificio, avvalendosi del supporto di schede di rilievo progettate appositamente. Tale metodologia si integra con il metodo semi-quantitativo degli indicatori di vulnerabilità sismica *(Indicator-Based Approach - IBA)*, che trova larga applicazione nell'ambito dell'analisi di vulnerabilità su larga scala. In questa tesi il metodo IBA è applicato

al caso specifico delle costruzioni in legno di grande luce, individuando quindi i criteri di vulnerabilità sismica tra le caratteristiche dell'edifico, come gli aspetti geometrici e tecnologici. Anche in questo caso la metodologia applicata è supportata da una scheda di rilievo, la scheda CARTIS GL di cui si mostra il contributo di aggiornamento della sezione 3D (Progetto Reluis WP2 Task 2.3.4). Successivamente le metodologie illustrate (GDFM e IBA) vengono applicate ad un set di casi studio, per valutarne l'efficienza e individuarne possibili criticità, nonché per testare l'efficacia delle schede di rilievo illustrate. Così da un insieme di 10 edifici di grande luce in legno sono individuati quelli più vulnerabili nei riguardi dell'azione sismica, mentre la vita utile di servizio è determinata per un set di 4 costruzioni in legno, riconoscendo quelle che versano nel peggior stato di conservazione.

Alla scala di dettaglio vengono forniti contributi e strumenti utili al rilievo, alla diagnosi e all'identificazione meccanica del legno. Dapprima viene proposta una scheda per il rilievo e la diagnosi di capriate lignee di pregio storico, frutto dell'attività di collaborazione scientifica con il comitato nazionale ICOMOS IIWC (Italian International Wood Committee). Infine si mostrano i contributi forniti e i risultati ottenuti nell'ambito di due campagne sperimentali volte alla caratterizzazione meccanica di tronchi di *Acacia dealbata* Link e di membrature in legno antico in Pino Laricio e Castagno. Dall'applicazione di tecniche d'indagine non distruttive e lo svolgimento di test a flessione sono stati elaborati modelli di correlazione utili all'identificazione meccanica in sito mediante tecniche non distruttive. Inoltre, sugli elementi di legno antico sono state applicate tecniche innovative di rilievo (fotogrammetria e rilievo laser scanner), per la definizione di modelli digitali utili alla stima delle proprietà geometriche e allo svolgimento dell'analisi di classificazione a vista in remoto. Vengono ampiamente descritte le procedure applicate e le strumentazioni impiegate, mostrando pro e contro delle due tecniche. Inoltre, su un numero ridotto di provini in legno antico sono state svolte prove a flessione di lungo termine, valutando il comportamento reologico del materiale attraverso la freccia differita e comparando i risultati ottenuti con quanto prescritto dalle norme per il calcolo delle strutture lignee. Infine, si confrontano i risultati ottenuti dall'analisi statistica dei dati delle prove a flessione con i profili prestazionali forniti dalle normative e dai documenti tecnici per la classificazione a vista delle specie lignee, valutandone la corrispondenza.

Parole chiave: Strutture in legno; analisi di vulnerabilità strutturale; vulnerabilità sismica; durabilità del legno; ispezione *in situ;* caratterizzazione meccanica.

Contents

List of Acronyms

The following acronyms are used throughout the thesis.

AHP	Analytical hierarchy process
BC	Building component
BET	Brunauer-Emmett-Teller theory
BF	Braced frame
CBF	Concentrically braced frame
CCA	Chromated copper arsenate
CLT	Cross laminated timber
Cr	Reference case
CS	Chestnut (*Castanea sativa* Mill.)
DLT	Dowel laminated timber
DM	Decision maker
DOL	Duration of load
DoP	Declaration of performance
DRM	Drilling resistance method
DS	Direct survey
DT	Destructive test
E	Exposure
EBF	Eccentrically braced frame
ESL	Estimated service life
FEM	Finite element method
FM	Factor method
GDFM	Global durability factor method
H	Hazard
ID	Identification
IP	Indicating properties
LSL	Laminated strand lumber
LSS	Laser scanner survey
LTT	Long-term test
LVL	Laminated veneer lumber
MCDM	Multi-criteria decision making method
MRF	Moment resisting frame

NDT	Non-destructive test
NLT	Nail laminated timber
OSB	Oriented strand board
PF	Pinned frame
PNL	Corsican Pine (*Pinus nigra* subsp. *laricio* Poir. Maire)
PS	Photogrammetric survey
PSL	Parallel strand lumber
PT	Pressure treatment
RC	Reinforced concrete
R_S	Specific risk
RSA	Response spectrum analysis
R_T	Total risk
StM	Structural member
StN	Structural node
StU	Structural unit
TBM	Timber-based material
TOF	Time of flight
TOPSIS	Technique for order of preference by similarity to ideal solution
UC	Use class
V	Vulnerability
VSG	Visual strength grading
WS	Wood species

List of Symbols

The following symbols are used within the thesis.

a	Distance between a loading position and the nearest support in bending test
A	Amplitude of drilling resistance method
$\mathbf{A^-}$	Ideal negative solution
$\mathbf{A^+}$	Ideal positive solution
b	Base of the rectangular cross-section
$\mathbf{d_1}$	Smallest diameter of the cross section
$\mathbf{d_{1,i}}$	Smallest diameter of the cross section at the i-th point
$\mathbf{d_{1,j}}$	Smallest diameter of the cross section at the j-th point
$\mathbf{d_2}$	Biggest diameter of the cross section
$\mathbf{d_{2,i}}$	Biggest diameter of the cross section at the i-th point
$\mathbf{d_{2,j}}$	Biggest diameter of the cross section at the j-th point
$\mathbf{d_h}$	Diameter in the direction perpendicular to the load direction at mid-span
$\mathbf{d_{ij}}$	Measure of the j-th criterion with respect to i-th alternative
$\mathbf{d_{nom}}$	Nominal diameter
$\mathbf{d_v}$	Diameter in the direction of the load at mid-span
$\mathbf{E_0}$	Modulus of elasticity parallel to the grain
$\mathbf{E_{0,12}}$	Modulus of elasticity parallel to the grain, at MC equal to 12%
$\mathbf{E_{0,mean}}$	Mean value of modulus of elasticity parallel to the grain
$\mathbf{E_{90}}$	Modulus of elasticity perpendicular to the grain
$\mathbf{E_L}$	Elastic modulus of elasticity in longitudinal (L) direction
$\mathbf{E_{m,0,12}}$	Modulus of elasticity parallel to the graina at MC equal to 12%
$\mathbf{E_{m,g}}$	Global modulus of elasticity obtained from bending test
$\mathbf{E_{m,l}}$	Local modulus of elasticity obtained from bending test
EMC	Equilibrium moisture content of wood
$\mathbf{E_R}$	Elastic modulus of elasticity in radial (R) direction
$\mathbf{E_T}$	Elastic modulus of elasticity in transversal (T) direction

f	Natural frequency of vibration in longitudinal direction
F	Cell load in bending test
$f_{c,0,12}$	Compression strength parallel to the grain, at MC equal to 12%
F_{LTT}	Applied load in long-term test in bending
f_m	Bending strength
$f_{m,k}$	Characteristic bending strength
F_{max}	Failure load in bending test
FSP	Fibre saturation point
G_{LR}	Tangential modulus of elasticity in LR direction
G_{LT}	Tangential modulus of elasticity in LT direction
G_{RT}	Tangential modulus of elasticity in RT direction
h	Heigth of the rectangular cross-section
I	Second moment of inertia
I'_v	Vulnerability index
I_1	Smallest second moment area of the cross-section along the gauge length
$i_{A(DS-LSS)}$	Index of relative variation between $MOE_{dyn,A,LSS}$ and $MOE_{dyn,A,DS}$
$i_{Em(l-g)}$	Index of relative variation between $E_{m,l}$ and $E_{m,g}$
I_{GD}	Global durability index
$i_{MOEdyn,A\ (L-D)}$	Index of relative variation between $MOE_{dyn,A,L}$ and $MOE_{dyn,A,D}$
$i_{SWS(L-D)}$	Index of relative variation between SWS_L and SWS_D
$i_{V(DS-LSS)}$	Index of relative variation between $MOE_{dyn,V,LSS}$ and $MOE_{dyn,V,DS}$
$i_{V(DS-LSS)}$	Index of relative variation between V_{LSS} and V_{DS}
$i_{\rho(DS-LSS)}$	Index of relative variation between ρ_{LSS} and ρ_{DS}
J_B	Set of the benefit (B) criteria
J_C	Set of the cost (C) criteria
k_{def}	Deformation factor
k_{mod}	Modification factor for duration of load and moisture content
L	Length of the specimen

l	Length between the support in bending test
l_1	Gauge length in bending test
L_p	Total length of drilling
l_p	Drilling depth
m	Wood mass
m	Mass of the specimen at a given moisture content
m_0	Mass of the oven dry specimen
MC	Moisture content of wood
MC_{max}	Maximum MC in long-term test
MC_{min}	Minimum MC in long-term test
MCt_0	Moisture content of wood at t_0 in long-term test
M_{gi}	Geometric mean
MOE_{dyn}	Dynamic modulus of elasticity
$MOE_{dyn,A}$	Dynamic modulus of elasticity obtained from acoustic test
$MOE_{dyn,A,D}$	Dynamic modulus of elasticity obtained from acoustic test in diagonal direction (from LSS)
$MOE_{dyn,A,DS}$	Dynamic modulus of elasticity obtained from acoustic test and direct survey
$MOE_{dyn,A,L}$	Dynamic modulus of elasticity obtained from acoustic test in longitudinal direction (from LSS)
$MOE_{dyn,A,LSS}$	Dynamic modulus of elasticity obtained from acoustic test and laser-scanner survey
$MOE_{dyn,V}$	Dynamic modulus of elasticity obtained from vibrational test
$MOE_{dyn,V,12}$	Dynamic modulus of elasticity obtained from vibrational test, at MC equal to 12%
$MOE_{dyn,V,DS}$	Dynamic modulus of elasticity obtained from vibrational test and direct survey
$MOE_{dyn,V,LSS}$	Dynamic modulus of elasticity obtained from vibrational test and laser-scanner survey
O	Cross-section ovality
$R_{(lp)}$	Drilling resistance as function of drilling depth
R^2	Coefficient of determination
RC_{Cr}	Relative closeness of the reference case (Cr) from the ideal solutions

$\mathbf{RC_i}$	Relative closeness of the i-th alternative from the ideal ones.
RH	Relative humidity
rij	Normalized measure of the j-th criterion with respect to i-th alternative
RLT	Recorded life time
Rm	Mean drilling resistance mesaure
RSL	Reference service life
S	Sweep of the specimen
$\mathbf{S_i^-}$	Euclidean distance between the real solution (A_i) and the ideal negative solution (A^-)
$\mathbf{S_i^+}$	Euclidean distance between the real solution (A_i) and the ideal positive solution (A^+)
SWS	Stress wave speed
$\mathbf{SWS_{12}}$	Stress wave speed at MC equal to 12%
$\mathbf{SWS_D}$	Stress wave speed in transversal direction
$\mathbf{SWS_L}$	Stress wave speed in longitudinal direction
t	Time in long-term test
T	Tapering of the specimen
$\mathbf{t_0}$	Time corresponding to the start of the long-term test
$\mathbf{TOF_D}$	Time of flight in diagonal direction
$\mathbf{TOF_L}$	Time of flight in longitudinal direction
TOG	Time of flight
V	Geometrical volume
$\mathbf{V_{DS}}$	Geometric volume obtained from direct survey
$\mathbf{v_{ij}}$	Weighted and normalized measure of the j-th criterion with respect to i-th alternative
$\mathbf{V_{LSS}}$	Geometric volume obtained from laser-scanner survey
W	Section modulus
w	Absolute displacement in bending test
$\mathbf{w_0}$	Displacement at t_0 in long-term test
$\mathbf{w_j}$	Weight related to j-th criterion
$\mathbf{w_{LVDT1}}$	Displacement of LVDT1 in bending test

w_{LVDT2}	Displacement of LVDT2 in bending test
w_{LVDT3}	Displacement of LVDT3 in bending test
w_{LVDT4}	Displacement of LVDT4 in bending test
w_{LVDT5}	Displacement of LVDT5 in bending test
w_{LVDT6}	Displacement of LVDT6 in bending test
w_{LVDT7}	Displacement of LVDT7 in bending test
w_{max}	Absolute displacement corresponding to specimen failure in bending test
$w_{max,LTT}$	Maximum displacement in long-term test
W_{rel}	Relative displacement in bending test
w_{side1}	Relative displacement measured on the specimen vertical side "1"
w_{side2}	Relative displacement measured on the specimen vertical side "2"
w_t	Displacemnet at time *t* in long-term test
$\Delta_{(DS-LSS)A}$	Difference between $MOE_{dyn,A,DS}$ and $MOE_{dyn,A,LSS}$
$\Delta_{(DS-LSS)V}$	Difference between $MOE_{dyn,V,DS}$ and $MOE_{dyn,V,LSS}$
$\Delta_{Em(l-g)}$	Difference between $E_{m,l}$ and $E_{m,g}$
$\Delta_{MOEdyn,A}$	Difference between $MOE_{dyn,A,L}$ and $MOE_{dyn,A,D}$
ν_{LR}	Poisson coefficient in LR direction
ν_{LT}	Poisson coefficient in LT direction
ν_{RL}	Poisson coefficient in RL direction
ν_{RT}	Poisson coefficient in RT direction
ν_{TL}	Poisson coefficient in TL direction
ν_{TR}	Poisson coefficient in TR direction
ρ	Wood density
ρ_{12}	Wood density at MC equal to 12%
ρ_{12}	Wood density at MC equal to 12%
ρ_{DS}	Wood density obtained from direct survey
ρ_k	Characteristic density
ρ_{LSS}	Wood density obtained from laser-scanner survey

List of Figures

List of Tables

Introduction

MOTIVATION AND GOALS

Today, the built-up area is exposed to many risks due to natural actions such as landslides, earthquakes and floods. The whole Italian territory is classified as seismic area. Therefore, given the great vulnerability of the built-up, risk assessment and analysis are fundamental for governance policy.

Methods and procedures for estimating vulnerability at the territorial scale are different from those at the detailed scale, where an in-depth survey of the building is necessary for an accurate assessment of the structural capacity. However, one factor that cannot be overlooked at both scales of analysis is the state of health of the structure. Indeed, the performance of a structure generally changes during the service life due to accidental events or modifications, such as alterations to the structural scheme, changes in the acting loads, or material decay. Especially timber structures suffer from decay phenomena that can significantly reduce the load-bearing capacity over time. For this reason, methods and tools for assessing the state of health and susceptibility to degradation are necessary for an accurate assessment of structural vulnerability.

In this context, the main topic of the PhD thesis is the characterization of the existing timber structures, aimed at structural vulnerability assessment, using methodologies at different scales. At the territorial scale, a quick-level method, based on purposely set up survey forms, is proposed for estimating the state of health of the structures, considering environmental and technological aspects, while at the detailed scale, procedures and tools for the identification of both the state of conservation and the mechanical behaviour of timber members are proposed.

Among the quick-level methods for structural vulnerability assessment, the indicator-based approach is taken into consideration. It is based on the application of multi-criteria decision-making methods (MCDM). It relies on the knowledge of building features, like typological, geometrical, mechanical and other aspects of the structure, which are related to the structural

vulnerability. For timber construction, specific criteria are identified and particular attention is paid to durability aspects. With regards to this, in order to assess the deterioration conditions of existing structures, a methodology for estimating the service life of timber structures is proposed. It consists in an innovative application of the Factorial Method (ISO 15686), based on the use of the MCDM as a supporting tool for the definition of the modification factors of the Factorial Method. Specifically, also aspects related to the durability of timber structures are assumed as modification factors. Based on this, a parameter for estimating the state of preservation of the timber structure is defined, for being integrated into the indicator-based approach as an additional vulnerability criterion.

To these purposes specific survey forms have been developed: 1) the Cartis GL 3D form, improved within the Reluis project (WP2 Task 2.3.4), for large-span timber buildings; 2) a survey form for existing timber structures (SHA-TS form), specifically devoted to assessing the state of conservation. The main aim of the forms is to support the researchers and the professional technician during the on-site assessment.

The survey forms and the indicator-based approach method set up have been tested on 10 large timber existing buildings located in Italy (Faggiano et al., 2021), leading to the assessment of the most vulnerable building, while the service life method has been applied to other four timber structures, achieving the assessment of the state of preservation.

At a detailed scale, the structural vulnerability assessment needs an in-depth investigation, for acquiring information related to the geometry, mechanical properties and state of preservation of the specific building. To this purpose, the survey forms proposed allow for providing a comprehensive description of the constructions. Further to the previous survey forms, an additional survey form specifically related to ancient timber trusses has been proposed, trusses being the most recurrent structural types for ancient timber roofs. This has been developed within the framework of cooperation within the Italian national committee ICOMOS IIWC (Italian International Wood Committee), whose mission is to promote the conservation, protection and sustainable management of the wooden built heritage. The application to case studies highlights the potential and critical aspects.

For the mechanical properties characterization of timber members in existing buildings, with the purpose to provide the most efficient procedure for the structural identification of in situ members, several non-destructive techniques and three different timber species have been taken into

consideration. In particular two experimental campaigns have been carried out on Acacia Dealbata Link timber logs and on ancient timber members in Corsican Pine (Pinus Nigra subsp. Laricio (Poir.) Maire) and Chestnut (Castanea Sativa Mill.). The typical steps of in situ detailed assessment, i.e., geometric survey, visual strength grading (VSG) and non-destructive tests (NDT), have been carried out in the laboratory on timber members. The sample of ancient timber has also been surveyed using digital techniques, such as photogrammetry and laser scanners. Pros and cons of the procedures and instrumentation have been extensively described, as well as the acquisition and processing times. Subsequently, four-point bending tests up to failure have been performed to evaluate the elastic modulus and bending strength. Only for the ancient timber sample long-term bending tests have been carried out to investigate the creep behaviour of the two wood species. From the statistical analysis of the results, linear regressions between destructive and non-destructive parameters have been determined, highlighting the most reliable relationships useful for the in situ mechanical identification through NDTs, validated through the valuation of the correspondence with the performance profiles assigned by VSG and the DT measures.

OUTLINE

Chapter 1 provides an introductory overview of the mechanical and physical characteristics of wood, with a specific focus on its application as a structural material. The chapter aims to emphasize the importance of durability in timber construction, as it significantly impacts its performance. It also seeks to analyze the current state of knowledge regarding wood decay phenomena, including their main causes and consequences. Additionally, the chapter intends to showcase a wide range of applications of timber in the construction field, including examples from vernacular architecture, modern construction and heritage architecture.

Chapter 2 provide a comprehensive overview of principles and methods for assessing the seismic vulnerability of timber structures, with a specific focus on the different methodologies at different scales of investigation. Additionally, it delves into methods for evaluating the health condition of timber structures and their susceptibility to decay. The concept of service life

is introduced, along with commonly employed evaluation methodologies. Moreover, the chapter addresses the detailed assessment of the state of health of timber structures, accomplished through specific surveying and diagnostic techniques. It thoroughly describes the procedures, standards, and common techniques employed in this process, which encompass visual strength grading (VSG), non-destructive (NDT), and destructive techniques (DT). In this framework we focus on the role and potential of survey form as a tool to support data acquisition, showing the models present in the state of the art and their purpose.

Chapter 3 presents and discuss three distinct survey forms for the analysis of existing timber structures at different scales of analysis. The three forms have been developed in different contexts and serve various purposes. First, the contribution to the update of the CARTIS form GL Section 3d, (Reluis project - WP2 Task 2.3.4), for the seismic risk prevention of large-span timber buildings is shown. The contribution aims to reorganize and improve the contents of the form, which is applied at the territorial scale as a tool to support the evaluation of the exposure, as well as to acquired data regarding the vulnerability aspects. Then, the SHA-TS survey form, designed specifically for surveying durability aspects of timber constructions, is presented. Along with the form, a user's manual has been proposed to guide the user in recognizing the phenomena of wood decay. This card can help the user at both scales of analysis (territorial and detailed): in the first case it facilitates the acquisition of data useful for assessing the state of conservation by mean of quick methods, while at the detailed scale it can guide the technician in the diagnosis of structural pathologies. In the end, as part of the collaboration activity with the ICOMOS IIWC (Italian International Wood Committee), a sheet has been developed for the survey and diagnosis of ancient timber trusses. The chapter is structured in such a way to firstly introduce the forms, providing insight into their contents and the context in which they have been developed. Then the practical application to case studies is illustrated. In this way, it offers tangible examples of how these forms can be used in the evaluation of existing timber structures. Lastly, the chapter provides a critical assessment of the survey forms by highlighting their potential benefits or limitations.

Chapter 4 introduce and delve into the application of an indicator-based approach for the assessment of the seismic vulnerability of large-span timber

buildings at territorial scale. This approach involves the identification of vulnerability criteria, such as building's general characteristics, technological features, geometric properties, etc., through the CARTIS form. The chapter outlines a systematic procedure for calculating the vulnerability index, employing multicriteria decision methods (MCDM). In addition to seismic vulnerability, the chapter also addresses durability concerns. It introduces a novel method (Global durability factor method - GDFM) based on the combined application of the Factorial Method (ISO 15686), for predicting the estimated service life (ESL), and the TOPSIS method (MCDM). In this way, the health of the structure can be evaluated through the estimated service life (ESL) and the proposed global durability index, which condenses the modifying factors of the FM method. These factors are to be recognized among the elements that influence the durability of timber constructions. Therefore, in the chapter, these methodologies are fully explained, furthermore the vulnerability criteria and durability factors are proposed. These aspects represent the authentic contribution to the combined assessment of seismic vulnerability and the state of health of the timber structures. In the end, the chapter takes a holistic approach by proposing the integration of the durability aspects into seismic vulnerability assessment.

Chapter 5 shows the application of the methods (exposed at Chapter 4) to the case studies. They are applied to different set of buildings, surveyed through the survey form showed in Chapter 3. Seismic vulnerability is assessed for a set of ten large-span timber buildings surveyed through the Cartis GL form, while the GDFM is applied to a set of four buildings surveyed through the SHA-TS form. Thus the most vulnerable buildings are selected through the evaluation of the vulnerability index, while the state of health of the four buildings is assessed through the estimated service life (ESL) and the global durability index.

Chapter 6 provide a comprehensive exploration of the mechanical properties of structural members made from various wood species. In particular two experimental campaigns have been carried out on *Acacia dealbata* Link timber logs and on ancient timber members in Corsican Pine (*Pinus Nigra* subsp. *Laricio* (Poir.) Maire) and Chestnut (*Castanea Sativa* Mill.). The standard procedures for *in situ* assessment, which include geometric survey, visual strength grading (VSG), and non-destructive tests (NDT), have been applied on timber members. Additionally, the research

conducted four-point bending tests on these samples to assess their elastic modulus and bending strength. For the ancient timber sample, long-term bending tests have been also carried out to investigate its creep behavior. The study's statistical analysis resulted in the identification of linear regressions between destructive and non-destructive parameters. These relationships provide reliable means for on-site mechanical identification through non-destructive testing (NDTs). The reliability of these NDT-based identifications was further validated by comparing them with performance profiles assigned using visual strength grading (VSG) and destructive testing (DT) measures.

Chapter

1

Timber in construction

Abstract: Timber is a traditional building material, as its first applications in architecture date back thousands of years. However, due to its excellent mechanical and physical properties, timber-based products currently find wide application in construction, making them attractive alternatives to modern materials. Nevertheless, it should be kept in mind that, unlike other structural materials, the behaviour of timber is very sensitive to environmental conditions. In fact, several factors, mainly insects and fungi, can affect its structural performance, drastically reducing its service life. On the other hand, under proper conditions, timber will provide service for centuries.

In this context, this introductory chapter shows the main mechanical and physical peculiarities of wood, focusing on the application of timber as a structural material. Wide emphasis is given to durability issues, which strongly affect timber performances. Thus, the state of the art related to the main phenomena of wood decay is analyzed, identifying main causes and consequences. In the end, a brief section of the chapter shows a wide variety of applications of timber in the construction field. Vernacular architectural examples are provided, in which some wood species continue to be used as local resources. In addition, the most common uses of timber in modern construction and in heritage architecture are discussed.

1.1 FORESTS IN THE TIMBER SUPPLY CHAIN

The timber products used in construction primarily originate from the sawmilling process within the wood supply chain. The wood supply chain is a complex process that involves various stages [1] to ensure sustainable and efficient utilization of the natural resource which is wood (Figure 1.1). It begins with the meticulous selection and harvesting of trees emphasizing sustainable forestry practices to preserve forest health and biodiversity. Logs

are transported to processing facilities, where they undergo sorting based on species, size, and quality. Sawmills then employ precision cutting technologies to transform logs into various wood products essential for construction, such as dimension lumber, boards, and veneers. Following the sawmilling stage, wood undergoes drying processes like kiln drying to enhance its strength and durability. Treatment procedures are applied to certain wood products to increase resistance against pests and decay, contributing to the longevity of final material. In the manufacturing and processing stage, advanced technologies and machinery are used to create specific products tailored to construction needs, including timber-based materials (TBM) such as glued laminated timber, cross laminated timber (CLT), etc.

Throughout this supply chain, adherence to sustainable forestry practices and certifications, such as those provided by organizations like the FSC [2] or the PEFC [3], is paramount. Indeed, despite their ecological importance, global forests face severe threats. Deforestation, driven by logging, and urbanization, poses a significant risk. The Global Forest Resources Assessment 2020 (Food and Agriculture Organization; [4]) indicates a net loss of 178 million hectares over the past three decades, underscoring the urgent need for conservation efforts. Nowadays the FSC and PEFC are the main internationally recognized certifications which verify that the wood used in construction has been sourced responsibly, supporting the global effort towards sustainable and ethical forest management. Indeed, forests are integral components of the Earth's ecological tapestry, playing a crucial role in maintaining biodiversity, regulating climate, and providing essential ecosystem services.

Understanding the extent of global forests and the diversity of tree species on different continents is paramount for effective conservation and sustainable management. According to the Food and Agriculture Organization of the United Nations [4], the total forest area worldwide is approximately 4.06 billion hectares, covering nearly 31% of the total land area. This expansive green mantle acts as the lungs of the planet, absorbing carbon dioxide and releasing life-enabling oxygen. The vast extent of global forests is not uniform, and the distribution of tree species varies significantly across continents. A large and well-known classification can be made between coniferous and broadleaf (deciduous) trees, to which softwood and hardwood correspond, respectively.

Asia, as the largest contributor to global forest cover, exhibits remarkable biodiversity. The diverse landscapes, from the taiga in Siberia to the lush

rainforests in Southeast Asia, contribute to the rich variety of tree life on the continent. The FAO [4] data reveals a mosaic of tree species in different climatic area: Teak (*Tectona grandis*) and Mahogany (*Swietenia spp.*) are spread in tropical rainforests whereas in the temperate forests area, such as Himalayan region, Himalayan cedar (*Cedrus deodara*) is the main tree species. In Boreal Forest, corresponding to Siberia and parts of Northeast Asia, Siberian pine (*Pinius sibirica*) and Siberian Larch (*Larix sibirica*) cover most of the forestry surface. According to the organization Amazon web services [5], the wood species most commonly used for the production of products for use in the construction industry are Siberian Larch, Scots Pine (*Pinus sylvestris*), Spruce (*Picea spp.*) and Douglas fir (*Pseudotsuga menziesii*).

Oceania, comprising Australia, New Zealand, and the Pacific islands, exhibits unique tree species adapted to the region's isolation. Australia, dominated by Eucalyptus (*Eucalyptus spp.*), showcases adaptability to diverse climates. New Zealand's forests feature iconic species like the Kauri tree (*Agathis australis*), and the Pacific islands host a diversity of indigenous hardwoods [4].

North America, characterized by a blend of temperate and boreal ecosystems, hosts a diverse array of tree species. The United States Forest Service [6] reports dominant conifers species such as Pine (*Pinus spp.*), Spruce (Picea spp.), Douglas fir (*Pseudotsuga menziesii*) and hardwoods (Oak, *Quercus spp.*; Maple, *Acer spp.*; Hickory, *Carya spp.)* The boreal forests of Canada add to this diversity, with Eastern White Pine (*Pinus strobus*), Western Red Cedar (*Thuja plicata*), White Spruce (*Picea glauca*), Douglas Fir, Yellow Birch (*Betula alleghaniensis*), Black Walnut (*Juglans nigra*) as prevalent species. Among these wood species, Douglas Fir, Southern Yellow Pine, and Spruce result as the most used species in the field of construction, being a source for the production of structural timber products and timber-based materials [7], [8].

South America, known for its expansive Amazon rainforest, houses an unparalleled wealth of biodiversity. Recent data from the Amazon Environmental Research Institute [9] underscores the prevalence of iconic species such as Brazil nut trees (*Bertholletia excelsa*), rubber trees (*Hevea brasiliensis*), and a myriad of hardwoods like mahogany (*Swietenia spp*.) and rosewood (*Dalbergia spp*.). The Amazon basin alone is home to over 16,000 different tree species [9].

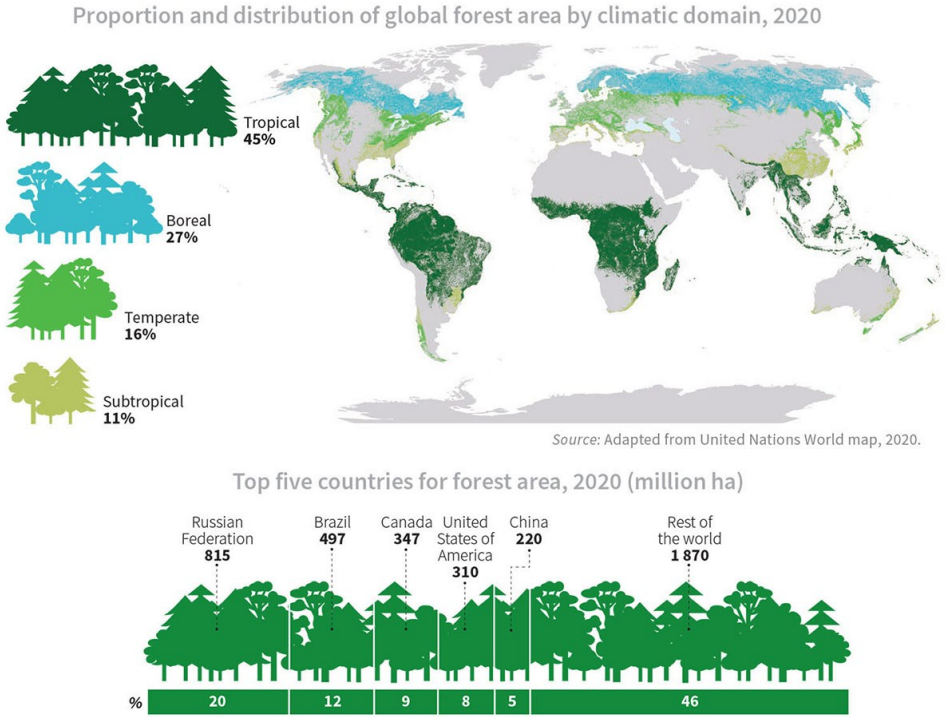

Figure 1.1. The distribution of global forest area by climatic domain and countries (extracted from: [10]).

Europe, with approximately 40% of its land covered by forests, showcases a mix of coniferous and deciduous trees. Data from the European Environment Agency [11] highlights several species from different climatic areas: in Boreal Forests, corresponding to most of the Northern and Central Europe, Norway spruce (*Picea abies*), Scots Pine (*Pinus sylvesttris*), Silver fir (*Abies alba*) are the widely softwoods species, whereas Oak (*Quercus spp.*), European beech (*Fagus sylvatica*), European ash (*Fraxinus excelsior*) are common in temperate deciduous forests, as well as in northern Mediterranean area. In Apline regions Swiss pine (*Pinus cembra*) and Mountain Ash (*Sorbus aucuparia*) are native in alpine and subalpine zones. In Mediterranean area the most spread softwoods are Maritime pine (*Pinus pinaster*), Stone pine (*Pinus pinea*), Aleppo pine (*Pinus halepensis*), Corsican pine (*Pinus nigra*) and Cypress (*Cupressus sempervirens*), whereas Castanea sativa (*Castanea sativa*), Holm oak (*Quercus ilex*), Downy oak (*Quercus pubescens*), Cork oak (*Quercus suber*), European beech are the most common hardwood species (Figure 1.2). For the production of sawn timber and timber-

based materials, the European continent makes greater use of softwood, such as Norway spruce, Silver fir, Larch (*Larix decidua*) and Scots pine [12].

Figure 1.2. Some of the wood species widespread in southern Italy.

Africa, with its diverse landscapes ranging from the Sahara Desert to the Congo rainforest, features a wide range of tree species. The World Wildlife Fund [13] notes Acacia trees (*Acacia spp.*) in the savannas, Baobabs (*Adansonia spp.*) in arid regions, and diverse hardwoods in the rainforests. The Congo Basin, the world's second-largest rainforest, is a hotspot of a huge biodiversity.

Among the species that are most widespread across continents, a distinction should be made between native and invasive tree species. Native wood species, evolving over time in specific regions, support local ecosystems and biodiversity, whereas invasive species, introduced to new environments, disrupt ecosystems, outcompete natives, and require active management to prevent ecological imbalances and protect biodiversity [14]. Invasive species can invade ecosystems through various modes, utilizing different mechanisms and pathways. The most common modes of invasion include: accidental introduction through trade, transport, etc., wind dispersal or water dispersal, wildlife-mediated dispersal, intentional introduction. Furthermore, climate change and habitats alterations due to land use changes (e.g., deforestation, urbanization) are causes that promote this process [15].

The most prevalent invasive wood species are certain exotic plants that, when introduced to new environments, can proliferate rapidly and displace indigenous flora. According to the regulation EU 1143/2014 [17] most of the invasive tree species in Mediterranean area are the Eucalyptus (*Eucalyptus spp.*), Acacia (*Acacia spp.*), Causarina (*Causarina spp.*) and Tree of heaven (*Ailanthus altissima*). In Italy *Acacia saligna* is a very invasive species

especially in Sardegna island, Liguria and Tuscany region (Figure 1.3) [18]. Further invasive species regards the Tree of Heaven (*Ailanthus altissima*) and the Chinese tallow (*Sapium sebiferum*) [16].

Figure 1.3. Some of the Italian invasive wood species according to (EU) 2022/1203 (extracted from: [16]).

1.2 MAIN CHEMICAL AND PHYSICAL CHARACTERISTICS OF WOOD

1.2.1 STRUCTURE OF WOOD

Wood is a natural material derived from the tree as a tissue generated to support the green parts (leaves and needles) in order to expose them to sunlight for the process of sugar synthesis to take place. During this process, sunlight or artificial light allows CO_2 and H2O molecules to be converted into a glucose molecule ($C_6H_{12}O_6$), which is essential for plant life, and into oxygen, which is released into the environment through the leaves. This process contributes to the plant's vegetative activity through growth in height and trunk diameter. Thus, from an anatomical point of view, it is effective to idealize a trunk as a succession of concentric cylinders, and to define three main directions: longitudinal L (medullary axis), radial R and tangential T (Figure 1.4.a).

The appearance of the cross-section of a plant's trunk is generally characterized by the presence of concentric rings each corresponding to a year of the plant's life. Generally, the rings formed in spring (earlywood) have lower density and lighter coloration than those in summer-autumn period (latewood). In addition, during the life of the plant, certain cells die, and

various phenomena are associated with their death, including the deposition of substances, often coloured. The area affected by this phenomenon is called heartwood, and it affects the inner part of the trunk for a large portion of the section; in addition, other layers such as sapwood, consisting of cells with sap transport function, cambium and bark, can be identified in the cross section of the trunk (Figure 1.4.b).

Within the trunk section, the structure and chemical composition gradually change moving from the inside to the outside. The composition of the cell wall can be seen as a composite material with a matrix (lignin), in which the fibrous elements with high mechanical strength (microfibrils) are present (Piazza et al., 2005). Thus, the main components of the cell wall are three: cellulose, hemicellulose and lignin (Figure 1.5.b). To these are added other components in smaller percentages, called extractives. This is a general and collective term to indicate a series of organic compounds present in certain wood species in relatively small quantity. They can affect colour characteristics and natural durability of wood. In terms of elementary chemical composition, wood has the dry weight percentages of 49% for Carbon, 6% for Hydrogen, 44% for Oxygen, while there are traces of other substances such as Nitrogen [19].

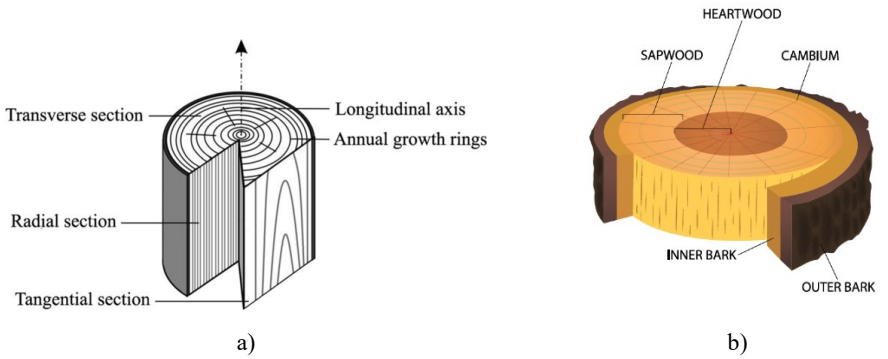

Figure 1.4. a) Anatomical direction of wood (extracted from: [21]); b) Basic structure of wood: tree cross-section [22].

The microstructure of wood should be analyzed by distinguishing the two major divisions that are commonly made in the botanical field, namely between angiosperms and gymnosperm. In fact, there are significant differences between angiosperms (hardwood) and gymnosperms (softwood)

in anatomical structure of wood (Figure 1.5.a). Tracheids make up the mass of wood cells in softwoods. They are positioned longitudinally within the trunk and make up the preponderance of the woody mass. In addition to conducting water, their primary functions are to support the tree's structure. Tracheids are not the only cells found in wood; parenchymal cells may also transport substances such as resins. Conversely, hardwood consists of two principal categories of wood cells: water conducting vessels (30% of wood volume) that facilitate high water conductance and fibres (which comprise 50% of the wood volume) that offer structural support [20]. Additionally, rays contain parenchymal cells, which serve a purpose analogous to that of softwoods.

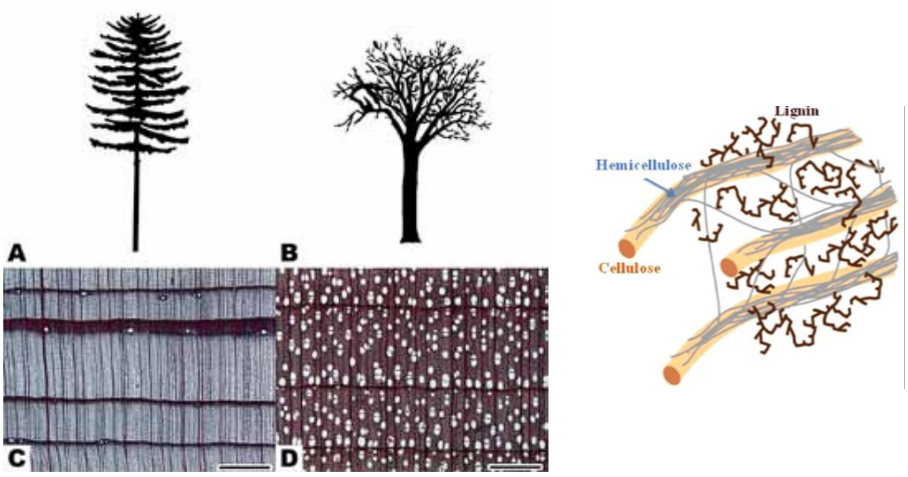

Figure 1.5. a) Difference in tree and microstructure between Softwood (A-C) and Hardwood (B-D) [24]; b) Main components of wood cell [20].

1.2.2 HYGROSCOPIC BEAHVIOUR

Wood, similar to numerous other organic materials, exhibits hygroscopic properties by absorbing moisture from its surrounding environment. The process of moisture exchange between wood and air is dependent by the relative humidity and temperature of the air, as well as the existing moisture content within the wood. The correlation between moisture and wood characteristics and performance is of significant importance. Numerous challenges associated with the utilisation of wood as an engineering material

come from variations in moisture content or excessive moisture present within the wood.

In the standing plant, water and other substances fill the wood cells. Following trunk cutting, the cell lumen is completely or partially filled with water (capillary domain of free water). After cutting down, the cell lumens of cut wood (green wood) begin to empty by evaporation of water into the external environment: this process, in low relative humidity environments, can progress until the cells are completely emptied, but also beyond; in this case the drying process involves water saturating the cell walls (hygroscopic domain of bound water). Thus, water molecules within cell walls can be called "bound water", while water in the macro-void structures is called "free water" or "capillary water" ([23]; Figure 1.6).

Most of the water in the cell wall is chemically bound to the molecular structure of cellulose. The process of losing the bound water is called desorption and results in the molecular chains moving closer together, with significant effects in terms of both dimensional variation and variation in physical mechanical properties. However, the desorption process is easily reversible and thus the microfibrils can capture water molecules again. Their saturation brings water into the capillary domain, resulting in the filling of the cell lumens with unbound free water. Variations in wood moisture within the capillary domain thus do not result in dimensional changes, only mass changes. The transition from the hygroscopic domain to the capillary domain is referred to as the fibre saturation point (FSP; [25], [26]). The moisture content at the FSP can vary depending on several factors, i.e., wood species, presence of extractives, bulk mass, percentages of late and early wood, etc. [27]. For different softwood the FSP values range from 38.5% to 42.5%, while Norway spruce *(Abies alba* Mill.*)* have a FSP of 42% at 20°C [26]. Conventional values of FSP are generally fixed in the range of about 25-30% for most of the wood species [27].

The quantification of water present within wood is referred to as the moisture content (MC), which is expressed as the mass of water relative to the weight of completely dry wood (Eq. 1.1):

$$MC = \frac{m\text{-}m_0}{m_0} \cdot 100 \qquad (1.1)$$

where:

MC moisture content of wood [-];

m mass of the specimen at a given moisture content [kg];

m_0 mass of the oven dry specimen [kg].

The moisture content of green wood can range from about 30% to more than 200% [27], furthermore the moisture content of sapwood is usually greater than that of heartwood. The physical and mechanical properties of timber are generally assessed "under normal conditions" or "standard condition", i.e. when the moisture content of the wood is 12%. For softwood, this value corresponds to an equilibrium condition with an ambient temperature of 20°C and 65% relative humidity [27].

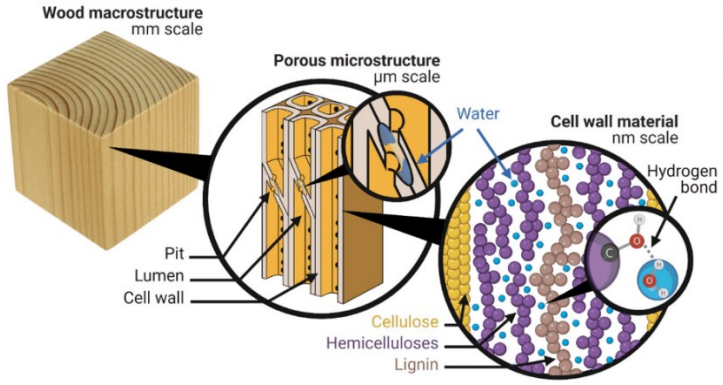

Figure 1.6. Water in different locations in wood: bound water and free water [23].

Moisture variations within the wood material are influenced by climatic environmental conditions, i.e. the temperature and relative humidity (RH) of the environment. In fact, it can be observed that a wood member placed in an environment with almost constant temperature and humidity, reaches a certain humidity value after a sufficiently long time. The material reaches a state of hygroscopic equilibrium with the environment when the quantity of water molecules bound by the material in a given period of time is equal to the quantity of water molecules released to the environment. The equilibrium moisture content (EMC) value depends not only on the climatic conditions, but also on the wood species and the history of moisture changes due to the hygroscopic hysteretic phenomenon [26]. Indeed, a difference between EMC reached by adsorption from the dry state and desorption from the saturation one can be found and it increases with decreasing temperature. This

dependence on moisture history is termed sorption hysteresis. This phenomenon can be easily recognized from the representation of the sorption isotherm, which is a discrete representation of equilibrium moisture states of wood when environmental temperature and RH are constant over time (Figure 1.7.a). Every equilibrium moisture state of wood, as depicted in the sorption isotherm (Figure 1.7.a), is attained through the process of water molecule absorption or desorption.

At the state of the art, there are numerous models for predicting the equilibrium moisture content of a wood element in a specific environment [26], [23]. These models describe the MC as a function of environmental temperature and humidity (Figure 1.7.b). Among these numerous models, experimental models can be distinguished from analytical models. Among the analytical models, two approaches can be identified: the first considers sorption as a surface exchange phenomenon, while the second considers it as a solution phenomenon [26]. Regarding the first approach, the best-known model is the BET sorption theory [28], later modified by Dent [29] into an expression identical to that given by [30]. However, the BET sorption model and the Dent model are inconsistent with the thermodynamic aspects of the sorption phenomenon [26]. The second approach [30] considers the phenomenon as a solution problem, considering wood in varying degrees of saturation (dry wood, wet wood, etc.) and provided the best degree of fit with the extensive experimental campaign conducted by Simpson [31]. The model of Hailwood and Horrobin, as well as the models obtained from the first approach, although they seem to adequately approximate the experimental findings, present contradictions with the principles of thermodynamics [26].

Recently Thybring et al. [32] fitted twelve equilibrium sorption models such as Hailwood-Horrobin [30], Dent [29], etc., to high-quality water vapor sorption isotherm data for wood at multiple temperatures [33], finding a disagreement between predicted values and experimental measurements. Although the models appear to be inadequate, their modelling according to a second-degree polynomial equation can approximate the experimental data, neglecting the theoretical background of the analytical models [23], [33]. However, the attainment of equilibrium for wood under real-life conditions is questionable due to the extended duration required to reach equilibrium under specific conditions and the inherent variability of the surrounding conditions, such as fluctuating air humidity [26].

Moisture variations within the wood material vary according to climatic conditions (temperature and RH). Changes in the moisture content of wood below FSP result in hygroscopic movements of shrinkage (shrinkage) and

swelling (swell). When water is absorbed by the cell wall, the wood swells, and when water is removed from the cell wall, the wood shrinks.

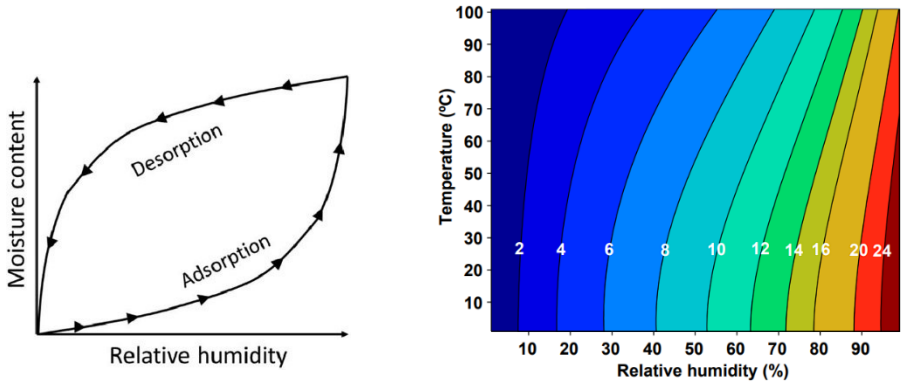

a) b)

Figure 1.7. a) Wood sorption hysteresis (extracted from: [34]) ; b) Equilibrium moisture content of wood (curves labelled with white values) as a function of relative humidity and temperature. (extracted from: [27]).

In general the wood shrinkage is influenced by a several variables, such as wood species and the wood density, since greater shrinkage is associated with greater density. Also the size and the shape of the wood member can affect shrinkage, as well as the rate of drying. Typical values for total volumetric shrinkage are in practice between approximately 9% and 23%. However, wood is an anisotropic material, therefore it shrinks (swells) most in the direction of the annual growth rings (tangentially and radially) and only slightly along the grain (longitudinally). The combination of radial and tangential shrinkage, coupled with the inclination of annual rings, may result in the deformation of wood parts into unintended forms. In addition, internal tensions can develop in the material, resulting in the formation of so-called shrinkage cracks (Figure 1.8.a). In elements containing the pith axis, the formation of cracks is practically unavoidable, as is the cupping of a board obtained from a tangential section. On the other hand, the deformations observed in bowed, bended and twisted boards are caused by wood defects such as reaction wood, spiral grains, etc., (Figure 1.8.b).

Average values for shrinkage from green to oven dry are between 0.1% and 0.2% for most species of wood, while reaction and juvenile wood can reach up to 2% of deformation; radial total shrinkage values vary between 3%

and 6% and transverse total shrinkage values between 6% and 12% [35].The difference between the shrinkage in the transverse plane between the radial and tangential direction is related to different aspects, such as the different microstructural properties of the wood fibres in the two planes or the mechanical action of the parenchymal rays that oppose movement in the longitudinal/radial plane [23]; in addition, the alternation of earlywood and latewood forces earlywood to shrink tangentially more due to its lower density than latewood.

1.3 TIMBER AS STRUCTURAL MATERIAL

1.3.1 NATURAL DEFECTS OF WOOD

In the field of timber structures, it is important to distinguish the behaviour of clear wood from that of members in structural dimensions that are to be placed in place. Indeed, the mechanical properties of timber in structural dimensions are influenced by the presence of "defects," which may be present within the timber member, and which can generally reduce the mechanical properties of the material. These are morphological singularities of the wood which are related to the vital needs of the plant. Therefore, the structural performance of a timber board can be influenced by the presence of the following defects: the presence of knots, the slope of grain, the ring shake, the shrinkage cracks, the reaction wood and the presence of pith.

Knots are formed by the change of wood structure that occurs when lateral bud development occurred. With increasing radial growth of the trunk, the branch bud is surrounded by a knot. In the case that the branch is still alive during the growth of the trunk, there is a continuous development of wood, resulting in a “adherent knot”. When the branch is died, a discontinuity may arise within the stem wood, resulting in a non-adherent knot. The mechanical properties of the timber member containing knots are generally inferior to those of clear wood, since they cause a discontinuity of the grain, as well as a grain deviation in the surrounding area. This discontinuity in the wood fibres leads to stress concentrations, which further contribute to the mechanical properties’ reduction in tension. Moreover, knots often lead to checking, a phenomenon characterised by the formation of cracks during the drying process. Knots have a much greater effect on strength in axial tension than in compression, and the effect on bending strength depends on the knots position with regard to the neutral axis: a knot at the tensile side has a greater effect on the capacity bearing than the knot at the compression side.

The wood grain refers to the longitudinal orientation of the primary components of timber, which include fibres or tracheid and vessels in the case of hardwoods. In numerous cases, the orientation of the wood fibres does not align parallel to the longitudinal axis, and it is commonly associated with irregular growth patterns exhibited by the tree. The slope of the grain mainly affects the bending strength of the timber member more than the axial strength (tension or compression). A general formulation for determining strength characteristics in the case of deviated fibres is Hankinso's equation [36].

The central part of the trunk comprising the pith and the wood is, from a mechanical point of view, a defect, as these areas generally have modest density and strength values. in addition, near the pith there is a high frequency of knots and splits.

Juvenile wood has anatomical peculiarities such as shorter cells, greater angles of inclination of microfibrils, and lower percentage of cellulose, which make it perform less well overall than normal wood, especially in terms of mechanical properties. In fast-growing woods generally, juvenile wood can account for a considerable portion of the section and thus affect the performance of the member.

Reaction wood is an abnormal wood tissue that originates as a result of persistent transverse loads acting on the standing tree, such as wind force. Reaction wood represents a serious defect within sawn timber because of the strong inhomogeneity of mechanical and deformation behaviour compared to normal wood. In particular, high axial shrinkage values can result in the formation of cracks and splits within structural elements, or undesirable deformations of boards related to the different shrinkage of the two faces (bow) or edges (spring) of a board, or a complete distortion of the whole board around its longitudinal axis (twist) (Figure 1.8.b).

Stress concentrations can be created within the standing tree and then released at cutting time, causing different deformations. Due to high stress gradients in the radial direction, crises in the material can occur, leading to the formation of ring shakes, i.e., separations between two consecutive growth rings, which are also favoured by the difference in strength between latewood and earlywood (Figure 1.8.b). This effect is very common in hardwood species such as chestnut, but also in spruce and larch [35].

The presence of lesions occurring at the cambium layer can lead to the integration of sections of the bark into the wood, which subsequently causes localised separations between growth rings. This process can result in the traumatic disruption of resin channels specifically in coniferous trees.

Consequently, the voids within the wood are filled with exudates that seep out from the injured conduits, resulting in the formation of resin pockets.

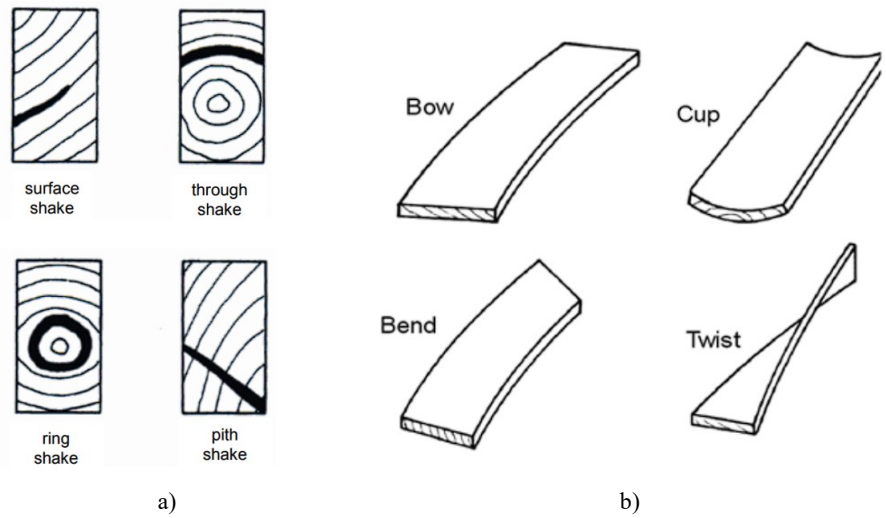

Figure 1.8. a) Main types of wood shake (modified from: [37]); b) Main deformation of sawn timber (modified from: [38]).

These resin pockets have the potential to adversely affect the overall quality of the sawn timber produced. The aesthetic damage primarily arises from the discontinuity of the fibres and the absence of heartwood formation in the central region of the trunk, instead being occupied by concentrations of sapwood.

1.3.2 MECHANICAL PROPERTIES

1.3.2.1 General properties

Mechanical anisotropy

As a result of its biological structure, wood is an anisotropic material; thus, its surface orientation in relation to its location in the trunk has a relevant impact on its properties. Given the morphology of the trunk, three directions can be identified: longitudinal, radial and transversal (Figure 1.9.a). The cross section is orthogonal to the longitudinal direction of the fibres, while the

section crossing the centre of the trunk is the radial section and the section parallel to the growth-ring tangential plane is the tangential section. The properties of wood are markedly affected by the orientation of the growth ring and fibre orientation. In order to describe the elastic behaviour of the material nine independent elastic parameter are needed: three modulus of elasticity (E_L, E_R, E_T), three tangential modulus of elasticity (G_{LR}, G_{RT}, G_{LT}) and six Poisson's rate (ν_{LR}, ν_{RL}, ν_{LT}, ν_{TL}, ν_{RT}, ν_{TR}). These parameters are illustrated in Table 1.1 [39].

Table 1.1. Modulus of elasticity for some wood species at moisture content MC:12% (extracted from: [39]).

Wood species	Modulus of elasticity E_0 [GPa]			Tangential modulus of elasticity G [GPa]		
	E_L	E_R	E_T	G_{LR}	G_{LT}	G_{RT}
Douglas fir	14.50	0.96	0.09	0.83	0.76	0.08
Fir red	11.71	0.83	4.94	0.70	0.66	0.07
Larch	14.13	1.05	0.69	0.84	0.78	0.09
Poplar	10.76	0.76	0.33	0.59	0.42	0.13
Pine	11.52	1.00	0.65	0.81	0.75	0.25
Beech	13.06	1.31	0.68	1.01	0.75	0.25
Oak	13.82	1.28	0.66	0.99	0.74	0.25
Birch	15.25	1.26	0.64	0.97	0.72	0.24
Balsa	3.30	0.27	0.08	0.21	0.14	0.03

However, for engineering applications, wood may be described as an orthotropic material, in which two main axes can be identified: longitudinal (0) and perpendicular (90) to the grain orientation (Figure 1.9.b). In this way the assumption of cylindrical-orthotropic material can be made confusing the radial and transversal anatomical direction. Based on these assumptions, the mechanical model of timber can be characterized by four independent properties: modulus of elasticity in parallel direction (E_0) and normal direction (E_{90}), tangential modulus of elasticity (G) and Poisson's ratio (ν). A general relationship for softwood is as follows: $G = E_0/16$ and $E_{90} = E_0/30$.

Failure mechanisms in compression, tension and shear

For the evaluation of the mechanical properties of wood, a distinction must be made between small clear wood and wood in structural dimensions. Small clear wood refers to the woods free from defects and irregularities on the macro level, whereas wood in structural dimensions is used to describe

members on a structural scale, where natural defects strongly affect the mechanical properties of timber. Therefore, an understanding of the mechanical behaviour of clear wood is fundamental to assessing the mechanical behaviour of wood in structural dimension. In order to better understand this detectable behaviour at the macroscopic level, it is useful to relate these properties to the anatomical characteristics of the material.

For compressive stresses parallel to the grain, wood can be seen as a set of fibre which, subjected to a compression load, reaches a buckling load and moves out of plane. In a timber element, this phenomenon can be recognized by the presence of local corrugations in the cell walls (Figure 1.10.b). In the stress-strain diagram (Figure 1.9.c) this mechanical behaviour corresponds to a curve with a first elastic branch and a second post-elastic softening branch (downward plastic branch).

When the wood is loaded orthogonally to the direction of the grain, the form of collapse observed at the anatomical level is associated with the lateral crushing of the wood cells, which occurs through instability crises of the cell side walls until the cell lumen is completely closed (Figure 1.10.d). In the stress-strain diagram (Figure 1.9.c) the linear elastic part is reached with very small deformations as soon as the first fibres begin to crush, while the subsequent pseudo-plastic zone is very long. Strength and deformability also depend on the arrangement of the growth rings with respect to the direction of the applied force. An important phenomenon contributing to the resistant mechanism is the so-called confinement effect, which is linked to the presence of unstressed lateral surfaces around the zone of load application.

With regard to shear strength, there are generally three modes of rupture that can be observed: orthogonal shear, parallel shear, rolling shear (Figure 1.12). In orthogonal shear, the cells tend to be stressed perpendicular to their axis; in practical cases, failures of this type are not frequent, since they are preceded by other modes of rupture (e.g., compression perpendicular to grain). More frequent are failure modes in which the shear acts parallel to the direction of the fibres, causing a slippage between the fibres parallel to their longitudinal axis. On the other hand, rolling shear consists of a separation of the fibres by rotation of one over the other. The resistance values for this type of stress are experimentally lower than those assumed in cases of parallel or orthogonal shear.

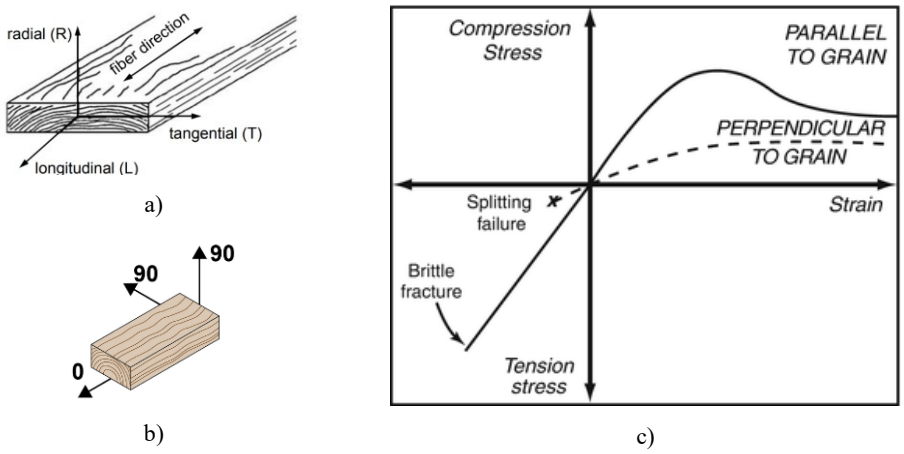

Figure 1.9. a) a) Three main directions in wood with respect to grain direction and growth rings; b) Two main direction in wood assuming a mechanical model of cylindrical-orthotropic material; c) Stress-strain relation for generic clear wood in compression and tension, parallel (continuous line) and perpendicular (dot line) to grain (modified from: [40]).

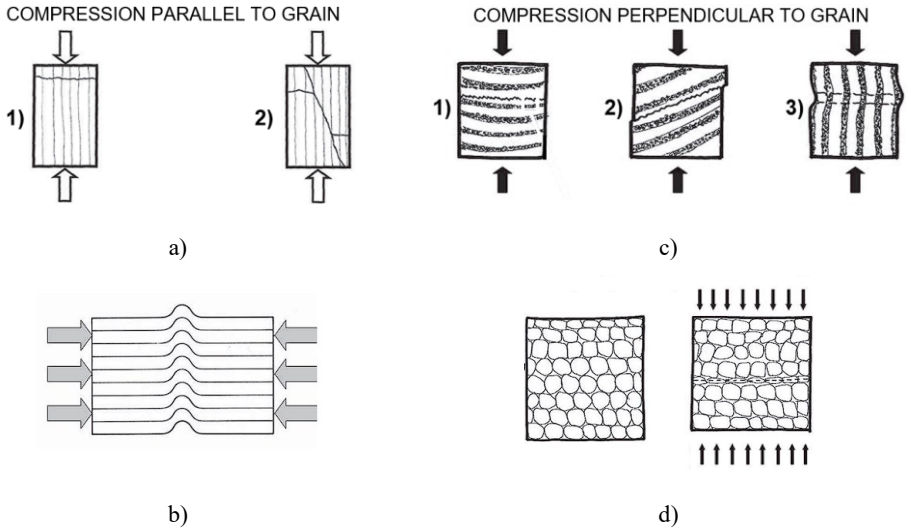

Figure 1.10. Failure in compression parallel (a-b) and perpendicular (c-d) to the grain: a) failure modalities - crushing (1), crushing and splitting (2); b) corrugation of the wood cells [35]; c) failure modalities as a function of load-growth ring orientation – perpendicular (1), transversal (2), parallel (3); d) wood cells before and after load application.

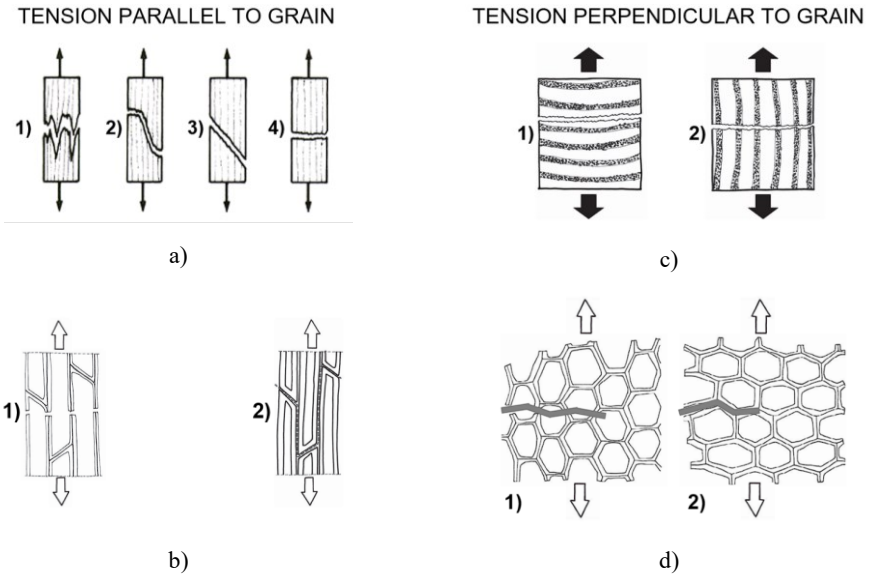

Figure 1.11. Failure in tension parallel (a-b) and perpendicular (c-d) to the grain: a) failure modalities – splintering tension (1), combined tension and shear (2), shear (3), brittle tension (4) [39]; b) anatomical failure modalities – rupture of the cell walls (1), separation of median lamella tissues (2)[35]; c) failure modalities as a function of load-growth ring orientation – parallel (1), perpendicular (2); d) anatomical failure modalities – rupture of the cell walls (1), separation of the cell walls (2).

The behaviour of wood in parallel tension is characterised by an elastic and fragile stress-strain law, with huge differences in ultimate load value as function of the inclination between the direction of the loads and the direction of the grain. For defect-free wood, the tensile strength parallel to the grain reaches the highest strength values, while in the perpendicular direction the lowest one. The high strength in the parallel direction is due to the mechanism at the macro-structural level, which consists of the elongation of the microfibril fibres in the direction parallel to the cell axis (Figure 1.11.b). In the perpendicular direction, the failure is externally brittle because the rupture generally occurs at the level of the early wood where the cell walls are thinner (Figure 1.11.d).

Failure mechanisms in bending

With regard to the bending behaviour of a clear wood member, collapse occurs according to one of the illustrated mechanisms in tension and compression, or as a combination of them. In general, 6 modes of bending failure can be identified for clear wood [39]. Failure type “a” is generally observed in high-density wood, while failure type “b” occurs in the presence

of fibre deviations; failure type “c” (splintering tension) occurs in specimens with low moisture content, while brittle failure of the through-bearing type (type “d”) indicates the presence of an atypical molecular structure. The presence of low-density wood can cause pseudo-ductile behaviour (type “e”), in which a compressive failure initially prevails, until tension fracture occurs. Fracture type “f” is observed in some species, due to the early wood strength being much lower than the late wood one [35].

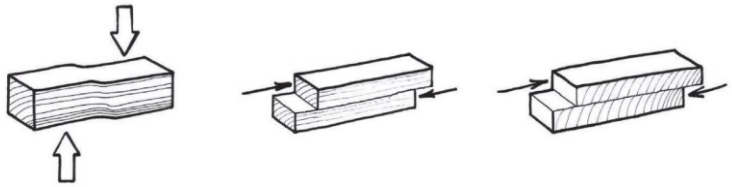

Figure 1.12. Shear failure with respect to different grain orientations [35]: a) perpendicular; b) longitudinal; c) rolling shear.

In general, the bending strength is determined according to the Navier theory, considering the assumption of elastic-linear material behaviour until failure and conservation of plane sections. However, in an experimental test in bending, it can be observed that a clear wood specimen can develop a pseudo-ductile behaviour, in which material shows a non-linear behaviour due to the plastic deformation in compression (Figure 1.13.b;[41]). By the analysis of the stress diagram during a monotonic bending test, it can be seen that the normal stresses increase until the maximum compressive stress parallel to grain is reached (Step 3 in Figure 1.13.a); then a redistribution of stresses occurs, and the neutral axis is progressively lowered (Step 4 in Figure 1.13.a). Thus, at the compression side the stress diagram is trapezoidal in shape due to the plastic deformation of the material, whereas at tension side the stress diagram is triangular in shape (Figure 1.13.a). Here the tensile stress continues to increase until the maximum value is reached, which results in the failure of the member (Step 5 Figure 1.13.a).

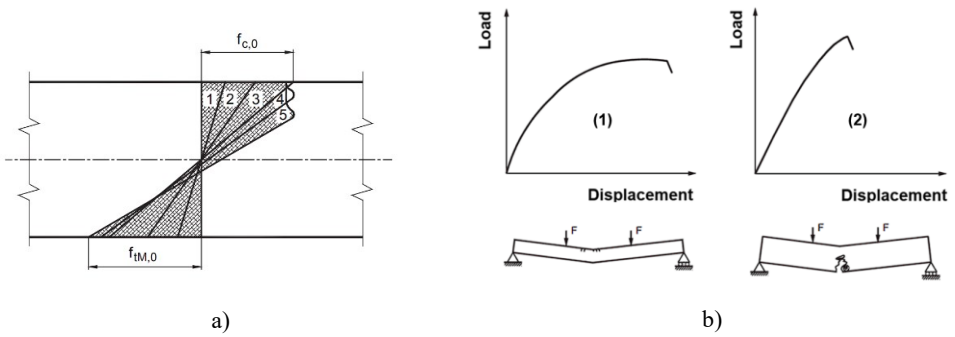

a) b)

Figure 1.13. a) Stress diagrams due to positive bending during a monotonic test [35]: linear behaviour (1, 2, 3) and non-linear behaviour (step 4 and 5); b) Load-displacement curve for bending test up to failure (modified from: [35]): pseudo-ductile (1) elastic (2) behaviour.

This pseudo-ductile behaviour is typical of clear wood, whereas for timber in structural dimension the failure generally occurs in elastic field (Figure 1.13.c), since wood defects such as knots, slope of the grain, ring shakes, shrinkage cracks, etc. strongly affect the bending strength.

Moisture content influencing mechanical properties

Many mechanical properties of timber are affected by changes in moisture content below the FSP. In fact, it has been observed that most of properties show an increase as the moisture content decreases and vice versa. However, the influence on the mechanical properties is reduced when moving closer to the FSP. This is due to the fact that water absorbed by cell walls cause a softening effect, while the presence of free water in the cell cavity does not have any noticeable impact on structural integrity contributing only to an overall increase in the weight.

The variations in strength and stiffness properties, resulting from changes in moisture content values, are primarily influenced by the wood species and the specific mechanical parameter being considered. Several authors conducted many studies in the past regarding the variation of the mechanical properties of wood as a function of moisture content, they mainly concern coniferous wood (Figure 1.14.a). McLain et al. [42] and Aplin et al. [43] performed several tests on structural members in Southern pine and Douglas fir respectively, studying the effects of moisture content on bending strength and modulus of elasticity. They found that the relationship between MC and the mechanical properties depends on timber size and quality, as well as the bending strength was much more affected by MC variations than the modulus of elasticity. Ido et al. [44] conducted a study to examine the influence of size

on the strength of timber in Sugi (*Cryptomeria japonica*). They found a relationship between the cross-section area and the strength variation in bending, evidencing that the strength variation as function of moisture content was higher for small specimens and high-quality timber.

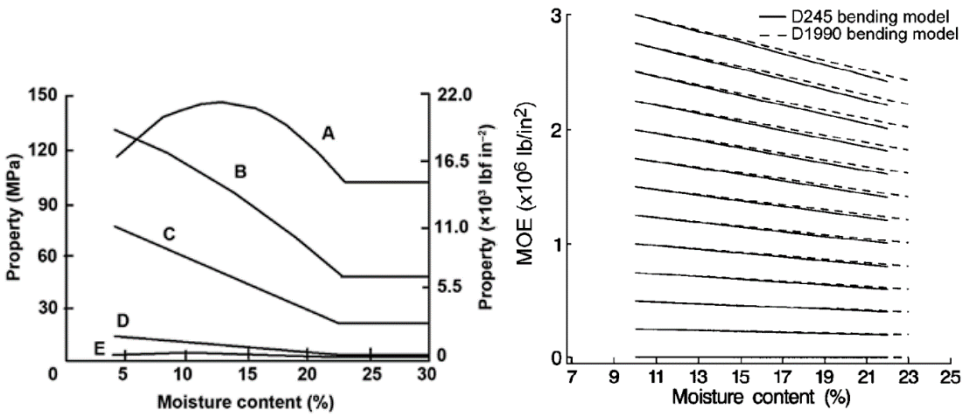

a) b)

Figure 1.14. a) Effect of moisture content on wood strength properties (A, tension parallel to grain; B, bending; C, compression parallel to grain; D, compression perpendicular to grain; and E, tension perpendicular to grain) [45]; b) Effect of moisture content on modulus of elasticity in bending comparing the ASTM D1990 and D245 model [46].

As results of several experimental tests analytical models were developed for estimating the bending strength and modulus elasticity at MC values from the standard condition (MC: 12%) [46], [47], [48]. Nowadays, the linear constant percentage adjustment model is widely acknowledged as the main method for evaluating mechanical properties at different MC values below the fibre saturation point (FSP). It is used in European standard UNI EN 384 [49]. According to UNI EN 384 [49], the wood density (ρ_{12}), compression strength parallel to grain ($f_{c,0,12}$) and modulus of elasticity parallel to grain ($E_{0,12}$) at MC:12% can be evaluated as follow (Eq. 1.2, 1.3, 1.4):

$$\rho_{12} = \rho_{(u)} \cdot [1+0.005 \cdot (MC-MC_{12})] \quad (1.2)$$

$$f_{c,0,12} = f_{c,0,(u)} \cdot [1+0.03 \cdot (MC-MC_{12})] \quad (1.3)$$

$$E_{0,12} = E_{0,(u)} \cdot [1+0.01 \cdot (MC-MC_{12})] \quad (1.4)$$

where:

ρ_{12} wood density at MC_{ref} [kgm^{-3}];

$f_{c,0,12}$ compression parallel to grain at MC_{ref} [MPa];

$E_{0,12}$ modulus of elasticity parallel to grain at MC_{ref} [MPa];

$\rho_{(u)}$ wood density at MC different from MC_{12} [kgm^{-3}];

$f_{c,0,(u)}$ compression parallel to grain at MC different from MC_{12} [MPa];

$E_{0,(u)}$ modulus of elasticity parallel to grain at MC different from MC_{12} [MPa];

MC moisture content of wood (8%≤MC≤18%) [%];

MC_{12} standard moisture content of wood (12%) [%].

Given the lack of studies about the Chestnut wood (*Castanea Sativa* Mill.), recently Nocetti et al. [50] investigate the influence of moisture content on the bending properties defining proper moisture content adjustment factors for density, static and dynamic modulus of elasticity. For density they found adjustment factor very close to that provided by UNI EN 384 (2022) below the FSP, while for modulus of elasticity they provide different equations for static and dynamic modulus below and above the FSP.

1.3.2.2 Time-dependent behaviour

Being wood a composite fibre material it has a viscoelastic behaviour, indeed mechanical properties of wood are time-dependent. As regard strain, if wood is subjected to a constant stress it shows increasing deformation over time. This phenomenon has been explained by various conceptual model; according to Boyd [51] viscoelasticity can be generally attributed to the yielding of the liquid substances embedded by wood fibre, while according to Grossman [52] the breaking of the hydrogen bonds between the cellulose chains is responsible for the creep in wood. However the creep behaviour is influenced by several factors, such as the load value, the duration of load (DOL), the loading history and the load direction, the moisture content and MC history, as well as the environmental temperature [53].

With regard the load direction Gressel [54] conducted creep tests on timber beams, revealing larger shear creep than compression or bending, whereas Ranta-Maunus [55] found transverse timber creep in Finnish spruce significantly higher than longitudinal creep. As regard the load and its duration, it has been seen that for a load time duration sufficiently long, a timber member can reach failure by showing lower strength values than in an instantaneous test. In other words, higher values of strength are obtained for wood loaded at a more rapid rate, and lower values are obtained at slower rates. Therefore, for a load value such that failure occurs, the typical creep behaviour curve is shown in Figure 1.15.a. The deformation-time curve is characterized by 4 branches corresponding to 4 creep stages: primary, secondary, tertiary and failure [56]. Usually creep deformations increases quickly in primary and tertiary stages. When the load is limited in time, the deformation-time curve is similar to the curve in Figure 1.15.b, in which 5 branches can be identified (A, B, C, D, E). Phase A corresponds to the elastic deformation, whereas in phase B the creep deformation increases due to the viscoelastic behaviour. When the load is removed, the elastic deformation component is immediately recovered (phase C), while creep deformation is gradually recovered (phase D), even though residual plastic deformation can remain.

In general under moderate loading the wood viscoelasticity can be considered linear, thus only primary and secondary creep happen, which means that contribution of each loading in different periods to timber creep is independent [57]. Conversely, if the stress level exceeds the threshold of linear creep, all three stages of timber creep will occur [58]. The occurrence of both visco-elastic and visco-plastic creep phenomena becomes evident when the applied stress exceeds the threshold of linear creep. This observation suggests that the deformation of timber due to creep is not only time-dependent but also dependent by the stress level (Navi and Stanzl-Tschegg, 2009).

The modelling of the viscoelastic behaviour of wood is a complex and still ongoing challenge, as many phenomena have to be taken into account. In addition to the relaxation phenomenon that develops under constant temperature and MC conditions, the creep induced by temperature variations and changes in moisture content, which is commonly recognised as mechano-sorptive creep, should also be taken into account [59]. Indeed, several experimental tests have shown the influence of temperature on creep [60] and several models have subsequently been proposed [61]. Other experiments consisting in the cyclic variation of the moisture content showed the effect of

mechano-sorptive creep [59]. However, the physical mechanisms governing the mechano-sorptive effects remain poorly understood [62].

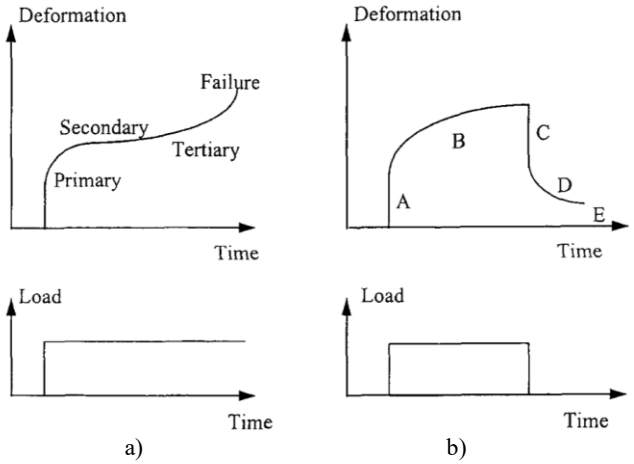

Figure 1.15. General creep behaviour [56]: a) for idealized long-term load; b) for a limited time duration load.

In order to simulate the creep behaviour of timber, several models have been proposed by many authors using different approaches. In general conceptual model can be distinguished by phenomenological model [58]. Conceptual models describe and simulate the phenomenon at the miscropic level, and these include models such as the hydrogen bond model, the polymer model, sliding face model, physical aging model [50], [63], [64]. These models allow an understanding of the essence of creep but are difficult to apply at the scale of the structural element as a large number of parameters are involved.

The phenomenological model can be further grouped in empirical and mechanistic models [58]. The empirical model employs mathematical functions like power, exponential, and logarithmic functions to describe timber creep [56], [65]. Among the empirical model, power law model is commonly adopted due to its suitability [66], [67], [69]. On the other hand, mechanistic models are based on rheological theory, according to which the model is made of series and parallel combinations of elastic springs and viscous dashpots [51]. Maxwell model and Kelvin-Voigt model are two typical mechanical models for creep behaviour [68].

Due to the impact of time-dependent behaviour of timber on deformation and load bearing capacity of structures, different national standards proposed simplified approach to take into account this phenomenon [70], [71], [72], [73]. This approach consist in providing creep coefficients as function of the load time-duration. In detail, standard approach focuses on strength reduction, in order to avoid the occurrence of the creep failure, and deformation, in order to account for the deformation increase due to viscoelastic behaviour. As regard the timber strength, the Eurocode 5 [70] takes into account the creep behaviour through the k_{mod} coefficient, which also considers the influence of moisture content variation on mechanical properties. The regulation provide different valus of k_{mod} as function of the service class and the load-duration class. UNI EN 1995-1-1 [70] defines three service classes to which correspond different values of relative humidity and environmental temperature to which the structure may be exposed during its service life, whereas five load duration classes are provided to take into account permanent, long, medium and short-term loads, as well as instantaneous loads. In this way if the duration of the load is longer the design strength is lower to avoid the occurrence of the failure due to creep. In Figure 1.16 values of k_{mod} are provided for different load duration classes and service classes. Instead, by multiplying the elastic modulus E for a reduction factor called k_{def} the deformation are increased in order to take into account the creep deformation. In other words, the material is considered more deformable to take into account the extra amount of deformation due to creep. Even the k_{def} values are provided for different service classes and materials (Figure 1.17).

Material	Standard	Service class	Load-duration class				
			Permanent action	Long term action	Medium term action	Short term action	Instanta-neous action
Solid timber	EN 14081-1	1	0,60	0,70	0,80	0,90	1,10
		2	0,60	0,70	0,80	0,90	1,10
		3	0,50	0,55	0,65	0,70	0,90
Glued laminated timber	EN 14080	1	0,60	0,70	0,80	0,90	1,10
		2	0,60	0,70	0,80	0,90	1,10
		3	0,50	0,55	0,65	0,70	0,90

Figure 1.16. Values of k_{mod} for solid timber and glulam (extracted from: [70]).

Material	Standard	Service class		
		1	2	3
Solid timber	EN 14081-1	0,60	0,80	2,00
Glued Laminated timber	EN 14080	0,60	0,80	2,00

Figure 1.17. Values of k_{def} for solid timber and glulam (extracted from: [70]).

1.3.3 TIMBER DURABILITY ISSUES

1.3.3.1 General

Durability is a fundamental requirement for a construction. It is influenced by several factors, like physical properties of materials, service condition, design, as well as protection and maintenance measures put in place to prevent degradation of materials and structures. Timber is particularly susceptible to the degradation due to several aspects. In order to understand which factors, influence the durability of a timber structure, it is necessary to identify the types of degradation that can affect it. A preliminary distinction should be made between wood degradation and wood decay – wood degradation is a collective term for major factors causing damage to wood, both biotic (e.g., fungi and bacteria, insects, etc.) and abiotic (e.g. weathering), while decay is more specific to biotic degradation caused by biotic agents such as fungi, bacteria and insect [74]. In general, the phenomenon of wood degradation is associated with causes and effects (Figure 1.18). Generally, the cause is to be found in the combination of intrinsic wood factors and external factors [75] that predispose the timber element to degradation (e.g., the presence of sapwood in some wood species is a major cause of insect attack). The resulting effects can be purely visual, as seen with superficial discoloration caused by exposure to ultraviolet radiation, without impacting the material's physical integrity or mechanical properties. Alternatively, degradation may manifest visually alongside physical and mechanical issues, as evidenced by insect attacks leaving galleries and flackery holes that reduce the cross-section of the member, thereby compromising its structural integrity.

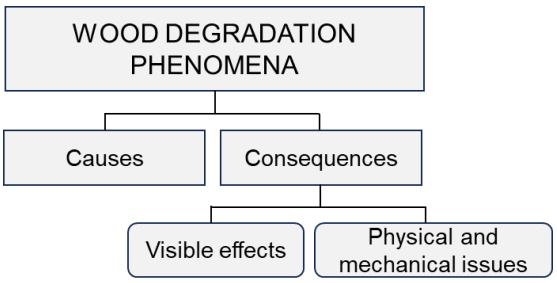

Figure 1.18. Conceptual scheme related to the causes and effects of wood degradation phenomena.

A decrease in the performance of a timber structure caused by deterioration can lead to a reduction in service life, i.e., non-fulfilment of expected performances over the design life. Therefore, in addition to verifying structural strength, the designer should conduct a verification of the structure's protection against durability issues by comparing demand and capacity in terms of durability [35]. Thus, as well as for loads, the durability demand consists of the wood degradation phenomena that can affect a given structure. On the other hand, capacity should be assessed by taking into account the natural durability of the wood member and any protective measures put in place by the designer, such as protective treatment or protection through care of construction details [35] (Figure 1.19).

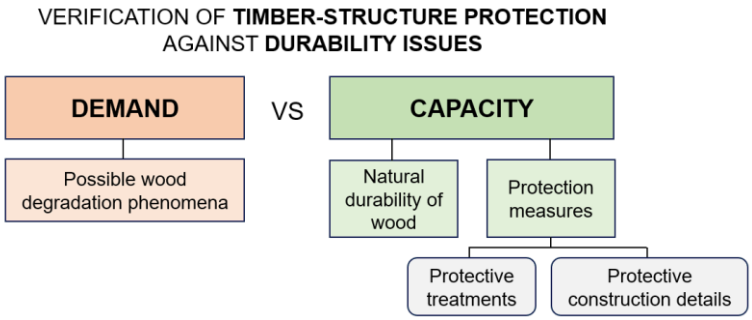

Figure 1.19. Conceptual scheme related to the causes and effects of wood degradation phenomena.

Beyond any protective measures, wood as an organic material has a certain resistance to degradation phenomena, the so-called natural durability. According to UNI EN 350 [76], wood durability is the “resistance of wood to destruction by wood-destroying organisms”. The term "natural durability" refers to the durability of a timber product or component that has not undergone any form of protection treatment or improvement to enhance its durability. Therefore, natural durability is a key factor to predicting the service life of a timber structure and it depends by several factors related to wood species. One of the primary determinants is the quantity and composition of heartwood extractives. However, other factors such as wood anatomy, wood density, lignin concentration, and moisture content also play a role in determining natural durability of wood [77], [78]. Standardised tests can be used to quantify the inherent resistance of wood to organisms such as wood-decay fungus and insects. In general wood species with differentiated

heartwood are more durable than those with no visual difference between heartwood and sapwood, as well as temperate gymnosperms are more durable than the angiosperms [80], [78]. As results of decades of experimentation regarding wood decay tests, UNI EN 350 [76] provide a classification of the wood species according to their natural durability. Five classes are defined for durability against fungi (1. Very durable, 2. Durable, …, 5. Not durable), two for insects (D. durable and S. susceptible) and three for termites and marine organisms (D. durable, M. moderately durable, S. susceptible).

As mentioned above, in addition to the natural durability of the wood species, the occurrence of decay phenomena is influenced by external factors, such as exposure to weathering. In this sense, structural elements placed outdoors and not protected from the weather are surely more exposed than those in covered and air-conditioned environments. To this end, UNI EN 335 [79] establishes the use classes (UC) or hazard classes, i.e., a five-class system that provides information regarding the exposure conditions to moisture of timber structures in service and the occurrence of different groups of decay organisms such as wood-discolouring and decaying fungi, beetles, termites, and marine borers seawater contact. This is presented on a scale of 1–5; UC 1: no soil contact, interior, dry to UC 5: seawater contact.

1.3.3.2 Biotic degradation phenomena

Insects

The biotic degradation phenomena of wood, or wood decay phenomena, due to insect attacks is common in timber structures. They can cause damages which severity depends on the type of insects [81], [82], but in general, insect attack results in a reduction of the residual section of the timber element due to the destructive action of the insects. A main distinction can be found between two groups of insects, which stand out for their impact on wood decay in Europe: beetles (*Coleoptera*) in the families *Anobidae, Cerambycidae, Lyctidae* and termites (*Isoptera*) in the families *Kalotermitidae and Rhinotermitidae* [81], [74] (Figure 1.20).

Anobiidae and *Bostrichidae* (to whose family *Lyctidae* belong) along with Cerambycidae are the most common families of beetles destroying timber heritage [74]. "Death-watch beetles", "woodworm beetles", and "furniture beetles" are common names for *Anobiidae* members. In temperate regions, they constitute one of the most significant families of wood-boring

insects [83]. Around fourteen anobiid species have been recognised as significant timber pests in Europe; among these, *Xestobium rufovillosum* and *Anobium punctatum* appear to be the most frequently documented [84] (Figure 1.21).

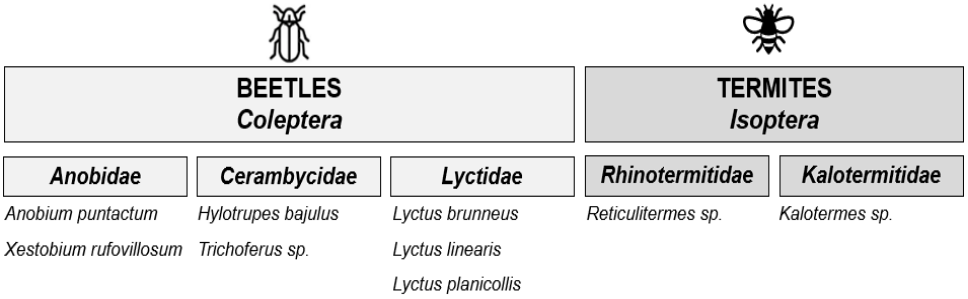

Figure 1.20. Common families of insects deteriorating wood in Europe.

In relation to wood species it appears that each anobiid species has its own preferences. *Anobium punctatum* attacks nearly all of the important temperate hardwoods and softwoods of Europe, however tropical wood species such as *Eucalyptus* appear to be immune to its attack. Sapwood is preferred by *Anobium punctatum* over heartwood, and the outermost sapwood with the highest nitrogen content in particular. *Xestobium rufovillosum*, conversely, inhabits damp, decaying hardwoods, predominantly oak and willow but also softwoods including pine and hawthorn, ash, beech, poplar, sweet, chestnut, white, and horn [74], [84], [85]. In general, all *Anobiidae* members attack wood at moisture contents over 15%, while the optimal moisture levels for their development is greater than the FSP [86]. During their development, wood-boring beetles undergo a complete metamorphosis, transforming from eggs to larvae to nymphaea to adults. The wood is exclusively consumed by the larvae, which further penetrate it using their highly developed mandibles, which are directed anteriorly. Upon hatching, the larvae of anobiids begin to feed and develop within the wood, forming an intricate network of numerous small, circular tunnels. Tunnels are closely packed with this mixture of wood fragments and faeces, known as “frass”, which fills up the burrow and varies in colour, shape and size according to species [74] (Figure 1.22.a). Typically, *Anobiidae* follow the wood grain, and they are 1–4 mm in diameter depending on the species [74]. They produce a

circular exit (flicker) hole (Figure 1.23.a), which varies in diameter according to species, but it generally range in size between 1 and 6 mm [74].

Lyctinae is a subfamily of *Bostrichidae* and it is a group of species which are common in attacking wood in structures. True-powderpost beetles are members of the *Lyctinae* subfamily; the name "true-powderpost beetles" is derived from the frass, which is an extremely fine, powdery substance resembling talcum powder or baking flour, and is generated throughout the feeding process [87]. The *Lyctinae* occurs mostly in the tropics, but it has been introduced and spread in Europe, the United States, Australia and Japan [84]. Larva length ranges from 3 to 20 mm and rarely reaches 60 mm. They attain a length of 2–7 mm as adults. Drywood pests, specifically *Lyctinae*, exhibit optimal growth in wood containing a relatively low moisture content (8% to 30%), with peak activity occurring between 10% and 20% [74]. Many significant timber species are vulnerable to *Lyctinae* members, including oak, walnut, ash, hickory, sycamore, sweet chestnut, elm, poplar and African mahogany and also imported tropical hardwoods like agba, obeche afara mahogany, iroko, ramin, seraya, meranti, teak and keruing and bamboo [84], [85], [87]. Wood damaged by true-powderpost beetles presents numerous small tunnels filled with frass similar to powder. The frass found in true-powderpost beetles exhibits a resemblance to talcum or flour and is loosely accumulated within galleries (Figure 1.22.b). *Bostrychids* tunnels vary greatly in size and shape. The true powderpost beetles create narrow, circular tunnels measuring 1-2 mm in width [74]. These tunnels can have a random direction but are primarily aligned parallel to the wood grains. They are found exclusively in the sapwood of hardwood trees [74]. Also the size of flicker holes varies among *Bostrichidae*, however true-powderpost beetles produce small circular exit holes ranging from 1 to 3 mm in diameter [85] (Figure 1.23.c).

Cerambycidae is one of the largest beetle families in the world and, due to their long antennae, *Cerambycidae* members are commonly known as “longicorn” or “longhorn-beetles” [74]. *Hylotrupes bajulus*, also referred to as the "European house borer" or the "old-house borer," is the most significant species that infests dry or seasoned wood [84] (Figure 1.21). *Cerambycids* are distributed worldwide, from sea level to 4200 m above [88], however the concentration is highest in the tropical and subtropical parts of the world. The *Cerambycidae* beetles are easily identifiable due to their distinctive long antennae and elongated bodies, which can range in length from 2 to 200 mm, although the typical range is 5-50 mm [89], [74]. Larva body has a lightly sclerotized surface and a length ranging from 5 to 220 mm [88]. The notorious

Hylotrupes bajulus typically attacks seasoned sound coniferous genera like Pinus, Picea and Abies [85]. A study examining the inherent resistance of different wood species to *Hylotrupes bajulus* revealed that *Pinus sylvestris* and *Abies nordmanniana*, both coniferous species, were the most susceptible, while *Fagus orientalis* and *Populus tremula*, both broadleaved species, exhibited the highest level of resistance [90].

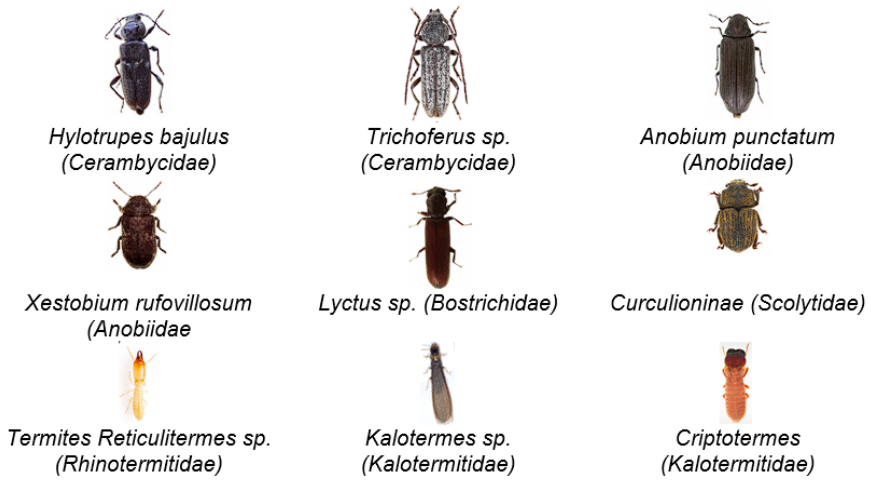

Figure 1.21. Main insect species deteriorating wood in Europe.

Hylotrupes bajulus requires wood moisture content above the fibre saturation point (30–40%) for optimal development, although can tolerate higher values up to 65% [74]. *Hylotrupes bajulus,* unlike most wood-boring cerambycids that typically inhabit forests, is capable of reproducing in seasoned wood. However, its development is significantly accelerated in recently felled timber. Moreover, whereas most longhorn beetles do not reinfest timber, several species, including *Hylotrupes bajulus*, it has the ability to repeatedly infest the same wood and result in significant structural damage [86]. Frequently parallel to the surface, the cavities of *Hylotupes bajulus* are demarcated by a thin layer that protrudes in a blister-like fashion. [74]. Initially cylindrical in cross-section, the tunnels beneath the sapwood's outer epidermis transform into oval, characteristically straight tunnels that follow the grain direction [8]4. The size of Cerambycid tunnels depends on the species and it varies greatly. *Hylotupes bajulus* galleries are of 7–12 mm diameter leading irregular oval exit holes of 3-9 mm diameter [74] (Figure

1.23.c). Its frass is uniformly yellowish, and the faecal pellets are typically cylindrical [84], [85], [91] (Figure 1.22.b). The walls of its tunnels often appear finely grooved, and they are frequently filled with the wood-dust left behind by the insects.

Termites are a monophyletic group of eusocial insects in the epifamily *Termitoidae*, order *Blattodea*, infraorder *Isoptera* [74]. In contrast to wood-boring beetles, termites are social insects, living in colonies organized through different castes and among them, only the workers significantly damage wood [92], [82] (Figure 1.24.a-b). In general, termites develop in environment characterized by relative humidity between 70% and 90% and temperatures between 26°C and 32°C [92]. As a result, tropical, subtropical, and temperate regions comprise most of their natural distribution. In Southern European countries like Spain, Portugal, Greece, Italy, and France, endemic infestation of termites occurs [75]. Two main groups take part in degrading wood: subterranean termites (*Rhinotermitidae*) and dry-wood termites (*Kalotermitidae*; Figure 1.21). Subterranean termites are the most widely distributed family of termites in Europe [93]. Subterranean termites form large colonies (from several hundred thousand to millions of individuals), they build their nests in the soil at 70–100 cm deep and explore wood sources in their surroundings, usually within a radius of less than 10 m [78].

On the other hand, dry-wood termites build their nests in wooden elements, forming small colonies (hundreds to thousands of individuals). They can live within structural timber and furniture inside buildings with very low moisture content and develop entirely within the wood [94]. Because Subterranean termites require high levels of moisture, damage by them is usually associated with high moisture contents of timber. Subterranean termites preferably attack decayed wood with MC higher than 20% [74]. In opposition to the subterranean termites, dry-wood termites do not require the soil and moisture supply. They may attack all untreated timber structures as low as 13% wood MC [74]. All termite species feed primarily on cellulose by the chewing action of their mandibles, in addition they degrade wood components by means of the production of endogenous cellulolytic enzymes and other substances [74]. They can attack hardwoods and softwoods and usually prefer feeding on earlywood, leaving intact thin layers of latewood due to its higher density (Figure 1.25.a-b). They can destroy not only solid wood, but any other product derived from wood, such as fibre and particleboard or paper. This results in the characteristic laminated appearance observed on termite-infested timber elements [74] (Figure 1.25.c). Furthermore, some species of termites, such as *Rhinotermitidae*, cover the

galleries in wood with moist mud (Figure 1.26.a-b) due to their characteristic of living in high-humidity environments. Instead *Kalotermitidae* leaving in the cavities release a characteristic dust in the form of hexagonal prisms[95] (Figure 1.26.c-d). Additionally, the existence of discarded wings or winged reproductive individuals serves as a reliable indicator of a previous wood infestation.

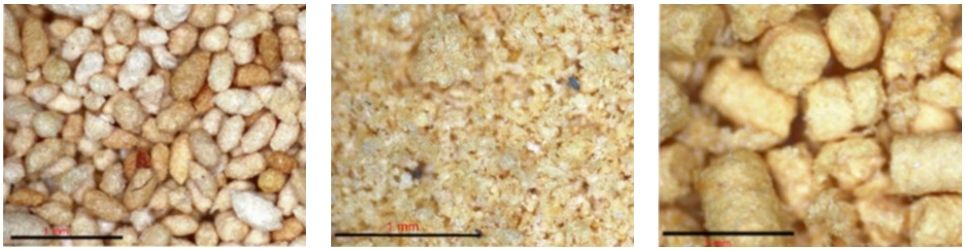

a) b) c)

Figure 1.22 Insect faeces from different insect species (modified from: [78]): a) *Anobium;* b) *Lyctidae*; c) *Cerambycidae.*

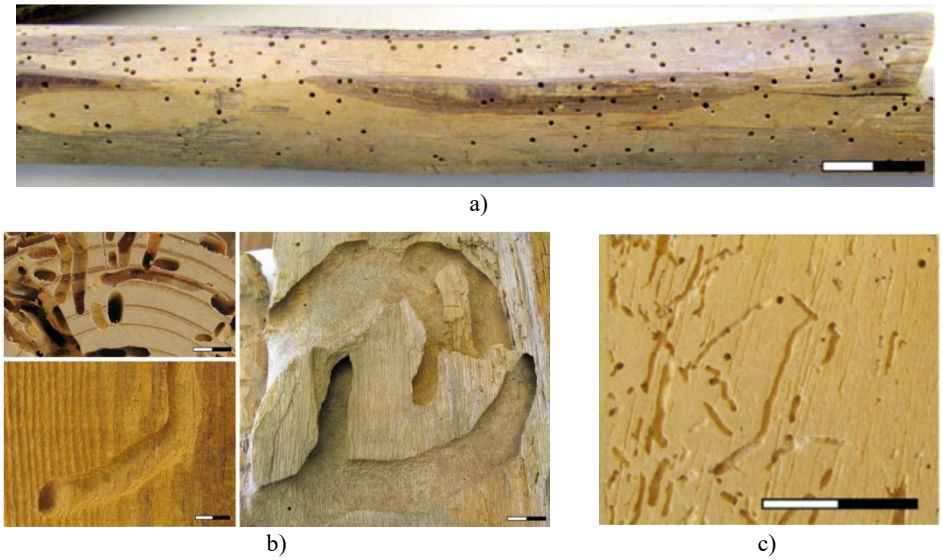

a)

b) c)

Figure 1.23 Visual effects due to insect attacks: a) Exit holes of *Anobium punctatum (Anobiidae;* modified from: [74]); b) Tunnels excavated by *Hylotrupes bajulus* (*Cerambycidae;* modified from: [74]); c) Tunnels and flicker holes produced by a *Lyctus spp.* (modified from: [74]).

a) b)

Figure 1.24 a) Termites' castes; (b) Royal cell of Cubitermes sp., with the queen, workers and soldiers (extracted from: [74]).

a) b) c)

Figure 1.25 a) Termites galleries following growth rings (transversal section view; extracted from: [74]); b) Termites galleries following growth rings (longitudinal section view; (extracted from: [74]; c) Damage by a dry-wood termite where galleries are separated by thin fragments of wood (extracted from: [74]).

a) b) c) d)

Figure 1.26 a-b) Detail of gallery of *Rhinotermitidae* covered by mud (modified from: [78]); c-d) Drywood termite faecal pellets (modified from: c. [74] d. [78]).

Microorganisms (fungi, mould, bacteria)

Timber is an organic material and its main components within the cell wall are hemicelluloses, cellulose and lignin, which provide the structural properties of wood. These compounds, along with others, are vulnerable to

degradation by specialised microorganisms, fungi and bacteria being the most prevalent. As a result, microorganisms capable of degrading wood utilise arrays of extraordinarily specialised enzymes and metabolites to gain access to resources within the cell wall; some of these microorganisms are exclusively capable of metabolising lignin and cellulose, while others are confined to polysaccharide metabolism [78].

Fungi can be found in a wide variety of aquatic and terrestrial habitats. Their modes of existence encompass parasitic (e.g., wood decomposers) and mutualistic (e.g., mycorrhizae in plants or mycobionts in lichens) conditions [78]. In order to cause damage to wood, decay fungi typically necessitate elevated moisture content (greater than 20%–30%), therefore the availability of water falls short of sustaining fungi below the fibre saturation point [96]. Consequently, the risk of decay due to fungi causing is minimal in environments where the wood component remains dry, such as air-conditioned indoor environments. A wide variety of enzymes, with the majority falling into the categories of hydrolases or oxidative enzymes, aid in the process of fungal cell wall polymer degradation [74].

In general wood-decaying fungi fall into three primary categories. The first includes the white-rot fungi, basidiomycetes, with the capability of degrading all cell wall components (polysaccharides and lignin) through hydrolases, oxidative enzymes, and low-molecular-weight mediators [97]. Moreover, certain white-rot fungi induce elongated cavities within the heartwood of living conifers, which serve as a preferential site for the degradation of lignin and hemicelluloses. This degradation process is commonly referred to as "white pocket rot" [98]. Various morphological decay patterns may be observed in cases of white rot; these patterns differ depending on factors such as fungal species, growth conditions, time, and the wooden substrate [74]. The most characteristic macroscopic feature, which coined the term for this fungal rot, is the whitish coloration that wood acquires as decay advances [84] (Figure 1.27). An additional characteristic at the macroscopic level is that white rotted wood undergoes a transformation into string-like fragments, resulting in a fibrous texture along the grain [84]. White-rot decay can occur uniformly or in concentrated areas known as "white pockets". These pockets can take the form of small, spindle-shaped, long narrow pockets or large patches of white tissue (Figure 1.27). These white pockets are separated by strips of brown wood that have not been degraded [99]. These decay patterns may refer to as “whitepiped rot”, “white-striped rot” or “honeycomb rot” [85].

The second group of wood-decay fungi includes the brown-rot fungi, basidiomycetes, able to metabolize cell wall polysaccharides but not lignin, although the arrangement of this last polymer can be modified during an attack [100]. Although brown-rot basidiomycetes are frequently linked to the deterioration of softwoods, white-rot fungi primarily impact hardwoods [78]. Brown-rot fungus decay is regarded as the most severe form of wood decay. The appearance of brown-rotted wood ranges from reddish brown to dark brown, and it becomes somewhat softer when wet [84]. In the final stages of decay, when cell wall polysacharides are lost, wood undergoes a severe, irregular shrinkage during drying. Additionally, it develops deep longitudinal and cross-sectional cracks, which contribute to the formation of cubical fragments [94], [96], [101] (Figure 1.27). A further distinguishing characteristic of brown-rotted wood that becomes apparent during the initial phases of decay is a significant deterioration in its strength properties [102].

The third group of wood-decay fungi includes the soft-rot fungi, ascomycetes, with the capacity to degrade both cell wall polysaccharides and lignin [103]. In contrast to white-rot and brown-rot fungi, which require free oxygen in wood pores for respiration, soft-rot fungi are adapted to environments with inadequate ventilation [78]. Therefore, wood susceptible to conditions that hinder the growth of white and brown-rot fungi (typically water-saturated wood, marine structures, railway ties, or wood with elevated moisture content) is often infected with soft-rot fungi [104]. Several species of soft-rot fungi have the capacity to attack wood structures, including preservative-treated wood [105]. In general, both European and tropical wood species are prone to soft-rot attack [74]. The term soft rot was originally coined by Savory [106] to express the soft appearance of the surface of wet decayed wood and differentiate this type of deterioration from brown or white rots caused by *Basidiomycetes* [74]. Soft-rotted wood when wet is very soft and appears dull brown, blue-grey or even black in advanced stages of decay [106], [102] (Figure 1.27).

Wood stain fungi and moulds are a polyphyletic group taxonomically placed in the Ascomycetes or that have yet to find a place in the modern fungal classification as they are imperfect fungi [78]. Wood stain fungi do not undergo degradation or induce only minor cell wall attacks; consequently, they do not substantially impact the majority of the mechanical properties of wood [78]. However, colour changes can significantly diminish the value of wood (Figure 1.27). This discoloration is caused by the modification of pigments produced by microorganisms, such as melanin [107].

In environments with high air humidity, inadequate ventilation, and warm temperatures, moulds are fungi that thrive on moist surfaces of various materials [78]. Moulds have a tendency to colonise newly cut wood subsequent to tree felling, specifically on moist sapwood, lumber, or wood products that have been stored in environments with inadequate ventilation, airtight sealed wood, or wood products [96]. Given that moulds usually do not penetrate inside the wood, they do not pose a risk to the wood's mechanical integrity [96].However, they can diminish its aesthetic value and hamper the drying process of wood [78]. In order to impart colour to the wood, they typically develop pigmented spores (black or green) on the surface and proliferate rapidly (Figure 1.27). Certain species are potentially hazardous to human health on account of their ability to generate mycotoxins [108].

Figure 1.27. Common microorganism attacking wood (extracted from: [74], [78]).

Bacteria are single-celled prokaryotic organisms found in almost all parts of the Earth [78]. Some specialized bacteria are able to degrade wood but at a much lower rate than saproxylic fungi. Many bacteria living on wood consume easily accessible compounds such as monosaccharides and pectin and may facilitate the subsequent activity of wood-decay fungi [109] but do not seriously affect the mechanical strength of wood. A few specialised bacteria, divided into erosion, tunnelling and cavity-forming bacteria, can also degrade lignified wood cell walls and can affect the mechanical properties of wood [112].

Marine borer

The term "marine borer" refers to a group of organisms classified as Bivalvia (*phylum Mollusca*) and subphylum Crustacea (*phylum Arthropoda*), which are capable of inflicting significant mechanical damage on timber members that are exposed to the marine environment [75] (Figure 1.28.a). Oxygen availability, water temperature, and salinity are the most influential determinants of their distribution and potential for wood infestation [111]. In temperate waters, different types of borers cause significant damage: *teredinids* (shipworms), *limnoriids* (gribbles) and *Sphaeromatidae* [74] (Figure 1.28.b-c). Marine borer infestation leads to the formation of intricate networks of apertures in wood, ultimately causing its total devastation and rendering it incapable of carrying out its designated purpose. Shipworm refers to a family of bivalve mollusks that are classified under the family *Teredinidae* [75].

a) b) c)

Figure 1.28. a) Attack of marine borers on a timber stump in seawater; b-c) *Sphaeroma spp.* attack on timber member across the wood grains (extracted from: [74]).

Shipworms have been observed in nearly all saline oceanic waters, and in recent times, have also been detected in the Baltic Sea, which is the largest brackish sea in the world, as a result of rising salinity [112]. Compared to shipworms, gribbles, which are crustaceous species classified within the *Limnoriidae* family, exhibit a reduced depth of penetration into wood, thereby impeding an inner degradation [113]. The marine borer poses the highest risk of degradation in wood applications in contact with the water body, as well as when the soil is in contact with the air above the water body. Nevertheless, oxygen levels below the ocean floor are insufficient for the sustenance of marine borers [114].

1.3.3.3 Abiotic degradation phenomena

Weathering

Wood weathering occurs as a result of the combination of sunlight, which causes the wood to dry out and be exposed to UV radiation, and rainwater that comes into contact with the surfaces of outdoor structural elements. Being both a hygroscopic and orthotropic material, wood is subject to swelling and shrinkage cycles mainly in the tangential and radial planes. Through drying and wetting cycles, the resulting high deformation of timber members can affect the service performances of the structure. Another problem resulting from drying and wetting cycles is the cracking of timber elements in the form of shakes, checks, splits, etc. Although their impact on the wood mechanical performances is minor in most cases, the presence of such cracks may lead to an increase of the wood water absorption, expanding susceptibility to attack by biotic agents. Outdoor timber structures may experience direct exposure to sunlight, resulting in significant photodegradation on their external surfaces due to UV radiation [115]. This process affects the optical and aesthetic performances of timber structures, resulting in the darkening softwood without modifying thermochemical performances. Such processes slightly affect the wood members in indoor environments due to changes in the sunlight spectrum caused by the window glasses.

Fire

Cellulose and lignin are substances characterized by a high carbon concentration, that is one of the principal combustion components of wood. Therefore, when timber is exposed to high temperature these substances undergo a thermal degradation called pyrolysis [116], [117]. The pyrolysis starts with hemicellulose decomposition (Bartlett et al., 2019), that is announced by a typically crack pattern of timber. Thanks to timber thermal proprieties, in a member exposed to fire the temperature gradient shows a high variation [116], so a cross section is formed by a charring outer layer, a thin layer exposed to an elevated temperature and a cool interior zone. The rate of charring is approximately constant over time and it is described by the charring rate [118], [119]. Given the relationship between mechanical proprieties and temperature of timber [120] can be state that the cooler zone retains its structural integrity.

1.3.3.4 Wood protection

When a timber structure is exposed to deterioration phenomena such that the natural durability of wood is not sufficient to ensure adequate protection, usually design strategies that increase protection, such as protective treatment and care of construction details, are employed. In addition, one of the key actions to ensure adequate durability is the monitoring of the state of health and scheduled maintenance of the construction [82], [121].

Timber can be subjected to various treatments, which improve certain characteristics (e.g., fire resistance, durability, impact resistance, etc.). For the purpose of protection against decay phenomena, among these technologies treatments for protection against weathering and biotic agents can be identified. The first group includes those products that simultaneously counteract the phenomenon of discoloration due to photo-oxidation and regulate the mechanism of water absorption in wood, by reducing the superficial permeability. The extensive range of products can be divided according to the type of binder polymer (e.g., wax, oil, resin), and according to the type of coating, impregnating products, primers, fillers, intermediate coating products and top coating products can be distinguished [122]. In addition, a further distinction can be made between film and non-film coatings [122].

A classification of wood protective treatment can be found on the base of the type of application, thus surface, physical and bulk treatment by impregnation can be identified [122]. While treatments against weathering are generally superficial, that is, they do not result in deep penetration and are applied by brushing, spraying, or dipping, treatments against biotic agents can be applied either superficially or by impregnation. Various combinations of pressure and vacuum are used to force adequate levels of chemical into the wood. Pressure treatment (PT) is the general term to describe the process for infusing/impregnating the wood fibres with preservative chemicals, removing any excesses, and leaving behind only enough chemical in the wood (retention) for protection [122]. In general, three pressure processes are commonly used: full cell, modified full cell, and empty cell [123]. However, not all wood species are impregnable to the same extent due to different anatomical structure and chemical composition [124]. In this regard a general reference is provided by the standard UNI EN 350 (2016), which classifies the major wood species according to treatability into 4 classes. Generally treatments against biotic agents involve impregnation of broadly active biocides into the wood. The testing of traditional biocide products started in

the in the mid-twentieth century with the introduction of the first generation of biocides, such as chromated copper arsenate (CCA), and later a second generation of products based on water-borne solution with complexed copper and organic cobiocide was brought to market at the end of the 1990s [125]. Due to environmental concerns about toxic chemicals and sustainability issues, chemical legislation gradually limited the use of traditional wood preservatives based on formulations containing heavy metals. Nowadays the use of biocides for wood in Europe is mainly regulated by the Biocidal Products Regulation (BPR) [126] and the Construction Products Regulation (CPR) [127]. The ECHA [128] rovides an overview of biocidal products under the category PT8 – Wood preservatives under the context of biocidal products being used for the preservation of wood. In general, these products can be distinguished in waterborne and oil borne products, as well as in curative and preservative products [129], [122].

In the last two decades, there has been growing attention to "modified wood" because of the negative environmental impact of traditional protective treatments [125]. *Modified wood* is a generic term that describes the application of chemical, physical, or biological methods that are used to alter the cellular structure of the wood in order to enhance specific features of wood. Wood modification has been defined by Hill [131] as a process that involves the action of a chemical, biological or physical agent upon the material, resulting in a desired property enhancement during the service life of the modified wood. Nowadays, various companies have introduced a diverse range of modified wood products, which can be categorized according to the following modification processes: acetylation, thermal modification and resin or polymer modification [132]. However, these treatments not only improve the performance of wood against decay phenomena but also alter the mechanical properties of wood. In general, a reduction in strength has been observed for the most common types of modified wood [133], [134], [135].

The protection of the timber members from possible degradation phenomena can also be increased through care for construction details by taking advantage of what is known as protection by design. It consist in avoiding any design solution whereby wood moisture content may rise above the normal content. Examples of construction details aimed at protecting wood from weathering are presented by Piazza et al. [35] (Figure 1.29) and Van Acker et al. [122].

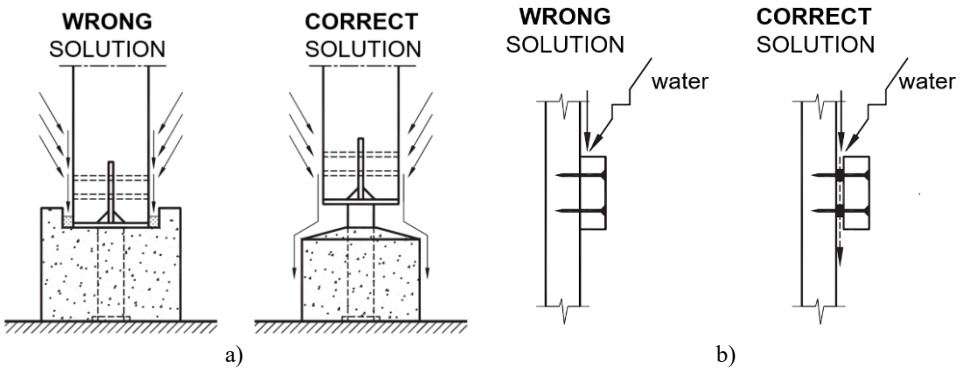

Figure 1.29. Timber construction solutions (wrong and correct) as regard durability issues (modified from: [35]): a) column to foundation joint; b) primary beam to secondary member joint.

1.4 TIMBER IN CONSTRUCTION: A BRIEF OVERVIEW

1.4.1 VERNACULAR ARCHITECTURE

In literature, vernacular architecture had its beginning in the studies of Bernard Rudofsky, who in 1964 inaugurated the exhibition *Architecture without Architects,* in which he illustrated artefacts of a spontaneous, indigenous, predominantly rural type from all parts of the world, built according to the climatic conditions of the place and with locally available materials and technologies [136]. Vernacular architecture is defined as those building artefacts that arise from primary housing needs, generally built by the community itself using local material resources and traditional techniques, and in total balance with the habitat [137]. These forms of architecture are fabricated to meet specific needs, values, economies, and ways of life typical of the cultures that make them. Thus, vernacular architecture refers to a variety of building configurations that have originated and evolved locally over the centuries in relation to different climatic conditions and available materials. In this contextual framework, the careful use of native wood species emerges as a distinctive element, emblematic of sustainable integration with regional ecosystems.

Emblematic applications of timber in vernacular architecture can be found in religious architecture and particularly in the Stave churches (Figure 1.30.a). These types are emblematic of medieval Nordic architecture from Scandinavia, showcases a distinctive construction method with vertical

timber staves supporting a steeply pitched roof. Characterized by elaborate post-and-beam techniques, the earliest applications of Stave Churches emerged in Norway during the 12th century [138]. These structures, marrying Norse and Christian influences, remain integral to the cultural and historical landscape of Scandinavian regions. Some wood species identification studies have shown the use of different wood species, however the huge application of Scots pine (*Pinus sylvestris*) has been recognized [138], [139].

Also, in the field of religious architecture, the eastern Spire-type churches (Figure 1.30.b) are a virtuous example of the application of timber. They are a hallmark of Eastern European architecture, employ a distinctive construction method featuring high spires and intricate timber frameworks. Originating in the Carpathian region during the 15th century, these churches reflect a fusion of Gothic and Byzantine influences. The construction relies on traditional carpentry techniques, highlighting the skilled craftsmanship prevalent in regions such as Ukraine and Poland [130].

Similar to the spire-type Eastern churches, Shinto architecture emphasizes the extensive utilization of timber in its construction, establishing a commonality in the vernacular use of this organic material. Shinto architecture, a distinctive Japanese vernacular style, employs post-and-beam construction with timber members, reflecting a harmonious blend of nature and spirituality. Originating in ancient Japan, the first applications date back to the 8th century [140]. Emphasizing simplicity and reverence, Shinto architecture is prevalent in the construction of temples (Figure 1.30.c), Shrines and Torii gates, exemplifying traditional craftsmanship and cultural continuity in locations such as Ise and Kyoto [141]. In addition to its application in the construction of temples and Torii gates, wood is also used for the production of ritual objects; in general, the most commonly used species are Japanese Cypress (*Hinoki*), Japanese Cedar (*Sugi*) and Japanese Pine (*Matsu*) [140]. In Japan, another example of vernacular architecture is residential architecture such as Minka houses (Figure 1.31.a). They are a representative example of traditional Japanese architecture characterized by a post-and-beam construction technique using timber elements. Characterized by thatched roofs and sliding doors, Minka originated in rural Japan during the Edo period, between the 17th and 19th century [142]. This architectural form, emphasizing functionality and craftsmanship, remains prevalent in various regions, reflecting the enduring cultural significance of Minka homes in Japanese countryside.

In the Eastern continent, India represents one of the countries where timber architecture is widely used in religious and civil construction.

Specifically, the northeastern region of India is characterised by dwellings built of local wood and bamboo. Northeast Indian huts (Figure 1.31.b), exemplifying vernacular architecture, employ bamboo and thatch in a traditional post-and-beam framework. Along with bamboo and Teak (*Tectona grandis*), which is the most common wood species, other tropical wood species are also found in this type of construction [143]. The huge presence of this type of architecture can be found in the regions of Assam and Meghalaya, where the construction methods date back centuries.

From the adobe structures of the Sahel to the thatched dwellings of tropical regions, vernacular architecture of Africa weave together local materials, cultural identities, and adaptive responses to different climatic conditions. The use of region-specific materials underscores the nuanced relationship between these structures and their environments, highlighting the resilience inherent in African vernacular architecture. The Masai Manyatta hut (Figure 1.31.c), a quintessential example of East African vernacular architecture, utilizes indigenous materials like timber poles, mud, and cow dung in a circular framework. Employing traditional techniques, it symbolizes Masai pastoralist culture. Originating in East Africa, particularly Kenya and Tanzania, the first applications of Manyatta houses date back centuries [144]. Small-diameter timber poles, mostly made of Acacia, are used in these constructions to make the framework, which is covered with straw and clay [143]. On the other hand, Sudano-Sahelian vernacular architecture, rooted in indigenous wisdom, employs sun-dried adobe bricks and timber members to craft distinctive structures (Figure 1.32.a). Utilizing traditional techniques, such as banco construction, this architectural style emerged in the ancient cities of Mali, notably Timbuktu, dating back to the 14th century [1454]. With a focus on sustainability and adaptation to the Sahelian climate, Malian architecture exemplifies a harmonious integration of craftsmanship, local materials, and environmental considerations. The wood species generally applied are local ones, in particular the Acacia wood. In Balat Town in Dakhla Oasis (Egypth) the typical house has bearing walls in sun-dried adobe mud bricks while Acacia wood is widely used in the dimensions of round members as support beams for the floors [146], [147] (Figure 1.32.b)

The first applications of timber in American architecture dates back to the colonial era, when balloon frame architecture developed with the earliest examples found in the 19th century [148]. European settlers, particularly in the New England region, brought with them the timber-framing techniques that were prevalent in their home countries. These early structures, often

simple and functional, laid the foundation for the widespread and enduring use of timber in American vernacular architecture. The availability of timber in the vast forests of North America contributed to its popularity as a primary building material, shaping the architectural landscape of the burgeoning colonies. Characterized by symmetrical layouts and steep roofs, the balloon frame techniques found in regions like New England, exemplify craftsmanship and durability, representing a foundational period in American architectural history [149] (Figure 1.32.c).

a) b) c)

Figure 1.30. a) Stave church [152]; b) Spire-type Russian church [153]; c) Shinto temple [154].

a) b) c)

Figure 1.31. a) Minka house [155]; b) North-east Indian hut [156]; c) Maasai hut [157].

Subsequently, an architecture type that has spread to the northern regions of North America and Canada is the log house. The log house construction system consists of walls mad of timber logs that are roughly cut to an almost round cross-section. These timber logs, made of several local wood species, are debarked and worked at the heads in order to create a connection to the corner of the building [150]. Notable for its resilience and insulation, log-

houses stand as enduring symbols of pioneer life, particularly across the wooded landscapes of Canada and North America.

Given the local climates and available resources, European vernacular architecture shows structures that are functional and culturally distinctive. A macro-distinction can be made between northern European and Mediterranean architecture. In the northern regions of Europe, abundant timber resources heavily influence construction. Timber framing, with visible timber frames filled with wattle and daub or brick infill, characterizes structures. The use of brick and stone, chosen for insulation in colder climates, is prevalent. Roofs are steeply pitched to shed snow, and high windows are strategically placed for insulation. Examples of this style include the iconic Half-Timbered Houses (Fachwerk in Germany; Figure 1.33.a), spread in Germany and parts of France and England, emphasizing the visibility of timber frames [151]. In contrast, Mediterranean vernacular architecture, prevalent in the Southern European countries, is notably influenced by the abundant availability of stone. Stone masonry, with thick walls providing thermal mass properties, is a predominant construction technique. Adobe and mud may also be used, particularly in regions where cooling effects are sought. Structures in the Mediterranean often feature flat roofs, suitable for the mild climate. Whitewashed stone houses with terracotta roofs, exemplified in Mediterranean villages of Greece, Italy, and Spain, embody the distinctive characteristics of this architectural style. In Central and Southern Europe, the frame system with infill masonry appears to be a building system developed as early as the 18th century as earthquake-resistant systems.

a) b) c)

Figure 1.32. a) Sudano-Sahelian construction [162]; b) House construction in Egypt (exraced from: [147]); c) Early balloon frame structure during construction [163].

The "Gaiola-pombalina" (Figure 1.33.b) and "Sistema-baraccato" (Figure 1.33.c) are the systems introduced in southern Portugal and Southern Italy, respectively, for post-earthquake reconstruction at the time [158], [159]. The origin of timber frame structures probably goes back to the Roman Empire, as in archaeological sites half-timbered houses were found and were referred to as Opus Craticium by Vitruvius. Half-timbered constructions later spread not only in Germany (Fachwerk), United-Kingdom (half-timber system), Italy (Sistema-baraccato) and Portugal (Gaiola-pombalina), but also in Greece, Scandinavia, Spain (Entramados), etc. [160], [161].

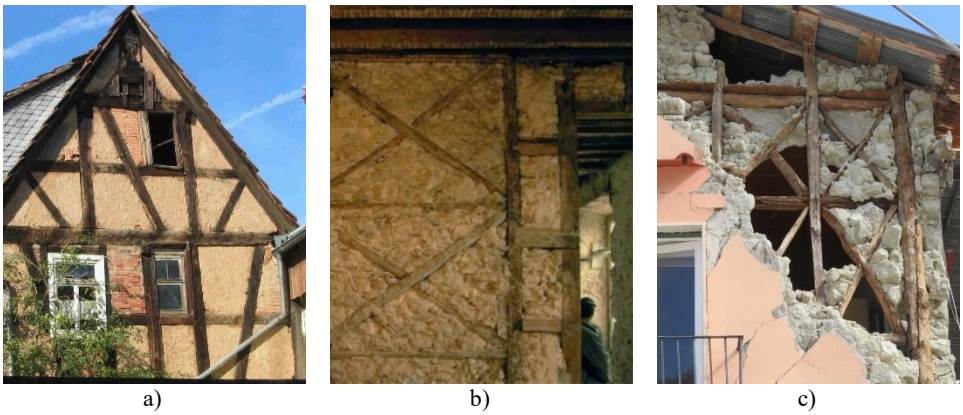

a) b) c)

Figure 1.33. Detail of the masonry-infilled timber frame from different construction typologies: a) Fachwek [164]; b) Gaiola pombalina [165]; c) Sistema baraccato [166].

1.4.2 CULTURAL HERITAGE ARCHITECTURE

Among the buildings that make up the architecture of a city, a distinction must be made between heritage buildings and cultural heritage buildings. In general, cultural heritage includes artefacts, monuments, a group of buildings and sites, museums that have a diversity of values including symbolic, historic, artistic, aesthetic, ethnological or anthropological, scientific and social significance [167]. Therefore, a distinction needs to be made between heritage/historic timber structures and other existing structures, since a greater value is placed on the fabric of heritage structures because of their historical significance [168]. Indeed, they are the evidence of craftworkers and builders'skill, they are the proof of traditional, cultural and ancestral knowledge [169]. Although the first applications of wood can be traced back to vernacular architecture thousands of years ago, over time people have gained increasing experience in carpentry, producing increasingly complex

and efficient structural types. Nowadays, in heritage buildings such as palaces, churches, bell towers, towers and villas, it is possible to enjoy remarkable timberwork, mainly roofs, vaults and ceilings structures (Figure 1.34).

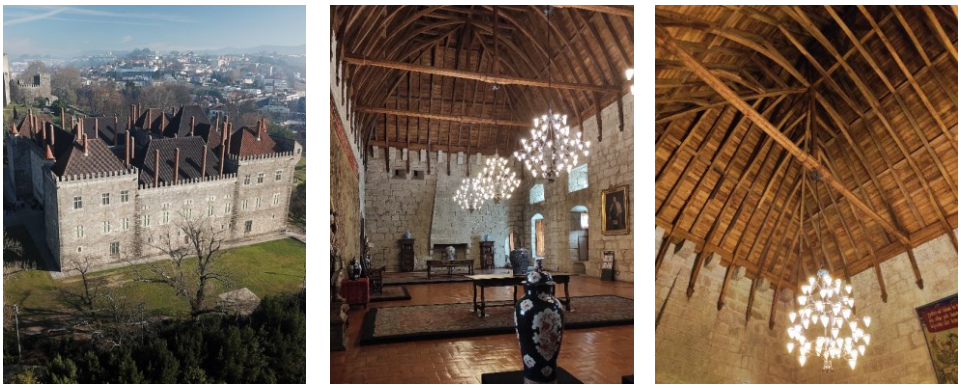

a) b) c)

Figure 1.34. Palace Duques de Bragançaa (Guimarães, Portugal): a) view of the Palace; b) the timber truss; c) the ceiling vault.

The most popular structural typology is undoubtedly the timber truss, which started to spread in early Christian times as a roof for the first Christian basilicas [170]. Throughout history, the primitive truss structure experienced significant development especially during the Middle Ages and the Renaissance, culminating in the complex trusses created by Andrea Palladio. In the so-called "Palladian truss" (Figure 1.35), an additional number of members were introduced, such as the collar, the queen posts, struts, etc. Over time, this scheme has undergone modifications, generating several complex variations (Figure 1.36.b). A general classification of the traditional Italian trusses can be made by dividing the open trusses from the closed trusses [170]. Basically, the Italian trusses show similar characteristics, such as the slight slope of the rafters, probably due to characteristics of the Mediterranean climate; however, in areas of northern Italy, roofs with a high pitch, supported by complexly shaped trusses, have been found [171], [172]. A wide inventory of roof and floor structural typologies used in monumental heritage buildings by referring to the iconic case-study of the Royal Palace of Naples (Figure 1.36.) have been carried out by Faggiano et al. [173].

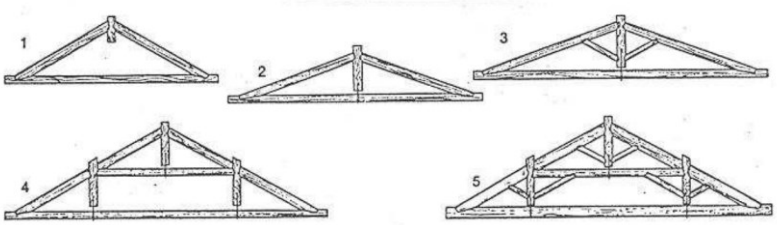

Figure 1.35. Common types of trusses in Italian architecture (1. triangular truss; 2. king-post truss; 3. traditional Italian truss; 4. Queen post truss; 5. Palladian truss) [174].

a) b) c)

Figure 1.36. Royal Palace of Naples (Italy): a) Palace's view from Plebiscite square; b) the Palladian truss of the Diplomatic Hall [173]; c) the ceiling vault of the Diplomatic Hall [173].

Outside Italy, some authors have investigated historical trusses and found types belonging to the collar beam truss, king-post truss and queen post truss type [175], [176], [177]. A distinctive character that can be found in Northern Europe architecture is the steep inclination of the roofs, usually around 60°, which facilitates outflow of rainwater and snow which has a positive effect on the durability of timber. Consequently, the trusses have more pitched struts. An example are the roofs of Central European Gothic churches and buildings built between the 14th and 16th centuries (Figure 1.37; Figure 1.39), characterised by collar beam trusses, which were later (Baroque architecture of the 16th and 17th centuries) followed by less pitched solutions supported by extra struts [178], [179] (Figure 1.38).

As regard the wood species used in Italian heritage-timber structures it varies based on the structure's location, unlike in France where oak is the dominant species [170]. In northern Italy the most diffuse wood species are the Norway spruce (*Picea abies*), Larch (*Larix decidua* sp.) [171]. In Florence, most of the monumental buildings show timber members in Silver

fir *(Albies alba*), while Chestnut (*Castanea Sativa Mill*.) can be found in Central-Southern Italy [170]. Appreciated for its strength and durability, chestnut wood has been extensively used for the roof and floor structures of historic buildings [173], [180]. Being a wood species typical of Calabria region, trusses with members of Corsican Pine (*Pinus Nigra* subsp. *laricio* (Poir.) Maire) have been found in historical buildings of Cosenza [181].

a) a) c)

Figure 1.37. Old Royal Palace of Prague (Czech Republic): a) view of the Palace; b) roofing trusses with evidence of the carpentry joints doweled with timber fasteners; c) roofing trusses with evidence of the double rafter.

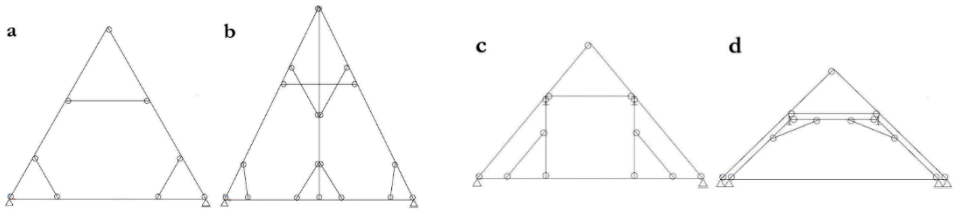

Figure 1.38. Scheme of trusses typical of central European Gothic (a. simple collar beam truss; b. collar beam truss with a king post; c. truss with supported collar beam by posts; d. collar beam truss supported by frame structure; (modified from: [178]).

Historical timber buildings have typically employed many types of wood species and structural joints. In the past carpentry joints did not have dowel-type connectors, such as nails, screws, or bolts, to effectively transmit shear and tensile stresses. Indeed, in the past, connections were not made to be subjected to tension, while shear was transmitted by friction of the contacting surfaces. In order to establish a connection between the timber members,

direct contact was facilitated by using specific cuttings and notches. Hence, these joints are commonly referred to as traditional carpentry joints. In the 18th century [182], the utilisation of steel connections emerged and assumed a significant role. However, the few metal fasteners that were used in parallel with traditional carpentry joints did not carry the loads.

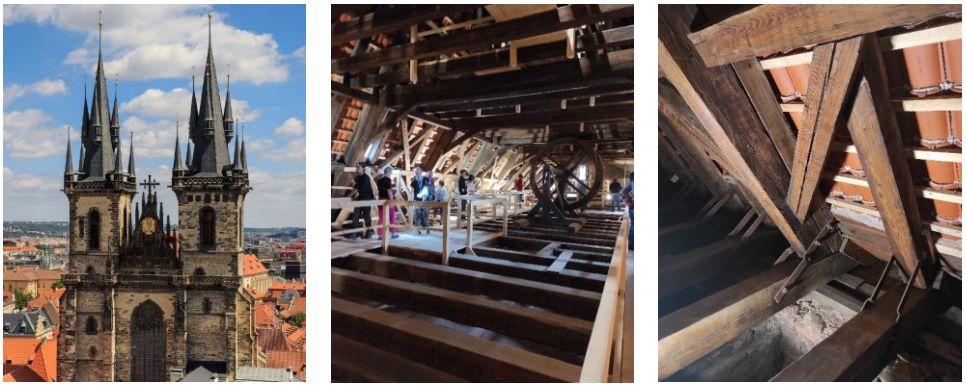

a) b) c)

Figure 1.39. The church of Our Lady before Týn (Prague, Czech Republic): a) view of the bell towers; b) inside view of the roofing structures of the bell tower; c) rafter to tie-beam joint aided by metallic plates.

The classification of common traditional carpentry joints found in historical timber frames can be organised into four primary categories based on their arrangement and geometric characteristics. They concern the tenon and mortise, the notched, the lap and scarf joints [183]. Other type of joints concerned the tabled, the heading and step joint (Figure 1.40) [184].

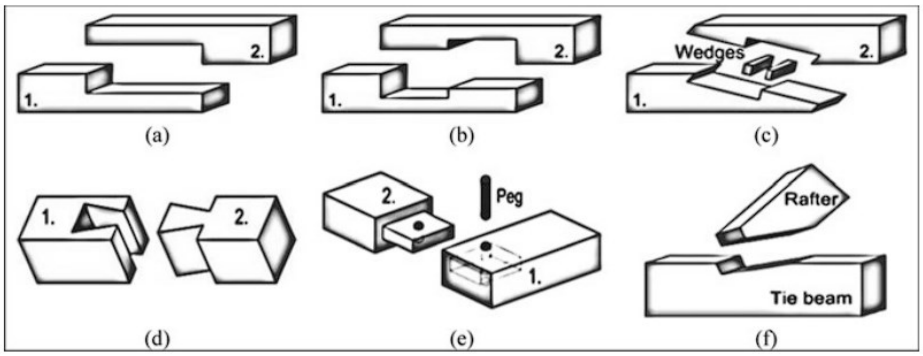

Figure 1.40. Most common traditional carpentry joints (a. simple half-lap splice joint; b. halved and tabled splice joint; c. scarf joint with edges; d. dovetailed heading joint; mortise-tenon joint with peg; single step joint) [184].

As regard to timber truss the connection between the rafters and tie-beam is generally the most stressed connection. In most cases this joint is made through a single, double or triple step joint [185], usually aided by a couple of nails or by U-plates, put in tension by metal wedges [170] (Figure 1.41.b). A timber hammerbeam is often placed below the tie-beam at the support, reducing the tie-beam span and improving the support on the masonry. The joint between rafters and king-post, as well as the joint between rafters and struts, are realized by simple notches, frequently aided by nails (Figure 1.41).

a) b) c)

Figure 1.41. a) Typical open truss from Italian architecture: evidence of the traditional carpentry joints; b) Rafter to tie-beam joint (single step joint) aided by metallic U-plates and supported by timber hammerbeam; c) Rafter to king post joint [170].

1.4.3 CONTEMPORARY ARCHITECTURE

The timber-based materials (TBM)

In contemporary construction field, there is a discernible trend toward the increasing utilization of timber and timber-based materials. This paradigm shift is underscored by the recognition of wood's inherent sustainability, structural and thermal efficiency. As technological advancements continue to enhance the structural and performance characteristics of timber, it emerges as a prominent and environmentally responsible material choice within the construction industry.

In fact, contemporary construction takes advantage of timber-based materials (TBM) or engineered wood products with high thermal and structural performance. This is a family of timber products created by layering veneers, chips, or laminated timber elements that are then sawn to specific dimensions [20] (Figure 1.42). The most widely used timber product is glulam (glued laminated timber), which is used to make one-dimensional elements such as columns and beams. It consists of individual lamellas of timber specially selected and positioned according to their performance

characteristics, then glued together with durable, moisture-resistant adhesives. It is often used for the construction of large-span buildings such as gyms, markets, swimming pools, etc., as well as for roofing structures. Another popular material in the building industry is CLT (cross laminated timber), used to make panels typically consisting of three, five, or seven layers of timber oriented with respect to each other orthogonally and then glued together to form structural panels with excellent strength, dimensional stability, and stiffness. Because of its structural properties and dimensional stability, this product is well suited for floors, walls, and roofs used in medium-to-high timber construction. LVL (laminated veneer lumber) is a high-performance structural product, often used as an alternative to glulam. It is generally used for the production of mainly one-dimensional members. It consists of dried softwood veneers joined together with adhesives in such a way that the grain of all veneers is parallel to the longitudinal direction. Oriented strand board (OSB) panels, consisting of thin fibre filaments oriented longitudinally, laid in mats, and then joined together with heat-sealed adhesives, are often used to make flat end elements. The low cost, combined with dimensional stability and durability, means that this material is widely used in construction. NLT (nail laminated timber) and DLT (dowel laminated timber) are other types of TBM obtained by the nails and dowel joints of timber boards, respectively, to make timber panels. PSL (parallel-strand lumber) and LSL (laminated-strand lumber), made from strip fibres, are used for mono-dimensional and bidimensional products.

Figure 1.42. Main timber-based materials (TBM).

The structural typologies

Generally, TBMs are applied for the construction of different structural types, finding application in the construction of load-bearing wall structural systems, frame systems, or in specific systems of timber construction technique. As regard the typological classification of the timber construction, at the state of art there are several proposal of classification [186], [187]. A first distinction can be made between "all timber" solutions, where the structure is entirely made of timber members connected by metal elements, and "hybrid timber," whose structure is also constituted by other materials such as steel or concrete [187].

Among contemporary constructions, i.e. those constructions intended for public and private buildings, a macro-classification can be made (Figure 1.43) by dividing the structural types in [186]:

- heavy timber framed structures (post-and-beam structures);
- shear-wall structures;
- blockhaus.
-

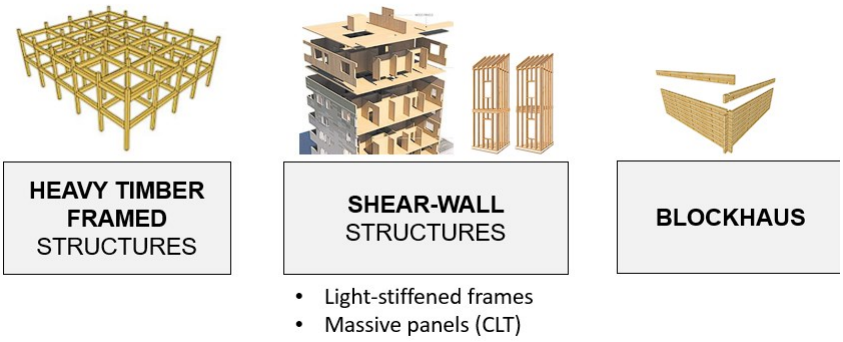

Figure 1.43. Macro-classification of the timber structural types for contemporary constructions.

The heavy timber framed system (also called post-and-beam), consisting of beams and columns, is probably one of the oldest building systems in the world. It has always been used in R.C. and steel structures, but only in the last decade is it finding wide application in timber structures [188], driven by the need for buildings with large and free interior spaces. The heavy timber framed structures provide a load-bearing frame of columns and beams (usually glulam) similar to R.C. or steel framed buildings where the members can be fully prefabricated or assembled on site (Figure 1.44). In this context, the columns transfer the vertical loads to the foundation while the beams

distribute the horizontal loads. Beam to column joints are typically built using steel fasteners. Given the variables stiffness of the connections, timber walls and brace are frequently employed to reinforce the structure. In general, the heavy framed structures can be classified according to their seismic-resistant system, identifying moment resisting frame (MRF), braced frame (BF) and frames with shear walls.

- In MRF structures, the frame has beam-column joints of rigid or semi-rigid type [189], [190]. Both vertical and horizontal loads are supported by the frame; therefore, the columns are subject to bending, shear and compression/tensile stresses;
- In BF structures, the joints are not sufficiently rigid to ensure lateral stability, therefore bracing is realised. In general, concentric (CBF; active tensioned diagonal, V-shaped, K-shaped, etc.) and eccentric (EBF; [190], [186]) bracing systems can be identified. The connections between the members are generally of the hinge type; therefore, all the members are mainly subjected to axial stresses, while due to vertical loads, the beams are under bending stress. The members are generally made of glulam, but hybrid structures with steel diagonals are often realised;

Figure 1.44. Heavy timber frame structure of CBF system type: construction steps [191].

- Shear wall structures are composed of two coupled structural systems: frame (beams and columns), designed for vertical loads only, and shear walls for horizontal actions [186]. In the case of coupled frame-wall systems, the connections are generally realised at the floors by means of

quite huge steel joints. The walls are generally made of CLT, or, in hybrid structures, reinforced concrete cores are built.

In order for the seismic behaviour of these structures to be regular, correct design requires a uniform distribution of the seismic-resistant systems in plan and elevation. This results in a uniform distribution of beams and columns in the MRF system, ensuring similar stiffness in both directions of earthquake action (longitudinal and transversal), while in BF and shear wall systems, the correct design includes a uniform distribution of bracing beams and shear walls in plan and elevation.

Shear wall type buildings can be divided into two groups: light stiffened frames and massive panels. Light timber frame buildings have ancient origins, belonging to Asian and American cultures. In general, the system features of light frames consisting of posts and beams made of solid wood or glulam, enclosed (or not) in panels made of wood or other materials that are connected to the frame by means of steel fasteners such as screws, nails and plates. The floors can be built with timber beams arranged in one direction only (one way system) or in both directions (two-way system). Two main systems are distinguished in construction practice: Ballon frame and Platform frame (Figure 1.45.a).

a) b) c)

Figure 1.45. a) Platform frame vs Balloon frame system; b) Platform frame building [193]; c) Balloon frame building [194].

The Balloon frame consists of vertical elements (columns) passing continuously from the foundation to the head of the building (Figure 1.45.c). The transfer of vertical loads from the floors to the foundation takes place by means of the load-bearing columns, while lateral stability is provided by shear

panels. Currently, the system is mainly used in the construction of small buildings in rural contexts as it does not have adequate characteristics to be used in the construction of multi-storey buildings. The platform frame system was born in North America in 1833 [192]. This system was conceived as a development of the Ballon frame system and it is one of the most commonly used systems for constructing multi-storey buildings. Unlike the Ballon frame system, the columns are not continuous along the height, but are interrupted at the floors (Figure 1.45.c). In this way, smaller and shorter timber members can be used, simplifying material handling on site. Typically, the uprights can be of different types: solid wood, glulam or LVL. The bracing panels can be made of OSB, chipboard, plywood or other timber-based materials. Any window and door openings must have a framework consisting of horizontal beams and vertical posts.

Massive panel systems generally consist of CLT panels, which are an optimal solution for the optimal combined structural-energetic performances, finding application in residential and office buildings [195]. Vertical panels ensure load bearing capacity against gravity loads and horizontal loads, such as wind and seismic loads. Often the horizontal structure is realised through panels of the same type, which are arranged to form a two-way system. The connections between vertical and horizontal panels are generally made with metal connectors, such as plates, screws and bolts. In particular, the connection of the vertical wall with the foundation is of crucial importance, as it is highly exposed to durability issues. The connection is made by means of steel plates and screw/bolts that transfer shear (angle plates) and tensile stresses resulting from the rocking of the panel (hold-down plates; Figure 1.46.b). Compressive stresses are generally transmitted directly through the timber-to-timber contact or timber-to-foundation contact. The construction process (Figure 1.46.a) is very fast, although transport can be more difficult, especially in construction site areas with limited accessibility. In the case of buildings of limited height (2 or 3 storeys), continuous panels are usually used in a vertical direction over the entire height of the building.

The Blockhaus structural system (also named as log-house) consists of walls made with overlapped horizontal timber logs. The cross-sections of timber logs can be round or square and can be made of solid or glued timber. The members are longitudinally notched at both the top and bottom to improve the beam-to-beam connections; in some cases, metallic fasteners are added to increase the walls' in-plane stability and stiffness. Carpentry joints serve as a technique of joining orthogonal log walls. Solid or glue-timber beams provide the structural support for wood-based panels, such as plywood

or OSB panels, but also CLT or timber-to-concrete composite floors. The panels are screwed to the beams to guarantee rigid diaphragms in plane. Metal fasteners are generally used to join the timber structure to the foundation transferring to it the bending and shear stresses.

a) b)

Figure 1.46. Wall structure in CLT: a) during construction [196]; b) hold-down joint [197]

Tall timber buildings

Over the past 10 years, there has been growing interest in tall buildings constructed from mass timber materials as a means to achieve greater urban density with more sustainable construction [198]. Nowadays in the world there are dozens of buildings with more than seven stories of timber construction. These buildings are all lower than a hundred meters and clearly cannot be compared to the tallest skyscraper in existence today. However, considering "all timber" buildings or timber hybrids these structures can be defined as tall buildings. A growing interest is direct to timber buildings thanks to the attention to sustainability for reducing the great environmental impact that buildings have during all their life. Both all timber and hybrid - timber structural solutions are competitive and largely used in the word for the realizations of high buildings.

Generally, the trend is that of use concrete-timber hybrid. In this way all the horizontal stability and resistance to horizontal loads is given by reinforced concrete core. Timber is used only for vertical loads. The same things happens in steel - timber hybrid where horizontal stability and resistance is given by steel braces and columns but, this structural solution is less used. However, it's interesting to notice that tallest all timber building (Mjøstårnet, Norway – 85.4 m; Figure 1.47.b) and timber hybrid (Ascent, USA – 86.6 m) reach more or less the same height. The following is a

description of the main characteristics of some tall timber buildings belonging to the category of all timber with shear walls in LVL (Lighthouse), heavy timber framed system (Mjøstårnet) and hybrid timber system (Ascent).

The Lighthouse building in Joensuu (Finland) is a 14-story building reaching a height of about 50 metres (Figure 1.47.a). The structure is composed of post tensioned LVL wall elements with a thickness of 126/162 millimetres. Floors are made of CLT panels and LVL support beams connected to the walls. Also stairs are made of CLT panels. Overturning forces are handled using tension rods bar connected to the concrete base, these rods connect also floors together each 3 levels. This is the example of a very innovative structural system applied in a timber structure.

The Mjøstårnet building in Brumunddal (Norway) is a 18-story building with a height of 85.4 meters (Figure 1.47.b). Built in 2019 this building is currently the tallest timber building in the world. The building has a vertical load resistant system based on timber beams and columns. Horizontal loads are resisted by large diagonals members that describes a K on the façade. These diagonals provide also stability to the whole structure. The floor construction technology varies depending on the storey level: floors 12 to 18 concrete floors are used to have more mass toward the top of the buildings and comply with comfort criteria for apartments, while floors 2 to 11 are prefabricated wooden decks based on Moelven's Trä8 building system derived from Metsä Woods RIPA deck systems [199].

The Ascent building in Wisconsin (U.S.A.) is the tallest concrete-timber hybrid building in the world with a height of 86.6 metres and 25 stories (Figure 1.47.c). This building present a central core in reinforced concrete and seven level parking made in reinforced concrete, eighteen residential levels with glulam beams and columns, as well as CLT slabs for floors. Lateral resistant system is composed of two concrete cores, while timber is used only for vertical loads.

Also in Italy, although with limited numbers, the construction of tall timber buildings is developing, representing an increasingly efficient solution for housing. Nowadays, one of the tallest buildings in Italy is in via Cenni in Milan, where a residential complex consisting of four 9-storey timber buildings with CLT structural walls has been built (Figure 1.48.a). The structure has both vertical and horizontal panels in CLT, and even the stairs and lift shafts are built in timbers. The *Panorama Giustinelli* luxury residential complex features a 6-storey timber building made entirely of timber (Figure 1.48.b). The load-bearing structure is of the post-and-beam

type, with glulam members. In the end, on the Caorle seafront the *Marina Verde Wellness Resort* is placed (Figure 1.48.c). The complex consists of two 6-storey buildings housing 73 residential units. This is one of the best examples of contemporary architecture in which sustainability, advanced technology and high living comfort are perfectly combined. The building's structural type is classified as hybrid timber systems, consisting of a post-and-beam system where most of the columns are in glulam. However, R.C. columns and cores are present to ensure lateral stability against seismic action.

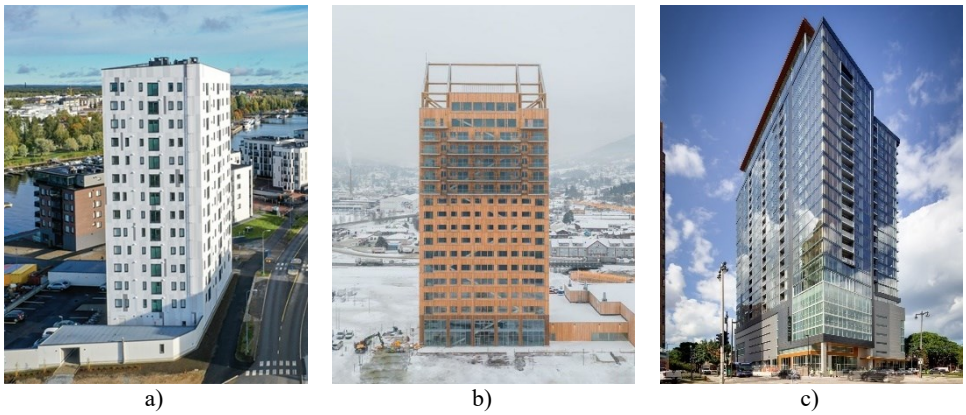

a) b) c)

Figure 1.47. Tall timber buildings with different structural system: a) Wall structure in CLT (Lighthouse, Joensuu, Finland; [200]; b) Heavy timber frame structure (Mjøstårnet, Brumunddal, Norway; [201]); c) Hybrid timber structure (Ascent, Wisconsin, U.S.A.; [202]).

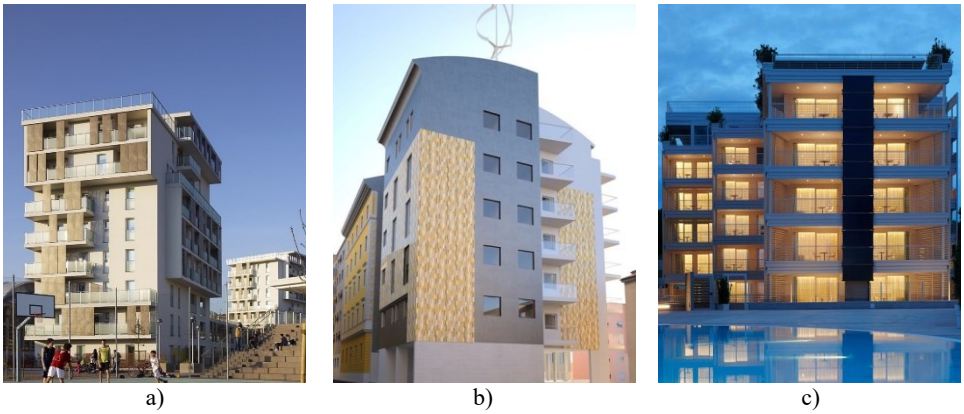

a) b) c)

Figure 1.48. Tall timber buildings with different structural system in Italy: a) Wall structure in CLT (Complesso via Cenni, Milano; [203]); b) Heavy timber frame structure [204]; c) Hybrid timber structure (Marina Verde Wellness Resort, Caorle; [205]).

Large-span timber buildings

Due to its high specific strength value and specific stiffness, obtained by dividing the material strength and the material elastic modulus by its density, respectively, timber is particularly appropriate for large-span structures [206]. The earliest example of man-made large-span timber structures are probably bridges. Until the first half of the 19th century, timber was basically the only material available for such a purpose, however from the late 19th century onwards, first steel and then R.C. took over in civil engineering. Nowadays timber is mainly used for pedestrian bridges, while it finds wide application in the construction of large-span roofing structures. Common applications include timber roof in industrial buildings (Figure 1.51.a)., agricultural buildings, sports structures such as arenas, swimming pools, pavilions, school gyms, as well as stadium and open space roofs (Figure 1.51.b). Among the wide list of examples, a great distinction can be made between the timber space frames or spatial structures, such as domes, and timber planar frames, such as trusses, arches structures, etc.

Space frame are conventional constructions comprised of a collection of linear members that are interconnected in three dimensions [207]. These structures withstand stresses that are applied either along their lengths or at their connections. Spatial structures include free-form configurations, braced barrel vaults, braced domes, flat double or multi-layer grids, and braced barrel vaults. Dome structures with geodesic geometry and radial rib dome are spread among the spatial timber structures [206]. Nowadays the world's largest timber dome is the Superior Dome, the stadium in the campus of Northern Michigan University in Marquette, Michigan, USA (Figure 1.49.a). It is a geodesic dome with glulam ribs made of Douglas fir (*Pseudotsuga menziesii*), having a diameter of 163 m and a height of 49 m (Figure 1.49.b). In Europe the largest timber dome is the "Federico II" dome located in Brindisi, Italy. It is a geodesic dome of 143 m in diameter and 46 m in height, realized as roofing structure of a coal storage building (Figure 1.50.a-b; Rubner, 2022). The spatial frame is made up of glulam members, while the covering surface is made of CLT, for a timber volume of 1.548 m^3 for glulam and a timber surface of 22.000 m^2 for CLT panels [208]. A special joint were designed for the nodes of this dome, consisting of steel plates and inclined self-tapping screws, designed to resist to bending moments and shear forces that arise during the construction steps [206].

a) b)

Figure 1.49. The Superiore Dome (Michigan, USA, 1991): a) outside [209]; b) inside [209].

a) b)

Figure 1.50. The Federico II dome during construction (Brindisi, Italy, 2013): a) outside [210]; b) inside [208].

Given the different flow of stresses, planar structures differ from spatial ones. Indeed, in a planar system, the force due to the roof load is transferred successively through the secondary elements, the primary elements, and then finally the foundation. Therefore, the loads are transferred from the elements of a lighter class to the elements of a heavier class. In large span timber constructions, the secondary members are generally one-dimensional as secondary beams or timber planks. These are single way-systems, while two-way systems, such as CLT and LVL panels, are characterized by a shell-type behaviour and they can be placed, as secondary members, directly in contact with the primary elements. In general, in timber large-span construction the primary members can be of different types: beam, truss, arch, frame. The performance of these structural types depends on several factors, however, considering only vertical loads, it can be said that the most efficiently timber structures are those with a greater number of tensioned members than compressed ones, and that overall, structures with members subjected to normal stress are more efficient than those subjected to bending [206].

Nowadays, glulam or LVL technology allows the realisation of elements of considerable dimensions, exceeding spans of more than 40 metres with a cross-section height of more than 2.0 metres. The possibility of curving the

lamellas allows the realisation of complex shapes, generating dynamic and very attractive architecture (Figure 1.51.a-b). In design practice, single-section glulam beams are frequently used up to spans of around 30 metres (Piazza et al., 2005) and are often realised with a variable height cross-section. These are generally bonded to steel or R.C. columns, R.C. or masonry walls. Single and double tapered beams, as well as pitched-cambered beam (Figure 1.52.a-c) are widely used in design practice, due to the sloped upper side which allows rainwater to run off. However, the state of tension and deformation to which a simple supported beam is subjected changes completely when the cross-section has a variable height or the axis of the element is no longer rectilinear, as in arched structures. Arched structures, with 2 or 3 hinges (Figure 1.53.a-b), are one of the main structural types used in timber large-span structures due to the structural performances, together with the ease of assembly on site, especially for the 3-hinged arch. However, the curvature of the lamellas implies additional orthogonal compressive or tensile stresses, which are greater the smaller the radius of curvature of the lamellas. Therefore, bending radius of less than 6 to 7 metres is difficult to realise [35].

When the span becomes large and production as well as transportability limitations prevent the use of single beams, the designer's choice is directed towards truss structural systems. Thanks to the truss configuration, the bending moment is translated into a compressive or tensile force in the members. In this way, the dimensioning of the members is generally governed by the verification of tensile or compressive strength, to which timber has high resistance. However, an important aspect is the lateral stabilisation of the compressed members, which is achieved through horizontal bracing structures to avoid buckling. A truss beam of primary importance, due both to its constructional evolution and diffusion, is the Palladian truss. However, “modern” Palladian trusses are currently preferred to “traditional” ones, where notched connections are not adequate to resist the reversal of stresses due to seismic action. Therefore, modern trusses are generally made with steel joints and often have steel ties instead of timber chains (Figure 1.54.a). Furthermore, the monk is not necessary as the connection between the rafters is not a carpentry joint. The more articulated truss structures make it possible to span considerable lengths. The range of feasible shapes and configurations is so wide that the design is not only guided by static considerations but also influenced by general aspects such as aesthetics, functionality, transport, and assembly aspects [35]. In general, the most common truss structures consist of an upper and a lower member connected by vertical and diagonal members

(Figure 1.54.b). Depending on the orientation of the diagonals, different stress distributions can occur. A particular type of truss beam is the lenticular truss, where two arched beams are connected by vertical struts (Figure 1.53.c).

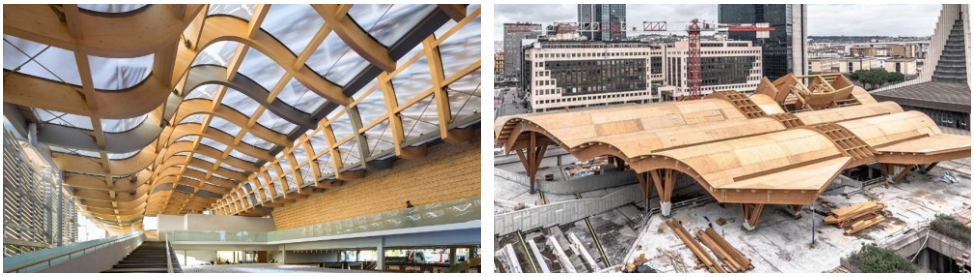

a) b)

Figure 1.51. a) China pavilion Expo 2015 in Milan (Italy; [211]); b) Metro station "Centro direzionale" (Naples, Italy; [212]).

Large span structures are often built with frames where both beams and columns are made of timber. 3-hinged frames are isostatic structures where the connection of the timber columns with the foundations and the central joint is of the hinge type. With reference to half of the structure, one can identify a column and a beam that are connected with a rigid joint to restore structural integrity. Generally, the rigid connection can be with external plates or with a single internal plate, as well as with a toothed steel plate joint (Figure 1.54.c).

In the design of large span structures great importance must be given to vertical and horizontal bracing structures. They fulfil the dual function of bracing against horizontal actions such as seismic and wind actions, as well as providing stability in order to avoid buckling occurring (Figure 1.55.a). Vertical bracings are systems arranged in vertical or sub-vertical planes and are responsible for the overall stability of the construction. In structural systems with rigid nodes (MRF) and cantilevers, stability is ensured by the frame itself, which has rigid or semi-rigid nodes. When the structure is labile, bracing systems such as timber or steel diagonals, as well as timber shear walls are generally introduced. The same applies to horizontal bracing where the different systems can be grouped into reticular bracing and diaphragms systems. In the first case, timber or steel diagonals are used (Figure 1.55.b), while in the second, roofing elements in CLT or LVL panels are generally used.

a) b) c)

Figure 1.52. Large-span timber typologies: a) Single-tapered beam [213]; b) Double-tapered beam [214]; c) Pitched-cambered beam [215].

a) b) c)

Figure 1.53. Large-span timber typologies: a) 2-hinged arch [216]; b) 3-hinged arch [217]; c) Lenticular truss [218].

a) b) c)

Figure 1.54. Large-span timber typologies: a) "Modern" Palladian truss [219]; b) Truss [220]; c) Timber frame with the toothed steel plate joint [221].

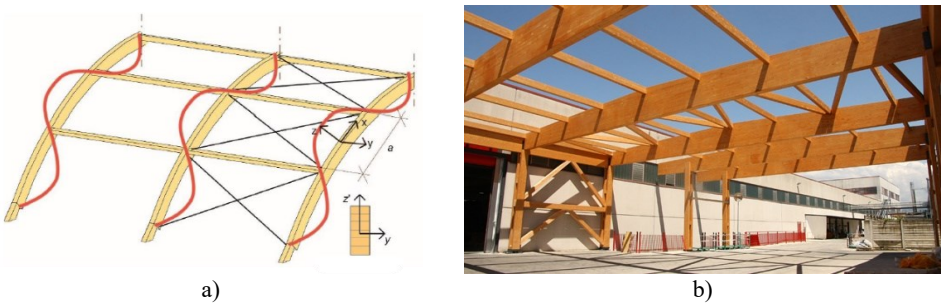

a) b)

Figure 1.55. a) Horizontal bracing system providing stability against buckling phenomena [206]; b) A large-span timber structure with both vertical and horizontal bracing systems with timber diagonals [222].

The proper arrangement and number of bracings are obviously a function of the geometry, the static scheme, the action intensity and the type of constraint between the members. The symmetry and uniform arrangement of these systems contributes to a regular and uniform structural response.

Chapter

2

Vulnerability assessment of existing timber structures at different scales: state of art

Abstract: Nowadays, the Italian territory is exposed to several risks, among which seismic risk is frequently the main cause of serious losses to the built heritage. Therefore, it is essential to implement policies aimed at increasing urban resilience by preventively assessing the vulnerability of the built heritage to seismic action. To achieve this goal, at the territorial scale, it is necessary to identify priority areas for intervention and then, at the building scale, perform an in-depth vulnerability assessment by acquiring adequate prior knowledge of the structure through the survey and diagnosis activities.

Regarding timber structures, vulnerability analysis should not be separated from a preliminary evaluation of preservation conditions. Therefore, at both the territorial and detailed scales, it is necessary to employ techniques and methods that integrate durability aspects of the timber constructions within the seismic vulnerability analysis methods.

In the following chapter, a brief description of principles and methods for the seismic vulnerability assessment of the timber structures is provided, highlighting the different methodologies at the two scales of investigation. At the same time, methods for assessing the health condition and susceptibility to decay of timber structures are shown. Therefore, the concept of service life is introduced, showing the methodologies commonly used for evaluation. On the other hand, the assessment of the state of preservation of timber structures at a detailed scale is carried out through specific surveying and diagnostic techniques. Therefore, the procedures and standards, as well as the investigative techniques such as visual strength grading and non-destructive and destructive techniques, are fully described.

2.1 VULNERABILITY IN THE FRAMEWORK OF RISK ASSESSMENT

The term risk follows the definition by the Office of the United Nations Disaster Relief Co-ordinator [223] and refers to the expected losses from a particular hazard to a specified element at risk in a particular future time period. As part of the risk assessment, the following terms can be identified:

Hazard (H) is the probability of occurrence of a potentially damaging phenomenon in a given period of time and within a specified territorial area;

Exposoure (E) denotes the population, facilities, economic activities, etc., at risk in a given area.

Vulnerability (V) means the degree of loss to a given element or set of elements at risk resulting from the occurrence of a natural phenomenon of a given magnitude.

Specific risk (R_S) means the expected degree of loss due to a particular natural phenomenon. It may be expressed by the product of H multiplied by V.

Total risk (R_T) means the expected losses in terms of lives lost, injured persons, damage to property, or disruption of economic activity due to a particular natural phenomenon and is therefore the product of specific risk (R_S) and elements at risk (E).

Thus, the total risk can be expressed as follows (Eq. 2.1; Figure 2.1):

$$R_T = E \cdot R_S = E \cdot H \cdot V \tag{2.1}$$

where:

R_T total risk [-];

E exposure [-];

R_S specific risk [-];

H hazard [-];

V vulnerability [-].

The risk management process generally consists of three components, as proposed by the framework of Fell et al. [224]: risk analysis, risk assessment and risk management. Risk analysis includes hazard, i.e., the process of

identification and characterisation of potential events and their corresponding frequency of occurrence, and consequence analysis. The latter analysis involves the identification and quantification of the elements at risk including property and peoples and the assessment of the vulnerability of the element at risk in terms of losses [224]. Risk assessment consists of comparing the risk analysis outputs (risk evaluation) to risk criteria and value judgements in order to determine whether the risks are tolerable levels. The risk assessment process can be done by comparing the calculated risk with socially "acceptable risk", taking into account several criteria, such as technical, social, economical and political criteria [225]. Once the risk in a given area is assessed, measures may be taken to mitigate the risk to the community, if necessary.

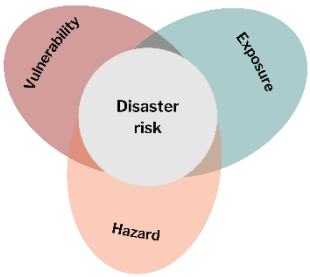

Figure 2.1. Elements of risk [226].

Losses may be estimated in terms of human lives, or damaged facilities or in financial terms. This is due to the different aspects related to the vulnerability. Indeed, most of definitions regarding natural disaster vulnerability concur that the term refers to the following: (1) multi-dimensional; (2) dynamic, because it changes over time; (3) intrinsic of any community; (4) scale-dependent, given that it can be expressed at different scales (e.g., from territorial to detailed); and (5) site-specific, which implies that each study area might need its own approach [227], [228].

One of the most remarkable aspects of the vulnerability pertain the multi-dimensionality, since it has several facets (e.g., physical, social, economic, environmental, institutional). Physical vulnerability, which is mainly accounted for in risk assessment, is defined with respect to direct damage to buildings, structures, infrastructure, networks, and other objects. In particular, it expresses the degree of loss or potential damage to a given element or set of elements stuck by an event of a given intensity. Social vulnerability expresses the rate of impact of the hazard on the exposed population

considering the phenomenon intensity (which is in relation to the warning time), the population sensitivity (depending on its age and capacity to anticipate a landslide) and the capacity of understanding the phenomenon and to move away from the exposed zone [229]. The economic vulnerability is determined by the indirect consequences of the phenomenon on a range of activities impacted by the damage, such as decreased tourist demand, increased travel distances for industrial goods, and depreciation of adjacent lands and buildings, etc. Furthermore, environmental vulnerability should be accounted for in phenomena (e.g., landslides) that impact the natural environment. Furthermore, also the environmental vulnerability should be accounted, for such hazard phenomena (e.g., landslide) impacts on the natural environment [229].

The territory in which we live is annually exposed to severe losses, both economic and social. Analysis of data recorded over the past 20 years (2001–2021) shows that the costliest disasters have been hurricanes and earthquakes [230]. Regarding to human losses, in these two decades, there were about 100 million people involved in natural disasters, and among them, thousands of deaths were recorded due to earthquakes; the most devastating were those in Haiti (220,000 deaths) and Sichuan (China; 87,000 death; [230]). Italy is a territory particularly exposed to seismic risk, due to the high rate of occurrence of seismic events as well as the fragility of the built-up. Indeed, Italian land partially extends along the contact zone between the Eurasian and African plates, whose movements result in the formation or reactivation of faults that can produce seismic events of considerable intensity [231]. Since 1900, there have been 30 very strong earthquakes (with magnitudes greater than 5.8), some of which have been catastrophic [232]. The strongest of these (magnitude 7.2) is the earthquake that destroyed Messina and Reggio Calabria in 1908 [232]. However, recent events such as the 2017 Casamicciola (Ischia Island, Naples) earthquake show how low-intensity seismic events can cause relevant damages to the built heritage, underscoring the fragility of the Italian territory [233], [166].

2.2 APPROACHES AND METHODS AT TERRITORIAL SCALE

2.2.1 SEISMIC-PHYSICAL VULNERABILITY

2.2.1.1 Assessment methods for timber structures

The assessment of the physical vulnerability of the built-up represents a fundamental action toward seismic risk analysis and management. This requires the use of reliable models that enable the prediction of losses associated with a given event, taking into account the exposed buildings. Commonly, at least three different methodologies are employed in the construction of vulnerability models: (1) Methods employing analytical methods, in which fragility is calculated using analytic estimations of the buildings' response and damage (2) Empirical methodologies in which models are developed using data statistically processed on the basis of damage caused by previous earthquakes. (3) Hybrid methodologies that integrate different assessment methods, such as analytical or expert-based evaluation, followed by empirical calibration using observational data [234]. As regard empirical fragility curves, various models have been proposed for masonry and reinforced concrete (R.C.) building typologies in Italy [235], [236], [237]. At the same time, analytical methods have been employed to derive analytical based fragility curves for masonry [238], [239] and RC buildings [240], [233]. An hybrid approach has been proposed by [241], which transformed the linguistic assignments of the EMS 98 scale into typological fragility curves using an hybrid-fuzzy approach. Several authors have applied the *indicator-based approach* [242] for assessing seismic vulnerability at the municipal and territorial scales, using a semi-quantitative method supported by the multi-criteria decision-making methods (MCDM) [243], [244], [245]. An exhaustive compilation of physical vulnerability models, which may be implemented in large-scale applications is showed in [246].

Regarding timber constructions, several vulnerability models related to constructions made of masonry walls and timber floors have been found in the literature [247], [248], [250], [251]. As regard full timber buildings a fragility model, evaluated through incremental dynamic analysis, has been obtained for structural systems in CLT, modelled through plane systems with an increasing number of stories from one to six [252]. The authors found that the vulnerability to earthquakes heavily depends on the number of stories and

the seismic scenario, rather than on the CLT wall panel typology [253] obtained fragility curves for hybrid steel structures with infilled CLT panels using nonlinear time-history analyses, evaluating the effectiveness of various panel arrangements. For Chinese ancient timber structures fragility curves, considering correlation among different failure modes, have been established by [254]. Gaspari et al. [255] analysed 101 large-span timber roof using a fast and straightforward approach. The authors performed a quantitative evaluation of the seismic vulnerability of the main beams and roofing bracing using simplified structural models and by applying the Italian building code. Then, the aspects not considered in the quantitative evaluation have been assessed through qualitative parameters inspired by damage identification forms (e.g. the AeDES form; [256]).

2.2.1.2 Survey forms for supporting vulnerability assessment

In seismic risk analysis, vulnerability analysis and exposure assessment require prior knowledge of a dataset inherent in the characteristics of the built environment. In large-scale analysis, such information can be quickly identified through databases constructed by institutional organisations, e.g., the census inventory provided by ISTAT in Italy (Instituto nazionale di statistica; [257]). In addition, image-processing techniques can support this, allowing the rapid and automatic collection of large-scale spatial information by using satellite data [258]. Nevertheless, the main parameters for vulnerability assessment, such as building age, quality of construction, materials and state of preservation, are not always suitable to collection via database or satellite. For such reason, in Italy the ReLUIS (Italian Network of Academic Laboratory of Earthquake and Structural Engineering; [259]) supported and funded by the Italian Civil Protection Department, developed a data management and acquisition system based on the CARTIS form, for the typological and structural characterization of the urban settlements [260].

The CARTIS method has two primary objectives: (1) Establishing a methodical approach to evaluate territorial-scale exposure and vulnerability by utilising typological-structural characteristics of existing buildings; (2) Constructing a database regarding typological-structural information of Italian buildings is useful for researchers intent on conducting vulnerability analyses towards earthquakes as well as other natural hazard phenomena [260], [261]. The CARTIS methodology relies primarily on the CARTIS form and its user's manual to characterise the residential building typologies in municipal or sub-municipal areas, called "Sectors" or “Compartments”.

These typologies are distinguished by factors such as the age of the first settlement, homogeneity of the building fabric, and construction and structural techniques. In addition, a validation survey form known as CARTIS BUILDING has been created to assess building by building inspections that align with the information gathered from the CARTIS form. In the end a software application allows the collection of the information acquired by the survey. Thus, the information are stored in a database which is accessible by the ReLUIS research units [261].

The CARTIS form is made by four sections, from 0 to 3. The section 0 is made by two parts, A and B. In the first one (A), the identification of the ReLUIS Research unit, interviewees, as well as general characteristics of the municipality is provided. The sectors into which the municipality has been subdivided are described in summary in Part B. Data pertaining to the primary typologies present in the sector, as well as the age of the initial urban settlement within the area, are necessary for each sector. The next section (section 2, 3) must be filled in for each typology. The identification of the general characteristics of the examined typologies, including the number of storeys, average floor height, average ground floor height, etc., are highlighted in the Section 2. The section 3 is devoted to the characterization of the typology's structural elements, including the collection of data concerning vertical and horizontal structures. Thus, the overall form contains the main parameters used in seismic vulnerability analysis [261]. The CARTIS form is filled out by one o more members of the Research Unit of ReLUIS organization by interviewing local experts (e.g., technician belonging of local public administration or private sectors) and operating in such a way as to first identify the sectors and then the types [260], [251]. About 383 municipalities of the Italian land (almost the 5% of the total number of municipalities) have been surveyed through the CARTIS form, for a total number of about 5,300 residential buildings [261].

The CARTIS methodology has also been extended to various types of buildings, including large-span buildings (CARTIS – LARGE-SPAN) and churches (CARTIS - CHURCH). The CARTIS LARGE-SPAN form consists of two main parts addressing the building and sector (or district) characterization respectively [262]. The first part (CARTIS “building”) is aimed at the identification of all the structural features, and it is divided into seven sections, from 0 to 3 (Table 2.1; [262]):

- Section 0 “Identification of municipality and building” is divided into subsections as follows: (a) localization; (b) identification data of the

ReLUIS research unit; (c) identification data of the interviewed technician; (d) identification data of the building.

- Section 1A, "Identification of the building constructive technology" enables the choice of the construction technology (R.C., precast R.C., steel, timber, masonry, etc.) associated to the vertical and horizontal structural elements, such as roof and foundation.

Table 2.1. Contents of the CARTIS form for large-span buildings (buildings; reproduced from: [262]).

CARTIS: "Buildings"	
0	Identification of municipality and building
1A	Identification of the building constructive technology
1B	Identification of the building typology
2A	Description of the building
2B	Presence of blocks added to the main structure
2C	Typology of connections, panels, special loads, other non-structural elements
3	Other information

- Section 1B, "Identification of the building typology" collects general metrics data (i.e., number and span of naves and bays, column height), information about the sub-systems (i.e., type of vertical seismic resistant system, connection, type of bracing system and members) and information about anti-seismic devices, the type of roofing system, closing elements, and foundations structures.
- Section 2A, "Description of the building" collects metrics data of the building, such as number of stories and underground stories, average inter-story heights, maximum column height, and average story area (m^2). Age of the building, use, and exposure, such as type and percentage of use, as well as ownership (if public or private) are also requested.
- Section 2A, "Description of the building" gathers building metric information, including the number of stories, average inter-story heights, maximum column height, and average story area. Further information regard the building's age, intended use, and usage.
- Section 2B, "Presence of blocks added to the main structure" enables the identification and characterization of the possible added blocks to the main structure.
- Section 2C, "Typology of connections, panels, special loads, other non-structural elements" enables the description of the type of connection between structural elements, the special loads, panels to

structure, the type of panels, the special loads, and the presence of other non-structural elements.

- Section 3, "Other information", gathers information regarding the building elevation and plan, openings in the facade, and the condition of preservation for both structural and non-structural components.

The CARTIS "Districts" is subdivided into four sections, from 0 to 3 (Table 2.2). Section 0 deals to the identification of the municipality and sectors ("districts"), whereas the description of the main typologies present in the district is provided in the following sections. A detailed description of the sections is given below [262]:

- Section 0, "Identification of the municipality (or province) and districts" collects data regarding (a) localization; (b) general data; (c) number of homogeneous districts; (d) identification data of the ReLUIS research Units; (e) identification data of the interviewed technicians; (f) constructive technologies present in the district; and (g) urban plan with delimitation and numbering of districts.

Table 2.2. Contents of the CARTIS form for large-span buildings (districts; reproduced from: [262]).

CARTIS: "Districts"	
0	Identification of the municipality (or province) and districts
1	Identification of the constructive technology
2	General features
3A	Characterization of masonry type
3B	Characterization of reinforced concrete type
3C	Characterization of steel type
3D	Characterization of timber type
3E	Characterization of precast reinforced concrete type
3F	Roofs and foundations
3G	Other information

- Section 1, "Identification of the constructive technology" must be filled out for each main construction typology identified in the district. It allows the selection of the construction technology (masonry, R.C., steel, precast R.C., or timber) and the recurrent position of the buildings into the district (e.g., isolated, in aggregate, etc.).
- Section 2, "General features", collects a set of data related to the main typology of the district; it can be subdivided into metrics data, general data and data related to the exposure.
- Sections 3A, 3B, 3C, 3D and 3E deal to the characterization of masonry, R.C., steel, timber and precast R.C. types. In general, they

collect data about the structural layout, structural system, structural members, and other further information specific to the construction technology.

- Section 3F, "Roofs and foundations", contains information about roofs, such as the overall stiffness, maximum span, presence of in plan braces, presence of ties and pushing elements, as well as the type of closing elements. Furthermore, it contains data about the type of foundation.
- Section 3G, "Other information" pertains to the requirements for regularities in the plan and elevation, the proportion of openings in the building facades, the condition of both structural and non-structural parts, potential retrofitting interventions for the structure, and the type of stairs present.

Currently the CARTIS form for large-span structures has been applied to a moderate number of buildings in steel and timber construction type [263], [265], and its improvement is still in progress. Indeed, the peculiarities of such constructions should be considered to improve the completeness and effectiveness of the form. The CARTIS form, along with other forms addressing the construction of an inventory of structural types, is not the only approach for supporting the seismic vulnerability assessment. Indeed, the forms for damage surveys during the post-event period are valuable tools for establishing databases supporting the seismic vulnerability assessment through an empirical approach. Nowadays in Italy the DaDO platform (DaDo – damage data observation), developed by Italian Civil Protection Department (ICPD), is the main common database containing information on damage and structural features on ordinary buildings for 11 national seismic events [264]. Such database has been built during time thanks to the data acquired through the AeDES form. In the years 1996-97 the joint working group of the National Seismic Survey (SSN) and National Group for the Defence against Earthquakes (GNDT) developed this survey form for damage assessment, short term countermeasures for damage limitation and evaluation of the post-earthquake usability of ordinary buildings [266]. Since the 2002 the form has become the official operational tool recognized by the DPC for the technical management of emergencies [266]. The most recent version of the AeDES, known as AeDES 07/2013 [267], has been implemented for the earthquake that took place in central Italy (2016) and in Casamicciola (Ischia Island, 2017). The form is composed of nine sections dealing to the: building identification and description, typology characterization and recognition of the damage. The damage is evaluated for structural and non-structural elements, furthermore the damage caused by other construction and short-

term countermeasures are identified. In the end the section 7 deals to the characterization of the soli and foundations, whereas the section 8 provides the information for the usability judgment [266]. Nowadays, the form is the main tool at the national level for assessing earthquake damage. Simultaneously, in combination with the DaDO database, it is a crucial element in providing support for vulnerability analysis through the application of empirical models [268], [269], [270].

2.2.2 DURABILITY ISSUES

2.2.2.1 Life-time concept in structures

Throughout its life cycle, every construction will experience degradation, which is influenced by many factors including ambient conditions, natural ageing, material quality, the execution of work, and planned maintenance. This decrease could result in a reduction in performance to the point where a structure is unable to satisfy the fundamental standards for functionality and safety before its intended life ends. The structural codes include different practical principles and application rules to prevent premature failure in construction. These include the implementation of protective systems for materials exposed to aggressive environments, construction detailing to prevent degradation, and regular maintenance actions.

As regard the structural performance of a building over time, both the applied loads and material resistance are time-dependent variables. Indeed, the loads generally tend to increase over time, whereas the resistance tends to decrease over time (Figure 2.2.a). Furthermore, the uncertainties related to the two variables tend to increase with time; thus, not only the mean values change but even the probability distributions show a larger scatter with time. For this reason, the probability of failure can be described as a function of time, which tends to reach the maximum value, i.e., the failure, for an infinite increase in the time variable.

Nowadays most of the European code for structure design provides rules for design according to the limit state method [71] using a semi-probabilistic approach. Thus, the partial safety factors [271] are applied to the characteristic value of both load and resistance, in order to achieve the proper degree of reliability. In this framework the concept of life-time is partially accounted, since only the loads are calculated taking into account the time dependence of variable action. Indeed, the load are defined considering the temporal variability of the action, which is accounted implicitly in the

definition of design value. On the contrary, the resistance is given by the characteristic value reduced through the partial safety factor, which take into account the scatter of material properties and uncertainties. Thus the effect of deterioration on the resistance is neglected in the current practise of design.

This results in independence of resistance from time, i.e., the design value of structural capacity does not consider the anticipated deterioration that may affect the structure. Therefore, if scheduled maintenance operations are insufficient or neglected, the reliability of the structure at the end of its service life may not meet the acceptable level of reliability fixed by standard rules.

However, tools for predicting the durability's performance of a structure are critical, especially for companies that own large sets of buildings or infrastructure, which often have to deal with unexpected maintenance interventions to extend the life of these structures. For example, in Figure 2.2.b progress of deterioration over time in two structures (A and B) is showed. Structure A has sufficient durability and exhibits higher resistance to deterioration prior to reaching an undesirable level of quality by the end of its service life. On the other hand, Structure B has a higher rate of decay and insufficient longevity, necessitating repairs throughout its operational lifespan.

This example clearly highlights the importance of maintenance to ensure a consistent level of quality. Furthermore, integrated design, aware of durability issues through the use of predictive models, can lead to sustainable management of the structure, avoiding unexpected and early interventions.

2.2.2.2 Principles and method for service life design

Since the end of the 1980s, the concept of durability has spread in the building sector. The Construction Products Directive (CPD) [272] was the first regulatory reference to introduce the concept of durability and sustainability in the production of building materials. The aim was to direct the building sector on a new path, based on the limited use of non-renewable resources, as well as the reduction of management and maintenance costs in the building life-time. Subsequently the topic was at the centre of the international research. Thus, a new regulation [273] was published in a short time, providing know-how about the methodologies for service life planning and introducing the concept of service life.

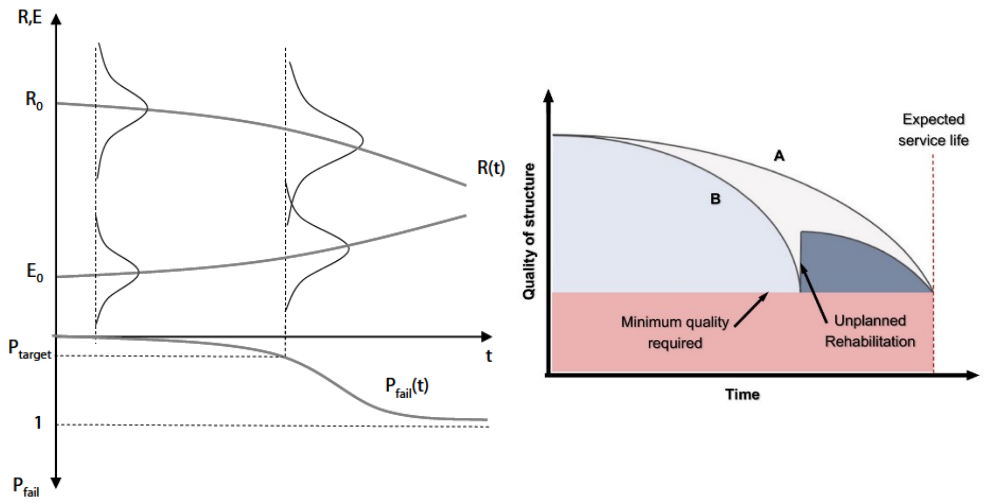

a) b)

Figure 2.2. a) Formal representation of a time-dependant reliability problem (R_0: resistance at time t_0; E: demand at time t_0; P_{fail}: probability of failure; t: time; extracted from: [274]); b) Schematic illustration of the concept of 'service life' of a structure (extracted from: [275]).

The service life can be defined as the actual period of time after manufacturing or installation during which relevant properties meet or exceed minimum acceptable values [276]. It is estimated from recorded performances, previous experience, tests or modelling [277]. As well as service life concept, also the following parameter assume a relevant weight in the field of service life design:

Target service life: required service life is fixed by general regulations, the client, or the structure's owner. It is the period of time during which a structure or component can be used for its intended purpose without requiring significant repairs [276].

Design service life: design value of service life. The reference value utilised in durability calculations incorporates the temporal variation and ensures the necessary level of safety to prevent falling below the target service life [276].

Residual service life: period of time, calculated after a durability assessment, for which the structure will keep a fixed level of performance [278].

Afterward, the concept of durability was also brought to the light in the field of structural design. It was understood that a material deterioration process could lead to such a performance decrease that a structure may not be

able to respond to service or safety requirements before the design life is over. First the Eurocode UNI EN 1990 [271], in 2002 introduced general guidance for design according to service life, specifying that degradation phenomena can be evaluated according to computational models, experimental tests, or empirically based methods. Subsequently, the International standard ISO 13823 [279] issued in 2008, was a first step toward codification of service life methods. Indeed, it provided a general framework for performing the verification of durability issues at different design levels, following an empirical, experimental or analytical approach. The ISO 13823 [279] defined the limit state method for the design and verification of durability following two steps: identifying and describing the significant degradation mechanisms that are expected to affect the structure, and then assessing the durability of the structure using a fully probabilistic, semi-probabilistic, or deterministic methodology [279]. The first step entails analysing the structural environment, determining the mode of transfer, and specifying environmental factors that may result in a decrease in structural performance. Regardless of the specified level of analysis, durability requirements can be verified by using one of the following approaches: service-life approach, which involves comparing the design life (t_d) with the target life (t_g), or limit state, which considers both demand and resistance of the structure as time-dependent variables [279].

Nowadays different approaches are spread for assessing the service life and they can be classified in prescriptive, deterministic, semi-probabilistic and full probabilistic approaches [274], [281]. The Factor Method (FM) was introduced by the ISO 15686 [273] Standard as a simple and deterministic method for evaluating the service life of building component or assembly of components. It is based on the identification of the main factors influencing service life, thanks to which the expected or estimated service life (ESL) can be calculated by adjusting the value of the reference service life (RSL). The approach does not offer a guarantee on the service life, but it provides an evaluation of the durability of components under specific conditions [274].

2.2.2.3 Methods for timber structures

The identification of possible material deterioration phenomena of a structure exposed to certain environmental conditions is a fundamental prerequisite for service life assessment. However, an analytical assessment needs the definition of reliable degradation models that capture the characteristics of degradation processes. Various performance models have been developed for different building materials, however they may not be

directly applicable to wood-based materials due to their organic nature. Methods and models for estimating service life of timber elements are very heterogeneous, since they differ in objective, governing variables and data sources [281]. At the state of the art, several authors have proposed models for predicting decay from fungi as well as models for climate conditions related to relative decay phenomena whereas biological decay from insect attacks has been modelled by a few authors, probably due to the complexity of the phenomena. T

Through work conducted in the early 1970s, Scheffer [282] proposed an index for modelling climatic conditions. Currently, this model still widely used to estimate the decay hazard related to thermo-hygrometric and geographical conditions [281]. Then, further climate indices have been developed and considered for service life prediction by other authors [283], [284].

As regard the model for predicting biological decay due to fungal, termite and marine borer attack, an extensive research project has been carried out in Australia, taking into account various sources of data [285], [286], [287], [288]. Thus, as a result of 10 years of research, the efforts have been realised in the "Timber service life design guide'' product and the *TimberLife* relative software tool, published by the Commonwealth Scientific and Industrial Research Organisation [289]. The software is based on a prediction model where the timber decay above the ground is estimated as decay depth over time considering several factors [290]. Although the CSIRO model [290] has been developed for applications in Australia's regions, several authors have adapted and simplified the model for applications outside of Australia [291], [292].

For decay by fungi different dose response model have been proposed [293], [294], [295]. The dose-response function is an instrument which describe the change in effect on an organism caused by different levels of exposure [295]. The dose-response relationship for fungal decay is generally expressed by a sigmoid function which fit the dose-decay data obtained by experimental tests, where the decay rate can be evaluated according to the standard EN 252 [296]. Viitanen et al. [293] defined a model expressed as mass loss of wood in accelerated tests at high humidity and at different temperatures. The idea of assuming the activation stage in the fungal degradation process led to the definition of subsequent models, in which this phenomenon was modelled through a time-lag [290] (Figure 2.3). Nofal and Kumaran [297] provided an alternative decay model, called "wood rotting mode", that relies primarily on laboratory test data obtained from literature.

The primary objective of their study was to establish the relationship between biological damage function models and hygrothermal models, enabling their use in design and performance evaluation.

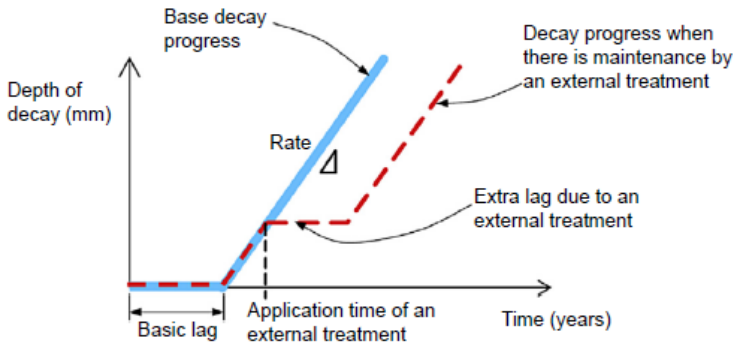

Figure 2.3. Idealized model for the progression of decay in timber elements with possibility of external treatments (extracted from: [82]).

Saito et al. [298] presented a model based on own test results with the brown rot fungus *Fomitopsis palustris*. Furthermore, they coupled the model with an hygrothermal simulations. The effect of fungal decay on mass loss and strength loss have been analysed by Van de Kuilen [299] and Montaruli et al. [300] through damage models and damage accumulation functiona. Furthermore Van de Kuilen and Gard [301] described a damage accumulation model for wooden pilings. Another relevant project on the service life design of timber structures concerns the European WoodWisdomNet project *WoodExter* [302], which is still ongoing. The project provided guidelines for design, in which the design condition against degradation issues is verified following a semi-probabilistic approach where demand (exposure) and capacity are compared. Both exposure and resistance are calculated following the dose-response approach. The exposure is expressed by the exposure index, evaluated through different factors taking into account exposure conditions [303], whereas the resistance is calculated by modifying the dose of the reference wood species by a set of parameters [304]. An innovative approach is proposed by Gaspari et al. [305] for evaluating the state of conservation of the balconies in timber CLT panel buildings. The proposed methodology allows estimating the amount of wooden material rotting over time, correlating the effect of design choices to the environmental conditions of the construction detail under analysis through a decision three method.

Then the rate of decay is evaluated through a model based on Wang et al. [290] model and the results are validated through onsite inspection.

2.3 APPROACHES AND METHODS AT BUILDING SCALE

2.3.1 GENERAL

At the building scale an in-depth knowledge of the structural features is needed to perform a structural analysis toward the seismic action and design proper retrofit interventions. In general, the structural analysis can be performed using different approaches and thanks to the development of calculation software, it is nowadays carried out using FEMA. According to Italian building regulation [71], seismic analysis can be performed using four methods: linear static analysis, response spectrum analysis (RSA), pushover analysis and the non-linear dynamic time-history analysis. Linear static analysis is a basic analysis that consists of applying static horizontal forces to the structural system, equivalent to the inertia forces induced by seismic action. The response spectrum analysis (RSA) utilizes a standardized ground motion input, called response spectrum, representing expected accelerations at different frequencies [306]. The structural model undergoes mode superposition analysis [307], breaking it into vibration modes, and then calculates the response for each mode independently. Then the response of the overall structural is determined. The pushover analysis is a static and nonlinear approach. Lateral loads are incrementally applied to the structure to simulate seismic forces. This method accounts for the nonlinear behaviour of materials and connections, providing a more realistic representation of the structure's response. The focus is on assessing the structure's deformation capacity and its ability to undergo significant lateral displacements [308]. The non-linear dynamic time-history analysis relies on actual ground motion records or synthetic earthquake accelerograms, providing a time-history of accelerations [309]. The analysis includes material yielding, stiffness changes, and potential structural damage, offering a realistic representation of the structure's response. It employs incremental time steps to calculate the structure's response throughout the seismic even. This analysis is valuable for structures with complex geometries or significant nonlinearities.

However, a sophisticated analysis does not ensure a correct assessment of the seismic vulnerability of an existing building. Indeed, key aspects concern the modelling of the structure's geometry, including constraints. In addition

to this, the assessment of the state of preservation of the structure plays a fundamental role, which must be taken into account both in the geometric model and in the evaluation of the physical-mechanical properties of the material. Indeed, the performance of a structure generally changes during its service life due to accidental events or modifications, such as alterations to the structural scheme, changes in the acting loads, or material decay. Especially timber structures suffer from decay phenomena that can significantly reduce the load-bearing capacity over time. For this reason, methods and procedures are needed for diagnosing existing structures and assessing their state of health.

2.3.2 SURVEY AND DIAGNOSIS OF EXISTING STRUCTURES

2.3.2.1 Standards and procedures

Structural assessment is also the first step towards an intervention that might itself range from mere preservation to the improvement of the structural performance, through a retrofit design, such as seismic retrofit. Each of these situations involves distinct requirements and procedures. According to Riggio et al. [310], standards and guidelines about the assessment of existing timber structures can be grouped according to their aims in: documentation for protection or conservation, vulnerability and damage assessment, documentation for serviceability, and safety evaluation. The ICOMOS [311] organisation has two scientific committees that specifically focus on the documentation and structural assessment of timber structures: the ISCARSAH committee, devoted to the assessment and restoration of the architectural heritage, and the International Wood Committee (IIWC), that is fully devoted to the timber structures. Both committees have formulated principles and guideline [312], [313]. These documents recommend inspection, recording and documentation and advocate the important principle that diagnosis and intervention should follow attentive and thorough study of present and past conditions. To this aim, guidelines for the assessment of historic timber structures have been drawn under the scope of the European Cooperation in Science and Technology – Wood Science for Conservation of Cultural Heritage [168]. The authors highlighted that a distinction needs to be made between heritage/historic structures and other existing structures, since a greater value is placed on the fabric of heritage structures because of their historical significance [168]. According to the author this value may justify greater expense both in the survey, diagnosis,

and assessment of the structure and in the subsequent repair methods that might be employed. Furthermore they drawn the process for assessing an historic timber structure, as well as for planning any interventions (Figure 2.4). This scheme highlights how the desk survey and preliminary survey constitute the initial stages, during which key documentation is obtained and a comprehensive overview of the structure is established. Then the measured survey or geometrical survey is carried out in order to perform a first structural analysis in which the aspects related to timber decay are not yet considered. A substantial increase in knowledge is achieved with the detailed survey, whereby information on the quality of the timber members is acquired through visual grading, possible areas of decay are detected, and an in-depth study of the connections is carried out. As a result of this analysis, a diagnosis report is generally produced and any repair, consolidation or retrofitting work is then designed. Starting from the flowchart proposed by Cruz et al. [168], recently Shabani et al. [314] showed a new procedure for the structural vulnerability assessment of heritage buildings. According to the author the methodology for vulnerability assessment and conservation of heritage timber buildings consists of a four main steps: preliminary survey, detailed methods, ex-situ methods and possible retrofitting suggestion. Other procedures for the assessment of existing timber structures with different purposes have been shown by several authors [121], [171], [315], [310]. Dietsch and Kreuzinger [121] proposed an articulated framework in which the number of phases necessary is dependent on the remaining level of doubt, the feasibility and simplicity of repair/strengthening (or demolition), always in combination with economic considerations. Parisi et al. [315] proposed a procedure for assessing the seismic vulnerability of timber roof structures by describing methods for on-site inspection and new approaches to the vulnerability analysis. An approach to the survey and diagnosis of heritage timber structures aimed at conservation and rehabilitation is shown by Bertolini Cestari and Marzi [171] through an extensive illustration of interventions carried out on 10 heritage timber structures located in northern Italy.

A further contribution to the definition of an ontological approach to the assessment of heritage timber, relating the scope of the assessment, information required, and necessary procedures, is provided by Riggio et al. [310]. Furthermore, the author presents an extensive review of state-of-the-art procedures, standards and guidelines in this field.

Nowadays in Italy several standards have been issued to define assessment at the level of the timber structural element, including the characterization of the material and its properties. UNI 11161 [316] provides comprehensive

instructions on various levels of intervention for heritage timber structures, encompassing conservation, restoration, and maintenance. The primary focus of UNI 11138 [317] is on interventions. The initial section of this document undertakes the essential preliminary examination of the artefact, encompassing tasks such as historical analysis and structural analysis. UNI 11119 [318] is exclusively focused on inspection for diagnostic purposes, while UNI 11118 [319] provides guidelines and techniques for identifying different wood species.

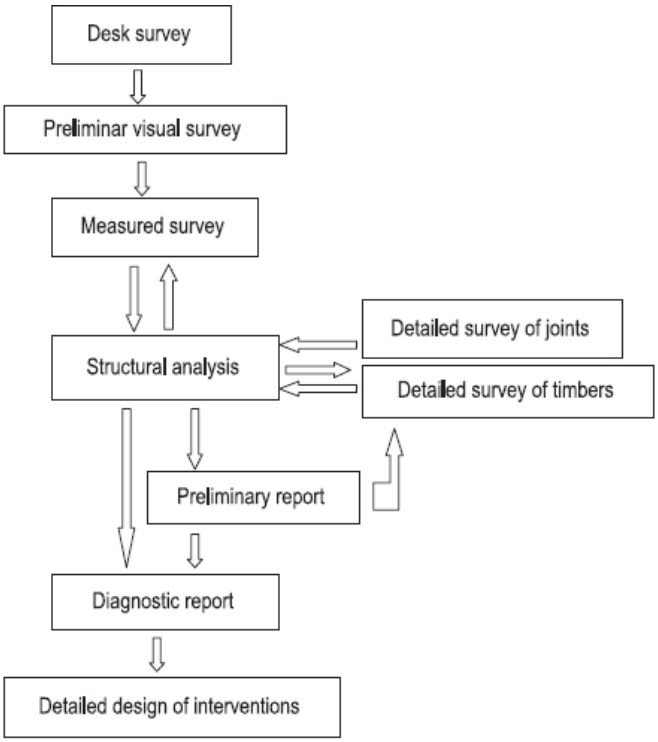

Figure 2.4. Steps required for the assessment and planning of interventions in historic timber structures (extracted from: [168]).

2.3.2.2 Visual inspection and geometrical survey

Visual inspection is the basis of any on-site assessment of timber structures and is intended to provide information about several aspects. It should include the surveys of geometry, joints, supports, materials, loads and any degradation phenomena or structural issue [320]. In a general framework, visual inspection should be carried out in several stages and to the aim of the

structural analysis at least, the following steps should be taken into account [168]:

- Geometrical survey;
- Technological survey;
- Recognition of degradation phenomena and structural issues.

Any of these steps can be conducted through simple visual inspection procedures and traditional surveying techniques. However, the technology available today allows for the application of advanced surveying and diagnostic techniques. On the other hand, the degree of depth of these steps should be calibrated according to the importance of the structure and the scope of the analysis, as well as the economic and time requirements.

The geometrical survey should involve the survey of the main members of the structures, i.e., the typical dimensions and shapes of the members; the survey of the joint types, materials, and typical dimensions; as well as the survey of the construction system supported by the structure, in order to determine the dead loads needed for the structural analysis. For structures characterised by quite regular geometry, the geometrical survey can be easily conducted using direct survey methodologies, i.e., using simple tools such as measuring tape, plumb lines, etc. However, the use of indirect surveying methodologies is becoming increasingly common in professional and research fields, especially when dealing with large structures with complex geometries. Two surveying techniques, photogrammetry and terrestrial laser scanner, have progressed significantly and implemented in recent years [321], [322], [323], [324]. These technologies not only enable accurate geometric surveying but can also work in combination with non-destructive techniques for the assessment of parts affected by biological decay [325] and abiotic degradation [326]. Thanks to the acquisition of textured digital models, these technologies are also finding application in visual strength grading analysis [324], [327]. By building digital models, these techniques contribute to the efficient and effective management of historic building information through the HBIM (Historic Building Information Modelling) process. It involves creating digital models that not only capture the physical aspects but also incorporate data, such as conservation, testing, and monitoring data [328], [329].

Visual site inspection as well as geometric surveying require the acquisition of a large amount of data. Therefore, an indispensable and base tool for the inspection of timber structures is the survey form, either hardcopy or digital document that allows the collection of all the necessary information. With regards to timber structures, many templates for inspection and

diagnosis are spread in literature, they differ in scope (damage, vulnerability, conservation assessment) and level of investigation (preliminary, general, detailed). Concerning the damage assessment, templates are proposed by Toratti [330] and Serafini et al. [331], the latter specifically devoted to the failure prevention of heritage timber roofs. For the vulnerability assessment on building scale, a survey form is provided by Riggio et al. [310]. Many authors suggested a multi-purpose inspection template, for guiding the expert in the collection and interpretation of data [324]. It is worth noticing that most of the aforementioned templates were conceived in digital form, in order to easily create consistent database for subsequent analyses [310].

2.3.2.3 Visual Strength Grading (VSG)

The timber classification according to its strength, stiffness and density is a crucial point for structural engineers and researchers working on existing timber structures or designing new timber structures since the structural safety, the efficient and economically sustainable use of this resource strongly depend on these findings. The physical and mechanical properties of wood are very different, since they vary from species to species and depend on the provenance. In order to distinguish wood members with better qualities (i.e., with higher physical and mechanical properties) from those with inferior characteristics, specific procedures and regulations are in place at the national and EU levels to regulate this selection, which is commonly called “strength grading." Although the terminology used in European grading standards may vary slightly and lack consistency, the “strength grade” can be defined as a category of timber describing its relative quality for construction. It is important to distinguish the latter definition from the “strength class," which refers instead to a specific category described by certain mechanical and physical properties that are used in calculations for design purposes [332].

At the European level, timber strength classes are described by three key physical and mechanical properties: strength, stiffness, and density. These are commonly estimated through destructive tests regulated in procedure by the Standards UNI EN 408 [333] and EN 384 [49]. On the other hand, for the purpose of strength grading, two parallel systems are currently used in the European system: visual and machine grading. Both latter systems operate in a way to relate non-destructive measures to the three grade determining properties based on relationships established by destructive testing. The two systems vary not just in terms of the parameters for grading timber, but also in terms of normative requirements.

Machine, or mechanical, strength grading can currently be carried out with predetermined machine settings (called ‘‘machine control’’) or by continuous testing of output (called ‘‘output control’’) [334]. Thanks to the machine test some properties of timber, commonly called “indicating properties” (IP), are measured for predicting the strength grade [332]. Nowadays several technologies are in use to this aim, they include longitudinal or flexural resonant frequency (with or without mass), X-ray measurement of density and knots and ultrasonic wave speed [332]. Regardless of the machine system and device type, an additional ‘‘visual override’’ step is always required to inspect the timber for strength-reducing defects that cannot be automatically identified by the machine. This highlights the durable efficiency of visual strength grading (VSG), despite its ancient roots.

VSG is carried out according to grading rules that are usually provided by national standards, considering the diversity of species, origins, quality, historic influences, requirements, and uses. The grading rules are based on the wood features that affect the quality, such as knots, slope of grain, ring width, reaction wood, etc. They specify limits for these features to assign pieces of timber into a grade. The grades are assigned to strength classes, together with species and growth area, based on the results of destructive testing. Nevertheless, the standardised EN 14081-1[335] establishes fundamental principles that the visual grading rules must conform to. A wide list of National Standards currently exists, some of the European standards are listed in Table 2.3. Generally, most of these standards are distinguished by wood species into hardwood (UNI 11035-2, [336]; UNE 56546, [337]; BS 5756, [338]) and softwood (UNI 11035-1, [339]; UNE 56544, [340]; BS 4978, [341]), in addition there are some that are specific to roundwood (DIN 4074 – 2, [342]) and others to existing wood in historic structures (UNI 11119, [318]). The wood species that can be employed for structural purposes in Europe are generally listed in standard UNI EN 1912 [343] which details the strength classes assigned to each. The mechanical properties of the strength classes are provided in the European standard UNI EN 338 [344] with their characteristic values for calculation according to the European standard UNI EN 1995-1-1 [70].

In Italy, timber members with squared cross-section can be graded through the grading rules provided by UNI 11035-1 [339] and UNI 11035-2 [336] standard, whose applicability is related to the visibility of at least three faces and one head of the timber member. The standard provides strength grades that can be related to the strength classes [344] by means of UNI EN 1912 [343]. The standard finds wide application in the classification of new timber, i.e., elements to be marketed, while application to existing structures is

limited by the very restrictive application requirements. On the other hand, a specific standard for existing timber structures is UNI 11119 [318], specifically addressing cultural heritage. In addition to providing classification rules for timber in existing structures, it specifies procedures for the inspection and on-site assessment. However, because the harmonised standard UNI EN 1912 [343] does not cover it, its applicability for structural calculations in accordance with current design codes is limited. Although the application requirements are restrictive, the Italian building regulations [71] indicate the UNI 11035-1 [339] and UNI 11035-2 [336] standards as the reference for the visual strength grading of existing timber structures aimed at diagnosis and structural safety checks.

Table 2.3. List of some national standard for visual strength grading in Europe.

Nation	Standard
France	NFB52-001 - Règles d'utilisation du bois dans la construction - Classement visuel pour l'emploi en structures des bois sciés français résineux et feuillus
Germany	DIN 4074 - Sortierung von Holz nach der Tragfähigkeit - Teil 1: Nadelschnittholz; Teil 2: Baurundholz (Nadelholz).
Italy	UNI 11035 - Legno strutturale - Classificazione a vista dei legnami secondo la resistenza meccanica - Parte 1: Conifere a sezione rettangolare; Parte 2: Latifoglie e sezione rettangolare.
	UNI 11119 - Beni culturali - Manufatti lignei - Strutture portanti degli edifici - Ispezione in situ per la diagnosi degli elementi in opera
Portugal	NP 4305 - Madeira serrada de pinheiro bravo para estruturas –Classificação visual.
Spain	UNE 56544 - Clasificación visual de la madera aserrada para uso estructural. Madera de Coníferas
	UNE 56546 - Clasificación visual de la madera aserrada para uso estructural. Madera de frondosas.
United Kingdom	BS 4978 - Visual strength grading of softwood.
	BS 5756 - Visual strength grading of hardwood

2.3.2.4 Non-destructive test (NDT)

NDT methods allow examining materials or components in ways that do not impair serviceability and future usefulness, in order to detect, locate, measure and evaluate flaws, to assess integrity, properties and composition, and to measure geometrical characteristics ASTM E1316 [348]. Nowadays, a wide range of NDT techniques and instrumentation can be applied to structural wood, and a comprehensive description of the main techniques has been performed by many authors [349], [320], [350], [351], [352], [353]. In

the literature, non-destructive investigation techniques are grouped according to different criteria. The most common classifications distinguish NDT between local and global, considering the area under investigation [353], [354] while other authors classify them between non-destructive and semi-destructive, taking into consideration the level of damage inflicted on the structure during the test [350], [355]. Among the semi-destructive techniques, resistance drilling [354], core drilling [356], [357] and penetration testing [355] are the most widely applied (Figure 2.5). Although these methods are called semi-destructive, they are often found in the literature under the generic group of NDTs.

Another relevant branch of NDTs involved the stress wave-based methods (also called acoustic methods by Palma and Steiger, [353]), which are mainly used for evaluating the stiffness of the existing members (Figure 2.6). A general distinction can be made between sonic stress wave techniques, commonly referred to simply as stress waves, and ultrasonic stress waves [349] based on the frequency of the wave. In general, ultrasonic stress waves have a frequency higher than 20,000 Hz [349]. Both techniques are based on the propagation of a sound waves through the material, which can be in longitudinal or transversal directions. Some of the characteristics of the sound waves are frequency, the wavelength and velocity of the wave [349]. An additional sub-grouping of the stress-wave methods can be obtained based on the type of analysis and postprocessing performed on the recorded data. As a result, frequency-based techniques (also called resonance-based acoustic methods, [358]) can be distinguished from techniques that are based on the time of flight of the stress wave (time domain; [352]). By utilising a Fourier transformation to analyse the spectrum of the recorded signal, frequency domain methods derive information regarding the material's conservation status or mechanical properties from the spectral characteristics [349].

Figure 2.5. NDT – semi-destructive methods: a) resistance drilling [359]; b) needle penetration [360]; b) core drilling (extracted from: [361]).

For detecting interior deterioration in wood, the sonic stress wave method is among the oldest and most widely used techniques still in use nowadays. By striking the wood surface (generally with a hammer) to generate sound

waves, defects, voids or defect can be recognized through the estimation of quantitative parameters. The time of flight (TOF) is the most common parameter, and it corresponds to the time required for the stress wave to propagate from the hitting point to the opposite side. In general, stresses waves propagate quickly through solid, dense materials; however, decay, voids, or cracks attenuate stresses. Therefore, fast stress wave propagation denotes sound and/or high-quality timber, whereas slow wave propagation indicates timber that has deteriorated and/or is of poor quality. Generally, two transducers a are used to detect passing stress waves and record time measurements. The measure can be in transversal or longitudinal direction. Transverse measurements are limited to a specific area of the specimen and only reveal quality aspects of that section of the timber member. On the other hand, longitudinal impact allows for the determination of the average global velocity of the stress wave along the entire specimen. By recording the TOF and measuring the distance between the impact site and the second sensor, it is possible to calculate the stress wave speed (SWS). This information can then be utilised to evaluate the internal physical conditions. An exhaustive list of SWS reference values for the main wood species can be found in the work of Dackermann et al. [351]. Regarding the positioning of sensors in investigations of existing structures, longitudinal measurements are rarely possible, so transverse, indirect longitudinal or semi-direct measurements are commonly used [351]. In the indirect measurements the slope of the sensor affect the evaluation of TOF, therefore standard values of sloping are suggested by Dackermann et al. [351]. A general procedure for carrying out the test is provided by the same authors, however the test set-up may change as function of the device. A list of common commercial devices is provided by Íñiguez-González et al. [352]. In addition to the sensor arrangement, other parameters such as the moisture content (MC) of the wood, the wood species, the presence of surface treatments, the grain orientation, influence the test results [351], [352]. Several authors studied the influence of MC on SWS and dynamic modulus of elasticity (E_{dyn} or MOE_{dyn}) by means of experimental tests [362] and literature review [363]. In addition to evaluating the decay of timber, stress wave measurements can also be utilised to predict the mechanical characteristics of timber, specifically the dynamic modulus of elasticity. The E_{dyn} can be calculated through the stress wave speed and timber density, according to a relation derived from the one-dimensional wave theory, which is reliable for wood [364]. The relationship between static and dynamic elastic modulus has been evaluated in many studies, finding very reliable linear correlations for several wood species [365], [366], [361], [367], [368].

Ultrasonic techniques use stress waves with high frequencies (above 20 kHz), which are not audible. Contrary to sonic methods, the stress wave is directly produced by a transmitting transducer and received by a receiving transducer. As seen for sonic methods, even in this case, the distance between the two transducers must be known in order to evaluate the SWS. The ultrasonic stress wave techniques have short wavelengths and can only travel shorter distances due to higher attenuation. The resolution of damage detection in stress-wave-based methods is heavily influenced by the wavelength of the sonic or ultrasonic waves that are produced. In general, ultrasonic waves are more effective than sonic stress waves in detecting small interior voids and defects. Typically, sonic stress wave methods are applicable for timbers that have a depth exceeding 89 mm, whereas ultrasonic testing is suitable for smaller dimensions [351]. The accuracy of measurement is significantly influenced by the coupling pressure, surface roughness, and alignment between the transducers and the surface [353]. Moreover, the MC of wood has a relevant influence on SWS, as showed by several studies [362], [363], [370], [371]. The ultrasonic technique finds wide application in the evaluation of the dynamic elastic modulus. Several experimental studies have been conducted to assess the mechanical properties of some wood species with destructive and ultrasonic techniques, finding reliable linear correlations between dynamic and static modulus [372], [373], [374], [375].

The application of vibration analysis, along with other methods, was initially used to determine the dynamic modulus of elasticity (E_{dyn}) of small clear specimens [378]. Sobue [376] proposed a technique to compute the E_{dyn} using Fourier transform of the power spectrum in the vibrating specimen. The primary parameter of the piece was its natural frequency. The natural frequency of vibration is determined by analysing the spectral frequency of vibration. A conventional method for evaluating the dynamic characteristics of a structure involves the installation of sensors, the application of an actuator to induce vibrations, and the subsequent analysis of the collected data. The most common sensors in vibration testing are accelerometers such as piezoelectric, piezoresistive, capacitive, and force-balance. In addition, the frequency of vibration can be measured by devices equipped with non-contact laser interferometer, such as ViSCAN devices (by MiCROTEC, Bressanone, Italy; [377]). Various types of actuators are used to impose forced vibrations on a structure. Impact hammers are typical actuators, and they can simulate an impulse with a very short duration, which results in all modes of vibration being excited with equal energy. The frequency of vibration is related to the stiffness properties of the member and its dimensions. The vibrational test can be performed in both longitudinal and transversal direction [378]. In

longitudinal application the stress wave speed can be calculated by multiplying two times the natural frequency of vibration and the wood density. Extensive literature exists regarding the evaluation of the mechanical properties of timber made from different wood species with this technique [379], [380], [381], [369], [382], [383], [372]. As a result of huge experimental tests, portable devices based on this technique received approval as grading machines for some wood species according to EN 14081-1 [335], [377], [384], [385]. The influence of moisture content has been studied by several authors, which found a relationship for calculating E_{dyn} at the reference MC [386], [381], [362], [363].

Figure 2.6. Ultrasound and stress wave devices (extracted from: [387]).

Due to its potentiality in assessing the extent and magnitude of decay, the drilling resistance technique or drilling resistance method (DRM) found large application in the on-site assessment of timber structures. A comprehensive discussion of the technique is provided by Tannert et al. [350] and Nowak et al. [354]. The device is mainly made of a drill with a small diameter drill pin (1.5–3.0 mm) to penetrate into wood member while measuring resistance to penetration [354]. The commercial device commonly used are [352]: Resistograph Rinntech (Rinntech, Germany) and the IML Resi (IML Instrumenta Mechanik Labor, Germany). Resistance to drilling is quite

proportional to wood density; therefore, DRM is suitable to estimate the wood density and locate zones with lower density. The latter zones may indicate internal decay, empty spaces, cracks, etc. Measurements are represented by a graphic profile characterized by two variables: drilling penetration (cm) and drilling resistance (%), the latter is a dimensionless parameter also called "amplitude" (A) or "resistance measure" (RM). Zones characterized by a lower drilling resistance are associated to a lower wood density. The main application of DRM in the diagnostic field concerns the detection and localization of the internal damage and discontinuities in timber elements, highlighted by voids and drop trend in the graphic profile provided by the DRM. Thanks to this feature DRM is largely used in technical community for estimating the resistant cross section reduced by damaged zone and voids, as well as for identifying the geometry of the cross section of timber members [388]. With this goal some authors have recently applied DRM in combination with the laser scanner [389], [390], [391]. Furthermore, DRM has been also lately applied in the field of post fire assessment, for estimating the residual cross section of members damaged by fire [180], [392], [393]. In addition to the aforementioned applications, DRM can be used for the prediction of the mechanical properties of timber, thanks to statistical correlations among the mean DRM output parameter (R_m) and the mechanical parameters obtained from destructive tests (DT). Several studies established relationships between R_m and timber mechanical properties, with different test-set up and an extensive description is provided by Nowak et al. [354]. In particular, it has been seen that the is influenced by the tool's settings (speed of rotation and sensitivity), the angle and direction of drilling (longitudinal or transversal), moisture content and timber species [350]. Both linear and multiple regressions are used in the estimation of timber mechanical properties [394]. Specifically, linear regression seems to be more reliable for the assessment of timber density and compression strength [395], [396], [397], [398], [399], [400], [401], [402].

Non-destructive testing also includes moisture content measurement test. The measurement of moisture content (MC) is crucial for accurate grading and calibration of non-destructive testing (NDT) results due to the significant impact of MC on various wood properties. Furthermore, elevated moisture content (MC) is related to the potential hazard of biological deterioration, such as the proliferation of fungi. MC in wood represents the proportion of water to the proportion of wood material, expressed as a percentage of the weight of oven-dry material. In general two methods can be applied to measure the moisture content of wood: direct method (or oven-dry method) and the indirect method [320]. The first one consist in measuring the quantity

of water in a wood sample or the weight of the sample when oven-dry. Therefore, the direct method requires removal of wood sample for analysis in laboratory and it doesn't permit the immediate MC measurement on-site. The test can be performed on small wood cores extracted from the timber member through a Pressler borer or similar tools [403]. On the other hand, the resistance or conductance method is an indirect method which is uses the relationship between MC and the electric conductance of wood. The basic measurement setup consists of a hand-held resistance type moisture meter equipped with two pin electrodes. In order to obtain accurate readings for the wood species/treatment and temperature under examination, it is crucial to calibrate the instrument or make corrections to the readings using external tables, reference functions integrated into the device, or information obtained from the literature [320]. With regard to the test procedure, multiple measurements should be taken along the length of the timber element, referring to the rules established by recognised standards [404].

2.3.2.5 Destructive Test (DT)

To achieve a thorough understanding of existing structures through testing, the most direct and effective approach is to carry out destructive test (DT), i.e., types of tests that can result in physical alteration or irreversible damage to the specimen. Destructive tests on existing structures are generally carried out in laboratory, by extracting the structure, or part of it, from the construction and then test it. Sometimes destructive tests are also conducted on-site, by testing the structure directly on-field with portable instruments and devices. In addition, another distinction must be made regarding the specimen dimension, which can be the whole structure, as is the case in full-scale testing, or a part of it (Figure 2.7). In this case, DT tests can be conducted on specimens in structural dimension (also called actual dimension) on specimens in small dimensions, which are typically defect-free. From the review of the state of the art about the destructive test on existing timber structures, it can be seen that the main focuses of the research are the mechanical characterization of the material and the evaluation of the global behaviour of the structural unit and its connections.

The mechanical characterization of the existing timbe members is generally performed on specimens in structural dimension or on small dimensions. These tests are generally carried out to evaluate the mechanical properties of different wood species in different anatomical directions and with reference to different stress states. Although there are experimental tests

conducted according to specific set-ups, UNI EN 408 [333] is the most used document for conducting tests on both new and ancient timber, since it defines test set-ups for the most common types of DTs, such as 4-point bending, compression, tensile, and shear tests. Often, these tests are preceded by visual strength grading analysis (VSG) and non-destructive investigations, in order to improve the relationships between these different types of tests. When referring to experimental tests on existing timber structures in the literature, we refer to tests on old, ancient, historical, or aged wood (or timber). A discussion about these terms as well as a huge critical review about experimental test performed on aged timber is carried out by Cavalli et al. [405]. The authors discussed the relevant primary research literature about the evaluation of mechanical properties of wood from different ages, summarising the current understanding of the problem and providing recommendations for future research. Although Cavalli et al. [405] emphasise the difficulty in providing solid comparisons due to the lack of standardization, they point out that mechanical properties in bending have been extensively investigated, and most research works agree that strength and stiffness in bending remain unchanged over time or decrease insignificantly. Indeed, most of the latest literature research about DT on ancient timber is focused on tests in bending. A comprehensive description of the bending tests carried out recently by several authors [406], [407], [408], [409], [410], [395], [411] is presented by Ruggieri [412], who beside focusing on the numerical results, also analyses the mechanisms of failure. A huge experimental campaign consisting in compression and bending test on ancient timber members made of Chestnut (*Castanaea sativa* Mill.) have been carried by Faggiano et al. [408], [410], [395]. Regarding the test in bending, a local modulus of elasticity in equal to 12.5 GPa and 14.0 GPa have been found for structural and small dimension samples respectively, whereas the bending strength have been seen equal to 41.1 MPa for structural dimension specimens and 39.7 MPa for small dimension specimens [395]. Ancient Chestnut wood have been also tested by Branco et al. [409] and Calderoni et al. [41] on a limited number of specimens in structural dimension, finding local elasticity modulus equal to 9.4 GPa and bending strength equal to 25.0 MPa [409] and 36.2 MPa [41].

In addition to the types of destructive testing seen so far, destructive testing also includes evaluating the impact of load duration on the mechanical properties of wood. As already seen, the duration of load (DOL) influences the performance of timber members both in the service state and in the ultimate condition (see Chapter 1, Section 1.3.2.2). As DOL increases, there is generally an increase in deformation and a reduction in strength. These

findings have been observed in experimental campaigns conducted since the mid-1990s aimed at evaluating and modelling creep (see Chapter 1, Section). As a result, standards have adopted simplified approaches to account for the effect of creep (see Chapter 1, Section 1.3.2.2). Nowadays, researchers' interest in wood creep is growing again because of the interest in understanding this effect on wood-based products in applications on high rise buildings and in innovative technological solutions [413], [414], [415].

a) b) c)

Figure 2.7. DT on specimens in different dimension: a) structural dimension (full-scale test; extracted from: [420]); b) actual dimension (extracted from: [417]); b) small dimension (specimen defect-free; extracted from: [417]).

Compared with laboratory testing, on-site test is less common, and few applications on timber structures are present at the state of the art [418], [419]. Instead, several authors performed full-scale test in laboratory [420], [421], [422], [423], [424], [177]. In their study, [420] examined a mid-19th century full-scale roof truss made of Silver fir (*Abies alba* Mill.). The objective was to calibrate and verify a numerical model that had been created to analyse timber structures under the influence of seismic forces. In order to identify suitable reinforcement methods, Branco et al. [424] examined the behaviour of two conventional kingpost trusses during a full-scale load-carrying test under symmetric and asymmetric loading. Barbari et al. [423] examined the mechanical behaviour of an original joint connection system between the top-chord and the tie beam by testing a full-scale prototype of a traditional timber truss. Before conducting full-scale load-bearing tests, two collar trusses were recently and thoroughly evaluated by Branco et al. [177] via visual inspection/grading and NDTs. Prior to testing the trusses in their current state of failure, they underwent testing once more after undergoing two different types of repairs.

Chapter

3

Vulnerability assessment of timber structures: proposal of survey forms for the seismic vulnerability and durability assessment

Abstract: The collection of general and metric information assumes significant importance in the assessment of existing structures for the purpose of territorial or detailed scale vulnerability assessment. In this task, survey forms can facilitate data collection and guide the surveyor to focus on crucial and critical aspects. However, they should be properly designed for a specific intent, being comprehensive in content, effective and efficient tools.

Therefore, three survey forms for the analysis of existing timber structures are proposed and discussed in this chapter. They differ in terms of contents and fields of application. The survey forms are firstly showed describing in detail each section, then the application to the case studies is discussed. Finally, the potential and criticalities of the survey forms are highlighted.

3.1 MOTIVATION AND GOALS

In the context of vulnerability analysis, adequate assessment of the structure is a fundamental prerequisite and indispensable step for understanding the individual criticalities and the behaviour of the structure. The reliability of the results of any structural analysis is therefore closely linked to the adequacy of knowledge of the structure, which is done through the collection of documentation, as well as the on-site inspection aimed at surveying and diagnosing the structure.

Among these activities, the collection of data concerning general, typological and technological aspects is a key aspect of the knowledge

process. Therefore, it is a common practice to use predefined survey forms for acquiring a set of information regarding different scope and contexts [310] Indeed, survey forms can facilitate data collection and ensure a more objective evaluation, even when several professionals are working, in addition, they can guide the surveyor in focusing on crucial and critical aspects for on-site assessment [310]. However, the form should be properly conceived. It should be designed to meet the assessment needs, considering the vulnerability analysis phenomenon, user purpose, and data usage. It should have an intuitive template, complete content, and focus on relevant data for assessment purposes. The form should be easy to fill in, time-saving, and suitable for data extrapolation, crucial for database creation and analysis.

The proposed survey forms are intended to serve two distinct contexts: seismic risk prevention and cultural heritage preservation. Each context has its own specific objectives, and these forms have been designed to meet the specific needs of each one.

The first contribution concerns the update of the Cartis form for the large span timber buildings (Cartis GL 3D). The form was born in the framework of the Italian project DPC–ReLUIS 2019-2021 for the development of activities related to the seismic prevention and protection of the built-up [262]. Indeed the form is designed to collect information related to the typological and structural characteristics of buildings and thus acquire information related to the exposure and vulnerability of buildings. The contribution to updating the section, starting with the version called "Rev. 09," resulted in a reorganization of most of the contents in order to achieve a more organic, simple and complete layout. The improvements facilitated the synthesis of information that was previously dispersed over multiple tables, resulting in a more condensed and informative form.

On the other hand the survey form for the Structural Health Assessment of existing Timber Structures (SHA-TS form) has been developed in the context of the seismic risk prevention of built-up structures, particularly in relation to timber structures. This form has been designed for the identification of structural types. Furthermore, the consideration of durability issues related to timber structures has been expanded to enhance the assessment of structural vulnerability in relation to the degradation factors. The main aim of the form is to support the researchers and the professional technician during the vulnerability assessment process of existing timber structures. In this respect, the form represents a practical tool for conducting on-site inspections. It guides users through a systematic process for gathering information about the construction type and technology, materials, and structural-health state of the

structure. Indeed, timber structures are particularly susceptible to decay, which can compromise their structural integrity. Therefore, the survey form includes specific sections, and a user's manual helps the users identify and diagnose various wood decay phenomena. Once the diagnosis is complete, the form and user manual offer practical guidance for illustrating and suggesting appropriate curative interventions. These recommendations are specifically adapted to the specific problems identified during the survey.

In a different context the IIWC form (Italian International Wood Committee form) has been designed. It serves the overarching aims and objectives of knowledge accumulation, education, and the enhancement of heritage timber structure conservation. The form has been developed within the framework of cooperation with the Italian national committee ICOMOS IIWC (Italian International Wood Committee; [311]), which mission is to promote the conservation, protection and sustainable management of the wooden built heritage [169]. In this framework the survey form acquires a twofold function: it is an operational tool for survey and diagnosis of the structures, as well as a support tool for the creation of a database from which an inventory of common ancient structural types and recurrent structural issues can be drawn. To this end, the form has been proposed in digital format as it enhances accessibility and versatility. Users can efficiently conduct surveys and diagnostics in the field using electronic devices, streamlining the process, improving data management, and facilitating easy sharing of findings within the community.

Thus, the SHA-TS has been primarily designed to cater to two main user groups: researchers and technicians involved in field of seismic vulnerability assessment. Researchers can utilize this form to gather valuable data on timber structures, aiding in their research efforts. It provides a structured and systematic approach to data collection. On the contrary, the technicians responsible for the maintenance, consolidation and strengthening of timber structures can benefit from the survey form's diagnostic capabilities and intervention recommendations. It helps them identify problems, make informed decisions and carry out the necessary measures to ensure the structural safety of timber buildings.

On the other hand, the IIWC form is intended for researchers and engineers working in the field of cultural heritage conservation. For researchers, the module is useful for data acquisition and sharing. Furthermore, consultation of the database enables knowledge of common types and structural issues. For professional technicians, the form is an operational tool for leading to the survey and diagnosis of valuable structures. Behind the dissemination of this

form there is also a didactic purpose, which is to inform less experienced technicians on how to approach the survey and diagnosis of this heritage.

A detailed descriptions of the forms (Cartis GL 3D, SHA-TS and IIWC) are provided below. These descriptions include the contents of the forms, instructions for their effective completion, and their practical application to noteworthy case studies. This comprehensive information is a useful resource for users who want an in-depth understanding of the forms and their relevance in real scenarios, offering insights into their potential impact and significance in various contexts.

3.2 IMPROVEMENT OF THE *CARTIS* FORM

3.2.1 DESCRIPTION

As part of the improvement of the Cartis large span buildings, the section 3D (large span timber buildings) has been updated, leading to the development of the version called "Rev. 10" The form has been reorganized and additional content has been included in order to achieve a more detailed and organic survey form.

The previous version of the form ("Rev. 09"), provided in Appendix A.1, had a total number of 12 tables, listed below:

- Structural grid parameters;
- Regular grid structure - Structural grid parameters;
- Non-regular grid structure – parameters;
- Vertical elevation structure and relationship to intermediate floors, vertical structure/seismic-resistant system, intermediate floors, type of wall bracing;

a. Classification of members - type of members;
b. Section of main members – columns, main beams;
c. Connections - connection type, materials, connectors, connector diameter, beam support length;
d. Horizontal bracing - bracing type, material, nx and ny braced spans, section area;
e. Horizontal bracing made with perforated tape;
f. Secondary beams restrained to end portals.

As a result of the revision work, the number of tables was reduced to 7; they are named as follows:

- Structural Grid Parameters;
a. Structural system;
b. Additional information on seismic-resistant systems;
c. Main structural members;
d. Bracing system;
e. Connections.

Each section of the updated form is described below, showing the critical issues found in the previous version (in red in the figures below) and highlighting the changes made (in yellow in the figures below).

Structural grid parameter

In the version "Rev.09", a general description of the timber structure is showed by means of two tables, the first providing identification of the main structural parameters, such as the number of n_x naves and n_y spans, the overall dimensions, such as the nave spacing L_x, the height of the columns H_c and the span spacing L_y; two other tables characterize the structure as either regular or non-regular grid (Figure 3.1).

The proposal is to keep the first table and merge the tables characterizing the regular and non-regular grid structure, preserving the corresponding schematic structural example (Figure 3.2).

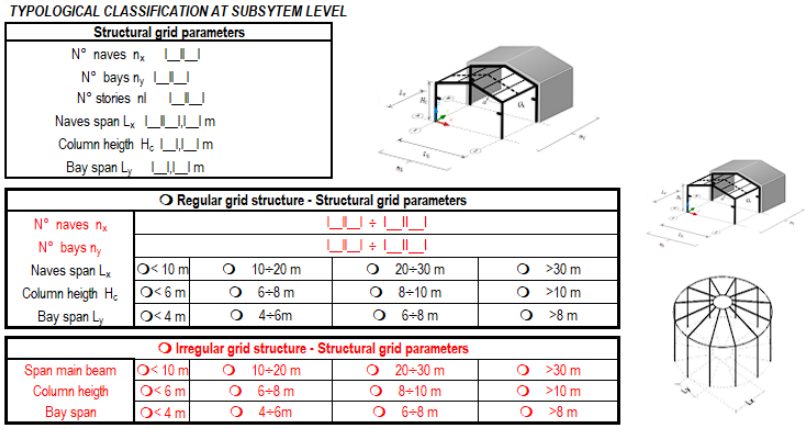

Figure 3.1. 3D Section CARTIS GL form: Structural grid parameters, regular and non-regular grid structure (rev. 09, ReLuis 2019-2021).

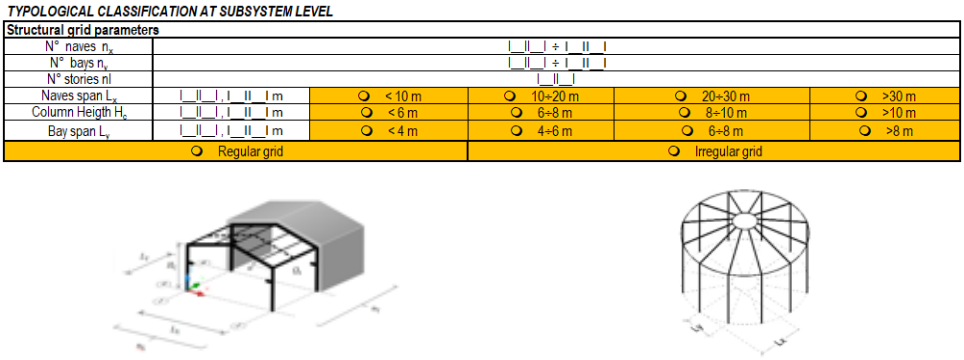

Figure 3.2. 3D Section CARTIS GL form: Structural grid parameters (proposal, Rev. 10).

a. Structural system

The version Rev. 09 illustrated the types of structural system, focusing on the seismic-resistant system (Figure 3.3).

In the proposed form, "structural system" is proposed instead of the title "seismic-resistant system" as the table deals with the identification of the structural system as a whole, regardless of the type of load (Figure 3.4).

Regarding vertical structures, the following structural types are given, which represent the generality of large span timber buildings: isolated columuns structures, heavy frame structures, wall structures and arched structures. Isolated columns correspond to the cantilever statical scheme, while heavy frame structures can be rigid node frames (MRF), or pinned frames (PF) with bracing, as well as wall structures can be solid panel, framed panel, or 3-D cell modules. Arch structures can be 2-hinged arches, 3-hinged arches, or fixed supported arches.

In this table, the fields for identifying the structural material have not been given, but only the type, referring the characterization of the geometry and material of individual members to subsequent tables. It is important to note that the type of selection is of the multichoice type (□), since several types can coexist in the same structure. As for intermediate floors, no changes are proposed.

b. Additional information on seismic-resistant systems

In the version Rev. 09, a further classification of the type of seismic-resistant structure is possible, whether hybrid or dual, with an indication of whether seismic devices are present (Figure 3.5.a). It should be noted that a

system is defined as hybrid if it is characterized by the coexistence in the same direction of seismic-resistant structures of different materials, for example, a heavy timber frame structure and a reinforced concrete wall; a system is defined as dual if it is characterized by the coexistence in the same direction of seismic-resistant structures of different types but of the same material. In both cases of hybrid system and dual system, seismic actions are distributed among the structures according to their lateral stiffness Anti-seismic devices referred to the possible presence of a dissipative devices, such as base isolators, dampers, etc.

1. Vertical structure and relationship with intermediate floors

Vertical structure / Intermediate floor	None	Seismic resitent system							
		Isolated column structures	Frame structures			Wall structures		
			Moment resisting frame (MRF)	Pinned frame (PF)	3 hinged arch	Coupled walls	Uncoupled walls	Modules or 3D cells
None	❍	❑	❑	❑	❑	❑	❑	❑
Not identified	❍	❑	❑	❑	❑	❑	❑	❑
In plane deformable floor	❑	❑	❑	❑	❑	❑	❑	❑
Rigid floor	❑	❑	❑	❑	❑	❑	❑	❑
	Without braces	With braces	Without braces	With braces				
	❍	❍	❍	❍				

Figure 3.3. 3D Section CARTIS GL form: Seismic-resistant system (Rev. 09, ReLuis 2019-2021).

a. Structural system										
Vertical structure / Intermediate floor		Isolated column structures	Frame structures		Wall structures			Arch structures		
			Moment resisting frames (MRF)	Pinned frames (PF)	Coupled walls	Uncoupled walls	Modules or 3D cells	2 hinged arch	3 hinged arch	fixed arch
None	❍	❑	❑	❑	❑	❑	❑	❑	❑	❑
Not identified	❍	❑	❑	❑	❑	❑	❑	❑	❑	❑
In plane deformable floor	❑	❑	❑	❑	❑	❑	❑	❑	❑	❑
Rigid floor	❑	With bracing system ❑	With bracing system ❑							
Bracing floor	❑									

Figure 3.4. 3D Section CARTIS GL form: Structural system (proposal, Rev. 10).

In the proposed tables (Figure 3.5.b) a title has been proposed and the multichoice type selection mode (□), for the purpose of generality, has been inserted, also introducing the percentage quantification in the case of earthquake-resistant devices (|__||__|%). In relation to the latter option, the percentage expresses the ratio between the number of spans equipped with dissipative device and the total number of seismic-resistant spans.

c. Main structural members

This table allows the characterization of structural members by identifying their type, cross-sectional geometry and material. The proposal has significant changes from the version Rev. 09 (Figure 3.6), however the approach is the same. Indeed, the same classification of the structural members (vertical, intermediate horizontal, and roofing) is proposed again. The novelty lies both in the introduction of the two classifications, referring to cross-section geometry and material, and in the elimination of the previous "Table b" (Main members Section). This last change is due to some critical issues in the table: only the indications related to columns and main beams is reductive as other structural system members (e.g. secondary beams, purlins, etc.) are left out; furthermore, the members were characterized with reference only to the dimensions "base" and "height", without any information about different types of cross sections.

Hybrid system	YES ❍	NO ❍
Dual system	YES ❍	NO ❍
Antisiesmic devices	YES ❍	NO ❍

a)

b. Additional information on seismic-resistant systems	
Hybrid system	❑
Dual system	❑
Antiseismic devices	❑ | | | %

b)

Figure 3.5. 3D Section CARTIS GL form: a) Hybrid-dual system and seismic device (Rev. 09, ReLuis 2019-2021); b) Additional information on seismic-resistant systems (proposal, Rev. 10).

a. Classification of members								
Member	Type of members							
	Linear	Single tapered	Double tapered	Tapered with arched bottom chord	Arch	Reticular	CLT	Other
Vertical	❍	❍	❍	❍	❍	❍	❍	
Horizontal Intermediate	❍	❍	❍	❍	❍	❍	❍	
Roof	❍	❍	❍	❍	❍	❍	❍	

Figure 3.6. 3D Section CARTIS GL form: Structural members (Rev. 09, ReLuis 2019-2021).

Thus, the proposed table is divided into four parts (Figure 3.7). The first part, corresponding to the first column, identifies the structural members, the second part characterizes the type (linear, reticular, single and double tapered, ribbed, arched, panel), the third part describes the geometry of the cross-section (squared, circular, coupled), and the fourth part defines the material, which can also be other than timber and its derivatives (glulam, solid timber, CLT, LVL, timber-based material, steel, reinforced concrete, etc.). Thus, also

the member made of material different from timber can be characterized (e.g., structure with reinforced concrete columns and wooden beams).

Regarding the dimensional characterization of the members, the introduction of additional fields useful for noting the main dimensions of structural elements has been proposed. In particular, for members with a square cross-section, the base and height of the cross-section are indicated, and for circular elements the diameter. The multichoice type with percentage (□||__||%) is given, since members with different shape, material and geometry can be generally found in the structure.

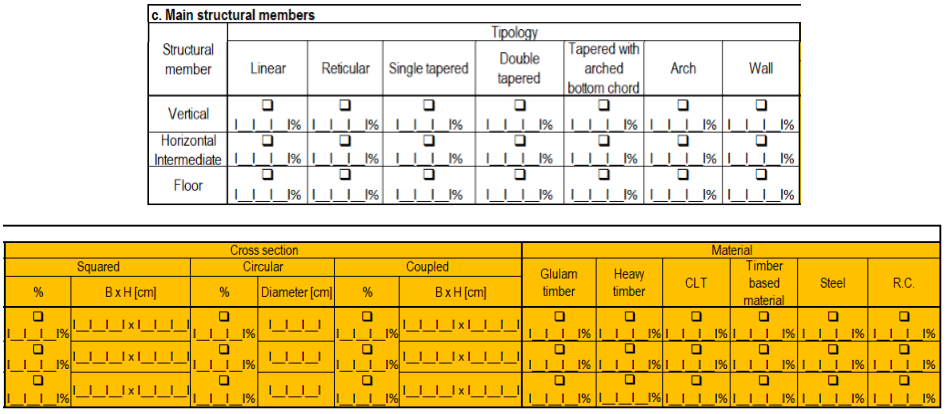

c. Main structural members

Structural member	Tipology						
	Linear	Reticular	Single tapered	Double tapered	Tapered with arched bottom chord	Arch	Wall
Vertical	☐ I_I_I_I%	☐ I_I_I_I%	☐ I_I_I_I%	☐ I_I_I_I%	☐ I_I_I_I%	☐ I_I_I_I%	☐ I_I_I_I%
Horizontal Intermediate	☐ I_I_I_I%	☐ I_I_I_I%	☐ I_I_I_I%	☐ I_I_I_I%	☐ I_I_I_I%	☐ I_I_I_I%	☐ I_I_I_I%
Floor	☐ I_I_I_I%	☐ I_I_I_I%	☐ I_I_I_I%	☐ I_I_I_I%	☐ I_I_I_I%	☐ I_I_I_I%	☐ I_I_I_I%

Cross section						Material					
Squared		Circular		Coupled		Glulam timber	Heavy timber	CLT	Timber based material	Steel	R.C.
%	B x H [cm]	%	Diameter [cm]	%	B x H [cm]						
☐ I_I_I_I%	I_I_I_I x I_I_I_I	☐ I_I_I_I%	I_I_I_I	☐ I_I_I_I%	I_I_I_I x I_I_I_I	☐ I_I_I_I%	☐ I_I_I_I%	☐ I_I_I_I%	☐ I_I_I_I%	☐ I_I_I_I%	☐ I_I_I_I%
☐ I_I_I_I%	I_I_I_I x I_I_I_I	☐ I_I_I_I%	I_I_I_I	☐ I_I_I_I%	I_I_I_I x I_I_I_I	☐ I_I_I_I%	☐ I_I_I_I%	☐ I_I_I_I%	☐ I_I_I_I%	☐ I_I_I_I%	☐ I_I_I_I%
☐ I_I_I_I%	I_I_I_I x I_I_I_I	☐ I_I_I_I%	I_I_I_I	☐ I_I_I_I%	I_I_I_I x I_I_I_I	☐ I_I_I_I%	☐ I_I_I_I%	☐ I_I_I_I%	☐ I_I_I_I%	☐ I_I_I_I%	☐ I_I_I_I%

Figure 3.7. 3D Section CARTIS GL form: Main structural members (proposal, Rev.10).

d. Bracing system

The characterisation of the vertical and horizontal seismic-resisting system (bracing system) assumes significant importance in the seismic vulnerability assessment of the structure. In the previous version (Rev. 09) two separate tables were intended to characterize the vertical and horizontal system (Figure 3.8). In the proposal, a single table (namely d. Bracing systems) has been conceived for characterizing both bracing systems (vertical and horizontal). For vertical systems the following systems have been indicated: rigid node frame, cantilever columns, single diagonal, concentric X, V, K bracing, eccentric bracing, walls. For horizontal systems can be choice: single diagonal, concentric X, V, K bracing, eccentric bracing, slabs, panels, spatial structures). The material (timber, steel, c. a.), the geometry of the cross-section (squared, circular, coupled, other), as well as the percentage of braced naves in x and y direction can be indicated.

Additional fields have been introduced to allow annotation of the main dimensions of the surveyed members. The selection mode is of the multiple-choice type with percentage (□||__||%) since, there may be a variable distribution of elements in the structure having different shape, material and geometry.

e. Connections

This table characterizes the connections between the members, indicating the type, the material and main dimensions of the possible fasteners. Moreover, the support length, a relevant geometric parameter for connections between overlapped members is given.

Type of vertical brace	
Concentric braces	❍
Concentric K braces	❍
Concentric V braces	❍
Eccentric braces	❍

d. Horizontal braces

Type of brace	Material			N° braced n_x naves [%]	N° braced n_y naves [%]	Cross-section area [cmq]
	Steel	Timber	R.C.			
Single diagonal	❑	❑	❑	I__II__II__I	I__II__II__I	I__II__II__I
S. Andrea Cross	❑	❑	❑	I__II__II__I	I__II__II__I	I__II__II__I
K	❑	❑	❑	I__II__II__I	I__II__II__I	I__II__II__I
Eccentric	❑	❑	❑	I__II__II__I	I__II__II__I	I__II__II__I
Slab	❑	❑	❑	I__II__II__I	I__II__II__I	I__II__II__I
Pannel	❑	❑	❑	I__II__II__I	I__II__II__I	I__II__II__I
Not necessary	❑	❑	❑	I__II__II__I	I__II__II__I	I__II__II__I

e. Horizontal bracing made with perforated tape	
YES ❍	NO ❍

f. Secondary beams restrained to end portals	
YES ❍	NO ❍

Figure 3.8. 3D Section CARTIS GL form: Bracing system (Rev. 09, ReLuis 2019-2021).

d. Bracing system

Typology		Material			Cross-Section							N° braced n_x naves [%]	N° braced n_y naves [%]
		Timber	Steel	R.C.	Squared		Circular		Coupled		Other		
					%	B x H [cm]	%	Diameter [cm	%	B x H [cm]			
Vertical system	Moment resisting frame (MRF)	❑	❑	❑	❑I_I_I_I%I_I_I_I x I_I_I_I		❑I_I_I_I%	I_I_I_I	❑I_I_I_I%	I_I_I_I x I_I_I_I	❑I I I I%	I_I_I_I	I_I_I_I
	Isolated column (cantilever)	❑	❑	❑	❑I_I_I_I%I_I_I_I x I_I_I_I		❑I_I_I_I%	I_I_I_I	❑I_I_I_I%	I_I_I_I x I_I_I_I	❑I I I I%	I_I_I_I	I_I_I_I
	Single diagonal	❑	❑	❑	❑I_I_I_I%I_I_I_I x I_I_I_I		❑I_I_I_I%	I_I_I_I	❑I_I_I_I%	I_I_I_I x I_I_I_I	❑I I I I%	I_I_I_I	I_I_I_I
	Concentric X braces	❑	❑	❑	❑I_I_I_I%I_I_I_I x I_I_I_I		❑I_I_I_I%	I_I_I_I	❑I_I_I_I%	I_I_I_I x I_I_I_I	❑I I I I%	I_I_I_I	I_I_I_I
	Concentric V braces	❑	❑	❑	❑I_I_I_I%I_I_I_I x I_I_I_I		❑I_I_I_I%	I_I_I_I	❑I_I_I_I%	I_I_I_I x I_I_I_I	❑I I I I%	I_I_I_I	I_I_I_I
	Concentric K braces	❑	❑	❑	❑I_I_I_I%I_I_I_I x I_I_I_I		❑I_I_I_I%	I_I_I_I	❑I_I_I_I%	I_I_I_I x I_I_I_I	❑I I I I%	I_I_I_I	I_I_I_I
	Eccentric braces	❑	❑	❑	❑I_I_I_I%I_I_I_I x I_I_I_I		❑I_I_I_I%	I_I_I_I	❑I_I_I_I%	I_I_I_I x I_I_I_I	❑I I I I%	I_I_I_I	I_I_I_I
	Walls	❑	❑	❑	❑I_I_I_I%I_I_I_I x I_I_I_I		❑I_I_I_I%	I_I_I_I	❑I_I_I_I%	I_I_I_I x I_I_I_I	❑I I I I%	I_I_I_I	I_I_I_I
Horziontal system	Single diagonal	❑	❑	❑	❑I_I_I_I%I_I_I_I x I_I_I_I		❑I_I_I_I%	I_I_I_I	❑I_I_I_I%	I_I_I_I x I_I_I_I	❑I I I I%	I_I_I_I	I_I_I_I
	Concentric X braces	❑	❑	❑	❑I_I_I_I%I_I_I_I x I_I_I_I		❑I_I_I_I%	I_I_I_I	❑I_I_I_I%	I_I_I_I x I_I_I_I	❑I I I I%	I_I_I_I	I_I_I_I
	Concentric V braces	❑	❑	❑	❑I_I_I_I%I_I_I_I x I_I_I_I		❑I_I_I_I%	I_I_I_I	❑I_I_I_I%	I_I_I_I x I_I_I_I	❑I I I I%	I_I_I_I	I_I_I_I
	Concentric K braces	❑	❑	❑	❑I_I_I_I%I_I_I_I x I_I_I_I		❑I_I_I_I%	I_I_I_I	❑I_I_I_I%	I_I_I_I x I_I_I_I	❑I I I I%	I_I_I_I	I_I_I_I
	Slab	❑	❑	❑	❑I_I_I_I%I_I_I_I x I_I_I_I		❑I_I_I_I%	I_I_I_I	❑I_I_I_I%	I_I_I_I x I_I_I_I	❑I I I I%	I_I_I_I	I_I_I_I
	Pannels	❑	❑	❑	❑I_I_I_I%I_I_I_I x I_I_I_I		❑I_I_I_I%	I_I_I_I	❑I_I_I_I%	I_I_I_I x I_I_I_I	❑I I I I%	I_I_I_I	I_I_I_I
	Spatial structure	❑	❑	❑	❑I_I_I_I%I_I_I_I x I_I_I_I		❑I_I_I_I%	I_I_I_I	❑I_I_I_I%	I_I_I_I x I_I_I_I	❑I I I I%	I_I_I_I	I_I_I_I

Figure 3.9. 3D Section CARTIS GL form: Bracing system (proposal, Rev.10).

c. Connection													
Type of connection		Materials			Connectors							Fasteners diameter [mm]	Beam support length [cm]
		Timber Timber	Timber Steel	Timber R.C.	Carpentry joint	Dowels	Bolts	Screws	Glue	Other	None		
1	Column/Wall - foundation	☐	☐	☐	☐	☐	☐	☐	☐	☐	☐	|_||_||_|	|_||_||_|
2	Beam - column/wall	☐	☐	☐	☐	☐	☐	☐	☐	☐	☐	|_||_||_|	|_||_||_|
3	Floor - beam	☐	☐	☐	☐	☐	☐	☐	☐	☐	☐	|_||_||_|	|_||_||_|
4	Roof - beam/roof - column	☐	☐	☐	☐	☐	☐	☐	☐	☐	☐	|_||_||_|	|_||_||_|
5	Column/wall -column/wall	☐	☐	☐	☐	☐	☐	☐	☐	☐	☐	|_||_||_|	|_||_||_|
6	Wall - structure	☐	☐	☐	☐	☐	☐	☐	☐	☐	☐	|_||_||_|	|_||_||_|
7	Vertical brace - column	☐	☐	☐	☐	☐	☐	☐	☐	☐	☐	|_||_||_|	|_||_||_|
8	Horizontal brace - beam	☐	☐	☐	☐	☐	☐	☐	☐	☐	☐	|_||_||_|	|_||_||_|

Figure 3.10. 3D Section CARTIS GL form: Connections (Rev. 09, ReLuis 2019-2021).

e. Connections									
Type of connection	**Materials**			**Cylinder fasteners**					
	Timber Timber	Timber Steel	Timber R.C.	Dowels		Bolts		Screws	
					Diameter [cm]		Diameter [cm]		Diameter [cm]
Column - foundation	☐	☐	☐	☐	|_|_|_|	☐	|_|_|_|	☐	|_|_|_|
Column/Wall - beam	☐	☐	☐	☐	|_|_|_|	☐	|_|_|_|	☐	|_|_|_|
Column/Wall - intermediate floor	☐	☐	☐	☐	|_|_|_|	☐	|_|_|_|	☐	|_|_|_|
Column/Wall - roof	☐	☐	☐	☐	|_|_|_|	☐	|_|_|_|	☐	|_|_|_|
Column - wall	☐	☐	☐	☐	|_|_|_|	☐	|_|_|_|	☐	|_|_|_|
Intermediate floor - purlin/main beam/secondary beam	☐	☐	☐	☐	|_|_|_|	☐	|_|_|_|	☐	|_|_|_|
Main beam - secondary beam	☐	☐	☐	☐	|_|_|_|	☐	|_|_|_|	☐	|_|_|_|
Purlin - secondary beam	☐	☐	☐	☐	|_|_|_|	☐	|_|_|_|	☐	|_|_|_|
Vertical brace - column	☐	☐	☐	☐	|_|_|_|	☐	|_|_|_|	☐	|_|_|_|
Horizontal brace - beam	☐	☐	☐	☐	|_|_|_|	☐	|_|_|_|	☐	|_|_|_|

Plates								**Other**			**Support legnth [cm]**
Plate		Toothed plate		Hold down		Angular plate		Carpentry joint	Glue	Other	
	Thickness [cm]		Thickness [cm]		Thickness [cm]		Thickness [cm]				
☐	|_|_|_|	☐	|_|_|_|	☐	|_|_|_|	☐	|_|_|_|	☐	☐	☐	|_||_||_|
☐	|_|_|_|	☐	|_|_|_|	☐	|_|_|_|	☐	|_|_|_|	☐	☐	☐	|_||_||_|
☐	|_|_|_|	☐	|_|_|_|	☐	|_|_|_|	☐	|_|_|_|	☐	☐	☐	|_||_||_|
☐	|_|_|_|	☐	|_|_|_|	☐	|_|_|_|	☐	|_|_|_|	☐	☐	☐	|_||_||_|
☐	|_|_|_|	☐	|_|_|_|	☐	|_|_|_|	☐	|_|_|_|	☐	☐	☐	|_||_||_|
☐	|_|_|_|	☐	|_|_|_|	☐	|_|_|_|	☐	|_|_|_|	☐	☐	☐	|_||_||_|
☐	|_|_|_|	☐	|_|_|_|	☐	|_|_|_|	☐	|_|_|_|	☐	☐	☐	|_||_||_|
☐	|_|_|_|	☐	|_|_|_|	☐	|_|_|_|	☐	|_|_|_|	☐	☐	☐	|_||_||_|
☐	|_|_|_|	☐	|_|_|_|	☐	|_|_|_|	☐	|_|_|_|	☐	☐	☐	|_||_||_|
☐	|_|_|_|	☐	|_|_|_|	☐	|_|_|_|	☐	|_|_|_|	☐	☐	☐	|_||_||_|

Figure 3.11. 3D Section CARTIS GL form: Connections (proposal, Rev.10).

The full version of the 3D section of the CARTIS GL version “Rev. 10” can be found in Appendix A.2.

3.2.2 APPLICATION TO THE CASE STUDIES OF LARGE SPANTIMBER STRUCTURES

A sample of 10 large span timber buildings placed in Northern Italy has been selected for applying the proposed survey form [262]. The buildings are close to the epicentres of the last three main earthquakes that occurred in Italy: Abruzzo 2009, Emilia 2012 and central Italy 2016 (Figure 3.12). The sample consists of buildings built between 1981 and 2014, having different intended use, public and private (Figure 3.13). The following 10 buildings have been studied (extrapolated from: [262]:

1. Bentivoglio—Shopping center (B-Sc);
2. Bentivoglio—Agricultural building (B-Ab);
3. Castello d'Argile—Industrial building (CA-Ib);
4. Correggio—Canteen of the Marconi state secondary school (C-Cs);
5. Correggio—School gym of the Luigi Einaudi Technical Institute (C-Gs);
6. Correggio—S. Francesco di Assisi State Primary School (C-S);
7. Correggio—Supermarket (C-Sm);
8. Crevalcore—Laboratory (C-L);
9. Galliera—Polisportiva gym (G-G);
10. San Giovanni in Persiceto—Mezzacasa secondary school gym (GP-Gs).

The proposed form (Cartis form GL 3D "Rev. 10") has been tested on these buildings to assess the form effectiveness and efficiency. The case studies have not been surveyed in on-site assessment, but thanks to the available documentation [262], the forms have been filled out remotely. However, due to the lack of information, only the table form "a" (structural system), "b" (additional information on seismic resistant systems), "c" (main structural members) and "d" (bracing systems) have been analysed.

Starting from the table "Structural grid parameter" it can be seen that most of the buildings have a single nave, while the case study B.Sc and C.Sm have 4 and 3 naves, respectively. Even though the buildings have variable number of spans, most of the buildings have 6 and 4 spans (6 out of 10). Except for case study B.Ab which has 9 spans, the rest of the buildings have a lower number of spans. Most of the buildings have rectangular floor plans with a maximum nave length between 10 and 30 meters, however, the C.Gs building exceeds 30 meters. Span length range from 4 to 6 meters, while the B.Sc, C.Sm and C.G buildings have spans length exceeding 8 meters. In the end, it

has been seen that the column height of most of the buildings (6 out 10) is lower than 6 meters, while for 4 buildings it range from 6 to 8 meters.

Figure 3.12. The sample of 10 large span timber buildings [262].

a) b)

Figure 3.13. Case study: a) 2. B.Ab [262]; b) 6. C.S [425].

The 10 buildings showed different types of structural systems, which has been characterized in the table "a". Among the buildings the most common structural system (5 out of 10 buildings) is the isolated columns system, i.e., cantilever static scheme. At the same time 2 buildings have a system with rigid node, i.e., moment resisting frame (MRF), while 4 buildings have load-bearing walls. No hybrid or dual systems have been identified for any buildings, just as no earthquake-resistant systems were found. As regard the storeys of the structural system it has been noted that only the building B.Sc has two storeys (intermediate floor and roof), while the remaining buildings have just one storey (roof).

As concern the main structural members, it has not been possible to fully describe the geometry, size, and material of the members; however, limited information has been collected, such as the member material. Indeed, it has been seen that all buildings have a roof with timber members, and the B.Sc building also has an intermediate floor made of timber. Except for the Gp.GS building, which has timber columns, most of the buildings have vertical R.C. members. The B.Sc building has both R.C. and steel vertical members. All buildings have sloping roofs; instead, the Gp.Gs and B.Sc buildings have flat roofs. At the same time, most of the buildings have beams with variable cross sections, except for buildings B.Sc., C.Sm and Gp.Gs, where beams with constant cross sections have been found.

In 6 out 10 building the concentric braces have been noted in the vertical bracing system. Among them, steel "X braces" have been found in 3 buildings, while the single timber diagonal have been used in 2 buildings and steel "V braces" have been identified in 1 building. The distribution of the bracing systems in the longitudinal and transverse directions is variable. In the transverse direction, five out of six buildings (83%) have braces on 100% of the length and one out of six buildings (17%) has braces on 60% of the length; in the longitudinal direction, one out of six buildings (17%) has braces on 100% of the length, one out of six buildings (17%) has braces on 80% of the length, one out of six buildings (17%) has braces on 70% of the length, and three out of six buildings (50%) have braces on 30% of the length (extrapolated from Faggiano et al., 2021). The remaining 6 buildings have vertical seismic-resistant structures characterised by walls (4 out of 6 buildings) and moment-resistant frames (MRF). In the end, the horizontal bracing system has been analysed, and it has been found that 7 out of 10 buildings have a bracing system; however, the geometrical and technological features have not been identified.

3.3 THE SHA-TS FORM

3.3.1 DESCRIPTION

The framework of the proposed form (SHA-TS – Structural Health Assessment of Timber Structures) is based on the Cartis form, for the seismic vulnerability assessment of timber large span structures [262]. Thus, the form is conceived through a top-down approach, going from the localization and

description of the building to the structural member characterization. The template is articulated in three main parts, corresponding to the following issues: building identification, timber decay detection, treatments/interventions (extrapolated from: [426]). The form contains seven sections (Table 1) dealing with the description of the building in terms of location and general future (section A and C), identification of the construction technology and typology, as well as characterization of the structural members (section D). The Section D should be filled for a single structural member, whose state of degradation is characterized in the subsequent section. Based on the state of art, the following section described the main effects of wood degradation (section E), from which the relevant phenomenon can be recognized (section F). In this diagnostic process the form-user is guided by a user manual conceived ad hoc. In the end the last section (section G) provide a list of possible measures for interventions and treatment for removing the effects of decay and fixing the relative causes. However, a more in-depth assessment of the state of conservation of the structure, also using non-destructive techniques, is mandatory for the design of an effective intervention. The following describes the sections of the form that are fully shown in Appendix B.1.

The Section A (Municipality and Building Identification) collects general information on the location of the building, the identification of the form user and any local technicians interviewed, as well as the information on the type of data available to the form filler. The above-mentioned parts of section A are made up of editable fields in text, numeric, multi-choice (❑) and single-choice (❍) modes.

Table 3.1. Outline of the SHA-TS survey form.

Scope	Section	Description
Building analysis	A	Identification of loca and building
	B	Identification of the building construction technology and structural typology
	C	Description of the building
Timber decay detection	D	Characterization of the structural members
	E	Decay effects identification
	F	Decay typology
Interventions and treatments	G	Possible interventions and treatments

The Section B of the form (Identification of the building construction technology and typology) is divided into further progressively numbered subsections B1 to B6. Sections B1, B2 and B3 contain information on the

classification of the structural system, while sections B4 and B5 aim at the structural characterisation of the intermediate floors and the roof system respectively. Finally, section B6 is aimed at the characterisation of the foundations. In section B1 the information necessary for the characterisation of the structural system are collected, identifying the construction material of the different building elements that make up the structure (Figure 3.14). Section B2 allows the characterisation of the structural typology through the selection of the most common types for timber structures (Figure 3.14). Furthermore, the intermediate floor is characterised in terms of in-plane stiffness, distinguishing between rigid and deformable floors. Finally, in section B3 the bracing system is defined, indicating its type, material and distribution along the main directions of the building (Figure 3.14).

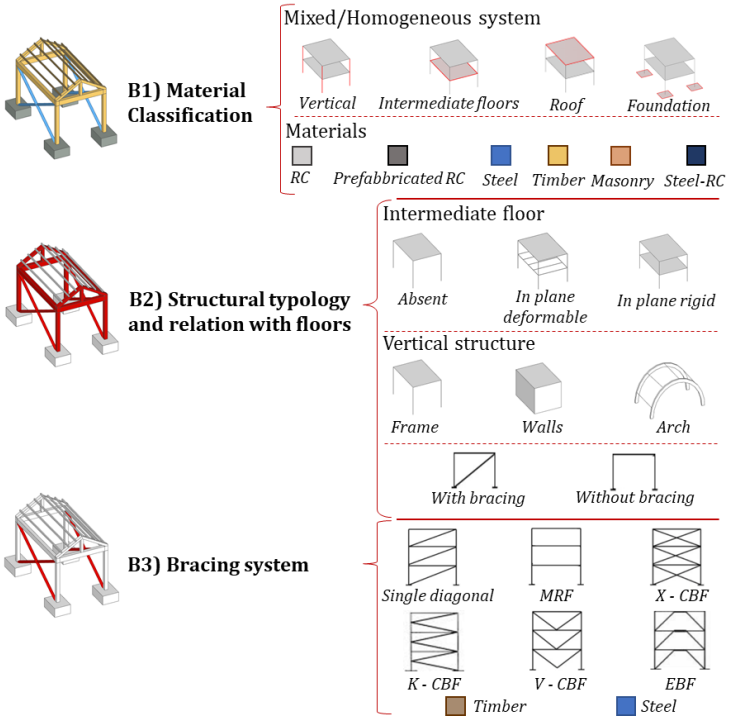

Figure 3.14. Section B of SHA-TS form (B1: Material classification; B2: Structural typology and relation with floors; B3: Bracing system).

The Section B4 allows the structural characterisation of intermediate floors; through subsections arranged according to an alphabetical index. The

section B4.A identifies the deformative characteristics in the plane of the floor deck (rigid/deformable floor). Section B4.B indicates the possible presence of bracing, pushing elements or chains and the type of single- or double-way structural system. Subsequently, it is possible to characterise the members constituting the single-way system by describing the geometric characteristics of the cross-section of the main members (B4.C) and of the secondary members (B4.D). Finally, section B4.E allows the description of the two-way system by selecting the type of plate or shell and the cross-section.

The Section B5 refers to the roof structure and it has a similar layout to section B4 (Figure 3.15). Thus, sections B5.A and B5.B identify the in-plane deformative behaviour of the roof. Furthermore, the presence of any possible bracing system, pushing elements or chains, as well as the type of structural system (single way or double way) can be selected. Additional information concerns the number of roof orders. With regard to the single-way structural system, described in section B5.C, a distinction is made between horizontal, pitched (single/double) and curved roofs. The same distinction is used for double-way systems, however a distinction is made between the curved single-way system and the curved double-way system (B5.F). For single-way structural systems, the cross-section geometry of the main and secondary members is characterised in Sections B5.D and B5.E respectively. For two-way structural systems in Section B5.G, the plate/shell type and the cross-section geometry of the members are described. In section B5.H, the roof closing members are characterised. Section B6 concludes with a description of the foundation structures, identifying the type of foundations and the information source (Figure 3.15).

The section C (Description of the building) describes the general features of the whole building: main geometric and metric characteristics, such as the number of storeys, average height and average floor area (C1), the age of the building (C2), as well as the destination and utilisation of the building (C3). In the end a box for inserting significant graphics and images (C4) of the building is provided.

The section D (Characterization of the structural members), as well as the section E, are filled for a single structural member, since the member is firstly characterized in terms of technology and then with regard to the state of conservation. In Section D, it is possible to identify the type of member (D1), the material in terms of wood product (D2) and wood species (D3), the year in which the element was placed (D4), and the member location (SD5). Concerning the exposure to the decay factors, the risk classes [79] and

durability classes [350] are identified in sections D6 and D8, respectively. In Section D7, the average environmental temperature is reported. This could be useful information for catching the possible biological decay phenomena affecting the members.

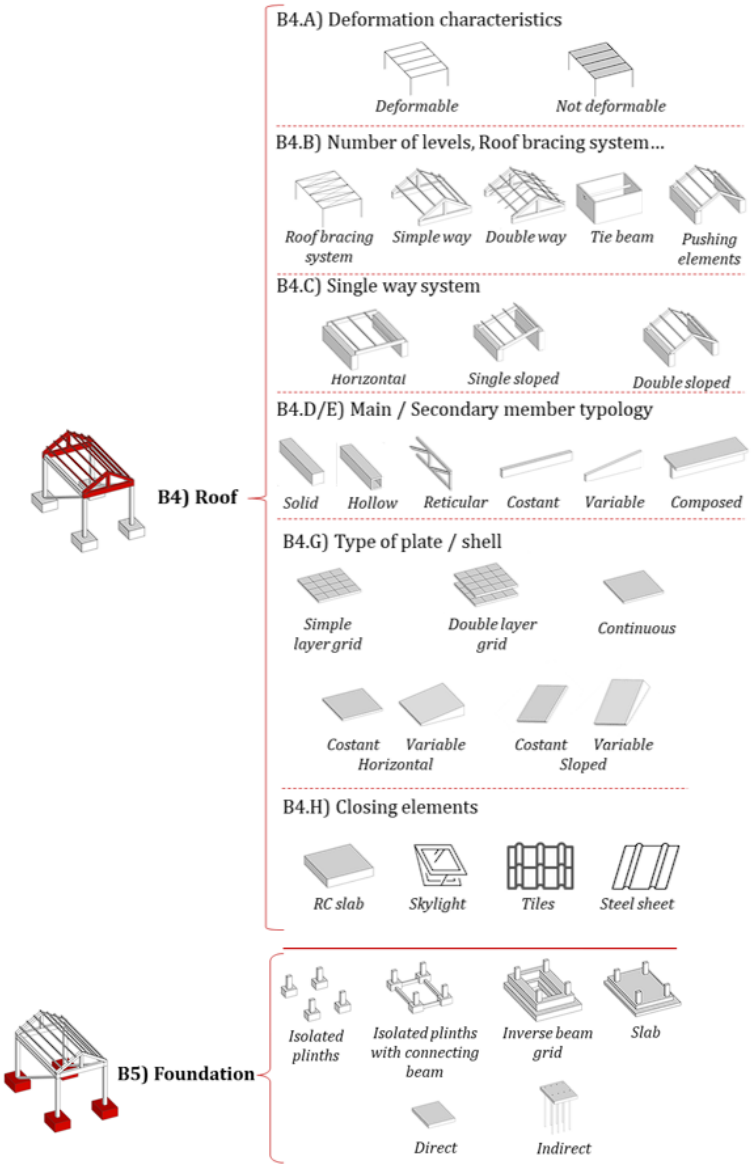

Figure 3.15. Section B of SHA-TS form (B4: Roof; B5: Foundation).

The Section E (Decay effects identification; Figure 3.16) is completely devoted to the characterisation of the state of conservation the members starting from the recognition of the effects (Figure 3.17). It contains a list of characteristic aspects of the main forms of degradation recognized in the state of the art, such as the color of the decayed area (E1), the appearance to the touch (E2), and the surface appearance (E3; Figure 3.17). A further description of the decay effect is provided in sections E4, E5, and E6. The presence of cracks, holes, and galleries can be remarked in these sections, providing indications about the geometry and dimensions (Figure 3.17). In section E8 it is possible to indicate the extent of the decayed zone, its location in relation to the member and the techniques used to identify these parameters. In section E9 other aspects leading to the diagnosis of the degradation phenomenon are indicated, such as the presence of insects, wood residues, mould. The presence of superficial or deep treatments (E10), as well as the moisture content, can be identified at the end.

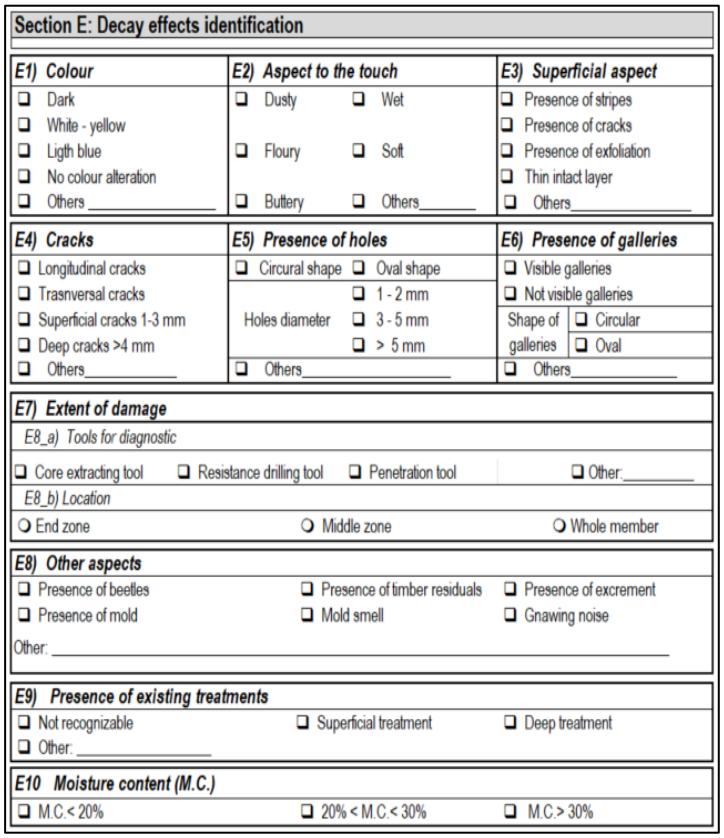

Section E: Decay effects identification

E1) Colour	***E2) Aspect to the touch***	***E3) Superficial aspect***
❑ Dark	❑ Dusty ❑ Wet	❑ Presence of stripes
❑ White - yellow		❑ Presence of cracks
❑ Ligth blue	❑ Floury ❑ Soft	❑ Presence of exfoliation
❑ No colour alteration		❑ Thin intact layer
❑ Others _____	❑ Buttery ❑ Others_____	❑ Others_____

E4) Cracks	***E5) Presence of holes***	***E6) Presence of galleries***
❑ Longitudinal cracks	❑ Circural shape ❑ Oval shape	❑ Visible galleries
❑ Trasnversal cracks	❑ 1 - 2 mm	❑ Not visible galleries
❑ Superficial cracks 1-3 mm	Holes diameter ❑ 3 - 5 mm	Shape of ❑ Circular
❑ Deep cracks >4 mm	❑ > 5 mm	galleries ❑ Oval
❑ Others_____	❑ Others_____	❑ Others_____

E7) Extent of damage

E8_a) Tools for diagnostic

❑ Core extracting tool ❑ Resistance drilling tool ❑ Penetration tool ❑ Other:_____

E8_b) Location

❍ End zone ❍ Middle zone ❍ Whole member

E8) Other aspects

❑ Presence of beetles ❑ Presence of timber residuals ❑ Presence of excrement
❑ Presence of mold ❑ Mold smell ❑ Gnawing noise

Other: _____

E9) Presence of existing treatments

❑ Not recognizable ❑ Superficial treatment ❑ Deep treatment
❑ Other: _____

E10 Moisture content (M.C.)

❑ M.C.< 20% ❑ 20% < M.C.< 30% ❑ M.C.> 30%

Figure 3.16. Extract from the SHA-TS form: Section E – Decay effect identification.

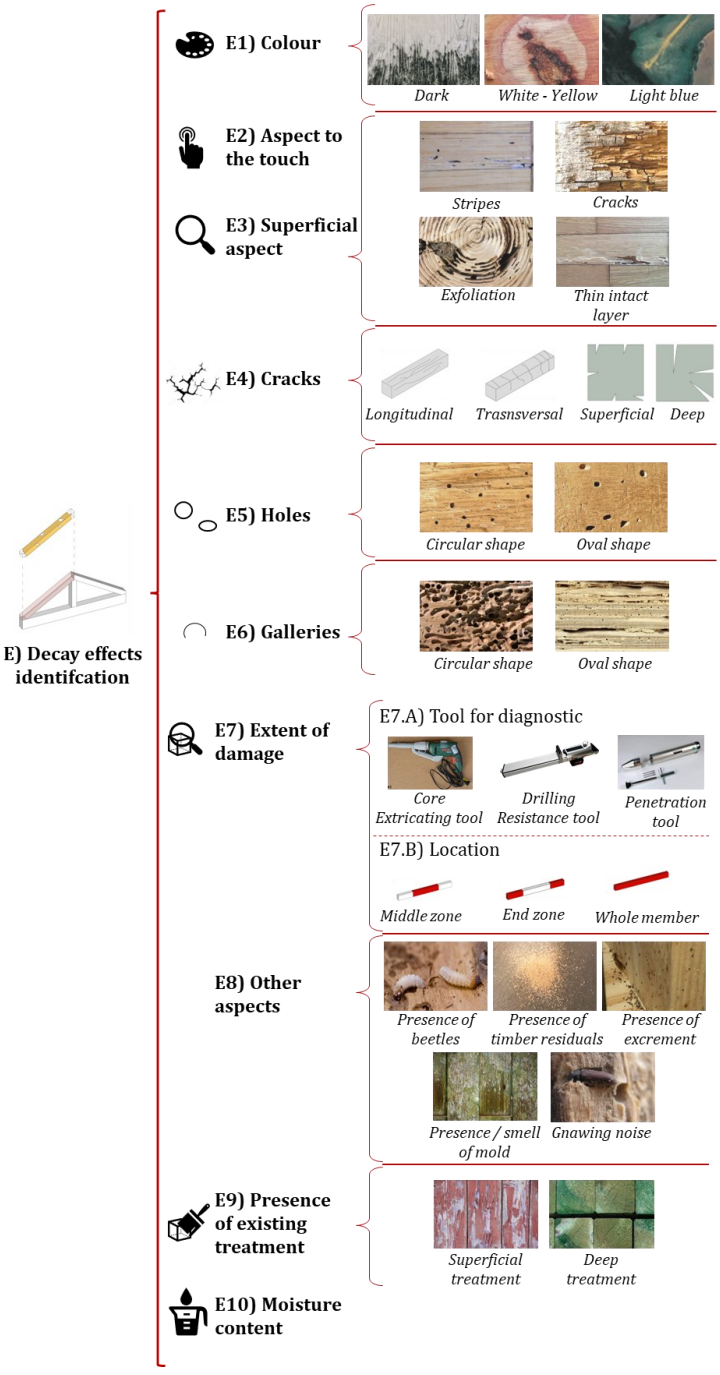

Figure 3.17. Section E of SHA-TS form (Decay effects identification).

Once the effects of degradation have been identified, the degradation phenomenon related to these effects can be selected in section F (Decay typology). This section is divided into two main parts concerning respectively biotic agents of degradation (F1) and abiotic one (F2), indicating the most common types. In the process of recognising the type of decay (through section E and F), the form user is supported by a user manual (Appendix B.2). The manual consists of forms illustrated by pictures and textual information. Each form refers to a single degradation phenomenon, listed by the causative agents (Figure 3.18)

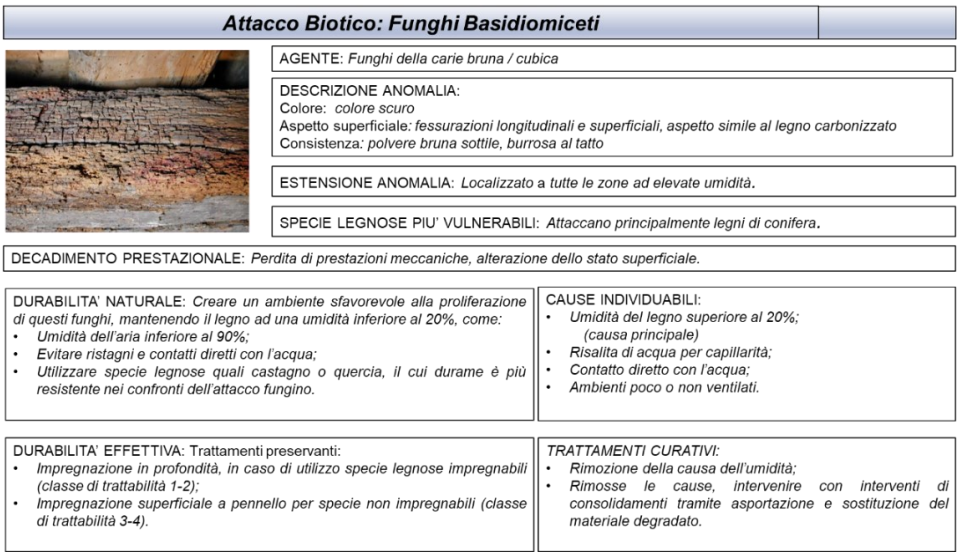

Attacco Biotico: Funghi Basidiomiceti

AGENTE: *Funghi della carie bruna / cubica*

DESCRIZIONE ANOMALIA:
Colore: *colore scuro*
Aspetto superficiale: *fessurazioni longitudinali e superficiali, aspetto simile al legno carbonizzato*
Consistenza: *polvere bruna sottile, burrosa al tatto*

ESTENSIONE ANOMALIA: *Localizzato a tutte le zone ad elevate umidità.*

SPECIE LEGNOSE PIU' VULNERABILI: *Attaccano principalmente legni di conifera.*

DECADIMENTO PRESTAZIONALE: *Perdita di prestazioni meccaniche, alterazione dello stato superficiale.*

DURABILITA' NATURALE: *Creare un ambiente sfavorevole alla proliferazione di questi funghi, mantenendo il legno ad una umidità inferiore al 20%, come:*
- *Umidità dell'aria inferiore al 90%;*
- *Evitare ristagni e contatti diretti con l'acqua;*
- *Utilizzare specie legnose quali castagno o quercia, il cui durame è più resistente nei confronti dell'attacco fungino.*

CAUSE INDIVIDUABILI:
- *Umidità del legno superiore al 20%; (causa principale)*
- *Risalita di acqua per capillarità;*
- *Contatto diretto con l'acqua;*
- *Ambienti poco o non ventilati.*

DURABILITA' EFFETTIVA: Trattamenti preservanti:
- *Impregnazione in profondità, in caso di utilizzo specie legnose impregnabili (classe di trattabilità 1-2);*
- *Impregnazione superficiale a pennello per specie non impregnabili (classe di trattabilità 3-4).*

TRATTAMENTI CURATIVI:
- *Rimozione della causa dell'umidità;*
- *Rimosse le cause, intervenire con interventi di consolidamenti tramite asportazione e sostituzione del materiale degradato.*

Figure 3.18. Extract from the user's manual supporting the survey form (form related to decay by *brown-rot fungi*).

Thus 7 forms have been made for the user manual, relating to degradation from fungi (brown-rot, soft-rot, white-rot) and insects (*Cerambycidae* Latreille, *Anobium* and *Lictus* Fabbricius). In each form the description of the effects visible on the member surface and detectable by touch, as well as the extent of degradation, are given. In addition, the most vulnerable wood species and the consequences in terms of performance decay are indicated in each form. Finally, the possible causes of the phenomenon and their remedies are identified. The section G (Interventions and treatments) ends the survey form with a list of possible interventions and curative treatments, selected according to the degradation phenomenon recognised. The section is divided

into two parts: in the section G1 the procedure for the removal of the cause and effects of degradation are indicated, while in section G2 the main protective treatments are listed. In this way, the user-form is supported in the recognition phase of the degradation phenomenon and in the planning phase of curative interventions.

3.3.2 APPLICATION TO THE CASE STUDIES OF TYPICAL EXISTING TIMBER STRUCTURES

The survey form has been applied to four case studies located in different areas of the Campania region (Southern Italy). The case studies “a” and “b” are in Gioia Sannitica, a municipality in Benevento province. The first one is a recently renovated building used as a public washhouse, and it consists of a timber roof characterised by glulam beams placed on reinforced concrete columns (Figure 3.19.a). Even the case study "b" is a public building, and it is entirely made of timber with a glulam frame structure partially enclosed by timber walls made of boards (Figure 3.19.b). On the other hand, the case studies “c” and “d” are placed in the centre of Naples, and they consist of historical buildings characterised by intermediate floors and roofs mainly made of timber (Figure 3.19.c-d). To assess the reliability and adaptability of the survey form, these case studies have been chosen to be representative of recurring building types, structural types and deterioration phenomena.

a) b) c) d)

Figure 3.19. The case studies: a) Public wash-house in Gioia Sannitica, Benevento; b) public kiosk in Gioia Sannitica, Benevento; c) residential building in Naples; d) Palazzo Petrucci in Naples [427].

It is important to note that the survey form sections A, B, and C have been filled out for all case studies, while the sections from D to G have only been completed for selected structural members. For the case studies “a” and “b”, the roof beam and column structure have been selected, respectively, whereas a beam of the intermediate floor and a rafter of the roofing trusses have been

chosen for cases “c” and "d." The compilation of the survey forms applied to all case studies is attached in Appendix B.3, while the application to case study “d” is shown herein.

The compilation of the form took place in situ, at the same time as the visual inspection of the timber structures. The case study “d”, namely Palazzo Caracciolo, is a prestigious building located in the historical centre of Naples (Figure 3.20.a). The building has masonry walls, as a vertical structural system, with the roof characterised by ancient timber trusses (section B1), with an average span of approximately 10 m (Figure 3.20.b-c). The intermediate floors and foundations were not identified as they were not inspected.

a) b) c)

Figure 3.20. Case study d (Palazzo Caracciolo): a) view of the building; b) the roof timber structures; c) the rafter-tie beam joint.

The roof consists of a single way system with secondary beams supported by main trusses. Thus, the main structural system is the truss showed in Figure 3.20.b. The roof structure is deformable in the plane, as it does not have a bracing system (section B5.a). In addition, it has been found the widespread presence of chains, even in correspondence with the roof slab. Both the main and secondary members of the structure have a single cross-section with a quite constant geometry. The closing elements of the roof are made of tiles. The building has four storeys, with an average height ranging from 3.5 m to 5 m. It is used for public utility activities (section C). The analysis of the state of conservation (sections D-G) concerned a timber truss located at the roof level. In detail, the struts and the tie-beams have been surveyed. Both are made of ancient timber, however the wood species has not been recognised. From the historical documentation, it has been determined that the truss dates back from the half of the XX century. Given the environmental condition where the structure is placed, the environmental risk class 2 (EN 335) has

been assigned to the surveyed members. Both struts and tie-beams showed the same type of decay (section E), consisting in degradation by insect attack. This phenomenon was recognized by the widespread presence of flickering holes characterized by oval shape, as well as by the timber surface signed stripes and exfoliation signs. From the decay effects the degradation phenomenon has been recognized thanks to the manual user. The whole structure was affected by the deterioration, which can be traced back to *Cerambycidea* and *Anobium* insect attack. This was probably caused by the presence of sapwood within the members. Subsequently, possible measure of interventions to remove the decay and preserve from further insect attacks have been identified through the user manual. It consisted in the surface cleaning and the subsequent application of biocide-type surface treatments.

3.4 THE IIWC FORM

3.4.1 DESCRIPTION

The survey form is organised in 5 macro-sections that progressively lead the user from the identification and description of the building to the survey and diagnosis of the structural member. The building analysis is conducted by gradually breaking down the building and structure into all its parts using a top-down approach. In this view, the building is considered as a set of several building components (BC) (e.g. the intermediate floor, the roof slab, the walls ec). In each building component, there can be more than one structural unit (StU). For example, a roof (BC) can be made up of several trusses (StU). Continuing the analysis from top to bottom, it is assumed that the structural unit is composed of several structural members (StM) and structural nodes (StN) (e.g. the truss is generally composed of struts, tie-beam, rafters and their relative nodes; Figure 3.21).

The form transposes this breakdown of the building through the organisation into sections and subsections (Table 3.2). The sections are aimed at the identification of the building (section 1), the description of the general and metric aspects (section 2), and the identification of the building components (BC) and structural units (StU; section 3). Section 4 (survey) is aimed at the typological and technological characterization of the StU and its components. Therefore, the structural unit is identified in Section 4.1, and then the structural elements (StM; Section 4.2) and structural nodes (StN;

Section 4.3) are characterised. The same procedure is provided for Section 5, devoted to the structural diagnosis of the StU (Section 5.1) and the StMs (Section 5.2).

From an operational point of view, the survey form in Microsoft Excel is organised into forms corresponding to the sections form. The forms can be repeated for the same section, as in the case of section 4 (survey) and 5 (diagnosis), for which the number of forms will be a function of the number of StUs, StMs and StNs to be surveyed or diagnosed. All the section of the survey forms are showed in the Appendix C.1. The form can be filled out on a computer or mobile device (such as a smartphone or tablet) using applications that can manage the ".xlsx" extension. Each section of the form is completed by manually entering numeric and textual data in the designated fields. However, some fields require the selection of an option from a predefined list. A detailed description of the section is reported in the following.

In Section 1 (Building identification), general information regarding the form is given, i.e., the ID, date of compilation, as well as data for the location of the building (e.g., city, address, building owner). In addition, the presence of any architectural and historical constraints to which the building is subject can be noted.

Section 2 (Building description) shows general information (e.g. intended use and utilisation) and metric information about the building, such as the number and height of floors. Images and graphic documentation can be inserted in the appropriate boxes.

The identification of building components (BC) and structural units (StU) is carried out in Section 3 (Identification of building components and structural units). The identification of these parts is carried out by means of summary tables, in which each BC and StU is required to be identified by a code. The tables are repeated according to the number of building elements in the building.

The information in Section 4.1 (Survey of the structural unit) is related to the survey of each StU. The section is divided into multiple tables. In the first, the structural unit is described by identifying the construction period and describing any previous works. In the following tables, the structural members and their corresponding IDs are listed. The same applies to structural nodes, with the addition of technological information such as the node's type of construction and the presence of metal or wood connectors. In addition, there are spaces for photographs and graphic documentation.

The purpose of this section (section 4.2; Survey of the structural member) is to characterize each StM. In the first part of the form, the StM is identified, followed by information on the timber species and the member's age, and then the principal geometric and dimensional characteristics are outlined (Figure 3.22). Finally, the wood-workings and surface treatments are described. The section is completed with a box for photographic documentation.

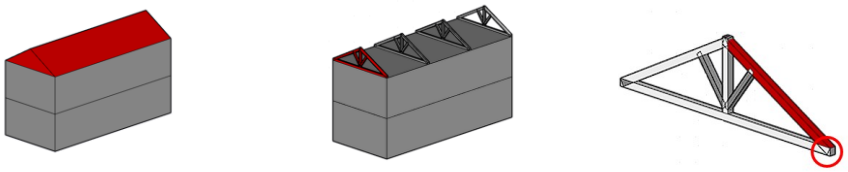

a) b) c)

Figure 3.21. Structure breakdown from building to the members: a) the building component (BC) in red (roof structures); b) the structural unit (StU) in red (truss); c) the structural member (StM) in red (the rafter) and the structural node (StN) circled in red (the rafter-tie beam node).

Table 3.2. Outline of the IIWC survey form.

Scope	Section	Description
Building analysis	1	Building identification
	2	Building description
	3	Identification of the building components and structural units
Typological and technological survey	4	Survey
	4.1	*Survey of the structural unit*
	4.2	*Survey of the structural member*
	4.3	*Survey of the structural nodes*
Assessment of the state of conservation	5	Diagonsis
	5.1	*Diagnosis of the structural unit*
	5.2	*Diagnosis of the structural member*

Section 4.3 (Survey of the Structural Node) is intended for the characterization of each StN part of the StU. The section contains useful information for the identification of the node, as well as a typological classification and general description of it. Finally, any metal or wooden means that make up the node are identified. The section is completed with a box for inserting the graphic documentation.

Section 5.1 (Diagnosis of the structural unit) provides information for the diagnosis of each StU. The section is divided into separate tables that aim to identify the stability issue of the StU, as well as the possibly mechanical damage and decay phenomenon involving the StMs and StNs. Finally, there

are special boxes for the insertion of photographic material relating to the identified issues.

4.2 SURVEY OF THE STRUCTURAL MEMBER (StM)	
Structural Member	-
ID	

Identification of the wood species		Note
through Macroscopic recognition		
through Microscopic recognition		
Existing documentation		
Age of the StM		

Geometry and dimension		Note
Type of cross section		
Geometry of the member		
Geometry of the cross-section		
Average dimension of the cross-section [cm]		
Member length [m]		

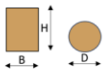

Type of woodworking		Note
Unbarked/Rounded		
Sawn finish	-	
Hewing finish	-	

Type of superficial treatment		Note
Not visible		
Wood oil		
Varnishing		
Painting		
Carving decoration		
Wax		
Other		

Figure 3.22. Extract from survey form: Section 4.2 – Survey of the structural member (StM).

Section 5.2 (Diagnosis of the structural member) aims at the diagnosis of the single StM. In the first section of the form, the StM is identified, and details about the wood species and visual strength class [318] are provided. Furthermore, the reference to specific documentation for the VSG analysis can be remarked herein. Then, it is possible to highlight the most significant wood defects on the member, i.e. those that, due to their type, size, and position within the member, may have the greatest impact on the structural behavior. A huge part of the form is devoted to non-destructive testing (NDT). The first column of the table indicates the type of test. In this regard, the thermo-hygrometric parameter measurement tests are listed first, followed by the traditional test. For each type of test, the following are provided: the date, the time, the testing tool, the number of measurements and their location, as well as the measured parameter. Furthermore, any notes or criticisms can be noted, and any specific test documents can be cited herein. In the last part of the form, a table designed for the description of the outcomes of the diagnostic analysis has been fixed, along with appropriate boxes for attaching photographic material and graphics.

3.4.2 APPLICATION TO THE CASE STUDY OF THE DIPLOMATIC HALL IN THE ROYAL PALACE OF NAPLES

In order to evaluate the feasibility and effectiveness of the survey form, it has been applied to a restricted part of the timber structures of the Royal Palace of Naples (Appendix C.2). The building is located in the historical centre of the town, in Plebiscito square. It was designed by the famous architect Domenico Fontana (1543-1607). The work started in 1600 and after about thirty years the main body of the building, consisting of three floors, was complete. During the eighteenth century, Luigi Vanvitelli was tasked with consolidating part of the building. In the first half of XIX century, a restoration project was undertaken to expand and standardize the structure following a fire event. Consequently, the palace underwent restoration under the supervision of Gaetano Genovese. During the second World War the building was damaged by the bombings and then some rooms were rebuilt. In 2009, further works were carried out on the timber structures of the Diplomatic Hall [173]. The Royal Palace served as a Royal Residence from 1600 to 1946. Nowadays the building has three levels and coexist within it: the museum of the Royal Palace, the National Library and the two Superintendencies for the city and the metropolitan area of Naples.

The survey activity focused on the complex roofing structures of the Diplomatic Hall. This room is located at the first floor, on the east side of the building, overlooking Plebiscite square. It is one of the most prestigious rooms since, in addition to the artistic value of the furnishings and flooring, it is covered by a vault painted by Francesco De Mura (1696-1782). The vault, which covers a rectangular surface of 16.70 m x 14.20 m, is supported by a complex structural system characterized by three main parts: the vaulted cieling, the floor beams and the Palladian truss [173]. In the early 2000s, these structures were involved in a huge retrofitting project, whose design and execution were guided by Prof. Emer. F. M. Mazzolani [173]. They mainly concerned the reinforcement of the floor beams through the execution of a R.C. slab connected to the floor beams through steel collars [417]. During this activity, the timber structures were involved in a huge investigation consisting of a detailed survey and a structural health assessment. After this, the timber structures were reinforced [417].

a) b)

Figure 3.23.a) The frontal view of Royal Palace of Naples from Plebiscito square [173]; b) Internal view of Diplomatic Hall [417].

Therefore, the filling out of the form has been carried out remotely on PC, thanks to the available documentation (courtesy of Prof. B. Faggiano and PhD M. R. Grippa). The survey and diagnosis of the timber structures (sections 4 and 5 of the form) concerned the Palladian truss, for which a detailed geometric survey and photographic material were available. The full version of the survey form completed for this case study can be found in Appendix C.2, while the process and results of the application are described below.

The information for the identification of the form and the location of the building has been provided in Section 1 (Building identification). Here it has been highlighted that the building is listed under the architectural and historical constraint by the ex. Italian law 1089/1939 [428]. Finally, a brief description of the building has been given, describing the main historical events.

In Section 2 (Building description), general and metric information about the building is given. In detail, Palace Royal was built in 1600 and has three floors with an average height of 4.5 meters. The average floor area is approximately 1000 m^2. In terms of its intended use, the building has several functions, such as a museum, library, and office, with more than 65% of the surface area being used.

Section 3 (Identification of the building components and structural units) for the identification of the building components (BC) and structural units (StU). Thus, the vertical structures, the floor structures (at ground, first, second, and third levels), and the roof structure have been identified as BC, and an ID has been assigned to them. For each BC, the StUs have been listed through the ID, and their construction typology has been noted. The vertical structures (BC.1) of the building consist of masonry walls (StU.1), as well as the floor slab (BC.2) consists mainly of reinforced concrete slabs (StU.2). The

roof structures (BC.6) show different types, since they were subjected to several works over the years; trusses in timber (StU.8), steel (StU.9) and R.C. (StU.10) types can be distinguished [173]. The intermediate floors present different construction technologies; however, only the floor structures of the Diplomatic Hall has been focused (BC.4). As already shown, the structural units of the floor structure are 3: the beam floors (StU.4), the Palladian truss (StU.5) and the ceiling vault (StU.6).

Section 4 (Survey), devoted to the survey of timber structures, has been applied to the Palladian truss of the (StU.5), being a complex typology, it was useful for evaluating the effectiveness of the proposed form (Figure 3.24). The characterization of the StU.5 has been carried out filling the section 4.1 (Survey of the structural unit). The identification of the StU has been first performed by identifying the period of construction (probably between the 17th and 18th centuries), describing the general aspects, and pointing out the interventions it underwent. The StU.5 is a composite Palladian truss that cover a length of about 16.70 m and it serves as mid-span beam of the floor slab. It was probably made between the 17^{th} and 18^{th} centuries, and it was only discovered during the survey activities in the early 2000s, as before it was enclosed in two partition brick walls supported by the floor slab [173]. Then, the walls were dismantled to facilitate the in-depth survey and diagnosis of the truss. Based on the results of the diagnosis and vulnerability assessment, the strut was involved in retrofitting interventions, which mainly consisted of the repair of the strut, which was damaged by biological attacks, and the restoration of all connections among truss elements [417]. The identification of all structural members (StM) composing the truss has been carried out in the second table of the form. Herein the StM can be chosen from a list of the members commonly spread in the context of timber structures of historical and architectural value. For each StM the number of elements and the ID has been provided, showing the ID code even on a carpentry drawing. As already mentioned, the StU.5 is a composed truss made of several StMs. In total, they are 23 StMs: 2 rafters, 2 secondary rafters, 1 tie-beam, 1 secondary tie-beam, 1 king post, 2 queen posts and 10 struts. The upper register of the truss consists of 2 struts and 1 king-post that are joined to the 2 main rafters. The lower and upper register are separated by the secondary tie-beam. In the lower register, secondary rafters are joined to the main rafters, making a composed cross-section. In addition, there are two queen posts and four pairs of struts. The tie-beam is simple supported on the masonry walls, and it is subject to bending stress state as well as tensile stress, as it also supports the floor beams. Then, the structural nodes (StN) have been

surveyed (in total 22 StNs), attributing the ID to each node identified by the converging StMs. In the last table of the section 4.1 a technological characterization of the StNs is provided through the identification of the construction typology and the presence of metallic/timber fasteners. The truss is characterized by carpentry joints, in which the transfer of stresses occurs through direct contact between the timber members (compression stress state). The notch joint without metal fasteners is the widespread type, whereas the joint between the tie-beam and the rafter, as well as the strut and queen-post, showed the presence of a couple of external timber chunks fixed with cast iron nails. A similar type has been discovered in the queen post-tie beam joint, however in that case the timber chunks are joined with metal stirrups. The struts at the bottom level of the truss are simply supported on the secondary tie-beam, which doesn't show any notches. However, the pair of struts is interspersed with external timber pieces fixed to the secondary tie-beam by metal stirrups. The photo of the joints described so far have been attached at the end of the form.

Section 4.2 (Survey of the structural member) deals with the characterisation of structural members. This section has been filled out for three representative members: the rafters (StM.1), the queen-post (StM.4) and the strut (StM.7; Figure 3.25). They have been selected for typological variety and state of preservation. The members are characterized by describing the wood species, the age and the geometrical and dimensional features. The wood species has been recognized by the visual analysis of the macroscopic aspects. It has been found that the three members are in Chestnut *(Castanea Sativa* Mill.) and they dates back to the 1600 [429]. The rafters (StM.1; Figure 3.25.a) have a circular cross section with an average diameter of 27 cm and a length of about 11.0 m. The queen-posts (StM.4; Figure 3.25.b) have a circular section with an average diameter of 18 cm and a length of 4.0 m, whereas the strut (StM.7; Figure 3.25.c) have a circular cross section, with a diameter of about 10 cm, and an overall length of 1.5 m. Then, the wood-working and surface treatments have been discussed. The rafters and queen-posts showed a same wood-working and finishing since the wood members were simply barked. Instead, the strut seems to be hewing finished. All the StMs didn’t show visible surface treatments.

The description of the structural nodes (StN) is provided in the section 4.3 (Survey of the structural nodes). In the same manner as the members, the application of the form to three StNs (rafter-tie beam, queen post-tie beam, rafter-strut) is shown herein (Figure 3.26). The StNs are first identified by means of IDs and the joined members are listed. Afterwards, a brief

description of the typological and technological aspects is given through textual fields and by selecting the alternatives from the predefined lists. The connection between the rafter and tie-beam (StN.1) is assured by direct contact of the members and thanks to the presence of external timber chunks that are joined to both rafter and tie-beam through cast iron nails. The two pairs of shafts are connected by means of a timber-to-timber joint with double step joint. Furthermore, the tie-beam is simple supported on the vertical masonry walls. Even the joint between the tie-beam and the queen-post (StN.21) is characterized by the presence of external timber chunks joined to the members through metal stirrups. In the end, the node where rafter and strut are joined has been analysed (StN.22). In this case, there are no metal fasteners, and the stress transfer occurs by direct contact between the members. The strut shows a notch in the connection with the strut.

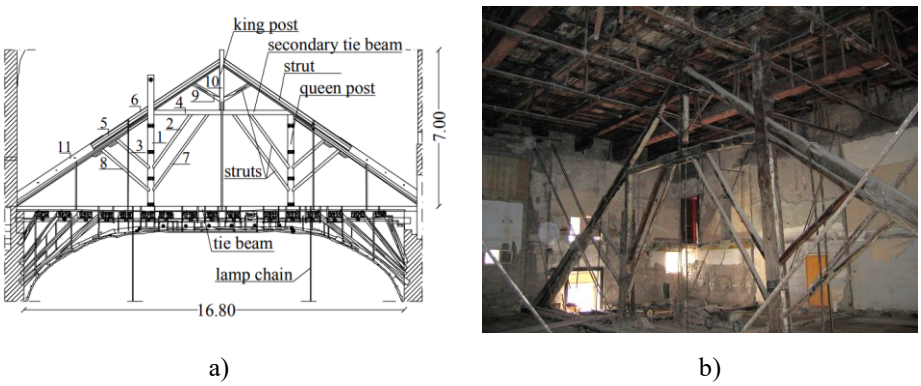

Figure 3.24.a) Frontal view of the structural units of the Diplomatic Hall: the beam floors (StU.4), the Palladian truss (StU.5) and the ceiling vault (StU.6; [417]); b) View of the Structural Unit StU.5 (Palladian composite truss; [417]).

In general Section 5 (Diagnosis) is devoted to is devoted to collecting the information indispensable for diagnosing the structural health state of the structure. Thus, two sections dedicated to this aspect have been proposed: section 5.1 for the diagnosis of pathologies affecting the whole structural unit and section 5.2 focusing on each structural member.

Section 5.1 (Diagnosis of the structural unit) has been applied to the Palladian truss (StU.5) considering the state of conservation at the time before the retrofitting project [417]. Therefore, the assessment has been carried out by consulting the huge database of photos and surveys. In the first part of the

section the StU is identified, and then the instability issues are noted by selecting from a list of the most common types. As easily detectable from Figure 3.27. the StU.5 is affected by instability issues mainly located in the queen-posts. Indeed, a relative rotation of the members has been noted and probably due to the disconnection of the external timber chunks. On the other hand, no warping and out of plane mechanisms have been recognized. Subsequently, the phenomena affecting structural members and nodes have been analysed. Thus, excessive deformations (deflection) has been identified for the StM.16 rafter and compression cracks have been noted for the rafter StM.1. in correspondence of the rafter-tie beam node. Due to the disconnection of the queen-posts, most of the structural nodes suffered a translation. With the exception of the structural nodes at the level of the tie-beam (nodes xx, yy, zz), all the remaining nodes showed a translation that is most evident for nodes StN.4 and StN.14. In the end the presence of compression cracks has been noted in correspondence of the node StN.1. where the rafter is joined with the tie-beam.

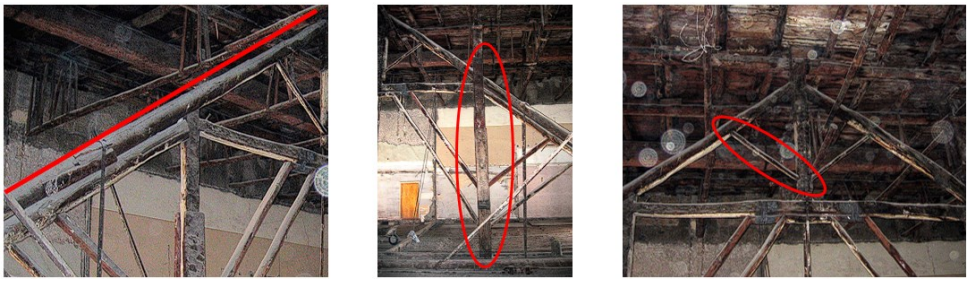

a) b) c)

Figure 3.25. Investigated structural members: a) the StM.1 (rafter); b) the StM.4 (queen-post); c) the StM.7 (strut; courtesy of Prof. B. Faggiano and PhD M.R. Grippa).

a) b) c)

Figure 3.26. Investigated structural nodes: a) the StN.1 (rafter-tie beam); b) the StN.21 (queen post-tie-beam); c) the StN.22 (rafter-strut; courtesy of Prof. B. Faggiano and PhD M.R. Grippa).

Section 5.2 has been filled out considering the same StMs (rafter, queen-post and strut) detected in section 4.2. For each members the main wood defects have been firstly detected by selecting from a list of the most common defects. Large wanes, small knots and superficial shrinkage cracks have been noted for the three members, however it has not been possible to measure the dimensions of them. The wood species has been recognised by watching the macroscopic aspects of wood and it has been seen that all members are in Chestnut wood *(Castanea Sativa* Mill*.)*. Subsequently, from the recognition of the effects produced on the members, the timber decay phenomena have been recognised. Whereas the StM.4 and StM.7showed no specific phenomena, in the StM.1, biological decay has been found in correspondence with the connection with the tie-beam. In fact, flickering holes and chromatic alterations, respectively, due to insect (*Anobiidae* and *Isoptera)* and fungi attacks, have been recognized. The fungi attack has certainly been caused by the high moisture content of the wood member, which, in contact with masonry, absorbed rising damp. Due to this attack the cross section has been significantly reduced. Furthermore, cracks due to an excessive compression stress state have been located in the same position.

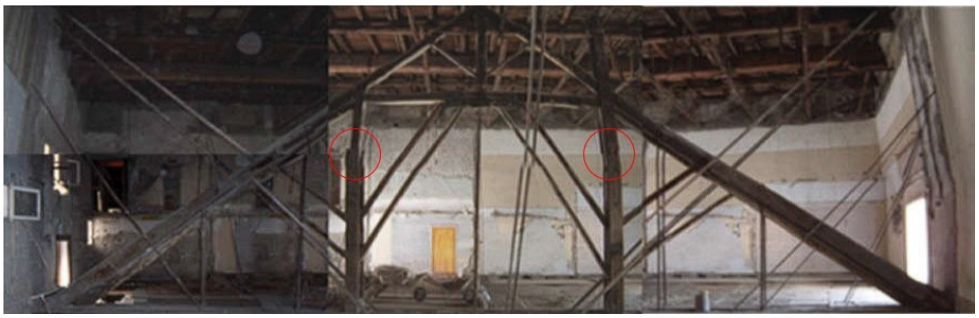

Figure 3.27. Frontal view of the StU.5 with evidence of the structural instability issues (cropped from Faggiano et al., 2018).

The excess of compression has probably been caused by the disconnection of some joints of the truss, probably in correspondence of the queen posts (Figure 3.27). Thus, the rafter suffered an increase in stress state. At the end the form provides information on NDT tests, describing the date of the test, the instrumentation, the number of tests and their location, and finally a field is given to refer to specific documents. As regard to the members subject to diagnosis, during the investigation carried out in the early 2000s, only drilling

resistance tests were performed. It was applied to perform the dendrochronological dating of the members, from which it was found that the members had an average age of 38 years and the residual cross section of member was evaluated [430].

Chapter

4

Vulnerability assessment at territorial scale: proposal of a semi-quantitative method for the seismic vulnerability and durability assessment of timber structures

Abstract: Assessing the physical vulnerability of built-up is a crucial step in seismic risk management. Institutions devoted to territorial governance need tools for identifying the most vulnerable buildings in order to manage resources for risk mitigation and emergency management. These tools should consider aspects that play a key role in seismic vulnerability assessment, and among them durability is a fundamental aspect for timber structures.

In this chapter the application of the *indicator-based approach* for assessing the physical vulnerability of large-span timber buildings exposed to seismic hazard is presented. The vulnerability criteria have been identified from the general, technological and geometrical aspects of the building, showing the procedure for calculating the vulnerability index through the TOPSIS method.

At the same time the durability issues have been evaluated through an innovative method. It is based on the Factorial Method [273] for predicting the estimated service life (ESL) and the TOPSIS method has been used as a supporting tool for defining the modification factors.

In the end, an approach to integrate durability aspects into seismic vulnerability assessment is proposed.

4.1 MOTIVATION AND GOALS

Italy is a territory particularly exposed to seismic risk, due to the high rate of occurrence of seismic events as well as the fragility of the built-up. For seismic risk management, the assessment of the physical vulnerability of the built-up represents a fundamental action. In this regard, territorial governance institutions require risk assessment tools at the territorial scale (large scale), in order to manage resources for risk mitigation and emergency management.

Methods and procedures employed at the territorial scale diverge from those utilised at the detailed scale, which requires a comprehensive survey and diagnosis of the structure to ensure a detailed evaluation of its structural capacity. Indeed, at the territorial scale, the main objective is to promptly identify the areas where the buildings most susceptible to damage are located, since following a given seismic event, there is the possibility of suffering greater losses in these areas. Therefore, it is crucial to employ quick level methods that use easily accessible building data as vulnerability parameters. In this way data can be easily acquired from databases shared by institutions or from expeditive on-site surveys. To this aim survey forms play a crucial role in facilitating the collection of information by focusing on factors of vulnerability [262].

Vulnerability parameters easily accessible at territorial scale include several aspects as the construction technology (e.g., R.C., masonry, steel, wood), the building geometry (e.g., number of floors, geometry in plan and height), the structural system, etc. However, one factor that cannot be overlooked is the state of health of the structure and especially timber structures suffer from decay phenomena that can significantly reduce the load-bearing capacity over time. For this reason, it is of primary importance to identify tools and methods to assess this aspect and integrate it into the overall vulnerability assessment, thus contributing to an integrated and comprehensive seismic vulnerability assessment.

This is the context for the proposed work, consisting in the application of the *indicator-based approach* to estimate the seismic vulnerability of selected buildings. In this way physical vulnerability is quantified through an index as measure of building susceptibility to damage. The index is determined through the definition of vulnerability criteria, while the computation of the index is based on the application of the *TOPSIS* method which is a multicriteria decision making method *(MCDM)*. At the same time an innovative method (Global durability factor method) for the evaluation of the

state of health and susceptibility to degradation of the timber building is proposed [427]. It is based on the combined application of the *Factor Method* (FM; [273]) and the *TOPSIS* method. In this way, the health of the structure has been evaluated through the estimated service life (ESL) and global durability index.

This chapter discusses the procedures of the two methodologies. In addition to the general description of the methodologies, two key aspects of the respective methods have been focused on: the definition of the seismic vulnerability criteria and the identification of durability factors. Vulnerability criteria has been calibrated to the peculiarities of timber buildings, and among the different building types, large span buildings such as sport facilities, gym, etc. have been analysed. Being facilities frequently used during the emergency as recovery buildings, the vulnerability analysis of such types is a task of great importance. At the same time, a qualitative and quantitative definition of the durability factors affecting the state of health of the timber buildings is proposed. In this context, it is important to note that the acquisition of data regarding both the vulnerability criteria and the durability aspects can be supported by the on-site survey through survey forms properly designed for the purpose.

In order to lead to an integrated and comprehensive assessment of the vulnerability of exposed buildings, a framework for integrating the two methodologies is proposed at the end of the chapter.

4.2 THE THEORETICAL BACKGROUND

4.2.1 THE TOPSIS METHOD

The framework

Both proposed methodologies are based on the multi-criteria decision-making method (MCDM), which uses the TOPSIS technique (Technique for Order Preferences by Similarity to Ideal Solution [431]. In general, MCDM methods are used to help the decision maker (DM) or a group of decision makers (DMs) make objective choices that are not influenced by the person responsible for the evaluation process. They are mathematical tools that help solve a complex decision-making problem by identifying the best alternative that satisfies a given number of criteria [432], [433].

All decision-making problems concerning a multi-criteria evaluation are analyzed by considering the following elements:

- An objective or set of objectives, which represent the goal to be achieved;
- A DM or group of DMs involved in the selection process, who are responsible for the evaluation procedure;
- A set of decision alternatives, which are the basic elements of the evaluation and selection process;
- A set of evaluation criteria, which are used by DMs to evaluate the performance of the alternatives;
- DMs' preferences, which are typically expressed in terms of weights assigned to the evaluation criteria;
- A set of scores, which express the value of alternative i with respect to criterion j.

The TOPSIS method is a simple and practical technique for immediately identifying the best solution and creating a ranking among all the alternatives considered (Bagga et al., 2019). This method allows the various alternatives to be represented as points in a vector in space having the number of criteria as dimensions, so that the performance of the various solutions becomes the coordinates in the assumed vector space. The TOPSIS method makes it possible to create two ideal alternatives, the best solution (A^+) and the worst solution (A^-), which have the best and worst performance, respectively, with respect to all criteria and are the DM's reference for identifying the best alternative among those considered. Thus, the solution to the decision problem is represented by the alternative having, at the same time, the least distance from A^+ and the greatest distance from A^- (Faggiano et al., 2011).

Specifically, any MCDM method relies on two basic elements, namely the decision matrix D, in which the performance of different alternatives against each defined criterion is reported, and the vector of criterion weights, which provides the importance that the DM attaches to each selected criterion with respect to the objective of the analysis. It is possible to summarise the procedure at the following points:

1. Definition of the decision matrix and its normalization;
2. Assignment of weights for each criterion;
3. Definition of the orders among the different alternatives;

Definition of the decision matrix and its normalization

The first step consists of constructing the decision matrix D_{mxn}, whose rows *m* correspond to the different alternatives (e.g., the buildings surveyed) and columns *n* are the criteria (e.g., the vulnerability elements acquired through the the survey forms).

The d_{ij} terms of the matrix are the indicators that quantify or qualify the criteria in each alternative, such as a measure of the alternative's performance against the criterion and can be of different natures. Some criteria are estimated from actual numerical values; other criteria can be associated with representative and quantifiable parameters; for some other criteria, which are expressed by judgements, numerical values can be assigned according to Saaty's scale [434], determining a hierarchical order by means of the *Analytical Hierarchy Process (AHP)* method [434].

For each category, the measures d_{ij} of criterion *j* with respect to alternative *i* are collected in the decision matrix D_{mxn} (*m:* number of alternatives; *n*: number of criteria for each category), whose generic terms (d_{ij}) are chosen on the basis of a direct measure (e.g., building height [cm]), a numerical score (poor: 2, mediocre: 5, good: 8, excellent: 10, ect.), or a numerical score determined through the AHP method.

Once the decision matrix D_{mxn} has been defined, the next step is its normalization, which is necessary due to the presence of qualified criteria with different units to obtain dimensionless terms for the purpose of data homogenization and comparison between criteria. Normalisation can be achieved through simple mathematical functions that operate on the terms of the matrix rows. This gives rise to the normalised decision matrix R, consisting of the parameters r_{ij} calculated as follows (Eq. 4.1):

$$r_{ij} = \frac{d_{ij}}{\sqrt{\sum_{i=1}^{n} d_{ij}^2}} \tag{4.1}$$

where:

r_{ij} normalized measure of the j-th criterion with respect to i-th alternative;

d_{ij} measure of the j-th criterion with respect to i-th alternative;

Assignment of weights for each criterion

The weights of each criterion measure the priorities assigned to the criterion on the vulnerability or durability assessment. The assignment can be made on the basis of binary comparisons (AHP) between two criteria according to a predetermined scale, such as the Saaty scale. The values thus determined are organised in the so-called matrix of weights, also called the matrix of binary comparisons, A_{nxn}, of which the rows and columns are the criteria and whose generic term a_{ij} has the following properties: $a_{ii}=1$ and $a_{ji}=1/a_{ij}$ and expresses the priority of one criterion over another.

Then the weights w_j to be assigned to each criterion are calculated as follow (Eq. 4.2):

$$w_j=\frac{M_{gi}}{\sum_{i=1}^{n} M_{gi}} \tag{4.2}$$

where:

w_j weight related to j-th criterion;

M_{gi} geometric mean (Eq. 4.3);

$$M_{gi}=\left(a_{1j}\cdot a_{2j}\cdot\ldots\cdot a_{nj}\right)^{\frac{1}{n}} \tag{4.3}$$

where:

a_{ji} generic term expressing the relation between the criteria.

Each column of the normalized decision matrix R must be multiplied by the weight of the criterion corresponding to it, thus obtaining a new matrix V_{mxn} (weighted normalized matrix), composed of the m alternatives and the n criteria, whose generic element is (Eq. 4.4):

$$v_{ij} = \frac{w_j \cdot d_{ij}}{\sqrt{\sum_{i=1}^{n} d_{ij}^2}} \quad (4.4)$$

where:

v_{ij} weighted and normalized measure of the j-th criterion with respect to i-th alternative;

w_j weight related to j-th criterion;

d_{ij} measure of the j-th criterion with respect to i-th alternative;

Definition of the orders among the different alternatives

According to the TOPSIS multicriteria method [431], the orders correspond to the total score associated with each alternative defining the final ranking. The best alternative has the highest score in case of Benefit criteria (B), the lowest score in case of Cost criteria (C). Each criterion will be identified as B or C in relation to its property of improving or worsening the final rating.

Considering for each criterion the best and worst performance offered by the examined alternatives, the ideal positive solutions (A^+; Eq. 4.5) and ideal negative solutions (A^-; Eq. 4.6) are respectively calculated:

$$A^+ = \left\{\left(\max v_{ij,j} \in J_B\right)\left(\min v_{ij,j} \in J_C\right)\right\} = \{v_{i,1+}; \ldots; v_{i,n+}\} \quad (4.5)$$

$$A^- = \left\{\left(\min v_{ij,j} \in J_B\right)\left(\max v_{ij,j} \in J_C\right)\right\} = \{v_{i,1-}; \ldots; v_{i,n-}\} \quad (4.6)$$

where:

A^+ ideal positive solution ;

A^- ideal negative solution;

J_B set of the benefit (B) criteria;

J_C set of the cost (C) criteria.

The vectors of the real ideal solutions (A_i) can be identified as follows (Eq. 4.7):

$$A_i = \{v_{i,1}; \ldots; v_{i,n}\} \tag{4.7}$$

The next step is to calculate the distance of each real alternative from the ideal ones. From this perspective, it is possible to calculate the Euclidean distances between the real solution A_i and the positive and negative ideal solutions as follows (Eq. 4.8; Eq. 4.9):

$$S_i^+ = |A_i - A^+| = \left[\sum_{j=1}^{n} \left(v_{i,j} - v_j^+\right)^2\right]^{\frac{1}{2}} \tag{4.8}$$

$$S_i^- = |A_i - A^-| = \left[\sum_{j=1}^{n} \left(v_{i,j} - v_j^-\right)^2\right]^{\frac{1}{2}} \tag{4.9}$$

where:

S_i^+ Euclidean distance between the real solution (A_i) and the ideal positive solution (A^+);

S_i^- Euclidean distance between the real solution (A_i) and the ideal negative solution (A^-).

In conclusion, the relative closeness of each alternative from the ideal ones is the benchmark for their ranking and it can be calculated as follow (Eq. 4.10):

$$RC = \frac{S_i^-}{S_i^+ + S_i^-} \tag{4.10}$$

where:

RC relative closeness of the i-th alternative from the ideal ones.

From the calculation of the relative closeness for each alternative the best one can be identified. When considering benefit criteria, it corresponds to the alternative with the highest score, whereas for cost criteria, it corresponds to the alternative with the lowest score. As will be seen below, the index RC will take meaning as the vulnerability index (I'_v) for seismic vulnerability

assessment, while it will correspond to the global durability index (I_{GD}) in durability assessment.

4.2.2 THE FACTORIAL METHOD AS SERVICE LIFE DESIGN METHOD

The factor method (FM; provides the service life estimation according to a deterministic approach. The factorial method is based on the identification of factors that can affect the service life of a component [273]. Once the modification factor are fully defined, the service life of a component can be determined through the following equation [273] (Eq. 4.11):

$$ESL = RSL \cdot (A \cdot B \cdot C \cdot D \cdot E \cdot F \cdot G) \quad (4.11)$$

where:

ESL estimated service life;

RSL reference service life;

(A, B, …, G) modification factors.

The ESL is the period of time (year) over which the component's performance remains above a predetermined level. The RSL is a predetermined period of time, fixed a priori on an empirical or experimental basis, as well as on expert judgment. The modification factors (A, B, …, G) can be linked to the following aspects [273]:

- factor A: quality of components;
- factor B: design level of a component or assembly installation;
- factor C: work execution level or skill level of the installers;
- factor D: indoor environment;
- factor E: outdoor environment;
- factor F: in-use conditions;
- factor G: maintenance level.

Each factor makes a more or less significant contribution to determining the durability of the component. For each factor, a numerical value lower than 1.00 can be attributed as a function of its weight, i.e., its influence with regard to the durability condition. The designer's task consists of computing the modification factors (A-G) in objective and effective manner, based on its judgment or real service data.

4.3 THE INDICATOR-BASED APPROACH FOR SEISMIC VULNERABILITY ASSESSMENT

4.3.1 GENERAL FRAMEWORK

The TOPSIS method has been applied to assess the seismic vulnerability of large span timber buildings by estimating the vulnerability index. This index is calculated after defining vulnerability criteria, i.e., aspects attributable to the typological and structural characteristics of the building that influence the structural response toward seismic action. Thus, the vulnerability index, expression of the building susceptibility to damage, has been evaluated.

The procedure of the TOPSIS method was shown in Section 4.2.1 In the application of this method in seismic vulnerability analysis, it is assumed that the criteria correspond to the vulnerability criteria or indicators of vulnerability, which should be defined qualitatively and quantitatively, as well as ranked according to their significance. In addition, the alternatives correspond to the buildings under analysis.

Therefore, the positive and negative ideal solutions correspond to the most and least vulnerable ideal buildings, respectively. The performance of each building is evaluated by using the seismic vulnerability index (Eq. 4.12), which represents how close the building in question is to the ideal cases (A^+ and A^-):

$$I'_V = \frac{S_i^-}{S_i^+ + S_i^-} \tag{4.12}$$

where:

I'_V vulnerability index.

It is clear that higher is the I'_V, higher the seismic vulnerability of the given building. It means that in a set of structures, the one with the highest I'_V is the most vulnerable to the seismic action.

4.3.2 VULNERABILITY CRITERIA FOR LARGE SPAN TIMBER STRUCTURES

4.3.2.1 Qualitative proposal

Vulnerability criteria have been developed specifically for large span timber buildings, considering their special characteristics and relevant aspects that influence structural response during an earthquake. Analysed criteria included those that could be identified using the Cartis GL form. In addition to structural aspects (Section 3D – Cartis GL), general aspects (Section 2 – Cartis GL) and aspects related to constructive technology (Section 1 – Cartis GL) have been also considered [262].

Although there are several criteria that play a significant role in assessing the seismic vulnerability of a structure, some of them have not been selected because they are not independent, but closely related to each other. For example, technological classification based on building materials corresponds to a qualitative criterion whose vulnerability depends on other criteria, such as the structural system, connections and state of preservation of buildings. In conclusion, 32 criteria have been selected and grouped into 4 categories. To facilitate the reading of the different processing tables, each category is identified by a color presented in Table 4.1 below.

Table 4.1. Category of criteria.

Category	**Colour**
Building regularity	
Building aspects	
Structural members	
Geometric features	

The following is a qualitative description of the vulnerability criteria, grouped for categories.

Building regularity

As regard building regularity 8 criteria have been proposed (Table 4.2). In fact, regularity allows to have a symmetrical distribution of the seismic loads and has a significant role in the stiffness and mass repartition and in the reduction of the torsion effect. Moreover, the design model is based on regular structure in order to simplify the structure model in plane model or in spatial model. The building's regularity in plane and in elevation are also well detailed in the last section of the CARTIS form GL.

Table 4.2. Criteria of building regularity.

Designation	Criteria
S1	Compact and symmetrical plan
S2	Ratio of the largest to the smallest side < 4
S3	Plants that do not exceed 5% of the total area
S4	External wall evenly and symmetrically distributed
S5	No eccentric core or blocks
S6	All the horizontal resistant systems extend over the entire height and without absence of any plane offset
S7	External walls evenly distributed in elevation and absence of continuous windows
S8	Symmetrical distribution of shear walls both continuous (panels) or reticular (vertical braces)

Building aspects

With regard to building aspects 7 criteria have been identified (Table 4.3). For example, the years of the construction (S9) is given to know which regulation was applied to realize the design. At the same time the state of conservation (S10, S11, S12, S13) is a significant data in the vulnerability assessment. In fact, this information allows to describe the structure before and after a seismic event and have an idea of its level of performance and if countermeasures are necessary. This general criterion has been specified for vertical, horizontal and non-structural elements, as well as for the whole building. The important class of the building (S14) is also specified in this section to have an idea of the performance level applied for the design and of the exposure [71].

Table 4.3. Criteria of building aspects.

Designation	Criteria
S9	Year of construction and renovation
S10	State of conservation: over all
S11	State of conservation: vertical structures
S12	State of conservation: horizontal structures
S13	State of conservation: non-structural element
S14	Importance class of building (0,1,2,3,4)
S15	Use of building
S16	Position of building (isolated, corner …)

There is also the use of the building (storage, sport hall, public services etc.) which defines the exposure and the loads, it is similar to the use code. Then, it is important to know if the building interacts with other structures and how many interactions there are to know the influence on the dynamic behavior and torsion effect and if it corresponds to a dynamically independent unit. This is translated by the following characteristic: isolated, extremity, corner and internal. All of this information can be collected on site through Section 2 of the CARTIS GL form.

Structural systems

Among the vulnerability criteria of great importance are those devoted to the characterization of the structure. Thus, 6 vulnerability criteria have been defined for this category (Table 4.4). The presence of horizontal bracing (S17) shows that the roof is equipped with a system resistant to seismic forces. In addition, it is necessary to know the deformational characteristics of the roof slab (S20; rigid or deformable), since they are closely related to the stiffness of the structural system, along with the distribution of the bracings in the two directions (S21-22) (longitudinal and transverse), which is important for characterising the distribution of seismic actions among the vertical seismic-resistant structures. Further criteria concern the presence of chains (S18), which improve the box effect of constructions in seismic zones, and pushing elements (S19), which, on the contrary, worsen seismic behaviour. The last criterion in this category is the description of the roofing system (S23), which defines the number of orders of the horizontal elements and the type of the single- or double-way system, significantly impacting the stress distribution and also the structural mass (Table 4.4).

Table 4.4. Criteria of structural members.

Designation	Criteria
S17	Braced roof (yes or no)
S18	Presence of chains (yes or no)
S19	Pushing elements (yes or no)
S20	Deformation characteristic (rigid, deformable)
S21	Repartition of bracing in transversal direction
S22	Repartition of bracing in longitudinal direction
S23	Way system (double or simple)

Geometrical features

These criteria make it possible to describe the geometry of the building, obviously characterising the dynamic behaviour of the structure. Eight criteria have been identified for this group (Table 4.5). Some of them affect the structural mass, such as the total number of floors with basements (S24), the number of spans (S29) and their spacing (S27), the average floor area (S31), the number of naves (S30) and their span length (S28), facade openings (S32), column height (S25), and average floor height (S26) (Table 4.5).

Table 4.5. Criteria of geometric features.

Designation	Criteria
S24	Total number of floors including undergrounds
S25	Column/wall height
S26	Average interstorey height
S27	Frame span
S28	Frame spacing
S29	Number of span
S30	Number of bay
S31	Average floor area
S32	Openings in the facade

The integral description of the vulnerability criteria is provided in the Appendix D.1.

4.3.2.2 Quantitative evaluation and ranking

After the vulnerability criteria have been defined, a quantitative value must be assigned to each set of options (qualitative) for each criterion. Thus, some criteria have been estimated from actual numerical values; other criteria can be associated with representative and quantifiable parameters; for some other

criteria, which are expressed by judgements, numerical values have been assigned according to Saaty's scale [434], determining a hierarchical order by means of the Analytical Hierarchy Process (AHP) method [434]. An extract of the list of criteria with evidence of qualitative and quantitative values is given in Table 4.6, while the complete list can be found in Appendix D.1.

Then it is necessary to define the hierarchy of vulnerability criteria, following what is defined within Section 4.2.1. For this purpose, 3 different classifications of the defined criteria categories have been considered (C1; C2; C3; Table 4.7). To this aim, three classifications have been created according to the following assumption: "For seismic analysis, a major importance is attributed to parameters influencing the global behaviour of structures, whereas geometrical features are considered less significant factors" (extrapolated from: [432]). The first two classifications aim to analyze the influence of the regularity, building aspects (use, conservation, and position) and structural elements criteria's categories on the structure vulnerability. The third classification allows the comparison when these three categories have the same importance. Thus, the three classifications are showed in Table 4.7.

Table 4.6. Extract of the list of criteria (category: Structural members) with evidence of the qualitative and quantitative value (integral table at Appendix D.1)

	Criteria	**Type of criteria d_{ij}**	**Qualitativa value d_{ij}**	**Quantitative value d_{ij}**
S17	Diaphragmatic floor (yes or no)	Binary	No / Yes	0.1
S18	Presence of chains (yes or no)	Binary	No / Yes	0.1
S19	Pushing elements (yes or no)	Binary	No / Yes	0.1
S20	Deformation characteristic	Feature	Deformable	2
			Rigid	1
S21 - S22	Repartition of bracing in transversal direction Repartition of bracing in longitudinal direction	Percentage	Continuos	2
			Discontinuos	1
S23	Way system	Feature	Double way	2
			One way	1

Table 4.7. Classification of the categories.

Classification 1 – C1		Classification 2 – C2		Classification 3 – C3	
1	Regularity	1	Structural elements		Structural elements
2	Building aspects	2	Regularity	1	Regularity
3	Structural elements	3	Building aspects		Building aspects
4	Geometry	4	Geometry	2	Geometry

Finally, an order among the criteria can be defined according to a predefined scale of importance by applying Piecewise Constant Sorting (PCO) [432]. Some criteria are considered to be of equal importance in the assessment of seismic vulnerability, such as all the building regularity criteria as well as the four building aspects related to the state of preservation. Furthermore, the structural members criteria, such as the distribution of bracings in the two main directions of the plan, the number of span and naves, their span length, and their wheelbase are considered to have same importance.

In the end, for the first (C1) and second (C2) classifications, each criterion was given a value from 1 to 14, derived from an analysis on the importance of each criterion relative to the other, thus defining, 14 different levels of importance. For the third classification (C3), where structure, regularity, and building have equal importance for seismic vulnerability, each criterion has been assigned a value ranging from 1 to 6. Thus, multiple criteria have the same importance, and there are six different levels of importance (Table 4.8).

From these ranks, the A_{mxn} weights matrix or matrix of binary comparisons of criteria is compiled (Appendix D.2, D.3, D.4, D.5, D.6, D.7). From this, the weights w_j (Table 4.9) to be assigned to each criterion are calculated according to the Equation 4.2. The weights correspond to the priorities assigned to each criterion in the seismic vulnerability assessment. Below is the weight matrix for the first, second and third classification (Table 4.9).

Table 4.8. Predefined order of criteria.

	Criteria	C1	C2	C3
S1	Compact and symmetrical plan	1	5	1
S2	Ratio of the largest to the smallest side < 4	1	5	1
S3	Plants that do not exceed 5% of the total area	1	5	1
S4	External wall evenly and symmetrically distributed	1	5	1
S5	No eccentric core or blocks	1	5	1
S6	All the horizontal resistant systems extend over the entire height and without absence of any plane offset	1	5	1
S7	External walls evenly distributed in elevation and absence of continuous windows	1	5	1
S8	Symmetrical distribution of shear walls both continuous (panels) or reticular (vertical braces)	1	5	1
S9	Year of construction and renovation	2	6	1
S10	State of conservation: over all	3	7	1
S11	State of conservation: vertical structures	3	7	1
S12	State of conservation: horizontal structures	3	7	1
S13	State of conservation: non-structural element	3	7	1
S14	Important class of building (0,1,2,3,4)	4	8	1
S15	Use of building	4	8	1
S16	Position of building (isolated, corner …)	5	9	1
S17	Braced roof (yes or no)	6	1	1
S18	Presence of chains (yes or no)	7	2	1
S19	Pushing elements (yes or no)	7	2	1
S20	Deformation characteristic (rigid, deformable)	8	3	1
S21	Repartition of bracing in transversal direction	8	3	1
S22	Repartition of bracing in longitudinal direction	8	3	1
S23	Way system (double or simple)	9	4	1
S24	Total number of floors including undergrounds	10	10	2
S25	Column height	11	11	3
S26	Average interstorey height	11	11	3
S27	Frame span	12	12	4
S28	Frame spacing	12	12	4
S29	Number of span	13	13	5
S30	Number of bay	13	13	5
S31	Average floor area	13	13	5
S32	Openings in the facade	14	14	6

Table 4.9. Weights w_j of criteria for the three classification.

	Criteria	C1	C2	C3
S1	Compact and symmetrical plan	0.074	0.044	0.039
S2	Ratio of the largest to the smallest side < 4	0.074	0.041	0.039
S3	Plants that do not exceed 5% of the total area	0.074	0.039	0.039
S4	External wall evenly and symmetrically distributed	0.074	0.036	0.039
S5	No eccentric core or blocks	0.074	0.034	0.039
S6	All the horizontal resistant systems extend over the entire height and without absence of any plane offset	0.074	0.031	0.039
S7	External walls evenly distributed in elevation and absence of continuous windows	0.074	0.029	0.039
S8	Symmetrical distribution of shear walls both continuous (panels) or reticular (vertical braces)	0.074	0.027	0.039
S9	Year of construction and renovation	0.056	0.023	0.039
S10	State of conservation: over all	0.044	0.019	0.039
S11	State of conservation: vertical structures	0.041	0.018	0.039
S12	State of conservation: horizontal structures	0.038	0.017	0.039
S13	State of conservation: non-structural element	0.036	0.016	0.039
S14	Important class of building (0,1,2,3,4)	0.029	0.013	0.039
S15	Use of building	0.027	0.012	0.039
S16	Position of building (isolated, corner …)	0.022	0.009	0.039
S17	Braced roof (yes or no)	0.017	0.112	0.039
S18	Presence of chains (yes or no)	0.014	0.091	0.039
S19	Pushing elements (yes or no)	0.013	0.087	0.039
S20	Deformation characteristic (rigid, deformable)	0.011	0.071	0.039
S21	Repartition of bracing in transversal direction	0.010	0.068	0.039
S22	Repartition of bracing in longitudinal direction	0.009	0.065	0.039
S23	Way system (double or simple)	0.008	0.055	0.039
S24	Total number of floors including undergrounds	0.006	0.007	0.022
S25	Column height	0.005	0.006	0.016
S26	Average interstorey height	0.005	0.006	0.014
S27	Frame span	0.004	0.005	0.011
S28	Frame spacing	0.004	0.005	0.010
S29	Number of span	0.003	0.004	0.008
S30	Number of bay	0.003	0.003	0.007
S31	Average floor area	0.003	0.003	0.007
S32	Openings in the facade	0.002	0.003	0.005
	Summ of weigths	1.000	1.000	1.000

4.4 THE DURABILITY ASSESSMENT METHOD

4.4.1 GENERAL FRAMEWORK

The selected approach for the quick assessment of the state of conservation of a timber structure and the estimation of susceptibility to degradation consists of the application of the factorial method. However, an innovative application is proposed, using the TOPSIS method to support the estimation of the modification factors provided by the FM method. In this view, the factors are evaluated through a single index (global durability index).

However, before the application of this procedure, it is necessary to qualitatively identify the modification factors. It has been seen that the modification factors can be traced to different aspects of the analysed component, such as quality of the component, main condition of the environment in which it is placed, maintenance conditions etc. In the case of timber structures, the component to analyse is the structural member and the factors to be defined refer to the durability aspects that influence the structural performances of the member.

Thus, various parameters (sub-factors) affecting the member's durability have been identified for each factor, considering the durability aspects that compromise the structural performance of the timber construction. Then, for each sub-factor, a value quantification has been proposed and they have been ranked according to their importance. In the end, the TOPSIS method has been applied to estimate the modification factors (FM method) through the quantification of the global durability index (Figure 4.1). It is important to understand that that in combining the TOPSIS method with the FM method, the sub-factors correspond to the TOPSIS method criteria (Section 4.2.1), while the alternatives are the structural elements under study.

Therefore, the main steps of the methodology are as follows:

- qualitative definition of modification factors for wood structures;
- quantitative evaluation of the sub-factors and ranking;
- application of the Global Durability Factor Method (GDFM).

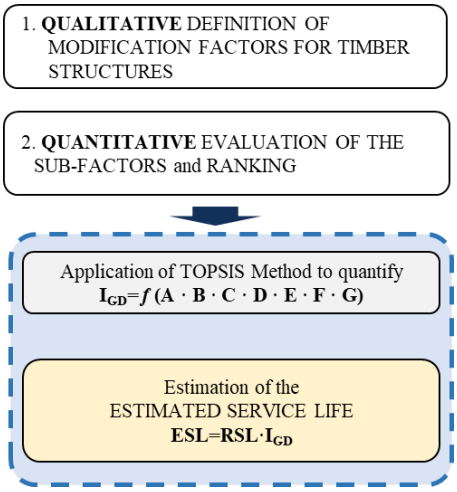

Figure 4.1. General framework of the proposed method

4.4.2 THE MODIFICATION FACTORS

4.4.2.1 Qualitative proposal for timber structures

At first, the qualitative definition of the factors that impact the durability of timber structures have been proposed, keeping the factor method grouping (A, B, …, G). For each factor a variable number of sub-factors have been proposed, up to a total number of sub-factors equal to 23 sub-factors. The list of sub-factors is provided in the Figure 4.2. Based on the judgment and thanks to the literature references, for each sub-factor the qualitative values have been defined. From the analysis of the state of the art, some of the durability aspects that most influence the state of preservation of a timber construction has been identified as sub-factors. The integral description of the sub-factors and their values is provided in the Appendix E.1.

For factor A (component quality), 9 sub-factors were identified. They express the different characteristics of the wood material that influence the durability of the component. Product type (A1) has been evaluated by distinguishing wood-based materials (e.g., CLT, glulam) from heavy wood elements. Subfactor A2 takes into account the possible presence of sapwood within the element, which is more susceptible to insect attack. The state of preservation (A2) takes into account the possible presence of cracks in timber member, which can cause an increasing water absorption. A key parameter for the durability of timber is the wood species, so the sub-factor A4 has been

proposed in ordet to take into account this aspect using the classification in durability classes provided by the standard UNI EN 350 [76]. The type of transport (A5) and storage of the material on site (A6) has also been evaluated, distinguishing between protected and unprotected transport and storage. Finally, aspects related to the quality of the timber product have been considered, with reference to the production chain. This included quality control (A7), the presence of the declaration of performance (DoP) (A8), and the quality of seasoning (A9), assessed on the basis of the residual moisture content of the wood, before installation.

For factor B (design level), two sub-factors have been identified that consider the quality of the design of the timber structure towards durability. Through sub-factor B1, the quality of the construction detail as designed is evaluated. In fact, often the incorrect design of the construction detail is the main cause of the degradation of the structure [35]. At the same time, factor B2 assesses the possible presence of protective, deep, or surface treatments.

Factor C (work execution) refers to the quality of the construction or assembly of the work. For this factor, 2 sub-factors have been identified. Through sub-factor C1, the correct execution of the work as designed is taken into account, while C2 considers the possible implementation of measures to protect the timber structure during the construction process.

For factor D (indoor environment), 2 sub-factors have been defined. The first (D1) considers the thermos-hygrometric conditions of the indoor environment, distinguishing cases of environments susceptible to the production of high humidity (e.g., gyms, kitchens, swimming pools) from standard ones. In addition, the possible presence of condensation phenomena, which is frequent in unconditioned indoor environments, is considered through sub-factor (D2).

Factor E (outdoor environment) takes into account the climatic characteristics of the site where the facility is located, and it has been characterised through five sub-factors. First, the climatic zone [435] of the site (E1) and the average rainfall have been considered, evaluating different ranges. Microclimatic conditions have been considered through sub-factors E3 and E5, identifying the service class [71] and use class [79], respectively. Finally, annual solar irradiance has been accounted for evaluating the level of exposure to solar radiation through different ranges of solar irradiance.

For the F-factor (conditions of use), a single sub-factor (F1) has been assumed. It takes into account the possible impacts to which the construction

could be subjected during its lifetime. This parameter is characterised by the impact class.

Factor	Sub-Factor	
A Quality of components	A1	Type of timber product
	A2	Presence of sapwood
	A3	State of conservation
	A4	Wood species
	A5	Quality of storage system at the building site
	A6	Quality of transport system (from industry to building site)
	A7	Presence of quality management system of industry (ISO 9001)
	A8	Presence of Declaration of Performance (DoP) (CPR 305/2011)
	A9	Quality of wood seasoning
B Design level of a component or assembly installation	B1	Quality of construction details (as designed)
	B2	Type of protective treatment
C Work execution level or skill level of the installers	C1	Quality of construction details (as built)
	C2	Quality of protection system during the construction steps
D Indoor environment	D1	Amount of environmental humidity
	D2	Water condensation risk
E Outdoor environment	E1	Climate zone
	E2	Average annual precipitation
	E3	Service class (NTC 18)
	E4	Average annual solar irradiance
	E5	Use class (EN 335)
F In-use condition	F1	Impact class
G Maintenance level	G1	Inspectability conditions
	G2	Quality of maintenance

Figure 4.2. List of the proposed sub-factors for timber construction.

In the end, the G factor (maintenance level) evaluates maintenance conditions through two sub-factors. The first one (G1) considers the conditions of inspectability of the construction, distinguishing different levels of accessibility, while the second (G2) evaluates the quality of maintenance, distinguishing preventive maintenance from corrective maintenance.

4.4.2.2 Quantitative evaluation and ranking

Once the factors have been identified as qualitatively defined sub-factors and their options, it is necessary to quantify the different options. Again, the

options differ in nature (e.g., numerical values, judgements, quantifiable parameters, etc.). For example, sub-factor A4 (wood species) is defined as a numerical value, as the various options correspond to the durability classes identified in UNI EN 350 [76], while sub-factor A1 (type of material) is defined by two options (heavy timber and timber-based products) identified through a judgment. In the latter case, the quantitative value has been attributed to the different options according to the Saaty's scale [434]. Quantitative values have been identified for all sub-factors, indicating their allocation criteria (Appendix E.1). An extract of the matrix is shown in Figure 4.3.

Sub-Factor		Qualitative value	Quantitative value	Best condition	Worst condition	Quantification criteria
A1	Type of material	Heavy timber	**1**	3	1	**Saaty 1990**
		Timber-based product	**3**			
A2	Exposed part	Sapwood	**1**	5	1	**Saaty 1990**
		Sapwood in higher percentage	**2**			
		Not-differiented	**3**			
		Hearthwood in higher percentage	**4**			
		Hearthwood	**5**			
A3	State of conservation	Un-cracked	1 mm	1	5	**Meausure**
		Superficial cracks	3 mm			
		Deep cracks	5 mm			
A4	Timber species	Not durable	1	5	1	**Meausure** **Durability classes** **UNI EN 350**
		Slightly durable	2			
		Moderately durable	3			
		Durable	4			
		Not durable	5			

Figure 4.3. Extract of the list of factors with evidence of the quantitative values and the quantification criteria (integral table at Appendix E.1)

In order to rank the sub-factors by importance, that is, by influence on the durability of the wooden element, it is necessary to assign a weight to the individual sub-factors. This is accomplished by identifying, on the basis of the state of the art and knowledge, a predetermination of orders of the sub-factors (Table 4.10.). It can be seen that maximum importance has been attributed to sub-factor E5 (Use Class) as it best expresses the degradation conditions to which the timber element is exposed, while less importance has been attributed to sub-factor F1 (Imapct class).

The next step consists of creating the matrix of pairwise comparisons using the Analytic Hierarchy Process (AHP) method. In this case, a rating scale with ratings ranging from 1 to 9 was considered [434]. Once the matrix of binary comparisons is determined (Appendix E.2), the weight w_j (Equation 4.2) of each sub-factor has been obtained (Table 4.10). From the latter table, it can be seen that the sum of the weights of all sub-factors is equal to 1.000.

Table 4.10. Predefined order of criteria and relative weights (w_j).

	Criteria	**Order**	**wj**
E5	Use Class (UNI EN 335)	1	0.121
E3	Service Class (NTC18)	2	0.114
A4	Wood species	3	0.106
A9	Quality of wood seasoning	4	0.088
A2	Presence of sapwood	5	0.074
E1	Climatic zone	6	0.064
B2	Type of protective treatment	7	0.059
G2	Quality of maintenance	8	0.055
A3	State of conservation	9	0.048
A1	Type of timber product	10	0.042
D1	Amount of environmental humidity	11	0.036
D2	Water condensation risk	12	0.032
E2	Average annual precipitation	13	0.028
B1	Quality of construction details (as designed)	14	0.025
C1	Quality of construction details (as built)	15	0.021
E4	Average annual solar irradiance	16	0.018
G1	Inspectiability conditions	17	0.016
A5	Quality of storage system at building site	18	0.013
A8	Presence of DoP (CPR 305/2011)	19	0.012
A7	Presence of quality system ISO 9001	20	0.010
C2	Quality of protection system during construction	21	0.009
A6	Quality of transport system	22	0.007
F1	Impact class	23	0.006
		Summ of weights	1.000

4.4.3 THE GLOBAL DURABILITY FACTOR METHOD (GDFM)

The Global Durability Factor Method (GDFM), herein proposed, is based on the combined application of the factor method (FM) and the TOPSIS method. So far, a list of modification factors has been proposed for evaluating the service life of timber structures. They have been qualitatively and quantitatively defined; moreover, they have been ranked by their relevance. Nevertheless, up to this moment, it remains unfeasible to ascertain the ESL

of a timber construction due to the absence of established criteria for assigning coefficients to each modification factor. Thus, the proposal intervenes at this stage, by introducing the TOPSIS for the determination of the modification factor of the RSL.

For this purpose, the TOPSIS method is applied by following its procedure, explained in Section 4.2.1. It is important to note that the j-th criterion corresponds to the sub-factors already defined for timber structures and that each alternative corresponds to a case study. It is also necessary to introduce and qualify the reference case (Cr) corresponding to ESL = RSL, further to the ideal positive and negative solutions. The Cr is an ideal, fictitious case study. Through the RC indexes calculated for each case study, it is possible to determine a single modification factor, called "Global Durability Index" (I_{GD}), according to Equation 4.12, which is a function of all the sub-factors (Eq. 4.12; Eq. 4.13):

$$I_{GD,i} = \frac{RC_i}{RC_{Cr}} \tag{4.12}$$

$$I_{GD,i} = f\,(A, B, C, D, E, F, G) \tag{4.13}$$

where:

I_{GD} Global durability index of the i-th case study.

RCi relative closeness of the i-th alternative (case study) from the ideal ones;

RC_{Cr} relative closeness of the reference case (Cr) from the ideal solutions;

(A, B, …, G) modification factors (ISO 15686).

Given for the reference case ESL=RSL, it is apparent that $I_{GD,Cr}$ is equal to 1.00. Therefore the ESL is calculated as it follows (Eq. 4.14):

$$ESL_i = RSL_i \cdot I_{GD,i} \tag{4.14}$$

where:

ESL_i estimated service life of the i-th case study;

RSL_i reference service life of the i-th case study;

$I_{GD,i}$ global durability factor of the i-th case study.

It is clear that higher is the I_{GD}, higher is the ESL of the structure. It means that in a set of structures, the one with the highest I_{GD} is the less vulnerable to the deterioration process. From the comparison of the ESL with the actual lifetime of a timber structure (recorded lifetime – RLT) the residual lifetime can be evaluated. It should correspond to the residual life of the element, upon reaching which irreversible performance decay should occur.

4.5 THE PROPOSAL FOR AN INTEGRATED APPROACH

One factor that cannot be overlooked in assessing the vulnerability of timber buildings is the state of health of the structure. Indeed, such structures are subject to decay phenomena that can significantly reduce their load-bearing capacity over time. Based on this assumption, the seismic vulnerability of timber buildings should be assessed through an integrated approach. To this aim it is necessary to combine the two methodologies described so far (Indicator based approach - Global durability factor method).

In the indicator-based approach, it was seen that the vulnerability index is assessed by establishing a set of vulnerability criteria, linked to structural, geometric and typological aspects of the structure. In the view of an integrated approach, a vulnerability criterion should be added in addition to these criteria, bringing into consideration durability aspects. The idea of an integrated approach (Figure 4.4) could be applied through the inclusion of the global durability factor (I_{GD}) in the vulnerability criteria.

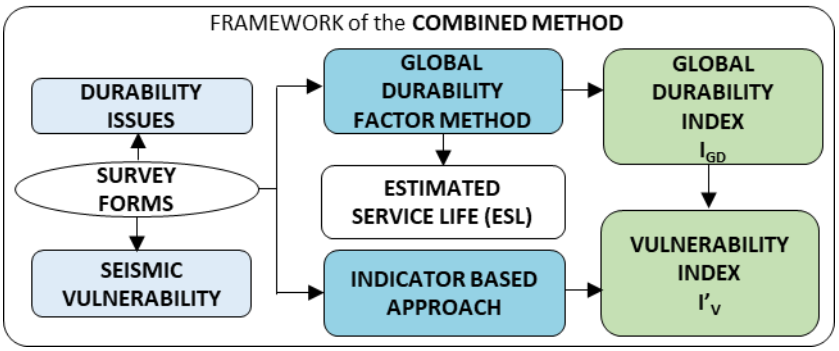

Figure 4.4. Framework of the combined method.

As shown so far, the state of conservation is already taken into account in the indicator-based approach by S10, S11, S12, S13 criteria whose values (Good, Medium, Low) are set on expert judgment. Thus, this measure has the cons of being assigned in a completely subjective manner. The idea of converting the IGD factor into a vulnerability criterion can lead to the assessment of conservation status in a more objective, comprehensive and effective manner. Since IGD is a numerical value, its inclusion as a criterion does not require the establishment of a qualitative scale; it would itself be a measure of the state of conservation.

However, the weight to assign to this criterion, i.e., the importance of the state of conservation among the vulnerability aspects of timber structures, should be evaluated. This exercise should be carried out iteratively, calibrating the weight of the I_{GD} criterion, in a general process of validation of the methodology through the comparison with other vulnerability assessment models.

Chapter

5

Application of the semi-quantitative methods to the case studies

Abstract: In this chapter, the *indicator-based approach* for seismic vulnerability assessment and the *Global durability factor method (GDFM)*, for state of conservation assessment, are applied to the case studies. The methodologies are applied to a different set of buildings, surveyed through the survey form showed in Chapter 3.

Seismic vulnerability is assessed for a set of 10 large-span timber buildings surveyed through the Cartis GL form, while the *GDFM* is applied to a set of 4 buildings surveyed through the SHA-TS form. They have been selected for the sake of representativeness of recurrent timber types of constructions and structural types, as well as different environmental exposure and age of construction.

In the first application, the most vulnerable buildings with regard to the seismic action are identified through the vulnerability index (I'_V), while in the second, the state of conservation is assessed through the I_{GD} index and service life (ESL).

5.1 SEISMIC VULNERABILITY ASSESSMENT OF LARGE-SPAN TIMBER BUILDINGS

The indicator-based approach for seismic vulnerability assessment has been applied on the sample of 10 large-span timber buildings (Figure 5.1; Table 5.1), which have been surveyed through the CARTIS form GL (see Chapter 3, Section 3.2.2). The aspects related to the structural system have been acquired through the application of the last version ("Rev. 10") of the CARTIS form GL Section 3D (Characterization of timber type). Other aspects related to the category of building regularity, building aspects, and geometric features have been surveyed by Faggiano et al. [262] by means of

additional sections of the CARTIS form GL. The principal findings regarding to the 10 buildings are outlined below:

- The materials used for the construction are reinforced concrete, steel, and timber. For almost all the cases studied that are homogeneous and mixed system, the timber is used for the roof. There is one case with a homogeneous system and vertical elements in timber and one case with mixed system and intermediate horizontal elements in timber. The vertical structure system corresponds to different systems: isolated columns, moment resisting frame or uncoupled walls. One structure has a bracing system with concentric V diagonal.
- All roof of the cases of the study have a simple way system. This simple way is, for eight buildings of the study, inclined. The sections of the inclined elements are mostly variable sections and for the horizontal elements its constant sections. A major part of the cases has a bracing system, no chains, and no pushing elements in the roof system. For all the buildings, the closing elements correspond to light elements.
- For all cases of the study, the foundations are not identified.
- In the sample, one building has two floors. However, all buildings have not underground floors. The average of the height floor is between 3,5 m and 14 m for a sport hall. The average of the floor area is really different according to the building: for example, the floor area is lower than 200 m² for the industrial hall and higher than 3.000 m² for the supermarket. All the construction or renovation on these buildings have been made between 1982 and 2011. The buildings of the sample have different use: production with industrial and agricultural hangar, market, public services with school and sport halls. The utilization of this building is higher than 65%, this corresponds to the use percentage in term of spatial and temporal occupation. The owners of the buildings are to 40% public owners and to 60% private owners. The study has also analyzed the presence of block added to the main structure. So, four buildings of the sample have one. These blocks are external to the structure except for one and all these blocks have an analogous function to the main structure use. To finish the building description, the typology of connections is indicated. The connections between the slap and the beams and the connections between the beams and the columns are hinged. Then, the connections columns/foundations, columns/ walls and panels/structure are not identified. Lastly, the connections between the roof and the beams and the columns are either hinged or support.

- All the structures are compact and symmetric, they respect the ratio of largest and of plant. They also present external wall and shear walls symmetrically distributed. Some structures have eccentric blocks added. The elevation regularity is also checked for all the building of the sample. Then, buildings have in maximum 19% of openings in the facade. Concerning the state of conservation, the overall, the vertical structures and the horizontal structures are in a good state for all the buildings and for a major part of the buildings of the sample, the non-structural element are also in a good state of conservation.

Figure 5.1. The 10 large-span timber building surveyed through the CARTIS form [262].

Definition of the decision matrix and its normalization

From the survey form (Chapter 3, Section 3.2.2) the characteristics of each building can be extracted. Therefore, the qualitative decision matrix can be filled. It is a matrix characterized by 10 rows (number of case studies) and the 32 columns (number of criteria). However, for some characteristics and for some cases, a lack of information have been noted; thus, in this case the worst

value among the values of other buildings has been used. For example, for the bracing criterion (S17), the worst condition is the lack of bracing system, so the choice "No" has been selected; similarly for the chain criterion (S18), whose worst condition is the absence of chains (No).

Table 5.1. The 10 large-span timber building surveyed through the CARTIS form.

City	Building	Designation
Bentivoglio	Agricultural hangar	1
Bentivoglio	Mall	2
Castello d'Argile	Industrial hangar	3
Correggio	School cafeteria	4
Correggio	School gym	5
Correggio	School	6
Correggio	Supermarket	7
Crevalcore	Laboratory	8
Galliera	Scool gym	9
San Giovanni in Perscieto	School gym	10

After defined each greatness of the qualitative decision matrix, it necessary to transform this in quantitative values. Therefore, the quantitative decision amatrix has been defined as shown in Section 4.3.2.2. The full version of the qualitative and quantitative decision matrix are given in Appendix D.9 and D.10, respectively. An extract of the quantitative decision matrix is showed in Table 5.2.

Table 5.2. Decision matrix (quantitative values) for the case studies (integral table at Appendix D.9)

Case Study	S1 [-]	S2 [-]	S3 [-]	S4 [-]	S5 [-]	S6 [-]	S7 [-]	S8 [-]	S9 [year]	S10 [-]
1	1	1	1	1	1	1	1	1	2001	3
2	1	1	1	1	1	1	0	1	2008	3
3	1	1	1	1	1	1	1	1	2008	3
4	1	1	1	1	0	0	1	1	2001	3
5	1	1	0	1	1	1	1	0	2001	3
6	1	1	0	1	0	0	1	0	2008	3
7	1	1	0	1	0	1	1	0	2008	3
8	1	1	0	1	1	0	1	0	2011	3
9	1	1	1	1	1	0	1	1	2001	3
10	1	1	1	1	1	1	1	0	1986	3

Once the decision matrix is defined the normalized decision matrix has been defined through the Equation 4.1. An extract of the normalized decision matrix is shown in Table 5.3, whereas the integral table can be found in Appendix D.11.

Assignment of weights for each criterion

The next step is the weighting of the matrix with the weights of each criteria defined before (Section 4.3.2.2). Since 3 classifications of criteria grouped by categories have been proposed, there will be 3 normalized-weighted decision matrices, corresponding to C1, C2 and C3 classifications. An extract of the decision matrix for the classification C1 is showed in Table 5.4 whereas the integral table is provided at Appendix D.12.

Table 5.3. Normalized decision matrix for the case studies (integral table at Appendix D.11)

Case Study	S1 [-]	S2 [-]	S3 [-]	S4 [-]	S5 [-]	S6 [-]	S7 [-]	S8 [-]	S9 [-]	S10 [-]
1	0.316	0.316	0.408	0.316	0.378	0.408	0.333	0.447	0.316	0.316
2	0.316	0.316	0.408	0.316	0.378	0.408	0.000	0.447	0.317	0.316
3	0.316	0.316	0.408	0.316	0.378	0.408	0.333	0.447	0.317	0.316
4	0.316	0.316	0.408	0.316	0.000	0.000	0.333	0.447	0.316	0.316
5	0.316	0.316	0.000	0.316	0.378	0.408	0.333	0.000	0.316	0.316
6	0.316	0.316	0.000	0.316	0.000	0.000	0.333	0.000	0.317	0.316
7	0.316	0.316	0.000	0.316	0.000	0.408	0.333	0.000	0.317	0.316
8	0.316	0.316	0.000	0.316	0.378	0.000	0.333	0.000	0.317	0.316
9	0.316	0.316	0.408	0.316	0.378	0.000	0.333	0.447	0.316	0.316
10	0.316	0.316	0.408	0.316	0.378	0.408	0.333	0.000	0.313	0.316

Table 5.4. Weighted-Normalized decision matrix according to the classification C1 (integral table at Appendix D.12)

Case Study	S1 [-]	S2 [-]	S3 [-]	S4 [-]	S5 [-]	S6 [-]	S7 [-]	S8 [-]	S9 [-]	S10 [-]
1	0.023	0.023	0.030	0.023	0.028	0.030	0.025	0.033	0.018	0.014
2	0.023	0.023	0.030	0.023	0.028	0.030	0.000	0.033	0.018	0.014
3	0.023	0.023	0.030	0.023	0.028	0.030	0.025	0.033	0.018	0.014
4	0.023	0.023	0.030	0.023	0.000	0.000	0.025	0.033	0.018	0.014
5	0.023	0.023	0.000	0.023	0.028	0.030	0.025	0.000	0.018	0.014
6	0.023	0.023	0.000	0.023	0.000	0.000	0.025	0.000	0.018	0.014
7	0.023	0.023	0.000	0.023	0.000	0.030	0.025	0.000	0.018	0.014
8	0.023	0.023	0.000	0.023	0.028	0.000	0.025	0.000	0.018	0.014
9	0.023	0.023	0.030	0.023	0.028	0.000	0.025	0.033	0.018	0.014
10	0.023	0.023	0.030	0.023	0.028	0.030	0.025	0.000	0.018	0.014

Definition of the orders among the different alternatives

To calculate the vulnerability index (I'_V) of each building, it is necessary to compare the real solution (A_i), i.e., consider the vector of each alternative corresponding to the rows of the matrix V_{mxn} for each criterion, and the positive (A^+) and negative (A^-) ideal solutions (Equation 4.5 and 4.6), i.e., the best and worst combination of criteria, representing the building characteristics. To know the positive and negative ideal solutions, each criterion is identified as Benefit criterion (B) or Cost criterion (C) (Appendix D.13). The best alternative has the highest score in case of Benefit criteria, the lowest score in case of Cost criteria. For example, if the structure's regularity checks (S1, S2, S3, S4, S5, S6, S7, S8) are met, its seismic vulnerability is reduced, so these criteria are of benefit.

Once the ideal solution are defined (Appendix D.14) for the three classifications (C1, C2, C3), the Euclidean distance of the real solution (A_i) from the ideal ones can be calculated using the Equation 4.8 and 4.9. In the end the vulnerability index can be evaluated as relative closeness using the Equation 4.10. It is important to underline that the higher the I'_V, the lower the building's vulnerability to seismic action.

Table 5.5. Euclidean distance and vulnerability index I'_V according to the 3 classifications.

	C1			C2			C3		
Case Study	Si^+ [-]	Si^- [-]	I'_V [-]	Si^+ [-]	Si^- [-]	I'_V [-]	Si^+ [-]	Si^- [-]	I'_V [-]
1	0.014	0.068	0.822	0.100	0.066	0.619	0.041	0.053	0.633
2	0.030	0.063	0.792	0.107	0.056	0.431	0.046	0.049	0.565
3	0.017	0.067	0.679	0.116	0.029	0.400	0.048	0.047	0.525
4	0.045	0.052	0.643	0.114	0.045	0.387	0.051	0.039	0.515
5	0.045	0.053	0.609	0.063	0.103	0.357	0.034	0.058	0.495
6	0.064	0.026	0.541	0.118	0.040	0.345	0.059	0.026	0.461
7	0.057	0.040	0.538	0.107	0.060	0.298	0.059	0.033	0.436
8	0.056	0.041	0.426	0.114	0.047	0.285	0.053	0.041	0.436
9	0.034	0.061	0.412	0.103	0.064	0.255	0.045	0.050	0.359
10	0.037	0.058	0.293	0.100	0.076	0.208	0.049	0.042	0.310

From the analysis of the results (Table 5.5), it can be observed that, first, for C2 and C3 classifications, the change in vulnerability index is smaller than for C1 classification ([0.619-0.208] = 0.411, [0.633-0.310] = 0.323, [0.822-0.293] = 0.529). The maximum value of the seismic vulnerability index, i.e., identifying the least vulnerable building, is lower for C2 and C3 than for C1,

i.e., when the Structure category is prioritized or when the latter has the same importance as the Regularity and Building categories. The C2 and C3 classifications generally result in similar seismic vulnerability indices for most cases. It can be seen that through C2 buildings are more vulnerable, while through C1 they are less vulnerable.

Table 5.6 shows the three rankings corresponding to the classifications. Specifically, vulnerability levels are defined through the following scales of Vulnerability Index values:

- High vulnerability (black): $I'_v \in [0\text{-}0.24]$;
- Medium-High vulnerability (dark grey): $I'v \in [0.25\text{-}0.50]$;
- Medium-Low vulnerability (grey): $I'v \in [0.51\text{-}0.75]$;
- Low vulnerability (white): $I'v \in [0.76\text{-}1.00]$.

It can be observed that for half of the cases, buildings have a similar position in all three classifications. For example, the school in Correggio (building 6) takes position 10 in C1 and C3 and position 9 in C2. However, for some buildings the order is totally different, presenting, therefore, significantly different vulnerabilities depending on the priority assigned to the vulnerability criteria. For example, the industrial hangar (building 3 – Castello d'Argile) is the most vulnerable building by considering the classification C2 (I'_V: 0.208), however it results to be the almost the less vulnerable according to the classification C1 (I'_V: 0.792). It assumed an intermediate position according to the classification C3, when the 3 categories have the same importance.

Table 5.6. Vulnerability index (I'v): comparison of results.

City	Intended use of building	Designation	I'_V		
			C1	C2	C3
Bentivoglio	Shopping center	1	0.822	0.400	0.565
Bentivoglio	Agricultural	2	0.679	0.345	0.515
Castello d'Argile	Industrial	3	0.792	0.208	0.495
Correggio	School canteen	4	0.541	0.285	0.436
Correggio	School gym	5	0.538	0.619	0.633
Correggio	School	6	0.293	0.255	0.310
Correggio	Market	7	0.412	0.357	0.359
Crevalcore	Laboratory	8	0.426	0.298	0.436
Galliera	School gym	9	0.643	0.387	0.525
San Giovanni in P.	School gym	10	0.609	0.431	0.461

The school in Correggio (building 6) is in the last rank for the three classifications, so according to this comparative study, this is the building the most vulnerable building. From reading the results, therefore, it is possible to say that Structure are the parameters that most influence the vulnerability of the structure (C2, C3). The third classification (C3) confirms this observation because the seismic vulnerability indexes of this classification are similar for the cases' majority to the second classification which give more importance to the structural elements. Moreover, as already said, all building aspects generate better value of vulnerability index.

5.2 DURABILITY ASSESSMENT OF TYPICAL EXISTING TIMBER STRUCTURES

The method is applied and validated on four simple case studies located in different municipalities of the Southern Italy (see Chapter 3, Section 3.3.2). They have been selected for the sake of representativeness of recurrent timber types of constructions and structural types, as well as different environmental exposure and age of construction (Recorded Lifetime: RLT). The proposed method is applied to specific members of the case studies, as shown in Figure 5.2. The application of the SHA-TS survey form assisted in the acquisition of the durability aspects needed for the application of the GDFM. Although a critical state of preservation has not been recorded, the investigated structures showed different types of degradation:

case a) It is placed outdoor, part of the member has fine cracks due to direct exposure to UV radiation and contact with rainwater;

case b) The roofing structure is placed outdoor; some parts are directly exposed to UV radiation and rainwater, showing discoloration, while columns show also fine cracks;

case c) The intermediate floor is placed inside a residential building; the beams show the evidence of insect attack (Cerambycidea), due to the presence of sapwood; however, the decay is confined to a thin layer of the cross-section.

case d) The structure is placed at the roof level; struts and ties show degradation by insect attack (Cerambycidea and Anobium), mainly due to the presence of sapwood in the members.

a) b) c) d)

Figure 5.2. The 4 case studies surveyed through the SHA-TS form [427]: a) case study a; b) case study b; c) case study c; d) case study d.

Definition of the decision matrix and its normalization

The decision matrix has been constructed considering the conditions of the case studies (a, b, c, d), the reference case (Cr) and the ideal cases, positive (A^+) and negative (A^-). It has been evaluated on the basis of the proposed sub-factors (Appendix E.1) and detected, for each case study, using the SHA-TS form. The decision matrix in quantitative values is shown in Table 5.7, whereas the qualitative decision matrix is provided in Appendix E.3.

Table 5.7. Decision matrix (quantitative values) for the case studies (continued)

Case study	A1 [-]	A2 [-]	A3 [mm]	A4 [-]	A5 [-]	A6 [-]	A7 [-]	A8 [-]	A9 [%]	B1 [-]	B2 [mm]	C1 [-]
a)	3	3	1	2	7	3	1	4	16	3	2	3
b)	1	4	3	4	7	3	1	4	16	3	3	3
c)	1	3	3	4	5	1	1	2	16	1	1	1
d)	1	5	5	4	3	1	1	2	16	1	1	1
C_r	3	3	1	3	7	3	1	5	16	1	3	1
A^+	3	5	1	5	9	3	1	6	8	3	5	3
A^-	1	1	5	1	1	1	1	1	24	1	1	1

Once the decision matrix D is defined (Table 5.7, Table 5.8), the normalized decision matrix R has been built through the Equation 4.1.

Table 5.8. Decision matrix (quantitative values) for the case studies (continued)

Case study	C2 [-]	D1 [-]	D2 [-]	E1 [-]	E2 [mm/yrs]	E3 [%]	E4 [KW/m^2]	E5 [-]	F1 [-]	G1 [-]	G2 [-]
a)	3	3	3	1150	850	75	700	7	6	5	1
b)	1	3	3	1150	850	75	700	5	6	5	1
c)	1	3	3	1150	900	55	700	9	6	3	1
d)	3	3	3	1150	1080	55	700	9	6	3	1
C_r	1	1	1	1150	850	75	700	7	6	5	3
A^+	3	3	3	500	400	55	700	9	6	7	3
A^-	1	1	1	3500	1300	95	100	1	1	1	3

Table 5.9. Normalized decision matrix for the case studies (continued)

C. S.	A1	A2	A3	A4	A5	A6 [10^3]	A7	A8	A9	B1	B2	C1
a)	1.88	1.88	0.63	1.25	4.39	1.88	0.63	2.51	10.04	1.88	1.25	1.88
b)	0.63	2.51	1.88	2.51	4.39	1.88	0.63	2.51	10.04	1.88	1.88	1.88
c)	0.62	1.85	1.85	2.47	3.09	0.62	0.62	1.23	9.87	0.62	0.62	0.62
d)	0.58	2.90	2.90	2.32	1.74	0.58	0.58	1.16	9.26	0.58	0.58	0.58
C_r	1.53	1.53	0.51	1.02	1.53	1.53	0.51	1.53	8.14	0.51	1.53	1.53
A^+	1.88	1.88	0.63	1.88	4.39	1.88	0.63	3.14	10.04	0.63	1.88	0.63
A^-	3.16	5.26	1.05	5.26	9.47	3.16	1.05	6.31	8.42	3.16	5.26	3.16

Table 5.10. Normalized decision matrix for the case studies (continued)

C. S.	C2	D1	D2	E1	E2	E3 [10^3]	E4	E5	F1	G1	G2
a)	1.88	1.88	1.88	721.41	533.22	47.05	439.12	4.39	3.76	3.14	0.63
b)	0.63	1.88	1.88	721.41	533.22	47.05	439.12	3.14	3.76	3.14	0.63
c)	0.62	1.85	1.85	709.66	555.39	33.94	431.97	5.55	3.70	1.85	0.62
d)	1.74	1.74	1.74	665.91	625.37	31.85	405.33	5.21	3.47	1.74	0.58
C_r	1.53	1.53	1.53	585.25	585.25	38.17	559.81	3.56	3.05	2.54	0.51
A^+	0.63	0.63	0.63	721.41	533.22	47.05	439.12	4.39	3.76	3.14	1.88
A^-	3.16	3.16	3.16	526.02	420.81	57.86	736.43	9.47	6.31	7.36	3.16

Assignment of weights for each criterion

By adjusting the decision matrix through the weights (w_j; Appendix E.1), the influence of different durability aspects (sub-factors) is taken into account. The weighted-normalized decision matrix is showed in Table 5.11, Table 5.12, Table 5.13.

Table 5.11. Weighted - normalized decision matrix for the case studies (continued)

Case Study	A1	A2	A3	A4	A5 [10^5]	A6	A7	A8	A9
a)	7.90	13.87	3.03	13.28	5.68	1.32	0.61	2.91	88.68
b)	2.63	18.49	9.08	26.57	5.68	1.32	0.61	2.91	88.68
c)	2.59	13.64	8.93	26.13	3.99	0.43	0.60	1.43	87.24
d)	2.43	21.33	13.97	24.52	2.25	0.40	0.56	1.34	81.86
C_r	6.41	11.25	2.46	10.78	1.97	1.07	0.49	1.77	71.95
A^+	7.90	13.87	3.03	19.92	5.68	1.32	0.61	3.63	88.68
A^-	13.25	38.75	5.08	55.69	12.24	2.21	1.02	7.31	74.36

Table 5.12. Weighted - normalized decision matrix for the case studies (continued)

Case Study	B1	B2	C1	C2 [10^5]	D1	D2	E1
a)	7.90	13.87	3.03	13.28	5.68	1.32	0.61
b)	2.63	18.49	9.08	26.57	5.68	1.32	0.61
c)	2.59	13.64	8.93	26.13	3.99	0.43	0.60
d)	2.43	21.33	13.97	24.52	2.25	0.40	0.56
C_r	6.41	11.25	2.46	10.78	1.97	1.07	0.49
A^+	7.90	13.87	3.03	19.92	5.68	1.32	0.61
A^-	13.25	38.75	5.08	55.69	12.24	2.21	1.02

Table 5.13. Weighted - normalized decision matrix for the case studies (continued)

Case Study	E2	E3	E4	E5 [10^5]	F1	G1	G2
a)	7.90	13.87	3.03	13.28	5.68	1.32	0.61
b)	2.63	18.49	9.08	26.57	5.68	1.32	0.61
c)	2.59	13.64	8.93	26.13	3.99	0.43	0.60
d)	2.43	21.33	13.97	24.52	2.25	0.40	0.56
C_r	6.41	11.25	2.46	10.78	1.97	1.07	0.49
A^+	7.90	13.87	3.03	19.92	5.68	1.32	0.61
A^-	13.25	38.75	5.08	55.69	12.24	2.21	1.02

Definition of the orders among the different alternatives

Once the normalized-weighted matrix has been determined, the distance of each real alternative (case studies a, b, c, d) and the reference alternative (Cr), from the two ideals positive (A^+) and negative (A^-) alternatives has been calculated. Thus the coefficient of relative closeness (RC_i) has been evaluated (Table 5.14).

Table 5.14. Euclidean distances and relative closeness

Case study	Si^+ [-]	Si^- [-]	RC_i [-]
a)	0.0156	0.0151	0.49
b)	0.0156	0.0151	0.49
c)	0.0150	0.0162	0.52
d)	0.0136	0.0194	0.59
C_r	0.0156	0.0151	0.49
A^+	0.0133	0.0263	1.00
A^-	0.0263	0.0115	0.00

It is interesting to note that for the positive ideal solution it has been found $RC_A{}^+$:1.00 since this ideal case represents the building least susceptible to degradation phenomena. In contrast, the negative ideal solution is the most susceptible, thus RC_{A-}: 0.00 has been found. In contrast, for the reference case (Cr), for which IGD: 1.00 (ESL=RSL) is assumed, a RC_i equal to 0.49 has been found. Then the IGD has been evaluated through the Equation 4.12 and the ESL has been calculated by previously defining the RSL (

Table 5.15). In absence of experimental tests and considering the design life prescribed by the Italian building Code [71] for ordinary buildings, a RSL equal to 50 years is assumed for all the buildings.

The longest ESL has been determined for case studies “c” and “d” (52 and 59 years respectively), probably because they are placed in indoor environment, although case studies “a” and “b” are made of new timber, but they are in outdoor environment.

Table 5.15. The results of GDFM application to the case studies (a, b, c, d).

Case study [-]	RSL [years]	RC_i [-]	I_{GD} [-]	ESL [years]	RLT [years]
a)	50	0.49	1.00	50	6
b)	50	0.49	1.00	50	11
c)	50	0.52	1.05	52	150
d)	50	0.59	1.19	59	200
C_r	50	0.49	1.00	50	-
A^+	-	1.00	1.74	-	-
A^-	-	0.00	0.76	-	-

Nevertheless, the ESL values obtained for cases “c” and “d” are far from the recorded lifetime (RLT), since they were built more than 150 years ago, and they are still in service. At the same time for cases “a” and “b” an ESL

equal to 50 years has been found. Hence, they should still keep in service for a lifetime respectively equal to 44 and 39 years.

Chapter

6

Vulnerability assessment at building scale: contributions for the diagnosis and analysis of existing timber structures

Abstract: To assess the vulnerability of existing structures, it is essential to conduct a thorough on-site assessment. For this purpose, geometric survey, characterization of mechanical properties, and diagnosis are key tasks. Visual strength grading (VSG) and non-destructive techniques (NDT) are the most common approaches for mechanical identification of existing timber structures. However, the lack of adequate correlations between destructive and non-destructive parameters, as well as the poor presence or absence of standards for VSG, make such methodologies ineffective.

The following chapter shows the mechanical characterization of structural members made of different wood species. Both experimental campaigns concerned the geometric survey with different techniques, the VSG analysis and NDT application. In the end the destructive test (DT) in bending and long-term test in bending have been performed.

Methodologies and procedure are extensively shown, highlighting the main findings for the different wood species. Linear regressions between NDT and DT are provided, highlighting the most reliable correlation useful for on-site mechanical identification. Furthermore, the performance profiles attributed by VSG analysis have been compared with the results of destructive tests. The creep behaviour has been evaluated in long-term test and a comparison with the Standard prescription has been carried out.

6.1 MOTIVATION AND GOALS

In order to evaluate the structural vulnerability, it is necessary to carry out a comprehensive structural analysis, which involves the application of various methodologies, ranging in complexity, to assess the structural performance. Fundamental elements of the structural model are the geometry, constraint conditions, and physical-mechanical properties, while the loads model are to be evaluated taking into account the hazards features. Therefore, the reliability of the vulnerability assessment is closely related to the degree of knowledge of the structure, as well as to the suitable structural and hazard modelling.

The knowledge of the structure is generally achieved through on-site assessment, where fundamental tasks as the geometrical survey, mechanical characterization and diagnosis of decay and structural issues are performed [168], [310], [314].

The geometrical survey consists in acquiring geometric attributes, as the cross-section dimension, member's length and the overall configuration of the structures, which are crucial both for structural and load modelling. However, the survey of existing timber structures, especially the historic one, is a challenging task as they are often characterized by complex and irregular geometries. In this field, innovative surveying techniques utilising instruments such as laser scanners and high-performance cameras can support the technicians in their work [326], [390]. However, the effectiveness of the methodologies depends on several parameters, as the test sample, the instrumentation and the operating conditions. As a consequence, these aspects should be analysed in order to carry out an effective geometrical survey.

As regard the mechanical characterization of existing timber structures the most common approach consist in performing visual strength grading (VSG) and non-destructive techniques (NDT), since they don't compromise the structural integrity. The first approach (VSG) address the evaluation of macroscopic characteristics of timber, assigning a performance profile established by the Standards to the investigated members. For this task, the techno-scientific community should be supported by guidelines or regulations that define grading criteria and performance profiles specifically adapted to the wood species in question, taking into account its geometric and anatomical characteristics. Thus, the visual analysis can provide an estimation that is closer to the actual capabilities of the investigated members.

On the other end NDTs are frequently used as a tool to support indirect evaluation of wood's mechanical properties and for diagnosing the state of

preservation. These techniques are effective to on-site assessment when reliable regression laws are available, enabling the prediction of wood mechanical properties (e.g., bending strength, modulus of elasticity in parallel compression, etc.) without the need for destructive testing. This approach is supportive of VSG evaluation, which is limited to visual analysis of the external part of the member. At the same time the use of these techniques should be supported by established and shared procedures.

Against this background, two experimental campaigns involving structural elements in different wood species have been performed. They regard Chestnut (*Castanea Sativa* Mill.) and Corsican Pine (*Pinus Nigra* subsp. *laricio* (Poir.) Maire) wood members extracted from an historical building in Southern Italy and wood logs in *Acacia dealbata* Link harvested from the Peneda-Gerês National Park (Portugal).

Nowadays these different wood species can be found in different existing buildings, within the framework of historical and vernacular architecture. Corsican Pine and Chestnut have been widely used in historical architecture, especially in Southern Italy, where timber was generally applied in floors and roofs [173], [180], [436], [181]. Typical application consisted of the hand-working of logs to obtain roughly squared members which were directly used as beams or connected to make trusses [173], [170]. Instead, the use of *Acacia* wood can be seen in the context of North African vernacular architecture, where round members are used in floors and roofs of buildings with clay walls [146], [147]. Although few applications of this material in construction field have been observed, preliminary research on related species indicates promising structural potential for *Acacia* wood.

Thus, with the purpose to provide the most efficient procedure for the in-situ mechanical characterization of timber members, several tests have been performed in both experimental campaigns. The typical steps of in situ detailed assessment, i.e., geometric survey, visual strength grading (VSG) and non-destructive tests (NDT), have been carried out in the laboratory on timber members. The sample of ancient timber has also been surveyed using digital techniques, such as photogrammetry and laser scanners. Pros and cons of the procedures and instrumentation have been extensively described, as well as the acquisition and processing times. Subsequently, four-point bending tests up to failure have been performed to evaluate the elastic modulus and bending strength. Only for the ancient timber sample long-term bending tests have been carried out to investigate the creep behaviour of the two wood species. From the statistical analysis of the results, linear regressions between destructive and non-destructive parameters have been determined, highlighting the most reliable relationships useful for the in situ mechanical

identification through NDTs, validated through the valuation of the correspondence with the performance profiles assigned by VSG and the DT measures.

6.2 MECHANICAL CHARACTERIZATION OF *CASTANEA SATIVA* MILL. AND *PINUS NIGRA* SUBSP. *LARICIO (POIR.) MAIRE*

6.2.1 GENERAL METHODOLOGY

The experimental campaign has been carried out on 18 specimens of timber in structural dimension which were extracted from a historical building placed in the historic city of Cosenza. The experimental campaign has been carried out at Labarotory "Grandi Modelli" of the Department of Civil Engineering at University of Calabria (Arcavacata di Rende, Cosenza, Italy). The experimental tests has been performed through a cooperation with the University of Calabria, University of Florence and the Italian National Research Council.

In the experimental activity the following methods and techniques has been performed:

- size survey performed through Direct (DS) and indirect techniques (3D digital acquisition methodologies), as Laser Scanner Survey (LSS) and Photogrammetric Survey (PS);
- Visual Strength Grading (VSG) analysis;
- Non-Destructive Test (NDT);
- Destructive Test (DT) in bending;
- Long-Term test (LTT) in bending.

The moisture content measurement, the density estimation, drilling resistance test, acoustic and vibrational test have been performed in the context of the NDT techniques.

The objectives and aims of this experimental work are manifold:

- evaluating the effectiveness and efficiency of 3D digital surveying techniques in the application on ancient timber, verifying pros and cons compared to traditional direct survey methods;

- Assessing the usefulness and effectiveness of 3D digital surveying method in assessing mechanical properties of timber through VSG and NDT;
- Evaluating the reliability of VSG analysis on existing timber structures comparing the results of visual grading with those of NDT and DT;
- Evaluating the reliability of NDT comparing the test results with those of DT and VSG;
- Estimating the influence environmental thermos-hygrometric properties on the creep behaviour of timber;
- Estimating correlation between NDT and DT parameters; experimental results are discussed and statistically analysed in order to calibrate novel correlations between NDT and DT parameters, based on linear regression model.

For each type of test, the methodology, the test-equipment and set-up are fully described. Then the results are showed and discussed, highlighting the main achievements of the work. The main aim of this study consists in providing new test procedures, correlations between NDT-DT parameters, relations between VSG and DT results, in order to support the technical-scientific community in the on-site assessment of the heritage timber.

6.2.2 THE SAMPLE OF STUDY

6.2.2.1 The ancient trusses of "Lyceum Gymnasium B. Telesio"

The experimental campaign has been carried out on 18 timber specimens in structural dimension. They are part of the structs extracted from the roof trusses of the XVI century building, the *lyceum gymnasium* Bernardino Telesio (Figure 6.1.a), in the historic centre of Cosenza, Italy [437]. The specimens date back approximately to the mid eighteenth century, since after the Cosenza earthquake (1854) the construction of the roof structures took place. In the 2020, as part of the building's safety works, the timber trusses were replaced and 18 struts were deposited at the Laboratory of "Grandi Modelli" at University of Calabria, in Cosenza.

In particular the ancient timber struts were extracted from the roof structures of the auditorium located in the *lyceum gymnasium* Bernardino Telesio. The roof structures consisted of nine Palladian trusses composed of two struts, one king post, one tie-beam and two diagonals, covering a span of

approximately 12 metres (Figure 6.1.b). All the nodes of the Palladian trusses were characterized by traditional notched joint and strengthening by metal stirrups (Figure 6.2). Furthermore, the king post was connected to the tie beam through a metal bracket, useful to keeping the truss in plane and preventing the excessive tie-beam deflection. The metal bracket was connected to the timber members through metal nails.

a) b)

Figure 6.1. a) The *lyceum gymnasium* Bernardino Telesio, Cosenza, Italy; b) The ancient timber trusses [437].

6.2.2.2 Main features of the identified wood species

The sample's species identification have been performed in macroscopic way. From the visual analysis have been found that most of the members (13) were in Corsican Pine (*Pinus nigra* subsp. *laricio* (Poir.) Maire) wood and the others (5) in Chestnut *(Castanea Sativa* Mill.*)*.

These two wood species are typically located in Mediterranean area. The Corsican Pine is a plant of preglacial origin found mainly in the mountains of Calabria, Corsica and Sicily, where it forms mountainous forests between about 600 m and 1500 m, on a generally siliceous substrate [438]. The Chestnut appears for the first time in some areas of the Italian peninsula during the first centuries of the Christian period and nowadays Chestnut trees are grown in many parts of the world, including Europe, North America, South America, Asia, and Africa [439].

The wood species have been recognized through the visual analysis of the macroscopic features of timber. The Corsican Pine (PNL) have been recognized thanks to the presence of resinous and rounded knots having

modest dimensions (Figure 6.3), as well as by the presence of differentiated heartwood in the transversal cross section. At the same time the 5 Chestnut struts (CS) have been identified for the presence of large and elliptical knots, characterized by the flaming (Figure 6.4); furthermore, the presence of porous rings and discoloration due to steel chain corrosion have been found in the cross section of the Chestnut members. In the end, members with irregular geometry and a non-squared cross-section have been identified for Chestnut; this is probably due to the modest dimension of the Chestnut trees typically spread in Italian land.

a) b)

Figure 6.2. a) The notched joint in correspondence of the diagonal-strut node (Ruggieri, 2019b); b) The node among king post, diagonals and tie-beam, with evidence of the metal bracket and nails (Ruggieri, 2019c).

6.2.3 THE GEOMETRICAL SURVEY

6.2.3.1 Direct survey (DS)

Firstly, a direct survey has been carried out with simple surveying instruments such as a folding ruler, a roller meter and squares. This methodology has been applied, since it is frequently used in on site assessment when conventional structures have to be surveyed. The aim is to obtain the main dimension of the specimens in order to get a benchmark model for the 3D acquisition method analysis.

Thus, the length (L) and the cross section of the struts have been measured. With regard to the cross-section, variable geometries have been found: many elements had almost square cross-sections, characterised by small and large wanes, while some elements had an almost circular cross-section. The latter characteristics has been frequently found in CS members.

Figure 6.3. The PNL specimen "3": evidence of resin, as well as small-rounded knots.

Figure 6.4. The CS specimen "10": evidence of large elliptical knots and variable geometry.

However, the cross-section of the whole sample have been approximated to an equivalent squared cross-section, having a base (b) and an height (h). Thus, the equivalent dimensions have been measured in the correspondence of the middle third of the members, so they results as the average value measured along the middle third of the member. In this way the volume (V_{DS}) of each member has been calculated as follow (Eq. 6.1):

$$V_{DS}=b \cdot h \cdot L \tag{6.1}$$

where:

V_{DS} geometric volume from direct survey measurement [mm^3];

b base of the cross-section [mm];

h height of the cross-section [mm];

L length of the member [mm].

In this step of analysis another fundamental task have been done for the purpose of destructive test (DT). The numbering of each face of the specimens according to a chosen nomenclature have been carried out. Nevertheless this nomenclature have been used also for the survey of the timber defects for visual strength grading analysis and for designing the NDT test set-up.

Thus, in accordance with standard UNI EN 408 [333], some fundamental points have been identified on the member: the middle point of the member (section "D"), the two supporting points (sections "A" and "B") and two points of load (section "C" and "E"). Thus, the numbering of the faces of the specimens was carried out, taking into account the type of stress acting when the member was in place. On the struts, the notch present necessary for the connection between the strut and the diagonal was identified in order to define the tensioned edge of the member. Thus the numeration have been assigned according to a clockwise increasing with direction from section A to section B (Figure 6.5). Anyway, distances and positions of the sections on the specimen will be discussed in more detail in the Section 6.3.6 (Destructive test in bending). The section have been fixed on the specimen through adhesive tapes (Figure 6.6.a).

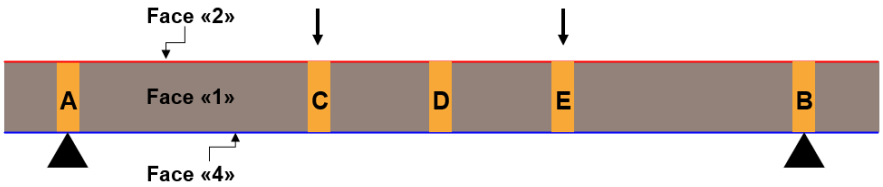

Figure 6.5. Nomenclature of the specimen.

a) b)

Figure 6.6. a) Identification of the sections on the specimens; b) Section A identified with adhesive tape.

Results

Thus, each specimen has been measured and the volume has been calculated (Table 6.1). The average dimensions of the cross-size are 220 mm in base and 200 mm in height. The length of the specimens range from 350 cm to 450 cm, while the average value is approximately equal to 420 cm.

6.2.3.2 Laser scanner survey (LSS)

Test equipment

The device *Focuss Plus 150* laser scanner manufactured by *FARO Technologies, Inc.*, have been used for LSS. It was furnished by the Architectural Survey laboratory of the Department of Civil Engineering of the University of Calabria. The scans have been processed using the software supplied with the *SCENE* detection tool from *FARO Technologies, Inc.,* version 2022.1.0.9661 and then elaborated in mesh with *software Geomagic Wrap 2021 di 3D Systems, Inc.*

Table 6.1 Results of direct size survey (DS): main dimension of the timber specimens.

Wood species [-]	Specimen [-]	b [mm]	h [mm]	L [mm]	V_{DS} [m^3]
CS	2	230	200	4403	0.203
	9	210	200	4373	0.184
	10	190	215	3834	0.157
	11	205	180	3965	0.146
	15	210	235	4180	0.206
PNL	1	210	190	4400	0.176
	3	245	180	4280	0.189
	4	230	195	3498	0.157
	5	230	195	4369	0.196
	6	220	200	4493	0.198
	7	205	190	4465	0.174
	8	220	215	4427	0.209
	12	240	198	4288	0.204
	13	245	175	4038	0.173
	14	235	205	3911	0.188
	16	220	180	4274	0.169
	17	195	180	4048	0.142
	18	215	205	4062	0.179

Procedure and test set-up

The survey operations took place in the Laboratory of "Grandi Modelli" at the University of Calabria. After the delimitation of the operation area, two

concrete supports have been positioned to support the specimens during the scanning operation. In each survey operation, 2 specimens have been surveyed at a time, so that the 18 struts were measured in 9 operations. This was due to the high performance of the instrumentation, equipped with 360° spherical scanning horizontally and 300° vertically. The LLS process has been thus standardised, defining a minimum number of stations and providing additional stations depending on the criticality and peculiarities of the specimens. In this way, the following standard positions have been identified:

- 3 bottom scans per specimen h: 0.80 m (Figure 6.7.a);
- 1 scan per head h: 2.00 m (Figure 6.7.b);
- 1 scan per outer side surface h: 2.00 m.

Variations in positions or the addition of further stations were determined on a case-by-case basis, anyway from eight to thirteen stations per single survey have been used.

a) b)

Figure 6.7. Laser scanner survey on specimen 16 and 17: a) station at height equal to 0.80 m; b) station at height equal to 2.00 m.

Acquisition consists of two moments: point detection and photographic acquisition. From the captured images has been possible to obtain the texture of the materials and spherical panoramic photos useful for the subsequent stages of exploration of the cloud. Thus, the following steps have been performed for each survey operation:

1. positioning of specimens on the supports;
2. identification of relevant notches or defects.
3. laser detection (from 8 to 13 stations for each specimen couple);
4. specimen storage (10 min).

The measurement method used has been time-of-flight calculated by means of phase difference. The following process steps have been done in order to obtain the editable point cloud: importing, registration and alignment of the scans, then points cloud exploration and exportation. The laser scanner surveys obtained in this way did not need any further scaling. Thus, after delimiting the point volume of the specimens by means of a clipbox, the exportable and editable point cloud has been obtained. Subsequently, the point clouds have been meshed to calculate the volume of the test specimens, resulting in a grid of connected polygons which nodes are the surveyed points. Thus, from *Geomagic Wrap software* the volume of the specimens have been estimated, as well as the cross-section geometry has been obtained and extrapolated in a CAD file.

Results

A total of 116 scans have been carried out from the survey of the 18 specimens. For each specimen 13 millions of points have been acquired, having a resolution of 1.75 point/mm^2 (Figure 6.8). As regard to the time of work the following results have been found for each specimen:

- acquisition operation: 75 minutes;
- cloud point construction: 60 minutes;
- mesh construction: 40 minutes.

Thus, in total LSS took 175 minutes for the data acquisition, processing and graphical restitution.

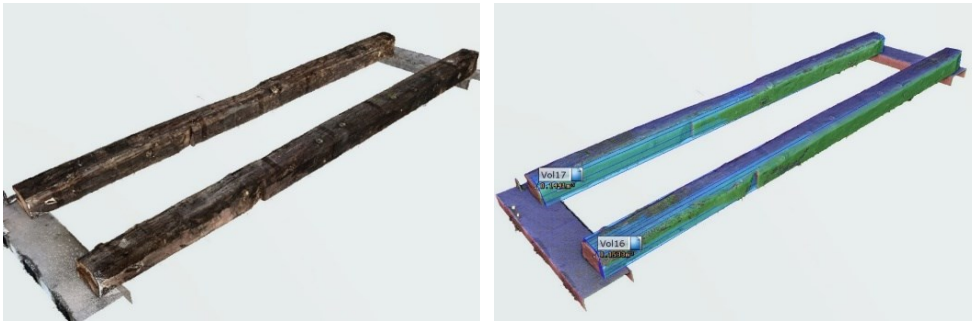

a) b)

Figure 6.8. a) Texturized point-cloud model of specimen 16 and 17 from LSS method; b) Mesh model of specimen 16 and 17 from LSS method.

Thus the volume (V_{LSS}) of each specimen has been calculated from the mesh models (Table 6.2).

6.2.3.3 Photogrammetric survey (PS)

Test equipment

The camera *Fujifilm X-T2*, in combination with optics *Fujifilm XF 18-55 f/2.8-4R LM OIS* lens, has been used for the photogrammetric survey. Furthermore, the software *Metashape Professional version 1.7.1* licensed by *Agisoft LLC.* have been used for the data elaboration and restitution.

Procedure and test set-up

The survey operations took place in the Laboratory of "Grandi Modelli" at the University of Calabria. In this case, the survey has been only carried out for specimen 16 and 17 and not for the whole sample. The location of the photo points have been chosen to take advantage of natural light and avoid problems such as incident light on the members. After positioning the specimens, the next step was to place the markers on the floor. These markers are provided by the software and are used to create a local coordinate system for orientating and dimensioning the digital model; the markers consist of QR codes in a circular format, with a 12-bit encryption. Relative distances between the targets were taken using a tape measure by taking 12 measurements in total. The use of artificial illuminators was not necessary, given the sufficient ambient light. Taking into account the specimens geometrical features, the survey has been carried out according to the following modalities:

- 1 series of orthogonal and horizontal photos for each face of the specimen (approximately 20 frames per series);
- 1 series of radial photos at approximately 45° for each angle between the specimen faces (approx. 20 frames per series);
- 1 photo for each head;
- 1 photo for each detail such as notches or geometrical irregularity;
- 1 set of photos for references and markers.

For each phothos a 40% overlap of each frame with respect to the next has been used; this applies both to shots taken inside overlap (i.e. moving horizontally with respect to the subject while keeping the camera orthogonal to it) and to shots in frontal overlap (i.e. taken in a vertical direction). Since

the camera used had an APS-C sensor (15.7mmx23.6mm), which was reduced compared to a full-frame sensor (24mmx36mm), a focal length of 35mm was set for each frame. The ISO value was varied from 200 to 800 using an f/3.6 stop aperture for the side and top shots of the specimen, having excellent ambient lighting and the stabilised lens. ISO values were increased from 3200 ISO up to 8000 ISO with an aperture of f/11stop for the lower shots of the specimens.

The software *Metashape Professional*, based on the Structure from Motion methodology, has been used for the data processing and restitution. The workflow used consists of the following phases:

1. uploading of photos;
2. photos inspection and deletion of unnecessary images;
3. photo alignment, generation of the sparse point cloud;
4. construction of the dense point cloud;
5. editing of dense point cloud points;
6. mesh construction (3D polygonal model);
7. mesh editing;
8. orthomosaic processing;
9. export of results.

In the software, the precision parameter for finding image characteristic points has been set equal to "high" in order to have the proper trade-off between quality and processing time. Once the dense cloud has been elaborated, the mesh model has been built always through the same software. Then the volume of the specimen has been calculated.

Results

For each specimen 45 millions of points have been acquired, having a resolution of 13.1 point/mm^2 (Figure 6.9). As regard to the time of work the following results have been found for each specimen:

- acquisition operation: 40 minutes;
- cloud point construction: 40minutes;
- mesh construction: 20 minutes.

Thus, in total PS took 100 minutes for the data acquisition, processing and graphical restitution.

Thus the volumes (V_{PS}) of specimen "16" and "17" have been calculated from the mesh models, it was found respectively equal to 0.1640 m^3 and 0.1535 m^3.

Table 6.2. Volume of specimen obtained from Laser Scanner Survey (LSS)

Wood Species [-]	ID [-]	V_{LSS} [m^3]
CS	2	0.1603
	9	0.1717
	10	0.1318
	11	0.1561
	15	0.1678
PNL	1	0.1567
	3	0.1759
	4	0.1757
	5	0.1740
	6	0.1770
	7	0.1932
	8	0.1908
	12	0.1867
	13	0.1731
	14	0.1704
	16	0.1616
	17	0.1517
	18	0.1756

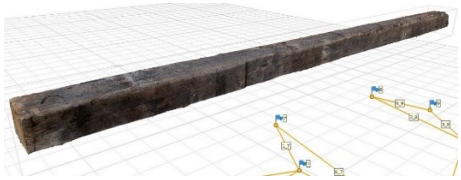

a)

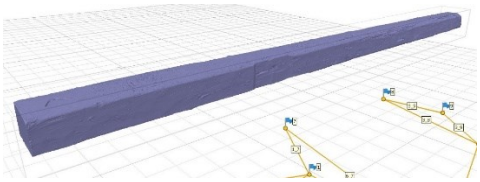

b)

Figure 6.9. a) Dense point cloud model of specimen 16 from PS method; b) Mesh model of specimen 16 from PS method.

6.2.3.4 Comparison of results and discussion

Three methodologies of survey have been applied for surveying the sample of timber struts: direct size survey (DS), Laser scanner survey (LSS) and Photogrammetric survey (PS). The DS and LSS methods have been applied on the whole sample whereas PS method has been applied only on specimen 16 and 17.

Starting from the comparison between the 3D acquisition methodologies (LSS and PS) it was found that:

- LSS took longer than PS, both in acquisition and processing time. The first one required an average time of 175 minutes for specimen while

PS required an average time of 100 minutes, thus the difference is equal to 75 minutes;

- LSS 3D model resulted in less detailed meshes than PS, but no appreciable differences in volume and section measurements have been found, since the differences in volume estimation is at most equal to 1.50% (Table 6.3);
- LSS returned a less refined texture, since a point cloud of 13 million points was obtained compared with 45 million for the PS (Figure 6.10); therefore PS is more effective than LSS for performing VSG on digital model.

a) b)

Figure 6.10. Textured digital model of specimen 16 acquired by: a) LSS method; b) PS method.

Given the same results in terms of geometry for both 3D acquisition methodologies (LSS and PS), a comparison between the LSS results (since it was applied on the whole sample) and direct survey (DS) has been carried out. The comparison has been performed in terms of volume, thus the volume variation obtained from the DS and LSS method have been evaluated through the parameter $i_{V(DS-LSS)}$ (Eq. 6.2):

$$i_{V(DS-LSS)}=(V_{DS}-V_{LSS})/V_{LSS} \quad (6.2)$$

where:

$i_{V(DS-LSS)}$ index of relative variation between V_{LSS} and V_{DS} [%];

V_{DS} volume calculated through direct survey [m^3];

V_{LSS} volume calculated through laser scanner survey [m^3].

This index expresses the relative increase in volume from the LSS technique to the DS technique (Table 6.3; Figure 6.11). When the index is greater than zero then the DS measurement is greater than the LSS

measurement and vice versa. At the same time, the index can be interpreted as an indicator of geometric irregularity as the higher the absolute value of $i_{V(DS\text{-}LSS)}$, the greater the geometric irregularity of the specimen.

Thus, it has been found that the highest value of $i_{V(DS\text{-}LSS)}$ is equal to 26.30% (specimen 2) whereas the lowest one is approximately equal to 0.00% (specimen 13). Furthermore, it has been found that for Chestnut (CS) and Corsican Pine (PNL) timber the average value of $i_{V(DS\text{-}LSS)}$ is respectively equal to 15.6% and 7.9%. It means that CS sample is characterised by specimens with more irregular geometry than the PNL specimens. At the same time the average value of the index is equal to 13.5% for CS and 3.4% for PNL, it means that the volumes calculated with DS method are on average higher than those with LSS method.

Table 6.3. Comparison of volume obtained from different methods.

W.S.	ID	V_{DS}	V_{LSS}	V_{PS}	Index of volume DS-LSS variation ($i_{V(DS\text{-}LSS)}$)			
					$i_{V(DS\text{-}LSS)}$	Min	Mean	Max
[-]	[-]	[m3]	[m^3]	[m^3]	[%]	[%]	[%]	[%]
	2	0.2025	0.1603	-	26.30			
	9	0.1837	0.1717	-	7.00			
CS	10	0.1566	0.1318	-	18.80	-6.30	13.7	26.30
	11	0.1463	0.1561	-	-6.30			
	15	0.2063	0.1678	-	22.90			
	1	0.1756	0.1567		12.1			
	3	0.1887	0.1759	-	7.30			
	4	0.1569	0.1757	-	-10.70			
	5	0.1959	0.1740	-	12.60			
	6	0.1977	0.1770	-	11.70			
PNL	7	0.1739	0.1932	-	-10.00	-10.70	4.1	12.60
	8	0.2094	0.1908	-	9.70			
	12	0.2038	0.1867	-	9.20			
	13	0.1731	0.1731	-	0.00			
	14	0.1884	0.1704	-	10.60			
	16	0.1693	0.1616	0.1640	4.80			
	17	0.1421	0.1517	0.1535	-6.30			
	18	0.1790	0.1756	-	1.90			

Thus, it has been seen that a significant variation occurs in the survey of ancient timber structures with traditional and 3D techniques. However, it has not been seen how these results can influence the estimation of the mechanical properties of the timber members and thus the assessment of structural performance. Therefore, in the following sections, the impact of the different

survey methods on timber mechanical properties estimation through Non-destructive test has been evaluated.

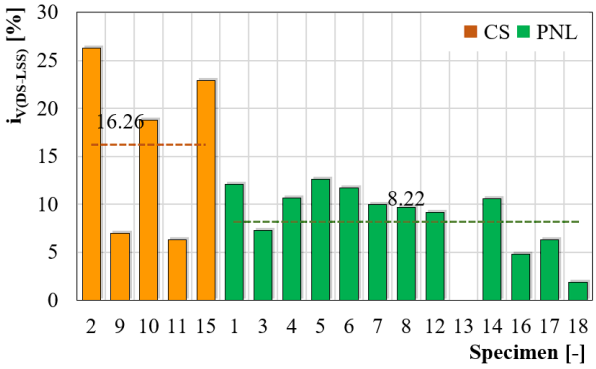

Figure 6.11. Index of volume variation.

6.2.4 VISUAL STRENGTH GRADING (VSG)

6.2.4.1 Procedure

The visual strength grading has been performed according to the two aforementioned regulations. The VSG has been carried out on the middle third of the member, as this is the area most subject to bending stress. However, the heads members have been also analysed, reporting only a qualitative description of the defects and degradation phenomena identified. Furthermore, from the list of the grading criteria identified by the two standards, some characteristics have not been measured for grading. This is due to the fact that some criteria are too penalising for the ancient timber structures that generally show different intrinsic characteristics from the case of new wood (e.g. geometry irregularities), at which the UNI 11035-1 and UNI 11035-2 [339], [336] dealing. This is the case of "wane", a geometrical characteristic of the cross section which is commonly spread in ancient timber members. This criterion is listed by both the regulations. However, it considerably limits the VSG of ancient timber [401], [380] and for this reason it has not been considered in this work. For the same reason, geometric irregularities (e.g. bowing, crooking, twisting) have been also not taken into account. In the end the criteria to be measured on the member heads (e.g. width of the grow rings, compression wood, ring shakes) have not been taken into account. As results the following characteristics have been considered:

knots, group of knots, slope of the grain, shrinkage cracks, insect and fungus attacks.

For both wood species, the classification rules given in UNI 11119 [318] have been used (Figure 6.12), while in accordance with [339] the category rules "Conifera 1" for Corsican Pine and "Latifoglie" for Chestnut have been adopted. According to [318] three visual grades (I, II, III) can be assigned both to Corsican Pine and Chestnut, whereas according to [339] three (S1, S2, S3) and only one (S) visual grades can be respectively assigned to Corsican Pine and Chestnut. Therefore, members that do not meet the classification criteria are rejected and a resistant profile cannot be associated with them.

CARATTERISTICA		CATEGORIA IN OPERA		
		I	II	III
Smussi		≤1/8	≤1/5	≤1/3
Lesioni varie Cretti da gelo Cipollature		assenti	assenti	ammissibili, purché in misura limitata
Nodi singoli		≤1/5 ≤50 mm	≤1/3 ≤70 mm	≤1/2
Gruppi di nodi		≤2/5	≤2/3	≤3/4
Inclinazione della fibratura (pendenza %)	in sezione radiale	≤1/14 (~7%)	≤1/8 (~12%)	≤1/5 (20%)
	in sezione tangenziale	≤1/10 (10%)	≤1/5 (20%)	≤1/3 (~33%)
Fessurazioni radiali da ritiro		ammissibili, purché non passanti		

Figure 6.12. Grading rules according to UNI 11119 (extracted from: [318]).

As regard to the macroscopic characteristics, it has been taken into account the general definitions and requirements dictated by UNI 11119 [318] and UNI 11035-1 [339]. However, it is important to note that as regard to knots, both standards set limits on the minimum knot diameter (d) for softwoods, while for hardwoods the UNI 11035 standard sets an additional limit on the maximum diameter (D). Furthermore, both standards consider a parameter (A) calculated as the ratio between the size of the knot and the width of the face on which it is located [339]. According to both standards the group of knots has been evaluated in a length of 150 mm and the ratio between the size of the knots and the width of the face on which they are located has been evaluated through the A_g parameter. The slope of the grain (i) has been measured on a length of 1000mm. In the end, based on the wood species a

visual strength grade has been assigned to each member following the criteria of the worst defect.

The visual strength grading has been performed on site, in the Laboratory "Grandi Modelli". Furthermore, in order to evaluate the potential of digital surveying techniques also in the field of VSG, the acquired digital models have been used to measure the visual characteristics and establish the visual grade. The classification has been carried out on the digital models obtained through LSS and PS methods, evaluating the pros and cons of both techniques.

6.2.4.2 Results and discussion

After visual analysis, the sample has been found to have heterogeneous quality. According to UNI 11119 [318] four out of five Chestnut specimens are classified as grade III while one specimen is grade II (Table 6.4). For Pine, four specimens have been found to be grade III, seven specimens' grade II and two specimens grade I.

Table 6.4. Visual strength grading according to UNI 11119 [318].

W.S.	ID	Knots		Group Knots	Slope grain	VSG (UNI 11119)	
		A	d	A_g	i	Grade	The worst defect
[-]	[-]	[-]	[mm]	[-]	[%]	[-]	[-]
CS	2	0.50	100	0.00	5%	III	Large knots
	9	0.49	98	0.21	9%	III	
	10	0.28	55	0.00	1%	III	Widespread insect attack
	11	0.28	55	0.00	9%	II	Large knots
	15	0.35	70	0.00	8%	III	
PNL	1	0.42	84	0.00	6%	III	Large knots
	3	0.25	50	0.00	6%	II	
	4	0.15	29	0.00	4%	I	-
	5	0.19	38	0.00	7%	I	-
	6	0.25	50	0.00	12%	II	Large knots and slope of the grain
	7	0.13	25	0.17	14%	II	Slope of the grain
	8	0.31	62	0.00	8%	II	Large knots
	12	0.37	74	0.00	15%	III	
	13	0.35	70	0.00	14%	III	
	14	0.27	53	0.00	15%	II	Large knots and slope of the grain
	16	0.25	50	0.00	11%	II	
	17	0.33	65	0.60	15%	II	
	18	0.40	80	0.26	12%	III	Large knots

In general, the defects that directed the grading were large knots for Chestnut and slope of the grain for Corsican Pine specimens. In detail, for specimen 2 and 9 knots having up to 100 mm of diameters have been found, whereas in the specimen 10, large zone of insect attack have been identified.

The insect species have been recognized by the morphology of the decayed areas. Indeed, *Cerambycidae* and *Anobiidae* species have been identified. In general, the degradation is concentrated in the edges of the strut, at least as far as the *Cerambicidae* are concerned, whereas for the insects belonging to the *Anobiidae* family the attack is widespread on all surfaces. More intense and extensive degradation has been observed in the CS specimens. The specimen most affected is the member 10. However, the maximum depth of the biotic attack is about 1 cm, and the attacks seem to have been extinct for a long time. The most common defect in samples of Corsican Pine is the slope of the grain evidenced by the shrinkage cracks. This is the case for specimens 6, 7, 14, 16, and 17, with a maximum deviation of 15%. At the same time, the knots influenced the classification of test specimens 1, 3, 8, 12, 13, 18, where the maximum diameter has been found to be equal to 84 mm (specimen 1). For the specimen 6, 14, 16, 17, both the knots and the slop of the grain influenced the grading. According to UNI EN 11035-2 [339] three out of five Chestnut specimens are classified as grade S while two specimens were rejected from grading (Table 6.5). As regard to Corsican Pine, seven specimens have been found to be grade S3, 4 specimens' grade S2 and two specimens' grade S1. Even in this case, large knots for Chestnut and slope of the grain for Corsican Pine specimens influenced the grading results.

In the end, as a result of the VSG the performance profiles in terms of mechanical properties have been obtained. From the visual grades obtained according to EN 11035-2 [339], a strength class [344] has been assigned to the sample according to the Standard UNI EN 1912 [343]. Thus, Italian Chestnut wood graded as S resulted as equivalent to a strength class D24. Corsican Pine grades S3, S2 and S1 correspond to strength class C14, C24 and C40, respectively.

Although the defects on the heads have not been considered for visual-grading purposes, an overview of the main defects is given. For most of the members, signs of degradation and defects have been found near to the heads (Figure 6.13). Ring shakes have been found on the head of specimens 2, 7 and 9. The ring shakes are arranged eccentrically to the heart in members 7 and 9. Furthermore, the presence of two piths has been noted in the specimens 2, 9,

16 and 18. Some limbs - 7, 9, 16 and 18 - seem to come from very old three, as the growth rings are very thin.

Table 6.5. Visual strength grading according to UNI 11035-2 [339].

W.S.	ID	Knots				Slope grain	VSG (UNI EN 11035-2)	
		A	d	D	A_g	i	Grade	The worst defect
[-]	[-]	[-]	[mm]	[mm]	[-]	[%]	[-]	[-]
	2	0.50	100	120	0.00	5%	NC	Large knots
	9	0.49	98	134	0.21	9%	NC	Lage knots
	10	0.28	55	70	0.00	1%	S	Widespread insect attack
CS	11	0.28	55	95	0.00	9%	S	-
	15	0.35	70	100	0.00	8%	S	
	1	0.42	84	95	0.00	6%	S3	Large knots
	3	0.25	50	54	0.00	6%	S2	
	4	0.15	29	33	0.00	4%	S1	
	5	0.19	38	56	0.00	7%	S1	-
	6	0.25	50	54	0.00	12%	S2	Large knots and slope of the grain
PNL	7	0.13	25	45	0.17	14%	S3	Slope of the grain
	8	0.31	62	67	0.00	8%	S2	Large knots
	12	0.37	74	97	0.00	15%	S3	Large knots and slope of the grain
	13	0.35	70	90	0.00	14%	S3	Slope of the grain
	14	0.27	53	69	0.00	15%	S3	
	16	0.25	50	70	0.00	11%	S2	Large knots and slope of the grain
	17	0.33	65	100	0.60	15%	S3	Slope of the grain
	18	0.40	80	120	0.26	12%	S3	Large knots

Table 6.6. Mechanical properties according to UNI EN 338 [344] derived from VSG analysis.

W.S.	ID	Grade UNI 11119	Grade UNI EN 11035-2	EN 338			
				Grade	$f_{m,k}$	$E_{m,0,mean}$	ρ_{mean}
[-]	[-]	[-]	[-]	[-]	[MPa]	[MPa]	[MPa]
	2	III	NC	-	-	-	-
	9	III	NC				
CS	10	III	S				
	11	II	S	D24	24	10000	580
	15	III	S				
	1	III	S3	C14	14	7000	350
	3	II	S2	C24	24	11000	420
	4	I	S1	C40	40	14000	480
	5	I	S1				
	6	II	S2	C24	24	11000	420
PNL	7	II	S3	C14			
	8	II	S2	C24	24	11000	420
	12	III	S3				
	13	III	S3	C14	14	7000	580
	14	II	S3				
	16	II	S2	C24	24	11000	420
	17	II	S3	C14	14	7000	350
	18	III	S3				

Some members are strongly tapering, such as specimen 10 which it takes on the conformation of freshly debarked and un-squared roundwood. In the end, sings of mechanical damage have been found on the heads and external face of the members. They are probably due to the excessive compression stresses in the struts, especially in correspondence of the strut-tie joint.

For specimen 16 and 17 the VSG has been also carried out on digital models acquired by laser scanner and photogrammetric survey techniques. The knots dimensions and slope of the grain have been measured on the textured models. These characteristics have been "manually" measured using the measurement tools of the digital model management software (*Geomagic Wrap software* for LSS and *Agisoft Metashape* for PS).

Comparing the two techniques, it has been seen that the model acquired with PS lends itself better to VSG analysis, as the point cloud has a greater resolution than LSS. In this way, the characteristics have been measured accurately without any differences from the traditional approach. On the model obtained with LSS, however, it has not been feasible to identify the wood grain and measure its inclination, and only a few knots have been discovered. In the following chapter, the data obtained with VSG will be compared with those derived from destructive testing.

a)

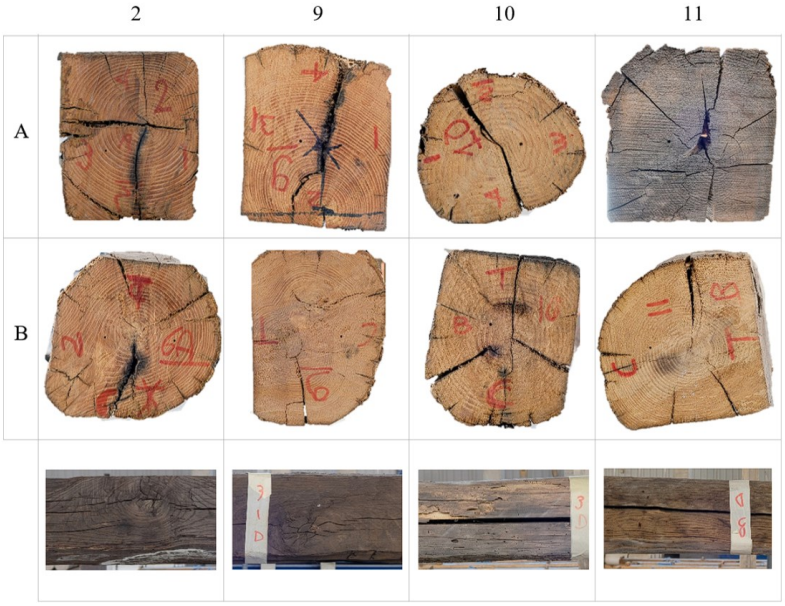

b)

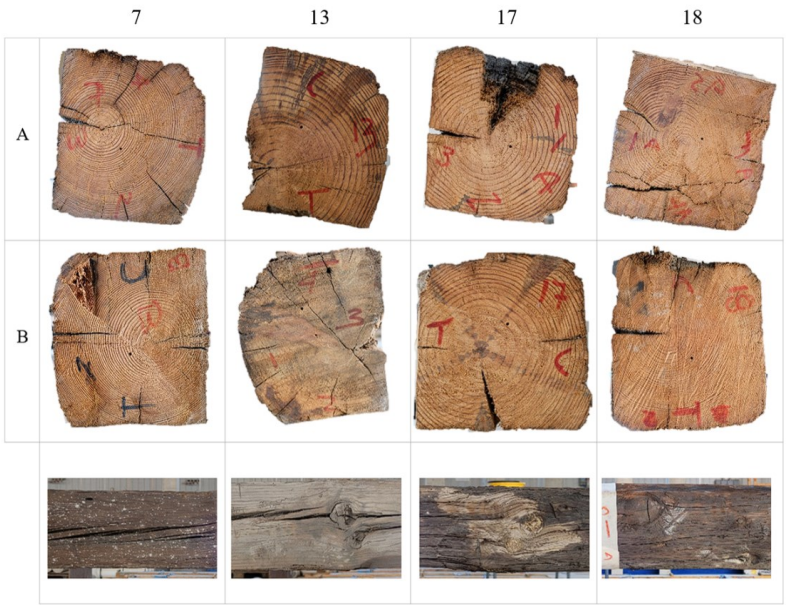

Figure 6.13. Visual macroscopic characteristics of specimens 2, 9, 10, 11 in *Castanea Sativa.* and specimens 7, 13, 17, 18 in *Pinus Nigra* subsp. laricio.

6.2.5 NON-DESTRUCTIVE TEST (NDT)

6.2.5.1 Moisture content measurement

Test equipment

The moisture content measurement have been performed by means of *Hydromette CH 17 GANN* device, which is a digital pin type resistance meter with built-in pins designed to take precise measurements of moisture content in wood (Figure 6.14). It mesaure variations of 1% moisture in a range from 7% to 40%. The total width of the electrodes is 60 mm.

The measurements are auto corrected by the device taking into account the ambient hygrometric conditions and the wood species. Indeed the moisture measurement are generally influenced by several factors as the environmental temperature and humidity, as well as the wood species and possible presence of wood superficial/deep treatment. As regards to the wood species, the electrical resistance can vary depending on the density of wood. This may affect meter readings for the same moisture content and may also be relevant for related species with different origins. When the test have been carried out the environmental temperature was 20°±2°C and relative humidity 65%±5%.

Procedure and test set-up

The test has been carried out on the whole sample by taking one transverse measurement per specimen at the middle span. The test have been performed inserting the electrode pin inside the timber member keeping the electrode couple aligned to the direction of wood grain. Specimen heads and zone characterized by wood defects have been excluded as a testing zone.

a)

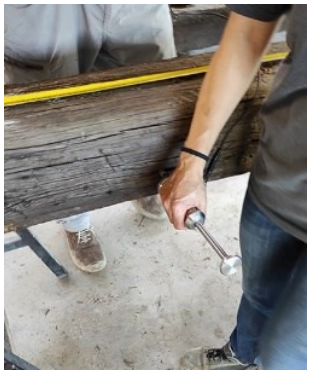

b)

Figure 6.14. a) The *Hydromette CH 17 GANN* device; b) The moisture content measurement.

Table 6.7. Moisture content (M.C.) measurements

W.S.	ID	Moisture Content (M.C.)					
		M.C.	Min	Mean	Max	σ	COV
[-]	[-]	[%]	[%]	[%]	[%]	[%]	[%]
	2	14.1					
	9	14.5					
CS	10	15.0	14.1	14.7	15.2	0.4	2.6
	11	15.2					
	15	14.7					
	1	17.0					
	3	14.4					
	4	13.1					
	5	27.0					
	6	16.9					
PNL	7	23.0	13.1	17.2	27.0	3.8	22.0
	8	15.9					
	12	16.0					
	13	15.9					
	14	16.7					
	16	19.2					
	17	13.9					
	18	14.0					

Results and discussion

The test results are provided in Table 6.7. In general, the moisture content of the specimen has been found higher than the normal content. The average value of MC is 15.1% for CS and 17.2% for PNL. The maximum value is 23.0% for specimen 7. This is probably due to the unprotected storage of material until it was transported to the laboratory. In general, a greater dispersion of M.C. has been found for CS (COV: 22.8). It is important to notice that M.C. is a fundamental parameter for timber, since it influences stiffness and strength.

6.2.5.2 Mass measurement and density estimation

Test equipment

The mass of each specimen has been measured through direct measurement using the platform scale *RHEWA* (Figure 6.15).

a)

b)

Figure 6.15. a) The platform scale *RHEWA* [442]; b) The mass measurement.

Procedure and test set-up

The tests have been carried out measuring the specimen one at time. Then, given the volume of the specimen the density has been calculate. Thus, the density have been estimated using the volume acquired through direct survey (DS) and laser scanner survey (LSS):

$$\rho_{DS} = \frac{m}{V_{DS}} \tag{6.3}$$

$$\rho_{LSS} = \frac{m}{V_{LSS}} \tag{6.4}$$

where:

ρ_{DS} density estimated through DS volume [kg m^{-3}];

ρ_{LSS} density estimated through LSS volume [kg m^{-3}];

m specimen mass [kg];

V_{DS} volume from DS [m^3];

V_{LSS} volume from LSS [m^3].

Results and discussion

The test results of mass measurement are provided in Figure 6.16. The results of density estimation obtained with DS and LSS technique are respectively shown in Table 6.8 and Table 6.9. It is evident how the use of the two different survey methods leads to very different density values, as shown in Figure 6.17.

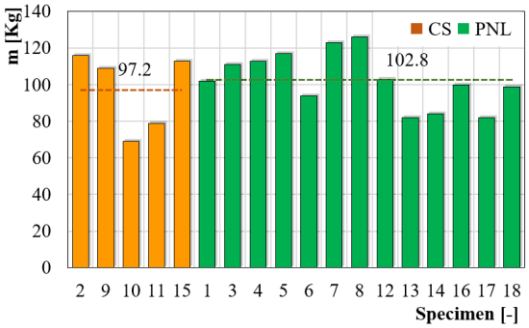

Figure 6.16. Mass measurements.

Given the volume estimate through LSS is a better approximation of the specimen's volume, it is possible to discuss these results (Table 6.9). In particular, the density is similar for both wood species, being in average approximately equal to 619 Kg for CS and 585 Kg for PNL. The highest mass values has been found for specimen 2, it is equal to 723 Kgm^{-3}. This is probably due to the presence of large knots inside the member. The same dispersion of data has been recorded for both CS (COV:12.7%) and PNL (COV:11.0%).

After the density of timber has been calculated and results are showed in Table 5.2 and Tale 5.4. It has been found that the from DS method to LSS method increases the dispersion of values for the Chestnut (from COV:9.2% to COV:12.7%) and decreases that of the Corsican Pine (from COV:14.5% to COV:11.0%).

In order to evaluate the differences between the two approaches an index of variation has been defined (Eq. 6.5):

$$i_{\rho(DS\text{-}LSS)}=(\rho_{DS}-\rho_{LSS})/\rho_{LSS} \tag{6.5}$$

where:

$i_{\rho(DS\text{-}LSS)}$ index of relative variation between ρ_{DS} and ρ_{LSS} [Kgm^{-3}];

ρ_{DS} density calculated through direct survey [m^3];

ρ_{LSS} density calculated through laser scanner survey [m^3].

Table 6.8. Density estimation through direct survey (DS) method

W.S.	ID	m	ρ_{DS}	Wood density from DS (ρ_{DS})				
				Min	Mean	Max	σ	COV
[-]	[-]	[Kg]	[Kgm^{-3}]	[Kgm^{-3}]	[Kgm^{-3}]	[Kgm^{-3}]	[Kgm^{-3}]	[%]
	2	116	573					
	9	109	593					
CS	10	69	441	441	539	593	52	9.7
	11	79	540					
	15	113	548					
	1	102	581					
	3	111	588					
	4	113	720					
	5	117	597					
	6	94	475					
PNL	7	123	707	446	570	720	79	13.9
	8	126	602					
	12	103	505					
	13	82	474					
	14	84	446					
	16	100	591					
	17	82	577					
	18	99	553					

The results variation between the two approaches has been highlighted in Table 5.2 and Figure 5.3. Given the average value of $i_{\rho(DS\text{-}LSS)}$ is negative for both CS and PNL, it is apparent that the density estimation by DS has led to a general underestimation of wood density. The density variation is on average equal to -11.0% for CS and -2.7% for PNL. The highest variation has been found for specimen "2" ($i_{\rho(DS\text{-}LSS)}$: 20.9%).

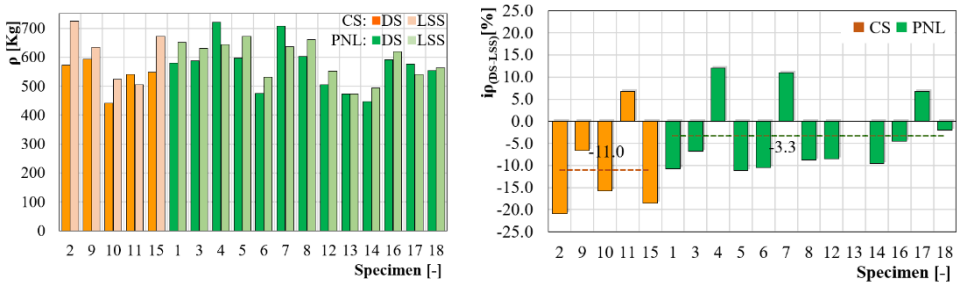

a) b)

Figure 6.17. a) Wood density estimated through Direct survey (DS) and Laser Scanner survey (LSS); b) Index of density variation.

Table 6.9. Density estimation through laser scanner survey (LSS) method

W.S.	ID	m	ρ_{LSS}	Wood density from LSS (ρ_{LSS})				
				Min	Mean	Max	σ	COV
[-]	[-]	[Kg]	[Kgm^{-3}]	[Kgm^{-3}]	[Kgm^{-3}]	[Kgm^{-3}]	[Kgm^{-3}]	[Kgm^{-3}]
	2	116	724					
	9	109	635					
CS	10	69	524	506	612	724	85	13.8
	11	79	506					
	15	113	673					
	1	102	651					
	3	111	631					
	4	113	643					
	5	117	672					
	6	94	531					
PNL	7	123	637	474	590	672	64	10.9
	8	126	660					
	12	103	552					
	13	82	474					
	14	84	493					
	16	100	619					
	17	82	541					
	18	99	564					

6.2.5.3 Drilling resistance test

Test equipment

The drilling resistance test have been performed using the *IML RESI PD400* device. It is an energy-based device for measuring the penetration resistance of wood to the drilling. The drilling needle have a diameter of about 3.0 mm, thus it doesn't damage the timber members during penetration. The max drilling penetration allowed by the device is equal to 400 mm. Every 0.1 mm, the drilling resistance is electrically monitored using the expended energy of the drilling tool that directly related to the drilling resistance. The pin rotation can be set from 1500 rpm to 5000 rpm, and the penetration speed from 25 cm/min to 200 cm/min. The data are recorded and instantly stored as graphic profiles, which can then be downloaded on a PC for further elaborations.

Table 6.10. Index of density variation

W.S.	ID	Index of density variation ($i_{\rho(DS-LSS)}$)					
		ρ_{DS}	ρ_{LSS}	$i\rho_{(DS-LSS)}$	Min	Mean	Max
[-]	[-]	[Kg m^{-3}]	[Kg m^{-3}]	[%]	[%]	[%]	[%]
	2	573	724	-20.90			
	9	593	635	-6.60			
CS	10	441	524	-15.80	-20.90	-11.0	6.70
	11	540	506	6.70			
	15	548	673	-18.60			
	1	581	651	-10.80			
	3	588	631	-6.80			
	4	720	643	12.00			
	5	597	672	-11.20			
	6	475	531	-10.50			
PNL	7	707	637	11.00	-11.20	-3.3	12.00
	8	602	660	-8.80			
	12	505	552	-8.50			
	13	474	474	0.00			
	14	446	493	-9.50			
	16	591	619	-4.50			
	17	577	541	6.70			
	18	553	564	-2.00			

Procedure and test set-up

The drilling resistance tests have been performed on all the sample of study. The experimental tests consisted of penetrations in perpendicular direction to the grain, with an advancing speed of 50 cm/minute. The

measurements have been carried out in correspondence of the head of the members, near the section "A" and "B" previously identified. Thus, 2 two measurements have been performed for each section, for a total number of 4 drillings per specimen. Given the nomenclature of timber faces defined in section Section6.2.3, the direction of drilling have been defined as direction "1-3" and direction "2-4".

From the drill graph wood defects have been located and the mean resistance drilling (R_m) has been calculated as (Eq. 6.6):

$$R_m = \int_0^{l_p} \frac{R_{(l_p)} \cdot dl_p}{L_p} \tag{6.6}$$

where:

R_m mean drilling resistance [%];

$R_{(lp)}$ drilling resistance as function of the drilling depth [%];

l_p drilling depth [mm];

L_p total length of drilling [mm].

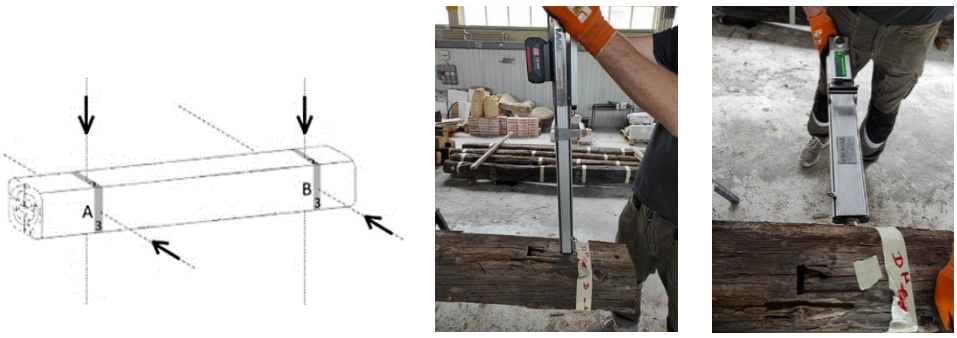

a) b) c)

Figure 6.18. a) Drilling resistance test set-up; b) Measurements in vertical direction; c) Measurements in horizontal direction.

The zones of the graph with low resistances, due to the presence of defects or decay, were not considered in the calculation of the average resistance R_m.

Results and discussion

For each specimen, the average resistance of R_m has been calculated as the average of the 4 measurements taken. The results are provided in Table 6.11 and Figure 6.20.

It is apparent that for CS R_m values are higher (R_m: 27.2%) than for PNL (R_m: 20.2%) and this is probably due to the higher density of CS than PNL. The highest value is for specimen 2 (R_m: 34.1%), it being closely related to the high density of the member.

A qualitative assessment of the drilling graphs have been carried out and an extract is showed in Figure 6.12 and Figure 6.19. From drill charts it is also apparent that rafters 7, 9 and 18 belonged to very old trees, since they have many growth rings. In specimen 2, 5, 6, 15 the reduction in strength recorded in the end portion shows the presence of biotic attacks.

Table 6.11. Mean Drilling Resistance measurements.

W.S.	ID	R_m	Mean Drilling Resistance measure (R_m)				
			Min	Mean	Max	σ	COV
[-]	[-]	[%]	[%]	[%]	[%]	[%]	[%]
CS	2	34.1	22.2	27.7	34.1	4.3	15.5
	9	27.4					
	10	22.2					
	11	24.2					
	15	30.7					
PNL	1	24.4	16.1	20.2	25.4	2.5	12.1
	3	19.7					
	4	18.6					
	5	21.5					
	6	16.1					
	7	25.4					
	8	17.6					
	12	21.9					
	13	19.2					
	14	19.5					
	16	19.6					
	17	19.2					
	18	20.0					

Table 6.12. Qualitative assessment of the drilling resistance graphs.

ID	Graph ID	Section	Drill direction	Graph description
1	a)	A	4-2	The pith is roughly centred, the peaks flatten out between a depth of about 10.5 cm and 12 cm. The width of the rings is fairly regular. In the middle zone there is the typical parabolic pattern where the resistance is lower due to presence of pith.
	b)	A	1-3	-
	c)	B	4-2	There is a sudden drop in resistance at a depth of 12 cm, probably due to the presence of a wood check.
	d)	B	1-3	There is a sudden drop in resistance at a depth of 14.5 cm, probably due to the presence of a wood check.

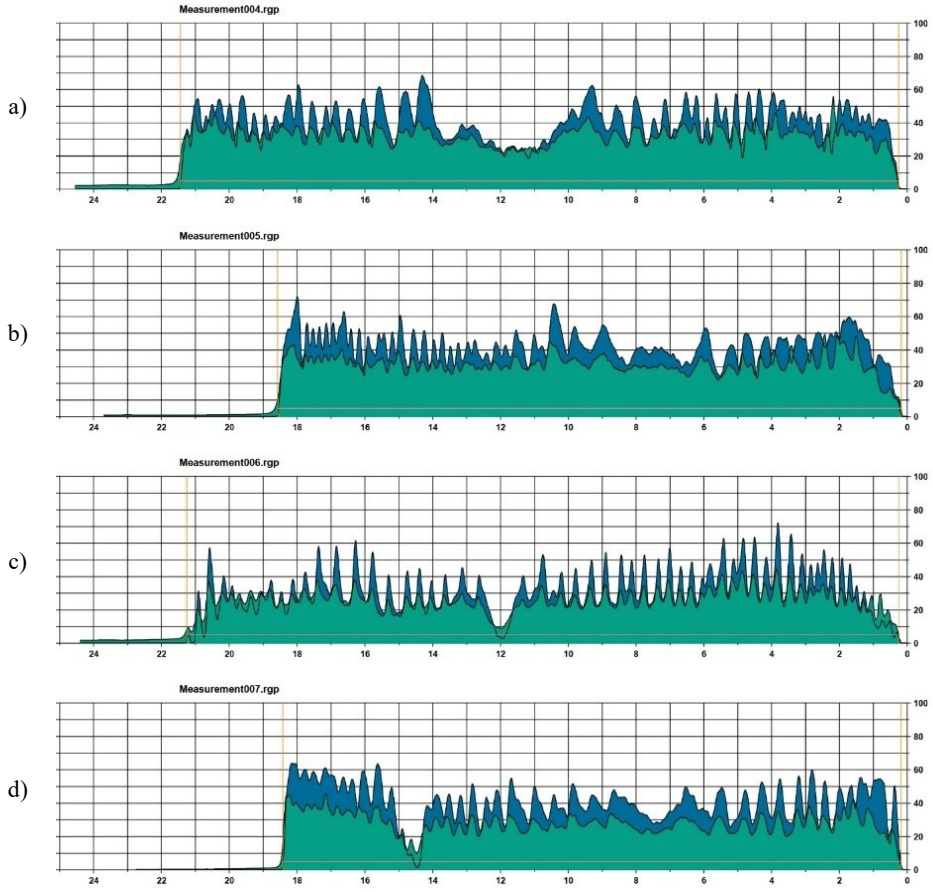

Figure 6.19. Drilling graph for specimen "1" (CS): a) in section "A" direction "4-2"; b) in section "A" direction "1-3"; c) in section "B" direction "4-2"; d) in section "B" direction "1-3".

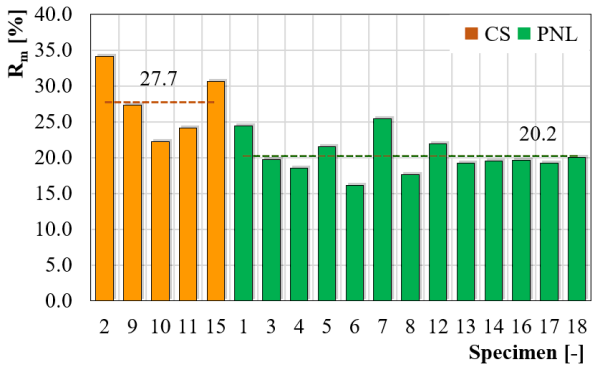

Figure 6.20. Mean Drilling resistance measure.

6.2.5.4 Acoustic test

Test equipment

The acoustic test has been performed with *Microsecond Timer Fakopp,* which aim to assess the elastic and dynamic properties of material. This kind of test are also called "Time of flight" test since the travel time of the acoustic wave as it passes from the transmitter to the receiver is measured by the device. Thus, the test equipment is made up of a data acquisition unit combined either with a couple of sensors, for transmitting and receiving the acoustic wave. Part of the equipment is also a hammer, used to hit the transmitter and generate the wave as a consequence. Thus the *Time of Flight* (TOF), which represents the time requires for the stress wave to travel between the sensors, is measured and stored by the acquisition unit that have an accuracy of ± 3 microseconds.

This test is especially useful for determining the homogeneity of the material under examination as well as the presence of any fractures or hollows. In general, stress waves propagate rapidly through dense and solid materials, while voids, cracks or decay attenuate and deflect stress waves. Therefore, a short TOF duration indicates healthy and/or high-quality wood, while long TOF duration suggests deteriorated and/or low-quality wood.

Procedure and test set-up

The acoustic tests have been performed on the whole sample. Since direct modes are generally not possible in on-site assessments, semi-direct

measurement has been also used in this experimental activity. Thus, direct and semi-direct transmission have been used. In the first case the sensors have been placed on the two opposite heads of the specimen in longitudinal direction (L). The second arrangement consist in a diagonal (D) orientation of the sensors, by positioning them on the same member face using an orientation of about 45° than the timber face (Figure 6.22.a). In this configuration the sensors are still placed near to section "A" and "B" of the specimen. Therefore 1 longitudinal (L) and 4 diagonal (D) measurements have been carried out per specimen (one diagonal measurements for each member face), for a total number of 5 measurements per specimen.

a) b)

Figure 6.21. The *Microsecond Timer Fakopp* device: a) Test equipment [443]; b) the general application on timber members [444].

During the test the correct orientation of the sensors have been maintained, as well as interference areas such as cracks, cavities, visibly decayed zone or metal nails have been avoided. As regard the procedure each measurement has been repeated 3 times, thus the TOF has been evaluated as the average of 3 hitting.

In both L and D arrangements the test has been carried out according to the following steps:

- Sensors positioning;
- Measuring distance between the sensors;
- Hiting the transmitter sensor (3 times);
- Reading of the TOF measures (3 times);

Based on the TOF and the known distance between the transmitting-receiving points, the "Stress Wave Speed" (SWS) has been calculated and

used to assess the internal physical conditions of the member. Therefore the SWS_L (Eq. 6.7) has been calculated for longitudinal test (L) and SWS_D (Eq. 6.8) for diagonal test (D):

$$SWS_L = \frac{L}{TOF_L} \tag{6.7}$$

$$SWS_D = \frac{L}{TOF_D} \tag{6.8}$$

where:

SWS_L stress wave speed in longitudinal direction [m s^{-1}];

SWS_D stress wave speed in diagonal direction [m s^{-1}];

TOF_L time of flight of the stress wave in longitudinal direction [s];

TOF_D time of flight of the stress wave in diagonal direction [s];

L length between transmitter-receiver sensors [m];

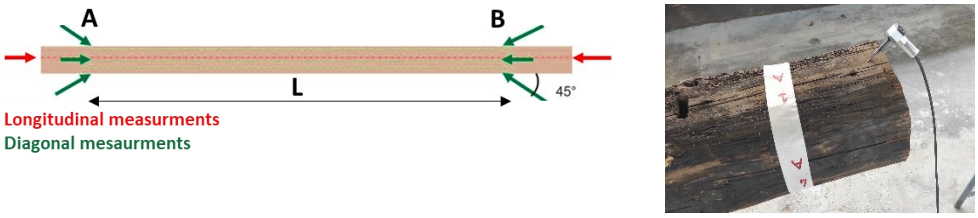

a) b)

Figure 6.22. a) The acoustic test set-up: b) The transmitter sensor.

The dynamic modulus of elasticity (MOE_{dyn}) has been calculated from SWS as follow (Eq. 6.9):

$$MOE_{dyn,A} = SWS^2 \cdot \rho \tag{6.9}$$

where:

$MOE_{dyn,A}$ modulus of elasticity derived from acoustic tests [MPa];

SWS stress wave speed [m s^{-1}];

ρ wood density [kg m^{-3}].

In this work the MOE_{dyn} has been calculated taking into account both the density estimated from DS and LSS, in order to evaluate the variations in stiffness due to the different geometrical survey methods. Furthermore, a comparison between longitudinal and diagonal MOE_{dyn} have been carried out using the different SWS values.

Results and discussion

The stress wave speed (SWS) measures for longitudinal (L) and diagonal (D) direction are respectively provided in and Figure 6.13. As regard to L measurements similar results have been found for both wood species, since the average speed is close to 4600 ms^{-1}. However for PNL a more data dispersion has been seen than CS (COV: 8.4% for PNL; COV: 3.7% for CS). The same remarks can be drawn also for diagonal results (D), since the average value of SWSD is quite the same (SWS_D: 4574 ms^{-1} for CS; SWS_D: 4583 ms^{-1} for PNL). Furthermore, the gap between the data dispersion of CS and PNL data remains about the same of the longitudinal test (Table 6.14).

For both testing direction (L and D) the minimum SWS value has been found for specimen "8" (SWS_L: 4039 ms^{-1}; SWS_D: 3889 ms^{-1}) while the maximum one for specimen "7" (SWS_L: 5506 ms^{-1}; SWS_D: 5344 ms^{-1}).

In order to account for the numerical variation of the results in the longitudinal and diagonal directions of testing, a variation index has been defined (Eq. 6.10):

$$i_{SWS(L-D)}=|(SWS_L - SWS_D)|/SWS_D \quad (6.10)$$

where:

$i_{SWS(L-D)}$ index of relative variation between SWS_L and SWS_D [m s^{-1}];

SWS_L stress wave speed in longitudinal direction measurement [m s^{-1}];

SWS_D stress wave speed in diagonal direction measurement [m s^{-1}];

The results are provided in Table 6.15 and Figure 6.23. It has been found that all the measurement in L direction are greater than D one, it means that the acoustic wave travels faster along the element in the longitudinal configuration than the diagonal one. This finding is in accordance with the state of art.

Table 6.13. Stress wave speed in Longitudinal direction.

W. S.	ID		Stress Wave Speed in Logitudinal direction (SWS_L)				
		SWS_L	Min	Mean	Max	σ	COV
[-]	[-]	[m s^{-1}]	[MPa]	[MPa]	[MPa]	[MPa]	[%]
	2	4823					
	9	4593					
CS	10	4922	4466	4670	4922	173	3.7
	11	4547					
	15	4466					
	1	4772					
	3	5144					
	4	4734					
	5	4812					
	6	4312					
PNL	7	5506	4039	4694	5506	393	8.4
	8	4039					
	12	4626					
	13	4167					
	14	4932					
	16	4738					
	17	4302					
	18	4936					

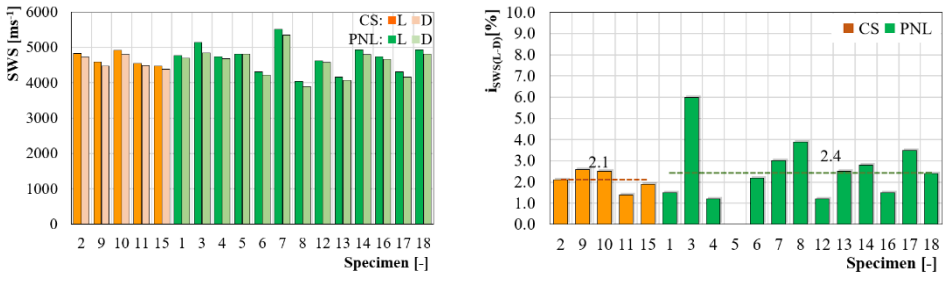

a) b)

Figure 6.23. a) Stress wave speed in longitudinal (L) and diagonal (D) direction; b) Index of variation of the stress wave speed.

Table 6.14. Stress wave speed in Diagonal direction

W. S.	ID		Stress Wave Speed in Diagonal direction (SWS_D)				
		SWS_D	Min	Mean	Max	σ	COV
[-]	[-]	[m s^{-1}]	[MPa]	[MPa]	[MPa]	[MPa]	[%]
	2	4726					
	9	4476					
CS	10	4801	4382	4574	4801	161	3.5
	11	4485					
	15	4382					
	1	4702					
	3	4851					
	4	4680					
	5	4811					
	6	4221					
PNL	7	5344	3889	4583	5344	382	8.3
	8	3889					
	12	4573					
	13	4064					
	14	4797					
	16	4666					
	17	4158					
	18	4819					

Table 6.15. Index of SWS variation for L and D direction.

W. S.	ID	SWS_L	SWS_D	Index of SWS variation ($i_{SWS(L-D)}$)			
				$i_{SWS(L-D)}$	Min	Mean	Max
[-]	[-]	[m s^{-1}]	[m s^{-1}]	[%]	[%]	[%]	[%]
	2	4823	4726	2.10			
	9	4593	4476	2.60			
CS	10	4922	4801	2.50	1.40	2.1	2.60
	11	4547	4485	1.40			
	15	4466	4382	1.90			
	1	4772	4702	1.50			
	3	5144	4851	6.00			
	4	4734	4680	1.20			
	5	4812	4811	0.00			
	6	4312	4221	2.20			
PNL	7	5506	5344	3.00	0.00	2.4	6.00
	8	4039	3889	3.90			
	12	4626	4573	1.20			
	13	4167	4064	2.50			
	14	4932	4797	2.80			
	16	4738	4666	1.50			
	17	4302	4158	3.50			
	18	4936	4819	2.40			

After calculating the SWS in the longitudinal and diagonal directions, the dynamic elastic modulus has been evaluated using Equation 6.9. It is important to note that density affect this evaluation. Given that density has been evaluated accurately through the LSS survey and coarsely through DS, the impact of this parameter on $MOE_{dyn,A}$ has been investigated. Thus $MOE_{dyn,A,LSS}$ and $MOE_{dyn,A,DS}$ have been calculated according to the equation 6.9 by using ρ_{LSS} and ρ_{DS} respectively. In this calculation has been used the stress wave speed in diagonal direction (SWS_D). Thus the variation have been calculated through the following index (Eq. 6.11; Eq. 6.12):

$$i_{A(LSS-DS)} = \frac{|\Delta_{(LSS-DS),A}|}{MOE_{dyn,A,DS}} \quad (6.11)$$

$$\Delta_{(LSS-DS),A} = MOE_{dyn,A,LSS} - MOE_{dyn,A,DS} \quad (6.12)$$

where:

$MOE_{dyn,A,LSS} = SWS_D \cdot \rho_{LSS}$

$MOE_{dyn,A,DS} = SWS_D \cdot \rho_{DS}$

The results are showed in Table 6.16 and Figure 6.24. It is clear that significant variations in MOE from DS to LSS have been found, with variation up to 3400 MPa (for specimen "2" in CS wood). In general it has been seen an average variation ($i_{MOEdyn,A,(LSS-DS)}$) of 13.70% for CS and 7.82% for PNL. The greater variation of the Chestnut than Corsican Pine is probably related to the greater geometric irregularity of the specimens.

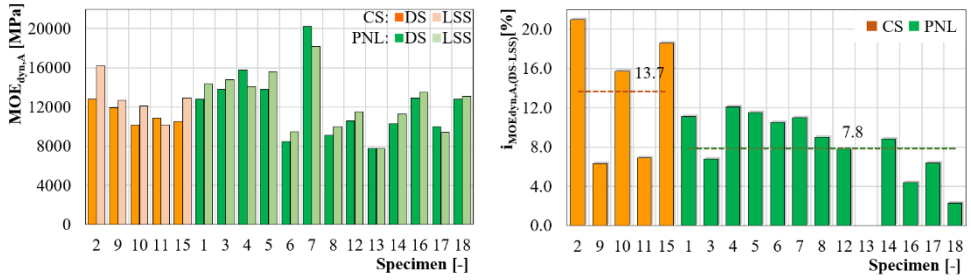

a) b)

Figure 6.24. a) Acoustic test - Dynamic Modulus of Elasticity ($MOE_{dyn,A}$) from ρ_{DS} and ρ_{LSS}; b) Index of $MOE_{dyn,A}$ variation for DS-LSS methods.

Table 6.16. Acoustic test - Dynamic Modulus of Elasticity ($MOE_{dyn,A}$) for DS-LSS methods and index of variation

W. S.	ID	$MOE_{dyn,A,DS}$	$MOE_{dyn,A,LSS}$	$\Delta_{(LSS-DS)A}$	Index of $MOE_{dyn,A}$ variation ($i_{,A,(LSS-DS)}$)			
					$i_{A(LSS-DS)}$	Min	Mean	Max
[-]	[-]	[MPa]	[MPa]	[MPa]	[%]	[%]	[%]	[%]
	2	12800	16200	-3400	21.00			
	9	11900	12700	-800	6.30			
CS	10	10200	12100	-1900	15.70	6.30	13.70	21.00
	11	10900	10200	700	6.90			
	15	10500	12900	-2400	18.60			
	1	12800	14400	-1600	11.10			
	3	13800	14800	-1000	6.80			
	4	15800	14100	1700	12.10			
	5	13800	15600	-1800	11.50			
	6	8500	9500	-1000	10.50			
PNL	7	20200	18200	2000	11.00	0.00	7.82	12.10
	8	9100	10000	-900	9.00			
	12	10600	11500	-900	7.80			
	13	7800	7800	0	0.00			
	14	10300	11300	-1000	8.80			
	16	12900	13500	-600	4.40			
	17	10000	9400	600	6.40			
	18	12800	13100	-300	2.30			

A comparison of $MOE_{dyn,A}$ in longitudinal (L) and diagonal (D) direction has been subsequently performed, using density data derived from the LSS method as they are more accurate than DS. Thus the variation of MOEdyn,A as function of L and D direction of testing has been evaluated through the following index (Eq. 6.13; Eq. 6.14):

$$i_{MOEdyn,A(L-D)} = \frac{\Delta MOE_{dyn,A}}{MOE_{dyn,A,D}} \tag{6.13}$$

$$\Delta MOE_{dyn,A} = MOE_{dyn,A,L} - MOE_{dyn,A,D} \tag{6.14}$$

where:

$MOE_{dyn,A,L} = SWS_L \cdot \rho_{LSS}$

$MOE_{dyn,A,D} = SWS_D \cdot \rho_{LSS}$

The results are showed in Table 6.17 and Figure 6.25. It has been found that from longitudinal to diagonal direction there is an average variation equal to 4.20% for CS and 4.90% for PNL. The maximum deviation between L and D dynamic MOE occurs for specimen "3" and it is equal to 1900 MPa ($i_{MOEdyn,A\ (L-D)}$: 12.80%).

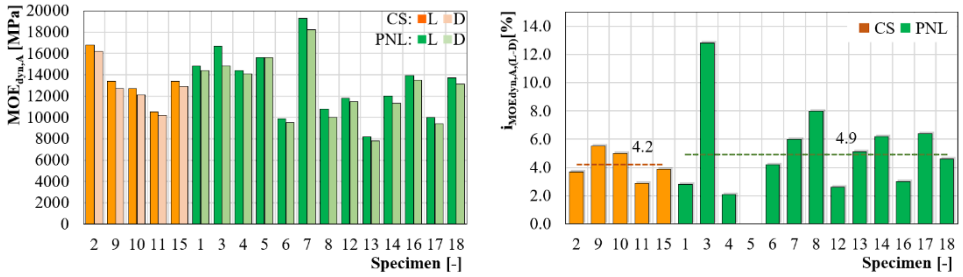

a) b)

Figure 6.25. Acoustic test: a) Dynamic Modulus of Elasticity ($MOE_{dyn,A}$) from longitudinal (L) and diagonal (D) direction; b) Index of $MOE_{dyn,A}$ variation for L-D directions.

Table 6.17. Acoustic test - Dynamic Modulus of Elasticity ($MOE_{dyn,A}$) for longitudinal (L) - diagonal (D) directions and index of variation.

W. S.	ID	$MOE_{dyn,A,L}$	$MOE_{dyn,A,D}$	$\Delta MOE_{dyn,A,}$	Index of $MOE_{dyn,A}$ variation ($i_{MOEdyn,A(L-D)}$)			
					$iMOE_{dyn,A\ (L-D)}$	Min	Mean	Max
[-]	[-]	[MPa]	[MPa]	[MPa]	[%]	[%]	[%]	[%]
	2	16800	16200	600	3.70			
	9	13400	12700	700	5.50			
CS	10	12700	12100	600	5.00	2.90	4.20	5.50
	11	10500	10200	300	2.90			
	15	13400	12900	500	3.90			
	1	14800	14400	400	2.80			
	3	16700	14800	1900	12.80			
	4	14400	14100	300	2.10			
	5	15600	15600	0	0.00			
	6	9900	9500	400	4.20			
	7	19300	18200	1100	6.00			
PNL	8	10800	10000	800	8.00	0.00	4.90	12.80
	12	11800	11500	300	2.60			
	13	8200	7800	400	5.10			
	14	12000	11300	700	6.20			
	16	13900	13500	400	3.00			
	17	10000	9400	600	6.40			
	18	13700	13100	600	4.60			

In the end, an overall outline of $MOE_{dyn,A}$ derived from diagonal tests (D) and LSS method is given in Table 6.18 and Figure 6.26. As can be seen from average $MOE_{dyn,A}$ values, both CS and PNL samples have medium-high stiffness ($MOE_{dyn,A}$: 12820 MPa for CS; $MOE_{dyn,A}$: 12554 MPa for PNL). A greater dispersion of data has been seen for PNL (COV: 22.6%) than CS (COV: 15.1%). The minimum value of $MOE_{dyn,A}$ has been found for specimen "13" ($MOE_{dyn,A}$: 7800 MPa) while the maximum one for specimen "7" ($MOE_{dyn,A}$: 18200 MPa) and it is in accordance with SWSs.

Table 6.18. Acoustic test – Dynamic Modulus of Elasticity.

W. S.	ID	Acoustic test - Dynamic Modulus of Elasticity ($MOE_{dyn,A}$)					
		$MOE_{dyn,A,D}$	Min	Mean	Max	σ	COV
[-]	[-]	[MPa]	[MPa]	[MPa]	[MPa]	[MPa]	[%]
CS	2	16200	10200	12820	16200	1941	15.1
	9	12700					
	10	12100					
	11	10200					
	15	12900					
PNL	1	14400	7800	12554	18200	2832	22.6
	3	14800					
	4	14100					
	5	15600					
	6	9500					
	7	18200					
	8	10000					
	12	11500					
	13	7800					
	14	11300					
	16	13500					
	17	9400					
	18	13100					

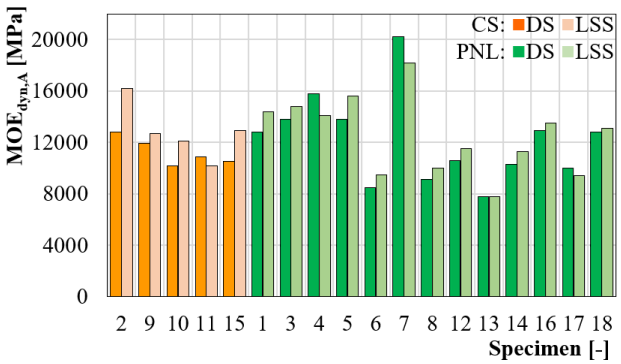

Figure 6.26. Acoustic test - Dynamic Modulus of Elasticity ($MOE_{dyn,A}$) from ρ_{DS} and ρ_{LSS}.

6.2.5.5 Vibrational test

Test equipment

The vibrational test has been performed with *ViSCAN Portable, MiCROTECH*. This kind of device, thanks to a laser interferometer, measure the natural frequency of vibration of a timber member in longitudinal direction after a percussion. The device is portable, thus the measurements can be made in any environment by placing the timber member above two supports and placing the device towards the head member. In this way the laser interferometer is and after hammering, the device measures the natural frequency of vibration (*f*).

Figure 6.27. The vibrational test device: *ViSCAN Portable MICROTEC*.

Thus, the test equipment is made up of a portable device (*ViSCAN Portable*) for data acquisition, connected to a PC that allows data visualisation and processing. Although the device is portable, this technique is not applicable *in situ* as the analysis requires the member to be free on the heads.

As the acoustic test, also vibrational one is useful for determining the quality of timber. In general, high frequencies generally indicate good wood quality while low frequencies indicate poor quality or presence of decay.

Procedure and test set-up

Also the vibrational tests have been carried out on the whole sample. A single measure in longitudinal direction have been acquired for each specimen. The test has been carried out through the following steps:

- device placing in a fixed position for the whole duration of the test;
- specimen positioning above the two supports and in front of the device;
- hitting the timber member on the head with a hammer (Figure 6.28.a);
- acquisition of measurement by device (Figure 6.28.b). After, the data have been stored and the dynamic Modulus of Elasticity (MOE_{dyn}) has been computed, combining the natural frequency of vibration (*f*) with the wood density and specimen dimensions (Eq. 6.15):

$$MOE_{dyn,V}=\rho\cdot(2\cdot f\cdot L)^2 \quad (6.15)$$

where:

$MOE_{dyn,A}$ modulus of elasticity derived from vibrational tests [MPa];

ρ wood density [kg m^{-3}];

f natural frequency of vibration in longitudinal direction [Hz];

L length of the specimen [m].

As for acoustic test, the MOE_{dyn} has been calculated taking into account both the density estimated from DS and LSS, in order to evaluate the variations in stiffness due to the different geometrical survey methods.

a) b)

Figure 6.28. The vibrational test set-up: a) back view; b) front view.

Results and discussion

The natural frequency of vibration (*f*) measured through vibrational test are listed in

Table 6.19 and depicted in Figure 6.29. In general, it can be noted that average frequencies for CS and LSS are quite similar (*f*: 521 Hz for CS; *f*: 505 Hz for PNL).

Table 6.19. Vibrational test – Natural frequency of vibration in longitudinal direction.

W. S.	ID	Vibrational test – Frequency (*f*)					
		f	Min	Mean	Max	σ	COV
[-]	[-]	[Hz]	[Hz]	[Hz]	[Hz]	[Hz]	[%]
	2	529					
	9	496					
CS	10	570	481	521	570	31	5.9
	11	530					
	15	481					
	1	506					
	3	533					
	4	494					
	5	524					
	6	455					
PNL	7	585	400	505	585	50	10.0
	8	400					
	12	516					
	13	462					
	14	572					
	16	521					
	17	449					
	18	550					

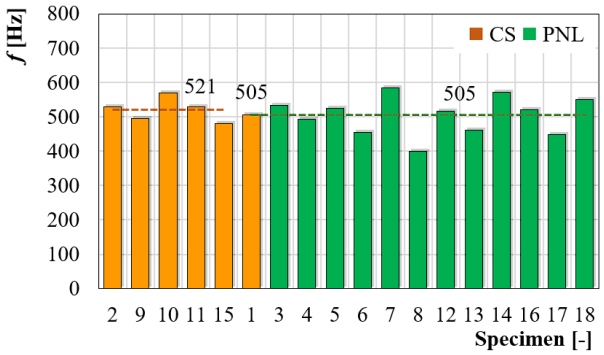

Figure 6.29. Vibrational test – Natural frequency of vibration in longitudinal direction.

Nevertheless a greater dispersion of data have been seen for PNL (COV: 10.0%) than CS (COV: 5.9%). The minimum value of frequencies has been found for specimen "8" (*f*: 400 Hz) while the maximum one for specimen "7" (*f*: 585 Hz).

As already shown for the acoustic test, also for the vibrational test the impact of survey methods has been evaluated by comparing $MOE_{dyn,V,LSS}$ and $MOE_{dyn,V,DS}$. Thus the index of relative variation has been calculated as follow (Eq. 6.16; Eq.6.17):

$$i_{V(LSS-DS)} = \frac{|\Delta_{(LSS-DS),V}|}{MOE_{dyn,V,DS}} \quad (6.16)$$

$$\Delta_{(LSS-DS),V} = MOE_{dyn,V,LSS} - MOE_{dyn,V,DS} \quad (6.17)$$

where:

$MOE_{dyn,V,LSS} = \rho_{LSS} \cdot (2 \cdot f \cdot L)^2$

$MOE_{dyn,A,DS} = \rho_{DS} \cdot (2 \cdot f \cdot L)^2$

The results are presented in Table 6.20 and Figure 6.30. It is apparent that remarkable variations in MOE from DS to LSS have been found, with differences up to 3300 MPa (for specimen "2" in CS wood). In general it has been found an average variation ($i_{MOEdyn,V,(DS-LSS)}$) equal to 13.60% for CS and 8.00% for PNL. As already discussed, high value of $i_{MOEdyn,V,(DS-LSS)}$ for CS are due to the geometrical irregularities of the specimens.

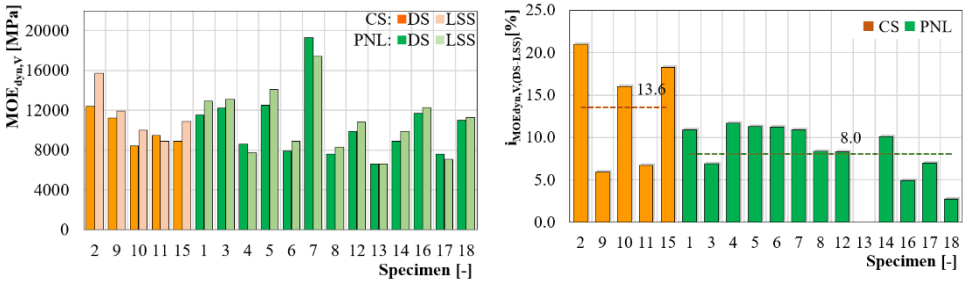

Figure 6.30. a) Vibrational test - Dynamic Modulus of Elasticity ($MOE_{dyn,V}$) from ρ_{DS} and ρ_{LSS}; b) Index of $MOE_{dyn,V}$ variation for DS-LSS methods.

Table 6.20. Vibrational test - Dynamic Modulus of Elasticity ($MOE_{dyn,V}$) for DS-LSS methods and index of variation

W. S.	ID	$MOE_{dyn,V,DS}$	$MOE_{dyn,V,LSS}$	$\Delta_{(DS-LSS)V}$	Index of $MOE_{dyn,V}$ variation ($i_{MOEdyn,V,(DS-LSS)}$)			
					$i_{V(DS-LSS)}$	Min	Mean	Max
[-]	[-]	[MPa]	[MPa]	[MPa]	[%]	[%]	[%]	[%]
	2	12400	15700	-3300	21.00			
	9	11200	11900	-700	5.90			
CS	10	8400	10000	-1600	16.00	5.90	13.60	21.00
	11	9500	8900	600	6.70			
	15	8900	10900	-2000	18.30			
	1	11500	12900	-1400	10.90			
	3	12200	13100	-900	6.90			
	4	8600	7700	900	11.70			
	5	12500	14100	-1600	11.30			
	6	7900	8900	-1000	11.20			
PNL	7	19300	17400	1900	10.90	0.00	8.00	11.70
	8	7600	8300	-700	8.40			
	12	9900	10800	-900	8.30			
	13	6600	6600	0	0.00			
	14	8900	9900	-1000	10.10			
	16	11700	12300	-600	4.90			
	17	7600	7100	500	7.00			
	18	11000	11300	-300	2.70			

In the end the $MOE_{dyn,V}$ has been calculated taking into account ρ_{LSS} the derived from LSS method, as it is a more accurate than ρ_{DS}. The results are shown in Table 6.21 and Figure 6.31. As can be seen from average $MOE_{dyn,V}$ values, both CS and PNL samples have medium-high stiffness ($MOE_{dyn,V,CS}$: 11480 MPa; $MOE_{dyn,V,PNL}$: 10800 MPa). A greater dispersion of data has been found for PNL (COV: 27.9%) than CS (COV: 20.3%).

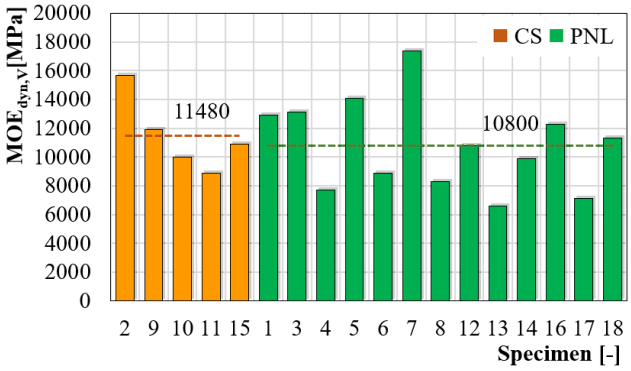

Figure 6.31. Vibrational test – Dynamic Modulus of Elasticity

Table 6.21. Vibrational test – Dynamic Modulus of Elasticity

W. S.	ID	Vibrational test - Dynamic Modulus of Elasticity ($MOE_{dyn,V}$)					
		$MOE_{dyn,V}$	Min	Mean	Max	σ	COV
[-]	[-]	[MPa]	[MPa]	[MPa]	[MPa]	[MPa]	[%]
	2	15700					
	9	11900					
CS	10	10000	8900	11480	15700	2331	20.3
	11	8900					
	15	10900					
	1	12900					
	3	13100					
	4	7700					
	5	14100					
	6	8900					
PNL	7	17400	6600	10800	17400	3016	27.9
	8	8300					
	12	10800					
	13	6600					
	14	9900					
	16	12300					
	17	7100					
	18	11300					

The minimum value of $MOE_{dyn,A}$ has been found for specimen "13" ($MOE_{dyn,A}$: 6600 MPa) while the maximum one for specimen "7" ($MOE_{dyn,A}$: 17400 MPa) and it is in accordance with frequencies results.

6.2.6 DESTRUCTIVE TEST (DT) IN BENDING

6.2.6.1 General procedures

In the field of ancient timber constructions, it is well known as the prediction of members strength is challenging for technicians and researchers. It is basically due to the fact that timber, especially ancient timber, exhibits significant strength fluctuation between and within its parts as function of several conditions. In general the strength variation along a timber beam depends on the length of the element, the geometrical features, the type of loading (distribution, stress rate, ec.), as well as defects and decay distribution of course. In addition to these parameters, other factors that affect strength include the moisture content of timber.

An extensive part of the experimental campaign has been dedicated to the destructive test in bending, that are described in this chapter. The whole sample has been tested: 5 specimens of Chestnut (CS) and 13 specimens of Corsican Pine (PNL). As already shown in the previous chapters, the specimens have been subjected to an extensive diagnostic campaign. An exhaustive geometrical survey of the elements and visual inspection has been performed in order get an accurate geometry model and to detect the extent of defects and decay. Thus, large knots and group of knots have been located on the specimens' lateral surfaces. Because the position of the knots in relation to the loading direction greatly affects the bending performance. Then, on the basis of the evidence gathered after the visual inspection, the visual strength grading (VSG) has been performed in order to assign a visual grade to the members according to the pertinent regulations. Hence, the mechanical properties of timber have been estimated following this approach. This was essential for the purposes of destructive test since a prediction of the failure loads has been done. After, these previsions has been validated thanks to the results of an extensive Non-Destructive (NDT) experimental campaign. It is important to notice that the bending test have been carried out after the NDT, therefore the moisture content of timber has been calculated again before the DT test.

The bending test have been carried out in the Laboratory "Grandi Modelli" at the University of Calabria (Arcavacata di Rende, Italy). The teste have been performed according to UNI EN 408 [333] regulation, that specifies test methods for determining the properties of structural timber and glued laminated timber for rectangular and circular shapes (of substantially constant cross section). The main purposes of testing investigations were the determination of the load-displacement curves, the stiffness in bending properties, such as local ($E_{m,l}$) and global ($E_{m,g}$) modulus of elasticity, flexural strength (f_m), together with the evaluation of relevant failure mechanisms under bending stress state. All these parameters are determined by means of a four-point bending test. This symmetrical application of load and restraint results in a central zone subject to constant moment and zero shear. This minimises the effects of shear stress in section where the moment reaches its maximum values.

The regulation UNI EN 408 [333] prescribe the following geometrical configuration for the test set-up: the minimum specimen length is equal to $19h \pm 1.5h$ (where h is the height of cross-section);

- the distance between the simple support points is equal to $18h \pm 3h$;
- the distance between the load application points is equal to $6h$;

- the distance between each load application points and the support is equal to 6h;

Furthermore, for the calculation of the $E_{m,l}$ the standard prescribes measuring the relative displacement of the specimen over a length of 5h placed in the middle-span (Figure 6.31).

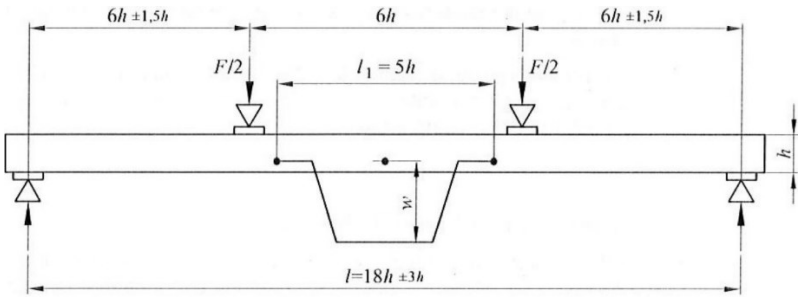

Table 6.34. Test set-up for local bending modulus of elasticity ($E_{m,l}$) estimation (modified from: [333]).

For determining the stiffness of the specimen both local and global modulus of elasticity are calculated in a load range that at most reaches the 40% of the load failure (0.40 F_{max}). The local modulus of elasticity ($E_{m,l}$) is calculated from the relative displacement (w) (Figure 6.31), measured at the central gauge length (Eq. 6.18):

$$E_{m,l}=\frac{a\cdot l_1^2\cdot(F_2-F_1)}{16\cdot I\cdot(w_2-w_1)} \tag{6.18}$$

where:

a distance between a loading position and the nearest support [mm];

l_1 gauge length (6h) [mm];

F_2-F_1 load increment on the straight-line portion until the value of 0.40 F_{max} [KN];

I second moment area of the cross-section [mm^4];

w_2-w_1 displacement increment on the straight-line portion corresponding to the F_2-F_1 force increment [mm].

At the same, the absolute displacement values (w) at the mid-span of the specimen (Figure 6.32) have been related to the actuator force (F) aiming at obtaining (F-w) curve and calculating the global modulus of elasticity ($E_{m,g}$) (Eq. 6.19):

$$E_{m,g}=\frac{3al^2-4a^3}{2bh^3\left(2\frac{w_2-w_1}{F_2-F_1}\right)} \tag{6.19}$$

where:

a distance between a loading position and the nearest support [mm];

l length between the simple supports [mm^4];

b base of the cross-section of the specimen [mm];

h height of the cross-section of the specimen [mm];

F_2-F_1 e load increment on the straight-line portion [KN];

w_2-w_1 displacement increment on the straight-line portion [mm].

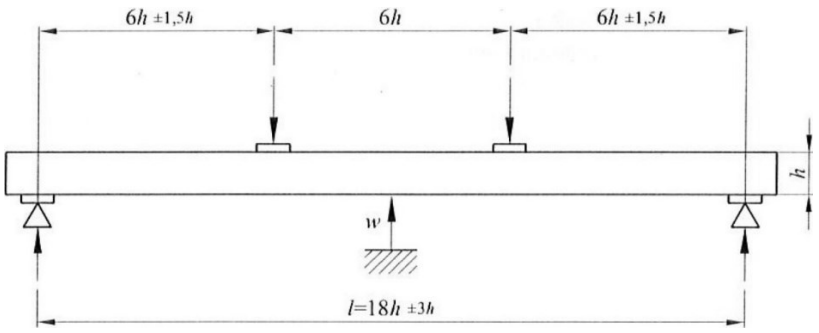

Figure 6.32. Test set-up for global bending modulus of elasticity ($E_{m,g}$) estimation (modified from: [333]).

Thus, the experimental tests showed in the following chapters are organized in two main sections: elastic and failure cycle tests. The first one deal with the calculation of the global and local modulus of elasticity, the second deal with the evaluation of the ultimate bending strength. In the follow a brief recapitulation of the main features of the specimens is firstly provided,

then the test equipment and test set-up are described. In the end the results are showed, analysed and discussed.

6.2.6.2 Elastic cycle

Test equipment

The bending test have been carried out using a quasi-static loading procedure. Thus the load have been applied through a hydraulic pump which was run manually. The load has been measured using a 100 KN load cell (class C1), with an accuracy of 1% of the load applied to the specimen. The test equipment consisted also of 7 displacement transducers (LVDT) with accuracy of of $1 \cdot 10^{-3}$, an acquisition system (HBM-Spider 8) and a PC for data recording.

a) b) c)

Figure 6.33. Bending test equipment: a) hydraulic pump; b) part of the test frame and the load cell; c) the load cell.

a) *b)*

Figure 6.34. Bending test equipment: a) acquisition system *Spider 8*; b) displacement transducers (LVDT)

a) b) c)

Figure 6.35. Views of test frame and specimen: a) diagonal view; b) lateral view; c) diagonal view.

The test have been carried out with a test frame which the laboratory is equipped. The load has been distributed to the two points of application by means of an IPE steel profile, effectively dimensioned.

Procedure and test set-up

The whole sample has been tested in elastic cycle bending test. The test set-up has been defined according to the standard prescriptions [333] and taking into account the geometrical features of specimens (Table 6.22).

In order to avoid variation in the test set-up and in view of the geometric uniformity of the test specimens, a single test set-up has been assumed for the whole sample. In this view the geometrical features of the test set-up have been fixed: the height of the specimen cross-section have been approximated to 200 mm (h: 200 mm), thus the length between the support points have been fixed equal to 3600 mm (18h) and distance between the load application points equal to 1200 mm (6h). The support points are external to the frame, they are located at 855 mm from the floor.

The load has been applied on timber specimen by mean of two steel rolls. Due to the geometrical irregularity of the specimen, the steel rolls was levelled by means of timber chocks. Furthermore, an steel subframe has been fixed to the test frame to support the LVDTs, while metal plates have been fixed on the specimens vertical sides in correspondence of the LVDT measurement points (Figure 6.36).

Table 6.22. Geometrical features and moisture content of the sample

Wood species [-]	Specimen [-]	b [mm]	h [mm]	L [mm]	MC [%]
CS	2	200	230	4403	12.0
	9	200	210	4373	12.7
	10	215	190	3834	12.0
	11	180	205	3965	12.1
	15	235	210	4180	12.9
PNL	1	190	210	4400	11.9
	3	180	245	4280	12.0
	4	195	230	3498	12.9
	5	195	230	4369	12.7
	6	200	220	4493	11.6
	7	190	205	4465	11.9
	8	215	220	4427	12.3
	12	198	240	4288	12.8
	13	175	245	4038	12.1
	14	205	235	3911	10.9
	16	180	220	4274	13.0
	17	180	195	4048	11.9
	18	205	215	4062	11.4

(M.C. referred to the time of DT tests)

a) b) c)

Figure 6.36. Test set-up for elastic cycle: a) LVDT arrangement on specimen vertical side "2"; b) "LVDT7" at tensile side; c) supporting point.

As regard to the LVDT, a single LVDT has been placed in the bottom side for measuring the global displacement, while a number of 6 LVDTs (3 for each specimen vertical side) have been fixed for measuring the local displacement on a length equal to 5h (5h: 1000 mm, with h equal to 200 mm). As results a total number of 7 LVDTs have been used for elastic cycle of the bending test.

On the specimen vertical side "1" three LVDT has been placed: "LVDT1, LVDT2, LVDT3" (Figure 6.37). While on the specimen vertical side "2" the following LVDT have been located: LVDT4, LVDT5, LVDT6. Thus the relative displacement at the central gauge length has been calculated as the average of the relative displacement measured on the two vertical side of the specimen (Eq. 6.20):

$$w_{rel}=\frac{w_{side1}+w_{side2}}{2} \tag{6.20}$$

where:

$$w_{side1}=w_{LVDT2}-\left(\frac{w_{LVDT1}+w_{LVDT3}}{2}\right)$$

$$w_{side2}=w_{LVDT5}-\left(\frac{w_{LVDT4}+w_{LVDT6}}{2}\right)$$

w_{side1} relative displacement measured on the specimen vertical side "1" [mm];

w_{side2} relative displacement measured on the specimen vertical side "2" [mm].

The absolute displacement for calculating $E_{m,g}$ correspond to the measure of the "LVDT7" (w_{LVDT7}).

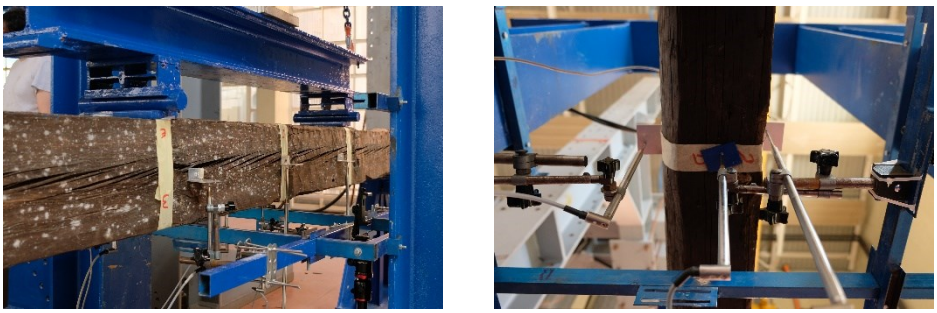

a) b)

Figure 6.37. Test set-up for elastic cycle: a) LVDT arrangement on specimen vertical side "2"; b) "LVDT7" at tensile side.

The elastic test have been carried out to calculate the local and global static modulus of elasticity. Thus, three cycles in elastic ranges have been carried out using a quasi-static loading procedure and limiting the maximum applied force within the conventional branch (0.4 F_{max}). The 3 cycles procedure has been applied to progressively reach the 40% of the failure force (Figure 6.38).

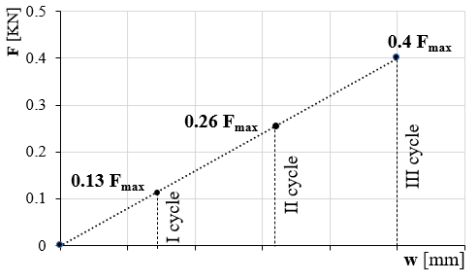

Figure 6.38. Elastic cycle test loading procedure.

In order to calculate the load steps of the three cycles, the failure load (F_{max}) has been estimated using the results of the VSG classification. Having noted the visual strength grade of each specimen according to UNI EN 11035-2 [349] the max bending strength (f_m) has been used to determine the failure moment (M_{max}) and then the F_{max}.

Results and discussion

On the basis of the data obtained from the measurements and their processing, the "load-relative displacement curve" and "load-absolute displacement curve" have been obtained (Figure 6.39). It is apparent as the relative displacement (max: 2 mm) are much smaller than the absolute displacement (max: 14 mm).

The main outputs of the elastic bending test are listed in Table 6.23, whereas the representative values of the global and local modulus of elasticity for the two wood species are provided in Table 6.24. The basic statistic of the measured mechanic properties is reported too, including minimum (min), Mean and maximum (Max) values, standard deviation (σ) and coefficient of variation (COV).

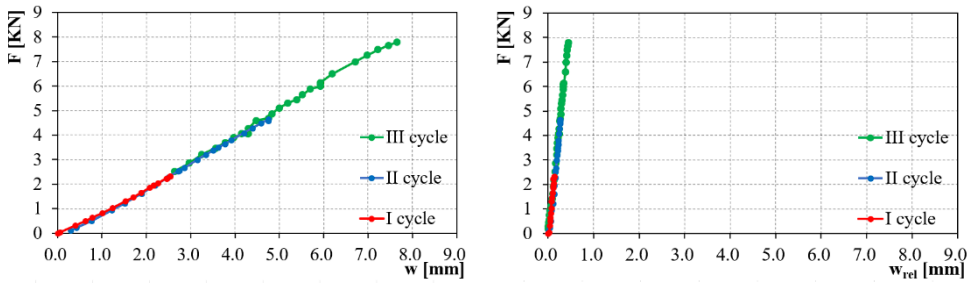

Figure 6.39. Elastic cycles – Specimen 2: a) load-absolute displacement curve; b) load-relative displacement curve.

Table 6.23. Main outputs of elastic cycle bending test

W. S.	ID	Local			Global		
		F_2-F_1	w_2-w_1	$E_{m,l}$	F_2-F_1	w_2-w_1	$E_{m,g}$
[-]	[-]	[KN]	[mm]	[MPa]	[KN]	[mm]	[MPa]
CS	2	5.84	0.50	4300	5.84	5.44	4400
	9	6.00	0.35	8200	6.00	3.74	8600
	10	5.02	0.73	4200	5.02	7.68	4400
	11	5.81	0.63	5400	5.81	5.47	7000
	15	7.01	0.41	7100	7.01	5.73	5600
PNL	1	6.46	0.25	13000	6.46	3.15	11600
	3	10.83	0.38	9800	10.83	4.13	9400
	4	10.31	0.36	10900	10.31	5.26	8200
	5	10.20	0.30	12700	10.20	4.04	10600
	6	8.08	0.44	7800	8.08	6.40	5900
	7	7.50	0.35	12000	7.50	3.34	13600
	8	8.81	0.31	11100	8.81	5.24	7300
	12	11.49	0.47	8000	11.49	6.19	6700
	13	7.80	0.63	4400	7.80	5.69	5300
	14	9.27	0.42	7500	9.27	5.38	6400
	16	6.97	0.29	11400	6.97	3.93	9200
	17	6.82	0.73	6300	6.82	7.31	6900
	18	7.16	0.23	14000	7.16	3.22	10900

It is evident that the values obtained for Corsican Pine are on average higher than those for Chestnut for both the local and global modulus of elasticity. Indeed, for CS the average value of $E_{m,l}$ and $E_{m,g}$ are respectively equal to 5840 MPa and 6000 MPa, while for PNL they are respectively equal to 9915 MPa and 8615 MPa. The maximum value of $E_{m,l}$ is equal to 8200 MPa for CS and 14000 MPa for PNL. The minimum value of $E_{m,l}$ is equal to 4200 for CS and 4400 for PNL.

It can be seen that there is homogeneity between the local and global elastic modulus. In fact $E_{m,l}$ and $E_{m,g}$ show a COV near to 27.5% for both wood species.

Table 6.24. Local and global modulus of elasticity.

	Wood species. [-]	Min [MPa]	Mean [MPa]	Max [MPa]	σ [MPa]	COV [%]
$E_{m,l}$	CS	4200	5840	8200	1576	27.0
	PNL	4400	9915	14000	2778	28.0
$E_{m,g}$	CS	4400	6000	8600	1615	26.9
	PNL	5300	8615	13600	2412	28.0

In order to evaluate the difference between local and global modulus, the difference ($\Delta E_{m\,(l\text{-}g)}$) has been calculated for each specimen and then the relative percentage variation has been evaluated as follow (Eq. 6.21):

$$i_{E_{m(l\text{-}g)}} = \left| \frac{\Delta E_{m(l\text{-}g)}}{E_{m,g}} \right| \tag{6.21}$$

where:

$i_{E_{m(l\text{-}g)}}$ index of relative variation between $E_{m,l}$ and $E_{m,g}$;

$\Delta E_{m(l\text{-}g)} = E_{m,l}\text{-}E_{m,g}$ difference between local and global modulus of elasticity (MPa);

$E_{m,l}$ local modulus of elasticity (MPa);

$E_{m,g}$ global modulus of elasticity (MPa).

From the Table 6.25 and Figure 6.40 it can be seen that there is a greater variation of $i_{Em(l\text{-}g)}$ for PNL sample (average value equal to 21.52%) than the CS sample (average value equal to 12.24%). The maximum variation has been found for specimen 8 in PNL, where the difference $\Delta E_{m(l\text{-}g)}$ is equal to 3800 MPa and the relative variation ($i_{E_{m(l\text{-}g)}}$) is equal to 52.1%. This huge difference is probably related to the evaluation of the local modulus, which is based on the measurement of displacements of a few millimeters and therefore its estimation can be affected by errors.

Table 6.25. Comparison between the local and global modulus of elasticity.

W. S.	ID	$E_{m,l}$	$E_{m,g}$	$\Delta E_{m\ (l-g)}$	Index of E_m variation ($i_{Em\ (l-g)}$)			
					$i_{Em\ (l-g)}$	Min	Mean	Max
[-]	[-]	[MPa]	[MPa]	[MPa]	[%]	[%]	[%]	[%]
	2	4300	4400	-100	2.30			
	9	8200	8600	-400	4.70			
CS	10	4200	4400	-200	4.50	2.30	12.24	26.80
	11	5400	7000	-1600	22.90			
	15	7100	5600	1500	26.80			
	1	13000	11600	1400	12.10			
	3	9800	9400	400	4.30			
	4	10900	8200	2700	32.90			
	5	12700	10600	2100	19.80			
	6	7800	5900	1900	32.20			
PNL	7	12000	13600	-1600	11.80			
	8	11100	7300	3800	52.10			
	12	8000	6700	1300	19.40	4.30	21.52	52.10
	13	4400	5300	-900	17.00			
	14	7500	6400	1100	17.20			
	16	11400	9200	2200	23.90			
	17	6300	6900	-600	8.70			
	18	14000	10900	3100	28.40			

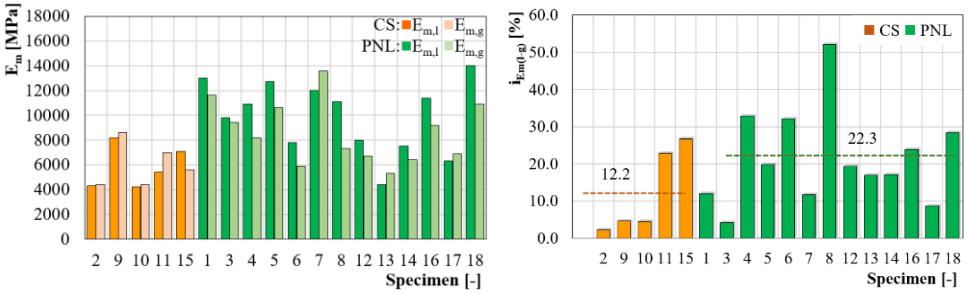

a) b)

Figure 6.40. a) Local and global modulus of elasticity in bending for CS and PNL; b) Index of variation between local and global modulus.

6.2.6.3 Failure cycle

Test equipment

The test equipment for failure cycle is the same of the elastic cycle, however, has been used a single displacement transducer ("LVDT7").

Procedure and test set-up

After the elastic cycles, the specimens have been tested in bending up to the failure through a quasi-static loading procedure. The test set-up consist in the same equipment arrangement used for elastic cycle, but a single displacement transducer has been used. This is the "LVDT7" placed at the tensile side of the specimen for measuring the absolute displacement. Hence, the steel subframe hasn't been applied.

Figure 6.41. Failure cycle test set-up.

The test procedure consisted in several loading-reloading cycles, thus the reduction of the load-bearing capacity and the stiffness degradation have been analysed. Destructive tests results are provided in terms of applied actuator force (F) versus loading w actuator displacement (w; LVDT7). Thus, the failure load and displacement are estimated, moreover the ultimate bending strength has been evaluated by (Eq. 6.22):

$$f_m = \frac{a \cdot F_{max}}{2 \cdot W} \tag{6.22}$$

where:

f_m ultimate bending strength [MPa];

a distance between a loading position and the nearest support [mm];

F_{max} failure load [N];

W section modulus [mm^3].

Results and discussion

The curve load displacement of specimens 2 and 10 are showed in Figure 6.42. In general, it can be seen that the first branch of the curve is linear and then non-linear. This behaviour is marked in Specimen 10, where there is a significant reduction in stiffness. After the first cycle of loading, additional cycles have been carried out to assess the residual strength of the member. In general, three to five loading cycles have been performed for each specimen. However, in specimen 6 the complete collapse occurred on the first cycle. In general, a reduction in stiffness and strength has been observed following the first cycle and this is related to the partialisation of the cross-section. However, some specimens (specimen 2) showed a large reserve of strength by reaching high load values even in cycles after the first one.

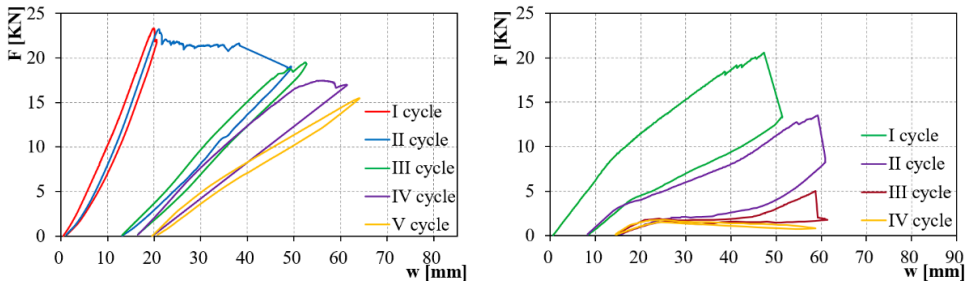

Figure 6.42. Load-displacement curves: a) Specimen 2; b) Specimen 10.

As regard to the strength values the results have been provided in Figure 6.42. In general, highly variable values have been found, as shown by the coefficients of variation. Indeed for both wood species an high dispersion of data has been observed (COV:37.3% for CS, COV:42.0% for PNL). The maximum load and bending moment have been noted respectively equal to 93.7 KN and 56.2 KNm (specimen 5 in PNL). It is clear that the values obtained for Corsican Pine are on average higher than those for Chestnut. Indeed, for CS the average value of f_m is equal to 13.5 MPa, while for PNL is equal to 22.9 MPa. As concern the PNL the maximum strength value is equal to 39.9 MPa (specimen 7), while the minimum is equal to 7.2 MPa. As regard to Chestnut the maximum is equal to 19.9 MPa while the minimum is equal to 7.9 MPa.

As regard the deformation, in general low values have been found for the global displacement, that have been measured at the middle span point. The average value is equal to about 35 mm and it range between a minimum of 12.5 mm (specimen 11) and a maximum of 54 mm (specimen 15).

Table 6.26. Main parameter and outputs of failure cycle bending test.

W.S. [-]	ID [-]	b [mm]	h [mm]	W [dm^3]	F_{max} [KN]	w_{max} [mm]	M_{max} [KNm]	f_m [MPa]
	2	200	230	1.76	23.3	20.0	14.0	7.9
	9	200	210	1.47	48.8	39.9	29.3	19.9
CS	10	215	190	1.29	20.6	46.2	12.4	9.6
	11	180	205	1.26	36.3	12.5	21.8	17.3
	15	235	210	1.73	37.3	54.1	22.4	13.0
	1	190	210	1.40	81.9	51.0	49.1	35.2
	3	180	245	1.80	90.4	40.0	54.2	30.1
	4	195	230	1.72	59.9	40.1	36.0	20.9
	5	195	230	1.72	93.7	46.8	56.2	32.7
	6	200	220	1.61	46.1	39.0	27.7	17.2
	7	190	205	1.33	88.6	33.6	53.1	39.9
PNL	8	215	220	1.73	39.9	24.4	23.9	13.8
	12	198	240	1.90	50.0	30.2	30.0	15.8
	13	175	245	1.75	21.0	16.4	12.6	7.2
	14	205	235	1.89	46.9	36.8	28.2	14.9
	16	180	220	1.45	58.6	37.6	35.1	24.2
	17	180	195	1.14	33.3	27.2	20.0	17.5
	18	205	215	1.58	73.9	43.7	44.4	28.1

Table 6.27. Bending strength values.

W.S. [-]	Min [MPa]	Mean [MPa]	Max [MPa]	σ [MPa]	COV [%]
CS	7.9	13.5	19.9	5.1	37.3
PNL	7.2	22.9	39.9	9.7	42.0

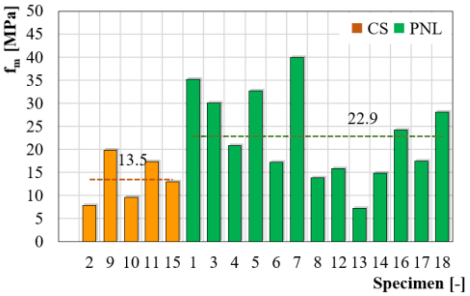

Figure 6.43. Bending strength values.

From the analysis of the failure modalities of the specimens, several types of failure have been identified. They can be traced back to those well known in the relevant scientific literature [35], [39], taking into account the peculiarities of the ancient timber [445]. However, no well-defined typologies have been identified, but often complex mechanisms resulting from the

concomitance of several phenomena. In general, all the specimens have been showed a fragile and pseudo-fragile failure mechanism due to fracture or its triggering at the tensioned side. Therefore, no mechanisms of collapse due to excessive compression have been identified. A total number of 4 failure mechanisms have been identified.

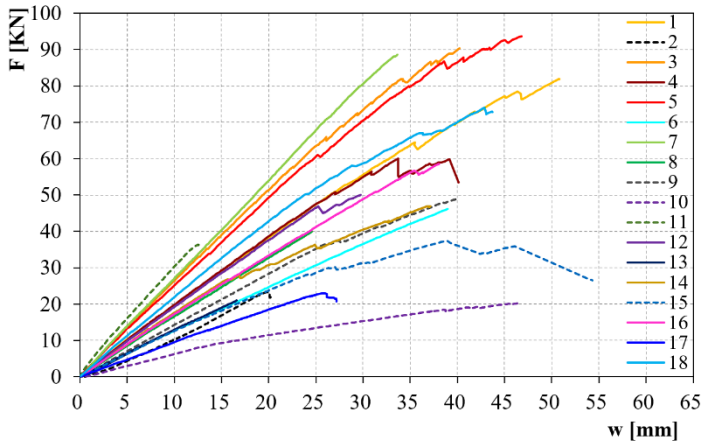

Figure 6.44. Bending test: Load-displacement curve of failure cycles (dot line: CS; continue line: PNL).

The first mechanism has been detected for the specimens 2, 9, 10 and 15 (CS), as well as for the specimens 1, 18 and 12 (PNL). For these specimens, the collapse occurred at the large nodes located within the middle third. In fact, for such specimens, the maximum knot sizes vary from 70 mm (specimen 15) to 100 mm (specimen 2) in minimum diameter. This modality affected almost all Chestnut specimens, as they were characterized by many large knots. However, two different types of fracture trigger were identified for this mechanism. For specimens 2, 9, 1, 18 the fracture trigger has been observed at the notch joint at the tension side. From here the fracture progressed to the knots. Here the final collapse occurred by rupture of the fibres adjacent to the knot, with a rotational kinematic motion (Figure 6.45.a). On the other hand, specimens 10, 15 and 12 showed crack trigger at the knots present at the tension side (Figure 6.45.b). For these collapse modes, strength values ranging from 7.9 MPa up to 35.2 MPa have been found, furthermore the ultimate displacements ranging from 20 mm up to 55 mm. It is important to note that the specimens 2, 10, 15 (CS) showed very low f_m values, due to the presence of large knots (2 and 15) and decay from widespread insect attack. At the same time the density ranges from 524 Kgm^{-3} to 724 Kgm^{-3}.

For most specimens (PNL: 3, 7, 17, 4, 5, 13, 14), a collapse mode characterized by crack fiber separation has been reached at the pre-existing shrinkage cracks. The main predisposing factor for this mode has been found in the presence of shrinkage cracks in the middle third. However, two different trigger modes have been recognized for this collapse mode. For specimens 3, 7, 17 (PNL) the trigger occurred at the notch joint (Figure 6.46.a). From here, the crack proceeded in a pattern like a staircase, until it reached failure by fiber separation at the shrinkage cracks. In contrast, for specimens 11 (CS), 4, 5, 13 and 14 (PNL) the trigger occurred by fiber fracture at the tension side, showing an initial vertical crack (Figure 6.46.b). From here, the crack proceeded in a staircase pattern. The collapse occurred by fiber divarication at a point characterized by shrinkage cracks. Highly variable values of both displacement (from 12.5 mm to 46.8 mm) and strength (from 7.2 MPa to 39.9 MPa) have been found for this failure mechanism. Furthermore, even for density a high variability has been noted (from 474 Kgm^{-3} to 637 Kgm^{-3}).

Figure 6.45. a) Failure of the specimen: a) 2; b) 12.

Figure 6.46. a) Failure of the specimen 3; b) Failure of specimen 11.

Instead, the brittle tension modality [35], [39] has been identified for specimen 16, where the failure affected a large volume at the tension side, reaching up to the neutral axis of the cross section (Figure 6.48.a). Moreover, the fracture surface has been characterized by the widespread presence of wood splinters. A similar modality has been observed for specimen 6, where the fracture surface has been characterized by many wood splinters. However, a sudden collapse has been observed, accompanied by a very loud sound. The specimen separated into two pieces and the observation of the fracture surface revealed the presence of 3 resin pockets radially arranged at the failure point (Figure 6.47). The ultimate displacement for both specimens were quite similar (39.0 mm for specimen 6 and 37.6 mm for specimen 16), whereas a bending strength values equal to 17.2 MPa and 24.2 MPa have been found for specimen 6 and 16 respectively. It is important to note that the force-displacement-to-breakage curves are similar to a straight line, indicating that the breakage was of the brittle type. Although this failure mode is associated with low wood density, moderate values have been observed for these specimens (531 Kgm^{-3} for specimen 6 and 619 Kgm^{-3} for specimen 16).

Figure 6.47. Failure specimen 6: a) Complete failure of the member; b) Evidence of the resin tasks in cross section.

Figure 6.48. a) Failure specimen 16; b) Failure specimen 8.

In the end, a failure mode typical of elements with sloped grain has been found for specimen 8 in PNL. Although the specimen had a moderately sloped grain (8%), the collapse mechanism has been characterized by crack trigger at the notch point and propagation in diagonal direction following the grain trend (Figure 6.48). A little displacement at failure (24.4 mm) and low bending strength (13.8 MPa) has been observed for this specimen.

6.2.7 LONG-TERM TEST IN BENDING

6.2.7.1 General

As seen at Chapter 1, Section 1.3.2.2., timber is characterized by visco-elastic mechanical behaviour. Specifically, a timber member subjected to a static load for a long time is subjected to deferred deformations (creep). In addition, since wood is a hygroscopic material, stiffness and strength are affected by the environmental temperature and moisture content.

In order to understand the effect of creep on the timber beam deformation a long-term test involving 4 specimens has been performed. A permanent load has been applied on the specimens, constantly measuring the vertical displacement and the moisture content of the beams, as well as the environmental thermo-hygrometric parameters. The test has been performed in Laboratory "Grandi Modelli" at University of Calabria and test duration was about 12 months.

6.2.7.2 Application and results discussion

Test equipment

The long-term test has been carried out through a four-point bending scheme, by applying a dead load on the specimens. The supports points have been made with masonry blocks and the dead load consists of masonry blocks and steel members. The test equipment consisted of devices for measuring the member's displacement and moisture content, as well as environmental temperature and humidity. For displacement measurement has been used a centesimal comparator with accuracy of $1 \cdot 10^{-2}$ mm. It was placed at midspan in order to measure the displacement at midspan. For the moisture content measurement the device *HYDROMETTE M2050 (Gann)* has been used. For

temperature and humidity measurements the digital device *ThermPro TP49 mini* has been used (Figure 6.49).

Procedure and test set-up

The geometrical features of the bending scheme are the same of the destructive test: the bending span is equal to 3600 mm, the distance between the load application points is equal to 1200 mm, as well as the distance between this point and the supporting points (Figure 6.50). The test has been carried out on 4 members: specimen 9 and 11 (*Castanea sativa* Mill.), specimen 7 and 13 (*Pinus nigra* subsp. *laricio*). The dead load (F_{LTT}) has been calculated by assuming it as the 15% of the expected ultimate load. The ultimate load has been calculated taking into account the results of both VSG and DT. As results a dead load equal to 2.5 KN has been fixed for specimen 9 – 11 and 3.5 KN for specimen 7 – 13 (Table 6.28).

a) b) c)

Figure 6.49. Long-term bending test equipment: a) centesimal comparator; b) wood hygrometer; c) digital device recorder for environmental temperature and humidity.

Table 6.28. Long-term bending test set-up.

Wood Species	ID [-]	b [mm]	h [mm]	I [dm^4]	$E_{m,l}$ [MPa]	$E_{m,g}$ [MPa]	$E_{m,l}$·I [Nm^2]	F_{LTT} [KN]
CS	9	210	200	1.40	8200	8600	1148000	2.5
	11	205	180	1.00	5400	7000	538002	2.5
PNL	7	205	190	1.17	12000	13600	1406095	3.5
	13	245	175	1.09	4400	5300	481451	3.5

The test duration was about 1 year (May 2022 to May 2023), during which two measurements per week have been recorded. For each member the moisture measurements have been done on two vertical side (Side 1 and 2) respectively, so that the data have been averaged later. The temperature and humidity of the environment have been measured near the specimen location and almost always in the time period from 11 a.m. to 4 p.m. Only in August have the measurements been taken from 6 p.m. to 7 p.m.

The following parameters have been measured:

RH relative humidity [%];

T environmental temperature [°C];

MC moisture content [%];

w_0 instantaneous displacement [mm];

$w_{(t)}$ displacement at time t [mm].

In this way the differential displacement has been calculated as the ratio of the displacement at time *t* to the instantaneous displacement ($w_{(t)}/w_0$).

Figure 6.50. Long-term bending test equipment: a) centesimal comparator; b) wood hygrometer; c) digital device recorder for temperature and humidity.

Results and discussion

During approximately one year of testing (360 days), 101 measurements have been taken. The test results are depicted in the following graphs, where time is the variable expressed in both months and days.

Starting from the environmental parameters showed in Figure 6.51, it can be noted that the maximum temperature (T:33°C) has been reached in July and August, while the minimum (T: 8°C) has been recorded in February. The average value has been found to be equal to 22°C. Furthermore, the maximum excursion between the two following dates of measurement has been recorded in May, and it is equal to 8 °C.

As regard relative humidity (RH), the maximum value (RH: 90%) has been recorded in December, whereas the minimum value has been found to be equal to 27% (month of May) and 27% is the average (Figure 6.51). Moreover, the humidity exceeded the threshold of 65% 14 days out of 101 days of test, while it exceeded 85% only once. The maximum excursion between the two following dates of measurement has been found to be equal to 37% and it has been recorded in September. Given the results of the thermo-hygrometric measurements, it can be said that the exposure conditions of the specimens during the test are comparable to those of Service Class 1 [71], [70].

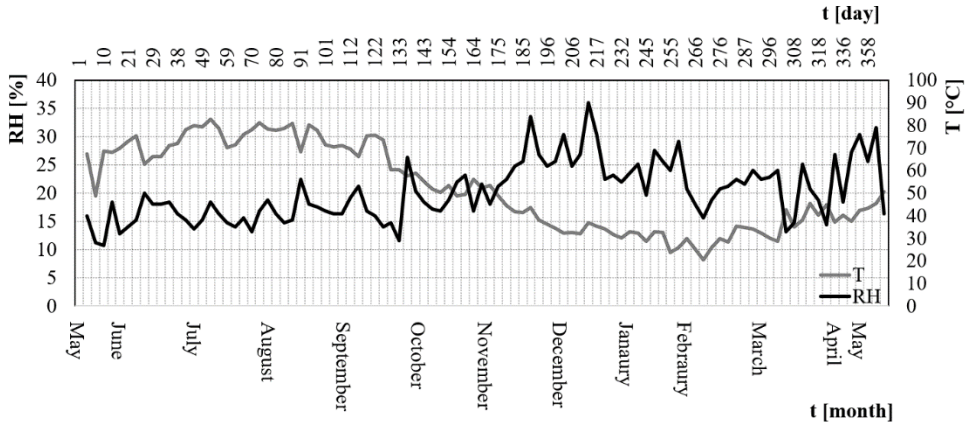

Figure 6.51. The environmental temperature (T) and relative humidity (RH) over time.

The four specimens started with different moisture contents (Table 6.29). The lowest moisture content (9.9%) was of specimen 13 in PNL, while the

highest (13.2%) was of specimen 9 in CS (Figure 6.52). For all specimens, the maximum content was reached in December and January, while the minimum content has been recorded between June and September. The maximum positive excursion has been observed for sample 13 in PNL and it was 2.2%. The lowest excursion has been found for specimen 7 in PNL and it was -2.7%. The highest moisture value has been observed to be 13.8% for specimen 9 (CS), which had a moisture value of 13.8% at the start of the test (t_0). The minimum has been reached by sample 13 (PNL), which had a moisture content of 9.9% at t = 0. From the analysis of the data obtained, it would appear that Corsican Pine was more susceptible to changes in moisture content, showing the greatest variations both upwards and downwards. In addition, the trend of the moisture content curve (Figure 6.52) of the PNL specimens (green and blue curve) seems to be more adherent to the environmental relative humidity curve.

Table 6.29. The moisture content (MC) of specimens: initial (t_0), minimum and maximum content.

Wood species	Chestnut		Corsican Pine	
ID	9	11	7	13
$MC_{t=0}$	13.2%	12.5%	12.2%	9.9%
MC_{min} (ΔMC)	10.9% (-2.4) September 2022	10.4% (-2.2) June 2022	9.5% (-2.7) July 2022	8% (-2.0) August 2022
MC_{max} (ΔMC)	13.8% (+0.6) January 2023	13.6% (+1.1) December 2022	12.8% (+0.6) January 2023	12.1% (+2.2) January 2023

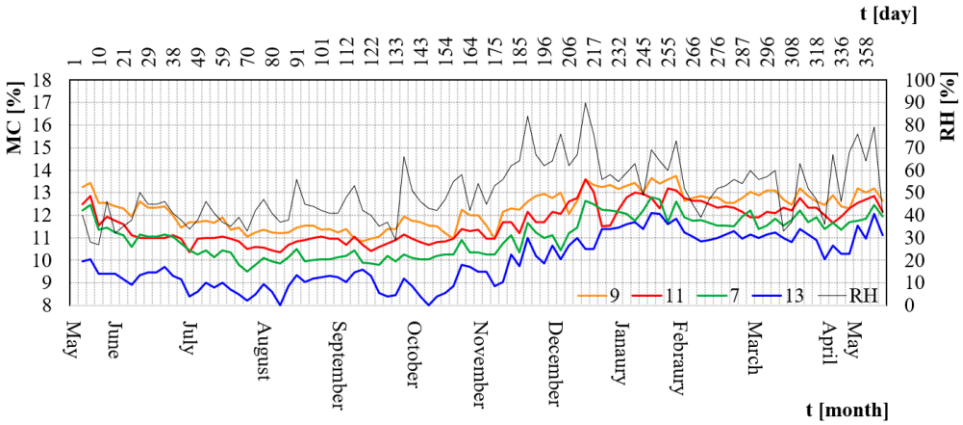

Figure 6.52. The environmental relative humidity (RH) and the moisture content (MC) of the timber specimens over time

Figure 6.53 shows the trend over time for vertical displacements. The instantaneous displacement (w_0) has been recorded in the few minutes after the start of the test, and then an increase in displacement has been recorded over the days. The specimens showed different values of w_0 (Table 6.30). The specimens 9 and 11 (CS) reported a w_0 of 2.57 mm and 3.93 mm, respectively, whereas specimens 7 and 13 (PNL) showed a w_0 of 1.88 mm and 4.12 mm, respectively. As expected, test specimens 11 and 13, having low elastic modulus values ($E_{m,l}$: 5400 MPa; 4400 MPa, respectively), reported a higher initial displacement.

The time-dependent behaviour of the specimens can be easily read from the curve showing the displacement trend over time, as the increase in deformation is progressively reduced until reaching the maximum displacement. More specifically, it is interesting to note that test specimens 9 (CS) and 7 (PNL), which have a greater elastic modulus, both reached their maximum displacement (3.59 mm and 3.15 mm, respectively) in July, approximately two months after the start of the test. On the other hand, specimens 11 (CS) and 13 (PNL) showed a conspicuous displacement (5.57 mm x 6.50 mm) after six and four months from the test staring, respectively. However, specimen 11 reached its maximum displacement in November (approximately 6 months after the start) and specimen 13 in September (approximately 4 months after the start).

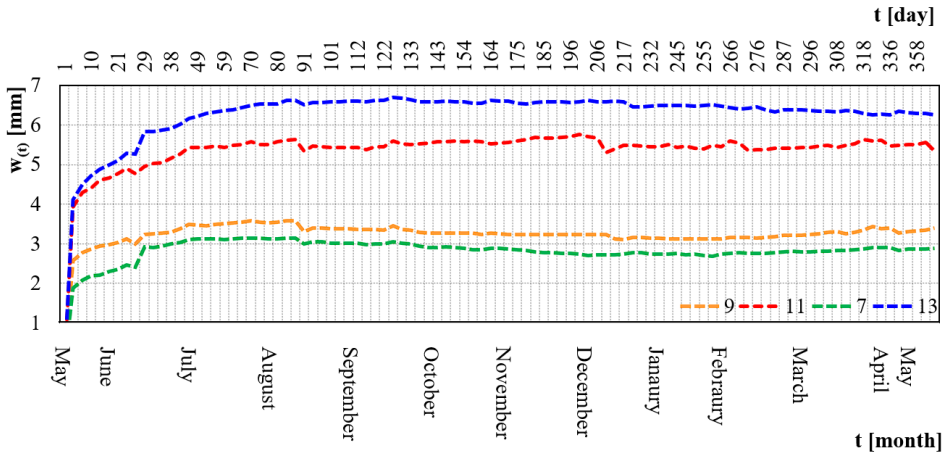

Figure 6.53. The vertical displacement over time ($w_{(t)}$).

Table 6.30. The displacement (w) and its relation to moisture content (MC).

Wood species	Chestnut				Corsican Pine			
ID	9		11		7		13	
w_0	2.57 mm		3.93 mm		1.88 mm		4.12 mm	
$w_{max,LTT}$ ($w_{(t)}/w_0$)	3.59 mm	(1.40)	5.76 mm	(1.47)	3.15 mm	(1.68)	6.69 mm	(1.62)
t (w_{max})	July 2022		November 2022		July 2022		September 2022	
MC (w_{max})	11.1%		12.1%		9.5%		8.5%	

It is also interesting to note that after reaching maximum displacement 2 months after the start of the test, test specimens 9 and 7 did not show any increase in displacement during the winter months when the moisture content reached its maximum value. On the contrary, the MC curves show a slightly decreasing average trend, followed by a slight rise until April 2023. Therefore, it would appear that timber elements with a higher modulus of elasticity reach their maximum displacement earlier (approximately 2 months after the start) and they maintain this displacement almost unchanged. In contrast, the specimens with a lower modulus of elasticity showed prolonged deferred displacements, with the maximum displacement being reached after a period of 4 to 6 months.

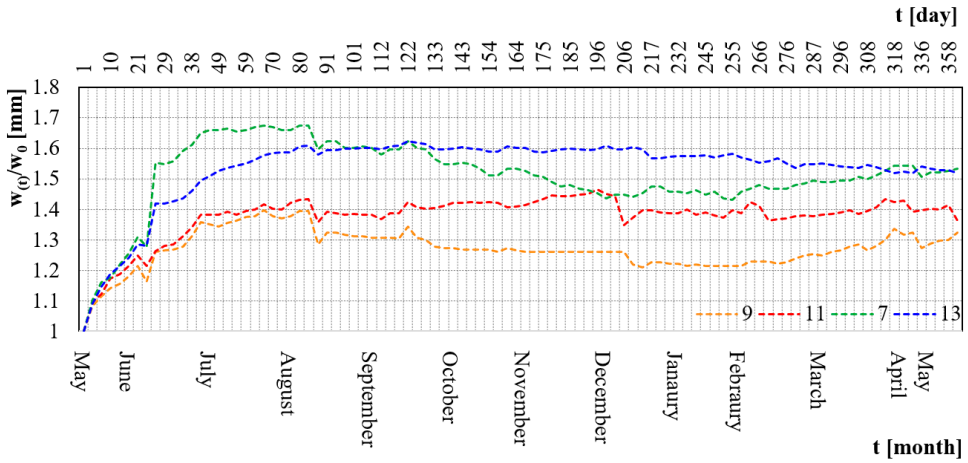

Figure 6.54. The ratio between the vertical displacement over time ($w_{(t)}$) and the instantaneous displacement (w_0)

In Figure 6.54, the ratio between the displacement at time t and the instantaneous displacement ($w_{(t)}/w_0$). It can be seen that specimen 13 (PNL), having a low modulus of elasticity, showed a maximum final displacement

equal to 1.62 times the instantaneous displacement (w_0). At the same time, it is interesting to note that the maximum final displacement of 1.68 (w_0) has been reported by the specimen 7 (PNL) and not by the specimen 11 (CS), as might be expected. In fact, the latter has a lower elastic modulus than specimen 7. Therefore, the maximum final displacements have been found for the specimens in Corsican Pine. They have been found to be equal to 1.62 and 1.68(w_0) for specimen 13 and 7, respectively. On the other hand, the Chestnut specimens showed a maximum final displacement of 1.40 and 1.47(w_0).

These values are comparable to what the standards for the design of timber structures provide [71]. For the calculation of the final displacement, both standards provide an increment equal to 1.60 ($w_{fin}=w_0 \cdot (1+k_{def})$, with k_{def} equal to 0.60 for Service Class 1). However, these values seem to underestimate the Corsican Pine wood displacement, for which values above 1.60 have been found in this work.

The relationship between moisture content and vertical displacement has been analysed for each specimen (Figure 6.55). It can be seen that for specimens 11 and 13, there is an anomalous reduction in the displacement values as the moisture content of the wood increases. At the same time, it has been seen that moisture content variations influenced the final deformation of specimens 7 and 9. At the same time, in accordance with the state of the art it has been seen that temperature did not influence the deformative behaviour of the specimens.

a)

b)

c)

d)

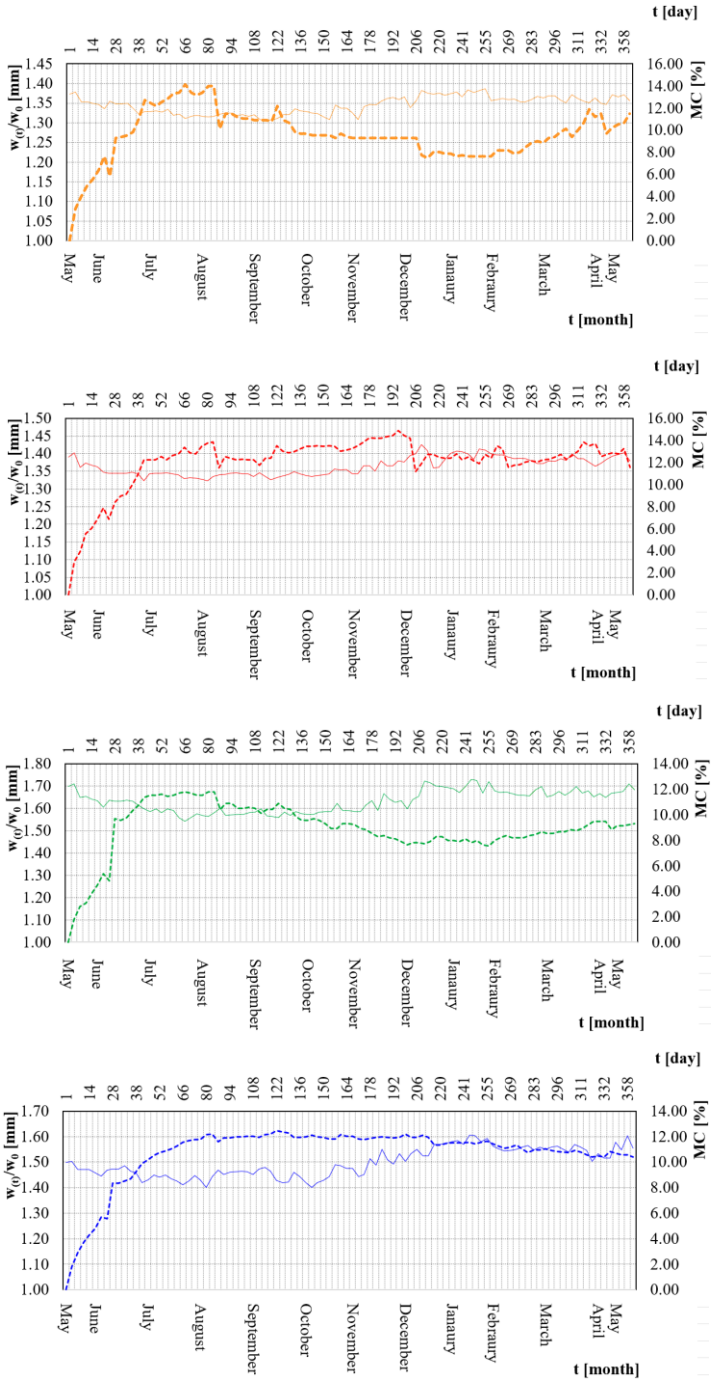

Figure 6.55. The ratio between the vertical displacement and the instantaneous displacement ($w_{(t)}/w_0$) over time for the specimens: a) 9 (CS); b) 11 (CS); c) 7 (PNL); d) 13 (PNL).

6.2.8 STATISTICAL ELABORATION OF RESULTS

6.2.8.1 General procedures

In the final phase of the research, the experimental results of non-destructive (NDT) investigations and destructive (DT) tests have been evaluated using statistical methods. Based on NDT and DT parameters, a set of relationships has been explored using linear regression. These models could provide an estimate of the physical and mechanical properties of the material, considering the randomness of the data sample. Thus, the correlations have been grouped into three classes: correlation between NDT, DT and NDT-DT parameters. Among them, the third group of models (NDT-DT correlations) is the most interesting set of tools for *in-situ* applications in order to predict the mechanical properties of wood. Given that NDT techniques are valuable for conducting structural health assessments of a structure without causing harm, correlating NDT results with the findings from DT is surely a valuable mission. Generally, the quality of the fit is evaluated using the goodness-of-fit index, R^2, which is a summary metric to evaluate the linear model's fit to a given set of data. R^2 is referred to as the coefficient of determination because it reflects the correlation between the dependent variable and the predicted variable, as explained by all predictors. The linear regression herein proposed are shown in terms of equations and R^2.

At the same time, a statistical analysis of DT parameters has been carried out, taking into account the results of the VSG analysis. Starting from the results of the destructive tests, the characteristic values of the mechanical properties (f_m, $E_{m,l}$) and density have been calculated for the sub-samples corresponding to the visual classes identified as a result of the VSG analysis, according to the procedures of Standard UNI EN 384 [49]. In this way, these characteristic values obtained for each visual class have been compared with those assigned by visual strength grading according to UNI 11035 [336], [339]. Therefore, the purpose of this analysis is to understand the efficiency of the results provided by visual classification through comparison with the results of destructive tests. The methodology applied consists of the following analyses. The results of the DT tests have been separated by wood species and by visual strength grade. Subsequently, the characteristic values have been calculated following the procedures of UNI EN 14358 [456] and UNI EN 384 [336], checking the degree of fit of the data with the probability distribution models. In the end, the characteristics properties have been compared with the performance profiles provided by UNI EN 338 [344].

6.2.8.2 VSG-DT relationship

Procedure

This chapter presents the statistical analysis of DT parameters in consideration of the findings of the VSG analysis. The purpose of the analysis is to analytically assess the correspondence between the visual strength classes assigned by VSG analysis and the mechanical and physical properties derived from destructive tests (i.e. density, bending strength, elastic modulus). This evaluation has been performed using descriptive statistics tools and fit tests.

The procedure consists firstly in the sample subdivision according to wood species. A subdivision has been made considering the strength classes (D24 for CS; C12, C24, and C40 for PNL). For each sub-sample, characteristic values of physical-mechanical properties (5^{th} percentile for $f_{m,k}$ and ρ_k; average value for $E_{0,mean}$) have been calculated using a log-normal distribution (for $f_{m,k}$) and normal distribution model (for $E_{0,mean}$ and ρ_k), as prescribed by UNI EN 14358 [446]. A first assessment has been carried out using descriptive statistics such as boxplots and frequency tables (histograms). Then the goodness of fit has been evaluated through the Kolmogorov-Smirnov (KS) normality test [447], which reveals that the data are normally distributed when p-value is higher than significance level. Both graphics and KS test have been performed using the software *IBM SPSS Statistics.*

Results and discussion

First of all, the sample has been analysed by means of the box plots depicted in figure Figure 6.56 for Corsican Pine and in figure Figure 6.57 for Chestnut. For each wood species, three graphs (a, b, c) corresponding to bending strength (f_m), elastic modulus (E_0), and density (ρ), respectively, have been drawn up.

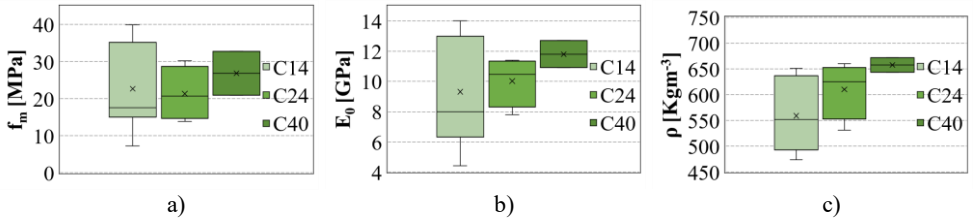

Figure 6.56. Boxplot for PNL sub-samples: a) bending strength; b) Elastic modulus; c) Density.

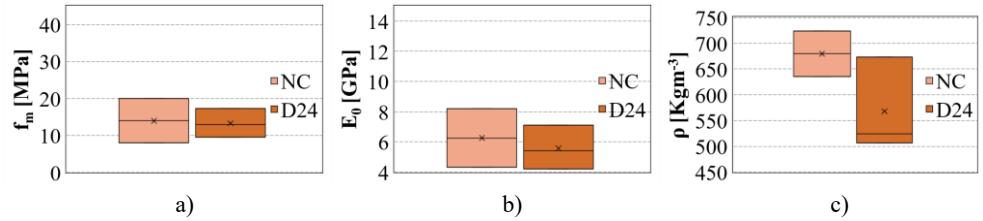

Figure 6.57. Boxplot for CS sub-samples: a) bending strength; b) Elastic modulus; c) Density.

Regarding Corsican Pine (Figure 6.56) it can be said that a similar trend has been noted for all the parameters taken into consideration (f_m, E_0, ρ): both the medians and the average values of each strength class showed an increasing trend as the quality of wood increased (from C14 to C40). Furthermore, class C14 showed a greater dispersion of the data than the other ones, as well as an asymmetric distribution for all the parameters analysed. These findings are probably due to the sample size, which is greater than the C24 and C40.

In contrast, for Chestnut (Figure 6.57), no increasing trend has been observed as the wood quality increased (from NC to D24). Moreover, both the average and median values of the NC sample have been found to be higher than those of the D24 class. This finding is in contrast to expectations and can be attributed to the lower density of some specimens (10 and 11) belonging to the D24 class, which showed intense insect attacks.

Frequency tables have been built considering the subdivision of the sample by wood species and strength classes, as well as considering the three parameters: f_m, E_0, ρ. For the PNL, histograms of classes C14 and C24 are shown in Figure 6.58 and Figure 6.59 respectively, while Figure 6.60 shows the histograms for class D24 of CS. On the same diagrams the probability density functions have been represented. For each sub-sample the number of specimen (n°), the characteristic values according to UNI EN 338 (2016) and the statistical values obtained through destructive tests are shown in Table 6.31, Table 6.32, and Table 6.33 for bending strength, modulus of elasticity a and density respectively. Furthermore, the p-value coefficient of KS test (p_{KS}) has been reported in order to assess the distribution normality [447].

With regard to bending resistance (Table 6.31), it can be seen that for both CS and PNL, the values corresponding to the 5th obtained by DT are much lower than the characteristic values prescribed by UNI EN 338 [344]. The greatest differences have been found for CS, where $f_{m,5th}$ is equal to 9.5 MPa against of 24.0 MPa prescribed by the Standard. The sub-sample C14 showed

the highest dispersion with a COV of 52.9%, whereas the remaining sub-samples showed COVs around 30%.

Table 6.31. Characteristics value of bending strength (f_m) for CS and PNL sub-samples.

W.S. [-]	Sub Sample [-]	n° [-]	$f_{m,k}$ (EN 338) [MPa]	f_m Min [MPa]	Mean [MPa]	Max [MPa]	5^{th} perc. [MPa]	σ [MPa]	COV [%]	p_{KS} [-]
CS	D24	3	24.0	9.6	13.3	17.3	9.5	3.9	29.3	0.198
	NC	2	-	7.9	13.9	19.9	-	-	-	-
PNL	C14	7	14.0	7.2	22.7	39.9	7.2	12.0	52.9	0.238
	C24	4	24.0	13.8	21.3	30.1	13.8	7.3	34.3	0.216
	C40	2	40.0	20.9	26.8	32.7	-	-	-	-

Regarding modulus of elasticity (Table 6.32), for both CS and PNL, the values corresponding to the 5^{th} (obtained from DT) are much lower than the characteristic values prescribed by UNI EN 338 [344]. The greatest differences have been found for CS, where $f_{m,\,5th}$ is equal to 9.5 MPa against of 24.0 MPa prescribed by the Standard.

Regarding modulus of elasticity (Table 6.32), CS showed an average value of 5570 MPa, whereas the value prescribed by the standard is 10000 MPa. On the other hand, for PNL, the values are partially in accordance with the standard. For class C14, the mean value is 9315 MPa, which is higher than the expected value of 7000 MPa. For class C24, the average value is 7800 MPa, while the standard's expected value is 11000 MPa. Finally, for class C40, $E_{0,Mean}$ has been found to be 11800 MPa, which is lower than the standard's expected value (14000 MPa). The class C14 has greatest data dispersion, having a COV of 39.4%.

For density, the values equal to the 5^{th} percentile of the probability distributions have been compared with the characteristic values prescribed by the standard. For CS, a value of 506 kgm^{-3} has been found. It is close to the standard prediction (485 kg m^{-3}). On the other hand, a larger discrepancy between DT results and the standard prescription has been seen for PNL. In general, a slight dispersion of the data has been found, with the maximum COV being 16.0% (for D24 CS).

Table 6.32. Characteristics value of elastic modulus (E_0) for CS and PNL sub-samples.

W.S. [-]	Sub Sample [-]	n° [-]	$E_{0,mean}$ (EN 338) [MPa]	Min [MPa]	Mean [MPa]	Max [MPa]	E_0 5th perc. [MPa]	σ [MPa]	COV [%]	p_{KS} [-]
CS	D24	3	10000	4200	5570	7100	4200	1460	26.2	0.212
	NC	2	-	4300	6250	8200	-	-	-	-
PNL	C14	7	7000	4400	9315	14000	4400	3675	39.4	0.183
	C24	4	11000	10025	7800	11400	7800	1640	21.0	0.244
	C40	2	14000	10900	11800	12700	-	-	-	-

Table 6.33. Characteristics value of wood density (ρ) for CS and PNL sub-samples.

W.S. [-]	Sub Sample [-]	n° [-]	ρ_k (EN 338) [kg m^{-3}]	Min [Kgm^{-3}]	Mean [Kgm^{-3}]	Max [Kgm^{-3}]	ρ 5th perc. [Kgm^{-3}]	σ [Kgm^{-3}]	COV [%]	p_{KS} [-]
CS	D24	3	485	506	568	673	506	92	16.0	0.350
	NC	2	-	635	679	724	-	-	-	-
PNL	C14	7	290	474	559	651	474	66	11.8	0.211
	C24	4	350	531	610	660	531	56	9.2	0.313
	C40	2	400	643	657	672	-	-	-	-

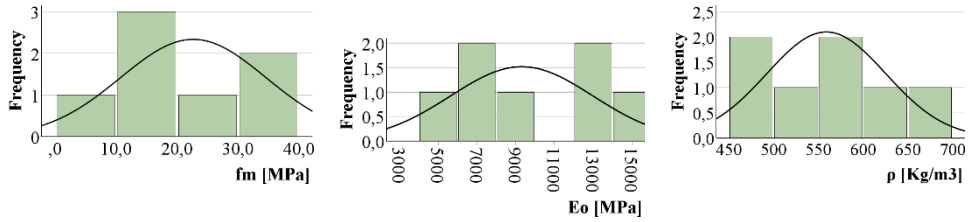

a) b) c)

Figure 6.58. Histogram and normal distribution for C14 PNL sub-samples: a) Bending strength; b) Elastic modulus; c) Density.

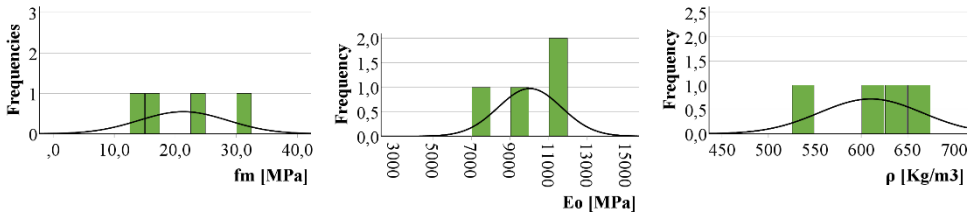

a) b) c)

Figure 6.59. Histogram and normal distribution for C24 PNL sub-samples: a) Bending strength; b) Elastic modulus; c) Density.

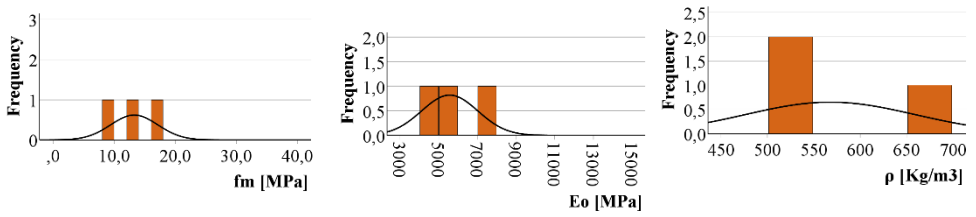

a) b) c)

Figure 6.60. Histogram and normal distribution for D24 NL sub-samples: a) Bending strength; b) Elastic modulus; c) Density.

In the end the Kolmogorov-Smirnov test has been conducted to assess whether each sub-sample of data follows a normal distribution. The p-value (p_{KS}) has been evaluated at a significance level set to 0.05. For all the three parameters (f_m, E_0, and ρ), the p_{KS} value ranges between 0.18 and 0.350. However, as several authors have shown [447], normality tests are very sensitive to sample size, especially when few data are available.

6.2.8.3 NDT and DT Correlations

NDT Correlations

The correlation between the non-destructive parameters themselves has been evaluated. Thus, correlations between the mean drilling resistance measure (R_m) and dynamic modulus of elasticity (MOE_{dyn}) have been evaluated, considering both acoustic ($MOE_{dyn,A}$) and vibrational methods ($MOE_{dyn,V}$). In both cases, the parameter calculated by ρ_{LSS} has been taken into account.

For both $MOE_{dyn,A}$ and $MOE_{dyn,V}$ good correlations have been found (Figure 6.61). R^2 values of 0.71 and 0.48, respectively, have been obtained for Chestnut and Corsican Pine in linear regression between $MOE_{dyn,A}$ and R_m. Slightly better results have been found in the prediction of $MOE_{dyn,V}$ using R_m. Indeed, a goodness of fit index equal to 0.72 and 0.58 have been found for CS and PNL (Table 6.34). A successful prediction of the dynamic modulus of elasticity by means of drilling resistance measurement is probably due to wood density, which is the needed parameter for MOE_{dyn} calculation according to Equation 6.9-6.15, and it is well correlated with R_m.

Table 6.34. NDT linear regression: parameters, coefficients of determination (R^2) and equations.

Parameters		Wood species	R^2	Equation
Dipendent (y)	Indipendent (x)			
$MOE_{dyn,A}$	R_m	CS	0.71	y = 379.12 x + 2314.48
		PNL	0.48	y = 801.03 x + 3643.52
$MOE_{dyn,V}$	R_m	CS	0.72	y = 457.66 x + 1201.74
		PNL	0.58	y = 931.65 x + 8038.60

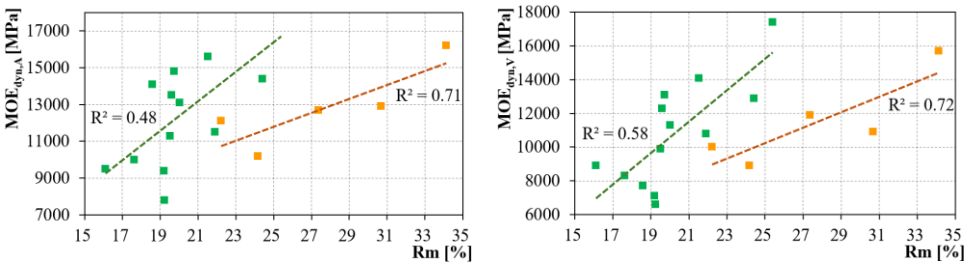

a) b)

Figure 6.61. Prediction of dynamic modulus of elasticity with drilling resistance measure: a) MOE_{dyn} from acoustic test; b) MOE_{dyn} from vibrational test.

DT Correlations

The correlation between the destructive parameters themselves has been assessed, considering the wood density, the bending strength and the global-local modulus of elasticity.

The regression analysis between DT parameters provided very interesting results (Table 6.35). A very, almost perfectly linear relationship has been found between bending strength and the global modulus of elasticity (Figure 6.62.a). In fact, for Chestnut and Corsican Pine, R^2 has been found to be 0.97 and 0.92 respectively. This finding also emerges from the force-displacement graph in Figure 6.44, as it can be seen that generally the curves that reach higher strength values are also the steepest ones (i.e., with highest modulus of elasticity). Consequently, the relationship between bending strength and local modulus of elasticity also showed a good result, with R^2 index of 0.61 for CS and 0.60 for PNL (Figure 6.62.b). Furthermore, from the graphs it is evident that the regression lines of the two wood species are almost overlapping and consequently the equations are very close. Therefore, it can be said that for the examined sample, the linear relationship between local/global elastic modulus and strength is independent of the wood species.

As regard to bending strength the correlation with density has been evaluated. Good results have been found for PNL where the R2 has been

found to be equal to 0.46, whereas a poor correlation has been noted for CS. Furthermore, it can be seen that the f_m-ρ relationship is inversely proportional, which is contrary to what is well known in the scientific literature. However, it can be seen from the Figure 6.63.b that the outliers correspond to the f_m-ρ value pair of specimens 2. Although it had a high density, it showed a low strength value due to the premature collapse triggered by the presence of large knots.

Table 6.35. DT linear regression: parameters, coefficients of determination (R^2) and equations.

Parameters		Wood species	R^2	Equation
Dipendent (y)	Indipendent (x)			
f_m	$E_{m,g}$	CS	0.97	y = 0.003 x - 3.00
		PNL	0.92	y = 0.004 x - 9.03
f_m	$E_{m,l}$	CS	0.61	y = 0.001 x + 0.42
		PNL	0.60	y = 0.001 x - 2.94
f_m	ρ	CS	0.09	y = -0.020 x + 23.17
		PNL	0.46	y = 0.100 x -35.05
$E_{m,l}$	$E_{m,g}$	CS	0.65	y = 0.790 x + 1109.94
		PNL	0.69	y = 0.960 x + 1657.57
$E_{m,g}$	ρ	CS	0.03	y = -3.050 x + 7865.97
		PNL	0.46	y = 25.510 x - 6431.87
$E_{m,l}$	ρ	CS	0.05	y = 4.180 x + 3278.66
		PNL	0.62	y = 34.060 x + 10172.01

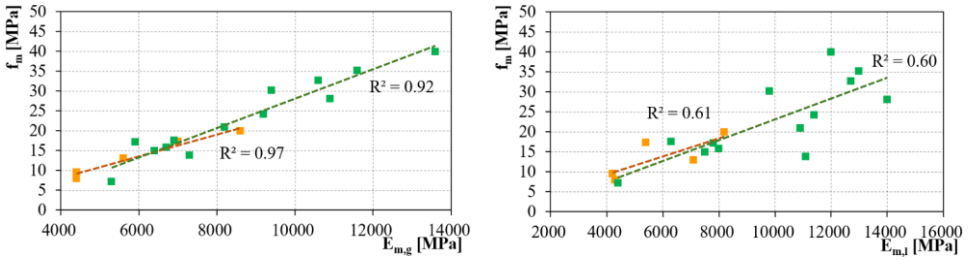

a) b)

Figure 6.62. Prediction of bending strength from a) global modulus of elasticity; b) local modulus of elasticity.

For wood Chestnut, the same results have been seen for the correlation between density and global and local modulus of elasticity, where the R^2 assumed values equal to 0.03 and 0.05. In contrast, for Corsican Pine, a strong correlation has been found between density and global modulus of elasticity (R^2=0.46), while a good correlation has been seen between density and local modulus (R^2=0.62).

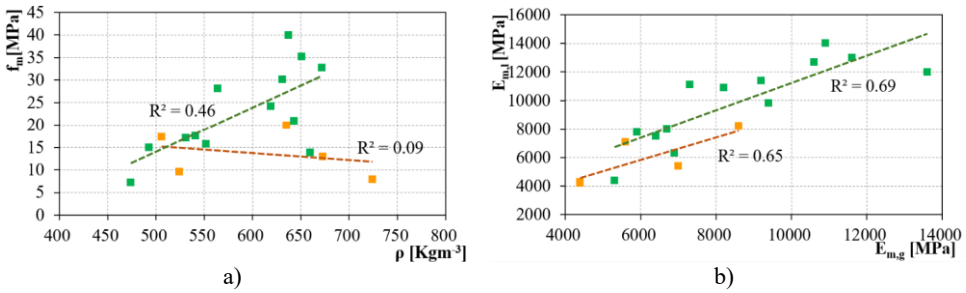

a) b)

Figure 6.63. Prediction of a) bending strength from density; b) local modulus of elasticity from global modulus.

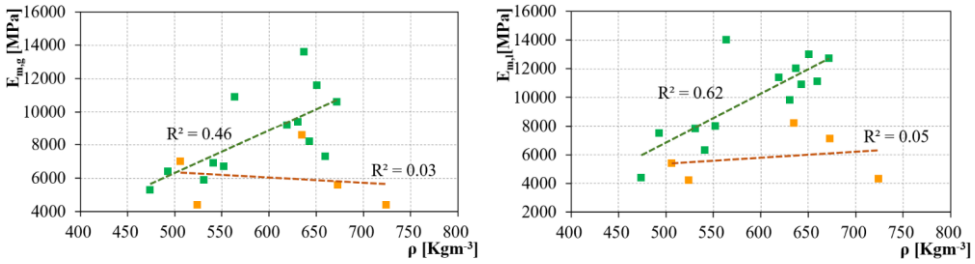

a) b)

Figure 6.64. Prediction of a) global modulus of elasticity from density; b) local modulus of elasticity from density.

In the end, for both wood species, a strong correlation has been found between the global and local moduli of elasticity. A goodness of fit index equal to 0.65 and 0.69 has been found for CS and PNL, respectively. In Figure 6.63.b the two regression lines are shown, and it can be seen that they are parallel. This means that the relationship between global and local modulus has the same proportionality for both species, although a greater stiffness in PNL than CS has been noted.

NDT-DT Correlations

The relationships between non-destructive and destructive parameters are the most interesting for on-site application in the structural health monitoring of timber structures. Therefore, many relations have been analysed in this work, considering all the mechanical and physical parameters shown so far.

In general, looking at the results in Table 6.36, it can be said that the correlations found for PNL are much more reliable than those for CS. The only exception has been seen for the correlations between mean drilling resistance measure (R_m) and density (Figure 6.65), where a strong correlation

(R^2: 0.92) has been noted for chestnut and a very poor for PNL (R^2: 0.12) for the rest, all correlations involving CS showed poor R^2 values. Furthermore, from Figure 6.65.b, Figure 6.66, Figure 6.67 it can be seen that the aforementioned relations between NDT and DT parameters are inversely proportional for Chestnut.

Table 6.36. NDT-DT linear regression: parameters, coefficients of determination (R^2) and equations.

Parameters		Wood species	R^2	Equation
Dependent (y)	Indipendent (x)			
ρ	R_m	CS	0.92	y = 18.850 x + 90.00
		PNL	0.12	y = 9.140 x + 405.08
f_m	R_m	CS	0.10	y = -0.034 x + 22.868
		PNL	0.51	y = 2.707 x – 31.853
f_m	$MOE_{dyn,A}$	CS	0.37	y = -0.001 x + 31.73
		PNL	0.85	y = 0.003 x – 15.14
f_m	$MOE_{dyn,V}$	CS	0.21	y = -0.001 x + 23.85
		PNL	0.79	y = 0.003 x – 6.756
$E_{m,l}$	R_m	CS	0.01	y = 38.680 x + 4768.2
		PNL	0.18	y = 475.840 x + 293.46
$E_{m,l}$	$MOE_{dyn,A}$	CS	0.04	y = -0.162 x + 7919.47
		PNL	0.57	y = 0.738 x + 651.10
$E_{m,l}$	$MOE_{dyn,V}$	CS	0.02	y = -0.098 x + 6970.76
		PNL	0.41	y = 0.590 x + 3508.99
$E_{m,g}$	R_m	CS	0.04	y = -76.456 x + 8118.6
		PNL	0.57	y = 744.060 x + 6430.03
$E_{m,g}$	$MOE_{dyn,A}$	CS	0.21	y = -0.383 x + 10916.10
		PNL	0.82	y = 0.769 x – 1045.00
$E_{m,g}$	$MOE_{dyn,V}$	CS	0.09	y = -0.208 x + 8383.22
		PNL	0.74	y = 0.689 x + 1168.81

As already shown, the regression laws for the Chestnut sample are strongly influenced by specimen 2. Although high values of R_m, $MOE_{dyn,A}$, $MOE_{dyn,V}$, and density have been found for it, at the same time poor values of f_m, $E_{m,g}$ and $E_{m,l}$ have been found due to the high knottiness of the specimen. For this reason, even though the relationships between $MOE_{dyn,A}$, $MOE_{dyn,V}$ and f_m gave an R^2 of 0.37 and 0.21, these equations are not valid because there is an inverse relationship between the aforementioned NDT and DT properties.

Regarding the correlation for PNL, a variable index of goodness has been seen, ranging from poor to very strong. Good relations have been found between the dynamic modulus of elasticity derived from acoustic test

($MOE_{dyn,A}$) and bending strength, since a R^2 equal to 0.85 has been found (Figure 6.66.a).

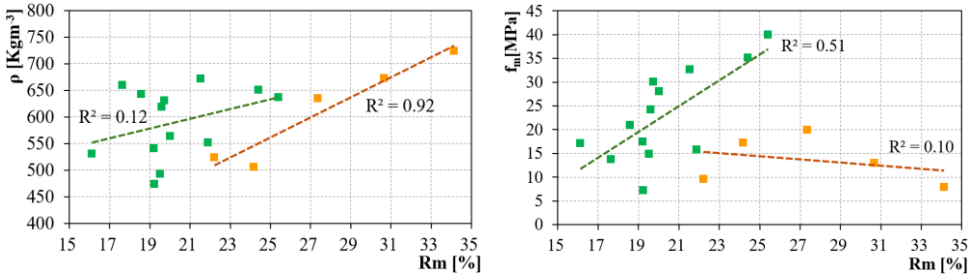

Figure 6.65. Prediction of a) density from mean drilling resistance measure; b) bending strength from mean drilling resistance measure.

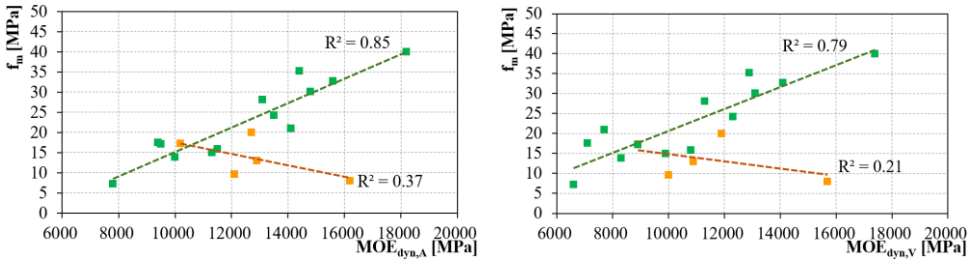

Figure 6.66. Prediction of a) bending strength from MOE_{dyn} from acoustic test; b) bending strength from MOE_{dyn} from vibrational test.

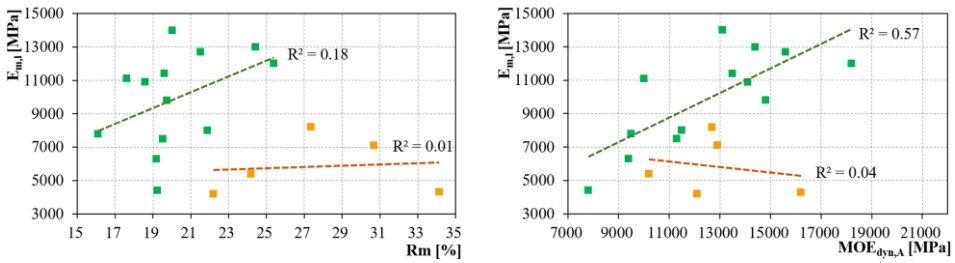

Figure 6.67. Prediction of a) local modulus of elasticity from mean resistance drilling measure; b) local modulus of elasticity from MOE_{dyn} from acoustic test.

Similar results have been found for correlations between the vibrational dynamic modulus ($MOE_{dyn,V}$) and f_m and $E_{m,g}$, with R^2 values of 0.79 and 0.74

(Figure 6.66.b). On the other hand, correlations for local modulus ($E_{m,l}$) prediction with $MOE_{dyn,A}$ and $MOE_{dyn,V}$ are slightly less reliable (R^2: 0.57; 0.41). These results are probably due to the greater randomness of the local form compared to the global form due to the difficulty of estimation. As regard the R_m, it has been already noted that a strong and poor correlation with density has been respectively found for CS and PNL. Looking at correlations with other parameters, good results have been obtained for the prediction of bending strength (R^2: 0.51) and global modulus of elasticity (R^2: 0.57) for the PNL sample. Instead, the prediction of $E_{m,l}$ with R_m results in a poor correlation, with R^2 equal to 0.18. This is probably due to the fact that the drilling resistance measurements have not been performed in the middle third, but near sections A–B.

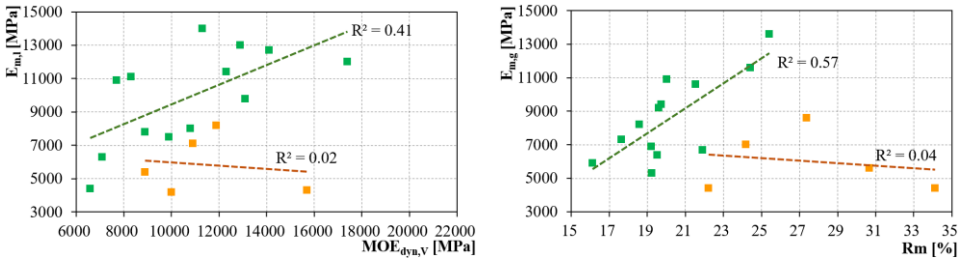

Figure 6.68. Prediction of a) local modulus of elasticity from MOE_{dyn} from vibrational test; b) global modulus of elasticity from mean drilling resistance measure.

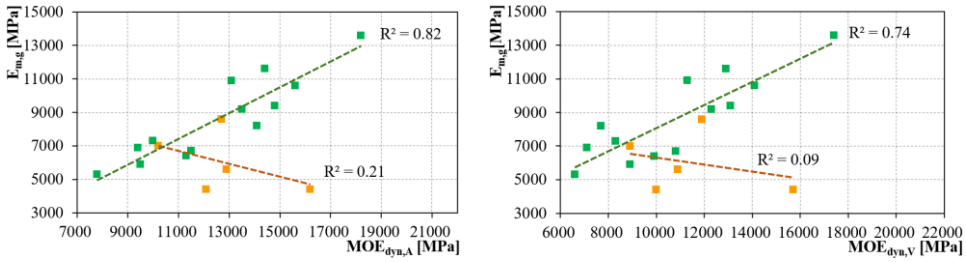

Figure 6.69. Prediction of a) global modulus of elasticity from MOE_{dyn} from acoustic test; b) global modulus of elasticity from MOE_{dyn} from vibrational test.

6.3 MECHANICAL CHARACTERIZATION OF TIMBER LOGS IN *ACACIA DEALBATA* LINK

6.3.1 GENERAL METHODOLOGY

The experimental activity has been performed on 16 wood logs from Acacia dealbata Link. The specimens were harvested from the National Park of Peneda-Gerês in North of Portugal. The experimental campaign has been carried out at Laboratory of the Department of Civil Engineering DEC-UM in Guimarães (Portugal).

Within the experimental activity, different procedures and techniques have been applied:

- Direct geometrical survey (DS);
- Visual Strength Grading (VSG) analysis;
- Non-Destructive Test (NDT);
- Destructive Test (DT) in bending;

The following NDT techniques have been applied: moisture content measurement, density estimation, drilling resistance test and vibrational test.

The objectives and aims of this experimental work are manifold:

- Evaluating the reliability of VSG analysis by comparing DT results for different visual grades, highlighting the most influential visual criteria and suggesting possible future developments in standardization;
- Evaluating the reliability of NDT comparing the test results with those of DT and VSG;

A comprehensive description of the methodology, test equipment, and set-up is provided for each test type. Subsequently, the findings are presented and analysed, emphasising the principal accomplishments of the study.

6.3.2 THE SAMPLE OF STUDY

6.3.2.1 The wood logs

The 16 wood logs in *Acacia dealbata* Link have been harvested in the December 2022 in the forest of the Park. They have been manually cut from plants with an approximate age of 15 to 20 years, having an average height of

about 20 meters. Then, they were subjected to a first kiln drying process. In detail, the sample was subjected to three cycles of drying: a first cycle was conducted before the experimental tests and immediately after the harvesting (Figure 6.70.). Then, VSG and NDTs were performed with exception of drilling resistance test (DRM). Due to the high moisture content recorded at the time of the NDT, the sample was subjected to two additional drying cycles. In the end the DT in bending and DRM were performed.

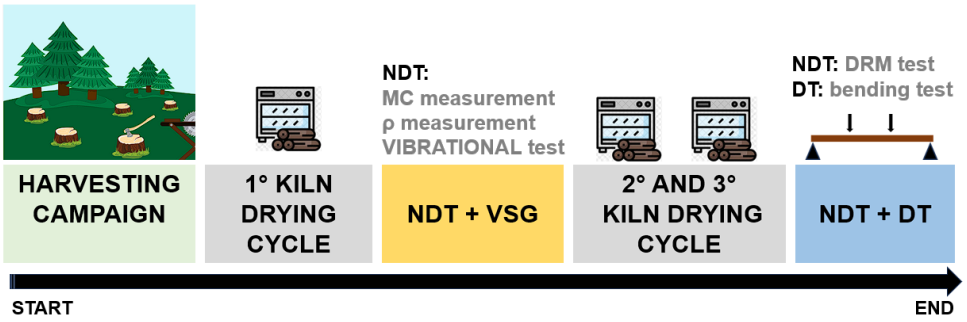

Figure 6.70. Steps of the experimental campaign

a) b)

Figure 6.71. a) The *A. dealbata* harvesting campaign in the National Park of Peneda-Gerês, Portugal [448]; b) Part of the wood logs stored in the Laboratory of School of Engineering at University of Minho, Guimaraes, Portugal.

Each specimen is characterized by a rounded cross section, an average diameter of about 110 mm and a length of about 2000 mm.

6.3.2.2 Main features of the identified wood species

The wood species was recognized at the time of harvesting in the forest, as the tree showed the typical characteristics of the *Acacia dealbata* plant [449], [450] i.e., the yellow and rounded flowers, as well as the bipinnate leaves (Figure 6.72). Generally, the average height of the Acacia D.L. tree is 15 m, however it can reach about 30 meters, whereas the diameter at breast height (DBH) can range from 5 up to 40 cm [451]. It is found in a variety of plant groups across its natural geographic range, including dry and wet forests, grassy and heathy woods and grasslands, furthermore, due to its biological attributes this wood species is particularly invasive [452].

a) b)

Figure 6.72. The *Acacia dealbata* Link: a) the tree [453]; b) the flowers and the leaves [454].

The Acacia wood is an Australian native wood species, that was introduced in Europe for the first time in 19th century [455]. After, due to its rapid proliferation it spread throughout the Southwest. The A. dealbata Link is the most widespread species of Acacia genus in Southern Europe territories (France, Italy, Portugal and Spain) [455], [452] as well as in Australia, South Africa, New Zealand, western USA (California), Asia (India, Sri Lanka), South America (Argentina, Chile) and Madagascar [449]. Usually, the invasiveness of this species is related to the occurrence of fires, since fire reduces the native species cover and reduces the viability of native seeds; at the same time the epicormic sprouting of *Acacia dealbata* Link is stimulated, thus this plant tends to increase its cover [451]. Given its invasiveness this plant is becoming a problem especially in Portugal and south-western Spain, as it is threatening native flora.

6.3.3 THE GEOMETRICAL SURVEY

With basic surveying tools as a folding ruler, a roller metre, and squares, a direct survey has been conducted with aim to determine the main dimension of specimen. Firstly, the length (L) of the specimen has been measured then the size of the cross-section. In order to take into account of the cross-section irregularities multiple dimensions have been measured according to the European standard UNI EN 14251 [456]. In addition to defining the test methods of round wood for the evaluation of strength and stiffness, the standard specifies the procedure for the determination of geometrical features, moisture content and density of timber logs. According to the regulation the minimum apparent diameter (d_1) and maximum one (d_2) have been measured. Then the nominal diameter (d_{nom}) of the specimen have been calculated taking into account the ovality (O) of the cross section. These measures have been taken in correspondence of the middle third of the specimen, since it is the most influential zone in bending behavior. In this way the volume (V) of each member has been calculated as follow (Eq. 6.22):

$$V=d_{nom} \cdot L \tag{6.22}$$

where:

d_{nom} nominal diameter of the specimen [mm];

L length of the member [mm].

In this phase of the study, the identification of different sections of the specimen has been also carried out following the specifications provided by the standard UNI EN 14251 [456] for the four-point bending test. Thus, a nomenclature has been defined in order to identify some fundamental points on each specimen: the middle point of the member (section “D”), the two supporting points (sections “A” and “B”) and two points of load (section “C” and “E”). The sections have been assigned taking to account the orientation of the tree from which the log has been extracted. Thus, the section “A” correspond to the base of the tree while the “B” corresponds to the top. This nomenclature have been used also for the survey of the timber defects for visual strength grading analysis and for designing the NDT test set-up.

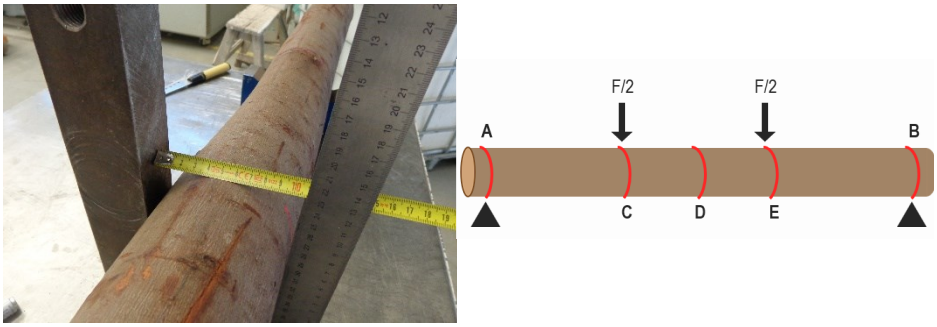

a) b)

Figure 6.73. a) Measurement of the log diameter [457]; b) Nomenclature adopted according to the bending test set-up.

Results

Thus, each specimen has been measured and the volume has been calculated (Table 6.37). The nominal diameter in average is equal to 111 mm, whereas the average length is equal to 2240 mm.

Table 6.37. Results of direct geometrical survey (DS): main dimension of the timber specimens.

ID [-]	L [mm]	d_2 [mm]	d_1 [mm]	d_{nom} [mm]	V [m^{-3}]
35	2390	116	105	114	0.0231
36	2406	120	99	112	0.0241
39	2410	115	102	115	0.0247
46	2410	115	110	117	0.0256
48	2428	123	104	113	0.0254
51	2400	132	105	115	0.0275
52	2395	108	103	123	0.0246
53	2407	110	97	110	0.0227
55	2400	124	106	122	0.0281
56	2400	105	101	110	0.0224
57	2400	117	103	122	0.0242
58	2410	102	92	122	0.0215
59	2388	111	90	106	0.0208
60	2400	124	102	113	0.0260
62	2404	117	100	105	0.0244
65	2390	110	97	110	0.0223

From the geometrical survey analysis, it is evident as the sample of study consisted in small diameter timber logs, characterized by a maximum nominal diameter of 123 mm.

6.3.4 VISUAL STRENGTH GRADING (VSG)

6.3.4.1 Procedure

As shown so far, the study sample consists of logs in small diameter, not sawn or squared and partly unbarked. The visual grading of these types of timber as structural elements falls within the field of round timber, for which there are various national and European standards. DIN 4074-2 [342] and UNI EN 1927-1 [458] define the visual grading rules for round timber. Although these standards are specifically designed for round timber products, they don't specifically limit its applicability to only large diameter or small diameter round timber. In Italy, UNI 11035-3 [459] deals with the visual characterization of the squared edged logs with wane from softwoods. However, it seems to be not applicable to timber logs as which of the sample of study. Another literature reference is the Finnish technical report VPS-SRT-2 [460]. In particular, the Annex A to the document aims at the visual grading of small round timber (diameter less than 200 mm) from Norway Spruce *(Picea Abies)* and Scots Pine *(Pinus Sylvestris)*.

As shown, at the state of art there are no specific regulations for the classification *Acacia Dealbata* Link, whose current applications do not fall in the field of construction. On the other hand, the existing standards (except the VPS-SRT-2, [460] are not specifically designed for small-diameter wood, which has certain peculiarities that influence its mechanical behaviour. Among them, the presence of juvenile wood seems to be a crucial factor to consider [461], however, the visual identification of this aspect seems to be not easy to evaluate [462].

Therefore, within the scope of this work, the visual grading has been performed according to the technical report VSP-SRT-2. The standard provides a list of criteria by which to classify the material based on macroscopic visual characteristics. According to VPS-SRT-2 [460], two visual grades classes (the best quality: “A”; the poorest quality: “B”) are prescribed. However, the standard does not provide the average or characteristic values corresponding to these visual grades classes.

Nevertheless, only some of the listed criteria have been taken into consideration, they are: ovality, tapering, sweep, knots and cracks. As concerned the ovality and knots, the analysis has been carried out in correspondence of the middle third of the specimen. The ovality (O) of the cross section is the parameter representing the cross-sectional shape. It has been measured as the difference between the maximum (d_2) and minimum

(d_1) diameter at a cross section expressed as a percentage of the minimum diameter (Eq. 6.23):

$$O = \frac{d_2 - d_1}{d_1} \tag{6.23}$$

where:

O ovality of the cross section [%];

d_2 biggest diameter of the cross section [mm];

d_1 smallest diameter of the cross section [mm].

The tapering consists of gradual change in diameter along the length of the specimen. It is measured as the difference of the two end diameters per each meter long (Figure 6.74). Thus, tapering parameter (T) can be measured as follow (Eq. 6.24):

$$T = \frac{1}{L}\left[\frac{d_{2,i} + d_{1,i}}{2} - \frac{d_{2,j} + d_{1,j}}{2}\right] \tag{6.24}$$

where:

T tapering of the specimen [mm/m];

L total length of the specimen [m];

$d_{2,i}$ biggest diameter of the cross section at the i-th point [mm];

$d_{1,i}$ smallest diameter of the cross section at the i-th point [mm];

$d_{2,j}$ biggest diameter of the cross section at the j-th point [mm];

$d_{1,j}$ smallest diameter of the cross section at the j-th point [mm];

The sweep (S) of the log consist of specimen deviation from a straight plane, curving to one side along the longitudinal axis (Figure 6.74). It has been measured as the maximum deflection within the concave profile of the log over a length of 2.00 m. As regard to knots, the ratio of the minimum diameter (d_k) of the largest knot to the cross-sectional nominal diameter (d_{nom}) has been considered for classifying the logs. The wood cracks are due to the

drying process. To visual grading, the standard requires the length and width of cracks to be measured. However, it does not place limits on the length of cracks, but rather on their width. Therefore, cracks have been evaluated through a parameter (C) calculated as the ratio of crack width to nominal diameter (d_{nom}) of the cross-section.

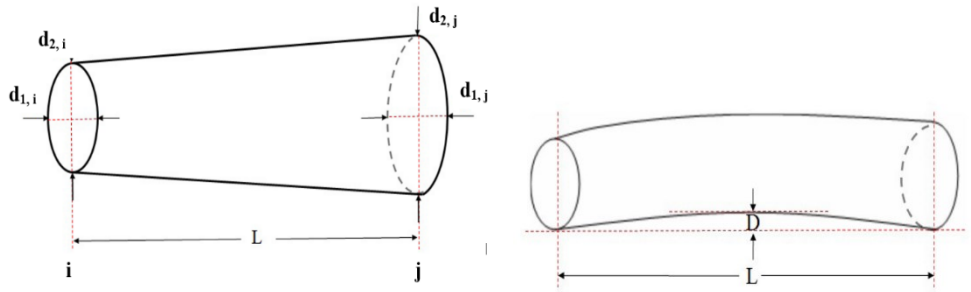

Figure 6.74. Part of the visual criteria for VSG according to VPS-SRT-2 [460]: (a) tapering; b) sweep.

Characteristic		Grade "A"	Grade "B"
Size of the knot in relation to the grading diameter, mm		25 %	30 %
Sum of knots, in relation to the grading diameter		75 %	100 %
Spiral grain		1:10	1:7
Rate of the growth, mm		3	5
Single crack, depth in relation to the grading diameter		50 %	50 %
Single crack, length		not limited	not limited
Sum of any two cracks at a cross-section, in relation to the diameter		75 %	75 %
Reaction wood, ratio to the cross-section		10 %	10 %
Tapering, mm/m	unmachined	5	10
	machined	3	5
Ovality	unmachined	10 %	20 %
	machined	5 %	10 %
Sweep, over 2 meters		5 mm	10 mm
Machining defects, maximum depth		5 mm	5 mm
Cambium		10 %	10 %
Insect holes		not permitted in the air-dried timber	not permitted in the air-dried timber

Figure 6.75. Grading rules established by technical report VPS-SRT-2 (extrapolated from: [460]).

6.3.4.2 Results and discussion

A set of macroscopic features of A. dealbata have been identified during the visual grading, such as cross-section ovality, tapering and sweep (Figure 6.76). Furthermore, large cracks have been located in correspondence of the head members (Figure 6.77). However, they are limited in length. This evidence is due to the fact that heads member are mainly involved in drying process.

Taking into account the visual macroscopic criteria defined by the VSP-SRT-2 [460] the measurement of defects have been carried out (Table 6.38). As concerned the ovality (O) an average value equal to 11.2% has been found, whereas maximum value is 19.3%. According to this criterion most of the sample (69%) is graded in B quality class, while the remaining 31% in A quality class. As regard to tapering (T) the average value has been found to be equal to 7.4 mm/m, whereas the maximum value is 10.4 mm/m. This criterion turns out to be more penalizing for the sample, since most of the sample (81%) is graded in B quality class, while the 6% in A grade class and the 13% (2 specimens) is rejected from the grading.

The most penalizing criterion is the sweep, since according to the Standard limits, all the specimens are rejected from the grading. The average sweep has been found to be equal to 33.5 mm/m, while the maximum is equal to 64.3 mm/m. Due to the characteristic of the knots, which are sparse and small in size, the “knots criteria” has been found as the least penalizing criterion. Indeed, all the sample has been graded in A quality class. As regard to the crack defects, long and width cracks have been found in correspondence of the head members. In some case it has been seen that crack length is equal to the 50% of the specimen total length. According to this criterion the 63% of the sample has been graded in B grade class while the remaining 31% has been rejected from grading.

In the end the sample has been graded according to the criteria of the worst defect and it has been found that all the specimens are rejected from graded (Table 5.1). As already mentioned, this is due to the sweep visual criterion that is the most penalizing for the sample. Avoiding this criterion, 50% of the sample turns out to be classified in B grade class, while the remaining 50% is rejected from the grading.

a) b)

Figure 6.76. Visual macroscopic characteristics of specimens: a) Tapering; b) Sweep.

a) b) c)

Figure 6.77. Visual macroscopic characteristics of specimens: a) Cracks (tangential view); b) Crack on head member; c) Knots.

Table 6.38. Results of visual strength grading.

Sp.	Ovality		Tapering		Sweep		Knots		Cracks	Gr.	Gr.*
	O	Gr.	T	Gr.	S	Gr.	d_k/d_{nom}	Gr.			
[-]	[%]	[-]	[mm/m]	[-]	[mm/m]	[-]	[%]	[-]	[-]	[-]	[-]
35	10.1	B	7.1	B	44.0	-	7.0	A	B	-	B
36	18.5	B	10.0	B	31.2	-	6.3	A	-	-	-
39	10.1	B	7.7	B	41.5	-	5.2	A	-	-	-
46	5.1	A	3.9	A	33.2	-	0.0	A	B	-	B
48	15.2	B	7.4	B	64.3	-	8.8	A	-	-	-
51	19.3	B	5.6	B	20.8	-	7.8	A	B	-	B
52	0.9	A	5.6	B	16.7	-	6.5	A	B	-	B
53	11.3	B	5.8	B	49.9	-	6.4	A	-	-	-
55	12.1	B	8.3	B	29.2	-	4.9	A	B	-	B
56	9.2	A	5.8	B	11.7	-	4.5	A	B	-	B
57	6.2	A	10.2	-	26.0	-	0.0	A	B	-	-
58	3.0	A	10.4	-	53.9	-	17.2	A	B	-	-
59	17.9	B	8.6	B	37.8	-	6.6	A		-	-
60	15.2	B	6.7	B	30.9	-	0.0	A	-	-	-
62	11.1	B	7.3	B	12.5	-	12.4	A	B	-	B
65	13.5	B	8.4	B	31.8	-	8.2	A	B	-	B

(Results of grading according to: Gr.) VSP-SRT2 [460]; Gr.) VSP-SRT2 without "sweep").*

6.3.5 NON-DESTRUCTIVE TEST (NDT)

6.3.5.1 Moisture content measurement

Test equipment

The moisture content measurement have been performed by means of hygrometer *Protimeter TimberMaster* device (Figure 6.78.a), which is a digital moisture meter. The device is equipped with pin with a length of about 60 mm. The instrument allows the measurement of wood moisture content in a reading range of 7.9% to 30% with accuracy of +/-1%, whereas measurements above or below this range are less accurate. When the test have been carried out the environmental temperature was equal to 13°±2°C and the relative humidity was equal to 68% ± 5%.

Procedure and test set-up

The test has been carried out on the whole sample by taking three transverse measurements per specimen at section "A" (base of the member), "B" (end of the member) and "D" (middle span point). The test have been performed inserting the electrode pin inside the timber member keeping the electrode couple aligned to the direction of wood grain (Figure 6.78.b). The log heads have been avoided from the measurement. The moisture content measurements have been carried before and after the double kiln drying process.

a) b)

Figure 6.78. a) The *Protimeter TimberMaster* device [463]; b) The moisture content measurement in the middle span section [464].

Results and discussion

A high value of moisture content has been found for the whole sample, as shown in Table 6.39. The mean value of MC is higher than the standard value (12%) and even above the fibre saturation point (FSP) value. The mean value it has been found to be equal to 59.5%, while the minimum and maximum value are respectively equal to 51.1% and 69.5%. A low dispersion of data has been noted (COV:7.9%).

Table 6.39. Moisture content (M.C.) measurements

	Moisture Content (M.C.)					
Specimen	M.C.	Min	Mean	Max	σ	COV
[-]	[%]	[%]	[%]	[%]	[%]	[%]
35	64.7					
36	64.3					
39	57.9					
46	57.7					
48	61.4					
51	63.0					
52	69.5					
53	60.5	51.1	59.9	69.5	4.7	7.9
55	59.3					
56	55.2					
57	51.1					
58	54.6					
59	57.2					
60	67.0					
62	56.1					
65	58.5					

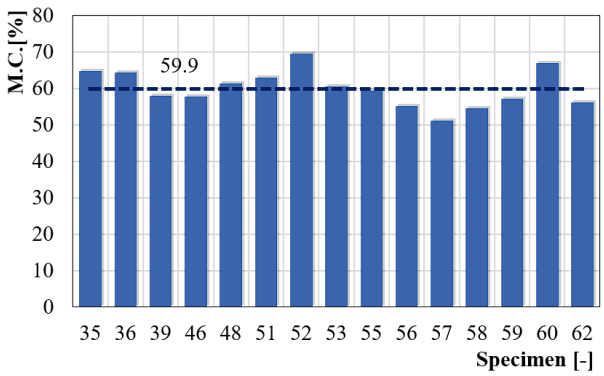

Figure 6.79. Moisture content (M.C.) measurements

These findings are attributed to the fact that only one kiln drying cycle was conducted before to this test.

6.3.5.2 Mass measurement and density estimation

Test equipment

The mass of each specimen has been measured through direct measurement using the platform scale *STEINBERG Classic,* with an accuracy of 0,1 g.

Procedure and test set-up

The tests have been carried out measuring the specimen one at time.

Then, given the volume of the specimen the density has been calculate. Thus, the density have been estimated using the volume acquired through direct survey (Eq. 6.25):

$$\rho_{DS} = \frac{m}{V_{DS}} \tag{6.25}$$

where:

ρ_{DS} density estimated through DS volume [kgm^{-3}];

m specimen mass [kg];

V_{DS} volume from DS [m^3].

Results and discussion

It has been found that the mass range from 16.2 kg to 26.0 kg, whereas the average values is equal to 21.3 kg (Figure 6.80). Then the density have been calculated and it has been seen that the average density value is equal to 882 kgm^{-3}, whereas the minimum and maximum density are respectively equal to: 709 kgm^{-3} and 1045 Kgm^{-3}, with a COV:12%; Table 6.40). From these results it can be said that being the MC over the fibre saturation point, the calculated density values should be higher than the same at normal content of moisture.

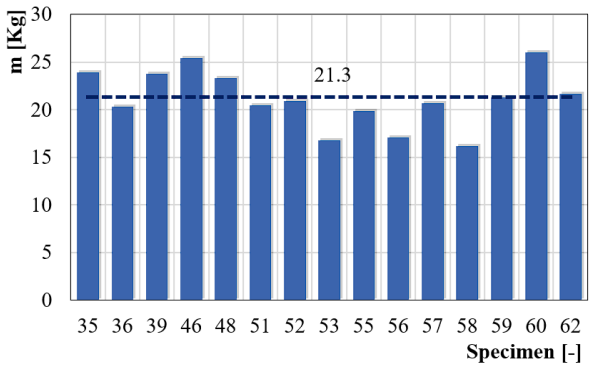

Figure 6.80. Mass measurements

Table 6.40. Density estimation through direct survey (DS) method

	Wood density from DS (ρ_{DS})					
Specimen	ρ_{DS}	Min	Mean	Max	σ	COV
[-]	[kgm^{-3}]	[kgm^{-3}]	[kgm^{-3}]	[kgm^{-3}]	[kgm^{-3}]	[%]
35	1033					
36	839					
39	961					
46	991					
48	914					
51	746					
52	849					
53	739	709	882	1045	113	12.9
55	709					
56	764					
57	854					
58	752					
59	1025					
60	999					
62	886					
65	1045					

In order to take into account this, a modification function has been applied for modifying the value of the density to the reference value (MC:12%) the applied equation is provided by the standard UNI EN 384 [344]. After the correction the value are drastically changed (Table 6.41). An average value of 756 kgm^{-3}, whereas the minimum and maximum are respectively equal to 610 kgm^{-3} and 900 kgm^{-3}. In Figure 6.81 both ρ and ρ_{12} values are showed.

Table 6.41. Wood density after the MC correction according to EN 384.

Specimen	Wood density at MC reference value (12%) ρ_{12}	Min	Mean	Max	σ	COV
[-]	[kgm^{-3}]	[kgm^{-3}]	[kgm^{-3}]	[kgm^{-3}]	[kgm^{-3}]	[%]
35	870					
36	707					
39	831					
46	857					
48	779					
51	632					
52	701					
53	632	610	756	900	96	12.8
55	610					
56	667					
57	757					
58	658					
59	888					
60	833					
62	771					
65	900					

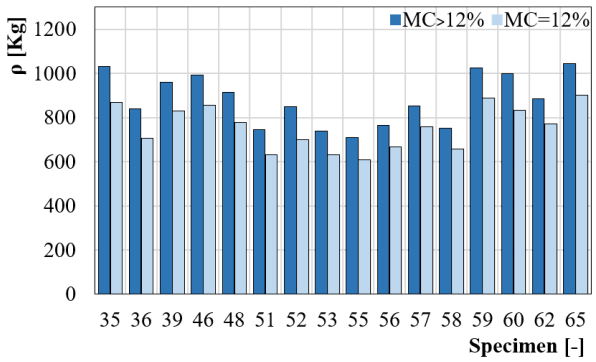

Figure 6.81. Wood density estimation considering MC>12% and MC=12%.

6.3.5.3 Vibrational test

Test equipment

The method of measurement of the actual frequency is also known as the vibrational test. For measuring the longitudinal frequency of vibration, the following device has been used: a contact piezoelectric accelerometer, a modal impact hammer *PCB IHC03* (*National Instruments Corporation, Austin, Texas-USA*), a dynamic signal acquisition device *NI-USB 4431* (*National Instruments Corporation, Austin, Texas-USA;* Figure 6.82) and a PC for data acquisition and elaboration. The impact hammer is a vibration

sensor for measuring the stimulus signals. The data have been acquired and collected through the software *Measurement & Automation Explorer v2022* (*National Instruments Corporation, Austin, Texas-USA*). The signals have been processed through the software *SeismoSignal* (Seismosoft ltd.).

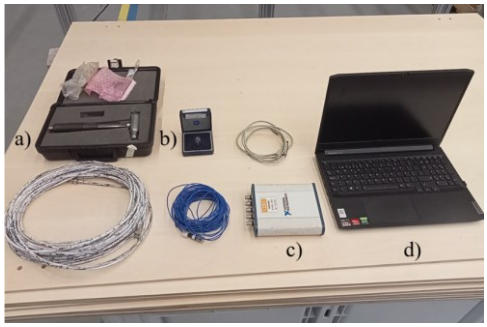

Figure 6.82. The vibrational test devices: a) modal impact hammer; b) contact piezoelectric accelerometer; c) dynamic signal acquisition device; d) PC.

Procedure and test set-up

The test consists of placing the accelerometer and hitting the timber logs through the impact hammer. To this end, the specimens have been placed on stands in order to allow the free vibration. The test has been carried out in the longitudinal direction, thus the specimen heads have been involved. For each measurement the hammer and accelerometer have been placed on the same head of the specimen (Figure 6.83). As regard the procedure each measurement has been repeated at least for 3 times, thus a minimum of 3 signals have been acquired for each specimen. Then, using the FFT (Brigham, 1988) the power spectrum have been obtained through the software *SeismoSignal* and the dominant frequency has been evaluated.

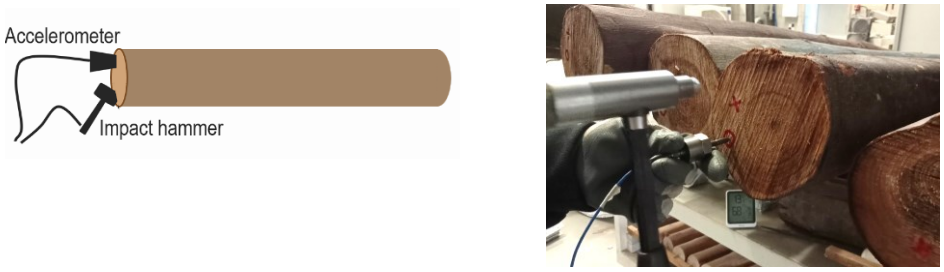

a) b)

Figure 6.83. The vibrational test: a) The test procedure; b) Performance of the test [465].

From frequency, the dynamic Modulus of Elasticity (MOE_{dyn}) has been computed according to the Equation 6.15 showed in Section 6.2.5.5.

Results and discussion

As regard to the natural frequency of vibration (*f*) it has been found that the minimum, average and maximum values are respectively equal to: 745 Hz, 826 Hz and 928 Hz (Figure 6.84; Table 6.42). A very low dispersion of data has been seen (COV: 5.8%).

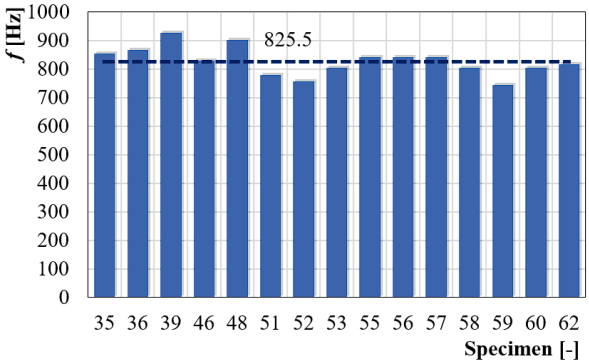

Figure 6.84. Vibrational test – Natural frequency of vibration in longitudinal direction.

Table 6.42. Vibrational test – Natural frequency of vibration in longitudinal direction.

	Vibrational test - Frequency (*f*)					
Specimen	*f*	Min	Mean	Max	σ	COV
[-]	[Hz]	[Hz]	[Hz]	[Hz]	[Hz]	[%]
35	854					
36	867					
39	928					
46	830					
48	903					
51	781					
52	757					
53	806	745	826	928	48	5.8
55	842					
56	842					
57	842					
58	806					
59	745					
60	806					
62	818					
65	781					

For $MOE_{dyn,V}$ it has been found that the minimum, average and maximum values are respectively equal to: 10500 MPa, 13931 MPa and 19200 MPa (Table 6.43). The dispersion has been found to be equal to COV: 18.0%.

Table 6.43. Vibrational test - Dynamic Modulus of Elasticity ($MOE_{dyn,V}$)

Vibrational test - Dynamic Modulus of Elasticity ($MOE_{dyn,V}$)						
ID	$MOE_{dyn,V}$	Min	Mean	Max	σ	COV
[-]	[MPa]	[MPa]	[MPa]	[MPa]	[MPa]	[%]
35	17200					
36	14600					
39	19200					
46	15900					
48	17600					
51	10500					
52	11200					
53	11100	10500	13931	19200	2502	18.0
55	11600					
56	12500					
57	14000					
58	11300					
59	13000					
60	14900					
62	13700					
65	14600					

In order to take into account the effect of the high moisture content on the vibrational properties of the specimen a modification function has been applied for modifying both the stress wave speed (SWS) [466]. Furthermore, by considering the value of wood density referred to reference value (MC:12%), the dynamic modulus of elasticity has been calculated as follows (Eq. 6.26):

$$MOE_{dyn,V,12}=\rho_{12}\cdot(SWS_{12})^2 \tag{6.26}$$

where:

$MOE_{dyn,V,12}$ dynamic modulus of elasticity referred to reference value (MC:12%) [MPa];

ρ_{12} wood density modified according to [344] [kgm^{-3}];

SWS_{12} stress wave speed modified according to Unterwieser and Schickhofer, [466] [ms^{-1}];

For dynamic MOE at MC:12% ($MOE_{dyn,V,12}$) it has been found that the minimum, average and maximum values are respectively equal to: 11600 MPa, 15934 MPa, 21300 MPa (Table 6.44; Figure 6.85).

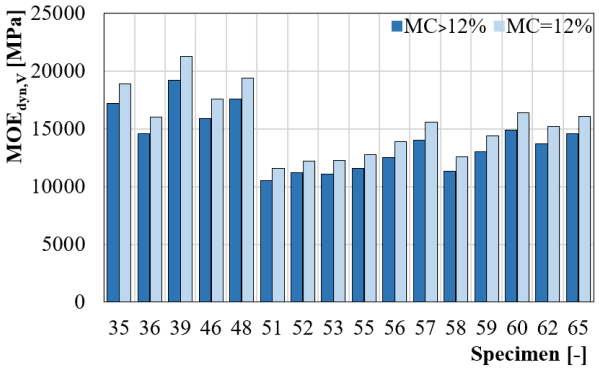

Figure 6.85. Dynamic Modulus of Elasticity ($MOE_{dyn,V}$) at MC>12% and MC=12%.

Table 6.44. Vibrational test - Dynamic Modulus of Elasticity ($MOE_{dyn,V}$)

	Vibrational test - Dynamic Modulus of Elasticity at M.C.: 12%					
ID	$MOE_{dyn,V}$	Min	Mean	Max	σ	COV
[-]	[MPa]	[MPa]	[MPa]	[MPa]	[MPa]	[%]
35	18900					
36	16000					
39	21300					
46	17600					
48	19400					
51	11600					
52	12200					
53	12300	11600	15394	21300	2761	17.9
55	12800					
56	13900					
57	15600					
58	12600					
59	14400					
60	16400					
62	15200					
65	16100					

6.3.5.4 Drilling resistance test

Test equipment

The drilling resistance test have been performed using the *IMLRESI PD400* device.

Procedure and test set-up

The experimental tests consisted of penetrations in perpendicular direction to the grain. In order to obtain an adequate resolution on the graph the advancing speed of the needle has been set equal to 50 cm/minute. It is important to notice that before the test the sample has been subjected to a second cycle of kiln drying process.

The measurements have been carried out in correspondence of 3 points of the member: in the section "A", "D" and "B" (Figure 6.86). Thus, one measurement have been performed for each section, for a total number of 3 measurements per specimen. From the drill graph the mean resistance drilling (R_m) has been calculated according to the (Eq. 6.6). Thus, from each specimen section the mean resistance Rm has been calculated and from these the average value has been estimated as follow (Eq. 6.22):

$$R_{m,av.} = \frac{R_{m,A} + R_{m,D} + R_{m,B}}{3} \tag{6.27}$$

where:

$R_{m,Mean}$ the average value of the mean drilling resistance measure [%];

$R_{m,A}$ the mean drilling resistance measure at section "A" [%];

$R_{m,D}$ the mean drilling resistance measure at section "D" [%];

$R_{m,B}$ the mean drilling resistance measure at section "B" [%];

The zones of the graph with low resistances, due to the presence of defects or decay, were not considered in the calculation of the average resistance R_m.

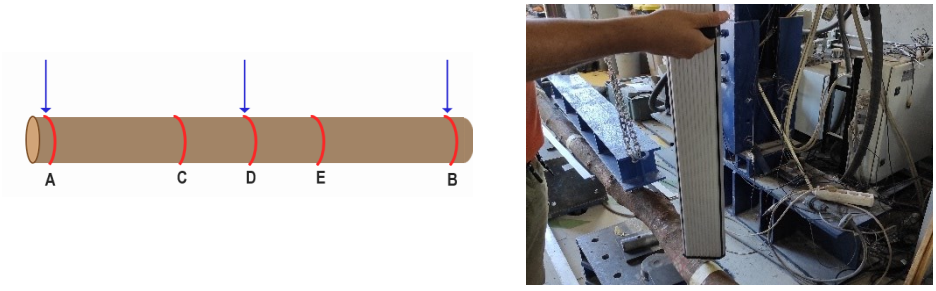

a) b)

Figure 6.86. The drilling resistance test: a) The test set-up; b) Performing the test.

Results and discussion

The results of the mean resistance drilling measure are provided Table 6.45. It is important to notice as for section "A" higher values (in average 18.4%) have been found than the section "B" (in average 16.7%) and "D" (in average 16.1%). This higher resistance is probably due to the fact that the section "A" correspond to the part of the tree closer to the base of the trunk. At the same time no relevant differences have been found for the section "B" and "D". As regard to the dispersion of the data for all the section similar values of coefficient of variation have been found: 19.2% for section "A", 17.6% for section "D" and 18.6% for section "B". As concern the average drilling measure ($R_{m,Mean}$) it ranges between the minimum value equal to 10.8% (specimen 51) and the maximum equal to 22.8% (specimen 35); the average value is equal to 17.0%.

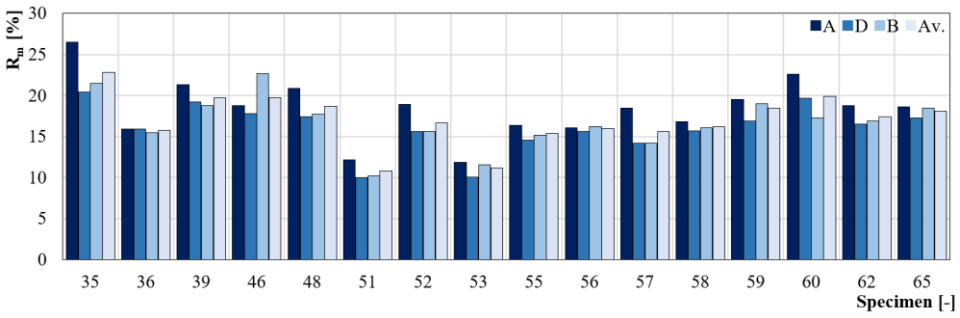

Figure 6.87. Mean Drilling resistance measure: Section "A", "D", "B", Average value.

Table 6.45. Mean Drilling Resistance measurements.

Specimen	Drilling resistance mesaure R_m [%]			
	Section A	Section D	Section B	Average
[-]	$R_{m,A}$	$R_{m,D}$	$R_{m,B}$	$R_{m,av}$
35	26.5	20.4	21.5	22.8
36	15.9	15.9	15.5	15.8
39	21.3	19.2	18.8	19.8
46	18.8	17.8	22.7	19.8
48	20.9	17.4	17.7	18.7
51	12.2	10.0	10.2	10.8
52	18.9	15.6	15.6	16.7
53	11.9	10.1	11.6	11.2
55	16.4	14.6	15.2	15.4
56	16.1	15.6	16.2	16.0
57	18.5	14.2	14.2	15.6
58	16.8	15.7	16.1	16.2
59	19.5	16.9	19.0	18.5
60	22.6	19.7	17.3	19.9
62	18.8	16.5	16.9	17.4
65	18.6	17.3	18.5	18.1
Min. [%]	11.9	10.0	10.2	10.8
Mean [%]	18.4	16.1	16.7	17.0
Max. [%]	26.5	20.4	22.7	22.8
σ [%]	3.5	2.8	3.1	3.0
COV [%]	19.2	17.6	18.6	17.6

Some of the drilling graphs are showed in Figure 6.88 and Figure 6.89. They respectively correspond to the specimen 35 (specimen with highest resistance) and 51 (specimen with lowest resistance).

From a qualitative assessment of the drilling graphs is apparent as the specimen 51 show low resistance values. At the same time the growth rings can be easily located and it is apparent as the specimen 51 has wider growth rings than the specimen 35. This evidence can be noticed in the all the three section of measurement, and this probably indicates that the specimen 51 is from a younger plant than the specimen 35. As concern the specimen 35, from the drilling graphs of section “A” and “B” (Figure 6.88 and Figure 6.89) can be easily identified the pith of the trunk, since low resistance are generally associated to it.

a)

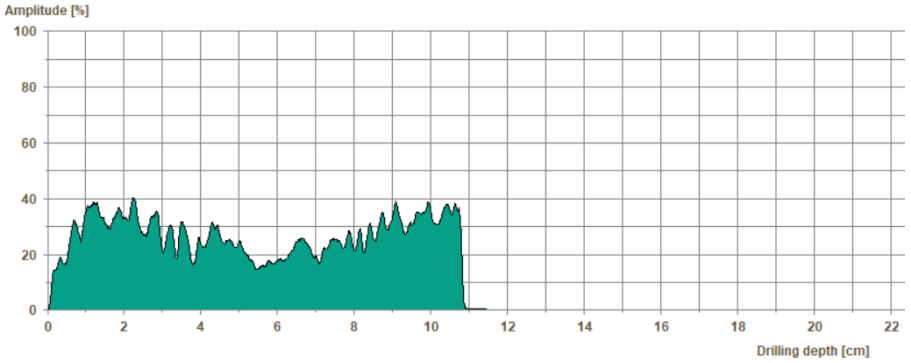

b)

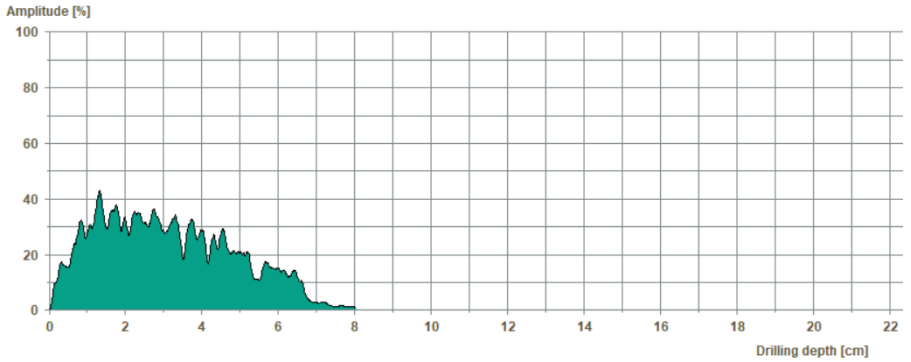

c)

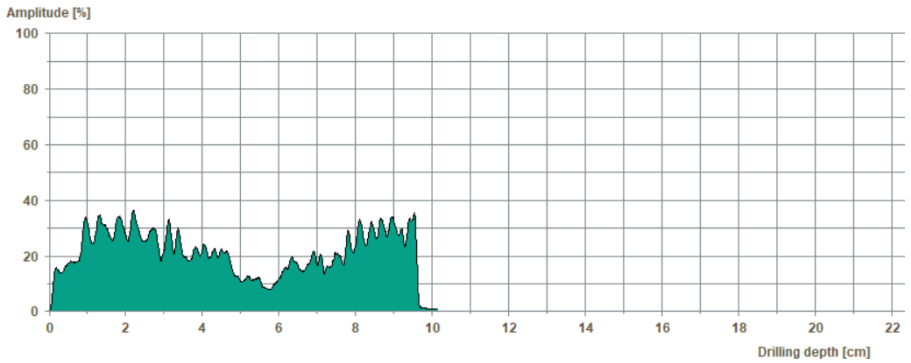

Figure 6.88. Drilling graph for specimen “35”: a) in section “A”; b) in section “D”; c) in section “B”.

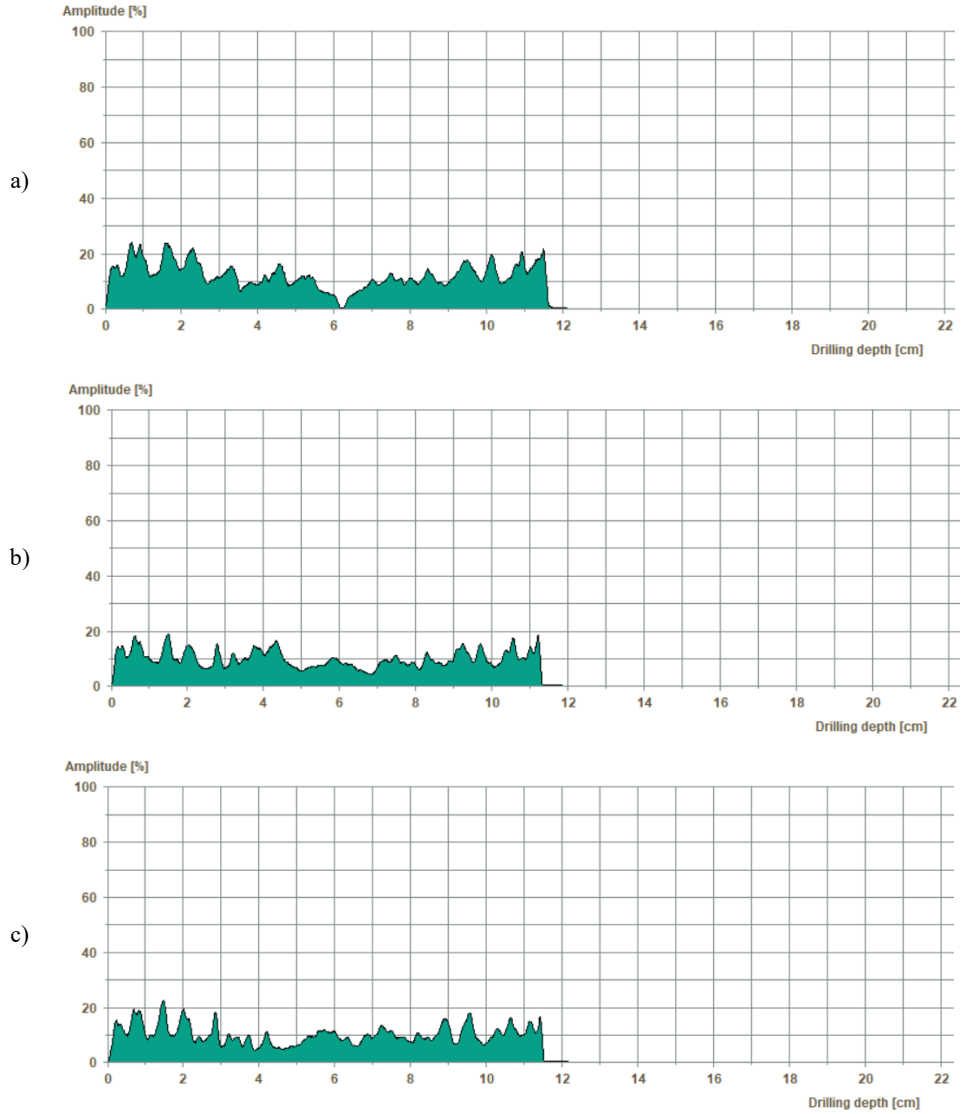

Figure 6.89. Drilling graph for specimen "51": a) in section "A"; b) in section "D"; c) in section "B".

6.3.6 DESTRUCTIVE TEST (DT) IN BENDING

6.3.6.1 General procedures

The bending test have been carried out in the Laboratory of Department of Civil Engineering at the University of Minho (Guimaraes, Portugal). The test

have been performed according to the Standard UNI EN 14251 [456], that specifies test methods for determining the properties of structural round timber. The main purposes of testing investigations are the determination of the load-displacement curves, the modulus of elasticity ($E_{m,0}$) and the bending strength (f_m), together with the evaluation of relevant failure mechanisms under bending stress state. All these parameters are determined by means of a four-point bending test.

The regulation UNI EN 14251 [456] prescribe the following geometrical configuration for the test set-up:

- the minimum specimen length is equal to $19d_{nom}\pm2d_{nom}$ (where d_{nom} is the nominal diameter of the log);
- the distance between the simple support points is equal to $18h\pm d_{nom}$;
- the distance between the load application points is equal to $6d_{nom}$;
- the distance between each load application points and the support is equal to $6d_{nom}$;

Furthermore, for the calculation of the $E_{m,0}$ the standard prescribes measuring the relative displacement of the specimen over a length of $5d_{nom}$ placed at the middle-span (Figure 6.90).

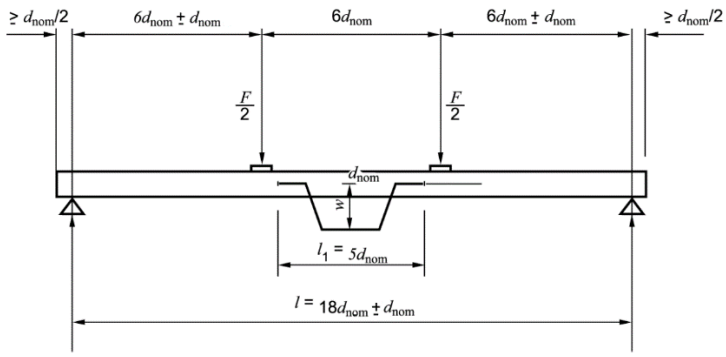

Figure 6.90. Test set-up for bending modulus of elasticity ($E_{m,0}$) estimation (modified from: [456]).

For determining the stiffness of the specimen, the local modulus of elasticity has been calculated in a load range that at most reaches the 40% of the load failure (0.40 F_{max}). The modulus of elasticity ($E_{m,0}$) is calculated from the relative displacement (w) (Figure 6.90), measured at the central gauge length (Eq. 6.28):

$$E_{m,0}=\frac{(M_1-M_2)c^4}{6(w_1-w_2)I_1}\left[-\frac{1}{\left(c+\frac{l_1}{2}\right)^2}-\frac{D}{2}+\frac{1}{c^2}\right] \quad (6.28)$$

where:

$$c=\frac{l_1 d_1}{(d_2-d_1)}$$

$$D=\left(\frac{1}{c^2}-\frac{1}{(c+l_1)^2}\right)$$

a distance between a loading position and the nearest support [mm];

l_1 gauge length ($6d_{nom}$) [mm];

M_2-M_1 bending moment increment on the straight-line portion until the value of 0.40 F_{max} [KNm];

I_1 the smallest second moment area of the cross-section along the gauge length [mm^4];

w_2-w_1 displacement increment on the straight-line portion corresponding to the F_2-F_1 force increment[mm].

For determining the bending strength, the load shall be applied at a constant rate and the maximum load should be reached within (300 ± 120) s. The bending strength (f_m) is calculated as follow (Eq. 6.24):

$$f_m=\frac{16\,F_{max}a}{\pi d_h d_v^2} \quad (6.24)$$

where:

F_{max} maximum total load [KN];

a distance between a loading position and the nearest support [mm];

d_v diameter in the direction of the load at mid-span [mm];

d_h diameter in the direction perpendicular to the load direction at mid-span [mm].

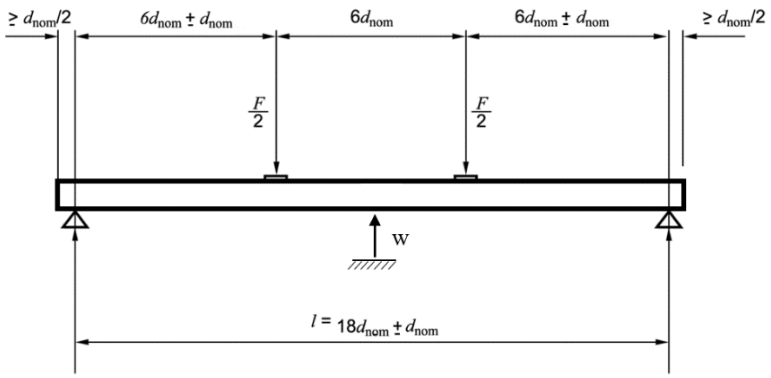

Figure 6.91. Test set-up for bending strength (f_m) estimation (modified from: [456]).

As already showed, the experimental tests are organized in two main sections: elastic and failure cycle tests. The first one deal with the calculation of the local modulus of elasticity, the second deal with the evaluation of the ultimate bending strength. Test equipment, test set-up and procedure are described in the following chapters. In the end the results are showed, analysed and discussed.

6.3.6.2 Elastic cycle

Test equipment

The bending test have been carried out using a displacement-controlled protocol. The load have been applied through a hydraulic machine and it has been measured using a 500 KN load cell. The test have been carried out with a test frame which the laboratory is equipped. Furthermore, the test equipment consisted of 2 displacement transducers (LVDT) with accuracy of of $1 \cdot 10^{-3}$, a data acquisition system and a PC for data recording.

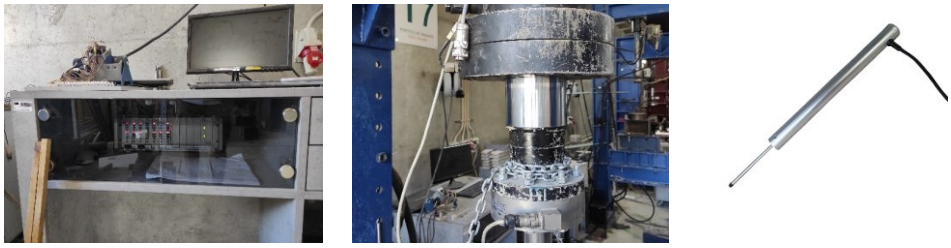

a) b) c)

Figure 6.92. Bending test equipment: a) PC and data acquisition system; b) load cell; c) LVDT.

a) b)

Figure 6.93. Views of test frame and specimen: a) lateral view; b) diagonal view.

Procedure and test set-up

The whole sample has been tested in elastic cycle bending test after a second kiln drying process, after that the moisture content has been measure according the procedure showed at the Section 6.3.5.1. The test set-up has been defined according to the standard prescriptions [456] and taking into account the geometrical features of specimens (Table 6.46).

The load has been distributed from the load actuator to the timber log by means of an IPE steel profile, steel plates and concrete blocks effectively dimensioned. Indeed, given the geometrical irregularities of the timber logs the reinforced concrete (R.C.) blocks have been used for distributing the load. The blocks have been fabricated ad-hoc for each specimen and they have been reinforced with the addition of steel fibres to the mixture.

In order to measure the relative displacement 2 LVDTs (1 for each specimen side) have been used. They have been located at the middle span of

the specimen (Figure 6.95) for measuring the local displacement on a length equal to $5d_{nom}$.

Table 6.46. Main geometrical features and moisture content of the sample after the three drying cycles.

ID [-]	d_{nom} [mm]	$18 \cdot d_{nom}$ [mm]	a [mm]	l_1 [mm]	M.C. [%]
35	114	2052	684	570	16.0
36	112	2016	672	560	17.7
39	115	2070	690	575	16.8
46	117	2106	702	585	21.5
48	113	2034	678	565	15.1
51	115	2070	690	575	19.4
52	123	2210	737	614	21.9
53	110	1980	660	550	15.5
55	122	2196	732	610	20.1
56	110	1980	660	550	13.1
57	122	2196	732	610	18.8
58	122	2199	733	611	18.4
59	106	1908	636	530	23.5
60	113	2034	678	565	22.4
62	105	1890	630	525	16.0
65	110	1980	660	550	21.8

As regard to the test protocol a displacement-controlled test has been carried out using a displacement rate of 0.30 mm/sec, according to the Standard instructions [456]. The test consist in 3 loading and unloading cycles with same amplitude equal to a displacement of 18 mm. These test parameters have been fixed taking into account the resulting maximum applied force, which falls within the elastic conventional branch (0.4 F_{max}).

a) b) c)

Figure 6.94. Test set-up for elastic cycle: a) R.C. block; b) steel plates over the R.C. block; c) steel support.

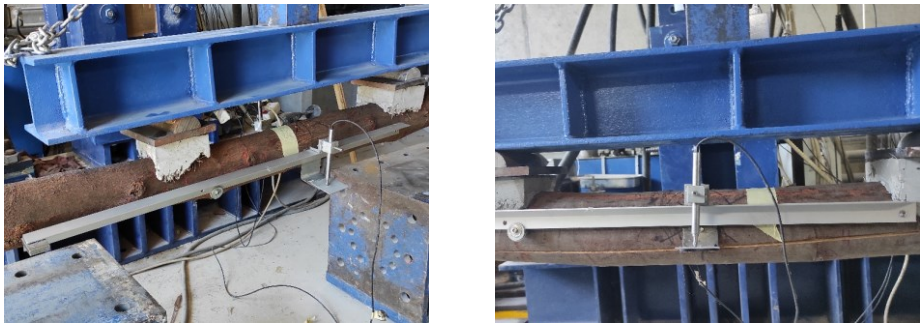

a) b)

Figure 6.95. Test set-up for elastic cycle with LVDT arrangement: a) diagonal view; b) frontal view.

Results and discussion

On the basis of the data obtained from the measurements and their processing, the "load-relative displacement curve" have been obtained. From this curve the modulus of elasticity ($E_{m,0}$) has been calculated (Table 6.47). The average value of $E_{m,0}$ has been found to be equal to 15.6 GPa, while the minimum and maximum are respectively equal to 11.9 GPa and 22.2 GPa. A quite dispersion of data has been found for the sample (COV: 16.5%), but it is clear that it is due to the heterogeneity of the wood quality.

Table 6.47. Modulus of Elasticity in bending at MC>12%

Specimen	F_2-F_1	w_2-w_1	Modulus of Elasticity ($E_{m,0}$)					
			$E_{m,0}$	Min	Mean	Max	σ	COV
[-]	[KN]	[mm]	[MPa]	[MPa]	[MPa]	[MPa]	[MPa]	[%]
35	6.82	0.89	16900					
36	6.14	1.18	11900					
39	6.84	0.89	18800					
46	8.77	0.86	22200					
48	7.01	1.04	13600					
51	6.76	0.84	13900					
52	5.66	1.21	13700					
53	3.92	0.80	13500	11900	15600	22200	2578	16.5
55	6.32	1.00	13300					
56	6.00	0.91	18200					
57	7.31	1.08	16900					
58	4.27	1.02	17300					
59	4.10	0.77	15500					
60	8.44	1.22	14000					
62	7.36	0.97	16000					
65	5.46	1.07	13900					

In order to take into account the effect of the high moisture content on the modulus of elasticity a modification function has been applied for adjusting the results according to the instructions of the EN 384. In this way the modulus of elasticity referred to the normal moisture content (MC:12%) has been calculated ($E_{m,0,12}$) and the results have been showed in Table 6.47.

As evident from Figure 6.96, the values of $E_{m,0,12}$ are found to be higher than $E_{m,0}$. This is clearly due to the fact that the specimens had a higher moisture content than the normal. Thus, the average value of $E_{m,0,12}$ has been found to be equal to 16.6 GPa, while the minimum and maximum are respectively equal to 12.6 GPa and 24.3 GPa

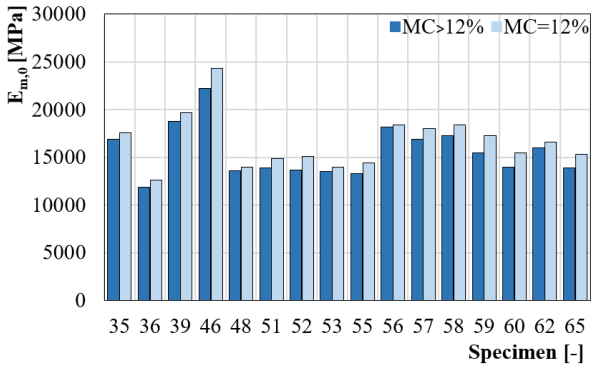

Figure 6.96. Modulus of Elasticity ($E_{m,0}$) estimation before (MC<12%) and after (MC=12%) the MC correction ($E_{m,0,12}$).

6.3.6.3 Failure cycle

Test equipment

The test equipment for failure cycle is the same of the elastic cycle, however, has been used a single displacement transducer.

Procedure and test set-up

After the elastic cycles, the specimens have been tested in bending up to the failure. The test set-up consist in the same equipment arrangement used for elastic cycle, but a single displacement transducer has been used. It has

been fixed on the steel frame in order to measure the global displacement of the log thanks to a steel plate fixed to it.

Table 6.48. Modulus of Elasticity in bending at MC: 12%

Specimen	Modulus of Elasticity ($E_{m,0}$) at M.C.: 12%					
	$E_{m,0,12}$	Min	Mean	Max	σ	COV
[-]	[MPa]	[MPa]	[MPa]	[MPa]	[MPa]	[%]
35	17600					
36	12600					
39	19700					
46	24300					
48	14000					
51	14900					
52	15100					
53	14000	12600	16631	24300	2752	16.5
55	14400					
56	18400					
57	18000					
58	18400					
59	17300					
60	15500					
62	16600					
65	15300					

The test protocol consists in a single load cycle in displacement control. The displacement rate have been set equal to 0.30 mm/sec, in order to reach the maximum load in (300 ± 120) seconds.

Results and discussion

The tests showed a very interesting results regarding both the strength and deformation capacity of the timber logs. Before commenting on the results, it is important to note how the R.C. blocks for load distribution fulfilled their function. In fact, even in the case of the most loaded specimen, they did not show conspicuous deformation or cracking (Figure 6.98).

As regard to the test results, in general very high strength values has been seen for the whole sample. The maximum load and bending moment have been noted respectively equal to 32.6 KN and 13.0 KNm (specimen 46). At the same time a load of 15.1 KN and a bending moment of 6.1 KNm have been found as the minimum value (specimen 53). The average values for load and bending strength are respectively equal to 26.1 KN (COV: 18.4%) and 10.4 KNm (COV: 18.8%). As concern the bending strength the average value

has been found to be equal to 83.0 MPa (COV: 16.9%). It ranges between 57.8 MPa (minimum value, specimen 53) and 121.3 MPa (maximum value, specimen 56).

a) b)

Figure 6.97. Failure cycle test set-up: a) diagonal view; b) lateral view.

a) b)

Figure 6.98. Verification of R.C. blocks integrity: a) before the failure test; b) after the failure test.

From Figure 6.100 is evident as the very high performance of the specimen 56 (f_m: 121.3 MPa) are an isolated case than the trend of the whole sample that showed values not exceeding the 94.6 MPa. This is probably due to the low moisture content of this specimen (13.1%), which is near to reference value (12%).

Table 6.49. Results of the failure tests.

ID [-]	F_{max} [KN]	w_{max} [mm]	M_{max} [KNm]	f_m [MPa]
35	26.8	81	10.6	90.2
36	25.6	92	10.3	84.1
39	29.0	104	11.6	91.5
46	32.6	106	13.0	85.3
48	29.0	80	11.8	88.2
51	26.8	115	10.6	63.5
52	23.1	119	8.8	67.9
53	15.1	50	6.1	57.8
55	26.9	101	10.3	74.7
56	31.2	143	12.6	121.3
57	28.9	110	11.0	86.0
58	20.9	130	8.0	94.6
59	17.9	143	7.3	79.7
60	29.9	154	12.0	81.3
62	30.7	149	12.7	85.8
65	22.8	138	9.2	76.4
Min	15.1	50	6.1	57.8
Av	26.1	113	10.4	83.0
Max	32.6	154	13.0	121.3
σ	4.8	28	2.0	14.0
COV	18.4	24.7	18.8	16.9

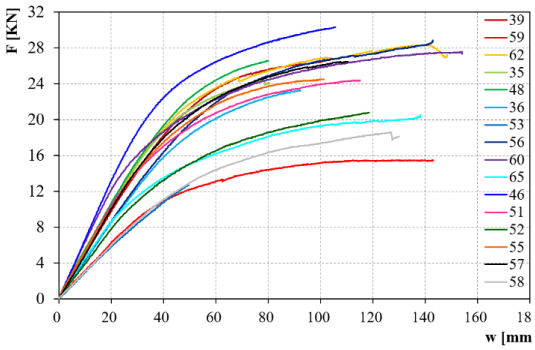

Figure 6.99. Load-displacement curve of the failure tests in bending.

As regard the deformation, in general high values have been found for the global displacement, that have been measured at the middle span point. The average value is equal to the 113 mm and it range between a minimum of 50 mm (specimen 53) and a maximum of 154 mm (specimen 60). It is significant to noticed that for displacements a greater variability (COV:24.7%) has been observed than for strength (COV: 16.9%). Furthermore, it is interesting to note that the minimum displacement (w_{max}: 50 mm) was found for specimen 53, which also reported the minimum strength (f_m: 57.8 MPa).

From the analysis of the failure modalities of the specimens during the failure test, several types of failure have been identified. They can be traced back to those well known in the relevant scientific literature [35], [39]. Therefore, the test specimen has been divided into 4 classes (Table 6.50) corresponding to the following failure mechanisms: compression, brittle tension, tension and longitudinal shear. Although the failure modes have different characteristics, during the tests for all the specimens with attached bark, it has been found that the bark broke at the tension side before the final failure of the log. The different failure mechanisms are discussed below,

describing the morphology and the physical-mechanical parameters associated with them.

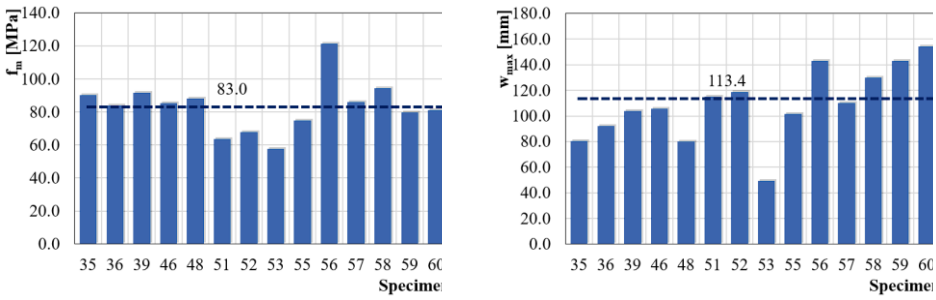

a) b)

Figure 6.100. Results of the failure tests: a) Bending strength (f_m); b) Maximum displacement (w_{max}).

Table 6.50. Failure mechanism and main outputs of the destructive test.

Specimen [-]	Failure mechanism [-]	MC [%]	ρ_{12} [Kgm^{-3}]	w_{max} [mm]	f_m [MPa]
39	Compression	16.8	831	104	91.5
59	Compression	23.5	888	143	79.7
62	Compression	16	771	149	85.8
56	Compression	13.1	667	143	121.3
60	Longitudinal shear	22.4	833	154	81.3
36	Brittle tension	17.7	707	92	84.1
51	Brittle tension	19.4	632	115	63.5
53	Brittle tension	15.5	632	50	57.8
35	Tension	16	870	81	90.2
46	Tension	21.5	857	106	85.3
48	Tension	15.1	779	80	88.2
52	Tension	21.9	701	119	67.9
55	Tension	20.1	610	101	74.7
57	Tension	18.8	757	110	86.0
58	Tension	18.4	658	130	94.6
65	Tension	21.8	900	138	76.4

The compression failure has been noted for the specimen 39, 59, 56 and 62. It has been recognized by different effects at the compression side; in specimens without bark the presence of conspicuous fractures distributed along the middle third of the specimen (Figure 6.101.a) have been seen, while the bark corrugation has been noted in specimen coated by the bark (Figure 6.101.b). These effects appear during the middle phase of the test, when the force-displacement curve exhibits its strongly non-linear branch. In any

event, it is essential to note that the final collapse has been caused by fiber fracture on the tension side. during the middle phase of the test, when the force-displacement curve presents its markedly non-linear branch. However, the behaviour until failure is governed by compression. In general, high displacement values have been found for this failure type (from 104 mm to 149 mm). Considering that the average value of density is ρ_{12} equal to 756 Kgm^{-3}, high wood density values are related to this failure mechanism (from 770 Kgm^{-3} to 888 Kgm^{-3}).

The brittle tension failure has been found for the specimen 36, 51 and 53. This mechanism has been recognized in specimens in which the failure affected a large volume of the tension side, reaching up to the neutral axis of the cross section (Figure 6.102.a). Moreover, the fracture surface is characterized by the widespread presence of wood splinters. In general, medium-low displacement values have been found for this failure mechanism (from 50 mm to 105 mm). Specifically, specimen 53 reported a very small displacement (w_{max}: 50 mm) compared with the average displacement of the sample (w_{max}: 113.4 mm). This type has been found in the specimens with a medium-low moisture content (from 15.5% to 19.4%). Furthermore, considering that the average value of density is ρ_{12}: 756 Kgm^{-3}, low wood density values are related to this failure mechanism (from 632 Kgm^{-3} to 707 Kgm^{-3}).

The most widespread mechanism is the tension failure type, since it has been found in 8 of the 16 specimens (35, 46, 48, 52, 55, 57, 58, 65). It is characterized by the fracture at the tension side with the separation of two main splinters (Figure 6.102.b). As respect to the brittle tension, this type of failure seems to be affecting a smaller volume at tension side. The specimens that reported this failure mechanism reached collapse with displacements ranging from 80 mm to 138 mm and a moisture content ranging from 15.1% to 21.9%. As regarding the density, the range of values associated with this type is very wide (from 610 Kgm^{-3} to 900 Kgm^{-3}).

The longitudinal shear failure mechanism have been recognized for the specimen 60, since it was characterized by the presence of long and wide splits at both heads. It consisted of the relative sliding of the two parts of the specimen along a plane arranged approximately at the height of the neutral axis (Figure 6.103). In particular this failure type occurred with the gradual development of the crack from the log heads to the middle-span point (Figure 6.103). The specimen 60 showed a large displacement until the failure (154 mm).

The results of the failure test have been qualitative analysed even in terms of deformative behaviour in order to understand which parameters affect the ductile/fragile failure of the logs and which failure mechanisms are ductile or fragile. The study has been carried out by examining the force-displacement curves and the related failure mechanisms.

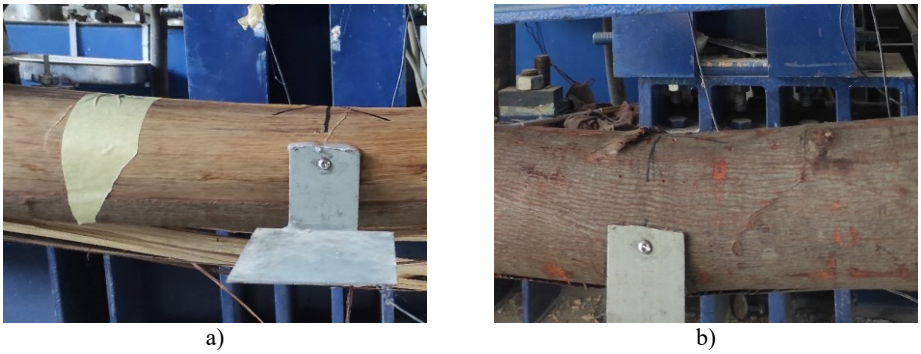

a) b)

Figure 6.101. Compression failure mechanism: a) specimen without bark (39); b) specimen with bark (59).

a) b)

Figure 6.102. a) The brittle failure mechanism (specimen 53); b) The tension failure mechanism (specimen 48).

a) b)

Figure 6.103. The longitudinal shear failure mechanism (specimen 60): a) global view of the split; b) the split propagation at the middle span point.

As is well known from the literature, timber does not exhibit ductile behaviour, however, pseudo-ductile collapse modes can be found under certain conditions. In this case the specimens 59 and 65 showed a pseudo-ductile failure mode evidenced by modest deformations under constant load (Figure 6.99). They reached long displacements (respectively equal to 143 mm and 138 mm) and showed two different failure mechanisms: compression (59) and tension (65). A similar behaviour has been identified for the specimens 56, 60 and 63, however the large displacement reached until failure (from 143 mm to 154 mm), do not occur under constant load. Indeed, after the linear branch the F-w curve shows an increasing trend of the non-linear type (Figure 6.99). The failure mechanism associated to this deformative behaviour are different: longitudinal shear (60) and compression (62, 56). This pseudo-ductile behaviour has been noted for specimen with a high wood density (from 667 kgm^{-3} to 900 kgm^{-3}) and high moisture content (23.5% for specimen 59 and 21.8% for specimen 65).

In contrast, a perfect fragile behaviour has been found only in specimen 53, whose load-displacement curve is a straight line until failure (Figure 6.99). It has been showed a very small displacement until failure (50 mm) and a failure type of the brittle tension. This behaviour is probably due to the wood characteristics of the specimen: a low wood density (632 kgm^{-3}) and low moisture content (15.5%).

The rest of the specimens have been showed a fragile behaviour. For those the first part the load-displacement curve is characterized by a linear branch and then by an increasing non-linear one. Furthermore, from the Figure 6.99 is evident as the length of the non-linear branch is related to the stiffness of the specimen (slope of the linear branch). Indeed, higher is the stiffness the lower is the length of the non-linear branch. Except for specimen 39 which failure mechanism is in compression, all specimens showed a failure mechanism of the brittle tension and tension type. The ultimate displacements (w_{max}) achieved by these logs range from 80 to 130 mm, while both density and MC vary in wide ranges.

6.3.7 STATISTICAL ANALYSIS OF RESULTS

6.3.7.1 General procedures

In the final phase of the research, the experimental results of non-destructive (NDT) investigations and destructive (DT) tests have been

evaluated using statistical methods. Based on NDT and DT parameters, a set of relationships has been explored using linear regression. These models could provide an estimate of the physical and mechanical properties of the material, considering the randomness of the data sample. Thus, the correlations have been grouped into three classes: correlation between NDT, DT and NDT-DT parameters. Among them, the third group of models (NDT-DT correlations) is definitely the most interesting set of tools for *in-situ* applications in order to predict the mechanical properties of wood. The quality of the fit has been evaluated using the goodness-of-fit index, R^2, which is a summary metric to evaluate the linear model's fit to a given set of data. R^2 is referred to as the coefficient of determination because it reflects the correlation between the dependent variable and the predicted variable, as explained by all predictors.

At the same time, a statistical analysis of NDT and DT parameters has been carried out, taking into account the results of the VSG analysis. Indeed, these parameters have been differentiated by visual grades, evidencing the variability and the mean values. In this way the influence of macroscopic visual characteristics of wood on physical and mechanical properties determined by destructive and non-destructive testing has been evaluated.

6.3.7.2 VSG-DT relationship

For the purposes of mechanical characterization of the material, it is essential to compare the results obtained from destructive testing with those obtained from visual classification. As the ultimate goal of VSG is to qualitatively classify the material according to its macroscopic characteristics and provide possible values (average or characteristics) for the mechanical properties. Thus, in this chapter, a variance analysis of the mechanical properties from the destructive tests has been done based on the exposed visual strength grades from the VSG. For this purpose, the results obtained in the absence of the sweep criterion have been used.

The sample has been divided in two groups (B and R) according the classification found in VSG analysis. For each of them the variability of the mechanical properties has been evaluated (Table 6.51)

As regard to the bending strength (f_m) it has been noted that:

- the average value of both groups are very close (83.1 MPa for grade B and 82.9 MPa for R group);

- grade B group has a greater dispersion of data (COV:20.2%) than the R group (COV:12.7%);
- for both groups the outliers have been found equal to 121.MPa (in grade B group) and 57.8 MPa (in R group) (Figure 6.104.a-b).
- both the group distribution observed in the Figure 6.104.a are asymmetrical and opposite.

Table 6.51. Mechanical properties for grade B (VSP-SRT-2)

Grade B			
	f_m [MPa]	$E_{m,0,12}$ [MPa]	ρ_{12} [Kgm^{-3}]
Min.	63.5	14400	610
Mean	83.1	17075	751
Max.	121.3	24300	900
5th perc.	61.0	14400	635
σ	16.8	3029	107
COV [%]	20.2	17.7	14.2

Table 6.52. Mechanical properties for specimens rejected from grading (VSP-SRT-2)

Rejected (R)			
	f_m [MPa]	$E_{m,0,12}$ [MPa]	ρ_{12} [Kgm^{-3}]
Min.	57.8	12600	632
Mean	82.9	16188	761
Max.	94.6	19700	888
5th perc.	57.8	12600	632
σ	10.6	2363	84
COV [%]	12.7	14.6	11.1

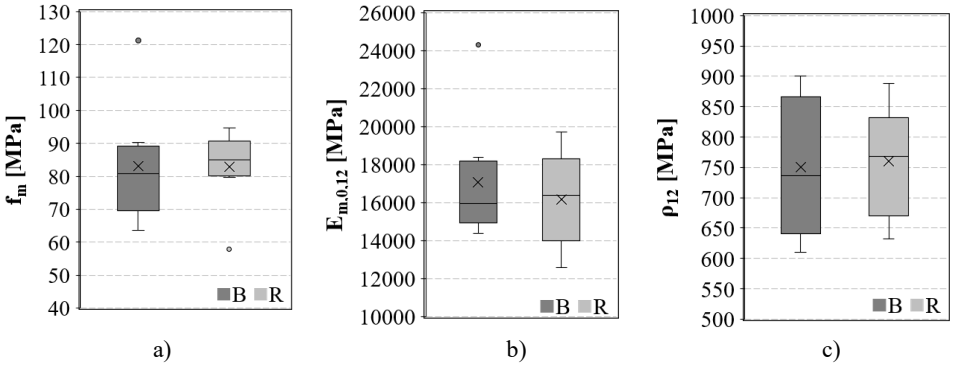

Figure 6.104. Box plot of mechanical properties per group of grade: a) bending strength; b) Modulus of elasticity at MC:12%; c) wood density at MC:12%.

As concern to the modulus of elasticity adjusted to MC:12% ($E_{m,0,12}$) it has been found that:

- there is a very slight difference between the average values of the two groups (17075 MPa for grade B and 16188 MPa for rejected group);
- B group has a greater dispersion (COV:17.7%) of data than R group (COV:14.6%), however this is probably due to the presence of an

outlier (24300 MPa) inside the B group (Figure 6.104.b); indeed, the quantiles of the distribution B are closer to the median than the R group;
- the distribution of the B group is asymmetrical whereas the R group one is quite symmetric.

As regard to density at MC:12% (ρ_{12}) it has been seen that:

- the average value of both groups are very close (751 MPa for grade B and 761 MPa for R group);
- grade B group has a greater dispersion of data (COV:14.2%) than the R group (COV:11.1%);
- for the group the graph are quite symmetric (Figure 6.104.c).

In the end, it can be said that the statistical analysis revealed some critical issues about the distribution of the f_m and $E_{m,012}$ values. In particular, the values found for the two visual grades (B and R) and their statistical distribution do not agree with what should result from the visual grades (i.e. group B should have higher strength and stiffness values than specimen rejected from VSG). As regard to bending strength, the fact that the average value of the B group is greater than the R group is only due to the presence of the outliers, while the quantile distribution is in contrast with this trend (Figure 6.104.a). Similar conclusion can be drawn for modulus of elasticity ($E_{m,0,12}$), since the outliers affect the average value estimation. Indeed, by removing the outliers from group B, group R has higher values than the previous one. As concern the density (ρ_{12}) the distribution seems to be quite similar and symmetric, and this finding is in agreement with what can be expected. The critical points found in this analysis could be related to the ineffectiveness of the VSG analysis. Other visual criteria should probably be considered, and the existing ones should be calibrated to the macroscopical characteristics found on a larger sample of *Acacia dealbata* Link. At the same time, the results examined refer to a small sample and can probably improve as the number of specimens increases.

6.3.7.3 NDT and DT Correlations

NDT Correlations

In the first class, the correlation between the non-destructive parameters themselves has been evaluated. Thus, correlations between the mean drilling resistance measure (R_m) and dynamic modulus of elasticity (MOE_{dyn}) have

been evaluated. In order to consider the moisture variation of the sample from the data of the vibrational test and the drilling test, the linear regression has been evaluated even for the adjusted dynamic modulus of elasticity at MC:12%. ($MOE_{dyn,12}$). As regard to R_m the regression equations have been evaluated considering the three sections of measurement separately ($R_{m,A}$, $R_{m,D}$, $R_{m,B}$) and the average value of these ($R_{m,Av}$).

A good direct relationship has been obtained for prediction of both MOE_{dyn} and $MOE_{dyn,12}$. A R^2 equal to 0.59 and 0.58 have been respectively found for their prediction with $R_{m,av}$ as independent parameter. Furthermore, similar values of coefficient of determination have been found for the regression based on $R_{m,A}$, $R_{m,D}$ and $R_{m,B}$.

Table 6.53. NDT-NDT correlations: parameters, coefficients of determination (R^2) and linear regression equations.

Parameters		R^2	Linear regression equation
Dipendent (y)	Indipendent (x)		
MOE_{dyn}	R_m	0.59	y = 642.37 x + 2989.51
$MOE_{dyn,12}$	R_m	0.58	y = 704.09 x + 3400.81

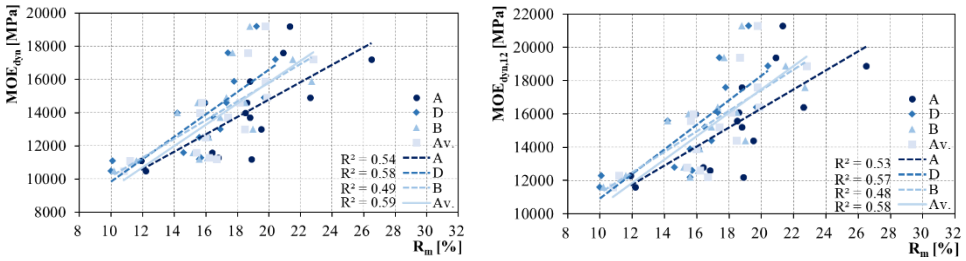

a) b)

Figure 6.105. NDT-NDT correlations: a) Prediction of dynamic modulus of elasticity with drilling resistance measure; b) Prediction of dynamic modulus of elasticity at MC:12% with drilling resistance measure.

A good prediction of the dynamic modulus of elasticity by mean of drilling resistance measure is probably due to the good relationship between R_m and density, a parameter that affect the MOE_{dyn} calculation.

DT Correlations

The correlation between the destructive parameters themselves has been evaluated in the second step of analysis. The correlations between the bending

strength, the modulus of elasticity and the density at MC:12% are provided in terms of equation and coefficient of determination. A moderate correlation between f_m and $E_{m,0}$ have been found (R^2:0.29).

At the same time, a poor relation has been found between density at MC:12% and bending strength (R^2:0.02). This result disagrees with the main literature, according to which density appears to be one of the main factors that influence material behaviour. This discrepancy is probably due to the density estimation that was not detected at the time of the bending test.

Table 6.54. DT-DT correlations: parameters, coefficients of determination (R^2) and linear regression equations.

Parameters		R^2	Linear regression equation
Dipendent (y)	Indipendent (x)		
f_m	$E_{m,0}$	0.29	y = 0.00291 x + 37.5845
f_m	ρ_{12}	0.02	y = 0.02 x + 66.12
$E_{m,0,12}$	ρ_{12}	0.16	y = 11.32 x + 8077.56

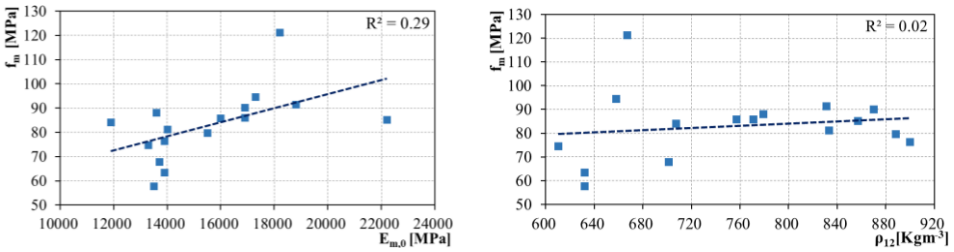

a) b)

Figure 6.106. DT-DT correlations: a) Prediction of bending strength with modulus of elasticity; b) Prediction of bending strength with density at MC:12%.

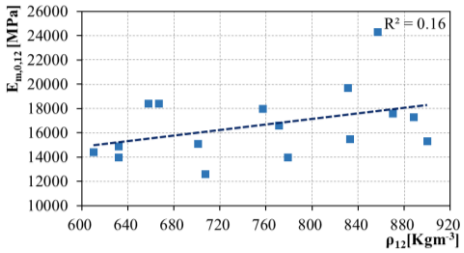

Figure 6.107. DT-DT correlations: Prediction of modulus of elasticity at MC:12% with density at MC:12%.

In the end the relation between ρ_{12} and $E_{m,0}$ has been investigated and a coefficient of determination equal to 0.16 has been seen.

NDT-DT Correlations

Firstly, the correlations between moisture content and the destructive parameters in bending (f_m and $E_{m,0}$) have been evaluated. The R^2 coefficient and the equations are provided in Table 6.55. A low relation has been found between MC and f_m (R^2:0.22); a very poor relation has been seen between MC and $E_{m,0}$ (R^2:0.01). These results are in contrast to the scientific literature, since it is well known that both modulus of elasticity and strength in general are inversely related to the moisture content until the fibre saturation point (FPS). This trend is evident from the Figure 6.108, however the dispersion of the data affects the goodness of the regression.

Table 6.55. NDT-DT correlations: parameters, coefficients of determination (R^2) and linear regression equations.

Parameters		R^2	Linear regression equation
Dipendent (y)	Indipendent (x)		
f_m	MC	0.22	y = -2.21 x + 124.23
$E_{m,0}$	MC	0.01	y = -81.34 x + 17114.64
f_m	*f*	0.20	y = 0.13 x - 26.82
$E_{m,0,12}$	*f*	0.01	y = 6.82 x + 11004.29
$E_{m,0,12}$	$MOE_{dyn,12}$	0.11	y = 0.33 x + 11481.49
f_m	$MOE_{dyn,12}$	0.14	y = 0.00189 x + 53.8539
ρ_{12}	R_m	0.66	y = 26.07 x + 311.69
f_m	R_m	0.24	y = 2.45 x + 43.66
$E_{m,0}$	R_m	0.32	y = 313.98 x + 10558.65

Aiming at evaluation the efficiency of longitudinal vibration test as useful supplement for mechanical characterization of timber, the correlation between frequency (*f*), dynamic modulus of elasticity at MC:12% ($MOE_{dyn,12}$) and DT parameters have been evaluated. Starting from frequency the linear regression with f_m and $E_{m,0}$ are provided in terms of equation and R^2 in Table 6.55. The results show as a poor relation has been founded for $E_{m,0}$ prediction (R^2:0.01). At the same time a low relation between f and f_m has been noted (R^2:0.22). The relations between $MOE_{dyn,12}$ and destructive parameters have been evaluated (). However, low values of coefficient of determination have been found: R^2:0.14 for bending strength (f_m) prediction and R^2:0.11 for modulus of elasticity ($E_{m,0}$) prediction. In contrast to the scientific literature,

which demonstrates a high correlation between static and dynamic modulus of elasticity, the latter results demonstrate a low correlation. The correlations between NDT and DT are unreliable probably due to the high difference in moisture content between the NDT tests (average MC:59.9%) and DT tests (average MC:18.6%).

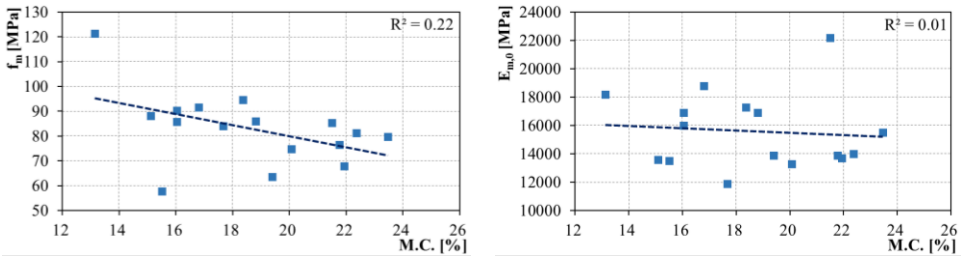

a) b)

Figure 6.108. NDT-DT correlations: a) Prediction of bending strength with moisture content; b) Prediction of modulus of elasticity with moisture content.

In the end, the correlations between the mean drilling resistance measure R_m and DT parameters have been assessed for evaluating the efficiency of this NDT. Relating the wood density with drilling resistance (R_m) at the different measurement sections, the regression lines are quite coincident with the average one (regression line of the $R_{m,av}$ parameter). Only the regression lines of the $R_{m,A}$ parameter deviate from this trend, and this is probably due to the fact that the values found in the section in A are on average higher than those found in B and D.

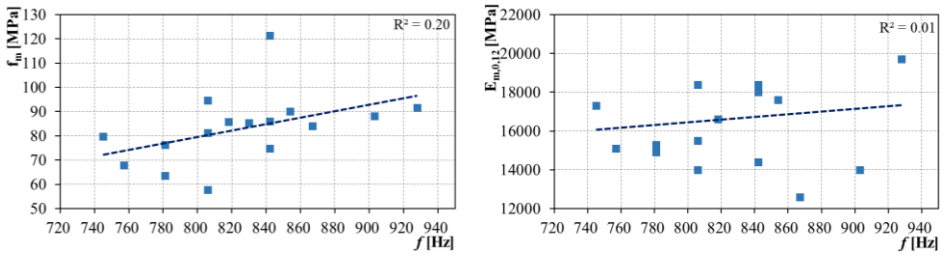

a) b)

Figure 6.109. NDT-DT correlations: a) Prediction of bending strength with frequency of vibration; b) Prediction of modulus of elasticity at MC:12% with frequency of vibration.

As regard to goodness of the fit the best results have been found for this analysis. Indeed a R^2 equal to 0.66 has been found for density prediction with the average drilling resistance ($R_{m,av}$). At the same time for the parameters calculated in sections A, B, and D, slightly lower indices of determination have been found but representative of a good fit. This finding is in good agreement with the main literature references and could be improved with the effective value of timber density.

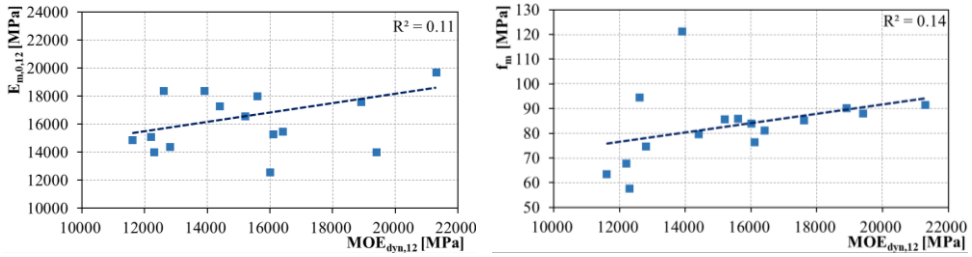

a) b)

Figure 6.110. NDT-DT correlations: a) Prediction of modulus of elasticity at MC:12% with MOE at MC:12%; b) Prediction of bending strength with dynamic modulus of elasticity at MC:12%.

Other interesting results have been noted for regression between Rm and both bending strength and modulus of elasticity. Starting from f_m, it has been found a moderate correlation with this parameters and the $R_{m,D}$ (R^2:0.24), whereas a slightly lower correlation have been found for the other parameters ($R_{m,A}$, $R_{m,B}$ and $R_{m,av}$).

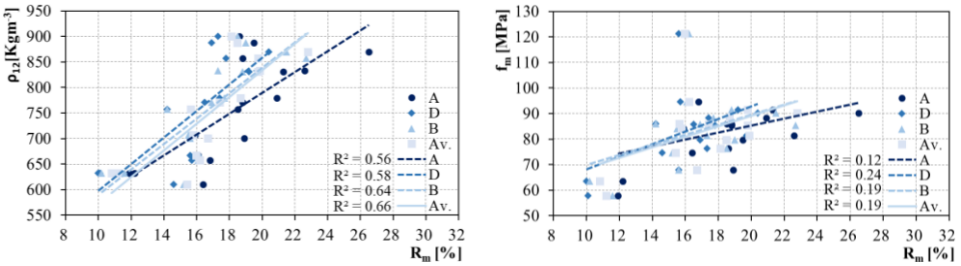

a) b)

Figure 6.111. NDT-DT correlations: a) Prediction of density at MC:12% with drilling resistance measure; b) Prediction of bending strength with drilling resistance measure.

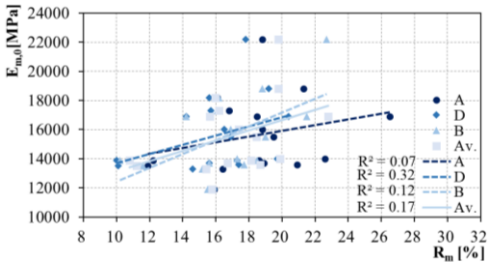

Figure 6.112. NDT-DT correlations: Prediction of modulus of elasticity with drilling resistance measure.

Similar results have been found for R_m-$E_{m,0}$ linear regressions, since the best coefficient of determination has been found for the drilling measurement in the section D (R^2:0.32) and lower values in the other sections. These results show that the measurement at the middle span point (section D) is more significant than the others for the purpose of predicting the bending strength and elastic modulus of the log with the drilling resistance test.

Conclusions

Nowadays the Italian territory is heavily exposed to many risks due to natural actions and the high vulnerability of the built-up. Among them seismic risk stand out due to the frequency and intensity of earthquakes affecting our territory.

Therefore, seismic prevention and risk mitigation policies assume great importance in national territorial planning. There are many actors in the field of prevention, and they act on two different levels: the territorial scale and the building scale. The institutions and the scientific community are generally dedicated to the identification of the most at-risk area and the quantification of resources for risk reduction; on the other hand, the community of professionals and technicians assumes a key role in the design of effective retrofit interventions. Based on these objectives, the two communities use different methods and approaches for assessing the vulnerability of the exposed built-up. To achieve this aim, the knowledge process of the exposed buildings is a fundamental step in the vulnerability assessment. It consists of the acquisition of the information required for vulnerability assessment using effective models suited to the scale of the analysis. As with vulnerability models, the approaches and methods for acquiring information must also be appropriate to the scale of the analysis. If at the territorial scale, it is sufficient to know the key aspects of building types, at the building scale, an in-depth geometric and technological survey, as well as a diagnosis of the state of health are necessary for assessing the vulnerability of the structure.

Based on this background, the attention has been focused on timber constructions, which are widespread in the field of vernacular, historic and contemporary architecture. A thorough review of the state of the art in material properties revealed that durability issues have a significant impact on structural performance of timber buildings, and degradation phenomena can significantly reduce their service life. At the same time, it has been seen that the heritage of timber structures is rich in different and often very complex structural types. Acquiring a comprehensive understanding of their functionality and examining their key aspects is crucial for preserving them and enhancing their structural performance. Therefore, it has been seen that analysing typological and durability aspects of timber structures is fundamental in order to perform effective structural vulnerability assessments at both territorial and building scale. To this end, methods and tools to

characterize existing timber structures at different scales have been proposed in this thesis.

At the territorial scale, an integrated approach to seismic vulnerability assessment of timber structures has been proposed. It is based on the integration of the indicator-based approach (IBA) for the seismic vulnerability assessment with the innovative "Global durability factor method – GDFM". The latter method has been proposed for assessing the state of preservation of the timber structures at territorial scale. Both methodologies are based on the MCDM methods, and they are supported by specific survey forms for the acquisition of data.

The indicator-based approach, which is widely used in large-scale vulnerability analysis, has been applied to the specific case of large-span timber buildings using an existing database related to a set of buildings surveyed through CARTIS form. To implement the methodology on large-span timber buildings, it was imperative to define vulnerability criteria including geometric, typological, and structural building aspects. These features have been identified in the set of data acquired through the CARTIS form GL. Thus, in a first step 32 vulnerability criteria have been qualitatively identified. Then, they have been quantified and ranked according to their importance using the MCDM techniques. In the end the methodology has been applied to a set of 10 large-span buildings. Thus, a classification of buildings according to the vulnerability index (I'_V) has been obtained, identifying the most vulnerable buildings. The distinctive features of the adopted methodology include its ease of implementation through the database acquired from CARTIS, quick application, and flexibility in updating, achieved through the easy calibration of the weights. However, to ensure the procedure's robustness and reliability, it is essential to validate the results through the application of different approaches.

The integration of the IBA method with durability aspects has been subsequently proposed. In terms of procedure, the proposed method consists of the integration of the 32 seismic vulnerability criteria with additional criteria related to the state of preservation and susceptibility to degradation, which are quantified through the global durability index (I_{GD}). This index gives the name to the proposed methodology (GDFM), which has its background in the factorial method (ISO 15686, [273]) and takes advantage of multi-criteria methods for the evaluation of the modification factors [273]. The potentiality of the method lies in the capability of identifying timber buildings more prone to degradation through service life (SL) and I_{GD} estimation, using a deterministic approach. However, this methodology

requires a prior definition of the set of environmental, typological, and technological parameters that most influence the state of preservation of a timber structure. Through the study of the state of the art concerning the timber durability issues, a list of durability factors has been qualitatively proposed. Following that, MCDM techniques have supported the quantification and ranking of these factors in accordance with their impact on durability, which is reflected in the I_{GD} calculation. Thus, the I_{GD} is conceived as a single parameter accounting for all the durability factors, which multiplied by reference service life (RSL) allow the estimation of the SL. The method has been applied on a sample of four case studies allowing for the evaluation of suitability of the proposed methodology. The application revealed both positive and negative aspects of the methodology. The calculated SL is distant from the actual age of the buildings, but there is proportionality between the recorded lifetime and SL, indicating an overall correct calibration of the coefficients. The calculation procedure is quick and integrates well with the predisposed survey form (SHA-TS form). However, the application of the method to a wide range of case studies would be beneficial for refining the durability factors and comprehensively evaluating the methodology's effectiveness.

In order to acquire the parameters necessary for the application of the methodologies shown so far, two survey forms have been used. They have been extensively described in Chapter 3 and detailed in the appendices attached to the thesis. The evaluation of the seismic vulnerability index using the indicator-based approach has been supported by CARTIS Large-span form. It allowed the acquisition and collection of the data necessary for the assessment of the vulnerability index for the sample of 10 large-span timber buildings [262]. Within the scope of this thesis, an activity has been carried out to update the latest version ("Rev.09") of the Cartis form for the large span timber buildings (Cartis GL 3D) in terms of content and organisation, leading to the development of a more organic, simple and complete layout. At the same time the SHA-TS form has been used as support tool to the application of the GDFM method in acquiring data related to the durability factors. However, the form has been conceived for a wider field of application, i.e., as a tool to support designers and technician during the diagnosis of existing timber structures. The form guides users through a systematic process for gathering information about the construction type and technology, materials, and structural-health state of the timber structure. Particular attention has been paid to the survey of degradation phenomena (sections E and F), providing an illustrated survey manual that guides users through the diagnosis of the phenomenon by recognizing the main visible

effects and identifying the main causes. The survey form has been applied and validated on four case studies, having positive feedback on the effectiveness of the form framework. However, more applications are needed in order to include any additional structural types. At the same time supplementary information could be added for including the decay effects and typologies spread in specific environmental condition.

At building scale, the effectiveness of vulnerability analysis is closely related to the degree of knowledge of the structure, which is generally acquired through on-site assessment. To this end geometrical and technological survey, characterization of mechanical properties and diagnosis of the state of health are key tasks. However, for existing timber constructions, on-site assessment is a challenging task because only the most recent constructions are engineered and standardised, while historical structures, which represent a large part of the built heritage, are particularly complex to analyse. Such complexity is generally due to the presence of non-regular geometries and technological solutions, material with physical-mechanical properties depending on the wood species, and the presence of possible mechanical and/or biotic degradation phenomena. Therefore, shared procedures and effective tools are necessary for the on-site assessment of these structures.

To this end a further survey form has been proposed in this thesis, specifically related to ancient timber trusses which are the main spread type in historic buildings. This form has been developed within the framework of cooperation within the Italian national committee ICOMOS IIWC. The aim of the form is twofold: it is an operational tool for survey and diagnosis of the structures, as well as a support tool for the creation of a database from which an inventory of common ancient structural types and recurrent structural issues can be drawn. In the three main sections of the form, typical aspects of ancient timber structures have been outlined, accompanied by a proposed nomenclature to identify the different parts of the structure. The form has then been used remotely in the case study of the Royal Palace, for which extensive and detailed documentation was acquired, kindly provided by Faggiano and Grippa. The application focused on the truss of the diplomatic room, a structural unit particularly complex in terms of geometry and technological solutions. Despite this, the form proved adequate in content, allowing for an analytical and complete survey of the structure. Future developments may consist in the on-site application of the form in order to evaluate its effectiveness and completeness of content.

Geometrical survey and mechanical material characterization are fundamental for the calculation of the load-bearing capacity. Regarding geometrical survey, nowadays the professional community can be supported by various innovative techniques. Especially in the structural field, their application is not limited to the mere geometric survey but can find a wider field of application. However, the effectiveness of these methodologies depends on several factors that can influence the output and processing times. At the same time, mechanical characterisation of existing structures is a very difficult task as wood, being a natural material, has physical-mechanical characteristics that depend on many parameters, including the thermo-hygrometric parameters of the environment in which it is placed. Strength properties of new timber member are usually determined by direct testing of timber elements according to a standardised protocol. Conversely the assessment of the mechanical properties of the existing timber members becomes difficult as it is usually not possible to remove large samples from an ancient structure for direct testing. Therefore, most common approach consist in performing visual strength grading (VSG) and non-destructive techniques (NDT), since they don't compromise the structural integrity of the construction. The first approach (VSG) address the evaluation of macroscopic characteristics of timber, assigning a strength grade according to grading rules provided by the pertinent Standard. On the other end NDTs are frequently used as a tool to support indirect evaluation of wood's mechanical properties and for diagnosing the state of preservation. Nevertheless, these techniques are effective to on-site assessment only when reliable regression laws are available, enabling the prediction of wood mechanical properties without the need for destructive testing. In addition, there is a noticeable lack of standardization about the non-destructive techniques on timber. At the same time safety assessment of ancient timber structures is usually not addressed by the current codes, which are conceptually oriented to new constructions. In Italy, there is a need for an update standard dedicated to the VSG of ancient wood that allows the assignment of strength grades in accordance with the design methods established by the current regulations.

Against this background, two experimental campaigns involving structural members in different wood species have been performed. They regard Chestnut (*Castanea Sativa* Mill.) and Corsican Pine (*Pinus Nigra* subsp. *laricio* (Poir.) Maire) wood members extracted from an historical building in Southern Italy and wood logs in Acacia dealbata Link harvested from the Peneda-Gerês National Park in Portugal. As testified by the literature review these wood species are typically spread in different fields as the cultural heritage and vernacular architecture. Thus, the typical steps of in situ detailed

assessment, i.e., geometric survey, visual strength grading (VSG) and non-destructive tests (NDT), have been carried out in the laboratory. Furthermore, destructive test (DT) in bending have been performed in order to assess stiffness and strength properties, post-elastic behaviour and collapse mechanisms of the timber elements. On ancient timber members long-term test in bending have been carried out for a time duration of one year, monitoring displacements, moisture content and environmental parameter as temperature and relative humidity. In this way the time-dependent behaviour of wood have been analysed taking into account the influence of environmental thermo-hygrometric parameters. After the analysis of the experimental results, including data processing and interpretation, statistical relationships between both NDT and DT parameters have been provided for the mechanical identification of timber, based on linear regression model.

On the basis of experimental investigations, the following conclusions can be drawn for ancient timber members.

Geometrical survey

Visual inspection revealed distinctive macroscopic features for Chestnut (CS) and Corsican Pine (PNL), allowing identification of the wood species in each specimen. PNL have been identified by resinous knots and differentiated heartwood, while CS specimens have been recognised by large knots with a pseudo-elliptical shape, as well as the presence of flaming in the cross-section. Irregular geometry, characterized by wane and distortion, has been found for CS specimens and it is could be related to smaller size of the CS trees than the PNL ones. Shape and geometrical size have been surveyed through different techniques: direct (DS) and indirect survey (laser scanner survey - LSS and photogrammetric survey - PS). Both indirect survey techniques have been found to provide digital models with accurate geometry for structural assessment scopes. From the digital model key geometrical features such as length, cross-sectional dimensions and volume have been easily measured. A comparison between the geometric volume of the specimen obtained from the different type of survey (DS and LSS) has been performed; by comparing the volume of each specimen a considerable difference has been seen, especially for Chestnut where an average percentage deviation of 13.7% have been found. As regard the performance of LSS and PS techniques, it has been found that LSS took longer timbe than PS, both in acquisition and processing time. Furthermore, it has been seen that PS provided a digital model more refined than LSS one, with a better resolution of the texture.

Visual strength grading (VSG)

Visual strength grading (VSG) has been carried out according to UNI 11119 and UNI 11035, without taking into consideration certain criteria that penalise ancient timber members (wane and geometrical irregularities) and those that can be measured at the heads, which are generally not accessible in on-site assessment. VSG analysis showed that almost the whole sample was characterised by poor-quality material. The defects influencing the grading varied according to the wood species. Large knots and widespread but shallow insect attacks have been found in CS, while slope of the grain has been found in most of the PNL specimens. In general CS showed poorer characteristics than PNL. As a result, 2 CS specimens (2 and 9) have been not assigned to a strength grade according to UNI 11035, and therefore they cannot be used for structural purposes. From VSG performed on digital model, it has been seen that LSS is not effective for this purpose due to the poor quality of the texture. On the other hand, digital model derived from PS was refined enough to easily measure all the features for VSG analysis. Therefore, it has been found that PS technique is very effective for such application purposes in daylight condition. However, the reliability of the technique should be evaluated under low illumination or artificial lighting conditions.

Non-destructive test (NDT)

In addition to direct weight measurement and indirect moisture measurement, 3 non-destructive techniques have been applied: drilling resistance, acoustic and vibrational methods. The mechanical parameters obtained through the NDT tests have been evaluated considering the specimen volume calculated by means of direct survey (DS) and LSS techniques. From the comparative analysis of the results, the influence of the survey accuracy in the determination of the mechanical parameters has been measured by means of a percentage variation index (i). It has been seen that direct surveying can lead to significant errors in the assessment of the physical and mechanical properties of ancient wood specimens, especially when very irregular geometries are present. The maximum variation has been recorded for the Chestnut sample, since a maximum error of 21% (3400 MPa) has been observed in the calculation of $MOE_{dyn,A}$. Using the acoustic technique, the stress wave speed has been calculated, and it has been seen that in the diagonal (D) measurement (or indirect longitudinal measurement), this parameter is on average lower than in the direct longitudinal measurement (L), with an average variation of approximately 2%. From this, the dynamic elastic modulus ($MOE_{dyn,A}$) has been calculated and an L-D variation of

approximately 4% has been found. The drilling resistance method has been helpful for the detection of the main defects of wood, such as cracks, pith, ring shakes, as well as for the qualitative assessment of ring width.

Destructive test (DT)

In relation to the elastic modulus, it has been fund that for CS, both the global and local elastic modulus are lower than for PNL. Although it is not possible to make analytical evaluations due to the different size of the two study samples, this result is certainly related to an overall better wood quality of PNL compared to CS.

For most of the elements (10 out of 18), it has been seen that the local elastic modulus is higher than the global elastic modulus. The percentage variation between global and local modulus has been assessed, finding wide dispersions and large differences for most of the sample (up to 52.10% for specimen 8 of NLP). This variation is probably related to the irregular geometry of the specimens, as well as the presence of the strut notch. The significant reduction in cross section due to this irregularity caused an higher deformability out of the middle third, where local modulus is measured.

In relation to the failure tests, a moderate dispersion of the bending strength data has been recorded for both wood species (COV: 37.3% for CS and COV: 42.0% for GNP), with the values of PNL on average higher than those of chestnut (13.5 MPa for CS and 22.9 MPa for PNL). This result is related to the fact that, overall, PNL had a higher wood quality than CS. Values higher than 30 MPa have been found in the best-quality specimens, up to 39.9 MPa (specimen 7).

Regarding failure modalities, a fragile and pseudo-fragile failure mechanism have been generally found for the whole sample, due to the failure at tension side without plastic deformation. In general, specimens with high bending strength simultaneously exhibited the highest displacements (e.g. specimens 5, 18, 1, 3 in NLP). Only a few CS specimens (10 and 15) achieved high displacements and were able to withstand more load cycles, even if they reached low failure loads. This capacity reserve is probably related to the intrinsic characteristics of the Chestnut wood, which is able to propagate the fracture. No strong cause-and-effect relationships have been found between collapse mode and f_m and w values; however, it can be observed that the lowest strength values (f_m<10 MPa) have been found in specimens where collapse was caused by presence of knots at the tensioned side (specimen 2, 10 and 15). Concerning the failure mechanisms and fracture, in most of the specimen (7 out 18) failure occurred in correspondence of large knots at

middle span, while for 5 specimen it occurred in correspondence of wide shrinkage cracks. At the same time a sudden collapse have been seen for specimen characterized by widespread resin pockets. In addition, different modes of fracture triggering and propagation have been observed. The presence of defects and irregularities on the tension side was the most influential factor in triggering modes. Indeed, knots and notch were the preferred points where fractures started. The fracture propagated along the grain, and failure occurred when it reached knots or shrinkage cracks.

Long-term test (LTT)

The long-term tests in bending have been performed on four specimens placed in the laboratory for a duration of about one year. The specimen displacement at middle span, wood moisture content (MC), environmental relative humidity (RH) and temperature have been measured. From thermo-hygrometric results, exposure conditions have been found to be close to Service Class 1 established by the Eurocode 5 [70]. For all specimens, the maximum MC has been reached in December and January, while the minimum one between June and September. The maximum absolute excursion have been found equal to -2.7% for specimen 9 in CS. In general, it has been found that Corsican Pine specimens were more susceptible to changes in moisture content than CS, showing the greatest variations both upwards and downwards. In addition, the trend of the moisture content curve of the PNL specimens seems to be more adherent to the environmental relative humidity curve. Regarding the displacement, similar beahviour have been found for specimen having similar value in bending stiffness. It has been found that timber members with a high stiffness reach their maximum displacement earlier (approximately 2 months after the test start) and they maintain this displacement almost unchanged. In contrast, the specimens with a lower modulus of elasticity showed prolonged deferred displacements, with the maximum displacement being reached after a period of 4 to 6 months. Regardless the bending stiffness, the highest displacement have been found for PNL. They have been found to be equal to 1.62 and 1.68(w0) for specimen 13 and 7, respectively. On the other hand, the Chestnut specimens showed a maximum final displacement of 1.40 and 1.47(w_0). These results are quite close to the prescription of Eurocode 5, which establishes an increasing initial displacement for a coefficient equal to 1.60 (considering k_{def}: 0.60) for solid wood in Service Class 1. However, the standard seems to underestimate the creep behaviour of Corsican pine wood. In this regard, conducting additional tests on a sufficient number of samples will enable the calculation of the

average and characteristic values of deferred displacement in order to make stronger comparisons.

VSG-DT relationship

The analytical assessment of the correspondence between the visual strength classes assigned by VSG analysis and the mechanical and physical properties derived from destructive tests has been performed. For this purpose, the specimens have been divided into sub-samples according to the strength classes of chestnut (D24) and those of larch pine (C14, C24, C40). In general, it has been found that both the strength and stiffness properties obtained through destructive testing are overall lower than the values assigned through VSG. Furthermore, a high dispersion of data can be observed especially for bending strength data. However, for PNL has been seen that average values of each strength class showed an increasing trend as the quality of wood increased (from C14 to C40). However, the comparison of strength in terms of characteristic values penalises the test result considerably. Chestnuts resulted in the worst finding since, a bad agreement has been found by comparing the results of destructive test ($f_{m,5th}$: 9.5 MPa; E0: 5570 MPa) and characteristics value provided by EN 338 ($f_{m,k}$: 24.0; E0,mean:10000 MPa). Also for PNL a bad agreement has been seen between bending strength from DT ($f_{m,5th}$: 7.4 MPa) and standard's value for class C14 ($f_{m,k}$: 14.0 MPa). On the other hand, the modulus of elasticity from DT test (E0: 9315 MPa) has been found to be higher than that prescribed by the Standard (7000 MPa). As regard density a lower dispersion of data have been found and value from direct measurements are close to the standard prescription. In general, these analyses reveal a high dispersion of data, therefore additional tests are required to conduct more robust comparisons.

NDT-DT correlations

The correlation between the non-destructive parameters themselves has been evaluated and the quality of correlation has been evaluated using the goodness-of-fit index R^2. For both CS and PNL good correlations ($R^2 > 0.48$) have been found between Rm and both $MOE_{dyn,A}$ and $MOE_{dyn,V}$. This good relation is probably due to the well-known relation between Rm and density, which is used for MOE_{dyn} calculation through the Eq. 6.9 and Eq. 6.11.

Successful findings have been seen in the correlation between DT parameters themselves. A strong correlation has been found between bending strength (f_m) and the global modulus of elasticity ($E_{m,g}$: R^2: 0.97 for CS; R^2: 0.92 for PNL). This finding also emerges from the load-displacement curve of the DT test, as generally the curves that reach the high failure load values

are also the steepest ones (i.e., with a high modulus of elasticity). Furthermore, it has been found that for the wood species, the regression laws have a similar equation. This result shows that there is a relationship between stiffness and strength that is independent of wood species. At the same time, for PNL, a good correlation has been found between density (ρ), local modulus of elasticity ($E_{m,l}$), showing a R^2 equal to 0.62. Moderate correlation have been seen also between ρ and $E_{m,g}$ (R^2: 0.46), as well as between ρ and fm (R^2: 0.46). On the contrary, CS showed poor correlation as respect these parameters. This result can be explained by considering that PNL exhibited a more homogeneous material than CS, showing smaller and less widespread knots, as well as less extensive areas of decay. Therefore, the density of the material had a greater influence on the bending behaviour of the members in terms of both strength and stiffness. In the end, for both wood species, a good correlation has been found between the $E_{m,g}$ and $E_{m,l}$ moduli of elasticity (R^2: 0.65 for CS; R^2: 0.69) for PNL.

In general strong correlations between NDT and DT have been found for Corsican Pine. Considering both acoustic (A) and vibrational method (V), good correlations has been noted between the dynamic elastic modulus and both the global (R^2: 0.82 for A-method; R^2: 0.74 for V-method) and local (R^2: 0.57 for A-method; R^2: 0.41 for V-method) static modulus. In addition, a strong correlation has been found between fm and $MOE_{dyn,A}$ (R^2: 0.85), as well as between f_m and $MOE_{dyn,V}$ (R^2: 0.79). The latter findings can be well explained by the proportionality between bending strength and static modulus, which has been found in the DT-DT correlation. On the contrary Chestnut showed poor correlation with R^2 lower than 0.37. Apart from the strong correlation between Rm and ρ (R^2 0.92), it has been observed that poor correlations emerge for the other parameters analysed in Chestnut, as evidenced by R^2 indices of lower than 0.38. This result, in contrast to what has been seen for PNL, shows how the widespread presence of defects affected the correlations between the physical and mechanical parameters of wood.

Based on experimental investigations, the following conclusions can be drawn for logs in *Acacia dealbata* Link.

Geometrical survey and visual inspection

The wood logs have been surveyed using traditional surveying techniques. The whole sample showed very irregular geometries characterised by sweep, twist, and taper. These characteristics are related to the features of the tree,

which are characterised by its tendency to grow tall and retain a small diameter. At the same time, small knots and shrinkage cracks limited to the beam heads have been found. Regarding the visual strength grading, there is no specific regulation for this wood species. Furthermore, using specific grading criteria for small-diameter wood, the whole sample has been found to be ungradable due to defects in geometry. In particular, the sweep criterion seems to be too restrictive for classification purposes. Therefore, the material classification has been carried out without considering this criterion, and it has been seen that both cracks and tapering are influential defects for classification purposes.

Non-destructive test (NDT)

Vibrational tests have been carried out before the kiln-drying process, when wood MC has been found to be equal to 59.9% on average. However, as the moisture content (MC) exceeds the fibre saturation point (FSP), it is considered that this measurement is only indicative. In general, high values have been found for both dynamic elastic modulus ($MOE_{dyn,V,12}$: 15394 MPa on average) and density (ρ_{12}: 756 kgm^{-3} on average) with low data dispersion (COV: 17.9% for $MOE_{dyn,V,12;}$ COV: 12.9%). The drilling resistance method test (DRM) has been performed after the kiln-drying process. It was useful for identifying wood macroscopical characteristics such as pith and growth rings. Furthermore, it has seen that the average resistance R_m, measured at the base of the tree, is higher than the other values. Also for DRM test low dispersion of data has been found (COV:19.2%). These findings are associated with the homogeneity of the material, which was evident since the visual inspection.

Destructive test (DT)

Destructive testing showed the high capabilities of this material in the structural field. High performance has been found in both stiffness ($E_{0.12}$: 16631 MPa on average) and strength (f_m: 83.0 MPa on average), reaching a maximum strength of 121.3 MPa. Furthermore, a low data dispersion has been seen (COV: 16.9%) in both properties. As regard to the deformation, in general large displacement have been found, ranging from 50 mm to 154 mm.

Different collapse modes have been observed and cause-and-effect relationships have been found between collapse mode and material properties. The specimen having high value of density showed a pseudo-ductile behavior, highlighted by small fractures and bark corrugation at compression side. The final collapse occurred by fiber fracture at the tension side, however the bending bahviour until failure was governed by compression. For these

specimens large displacement (maximum w_{max}: 149 mm) and high strength (maximum f_m: 121.3 MPa) have been found. On the contrary specimens characterized by density values below the average threshold showed a fragile behavior, marked by the sudden collapse and wide fractures at tension side. However, the influence of density on bending behaviour should also be related to the moisture content of the specimens, which at the time of the test showed values within a wide range.

VSG-DT relationship

Variance analyses revealed some critical issues about the distribution of bending strength and modulus of elasticity values as function of the visual grading classification. It has been seen that for specimens in class R (i.e., the class of specimens rejected by the VSG), the quantile distribution of f_m and $E_{m,0,12}$ have been found to be higher than for those belonging to class B. The fact that the average value of the B group is greater than the R group is only due to the presence of the outliers, which affect the calculation of the average values. On the other hand, as concern the density (ρ_{12}) the distribution seems to be quite similar and symmetric, and this finding is in agreement with what can be expected.

This finding refers to a small sample, and probably, by carrying out this analysis on a larger sample, these relationships might change. At the same time these results could be related to the ineffectiveness of the adopted visual grading criteria. Therefore, other visual criteria should be considered, and the existing ones should be calibrated to the macroscopical characteristics found on a larger sample of *Acacia dealbata* Link.

NDT-DT correlations

In general poor regression laws have been found between the DT and NDT properties. The main cause is probably due to the different moisture content of the specimens at the time of the DT and NDT test. Indeed the destructive test was performed after the kiln drying process, in contrast to the NDT tests which were performed before. Only the DRM investigation was carried out at the same time as the destructive tests. In fact, it has been found that the correlations between R_m and mechanical properties are the most reliable. The most robust correlation has been found between R_m and ρ_{12}, in accordance with what has been reported in the literature. The correlation between $E_{0,12}$ and R_m performed at the midspan section showed a good result ($R^2 = 0.32$) if compared to the values obtained at other points of the log, where R^2 has been found to be lower than 0.12. This result highlights the importance of conducting the drilling measurement at midspan of the beam if the bending

modulus of elasticity is to be effectively predicted. Regardless of moisture content, the correlations between $MOE_{dyn,V,12}$ and R_m showed a good correlation, with an R^2 value of 0.58. As found for ancient timber members, this result can be attributed to the relationship between dynamic MOE and density. Contrary to expectation, very poor correlation (R^2: 0.02) have been found between the ρ_{12} and f_m. As mentioned so far, these results can be related to the moisture content variation between DT and NDT test. In the end correlation between DT properties (E_0 and f_m) and MC have been investigated, but R^2 lower than 0.22 have been observed.

These findings indicate that additional bending tests should be conducted after deeply drying the specimens to ensure a uniform moisture content in the sample. This would allow a more robust evaluation of the influence of wood density, which seems to be the key parameter in the determination of bending strength, given the homogeneity of the material and the lack of significant wood defects. Furthermore, relationships between the strength and moisture content of wood should be investigated in order to obtain modifying equations such as those provided by the standard for density and modulus of elasticity.

Bibliography

[1] Weintraub, A., & Epstein, R. (2005). The supply chain in the forest industry: models and linkages. Supply chain management: Models, applications, and research directions, 343-362.

[2] Forest Stewardship Council. (n.d.). Home page. FSC. https://search.fsc.org/it/

[3] Programme for Endorsement of Forest Certification. (n.d.). Home page. PEFC. https://www.pefc.org/

[4] Food and Agriculture Organization. (2020). Global Forest Resources Assessment 2020: Main report (No. CA9825EN). FAO. https://www.fao.org/3/ca9825en/ca9825en.pdf

[5] Fedorov, A., Babko, A., Sukharenko, A., Emelin, V. (2021). Illegal logging and trade in forest products in the Russian federation. Amazon web Services. https://gridarendal-website-live.s3.amazonaws.com/production/documents/:s_document/310/original/RusLog_screen_(1).pdf?1488216205

[6] Butler, B. J., Butler, S. M., Caputo, J., Dias, J., Robillard, A., & Sass, E. M. (2021). Family forest ownerships of the United States, 2018: Results from the USDA Forest Service, national woodland owner survey. Gen. Tech. Rep. NRS-199. Madison, WI: USDA Forest Service, Northern Research Station, 52.

[7] American Wood Council. (n.d.). Homepage. AWC. https://awc.org/

[8] Canadian Wood Council. (n.d.). Homepage. https://cwc.ca/en/home/

[9] Amazon Environmental Research Institute. (2023). Homepage. IPAM. https://ipam.org.br/en/

[10] Meloni, E. (03/10/2022). FSC e PEFC: le certificazioni ambientali dei prodotti in legno. Infobuildenergia. https://www.infobuildenergia.it/approfondimenti/fsc-pefc-certificazioni-ambientali-prodotti-in-legno/

[11] European Environment Agency. (2019). The European environment - state and outlook 2020. EEA. https://www.eea.europa.eu/publications/soer-2020

[12] European Optical Society. (2023). EOS Annual Report 2021-2022. EOS. https://eos-oes.eu/wp-content/uploads/2023/04/eos-annual-report-2021-2022_web.pdf

[13] WWF – World Wide Fund for Nature. (2011). WWF LIVING FORESTS REPORT: CHAPTER 2 - FOREST AND ENERGY. WWF. https://wwfeu.awsassets.panda.org/downloads/living_forests_chapter2_report.pdf

[14] Hejda, M., Pyšek, P., & Jarošík, V. (2009). Impact of invasive plants on the species richness, diversity and composition of invaded communities. Journal of ecology, 97(3), 393-403.

[15] Didham, R. K., Tylianakis, J. M., Hutchison, M. A., Ewers, R. M., & Gemmell, N. J. (2005). Are invasive species the drivers of ecological change ?. Trends in ecology & evolution, 20(9), 470-474.

[16] European Commission. (2022). Regulation (EU) 2022/1203 of the European Parliament and of the Council of 12 July 2022 amending Implementing Regulation (EU) 2016/1141 to update the list of invasive alien species of Union concern. C/2022/4773. http://data.europa.eu/eli/reg_impl/2022/1203/oj

[17] European Commission. (2014). Regulation (EU) 2014/1143 of the European Parliament and of the Council of 22 October 2014 on the prevention and management of the introduction and spread of invasive alien species. http://data.europa.eu/eli/reg/2014/1143/oj
[18] Specieinvasive. (2023). https://www.specieinvasive.it/
[19] Giordano, G. (1999). Tecnica delle costruzioni in legno. Hoepli Editore.
[20] Ramage, M. H., Burridge, H., Busse-Wicher, M., Fereday, G., Reynolds, T., Shah, D. U., Wu, G., Yu, L., Fleming, P., Densley-Tingley, D., Allwood, J., Dupree, P., Linden, P. F., & Scherman, O. (2017). The wood from the trees: The use of timber in construction. Renewable and Sustainable Energy Reviews, 68(October 2015), 333–359.
[21] Geus, A. R., Silva, S. F. D., Gontijo, A. B., Silva, F. O., Batista, M. A., & Souza, J. R. (2020). An analysis of timber sections and deep learning for wood species classification. Multimedia Tools and Applications, 79, 34513-34529.
[22] The sandalwood shop. (n.d.). Homepage. The sandalwood shop. https://www.thesandalwoodshop.com.au/
[23] Thybring, E. E., Fredriksson, M., Zelinka, S. L., & Glass, S. V. (2022). Water in Wood: A Review of Current Understanding and Knowledge Gaps. Forests, 13(12).
[24] Wiedenhoeft, A. and Eberhardt, T. (2021). Chapter 3: Structure and function of wood. In: Wood handbook wood as an engineering material. General Technical Report FPL-GTR-282. Madison, WI: U.S. Department of Agriculture, Forest Service, Forest Products Laboratory. 20 pp.
[25] Hoffmeyer, P., Engelund, E. T., & Thygesen, L. G. (2011). Equilibrium moisture content (EMC) in Norway spruce during the first and second desorptions. Holzforschung, 65, 875–882.
[26] Engelund, E. T., Thygesen, L. G., Svensson, S., & Hill, C. A. S. (2013). A critical discussion of the physics of wood-water interactions. Wood Science and Technology, 47(1), 141–161.
[27] Glass, S. V., & Zalinka, L. (2010). Moisture Relations and Physical Properties of Wood (Chapter 4). In Forest Products Laboratory, Wood Handbook – Wood as an engineering material. General Technical Report FPL–GTR–190. Department of Agriculture, Forest Service, Forest Products Laboratory, Madison, WI: U.S.A.
[28] Brunauer, S., Emmet, P. H., & Teller, E. (1938). Adsorption of gases in multimolecular layers. Am Chem Soc, 35(2), 30–39.
[29] Dent, R. W. (1977). Multilayer theory for gas sorption—1. Sorption of a single gas. Text Res J, 47(3), 145–152.
[30] Hailwood, A. J., & Horrobin, S. (1946). Absorption of water by polymers—analysis in terms of a simple model. Trans Faraday Soc, 42B, 84–102.
[31] Simpson, W. T. (1973). Predicting equilibrium moisture content of wood by mathematical models. Wood Fiber Sci, 5(1), 41–49.
[32] Thybring, E. E., Boardman, C. R., Zelinka, S. L., & Glass, S. V. (2021). Common sorption isotherm models are not physically valid for water in wood. Colloids and Surfaces A: Physicochemical and Engineering Aspects, 627(July), 127214.
[33] Zelinka, S. L., Glass, S. V., & Thybring, E. E. (2018). Myth versus reality: Do parabolic sorption isotherm models reflect actual wood–water thermodynamics? Wood Science and Technology, 52(6), 1701–1706.
[34] Hamdaoui, M. A., Benzaama, M. H., El Mendili, Y., & Chateigner, D. (2021). A review on physical and data-driven modeling of buildings hygrothermal behavior: Models, approaches and simulation tools. Energy and Buildings, 251, 111343.

[35] Piazza, M., Modena, R., & Tomasi, R. (2005). Strutture in legno. Materiale, calcolo e progetto secondo le nuove normative europee. Hoepli Editore.
[36] Hankinson, R. L. (1921). Investigation of crushing strength of spruce at varying angles of grain. U.S. Air Service, Inform. Cir.3 no. 259.
[37] Forestrypedia. (n.d.). Timber defects. Forestrypedia. https://forestrypedia.com/wood-defects/#google_vignette
[38] Haque, N. (2010). Delamination in timber induced by drying. In Delamination in Wood, Wood Products and Wood-Based Composites (pp. 197-212). Dordrecht: Springer Netherlands.
[39] Bodig, J. and Jayne, B. A. (1982) Mechanics of wood and wood composites.
[40] Buchanan, A., Deam, B., Fragiacomo, M., Pampanin, S., & Palermo, A. (2008). Multi-storey prestressed timber buildings in New Zealand. Structural Engineering International, 18(2), 166-173
[41] Calderoni, C., De Matteis, G., Giubileo, C., & Mazzolani, F. M. (2006). Flexural and shear behaviour of ancient wooden beams: Experimental and theoretical evaluation. Engineering Structures, 28(5), 729–744.
[42] McLain, T. E., DeBonis, A. L., Green, D. W., Wilson, F. J., & Link, C. L. (1984). The influence of moisture content on the flexural properties of Southern pine dimension lumber. United States Department of Agriculture, Forest Service, Forest Products Laboratory, Res Pep FPL-447.
[43] Aplin, E. N., Green, D. W., Evans, J. W., & Barrett, J. D. (1986). The influence of moisture content on the flexural properties of Douglas fir dimension lumber. United States Department of Agriculture, Forest Service, Forest Products Laboratory, Res Pep FPL-475.
[44] Ido, H., Nagao, H., Kato, H., & Miura, S. (2013). Strength properties and effect of moisture content on the bending and compressive strength parallel to the grain of sugi (Cryptomeria japonica) round timber. J Wood Sci, 59(1), 67–72.
[45] Kretschmann D.E. (2010). Mechanical properties of wood. Wood handbook: wood as an engineering material (Centennial ed.), U.S. Dept. of Agriculture, Forest Service, Forest Products Laboratory, Madison, WI, USA, p. 5-46.
[46] Green, D. W., & Evans, J. W. (2001). Evolution of standardized procedures for adjusting lumber properties for change in moisture content (Gen Tech Rep FPL-GRT-127). United States Department of Agriculture, Forest Service, Forest Products Laboratory.
[47] Barrett, J. D., & Lau, W. (1991). Bending strength adjustment for moisture content for structural lumber. Wood Sci Technol, 25(6), 433–447.
[48] Zhou, H., Ren, H., Lv, J., Jiang, J., & Wang, X. (2010). Bending strength adjustment for moisture content for Chinese fir structural lumber. In Proceedings of the World Conference on Timber Engineering. June 20–24, Riva del Garda, Trento.
[49] UNI - Ente Italiano di Normazione. (2022). Legno strutturale - Determinazione dei valori caratteristici delle proprietà meccaniche e della massa volumica (UNI EN 384: 2022). UNI.
[50] Nocetti, M., Brunetti, M., & Bacher, M. (2015). Effect of moisture content on the flexural properties and dynamic modulus of elasticity of dimension chestnut timber. European Journal of Wood and Wood Products, 73, 51-60.
[51] Boyd, J. D. (1982). An anatomical explanation for visco-elastic and mechano-sorptive creep in wood, and effects of loading rate on strength. In New Perspectives in Wood Anatomy: Published on the occasion of the 50th Anniversary of the International Association of Wood Anatomists (pp. 171-222). Dordrecht: Springer Netherlands.

[52] Grossman, P. U. A. (1978). Mechano-sorptive behaviour. General constitutive relations of wood and wood-based materials, 313-325.
[53] Morlier, P. (1994). Creep in Timber Structures. E&FN SPON
[54] Gressel, P. (1984). Kriechverhalten von holz und holzwerkstoffen. bauen mit holz, 4(84), 216-223.
[55] Ranta-Maunus, A. (1993). Rheological behaviour of wood in directions perpendicular to the grain. Materials and Structures, 26(6), 362–369.
[56] Cai, Z., Fridley, K. J., Hunt, M. O., & Rosowsky, D. V. (2002). Creep and creep-recovery models for wood under high stress levels. Wood and Fiber Science, 34(3), 425–433.
[57] Schniewind, A. P., & Barrett, J. D. (1972). Wood as a linear orthotropic viscoelastic material. Wood Science and Technology, 6(1), 43–57.
[58] Zheng, X., Li, Z., He, M., & Lam, F. (2021). Experimental investigation on the rheological behavior of timber in longitudinal and transverse compression. Construction and Building Materials, 304(June), 124633.
[59] Navi, P., & Stanzl-Tschegg, S. (2009). Micromechanics of creep and relaxation of wood. A review. COST Action E35 2004-2008: Wood machining - Micromechanics and fracture. Holzforschung, 63(2), 186–195. https://doi.org/10.1515/HF.2009.013
[60] Salmén, L. (1982) Temperature and water induced softening behaviour of wood fibre-based materials. PhD thesis, Royal Ins. Technology, Stockholm, Sweden.
[61] Huet, C. (1992). Minimum theorems for viscoelasticity. European journal of mechanics. A. Solids, 11(5), 653-684.
[62] Navi, P., Pittet, V., Plummer, C.J.G. (2002) Transient moisture effects on wood creep. Wood Sci. Technol. 36:447–462.
[63] Hoffmeyer, P., & Davidson, R. W. (1989). Mechano-sorptive creep mechanism of wood in compression and bending. Wood Science and Technology, 23(3), 215-227.
[64] Hunt, D., Gril, J. (1996) Evidence of a physical ageing phenomenon in wood. J. Mater. Sci. Lett. 15:80–82.
[65] Wanninger, F., Frangi, A., Fragiacomo, M. (2015). Long-term behavior of posttensioned timber connections. Journal of Structural Engineering, 141(6), 04014155.
[66] Toratti, T. (1992). Creep of timber beams in a variable environment. PhD Thesis, University of Technology, Helsinki.
[67] Davies, M., & Fragiacomo, M. (2011). Long-term behavior of prestressed LVL members. I: Experimental tests. Journal of Structural Engineering, 137(12), 1553-1561.
[68] Bengtsson, R., Afshar, R., & Gamstedt, E. K. (2022). An applicable orthotropic creep model for wood materials and composites. Wood Science and Technology, 56(6), 1585–1604. https://doi.org/10.1007/s00226-022-01421-x
[69] Granello, G., & Palermo, & A. (2019). Creep in timber: research overview and comparison between code provisions. New Zealand Timber Design Journal, 27(1), 6–22.
[70] UNI - Ente Italiano di Normazione. (2014). Eurocodice 5 - Progettazione delle strutture di legno - Parte 1-1: Regole generali - Regole comuni e regole per gli edifici (UNI EN 1995-1-1:2014). UNI.
[71] NTC18 (2018). Decreto Ministeriale del 17/1/2018 Aggiornamento delle "norme 36 tecniche per le costruzioni," G.U. n. 42 del 20/2/2018,.
[72] NZS - New Zeland Standard. (1993). Timber Structures Standard (NZS 3603: 1993). NZS.
[73] AS - Australian Standards. (2010). Timber structures, Part 1: Design methods (AS 1720.1-2010). AS.

[74] Pournou, A. (2020). Biodeterioration of wooden cultural heritage. In Organisms and Decay Mechanisms in Aquatic and Terrestrial Ecosystems. Springer International Publishing Cham, Switzerland.
[75] Marais, B. N., Brischke, C., & Militz, H. (2022). Wood durability in terrestrial and aquatic environments–A review of biotic and abiotic influence factors. Wood Material Science & Engineering, 17(2), 82-105.
[76] UNI - Ente Italiano di Normazione. (2016). Durabilità del legno e dei prodotti a base di legno - Prove e classificazione della durabilità agli agenti biologici del legno e dei materiali a base di legno (UNI EN 350: 2016). UNI.
[77] Hillis, W.E. (2012). Heartwood and Tree Exudates (Vol. 4). Springer Science & Business Media: Berlin/Heidelberg, Germany.
[78] Martín, J. A., & López, R. (2023). Biological Deterioration and Natural Durability of Wood in Europe. Forests, 14(2), 283.
[79] UNI - Ente Italiano di Normazione. (2013). Durabilità del legno e dei prodotti a base di legno - Classi di utilizzo: definizioni, applicazione al legno massiccio e prodotti a base di legno (UNI EN 335: 2013). UNI.
[80] Kahl, T., Arnstadt, T., Baber, K., Bässler, C., Bauhus, J., Borken, W., Buscot, F., Floren, A., Heibl, C., Hessenmöller, D., & others. (2017). Wood Decay Rates of 13 Temperate Tree Species in Relation to Wood Properties, Enzyme Activities and Organismic Diversities. Forest Ecology and Management, 391, 86–95.
[81] Bravery, A. F., Berry, R. W., Carey, J. K., & Cooper, D. E. (1987). Recognising wood rot and insect damage in buildings (Vol. 3). Watford: Building Research Establishment.
[82] Verbist, M., Nunes, L., Jones, D., & Branco, J. M. (2019). Service life design of timber structures. In Long-term performance and durability of masonry structures (pp. 311-336). Woodhead Publishing.
[83] Arango, R. A., & Young, D. K. (2012). Death-watch and Spider Beetles of Wisconsin, Coleoptera: Ptinidae (Vol. 209). United States Department of Agriculture, Forest Service, Forest Products Laboratory.
[84] Eaton, R. A., & Hale, M. D. (1993). Wood: Decay, pests and protection. Chapman and Hall.
[85] Unger, A., Schniewind, A., & Unger, W. (2001). Conservation of wood artifacts: A handbook. Berlin: Springer.
[86] Zabel, R. A., & Morrell, J. J. (2012). Wood microbiology: decay and its prevention. Academic press.
[87] "Lewis, V. R., & Seybold S. J. (2010). Wood-boring beetles in homes – Integrated pest management in the home. Pest Notes, Publication 7418, Statewide Integrated Pest Management Program Agriculture and Natural Resources."
[88] Wang, X., & Allison, R. B. (2008). Decay detection in red oak trees using a combination of visual inspection, acoustic testing, and resistance microdrilling. Arboriculture and Urban Forestry, 34(1), 1.
[89] Slipinski, A., & Escalona, H. (2013). Australian longhorn beetles (Coleoptera: Cerambycidae): Vol. 1. Introduction and subfamily lamiinae. CSIRO.
[90] Yalçın, M., Doğan, H. H., & Akçay, Ç. (2019). Identification of wood-decay fungi and assessment of damage in log depots of Western Black Sea Region (Turkey). Forest pathology, 49(2), e12499.
[91] Reinprecht, L. (2016). Wood deterioration, protection, and maintenance. London: Wiley Blackwell.

[92] Becker, G. (1976) Concerning termites and wood. Unasylva, the FAO Journal of Forestry and Forest Industries - No. 111 - Termites, 28(I), 2–11.
[93] Abe, T., Bignell, D.E. Termites: Evolution, Sociality, Symbioses, Ecology; Higashi, M., Ed.; Springer: Dordrecht, The Netherlands, 2000; ISBN 978-90-481-5476-0.
[94] Steward, R.C. (1982). Comparison of the Behavioural and Physiological Responses to Humidity of Five Species of Dry-Wood Termites, Cryptotermes Species. Physiological Entomology, 7, 71–82.
[95] Bobadilla, I.; Martínez, R.D.; Martínez-Ramírez, M.; Arriaga, F. Identification of Cryptotermes brevis (Walker, 1853) and Kalotermes flavicollis (Fabricius, 1793) Termite Species by Detritus Analysis. Forests 2020, 11, 408.
[96] Schmidt, O. (2006). Physiology. In Wood and Tree Fungi (pp. 53–85). Springer: Berlin/Heidelberg, Germany.
[97] Leonowicz, A., Matuszewska, A., Luterek, J., Ziegenhagen, D., Wojta´s-Wasilewska, M., Cho, N.-S., Hofrichter, M., & Rogalski, J. (1999). Biodegradation of Lignin by White Rot Fungi. Fungal Genetics and Biology, 27, 175–185.
[98] Blanchette, R.A. (1991). Delignification by Wood-Decay Fungi. Annual Review of Phytopathology, 29, 381–403.
[99] "Eriksson K.-E. L., Blanchette, R. A., & Ander, P. (1990). Microbial and enzymatic degradation of wood and wood components. Berlin: Springer, 407 pp."
[100] Arantes, V., Jellison, J., & Goodell, B. (2012). Peculiarities of Brown-Rot Fungi and Biochemical Fenton Reaction with Regard to Their Potential as a Model for Bioprocessing Biomass. Applied Microbiology and Biotechnology, 94, 323–338.
[101] Schwarze, F. W., Engels, J., & Mattheck, C. (2004). Fungal strategies of wood decay in trees (1st ed., 2nd printing). Berlin: Springer.
[102] "Blanchette, R. A., Nilsson, T., Daniel, G., & Abad, A. R. (1990). Biological degradation of wood.Biological degradation of wood, in archaeological wood properties, chemistry, and preservation, (Eds R. M. Rowell and R. J. Barbour). Advances in Chemistry, 225, 141–174."
[103] Nelson, B.C., Goñi, M.A., Hedges, J.I., & Blanchette, R.A. (1995). Soft-Rot Fungal Degradation of Lignin in 2700 Year Old Archaeological Woods. Holzforschung, 49, 1–10.
[104] "Gao, J.; Kim, J.S.; Terziev, N.; Cuccui, I.; Daniel, G. Effect of Thermal Modification on the Durability and Decay Patterns of Hardwoods and Softwoods Exposed to Soft Rot Fungi. Int. Biodeterior. Biodegrad. 2018, 127, 35–45"
[105] Goodell, B., Zhu, Y., Kim, S., Kafle, K., Eastwood, D., Daniel, G., Jellison, J., Yoshida, M., Groom, L., Pingali, S.V., & others. (2017). Modification of the Nanostructure of Lignocellulose Cell Walls via a Non-Enzymatic Lignocellulose Deconstruction System in Brown Rot Wood-Decay Fungi. Biotechnology for Biofuels, 10, 179.
[106] Savory, J. G. (1954). Breakdown of timber by Ascomycetes and fungi Imperfecti. Annals of Applied Biology, 41(2), 336–347
[107] Zink, P., & Fengel, D. (1989). Studies on the Colouring Matter of Blue-Stain Fungi Part 2. Electron Microscopic Observations of the Hyphae Walls. Holzforschung, 43, 371–374.
[108] Rea, W.J., Didriksen, N., Simon, T.R., Pan, Y., Fenyves, E.J., & Griffiths, B. (2003). Effects of Toxic Exposure to Molds and Mycotoxins in Building-Related Illnesses. Archives of Environmental Health: An International Journal, 58, 399–405.
[109] Rayner, A.D., & Boddy, L. (1988). Fungal Decomposition of Wood: Its Biology and Ecology. John Wiley & Sons, Ltd.: Chichester, UK.

[110] Singh, M. K., Mahapatra, S., & Atreya, S. K. (2009). Bioclimatism and vernacular architecture of north-east India. Building and Environment, 44(5), 878–888.
[111] "Cragg, S. M., Pitman, A. J. and Henderson, S. M. (1999) Developments in the understanding of the biology of marine wood boring crustaceans and in methods of controlling them. International Biodeterioration and Biodegradation, 43, 197–205."
[112] Appelqvist, C., Havenhand, J. N., & Toth, G. B. (2015). Distribution and abundance of teredinid recruits along the Swedish coast: Are shipworms invading the Baltic Sea? Journal of the Marine Biological Association of the United Kingdom, 95(4), 783–790.
[113] Treu, A., Zimmer, K., Brischke, C., Larnøy, E., Gobakken, L. R., Aloui, F., Cragg, S. M., Flæte, P.-O., Humar, M., Westin, M., Borges, L. and Williams, J. (2019) Durability and protection of timber structures in marine environments in Europe: A review. Bioresources, 14(4), 10161–10184.
[114] "Björdal, C. G. and Nilsson, T. (2008) Reburial of shipwrecks in marine sediments: a long-term study on wood degradation. Journal of Archaeological Science, 35(4), 862–872."
[115] Papp, G., Preklet, E., Košıková, B., Barta, E., Tolvaj, L., Bohus, J., ... & Berkesi, O. (2004). Effect of UV laser radiation with different wavelengths on the spectrum of lignin extracted from hard wood materials. Journal of Photochemistry and Photobiology A: Chemistry, 163(1-2), 187-192.
[116] White, R.H., & Dietenberger, M.A. (2010). Fire safety of wood construction. In Wood Handbook: Wood as an Engineering Material (Centennial ed.), U.S. Dept. of Agriculture, Forest Service, Forest Products Laboratory, Madison, WI, USA, pp. 18-46.
[117] Bartlett, A.I., Hadden, R.M., & Bisby, L.A. (2019). A Review of Factors Affecting the Burning Behaviour of Wood for Application to Tall Timber Construction. Fire Technology, 55(1), 1-49.
[118] Babrauskas, V. (2015). Charring rate of wood as a tool for fire investigations. Fire Safety Journal, 40(6), 528–554
[119] Friquin, K.L. (2011). Material properties and external factors influencing the charring rate of solid wood and glue - laminated. Fire and materials, 35(5) p. 303-327.
[120] Hopkin, D.J. (2011). The Fire Performance of Engineered Timber Products and Systems, PhD Thesis Loughborough University (in England).
[121] Dietsch, P., & Kreuzinger, H. (2011). Guideline on the assessment of timber structures: Summary. Engineering structures, 33(11), 2983-2986.
[122] Van Acker, J., Van den Bulcke, J., Forsthuber, B., & Grüll, G. (2023). Wood Preservation and Wood Finishing. In Springer Handbook of Wood Science and Technology (pp. 793-871). Cham: Springer International Publishing.
[123] Lebow, S. T. (2010). Wood preservation. In: Wood handbook: wood as an engineering material (Centennial ed.), U.S. Dept. of Agriculture, Forest Service, Forest Products Laboratory, Madison, WI, USA, p. 18-46.
[124] Tarmian, A., Zahedi Tajrishi, I., Oladi, R., & Efhamisisi, D. (2020). Treatability of wood for pressure treatment processes: a literature review. European Journal of Wood and Wood Products, 78, 635-660.
[125] Schultz, T.P., Nicholas, D.D., & Preston, A.F. (2007). A brief review of the past, present, and future of wood preservation. Pest Management Science, 63, 784–798.
[126] Regulation (EU) No 528/2012 of the European Parliament and of the Council. (2012). https://eur-lex.europa.eu/LexUriServ/LexUriServ.do?uri=OJ:L:2012:167:0001:0123:en:PDF

[127] Regulation (EU) No 305/2011 of the European Parliament and of the Council. (2011). https://eur-lex.europa.eu/legal-content/EN/TXT/?uri=celex%3A32011R0305
[128] European Chemical Agency. (n.d.). Substances of very high concern identification. ECHA. https://echa.europa.eu/substances-of-very-high-concern-identification
[129] Clausen, C. A. (2010). Biodeterioration of wood. Wood handbook: wood as an engineering material, 190, 14-1.
[130] Herych, V. (2013). Wooden Tserkvas of the Carpathian Region in the UNESCO World Heritage List. Common Problems and Local Solutions. Barometr Regionalny. Analizy i Prognozy, 11(4), 43–51.
[131] Hill, C.A.S. (2006). Wood Modification—Chemical, Thermal and Other Processes (Wiley Series in Renewable Resources). John Wiley & Sons: Chichester, UK.
[132] Spear, M. J., Curling, S. F., Dimitriou, A., & Ormondroyd, G. A. (2021). Review of functional treatments for modified wood. Coatings, 11(3), 327.
[133] Lee, S. H., Ashaari, Z., Lum, W. C., Halip, J. A., Ang, A. F., Tan, L. P.,.. & Tahir, P. M. (2018). Thermal treatment of wood using vegetable oils: A review. Construction and Building Materials, 181, 408-419.
[134] Boonstra, M. J., Van Acker, J., Tjeerdsma, B. F., & Kegel, E. V. (2007). Strength properties of thermally modified softwoods and its relation to polymeric structural wood constituents. Annals of forest science, 64(7), 679-690.
[135] Rowell, R. M. (2017). Physical and mechanical properties of chemically modified wood. In Chemical modification of lignocellulosic materials (pp. 295-310). Routledge.
[136] Rudofsky, B. (1964). Architecture Without Architects: A Short Introduction to Nonpedigreed Architecture. Doubleday: New York.
[137] Oliver, A. C. (1974) Timber for Marine and Freshwater Construction (High Wycombe, UK: Timber Research and Development Association).
[138] Kristjansdottir, S., Lazzeri, S., & Macchioni, N. (2001). An Icelandic medieval stave church made of drift timber: The implications of the wood identification. Journal of Cultural Heritage, 2(2), 97–107.
[139] Aune, P., Sack, R. L., & Selberg, A. (1983). The stave churches of Norway. Scientific American, 249(2), 96-105.
[140] Satoshi, Y. (2006). The Tradition of Wooden Architecture in Japan. Cultural Heritage Protection Cooperation Office. UNESCO Asia-Pacific Cultural Centre (ACCU).
[141] Young, D., & Young, M. (2019). The Art of Japanese Architecture: History/Culture/Design. Tuttle Publishing.
[142] Locher, M. (2012). Traditional Japanese architecture: an exploration of elements and forms. Tuttle Publishing.
[143] Puspita, A. A., Sachari, A., & Sriwarno, A. B. (2018). Knowledge from Javanese Cultural Heritage: How They Manage and Sustain Teak Wood. Cultura, 15(1), 23-48.
[144] Rukwaro, R. W., & Mukono, K. M. (2001). Architecture of societies in transition—the case of the Maasai of Kenya. Habitat International, 25(1), 81-98.
[145] Sacko, O. (2021). The involvement of local communities in the conservation process of earthen architecture in the Sahel-Sahara region – the case of Djenné, Mali. Built Heritage, 5(26).
[146] De Filippi, F. (2006, September). Traditional architecture in the Dakhleh Oasis, Egypt: space, form and building systems. In Proceedings of The 23rd Conference on Passive and Low Energy Architecture. Geneva: PLEA2006 (pp. 1-6).

[147] Dabaieh, M., Maguid, D., & El-Mahdy, D. (2021). Circularity in the New Gravity—Re-Thinking Vernacular Architecture and Circularity. Sustainability, 14(1), 328.
[148] Sprague, P. E. (1981). The origin of balloon framing. The Journal of the Society of Architectural Historians, 40(4), 311-319.
[149] Peterson, F. W. (2000). Anglo-American wooden frame farmhouses in the Midwest, 1830-1900: Origins of balloon frame construction. Perspectives in vernacular architecture, 8, 3-16.
[150] Wonders, W. C. (1979). Log dwellings in Canadian folk architecture. Annals of the Association of American Geographers, 69(2), 187-207.
[151] Bostenaru Dan, M. (2014). Timber frame historic structures and the local seismic culture—an argumentation. Earthquake hazard impact and urban planning, 213-230.
[152] Rieiser, L. (2010). Outside of the stave church of heddal. Wikipedia. https://en.wikipedia.org/wiki/File:Stavechurch-heddal.jpg
[153] Colorshadow. (n.d.). Traditional Russian wooden church of the Resurrection from village of Patakino. Adobe Stock.https://stock.adobe.com/ch_it/images/traditional-russian-wooden-church-of-the-resurrection-from-village-of-patakino-the-monument-of-russian-wooden-architecture-of-the-late-xviii-century-domestic-geese-suzdal-russia/1890768294
[154] SeanPavone. (n.d.). Outside of Santuario di nachi taisha a nachi wakayama. Freepik.https://commons.wikimedia.org/wiki/File:Stavechurch-heddal.jpg
[155] Yosemite. (n.d.). World Heritage site Historic Villages of Shirakawa-go and Gokayama. Wikipedia. https://commons.wikimedia.org/wiki/File:Shirakawago_Japanese_Old_Village_001.jpg
[156] Swapnil. (18/01/2011). Typical Mizo House. India mike.https://www.indiamike.com/india-images/pictures/typical-mizo-house
[157] Waltyao. (2011). Traditional Maasai house. Flickr. https://www.flickr.com/photos/waltyao/5347542894
[158] Stellacci, S., Ruggieri, N., & Rato, V. (2016). Gaiola vs. Borbone system: A comparison between 18th century anti-seismic case studies. International Journal of architectural heritage, 10(6), 817-828.
[159] Ruggieri, N. (2016). Reliability of timber framed constructions in seismic prone areas in the practice codes issued from 18th to 19th Century. In Historical Earthquake-Resistant Timber Framing in the Mediterranean Area: HEaRT 2015 (pp. 229-240). Springer International Publishing.
[160] Vasconcelos, G., Poletti, E., Salavessa, E., Jesus, A. M., Lourenço, P. B., & Pilaon, P. (2013). In-plane shear behaviour of traditional timber walls. Engineering Structures, 56, 1028-1048.
[161] Parisse, F., Poletti, E., Dutu, A., & Rodrigues, H. (2021). Numerical modeling of the seismic performance of Romanian timber-framed masonry walls. Engineering Structures, 239, 112272.
[162] Taguelmoust. (18/12/2006). Mosquée Djingareyber de Tombouctou - Le minaret.https://commons.wikimedia.org/wiki/File:Mosqueetombou_01.JPGhttps://www.flickr.com/photos/waltyao/5347542894
[163] Stouhi, D. (2021). Wood-Framed Construction in American Architecture. Archdaily. https://www.archdaily.com/960940/the-us-pavilion-at-the-2021-venice-biennale-curated-by-paul-andersen-and-paul-preissner-explores-wood-framed-construction-in-american-architecture

[164] Kaiser, B. (n.d.). Hause. Bruno Kaiser. https://www.bruno-kaiser.de/sanierung/sanierung-schwarzwaldhof-in-holzbauweise-2/

[165] Elena. (2018). La GAIOLA POMBALINA e la CASA BARACCATA, due sistemi costruttivi antisismici del '700. Il Capochiave. https://ilcapochiave.it/2018/04/27/la-gaiola-pombalina-e-la-casa-baraccata-due-sistemi-costruttivi-antisismici-del-700/

[166] D'Ambra, C., Prota, A., Di Ludovico, M., & Manfredi, G. (2017). Rapporto fotografico relativo ai danni subiti da alcuni edifici a seguito dell'evento sismico del 21 Agosto 2017 presso isola d'Ischia-M= 4.0.

[167] UNESCO - Institute for Statistics. (2009). UNESCO Framework for Cultural Statistics. https://uis.unesco.org/en/glossary-term/cultural-heritage

[168] Cruz, H., Yeomans, D., Tsakanika, E., Macchioni, N., Jorissen, A., Touza, M., ... & Lourenço, P. B. (2015). Guidelines for on-site assessment of historic timber structures. International Journal of Architectural Heritage, 9(3), 277-289.

[169] ICOMOS International Wood Committee. (2017). Principles for the conservation of wooden built heritage. Delhi, India.

[170] Macchioni, N., & Mannucci, M. (2018). The assessment of Italian trusses: survey methodology and typical pathologies. International Journal of Architectural Heritage, 12(4), 533–544.

[171] Bertolini Cestari, C., & Marzi, T. (2018). Conservation of historic timber roof structures of Italian architectural heritage: diagnosis, assessment, and intervention. International Journal of Architectural Heritage, 12(4), 632–665. https://doi.org/10.1080/15583058.2018.1442523

[172] Parisi, M. A., & Piazza, M. (2007). Restoration and strengthening of timber structures: Principles, criteria, and examples. Practice periodical on structural design and construction, 12(4), 177-185.

[173] Faggiano, B., Marzo, A., Grippa, M. R., Iovane, G., Mazzolani, F. M., & Calicchio, D. (2018). The inventory of structural typologies of timber floor slabs and roofs in the monumental built heritage: the case of the Royal Palace of Naples. International Journal of Architectural Heritage, 12(4), 683-709.

[174] Koenig, G. K., Furiozzi, B., & Brunetti, F. (1995). Tecnologia delle costruzioni 2. Le Monnier, Firenze.

[175] Branco, J. M., Cruz, P. J., Piazza, M., & Varum, H. (2008). Field tests of a timber queen-post truss and numerical analysis.

[176] Branco, J. M., Piazza, M., & Cruz, P. J. (2010). Structural analysis of two King-post timber trusses: Non-destructive evaluation and load-carrying tests. Construction and Building Materials, 24(3), 371-383.

[177] Branco, J. M., Sousa, H. S., & Tsakanika, E. (2017). Non-destructive assessment, full-scale load-carrying tests and local interventions on two historic timber collar roof trusses. Engineering Structures, 140, 209-224.

[178] Kunecký, J., Hasníková, H., Kloiber, M., Milch, J., Sebera, V., & Tippner, J. (2018). Structural assessment of a lapped scarf joint applied to historical timber constructions in central Europe. International Journal of Architectural Heritage, 12(4), 666-682.

[179] Bláha, J., Kloiber, M., & Serafini, A. (2018). A comparison of two distinct roof timber frame systems implemented in the past in house no. 414/I in Prague. International Journal of Architectural Heritage, 12(4), 749-759.

[180] Marranzini, D., Iovane, G., Vitiello, V., Castelluccio, R., & Faggiano, B. (2022). Post-fire Assessment of Heritage Timber Structures. In INTERNATIONAL SYMPOSIUM: New Metropolitan Perspectives (pp. 2597-2606). Cham: Springer International Publishing.

[181] Verre, S., Cauteruccio, G. F., Fortunato, G., Zappani, A. A., Ombres, L., Brunetti, M., ... & Faggiano, B. (2023). Assessment of mechanical properties for ancient timber through visual and ND methods. In Life-Cycle of Structures and Infrastructure Systems (pp. 3920-3926). CRC Press.

[182] Holzer, S. M. (2008). Structural iron elements in German timber roofs (1600-1800). Construction History, 23, 33-57.

[183] Branco, J. M., & Descamps, T. (2015). Analysis and strengthening of carpentry joints. Construction and Building Materials, 97, 34–47. https://doi.org/10.1016/j.conbuildmat.2015.05.089

[184] Branco, J.M., Verbist, M., Tsakanika, E. (2021). Reinforcement of Traditional Carpentry Joints. In: Branco, J., Dietsch, P., Tannert, T. (eds) Reinforcement of Timber Elements in Existing Structures. RILEM State-of-the-Art Reports, vol 33. Springer, Cham. https://doi.org/10.1007/978-3-030-67794-7_12

[185] Branco, J. M., Verbist, M. P., & Descamps, T. (2018). Design of three typologies of step joints–Review of European standardized approaches. Design of Connections in Timber Structures, 297.

[186] Faggiano, B., Sandoli, A., Iovane, G., Fragiacomo, M., Bedon, C., Gubana, A., Ceraldi, C., Follesa, M., Gattesco, N., Giubileo, C., Pio Lauriola, M., Podestà, S., & Calderoni, B. (2022). The Italian instructions for the design, execution and control of timber constructions (CNR-DT 206 R1/2018). Engineering Structures, 253(December 2021).

[187] Premrov, M., & Žegarac Leskovar, V. (2023). Innovative Structural Systems for Timber Buildings: A Comprehensive Review of Contemporary Solutions. Buildings, 13(7), 1820.

[188] Tlustochowicz, G., Serrano, E., & Steiger, R. (2011). State-of-the-art review on timber connections with glued-in steel rods. Materials and structures, 44, 997-1020.

[189] Gohlich, R., Erochko, J., & Woods, J. E. (2018). Experimental testing and numerical modelling of a heavy timber moment-resisting frame with ductile steel links. Earthquake Engineering & Structural Dynamics, 47(6), 1460-1477.

[190] Iovane, G., Oliva, V., & Faggiano, B. (2023). Design and analysis of dissipative seismic resistant heavy timber frame structures equipped with steel links. Procedia Structural Integrity, 44, 1864-1869.

[191] Fletcher, J. (28/08/2018). (n.d.). Stuff.https://www.stuff.co.nz/business/106598828/canterbury-technology-behind-the-future-of-earthquakeresistant-construction

[192] Isaacs, N. (2013). " Balloon to Platform Framing": a change of the 1880s?. Architectural History Aotearoa, 10, 35-43.

[193] Ottavi, E. (13/10/2016). (n.d.). Albertani.https://www.albertani.com/wp-content/uploads/2016/10/5.800x430-800x430.jpg

[194] Crivellaro, P. (n.d.). Due telai leggeri in legno.https://caseprefabbricateinlegno.it/2014/07/due-telai-leggeri-in-legno.html#lightbox/0/

[195] Brandner, R., Flatscher, G., Ringhofer, A., Schickhofer, G., & Thiel, A. (2016). Cross laminated timber (CLT): overview and development. European Journal of Wood and Wood Products, 74, 331-351.

[196] Geminit. (n.d.). x-lam-05. My house legno.https://www.myhouselegno.it/author/geminit/page/3/
[197] Costantini. (n.d.). Attacchi-02. Costantini.https://www.costantinilegno.it/chi-siamo/tecnologie-costruttive-legno-x-lam/
[198] Svatoš-Ražnjević, H., Orozco, L., & Menges, A. (2022). Advanced timber construction industry: a review of 350 multi-storey timber projects from 2000–2021. Buildings, 12(4), 404.
[199] Council of tall building and Urban Habitat. (n.d.). The Mjøstårnet building. CTBUH. https://www.ctbuh.org/buildings-of-distinction/mjostarnet
[200] Puuinfo. (2020). Lighthouse Joensuu. Puuinfo. https://puuinfo.fi/arkkitehtuuri/block-of-flats/lighthouse-joensuu/?lang=en
[201] Surfaces Reporter. (18/03/2019). Norway constructs the worlds tallest all-timber building.https://surfacesreporter.com/articles/41099/subscribe
[202] Okler, N. (n.d.). Ascent. Council on Tall Buildings and Urban Habitat.https://www.skyscrapercenter.com/building/ascent/34292
[203] Soverelli. (n.d.). Housing complex with four towers and 124 apartments. Triple wood. https://www.triplewood.eu/projects/social-housing-via-cenni
[204] Panorama Giustinelli. (n.d.). Vista laterale.http://www.panoramagiustinelli.it/it/render
[205] Arketipo. (n.d.). 4 of 23. Arketipo magazine.https://www.arketipomagazine.it/marina-verde-wellness-resort-a-caorle-venezia-carlo-falconera-e-simone-micheli/
[206] Crocetti, R. (2016, March). Large-span timber structures. In Proceedings of the World Congress on Civil, Structural, and Environmental Engineering (pp. 1-23).
[207] Lan, T. T. (1999). Space frame structures. Structural engineering handbook, 13(4).
[208] Rubner. (n.d.). Centrale Enel di Brindisi "Federico II".https://www.rubner.com/it/riferimenti/costruzioni-legno/centrale-enel/
[209] TMP architecture. (n.d.). Superior Dome. TMP. https://www.tmp-architecture.com/project/superior-dome/
[210] Tecnowood. (23/03/2017). Strutture in legno lamellare, l'utilizzo è sempre maggiore.https://www.tecnowood.info/blog/strutture-tetti-legno-lamellare
[211] Grazla, S. (13/05/2015). Tsinghua University & Studio Link-Arc, Padiglione Cinese, Terra di speranza, cibo per la vita, Expo Milano 2015. Domusweb.https://www.domusweb.it/it/interviste/2015/05/13/link_arc_padiglione_cinese.html
[212] Fassoli, P. (2021). Miralles Tagliabue, EMBT, Stazione di Napoli, Centro Direzionale, in progress. Domusweb.https://www.domusweb.it/it/architettura/gallery/2021/05/03/work-in-progress-la-stazione-metropolitana-di-napoli.html
[213] Saiebologna. (n.d.). Strutture in legno lamellare: i pregi di un materiale da costruzione unico.https://www.saiebologna.it/it/trend/strutture-legno-lamellare-pregi-materiale-costruzione-unico/
[214] Subissati. (30/10/2013). Lamellar wood cover for the new swimming pool in Maiolati Spontini (AN).https://subissati.it/en/lamellar-wood-cover-for-the-new-swimming-pool-in-maiolati-spontini-an
[215] Legnofab. (n.d.). Copertura in legno edificio industriale a Pisa.https://www.legnofab.com/portfolio-category/tetti-in-legno/
[216] Olimpiacostruzioni. (n.d.). Coperture in legno lamellare. Olimpiacostruzioni. https://www.olimpiacostruzioni.it/coperture/legno-lamellare/

[217] Icurvi. (n.d.). Struttura in legno lamellare.https://www.icurvi.com/application-fields/laminated-wood-structures/
[218] Abita. (n.d.). Montaggio della copertura realizzata con travi lenticolari in legno lamellare.https://www.facebook.com/345003629004994/photos/montaggio-della-copertura-realizzata-con-travi-lenticolari-in-legno-lamellare/546217052216983/
[219] Cgedilservice. (n.d.). Cantine fattori bastia san Giovanni Ilarione, Verona. Cgedilservice.https://www.cgedilservice.it/realizzazioni-e-cantieri/cantine-fattori/
[220] Bossi, S. (27/04/2021). Palaluxottica vince il XVII Premio Architettura Oderzo. Archiportale.https://www.archiportale.com/news/2021/04/architettura/palaluxottica-vince-il-xvii-premio-architettura-oderzo_82340_3.html
[221] AB-Engineering. (n.d.). Bureau d'étude charpente bois.https://www.ab-engineering.fr/bureau-d-etude-charpente-bois.html/charpente-en-bois
[222] Studio Fornalè. (n.d.). Portfolio. Studio Fornalè. https://studiofornale.it/progetti/
[223] UNDRO: "Natural Disasters and Vulnerability Analysis": Report of Expert Group Meeting, 9–12 July 1979.
[224] Fell, R., Ho, K. K., Lacasse, S., & Leroi, E. (2005). A framework for landslide risk assessment and management. Landslide risk management, 3-25.
[225] Fell, R. (1994). Landslide risk assessment and acceptable risk. Canadian Geotechnical Journal, 31, 261-272.
[226] HazNet. (2023). Elements of disaster risk. HazNet. https://haznet.ca/wp-content/uploads/2023/04/Elements-of-disaster-risk.png
[227] Thywissen, K. (2006). Components of Risk: A Comparative Glossary. UNU-EHS: Bonn, Germany.
[228] Guillard-Gonçalves, C., & Zêzere, J. L. (2018). Combining social vulnerability and physical vulnerability to analyse landslide risk at the municipal scale. Geosciences, 8(8), 294.
[229] Amatruda G, Bonnard Ch, Castelli M, Forlati F, Giacomelli L, Morelli M, Paro L, Piana F, Pirulli M, Polino R, Prat P, Ramasco M, Scavia C, Bellardone G, Campus S, Durville J-L, Poisel R, Preh A, Roth W, Tentschert EH (2004) A key approach: the IMIRILAND project method. In: Bonnard, Ch, Forlati F, Scavia C (Eds.), Identification and mitigation of large landslide risks in Europe. Advances in risk assessment. A. A. Balkema Publishers, pp. 13–43
[230] CRED - Centre for Research on the Epidemiology of Disasters. (2022). 2021 Disasters in numbers. Emergency Events Database (EM-DAT). https://www.emdat.be/categories/adsr/
[231] Meletti, C., Patacca, E., & Scandone, P. (2000). Construction of a seismotectonic model: the case of Italy. Pure and applied Geophysics, 157, 11-35.
[232] Rovida A., Locati M., Camassi R., Lolli, B., Gasperini P., 2020. The Italian earthquake catalogue CPTI15. Bulletin of Earthquake Engineering 18, 2953-2984. https://doi.org/10.1007/s10518-020-00818-y
[233] Del Gaudio, C., Di Domenico, M., Ricci, P., & Verderame, G. M. (2018). Preliminary prediction of damage to residential buildings following the 21st August 2017 Ischia earthquake. Bulletin of Earthquake Engineering, 16, 4607-4637.
[234] Dolce, M., Prota, A., Borzi, B., da Porto, F., Lagomarsino, S., Magenes, G., ... & Zuccaro, G. (2021). Seismic risk assessment of residential buildings in Italy. Bulletin of Earthquake Engineering, 19, 2999-3032.
[235] Zuccaro G, Cacace F (2015) Seismic vulnerability assessment based on typological characteristics. The first level procedure "SAVE". Soil Dyn Earthq Eng 69:262–269

[236] Del Gaudio C, De Martino G, Di Ludovico M, Manfredi G, Prota A, Ricci P, Verderame GM (2019) Empirical fragility curves for masonry buildings after the 2009 L'Aquila, Italy, earthquake. Bull Earthq Eng 17(11):6301–6330

[237] Del Gaudio C, Di Ludovico M, Polese M, Manfredi G, Prota A, Ricci P, Verderame GM (2020) Seismic fragility for Italian RC buildings based on damage data of the last 50 years. Bull Earthq Eng 18(5):2023–2059

[238] D'Ayala D, Speranza E (2003) Definition of collapse mechanisms and seismic vulnerability of historic masonry buildings. Earthq Spectra 19(3):479–509

[239] Rota M, Penna A, Magenes G (2010) A methodology for deriving analytical fragility curves for masonry buildings based on stochastic nonlinear analyses. Eng Struct 32(5):1312–1323

[240] Polese M, Verderame GM, Mariniello C, Iervolino I, Manfredi G (2008) Vulnerability analysis for gravity load designed RC buildings in Naples-Italy. J Earthq Eng 12(S2):234–245

[241] Lagomarsino S, Giovinazzi S (2006) Macroseismic and mechanical models for the vulnerability and damage assessment of current buildings. Bull Earthq Eng 4:415–443

[242] Kappes, M. S., Papathoma-Koehle, M., & Keiler, M. (2012). Assessing physical vulnerability for multi-hazards using an indicator-based methodology. Applied Geography, 32(2), 577-590.

[243] Armaș, I. (2012). Multi-criteria vulnerability analysis to earthquake hazard of Bucharest, Romania. Natural hazards, 63, 1129-1156.

[244] Peng, Y. (2015). Regional earthquake vulnerability assessment using a combination of MCDM methods. Annals of Operations Research, 234, 95-110.

[245] Alizadeh, M., Hashim, M., Alizadeh, E., Shahabi, H., Karami, M. R., Beiranvand Pour, A., ... & Zabihi, H. (2018). Multi-criteria decision making (MCDM) model for seismic vulnerability assessment (SVA) of urban residential buildings. ISPRS International Journal of Geo-Information, 7(11), 444.

[246] Yepes-Estrada, C., Silva, V., Rossetto, T., D'Ayala, D., Ioannou, I., Meslem, A., & Crowley, H. (2016). The global earthquake model physical vulnerability database. Earthquake Spectra, 32(4), 2567-2585.

[247] Novelli, V. I., D'Ayala, D., Makhloufi, N., Benouar, D., & Zekagh, A. (2015). A procedure for the identification of the seismic vulnerability at territorial scale. Application to the Casbah of Algiers. Bulletin of Earthquake Engineering, 13, 177-202.

[248] Cocco, G., D'Aloisio, A., Spacone, E., & Brando, G. (2019). Seismic vulnerability of buildings in historic centers: From the "urban" to the "aggregate" scale. Frontiers in Built Environment, 5, 78.

[249] Martins, L., & Silva, V. (2021). Development of a fragility and vulnerability model for global seismic risk analyses. Bulletin of Earthquake Engineering, 19(15), 6719-6745.

[250] Matteis, G. D., Brando, G., Corlito, V., Criber, E., & Guadagnuolo, M. (2019). Seismic vulnerability assessment of churches at regional scale after the 2009 L'Aquila earthquake. International Journal of Masonry Research and Innovation, 4(1-2), 174-196.

[251] Brando, G., Cianchino, G., Rapone, D., Spacone, E., & Biondi, S. (2021). A CARTIS-based method for the rapid seismic vulnerability assessment of minor Italian historical centres. International Journal of Disaster Risk Reduction, 63, 102478.

[252] Aloisio, A., Alaggio, R., & Fragiacomo, M. (2021). Fragility functions and behavior factors estimation of multi-story cross-laminated timber structures characterized by an energy-dependent hysteretic model. Earthquake Spectra, 37(1), 134-159.

[253] Tesfamariam, S., Stiemer, S. F., Dickof, C., & Bezabeh, M. A. (2014). Seismic vulnerability assessment of hybrid steel-timber structure: Steel moment-resisting frames with CLT infill. Journal of Earthquake Engineering, 18(6), 929-944.

[254] Huan, J., Ma, D., & Wang, W. (2018). Vulnerability analysis of ancient timber architecture by considering the correlation of different failure modes. Mathematical Problems in Engineering, 2018, 1-10.

[255] Gaspari, A., Modena, R., Giongo, I., & Piazza, M. (2023). Vulnerability analysis on a dataset of long-span timber structures in Italy. Proceedings of the Institution of Civil Engineers-Structures and Buildings, 1-14.

[256] DPC - Dipartimento di Protezione Civile. (n.d.). Scheda AeDES. Protezione Civile. https://www.protezionecivile.gov.it/it/approfondimento/scheda-aedes/

[257] ISTAT - Istituto Nazionale di Statistica. (2023). https://www.istat.it/

[258] Ehrlich, D., Kemper, T., Blaes, X., & Soille, P. (2013). Extracting building stock information from optical satellite imagery for mapping earthquake exposure and its vulnerability. Natural Hazards, 68, 79-95.

[259] ReLUIS - Consorzio della Rete dei Laboratori Universitari di Ingegneria Sismica e Strutturale. (2023). https://www.reluis.it/it/

[260] Zuccaro, G., Dolce, M., De Gregorio, D., Speranza, E., & Moroni, C. (2015, November). The CARTIS form for the typological and structural characterization of urban areas composed by ordinary buildings. In Proceedings of the 34th National Conference GNGTS, Trieste, Italy (pp. 281-7).

[261] Zuccaro G, Dolce M, Perelli FL, De Gregorio D and Speranza E (2023), CARTIS: a method for the typologicalstructural characterization of Italian ordinary buildings in urban areas. Front. Built Environ. 9:1129176. doi: 10.3389/fbuil.2023.1129176

[262] Faggiano, B., Iovane, G., Gaspari, A., Fournely, E., Bouchair, A., Landolfo, R., & Piazza, M. (2021). The CARTIS form for the seismic vulnerability assessment of timber large-span structures. Buildings, 11(2), 45.

[263] Meglio, E., Formisano, A., & Landolfo, R. (2023, September). Seismic behaviour of steel industrial buildings built in the late 80's in the Campania region of Italy. In AIP Conference Proceedings (Vol. 2849, No. 1). AIP Publishing.

[264] Dolce, M., Speranza, E., Giordano, F., Borzi, B., Bocchi, F., Conte, C., ... & Pascale, V. (2019). Observed damage database of past Italian earthquakes: the Da. DO WebGIS. Bollettino di Geofisica Teorica ed Applicata, 60(2).

[265] Liguori, F. S., Madeo, A., & Formisano, A. (2023). Seismic vulnerability of industrial steel structures with masonry infills using a numerical approach. Bulletin of Earthquake Engineering, 1-27.

[266] Baggio, C., Bernardini, A., Colozza, R., Corazza, L., Della Bella, M., Di Pasquale, G., ... & Zuccaro, G. (2007). Field manual for post-earthquake damage and safety assessment and short term countermeasures (AeDES). European Commission—Joint Research Centre—Institute for the Protection and Security of the Citizen, EUR, 22868.

[267] DPC - Dipartimento di Protezione Civile. (2014, July 8). DPCM dell'8 luglio 2014. Protezione Civile. https://www.protezionecivile.gov.it/it/normativa/dpcm-dell8-luglio-2014-0/

[268] Sisti, R., Argiento, L. U., Ceroni, F., da Porto, F., Prota, A., & Casapulla, C. (2023, November). Empirical fragility curves for masonry churches and their macro-elements using a large database: Proposal of a new likelihood function. In Structures (Vol. 57, p. 105164). Elsevier.

[269] Rosti, A., Rota, M., & Penna, A. (2021). Empirical fragility curves for Italian URM buildings. Bulletin of Earthquake Engineering, 19, 3057-3076.
[270] Zucconi, M., & Sorrentino, L. (2022). Census-Based Typological Damage Fragility Curves and Seismic Risk Scenarios for Unreinforced Masonry Buildings. Geosciences, 12(1), 45.
[271] UNI - Ente Italiano di Normazione. (2006). Eurocodice - Criteri generali di progettazione strutturale (UNI EN 1990: 2006). UNI.
[272] EU: 1988. Council Directive of 21 December 1988 on the approximation of laws, regulations and administrative provisions of the Member States relating to construction products. Brussels: European Union.
[273] ISO - International Organization for Standardization (2011): ISO 15686-1:2011. Buildings and constructed assets - Service life 1 planning - Part 1: General principles and framework. Genève : International Organization for Standardization.
[274] Cascini, L. (2009). Atmospheric corrosion and durability design of metal structures. (PhD thesis). University of Naples Federico II. http://www.fedoa.unina.it/3058/
[275] Alexander, M., & Beushausen, H. (2019). Durability, service life prediction, and modelling for reinforced concrete structures–review and critique. Cement and Concrete Research, 122, 17-29.
[276] Sarja, A., & Vesikari, E. (1996). Rilem Report 14: durability design of concrete structures. E & FN Spon, London.
[277] Moser, K., & Edvardsen, C. (2002, March). Engineering design methods for service life prediction. In Proceedings of the 9th International Conference on the Durability of Building Materials and Components, Brisbane, Australia (pp. 17-20).
[278] SB-LRA (2007). Guideline for Load and Resistance Assessment of Existing European Railway Bridges Advices on the use of advanced methods. Deliverable D4.2 of the Research Project "Sustainable Bridges - Assessment for Future Traffic Demands and Longer Lives". 6th Framework Programme. Contract number TIP3-CT-2003-001653.
[279] ISO - International Organization for Standardization (2008). General principles on the design of structures for durability (ISO 13823: 2008). Genève : International Organization for Standardization.
[280] Trinius, W., & Sjöström, C. (2005). Service life planning and performance requirements. Building research & information, 33(2), 173-181.
[281] Brischke, C., & Thelandersson, S. (2014). Modelling the outdoor performance of wood products–A review on existing approaches. Construction and Building Materials, 66, 384-397.
[282] Scheffer, T. C. (1971). A climate index for estimating potential for decay in wood structures above ground. Forest Products Journal, 21, 25–31.
[283] Creemers, J., de Meijer, M., Zimmermann, T., & Sell, J. (2002). Influence of climatic factors on the weathering of coated wood. Holz als Roh- und Werkstoff, 60, 411–420.
[284] Morris, P. I., & Wang, J. (2011). Scheffer Index as the preferred method to define decay risk zones for above ground wood in building codes. International Wood Products Journal, 2, 67–70.
[285] Leicester, R. H., Wang, C. H., & Cookson, L. J. (2003). A risk model for termite attack in Australia.
[286] Leicester, R. H., Wang, C. H., & Cookson, L. J. (2008). A reliability model for assessing the risk of termite attack on housing in Australia. Reliability Engineering & System Safety, 93(3), 468-475.

[287] Leicester, R. H., Wang, C. H., Nguyen, M. N., & MacKenzie, C. E. (2009). Design of exposed timber structures. Australian Journal of Structural Engineering, 9(3), 217-224.

[288] Nguyen, M. N., Leicester, R. H., Wang, C. H., & Foliente, G. C. (2008). Timber Service Life Design Code.

[289] CSIRO - Commonwealth Scientific and Industrial Research Organization. (2023). Engineered performance of timber publications. CSIROpedia. https://csiropedia.csiro.au/engineered-performance-of-timber-publications/

[290] Wang, C. H., Leicester, R. H., & Nguyen, M. N. (2008). Decay above ground. Manual No. 4. CSIRO Sustainable Ecosystems, Urban Systems Program, Highett, Victoria.

[291] Freitas, R. R., Molina, J. C., & Júnior, C. C. (2010). Mathematical model for timber decay in contact with the ground adjusted for the state of São Paulo, Brazil. Materials Research, 13, 151–158.

[292] Lourenço, P. B., Sousa, H. S., Brites, R. D., et al. (2013). In situ measured cross section geometry of old timber structures and its influence on structural safety. Materials and Structures, 46, 1193–1208.

[293] Viitanen, H., Toratti, T., Makkonen, L., et al. (2010). Towards modelling of decay risk of wooden materials. European Journal of Wood and Wood Products, 68, 303–313.

[294] Toratti, T., Viitanen, H., Peuhkuri, R., Makkonen, L., Ojanen, T., & Jämsä, S. (2009). Modelling of durability of wooden structures. In 4th International Building Physics Conference, IBPC 2009 (pp. 127-134).

[295] Brischke, C., & Rapp, A. O. (2010). Service life prediction of wooden components-Part 1: Determination of dose-response functions for above ground decay. In 41st Annual Meeting of the International Research Group on Wood Protection, Biarritz, France, 9-13 May 2010. IRG Secretariat.

[296] European Committee for Standardization. (2014). EN 252. Field test method for determining the relative protective effectiveness of a wood preservative in ground contact. Brussels, Belgium: CEN.

[297] Nofal, M., & Kumaran, K. (2011). Biological damage function models for durability assessments of wood and wood-based products in building envelopes. European Journal of Wood and Wood Products, 69, 619–631.

[298] Saito, H., Fukuda, K., & Sawachi, T. (2012). Integration model of hygrothermal analysis with decay process for durability assessment of building envelopes. Building Simulation, 5, 315–324.

[299] Van de Kuilen, J. W. G. (2007). Service life modelling of timber structures. Materials and Structures, 40, 151–161.

[300] Montaruli, N. E., van de Kuilen, J. W. G., & Gard, W. F. (2007). Weight loss prediction in wood decay processes. In International conference" Biodeterioration of wood and wood products" BWWP 2007, Riga, Latvia (pp. 50-60). Latvian State Institute of Wood Chemistry.

[301] Van de Kuilen, J. W. G., & Gard, W. F. (2012). Residual service life estimation using damage accumulation models. In World conference on timber engineering WCTE, Auckland, New Zealand (pp. 109-116).

[302] Thelandersson, S., Isaksson, T., Frühwald Hansson, E., Toratti, T., Viitanen, H., Grüll, G., Jermer, J., & Suttie, E. (2011). Service Life of Wood in Outdoor above Ground Applications Engineering Design Guideline (p. 29). Lund University: Lund, Sweden.

[303] Meyer-Veltrup, L., Brischke, C., Niklewski, J., & Frühwald Hansson, E. (2018). Design and performance prediction of timber bridges based on a factorization approach. Wood material science & engineering, 13(3), 167-173.
[304] Isaksson, T., Thelandersson, S., Jermer, J., & Brischke, C. (2014). Beständighet för utomhusträ ovan mark. Guide för utformning och materialval (Rapport TVBK–3066).
[305] Gaspari, A., Gianordoli, S., Giongo, I., & Piazza, M. (2024). A decay prediction model to minimise the risk of failure in timber balconies. Engineering Failure Analysis, 155, 107719.
[306] Gupta, A. K. (2017). Response spectrum method in seismic analysis and design of structures. Routledge.
[307] Wilson, E. L., Yuan, M. W., & Dickens, J. M. (1982). Dynamic analysis by direct superposition of Ritz vectors. Earthquake Engineering & Structural Dynamics, 10(6), 813-821.
[308] Hasan, R., Xu, L., & Grierson, D. E. (2002). Push-over analysis for performance-based seismic design. Computers & structures, 80(31), 2483-2493.
[309] Wilson, E. L., Farhoomand, I., & Bathe, K. J. (1972). Nonlinear dynamic analysis of complex structures. Earthquake Engineering & Structural Dynamics, 1(3), 241-252.
[310] Riggio, M., D'ayala, D., Parisi, M. A., & Tardini, C. (2018). Assessment of heritage timber structures: Review of standards, guidelines and procedures. Journal of Cultural Heritage, 31, 220-235.
[311] ICOMOS. (n.d.). Home. International Council on Monuments and Sites. https://www.icomos.org/en
[312] ICOMOS, International Wood Committee. (1999). Principles for the Preservation of Historic Timber Buildings. https://www.icomos.org/images/DOCUMENTS/Charters/wood e.pdf
[313] ICOMOS, International Scientific Committee for the Analysis and Restoration of Structures of Architectural Heritage (ISCARSAH). (2003). Principles for the analysis, conservation, and structural restoration of architectural heritage. https://iscarsah.files.wordpress.com/2014/11/iscarsah-principles-english.pdf.
[314] Shabani, A., Kioumarsi, M., Plevris, V., & Stamatopoulos, H. (2020). Structural vulnerability assessment of heritage timber buildings: A methodological proposal. Forests, 11(8), 881.
[315] Parisi, M. A., Chesi, C., Tardini, C., & Vecchi, D. (2017). Seismic vulnerability of timber roof structures: an assessment procedure. In Proceedings of the 16th World Conference on Earthquake Engineering, Santiago, Chile (No. 4397).
[316] UNI - Ente Italiano di Normazione. (2005). Beni culturali - Manufatti lignei - Linee guida per la conservazione, il restauro e la manutenzione testing (UNI EN 11161: 2005). UNI.
[317] UNI - Ente Italiano di Normazione. (2004). Beni culturali - Manufatti lignei - Strutture portanti degli edifici - Criteri per la valutazione preventiva, la progettazione e l'esecuzione di interventi (UNI EN 11138: 2004). UNI.
[318] UNI - Ente Italiano di Normazione. (2004). Beni culturali - Manufatti lignei - Strutture portanti degli edifici - Ispezione in situ per la diagnosi degli elementi in opera (UNI EN 11119: 2004). UNI.
[319] UNI - Ente Italiano di Normazione. (2004). Beni culturali - Manufatti lignei - Criteri per l'identificazione delle specie legnose (UNI EN 11118: 2004). UNI.
[320] Riggio, M., Anthony, R. W., Augelli, F., Kasal, B., Lechner, T., Muller, W., & Tannert, T. (2014). In situ assessment of structural timber using non-destructive techniques. Materials and structures, 47, 749-766.

[321] Arias, P., Carlos Caamaño, J., Lorenzo, H., & Armesto, J. (2007). 3D modeling and section properties of ancient irregular timber structures by means of digital photogrammetry. Computer-Aided Civil and Infrastructure Engineering, 22(8), 597-611.

[322] Koehl, M., Viale, A., & Reeb, S. (2013). A historical timber frame model for diagnosis and documentation before building restoration. ISPRS Annals of the Photogrammetry, Remote Sensing and Spatial Information Sciences, 2, 201-212.

[323] Bertolini-Cestari, C., Chiabrando, F., Invernizzi, S., Marzi, T., & Spanò, A. (2013). Terrestrial laser scanning and settled techniques: A support to detect pathologies and safety conditions of timber structures. Advanced materials research, 778, 350-357.

[324] Riggio, M., Sandak, J., & Franke, S. (2015). Application of imaging techniques for detection of defects, damage and decay in timber structures on-site. Construction and Building Materials, 101, 1241-1252.

[325] Abraldes, P., Cabaleiro, M., Sousa, H. S., & Branco, J. M. (2022). Use of polar coordinates for improving the measurement of resistant cross-sections of existing timber elements combining laser scanner and drilling resistance tests. Measurement, 204, 112027.

[326] Cabaleiro, M., Suner, C., Sousa, H. S., & Branco, J. M. (2021). Combination of laser scanner and drilling resistance tests to measure geometry change for structural assessment of timber beams exposed to fire. Journal of Building Engineering, 40, 102365.

[327] Olsson, A., & Oscarsson, J. (2017). Strength grading on the basis of high resolution laser scanning and dynamic excitation: a full scale investigation of performance. European Journal of Wood and Wood Products, 75, 17-31.

[328] Wang, J., You, H., Qi, X., & Yang, N. (2022). BIM-based structural health monitoring and early warning for heritage timber structures. Automation in Construction, 144, 104618.

[329] Mol, A., Cabaleiro, M., Sousa, H. S., & Branco, J. M. (2020). HBIM for storing life-cycle data regarding decay and damage in existing timber structures. Automation in Construction, 117, 103262.

[330] Toratti, T. (2011). Proposal for a failure assessment template. Engineering Structures, 33, 2958–2961.

[331] Serafini, A., Riggio, M., González-Longo, C. (2017). A Database Model for theAnalysis and Assessment of Historic Timber Roof Structures. InternationalWood Products Journal. Assessment, Reinforcement and Monitoring of Tim-ber Structures: Research outputs from the COST ACTION FP1101. 8 (1): 3-8.

[332] Ridley-Ellis, D., Stapel, P., & Baño, V. (2016). Strength grading of sawn timber in Europe: an explanation for engineers and researchers. European journal of wood and wood products, 74, 291-306.

[333] UNI - Ente Italiano di Normazione. (2012). Strutture di legno - Legno strutturale e legno lamellare incollato - Determinazione di alcune proprietà fisiche e meccaniche (UNI EN 408: 2012). UNI.

[334] Kovryga, A., Stapel, P., & Van de Kuilen, J. W. G. (2017). Quality control for machine strength graded timber. European Journal of Wood and Wood Products, 75, 233-247.

[335] European Committee for Standardization. (2005). Timber structures—strength graded structural timber with rectangular cross section—part 1: general requirements (EN 14081-1: 2005). Brussels, Belgium: CEN.

[336] UNI - Ente Italiano di Normazione. (2022). Legno strutturale - Classificazione a vista dei legnami secondo la resistenza meccanica - Parte 2: Latifoglie e sezione rettangolare (UNI 11035-2: 2022). UNI.

[337] UNE - Asociación Española de Normalización. (2022). Clasificación visual de la madera aserrada para uso estructural. Madera de frondosas (UNE 56546: 2022). UNE.
[338] BS - British Standards. (2007). Visual strength grading of hardwood (BS 5756: 2007). BS
[339] UNI - Ente Italiano di Normazione. (2022). Legno strutturale - Classificazione a vista dei legnami secondo la resistenza meccanica - Parte 1: Conifere a sezione rettangolare (UNI 11035-1: 2022). UNI.
[340] UNE - Asociación Española de Normalización. (2011). Clasificación visual de la madera aserrada para uso estructural. Madera de Coníferas (UNE 56544: 2011). UNE.
[341] BS - British Standards. (2007). Visual strength grading of softwood (BS 4978: 2007). BS
[342] DIN - Deutsches Institut für Normung. (2021). Sortierung von Holz nach der Tragfähigkeit - Teil 2: Baurundholz (Nadelholz; DIN 4074-2: 2021). DIN.
[343] UNI - Ente Italiano di Normazione. (2012). Legno strutturale - Classi di resistenza - Assegnazione delle categorie visuali e delle specie (UNI 1912: 2012). UNI.
[344] UNI - Ente Italiano di Normazione. (2016). Legno strutturale - Classi di resistenza (UNI 338: 2016). UNI.
[345] NFB - Association Francaise de Normalisation. (2007). Règlesd'utilisationduboisdans les constructions—Classementvisuel pour l'emploi en structure pour les principales essences résineuses et feuillues (NFB 52 001: 2007). NFB.
[346] DIN - Deutsches Institut für Normung. (2012). Sortierung von Holz nach der Tragfähigkeit - Teil 1: Nadelschnittholz (DIN 4074-1: 2012). DIN.
[347] NP - Norma Portuguesa. (1995). Madeira serrada de pinheiro bravo para estruturas – Classificação visual (NP 4305:1995). NP.
[348] ASTM E1316 – 00. Standard Terminology for Nondestructive Examinations, ASTM International, 2000.
[349] Kasal, B., Lear, G., & Tannert, T. (2011). Stress waves. In Situ Assessment of Structural Timber: State of the Art Report of the RILEM Technical Committee 215-AST, 5-24.
[350] Tannert, T., Anthony, R. W., Kasal, B., Kloiber, M., Piazza, M., Riggio, M., ... & Yamaguchi, N. (2014). In situ assessment of structural timber using semi-destructive techniques. Materials and structures, 47, 767-785.
[351] Dackermann, U., Crews, K., Kasal, B., Li, J., Riggio, M., Rinn, F., & Tannert, T. (2014). In situ assessment of structural timber using stress-wave measurements. Materials and structures, 47, 787-803.
[352] Íñiguez-González, G., Arriaga, F., Esteban, M., & Llana, D. F. (2015). Reference conditions and modification factors for the standardization of nondestructive variables used in the evaluation of existing timber structures. Construction and Building Materials, 101, 1166-1171.
[353] Palma, P., & Steiger, R. (2020). Structural health monitoring of timber structures–Review of available methods and case studies. Construction and Building Materials, 248, 118528.
[354] Nowak, T. P., Jasieńko, J., & Hamrol-Bielecka, K. (2016). In situ assessment of structural timber using the resistance drilling method–Evaluation of usefulness. Construction and Building Materials, 102, 403-415.
[355] Kloiber, M., Tippner, J., & Hrivnák, J. (2014). Mechanical properties of wood examined by semi-destructive devices. Materials and Structures, 47, 199–212
[356] Llana, D. F., Íñiguez-González, G., Montón, J., & Arriaga, F. (2018). In-situ density estimation by four nondestructive techniques on Norway spruce from built-in wood structures. Holzforschung, 72(10), 871-879.

[357] Martínez, R. D., Balmori, J. A., F. Llana, D., & Bobadilla, I. (2020). Wood density determination by drilling chips extraction in ten softwood and hardwood species. Forests, 11(4), 383.

[358] Arriaga, F., Wang, X., Íñiguez-González, G., Llana, D. F., Esteban, M., & Niemz, P. (2023). Mechanical Properties of Wood: A Review. Forests, 14(6), 1202.

[359] IML Service. (n.d.). IML PowerDrill. IML Service. https://www.iml-service.com/wp-content/uploads/2013/08/iml-resi_pd300_5786.jpg

[360] Novatest. (n.d.). Woodtester. Novatest. https://www.novatest.it/civil-engineerings/woodtester/

[361] Arriaga, F., Osuna-Sequera, C., Bobadilla, I., & Esteban, M. (2022). Prediction of the mechanical properties of timber members in existing structures using the dynamic modulus of elasticity and visual grading parameters. Construction and Building Materials, 322, 126512.

[362] Llana, D. F., Íñiguez-González, G., Martínez, R. D., & Arriaga, F. (2018). Influence of timber moisture content on wave time-of-flight and longitudinal natural frequency in coniferous species for different instruments. Holzforschung, 72(5), 405-411.

[363] Llana, D. F., Íñiguez-González, G., Esteban, M., Hermoso, E., & Arriaga, F. (2020). Timber moisture content adjustment factors for nondestructive testing (NDT): Acoustic, vibration and probing techniques. Holzforschung, 74(9), 817-827.

[364] Wang X, Ross RJ, Mattson JA, Erickson JR, Forsman JW, Geske EA, Wehr MA (2001) Several nondestructive evaluation techniques for assessing stiffness and MOE of small-diameter logs. USDA forest service, FPL-RP-600

[365] Wang, S. Y., Chen, J. H., Tsai, M. J., Lin, C. J., & Yang, T. H. (2008). Grading of softwood lumber using non-destructive techniques. Journal of materials processing technology, 208(1-3), 149-158.

[366] Morales-Conde, M. J., & Machado, J. S. (2017). Evaluation of cross-sectional variation of timber bending modulus of elasticity by stress waves. Construction and Building Materials, 134, 617-625.

[367] França, T. S., França, F. F., Daniel Seale, R., Ross, R. J., & Shmulsky, R. (2022). Flexural Properties of Visually Graded Southern Pine 2x4 and 2x6 Structural Lumber. BioResources, 17(1).

[368] Martins, C., Monteiro, S., Knapic, S., & Dias, A. (2020). Assessment of bending properties of Sawn and Glulam blackwood in Portugal. Forests, 11(4), 418.

[369] Nocetti, M., Aminti, G., Wessels, C. B., & Brunetti, M. (2021). Applying Machine Strength Grading System to Round Timber Used in Hydraulic Engineering Works. Forests, 12(3), 281.

[370] Montero, M.J., de la Mata, J., Esteban, M., Hermoso, E. (2015) Influence of moisture content on the wave velocity to estimate the mechanical properties of large cross-section pieces for structural use of Scots pine from Spain. Maderas-Cienc. Tecnol. 17:407–420.

[371] Gonçalves, R., Mansini-Lorensani, R.G., Negreiros, T.O., Bertoldo, C. (2018) Moisture-related adjustment factor to obtain a reference ultrasonic velocity in structural lumber of plantation hardwood. Wood Mater. Sci. Eng. 13:254–261.

[372] Kovryga, A., Chuquin Gamarra, J. O., & van de Kuilen, J. W. G. (2020). Strength and stiffness predictions with focus on different acoustic measurement methods. European Journal of Wood and Wood Products, 78, 941–949

[373] Morales-Conde, M. J., Rodríguez-Liñán, C., & Rubio de Hita, P. (2013). Application of non-destructive techniques in the inspection of the wooden roof of historic buildings: A case study. Advanced Materials Research, 778, 233-242.

[374] Baar, J., Tippner, J., & Rademacher, P. (2015). Prediction of mechanical properties-modulus of rupture and modulus of elasticity-of five tropical species by nondestructive methods. Maderas. Ciencia y tecnología, 17(2), 239-252.

[375] Riveiro, B., González-Jorge, H., Varela, M., & Jáuregui, D. V. (2013). Validation of terrestrial laser scanning and photogrammetry techniques for the measurement of vertical underclearance and beam geometry in structural inspection of bridges. Measurement, 46(1), 784-794.

[376] Sobue, N. (1986). Measurement of Young's modulus by the transient longitudinal vibration of wooden beams using a fast Fourier transformation spectrum analyzer. Mokuzai Gakkaishi, 32, 744-747.

[377] Bacher, M. (2008, October). Comparison of different machine strength grading principles. In COST E53 Conference 29th–30th October, Delft, The Netherlands (pp. 183-193).

[378] Arriaga, F., Monton, J., Segues, E., & Íñiguez-Gonzalez, G. (2014). Determination of the mechanical properties of radiata pine timber by means of longitudinal and transverse vibration methods. Holzforschung, 68(3), 299-305.

[379] Bucur, V. (2017). The Acoustics of Wood (1995). CRC press.

[380] Nocetti, M., Bacher, M., Berti, S., Brunetti, M., & Burato, P. (2013). Machine grading of chestnut structural timber with wane. In Proceedings of the 4rd International Scientific Conference on Hardwood Processing (pp. 7-9).

[381] Nocetti, M., Brunetti, M., & Bacher, M. (2016). Efficiency of the machine grading of chestnut structural timber: prediction of strength classes by dry and wet measurements. Materials and Structures, 49, 4439-4450.

[382] Brunetti, M., Nocetti, M., Pizzo, B., et al. (2020). Structural products made of beech wood: quality assessment of the raw material. European Journal of Wood and Wood Products, 78, 961–970.

[383] Sciomenta, M., Spera, L., Peditto, A., Ciuffetelli, E., Savini, F., Bedon, C., ... & Fragiacomo, M. (2022). Mechanical characterization of homogeneous and hybrid beech-Corsican pine glue-laminated timber beams. Engineering Structures, 264, 114450.

[384] Nocetti, M., Bacher, M., Brunetti, M., Crivellaro, A., & Van De Kuilen, J. W. G. (2010, June). Machine grading of Italian structural timber: preliminary results on different wood species. In Proceedings of the World Conference on Timber Enginnering (WCTE).

[385] Brunetti, M., Aminti, G., Nocetti, M., & Russo, G. (2021). Validation of visual and machine strength grading for Italian beech with additional sampling. iForest-Biogeosciences and Forestry, 14(3), 260.

[386] Rais, A., Pretzsch, H., & van de Kuilen, J. W. G. (2020). European beech log and lumber grading in wet and dry conditions using longitudinal vibration. Holzforschung, 74(10), 939-947.

[387] Llana, D. F., Íñiguez-González, G., Díez, M. R., & Arriaga, F. (2020). Nondestructive testing used on timber in Spain: A literature review. Maderas. Ciencia y tecnología, 22(2), 133-156.

[388] Degl'Innocenti, M., Nocetti, M., Kovačević, V. C., Aminti, G., Betti, M., Lauriola, M. P., & Brunetti, M. (2022). Evaluation of the mechanical contribution of wood degraded by insects in old timber beams through analytical calculations and experimental tests. Construction and Building Materials, 339, 127653.

[389] Cabaleiro, M., Branco, J. M., Sousa, H. S., & Conde, B. (2018). First results on the combination of laser scanner and drilling resistance tests for the assessment of the geometrical condition of irregular cross-sections of timber beams. Materials and Structures, 51, 1-15.

[390] Santos, D., Cabaleiro, M., Sousa, H. S., & Branco, J. M. (2022). Apparent and resistant section parametric modelling of timber structures in HBIM. Journal of Building Engineering, 49, 103990.

[391] Cuartero, J., Cabaleiro, M., Sousa, H. S., & Branco, J. M. (2019). Tridimensional parametric model for prediction of structural safety of existing timber roofs using laser scanner and drilling resistance tests. Engineering Structures, 185, 58-67.

[392] Marranzini, D., Iovane, G., & Faggiano, B. (2021). Methodology for the 8 assessment of timber structures exposed to fire through NDT. In Applications of Structural Fire Engineering ASFE21 (pp. 9-11). Ljubljana, Slovenia.

[393] Cabaleiro, M., Suner, C., Sousa, H. S., & Branco, J. M. (2021). Combination of laser scanner and drilling resistance tests to measure geometry change for structural assessment of timber beams exposed to fire. Journal of Building Engineering, 40, 102365.

[394] Faggiano, B., Grippa, M. R., Marzo, A., & Mazzolani, F. M. (2011). Experimental study for non-destructive mechanical evaluation of ancient chestnut timber. Journal of Civil Structural Health Monitoring, 1, 103-112.

[395] Faggiano, B., Grippa, M. R., & Calderoni, B. (2013). Non-destructive tests and bending tests on chestnut structural timber. Advanced Materials Research, 778, 167-174.

[396] Faggiano, B., Marzo, A. (2015). A method for the determination of the timber density through the statistical assessment of ND transverse measurements aimed at in situ mechanical identification of existing timber structures. Constr. Build. Mater., 101, 1235–1240.

[397] Feio, A. O., Lourenço, P. B., Machado, J. S. (2005). Parallel to the grain behaviour and NDT correlations for chestnut wood (Castanea sativa Mill.). In: C. Modena, P.B. Lourenço, P. Roca (Eds.), Proceedings of the IVth Int. Seminar on Structural Analysis of Historical Constructions, Padova, Italy, 10-13 November, 2004, Taylor & Francis Group, London, 369-375.

[398] Feio, A. O., Lourenço, P. B., Machado, J. S. (2007). Non-Destructive evaluation of the mechanical behavior of chestnut wood in tension and compression parallel to grain. Int. J. Archit. Herit., 1, 272–292.

[399] Acuña, L., Basterra, L. A., Casado, M. M., López, G., Ramón-Cueto, G., Relea, E., ... González, A. (2011). Aplicación Del Resistógrafo a La Obtención De La Densidad Y La Diferenciación De Especies De Madera. Mater. Constr., 61, 451–464.

[400] Lourenço, P. B., Feio, A. O., Machado, J. S. (2007). Chestnut wood in compression perpendicular to the grain: Non-destructive correlations for test results in new and old wood. Constr. Build. Mater., 21, 1617–1627.

[401] Piazza, M., Riggio, M. (2008). Visual strength-grading and NDT of timber in traditional structures. J Build Apprais, 3, 267–296.

[402] Marranzini, D., Iovane, G., Cozzolino, F., Faggiano, B. (2022). In situ assessment of mechanical properties of timber using the drilling resistance method. In: 6th International Conference on Structural Health Assessment

[403] Caetano-Andrade, V. L., Schöngart, J., Ayala, W. E., Melinski, R. D., Silva, F., Dobrindt, R., & Roberts, P. (2021). Advances in increment coring system for large tropical trees with high wood densities. Dendrochronologia, 68, 125860.

[404] European Committee for Standardization. (2002). EN 13183-2:2002. Moisture content of a piece of sawn timber - Part 2: Estimation by electrical resistance method. Brussels, Belgium: CEN.

[405] Cavalli, A., Cibecchini, D., Togni, M., & Sousa, H. S. (2016). A review on the mechanical properties of aged wood and salvaged timber. Construction and Building Materials, 114, 681-687.

[406] Ceccotti, A., & Togni, M. (1996, August). NDT on ancient timber beams: Assessment of strength/stiffness properties combining visual and instrumental methods. In Proceedings of the 10th International Symposium on Nondestructive Testing of Wood, Lausanne, Switzerland (pp. 26-28).

[407] Branco, J., Cruz, P., & Dias, S. (2005). Old timber beams: diagnosis and reinforcement. In Conservation of historic wooden structures: proceedings of the international conference, Florence 22-27 February, 2005. Vol. 1 and 2 (pp. 417-422).

[408] Faggiano, B., Grippa, M. R., Marzo, A., & Mazzolani, M. F. (2010). Structural grading of old chestnut elements by bending and compression tests. In 11th World Conference on Timber Engineering 2010, WCTE 2010 (Vol. 2, No. ID 758, pp. 1505-1510).

[409] Branco, J. M., Peixoto, T. P., Lourenço, P. B., & Medeiros, P. (2011). Mechanical characterization of old chestnut beams. In Proceedings of the SHATIS'11 International Conference on Structural Health Assessment of Timber Structures, June 16–17, 2011, Lisbon, Portugal.

[410] Faggiano, B., & Grippa, M. R. (2012). Mechanical characterization of old chestnut clear wood by non-destructive and destructive tests. In Timber engineering challenges and solutions, part 2 (Vol. 5, pp. 359-364).

[411] Cavalli, A., & Togni, M. (2013). The influence of routed grooves on the bending behavior of old timber beams. Advanced Materials Research, 778, 393-401.

[412] Ruggieri, N. (2021). In Situ Observations on the Crack Morphology in the Ancient Timber Beams. Sustainability, 13(1), 439.

[413] Dubois, F., Dopeux, J., Pop, O., & Metrope, M. (2023). Long-term creep behavior of timber columns: Experimental and numerical protocols. Engineering Structures, 275, 115283.

[414] Jockwer, R., Grönquist, P., & Frangi, A. (2021). Long-term deformation behaviour of timber columns: Monitoring of a tall timber building in Switzerland. Engineering Structures, 234, 111855.

[415] Fragiacomo, M., & Lukaszewska, E. (2013). Time-dependent behaviour of timber–concrete composite floors with prefabricated concrete slabs. Engineering Structures, 52, 687-696.

[416] Wanninger, F., Frangi, A., & Fragiacomo, M. (2015). Long-term behavior of posttensioned timber connections. Journal of Structural Engineering, 141(6), 04014155.

[417] Grippa, M. R. (2009). Structural identification of ancient timber constructions by non-destructive techniques.. (PhD thesis). University of Naples Federico II. http://www.fedoa.unina.it/3877/

[418] Branco, J. M., Varum, H., & Matos, F. T. (2018). On-site full-scale tests of a timber queen-post truss. International Journal of Architectural Heritage, 12(4), 545-554.

[419] Arriaga, F., Osuna-Sequera, C., Esteban, M., Iniguez-Gonzalez, G., & Bobadilla, I. (2021). In situ assessment of the timber structure of an 18th century building in Madrid, Spain. Construction and Building Materials, 304, 124466.

[420] Parisi, M. A., & Piazza, M. (2002). Seismic behavior and retrofitting of joints in traditional timber roof structures. Soil Dynamics and Earthquake Engineering, 22(12), 1183–1191.

[421] Piazza, M., G. Brentari, and M. P. Riggio. 2004. Strengthening and control methods for old timber trusses: The queen-post truss of the Trento theatre. In SAHC 2004: Structural analysis of historical constructions, Dina D'Ayala, Enrico Fodde (eds). Vol. II, 957–65. Padova, IT

[422] Branco, J. M., Cruz, P. J. S., & Piazza, M. (2008). Diagnosis and analysis of two king-post trusses. In D'Ayala, D., & Fodde, E. (Eds.), SAHC 2008: Structural analysis of historical constructions. Proceedings of the 6th International Conference on Structural Analysis of Historical Constructions (pp. 2–4). Bath, UK: July 2–4.

[423] Barbari, M., A. Cavalli, L. Fiorineschi, M. Monti, and M. Togni. 2014. Innovative connection in wooden trusses. Construction and Building Materials 66:654–63.

[424] Branco, J. M., Varum, H., Ramisote, V., & Costa, A. (2016). Load-carrying capacity test of a long-span timber truss. Structures and Buildings, 169(5), 373–387.

[425] Marranzini, D. (2023). Vista da strada della scuola di Correggio. Google Maps. https://www.google.com/maps/@44.7769513,10.7799884,3a,75y,87.1h,90t/data=!3m7!1e1!3m5!1sHWI5ljdw057S75bR3zjWqg!2e0!6shttps:%2F%2Fstreetviewpixels-pa.googleapis.com%2Fv1%2Fthumbnail%3Fpanoid%3DHWI5ljdw057S75bR3zjWqg%26cb_client%3Dmaps_sv.tactile.gps%26w%3D203%26h%3D100%26yaw%3D85.91993%26pitch%3D0%26thumbfov%3D100!7i16384!8i8192?entry=ttu

[426] Faggiano, B., Nicolella, M., Iovane, G., & Marranzini, D. (2022). A survey form for the structural health assessment of timber constructions. In Proceedings of the 6th International Conference on Structural Health Assessment of Timber Constructions (SHATIS22), September 7-9, 2022, Prague, Czech Republic.

[427] Marranzini, D., Iovane, G., Cascini, L., Landolfo, R., Nicolella, M., Faggiano, B. (2023). A methodology for the service life estimation of timber buildings. In Proceedings of the 8th International Symposium on Life-Cycle Civil Engineering (IALCE 2023), June 2-6, 2023, Milan, Italy.

[428] L. 1 giugno 1939, n. 1089 Tutela delle cose d'interesse artistico o storico.

[429] Mazzolani, F. M., Faggiano, B., Marzo, A., & Grippa, M. R. (2010). The ancient timber structures of the Royal Palace of Naples: diagnosis, analysis and retrofitting. In Proceedings of the World Conference on Timber Structures, Riva del Garda, Italy.

[430] Macchioni, N., Bernabei, M., Brunetti, M., Pollini, C., Calicchio, D., & Crivellaro, A. (2011, June). Structural diagnosis on ancient timber structures: the example of the Diplomatic Room at the Royal Palace in Naples. In SHATIS'11 International Conference on Structural Health Assessment of Timber Structures, Lisbon, Portugal.

[431] Hwang, C. L., Yoon, K., Hwang, C. L., & Yoon, K. (1981). Methods for multiple attribute decision making. Multiple attribute decision making: methods and applications a state-of-the-art survey, 58-191.

[432] Formisano, A., Florio, G., Landolfo, R., & Mazzolani, F. M. (2014). Seismic and volcanic vulnerability assessment of a monumental building in the Vesuvius area. NED University Journal of Research, 11(1), 1.

[433] Faggiano, B., Formisano, A., De Gregorio, D., De Lucia, T., Mazzolani, F. (2012). The structural behaviour assessment of Golden Miles Vesuvian villas through a seismic-volcanic quick procedure. WIADOMOSCI KONSERWATORSKIE, 807-815.

[434] Saaty, T. (1980, November). The analytic hierarchy process (AHP) for decision making. In Kobe, Japan (Vol. 1, p. 69).

[435] Decreto del Presidente della Repubblica 26 agosto 1993, n. 412. Regolamento recante norme per la progettazione, l'installazione, l'esercizio e la manutenzione degli impianti

termici degli edifici ai fini del contenimento dei consumi di energia, in attuazione dell'art. 4, comma 4, della L. 9 gennaio 1991, n. 10

[436] Stellacci, S., & Rato, V. (2021). Timber-framing construction in herculaneum archaeological site: Characterisation and main reasons for its diffusion. International Journal of Architectural Heritage, 15(9), 1301-1319.

[437] Ruggieri, N., & Serra, D. (2019). Il complesso Bernardino Telesio a Cosenza: Note storiche e costruttive. In Monére: rivista dei beni culturali e delle istituzioni politiche, 105–114. Il Menabò edizioni, Santa Maria a Vico (CE), Italy.

[438] Picchio, R., Neri, F., Maesano, M., Savelli, S., Sirna, A., Blasi, S., ... & Marchi, E. (2011). Growth effects of thinning damage in a Corsican pine (Pinus laricio Poiret) stand in central Italy. Forest Ecology and Management, 262(2), 237-243.

[439] Conedera, M., Krebs, P., Tinner, W., Pradella, M., & Torriani, D. (2004). The cultivation of Castanea sativa (Mill.) in Europe, from its origin to its diffusion on a continental scale. Vegetation history and archaeobotany, 13, 161-179.

[440] Brunetti, M., Nocetti, M., & Burato, P. (2013). Strength properties of chestnut structural timber with wane. Advanced Materials Research, 778, 377-384.

[441] GANN. (n.d.). HYDROMETTE CH17. GANN. https://www.gann.de/en/products/handhelds/electronic-moisture-meters/ch-17

[442] RHEWA. (n.d.). Platform scale. RHEWA. https://www.rhewa.com/en/products/weighing-platforms/bench-scales/

[443] FAKOPP. (n.d.). Microsecond timer 1. Fakopp. https://fakopp.com/en/product/mstimer/

[444] FAKOPP. (n.d.). Microsecond timer. Fakopp. https://fakopp.com/en/product/mstimer/

[445] Tampone, G. (2007, November). Mechanical failures of the timber structural systems. In Proceedings of ICOMOS IWC–XVI international symposium, Florence, Venice and Vicenza.

[446] UNI - Ente Italiano di Normazione. (2016). Strutture di legno - Calcolo e verifica dei valori caratteristici (UNI EN 14358: 2016). UNI.

[447] Steinskog, D. J., Tjøstheim, D. B., & Kvamstø, N. G. (2007). A cautionary note on the use of the Kolmogorov–Smirnov test for normality. Monthly Weather Review, 135(3), 1151-1157.

[448] Uribe, S. M. (2022). The A. dealbata harvesting campaign in the National Park of Peneda-Gerê [Photpgraph]. Guimarães, Portugal: Manuel Suazo Uribe.

[449] Raposo, M. A. M., Pinto Gomes, C. J., & Nunes, L. J. R. (2021). Evaluation of Species Invasiveness: A Case Study with Acacia dealbata Link. on the Slopes of Cabeça (Seia-Portugal). Sustainability 2021, 13, 11233.

[450] Giuliani, C., Giovanetti, M., Foggi, B., & Mariotti Lippi, M. (2016). Two alien invasive acacias in Italy: differences and similarities in their flowering and insect visitors. Plant Biosystems-An International Journal Dealing with all Aspects of Plant Biology, 150(2), 285-294.

[451] Nunes, L. J., Raposo, M. A., Meireles, C. I., Pinto Gomes, C. J., & Almeida Ribeiro, N. M. (2021). Carbon sequestration potential of forest invasive species: a case study with Acacia dealbata Link. Resources, 10(5), 51.

[452] Lorenzo, P., Palomera-Pérez, A., Reigosa, M. J., & González, L. (2011). Allelopathic interference of invasive Acacia dealbata Link on the physiological parameters of native understory species. Plant Ecology, 212, 403-412.

[453] Crespogarden. (2022). La Mimosa, simbolo della Primavera e della Donna. Crespogarden. https://www.crespogarden.com/la-mimosa-simbolo-della-primavera-e-della-donna/

[454] Publico. (2022).A mimosa da espécie Acacia dealbata. Publico. https://www.publico.pt/2022/02/25/ciencia/noticia/mimosas-floridas-sao-lado-belo-invasora-veio-ficar-1996618

[455] Sheppard, A., Shaw, R., & Sforza, R. (2006). Top 20 environmental weeds for classical biological control in Europe: A review of opportunities, regulations and other barriers to adoption. Weed Research, 46, 93-117.

[456] UNI - Ente Italiano di Normazione. (2004). Legno tondo strutturale - Metodi di prova. (UNI EN 14251: 2004). UNI.

[457] Uribe, S. M. (2022). Measurement of the log diameter [Photpgraph]. Guimarães, Portugal: Manuel Suazo Uribe.

[458] UNI - Ente Italiano di Normazione. (2008). Classificazione qualitativa del legno tondo di conifere - Parte 1: Abeti rossi e Abeti bianchi (UNI EN 1927-1: 2008). UNI.

[459] UNI - Ente Italiano di Normazione. (2010). Legno strutturale - Classificazione a vista dei legnami secondo la resistenza meccanica - Parte 3: Travi Uso Fiume e Uso Trieste (UNI 11035-3: 2010). UNI

[460] Ranta-Maunus, A. (Ed.) (1999). Round small-diameter timber for construction. Final report of project FAIR CT 95-0091 (VTT Publications No. 383). Espoo: VTT, Technical Research Centre of Finland

[461] Guler, C., Copur, Y., Akgul, M., & Buyuksari, U. (2007). Some chemical, physical and mechanical properties of juvenile wood from black pine (Pinus nigra Arnold) plantations. Journal of Applied Sciences, 7(5), 755-758.

[462] Vega, A., González, L., Fernández, I., & González, P. (2019). Grading and mechanical characterization of small-diameter round chestnut (Castanea sativa Mill.) timber from thinning operations. Wood Material Science & Engineering, 14(2), 81-87.

[463] Protimeter. (2022). TimberMaster. Protimeter. https://www.protimeter.com/hygromaster2-kit-0

[464] Uribe, S. M. (2022). The moisture content measurement in the middle span section. [Photpgraph]. Guimarães, Portugal: Manuel Suazo Uribe.

[465] Uribe, S. M. (2022). Performance of the vibrational test. [Photpgraph]. Guimarães, Portugal: Manuel Suazo Uribe.

[466] Unterwieser, H., & Schickhofer, G. (2010). Influence of moisture content of wood on sound velocity and dynamic MOE of natural frequency-and ultrasonic runtime measurement. European Journal of Wood and Wood Products, 69(2), 171-181.

Author's publications

1. Uribe M. S., Opazo, A., Marranzini, D., Louzada, J. L., Branco, J. M. (2024). Estudio preliminar de trozas de *Acacia dealbata* link para uso en contrucción: caracterización visual y ensayos no destructivos. In: 3th Congreso Ibero-Latinoamericano de la Madera en la Constructiòn (CIMAD23), 10 – 14 June 2024, Madrid, Spain.
   [Abstract submitted].
2. Iovane G., Zoccolillo A., Marranzini D., Landolfo R., Prota A., Sandoli A., Faggiano B. (2024). "Innovative CLT endoskeletons for integrated structural and energetic retrofit of ancient masonry buildings". In: 18th World Conference on Earthquake Engineering (WCEE2024), 30 June - 5 July 2024, Milan, Italy. [Abstract submitted].
3. Verre S., Marranzini D., Brunetti M., Nocetti M., Ruggieri N., Cauteruccio G. F., Iovane G., Togni M., Ombres L. (2023). "Assessment of strength and stiffness properties for ancient timber members combining visual and non-destructive methods". In: 8th International Symposium on Life-Cycle Civil Engineering (IALCE 2023), 02-06 June 2023, Milan, Italy.
4. Marranzini D., Iovane G., Cascini L., Landolfo R., M. Nicolella, Faggiano B. (2023). "A methodology for the service life estimation of timber buildings". In: 8th International Symposium on Life-Cycle Civil Engineering (IALCE 2023), 02-06 June 2023, Milan, Italy.
5. Iovane G., Sandoli A., Marranzini D., Landolfo R., Prota A., Faggiano B. (2023). Timber based systems for the seismic and energetic retrofit of existing structures. In: Procedia Structural Integrity, 44 (2023) 1870–1876.
6. Amarone, N., Iovane, G., Marranzini, D., Sessa, R., Guedes, M. C., & Faggiano, B. (2023). Arundo donax L. as sustainable building material. Sustainable Buildings, 6, 2.
7. Faggiano B., Nicolella M., Iovane G., Marranzini D. (2022). "A survey form for the structural health assessment of timber constructions". In: 6th International Conference on Structural Health Assessment of Timber Constructions (SHATIS22), 7-9 September 2022, Prague, Czech Republic.
8. Marranzini, D., Iovane, G., Cozzolino, F., Faggiano, B. (2022). "In situ assessment of mechanical properties of timber using the drilling resistance method". In: 6th International Conference on Structural Health Assessment of Timber Constructions (SHATIS22), 7-9 September 2022, Prague, Czech Republic.
9. Marranzini, D., Iovane, G., Vitiello, V., Castelluccio, R., & Faggiano, B. (2022). Post-fire Assessment of Heritage Timber Structures. In INTERNATIONAL SYMPOSIUM: New Metropolitan Perspectives (pp. 2597-2606). Cham: Springer International Publishing.
10. Marranzini, D., Iovane, G., & Faggiano, B. (2021). Methodology for the assessment of timber structures exposed to fire through NDT. In Applications of Structural Fire Engineering ASFE21 (pp. 9-11). Ljubljana, Slovenia.

APPENDIX A – The improvement of the CARTIS form GL (Large span buildings) – Section 3D (Timber type)

A.1 3D Section CARTIS GL form version "Rev. 09" (ReLuis 2019-2021)

PROTEZIONE CIVILE
Presidenza del Consiglio dei Ministri
Dipartimento della Protezione Civile

CARTIS Large Span

reluis
Rete dei Laboratori Universitari di Ingegneria Sismica

Sezione 3D: Characterization of timber type (to be completed as an alternative to Sections 3A.B.C.E.)

IDT I__II__I I__II__II__I I__II__II__I I__II__II__II__I I__II__II__II__I

TYPOLOGICAL CLASSIFICATION AT SUBSYTEM LEVEL

Structural grid parameters
N° naves n_x I__II__I
N° bays n_y I__II__I
N° stories nl I__II__I
Naves span L_x I__II__I,I__I m
Column heigth H_c I__I,I__I m
Bay span L_y I__I,I__I m

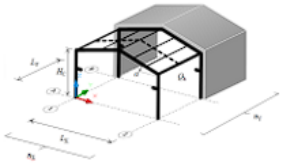

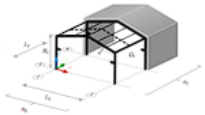

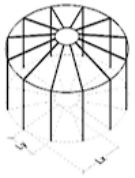

❍ Regular grid structure - Structural grid parameters				
N° naves n_x	I__II__I ÷ I__II__I			
N° bays n_y	I__II__I ÷ I__II__I			
Naves span L_x	❍ < 10 m	❍ 10÷20 m	❍ 20÷30 m	❍ >30 m
Column heigth H_c	❍ < 6 m	❍ 6÷8 m	❍ 8÷10 m	❍ >10 m
Bay span L_y	❍ < 4 m	❍ 4÷6m	❍ 6÷8 m	❍ >8 m

❍ Irregular grid structure - Structural grid parameters				
Span main beam	❍ < 10 m	❍ 10÷20 m	❍ 20÷30 m	❍ >30 m
Column heigth	❍ < 6 m	❍ 6÷8 m	❍ 8÷10 m	❍ >10 m
Bay span	❍ < 4 m	❍ 4÷6m	❍ 6÷8 m	❍ >8 m

1. Vertical structure and relationship with intermediate floors

Vertical structure / Intermediate floor	None	*Seismic resitent system*						
		Isolated column structures	Frame structures			Wall structures		
			Moment resisting frame (MRF)	Pinned frame (PF)	3 hinged arch	Coupled walls	Uncoupled walls	Modules or 3D cells
None	❍	❑	❑	❑	❑	❑	❑	❑
Not identified	❍	❑	❑	❑	❑	❑	❑	❑
In plane deformable floor	❑	❑	❑	❑	❑	❑	❑	❑
Rigid floor	❑	❑	❑	❑	❑	❑	❑	❑
	Without braces	With braces	Without braces	With braces				
	❍	❍	❍	❍				

Type of vertical brace	
Concentric braces	❍
Concentric K braces	❍
Concentric V braces	❍
Eccentric braces	❍

Hybrid system	YES ❍	NO ❍
Dual system	YES ❍	NO ❍
Antisiesmic devices	YES ❍	NO ❍

APPENDIX A – The improvement of the CARTIS form GL (Large span buildings) – Section 3D (Timber type)

PROTEZIONE CIVILE
Presidenza del Consiglio dei Ministri
Dipartimento della Protezione Civile

CARTIS Large Span

reluis
Rete dei Laboratori Universitari di Ingegneria Sismica

Sezione 3D: Characterization of timber type (to be completed as an alternative to Sections 3A.B.C.E.)

IDT |__||__| |__||__||__| |__||__||__| |__||__||__||__| |__||__||__||__|

a. Classification of members

Member	Type of members							
	Linear	Single tapered	Double tapered	Tapered with arched bottom chord	Arch	Reticular	CLT	Other
Vertical	❍	❍	❍	❍	❍	❍	❍	
Horizontal Intermediate	❍	❍	❍	❍	❍	❍	❍	
Roof	❍	❍	❍	❍	❍	❍	❍	

b. Section of main members

Columns	
Base [mm]	|__||__||__| ÷ |__||__||__|
Heigth [mm]	|__||__||__| ÷ |__||__||__|
Main beams	
Base [mm]	|__||__||__| ÷ |__||__||__|
Heigth [mm]	|__||__||__| ÷ |__||__||__|

c. Connection

	Type of connection	Materials			Connectors							Fasteners diameter [mm]	Beam support length [cm]
		Timber Timber	Timber Steel	Timber R.C.	Carpentry joint	Dowels	Bolts	Screws	Glue	Other	None		
1	Column/Wall - foundation	❑	❑	❑	❑	❑	❑	❑	❑	❑	❑	|__||__|	|__||__|
2	Beam - column/wall	❑	❑	❑	❑	❑	❑	❑	❑	❑	❑	|__||__|	|__||__|
3	Floor - beam	❑	❑	❑	❑	❑	❑	❑	❑	❑	❑	|__||__|	|__||__|
4	Roof - beam/roof - column	❑	❑	❑	❑	❑	❑	❑	❑	❑	❑	|__||__|	|__||__|
5	Column/wall -column/wall	❑	❑	❑	❑	❑	❑	❑	❑	❑	❑	|__||__|	|__||__|
6	Wall - structure	❑	❑	❑	❑	❑	❑	❑	❑	❑	❑	|__||__|	|__||__|
7	Vertical brace - column	❑	❑	❑	❑	❑	❑	❑	❑	❑	❑	|__||__|	|__||__|
8	Horizontal brace - beam	❑	❑	❑	❑	❑	❑	❑	❑	❑	❑	|__||__|	|__||__|

d. Horizontal braces

Type of brace	Material			N° braced n_x naves [%]	N° braced n_y naves [%]	Cross-section area [cmq]
	Steel	Timber	R.C.			
Single diagonal	❑	❑	❑	|__||__|	|__||__|	|__||__|
S. Andrea Cross	❑	❑	❑	|__||__|	|__||__|	|__||__|
K	❑	❑	❑	|__||__|	|__||__|	|__||__|
Eccentric	❑	❑	❑	|__||__|	|__||__|	|__||__|
Slab	❑	❑	❑	|__||__|	|__||__|	|__||__|
Pannel	❑	❑	❑	|__||__|	|__||__|	|__||__|
Not necessary	❑	❑	❑	|__||__|	|__||__|	|__||__|

e. Horizontal bracing made with perforated tape

YES ❍ NO ❍

f. Secondary beams restrained to end portals

YES ❍ NO ❍

A.2 3D Section CARTIS GL form version "Rev. 10" (Proposal)

PROTEZIONE CIVILE
Presidenza del Consiglio dei Ministri
Dipartimento della Protezione Civile

CARTIS Large Span

reluis
Rete dei Laboratori Universitari di Ingegneria Sismica

Sezione 3D: Characterization of timber type (to be completed as an alternative to Sections 3A.B.C.E.)

IDT I__II__I I__II__II__I I__II__II__I I__II__II__II__I I__II__II__II__I

TYPOLOGICAL CLASSIFICATION AT SUBSYSTEM LEVEL

Structural grid parameters					
N° naves n_x	I__II__I ÷ I__II__I				
N° bays n_y	I__II__I ÷ I__II__I				
N° stories nl	I__II__I				
Naves span L_x	I__II__I , I__II__I m	❍ < 10 m	❍ 10÷20 m	❍ 20÷30 m	❍ >30 m
Column heigth H_c	I__II__I , I__II__I m	❍ < 6 m	❍ 6÷8 m	❍ 8÷10 m	❍ >10 m
Bay span L_y	I__II__I , I__II__I m	❍ < 4 m	❍ 4÷6 m	❍ 6÷8 m	❍ >8 m
❍ Regular grid			❍ Irregular grid		

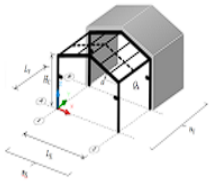

a. Structural system

Intermediate floor \ Vertical structure		Isolated column structures	Frame structures		Wall structures			Arch structures		
			Moment resisting frames (MRF)	Pinned frames (PF)	Coupled walls	Uncoupled walls	Modules or 3D cells	2 hinged arch	3 hinged arch	fixed arch
None	❍	❑	❑	❑	❑	❑	❑	❑	❑	❑
Not identified	❍	❑	❑	❑	❑	❑	❑	❑	❑	❑
In plane deformable floor	❑	❑	❑	❑	❑	❑	❑	❑	❑	❑
Rigid floor	❑	With bracing system ❑	With bracing system ❑							
Bracing floor	❑									

b. Additional information on seismic-resistant systems

Hybrid system	❑
Dual system	❑
Antiseismic devices	❑ I I I I%

c. Main structural members

Structural member	Tipologia							Cross section						Material					
								Squared		Circular		Coupled							
	Linear	Reticular	Single tapered	Double tapered	Tapered with arched bottom chord	Arch	Wall	%	B x H [cm]	%	Diameter [cm]	%	B x H [cm]	Glulam timber	Heavy timber	CLT	Timber based material	Steel	R.C.
Vertical	❑ I__I__I%	❑ I__I__I%	❑ I__I__I%	❑ I__I__I%	❑ I__I__I%	❑ I__I__I%	❑ I__I__I%	❑ I__I__I%	I__I__I x I__I__I	❑ I__I__I%	I__I__I	❑ I__I__I%	I__I__I x I__I__I	❑ I__I__I%	❑ I__I__I%	❑ I__I__I%	❑ I__I__I%	❑ I__I__I%	❑ I__I__I%
Horizontal Intermediate	❑ I__I__I%	❑ I__I__I%	❑ I__I__I%	❑ I__I__I%	❑ I__I__I%	❑ I__I__I%	❑ I__I__I%	❑ I__I__I%	I__I__I x I__I__I	❑ I__I__I%	I__I__I	❑ I__I__I%	I__I__I x I__I__I	❑ I__I__I%	❑ I__I__I%	❑ I__I__I%	❑ I__I__I%	❑ I__I__I%	❑ I__I__I%
Floor	❑ I__I__I%	❑ I__I__I%	❑ I__I__I%	❑ I__I__I%	❑ I__I__I%	❑ I__I__I%	❑ I__I__I%	❑ I__I__I%	I__I__I x I__I__I	❑ I__I__I%	I__I__I	❑ I__I__I%	I__I__I x I__I__I	❑ I__I__I%	❑ I__I__I%	❑ I__I__I%	❑ I__I__I%	❑ I__I__I%	❑ I__I__I%

APPENDIX A – The improvement of the CARTIS form GL (Large span buildings) – Section 3D (Timber type)

CARTIS Large Span

Sezione 3D: Characterization of timber type (to be completed as an alternative to Sections 3A.B.C.E.)

IDT I__II__I I__II__II__I I__II__II__I I__II__II__II__I I__II__II__II__I

d. Bracing system

Typology		Material			Cross-Section							N° braced n_x naves [%]	N° braced n_y naves [%]
		Timber	Steel	R.C.	Squared		Circular		Coupled		Other		
					%	B x H [cm]	%	Diameter [cm]	%	B x H [cm]			
Vertical system	Moment resisting frame (MRF)	❑	❑	❑	❑ I__I__I__I%	I__I__I__I x I__I__I__I	❑ I__I__I__I%	I__I__I__I	❑ I__I__I__I%	I__I__I__I x I__I__I__I	❑ I__I__I__I%	I__I__I__I	I__I__I__I
	Isolated column (cantilever)	❑	❑	❑	❑ I__I__I__I%	I__I__I__I x I__I__I__I	❑ I__I__I__I%	I__I__I__I	❑ I__I__I__I%	I__I__I__I x I__I__I__I	❑ I__I__I__I%	I__I__I__I	I__I__I__I
	Single diagonal	❑	❑	❑	❑ I__I__I__I%	I__I__I__I x I__I__I__I	❑ I__I__I__I%	I__I__I__I	❑ I__I__I__I%	I__I__I__I x I__I__I__I	❑ I__I__I__I%	I__I__I__I	I__I__I__I
	Concentric X braces	❑	❑	❑	❑ I__I__I__I%	I__I__I__I x I__I__I__I	❑ I__I__I__I%	I__I__I__I	❑ I__I__I__I%	I__I__I__I x I__I__I__I	❑ I__I__I__I%	I__I__I__I	I__I__I__I
	Concentric V braces	❑	❑	❑	❑ I__I__I__I%	I__I__I__I x I__I__I__I	❑ I__I__I__I%	I__I__I__I	❑ I__I__I__I%	I__I__I__I x I__I__I__I	❑ I__I__I__I%	I__I__I__I	I__I__I__I
	Concentric K braces	❑	❑	❑	❑ I__I__I__I%	I__I__I__I x I__I__I__I	❑ I__I__I__I%	I__I__I__I	❑ I__I__I__I%	I__I__I__I x I__I__I__I	❑ I__I__I__I%	I__I__I__I	I__I__I__I
	Eccentric braces	❑	❑	❑	❑ I__I__I__I%	I__I__I__I x I__I__I__I	❑ I__I__I__I%	I__I__I__I	❑ I__I__I__I%	I__I__I__I x I__I__I__I	❑ I__I__I__I%	I__I__I__I	I__I__I__I
	Walls	❑	❑	❑	❑ I__I__I__I%	I__I__I__I x I__I__I__I	❑ I__I__I__I%	I__I__I__I	❑ I__I__I__I%	I__I__I__I x I__I__I__I	❑ I__I__I__I%	I__I__I__I	I__I__I__I
Horziontal system	Single diagonal	❑	❑	❑	❑ I__I__I__I%	I__I__I__I x I__I__I__I	❑ I__I__I__I%	I__I__I__I	❑ I__I__I__I%	I__I__I__I x I__I__I__I	❑ I__I__I__I%	I__I__I__I	I__I__I__I
	Concentric X braces	❑	❑	❑	❑ I__I__I__I%	I__I__I__I x I__I__I__I	❑ I__I__I__I%	I__I__I__I	❑ I__I__I__I%	I__I__I__I x I__I__I__I	❑ I__I__I__I%	I__I__I__I	I__I__I__I
	Concentric V braces	❑	❑	❑	❑ I__I__I__I%	I__I__I__I x I__I__I__I	❑ I__I__I__I%	I__I__I__I	❑ I__I__I__I%	I__I__I__I x I__I__I__I	❑ I__I__I__I%	I__I__I__I	I__I__I__I
	Concentric K braces	❑	❑	❑	❑ I__I__I__I%	I__I__I__I x I__I__I__I	❑ I__I__I__I%	I__I__I__I	❑ I__I__I__I%	I__I__I__I x I__I__I__I	❑ I__I__I__I%	I__I__I__I	I__I__I__I
	Slab	❑	❑	❑	❑ I__I__I__I%	I__I__I__I x I__I__I__I	❑ I__I__I__I%	I__I__I__I	❑ I__I__I__I%	I__I__I__I x I__I__I__I	❑ I__I__I__I%	I__I__I__I	I__I__I__I
	Pannels	❑	❑	❑	❑ I__I__I__I%	I__I__I__I x I__I__I__I	❑ I__I__I__I%	I__I__I__I	❑ I__I__I__I%	I__I__I__I x I__I__I__I	❑ I__I__I__I%	I__I__I__I	I__I__I__I
	Spatial structure	❑	❑	❑	❑ I__I__I__I%	I__I__I__I x I__I__I__I	❑ I__I__I__I%	I__I__I__I	❑ I__I__I__I%	I__I__I__I x I__I__I__I	❑ I__I__I__I%	I__I__I__I	I__I__I__I

e. Connections

Type of connection	Materials			Cylinder fasteners						Plates								Other			Support legnth [cm]
	Timber Timber	Timber Steel	Timber R.C.	Dowels	Diameter [cm]	Bolts	Diameter [cm]	Screws	Diameter [cm]	Plate	Thickness [cm]	Toothed plate	Thickness [cm]	Hold down	Thickness [cm]	Angular plate	Thickness [cm]	Carpentry joint	Glue	Other	
Column - foundation	❑	❑	❑	❑	I__I__I__I	❑	I__I__I__I	❑	I__I__I__I	❑	I__I__I__I	❑	I__I__I__I	❑	I__I__I__I	❑	I__I__I__I	❑	❑	❑	I__I__I__I
Column/Wall - beam	❑	❑	❑	❑	I__I__I__I	❑	I__I__I__I	❑	I__I__I__I	❑	I__I__I__I	❑	I__I__I__I	❑	I__I__I__I	❑	I__I__I__I	❑	❑	❑	I__I__I__I
Column/Wall - intermediate floor	❑	❑	❑	❑	I__I__I__I	❑	I__I__I__I	❑	I__I__I__I	❑	I__I__I__I	❑	I__I__I__I	❑	I__I__I__I	❑	I__I__I__I	❑	❑	❑	I__I__I__I
Column/Wall - roof	❑	❑	❑	❑	I__I__I__I	❑	I__I__I__I	❑	I__I__I__I	❑	I__I__I__I	❑	I__I__I__I	❑	I__I__I__I	❑	I__I__I__I	❑	❑	❑	I__I__I__I
Column - wall	❑	❑	❑	❑	I__I__I__I	❑	I__I__I__I	❑	I__I__I__I	❑	I__I__I__I	❑	I__I__I__I	❑	I__I__I__I	❑	I__I__I__I	❑	❑	❑	I__I__I__I
Intermediate floor - purlin/main beam/secondary beam	❑	❑	❑	❑	I__I__I__I	❑	I__I__I__I	❑	I__I__I__I	❑	I__I__I__I	❑	I__I__I__I	❑	I__I__I__I	❑	I__I__I__I	❑	❑	❑	I__I__I__I
Main beam - secondary beam	❑	❑	❑	❑	I__I__I__I	❑	I__I__I__I	❑	I__I__I__I	❑	I__I__I__I	❑	I__I__I__I	❑	I__I__I__I	❑	I__I__I__I	❑	❑	❑	I__I__I__I
Purlin - secondary beam	❑	❑	❑	❑	I__I__I__I	❑	I__I__I__I	❑	I__I__I__I	❑	I__I__I__I	❑	I__I__I__I	❑	I__I__I__I	❑	I__I__I__I	❑	❑	❑	I__I__I__I
Vertical brace - column	❑	❑	❑	❑	I__I__I__I	❑	I__I__I__I	❑	I__I__I__I	❑	I__I__I__I	❑	I__I__I__I	❑	I__I__I__I	❑	I__I__I__I	❑	❑	❑	I__I__I__I
Horizontal brace - beam	❑	❑	❑	❑	I__I__I__I	❑	I__I__I__I	❑	I__I__I__I	❑	I__I__I__I	❑	I__I__I__I	❑	I__I__I__I	❑	I__I__I__I	❑	❑	❑	I__I__I__I

APPENDIX B - The SHA-TS form (Structural Health Assessment – Timber Structures)

B.1 The proposed survey form

SHA-TS form

Structura health assessment - Timber Structures

Section A: Identification of municipality and building

DATE /__/__//__/__//__/__/__/__/

A1) Building location

Region: ____________________ ISTAT Code I__I__I

Province: ____________________ ISTAT Code I__I__I__I

Municipality: ____________________ ISTAT Code I__I__I__I

A2) Surveyor identification data

Name and surname: ________________________________

Affiliation: ________________________________

Title: ________________________________

Degree: ________________________________

Address: ________________________________

Telephone number: ________________________________

Mail: ________________________________

Signature: ________________________________

A3) Data of the interviewed thecnician *(optional)*

Name and surname: ____________________

Affiliation: ____________________

Title: ____________________

Degree: ____________________

Address: ____________________

Mail: ____________________

Telephone number: ____________________

A4) Source of data

❑ Documentation / Drawings

❑ On-site survey

❑ Interview

❑ Others ____________________

A5) Identification data of the build

Name of the building or name of its owners	I__I__I__I__I__I__I__I__I__I__I__I__I__I__I__I__I__I__I__I
Class of use (NTC18)	❍ I Class ❍ II Class ❍ III Class ❍ IV Class
Code of use (DPC Italy)	I_S_I__I__I
Building location as respect to the other buildings	❍ Isolated ❍ Internal ❍ At the end ❍ At the corner

Section B: Identification of the building constructive technology and typology

B1) Material classification

Mixed/Homogeneous system				
Materials	***Vertical***	***Intermediate floors***	***Roof***	***Foundation***
R.C.	❑	❑	❑	❑
Prefabricated R.C.	❑	❑	❑	❑
Steel	❑	❑	❑	❑
Timber	❑	❑	❑	❑
Masonry	❑	❑	❑	❑
Composite Steel-RC	❑	❑	❑	❑
Absent	❑	❑	❑	❑
Not identified	❑	❑	❑	❑
Other materials				

B2) Structural typology and relation with floors

Vertical structure / *Intermediate floor*	Absent	***Seismic resistant system***				
		Frame		Walls	Archs	
Absent	❍	❑		❑	❑	
Not identified	❍	❑		❑	❑	
In plane deformable floor	❑	❑		❑	❑	
In plane rigid floor	❑	❑		❑	❑	
		Without bracing ❍	With bracing ❍		Without bracing ❍	With bracing ❍

B3) Bracing system

	Materials		**Transv. Dir.**	**Long. Dir.**
	Timber	Steel		
Single diagonal	❑	❑	❑ ___ [%]	❑ ___ [%]
MRF	❑	❑	❑ ___ [%]	❑ ___ [%]
Concentric X braces	❑	❑	❑ ___ [%]	❑ ___ [%]
Concentric K braces	❑	❑	❑ ___ [%]	❑ ___ [%]
Concentric V braces	❑	❑	❑ ___ [%]	❑ ___ [%]
Eccentric braces	❑	❑	❑ ___ [%]	❑ ___ [%]

Section B: Identification of the building constructive technology and typology

B4) Roof

B4_A) Deformation characteristics		B4_B) Number of levels: I__I			Simple way system	Double way system	Presence of tie beam	Pushing elements
Not identified	❍							
Deformable	❍	Roof bracing system:	YES ❍	NO ❍	❍	❍	YES ❍ NO ❍	YES ❍ NO ❍
Rigid	❍							

B4_C) Simple way system		B4_D) Main member typology	Costant section	Variable section	Single section	Composed section
Horizontal ❍		Not identified	❍	❍	❍	❍
		Solid section	❑	❑	❑	❑
Sloped	Single ❍	Hollow section	❑	❑	❑	❑
	Double ❍	Reticular	❑	❑	❑	❑
Curved ❍		Other: _____	❑	❑	❑	❑

B4_E) Secondary member typology	Costant section	Variable section	Single section	Composed section
Not identified	❍	❍	❍	❍
Solid section	❑	❑	❑	❑
Hollow section	❑	❑	❑	❑
Reticular	❑	❑	❑	❑
Other: _____	❑	❑	❑	❑

B4_F) Double way system		B4_G) Type of plate / shell	Horizontal		Sloped	
			Cost. sect.	Var. sect.	Cost. sect.	Var. sect.
Horizontal ❍		Not identified	❍	❍	❍	❍
Sloped ❍		Simple layer grid	❑	❑	❑	❑
		Double layer grid	❑	❑	❑	❑
Curved	*Single curvature* ❍	Contiunous	❑	❑	❑	❑
	Double curvature ❍	Other: _____	❑	❑	❑	❑

B4_G) Closing elements					
Not identified ❍	R.C. slab ❑	Skylight ❑	Tiles ❑	Steel sheet ❑	Other _____

B5) Foundation

Type of foundation	Not Identified	Presumed	From interview	From drawings	From inspection	Direct / superf. foundation	Indirect / deep foundation
Not identified	❍	❑	❑	❑	❑	❑	❑
Isolated plinths	❑	❑	❑	❑	❑	❑	❑
Isolated plinths with connecting beams	❑	❑	❑	❑	❑	❑	❑
Inverse beam grid	❑	❑	❑	❑	❑	❑	❑
Slabs	❑	❑	❑	❑	❑	❑	❑

Section C: Description of the building

C1) Metrics data

N° total floors with underground ones	Average interstory height (m)	Floor average area (m^2)	
❍ 1	❍ < 2.50	❍ < 200	❍ 2500 ÷ 3000
❍ 2	❍ 2.50 ÷ 3.49	❍ 200 ÷ 250	❍ 3000 ÷ 3500
❍ 3	❍ 3.50 ÷ 4.99	❍ 250 ÷ 300	❍ 3500 ÷ 4000
❍ 4	❍ 5.00 ÷ 6.99	❍ 300 ÷ 400	❍ 4000 ÷ 4500
❍ 5	❍ 7.00 ÷ 9.99	❍ 400 ÷ 500	❍ 4500 ÷ 5000
❍ 6	❍ 10 ÷ 14.00	❍ 500 ÷ 650	❍ 5500 ÷ 6000
Underground floors	❍ > 14.00	❍ 650 ÷ 900	❍ 6000 ÷ 7000
❍ 0		❍ 900 ÷ 1200	❍ 7000 ÷ 10000
❍ 1		❍ 1200 ÷ 1600	❍ 10000 ÷ 15000
❍ 2		❍ 1600 ÷ 2000	❍ 15000 ÷ 20000
❍ ≥ 3		❍ 2000 ÷ 2500	❍ > 2000

C2) Age

Construction and renovation age
❑ < 1950
❑ 1950 ÷ 61
❑ 1962 ÷ 71
❑ 1972 ÷ 75
❑ 1976 ÷ 81
❑ 1982 ÷ 86
❑ 1987 ÷ 91
❑ 1992 ÷ 96
❑ 1997 ÷ 01
❑ 2002 ÷ 08
❑ 2009 ÷ 11
❑ > 2011

C3) Use - Exposure

Use	Use - Exposure
❑ Residential	❍ > 65%
❑ Productive	❍ 30 ÷ 65%
❑ Commercial	❍ < 30%
❑ Offices	❍ Not used
❑ Public utility activities	❍ In costruction
❑ Storehouses	❍ Not finished
❑ Strategic	❍ Abandoned
❑ Tourist	**Ownership**
❑ Parking aerea	❑ Public ❑ Private
❑ Exposition space	I_1_I_0_I_0_I % I__I__I__I %
❑ Sport facilities	

C4) Plan and section

Section D: Characterization of the structural members

D1) Typology

❑ Column	❑ Strut	
❑ Primary beam	❑ Diagonal	
❑ Secondary beam	❑ King post	
❑ Brace	❑ Tie	
❑ Plank	❑ Other:_____	
❑ Panel		
❑ Other:_____		

D2) Material

- ❑ Massive timber
- ❑ Glulam timber
- ❑ CLT
- ❑ MDF
- ❑ OSB
- ❑ LVL
- ❑ Other:_____

D3) Timber species

❍ Softwood ❍ Hardwood ❍ Not recognized

D4) Year of construction

❑ < 1950	❑ 1972 ÷ 75	❑ 1987 ÷ 91	❑ 2002 ÷ 08	❑ 2015 ÷ 17
❑ 1950 ÷ 61	❑ 1976 ÷ 81	❑ 1992 ÷ 96	❑ 2009 ÷ 11	❑ 2018 ÷ 20
❑ 1962 ÷ 71	❑ 1982 ÷ 86	❑ 1997 ÷ 01	❑ 2012 ÷ 14	❑ > 2020

D5) Floor

Above ground

- ❍ 1
- ❍ 2
- ❍ 3
- ❍ 4
- ❍ 5
- ❍ 6

Underground

- ❍ 0
- ❍ 1
- ❍ 2
- ❍ ≥ 3

D6) Hazard class [335-

	Service condition / Exposure to wetting in service	Moisture Content (M.C.)
❍ 1	Indoor, dry	M.C. < 20%
❍ 2	Indoor or coovered, not exposed to environmental agents	M.C.occasionaly > 20%
❍ 3	Outdoor, not in contact with the ground, exposed to environmental agents	M.C.frequently > 20%
❍ 4	Outdoor, in contact with the ground and or water	M.C.permanently > 20%
❍ 5	Permanently and regularly immersed in salt water	M.C.permanently > 20%

D7) Average environmental temperature

❑ < 10° ❑ 10° ÷ 20° ❑ 20° ÷ 30° ❑ > 30°

D8) Class of durability [EN 350-1]

❑ 1 - Very durable ❑ 2 - Durable ❑ 3 - Moderately durable ❑ 4 - Slightly durable ❑ 5 - Not durable

Section E: Decay effects identification

E1) Colour	***E2) Aspect to the touch***	***E3) Superficial aspect***
❑ Dark	❑ Dusty ❑ Wet	❑ Presence of stripes
❑ White - yellow		❑ Presence of cracks
❑ Ligth blue	❑ Floury ❑ Soft	❑ Presence of exfoliation
❑ No colour alteration		❑ Thin intact layer
❑ Others _____	❑ Buttery ❑ Others_____	❑ Others_____

E4) Cracks	***E5) Presence of holes***	***E6) Presence of galleries***
❑ Longitudinal cracks	❑ Circural shap ❑ Oval shape	❑ Visible galleries
❑ Trasnversal cracks	❑ 1 - 2 mm	❑ Not visible galleries
❑ Superficial cracks 1-3 mm	Holes diameter ❑ 3 - 5 mm	Shape of ❑ Circular
❑ Deep cracks >4 mm	❑ > 5 mm	galleries ❑ Oval
❑ Others_____	❑ Others_____	❑ Others_____

E7) Extent of damage

E8_a) Tools for diagnostic

❑ Core extracting tool ❑ Resistance drilling tool ❑ Penetration tool ❑ Other:_____

E8_b) Location

❍ End zone ❍ Middle zone ❍ Whole member

E8) Other aspects

❑ Presence of beetles ❑ Presence of timber residuals ❑ Presence of excrement

❑ Presence of mold ❑ Mold smell ❑ Gnawing noise

Other: _____

E9) Presence of existing treatments

❑ Not recognizable ❑ Superficial treatment ❑ Deep treatment

❑ Other: _____

E10 Moisture content (M.C.)

❑ M.C.< 20% ❑ 20% < M.C.< 30% ❑ M.C.> 30%

Section F: Decay typology

F1) Biological decay

F1_A) Fungi	❑ Basidiomycetes	❑ Brown caries fungi
		❑ Soft caries fungi
	❑ Ascomycetes	❑ White caries fungi
		❑ Chromogen fungi
F1_B) Xylophagous insects	❑Coleoptera	❑ Cerambycidae
		❑ Anobium
		❑ Lyctus
	❑ Isoptera	❑ Rhinotermitidae / Kalotermitidae

F2) Abiotic decay

- ❑ Decay by marine organisms
- ❑ Decay by UV radiation
- ❑ Other:_____

Section G: Possible interventions and treatments

G1) Criteria of Interventions	G2) Treatments
❑ Reduction of the enviromental humidity RH < 90%	❑ Impregnation with fungicidal substances
❑ Avoid stagnation and direct contact with water	❑ Fumigation treatment
❑ Surface cleaning	❑ Permethrin and Boron treatments
❑ Avoid direct exposure to UV radiation	❑ Heat treatment
❑ Avoid rising damp for capillarity	❑ Other_____
❑ Removal and replacement of degraded parts	
❑ Replacement, if possible, of the whole timber member, using timber with greater durability class	
❑ Other_____	

B.2 User's manual supporting the SHA-TS form

Attacco Biotico: Funghi Basidiomiceti

AGENTE: *Funghi della carie bruna / cubica*

DESCRIZIONE ANOMALIA:
Colore: *colore scuro*
Aspetto superficiale: *fessurazioni longitudinali e superficiali, aspetto simile al legno carbonizzato*
Consistenza: *polvere bruna sottile, burrosa al tatto*

ESTENSIONE ANOMALIA: *Localizzato a tutte le zone ad elevate umidità.*

SPECIE LEGNOSE PIU' VULNERABILI: *Attaccano principalmente legni di conifera.*

DECADIMENTO PRESTAZIONALE: *Perdita di prestazioni meccaniche, alterazione dello stato superficiale.*

DURABILITA' NATURALE: *Creare un ambiente sfavorevole alla proliferazione di questi funghi, mantenendo il legno ad una umidità inferiore al 20%, come:*
- *Umidità dell'aria inferiore al 90%;*
- *Evitare ristagni e contatti diretti con l'acqua;*
- *Utilizzare specie legnose quali castagno o quercia, il cui durame è più resistente nei confronti dell'attacco fungino.*

CAUSE INDIVIDUABILI:
- *Umidità del legno superiore al 20%; (causa principale)*
- *Risalita di acqua per capillarità;*
- *Contatto diretto con l'acqua;*
- *Ambienti poco o non ventilati.*

DURABILITA' EFFETTIVA: Trattamenti preservanti:
- *Impregnazione in profondità, in caso di utilizzo specie legnose impregnabili (classe di trattabilità 1-2);*
- *Impregnazione superficiale a pennello per specie non impregnabili (classe di trattabilità 3-4).*

TRATTAMENTI CURATIVI:
- *Rimozione della causa dell'umidità;*
- *Rimosse le cause, intervenire con interventi di consolidamenti tramite asportazione e sostituzione del materiale degradato.*

Decay by Brown-rot fungi

Attacco Biotico: Funghi Ascomiceti

AGENTE: *Funghi cromogeni o dell'azzurramento*

DESCRIZIONE ANOMALIA:
Colore: *colore azzurro*
Aspetto superficiale: *alterazione cromatica*
Consistenza: *legno umido al tatto*

ESTENSIONE ANOMALIA: *Localizzato a tutte le zone ad elevate umidità.*

SPECIE LEGNOSE PIU' VULNERABILI: *Attaccano principalmente legni di latifoglie più ricche di lignina*

DECADIMENTO PRESTAZIONALE: *Alterazione cromatica dello stato superficiale, non interessa la resistenza meccanica.*

DURABILITA' NATURALE:
Creare un ambiente sfavorevole alla proliferazione di questi funghi, mantenendo il legno ad una umidità inferiore al 30%, come:
- *Umidità dell'aria inferiore al 95%;*
- *Evitare ristagni e contatti diretti con l'acqua;*

CAUSE INDIVIDUABILI:
- *Tronchi appena abbattuti e non ancora stagionati;*
- *Umidità del legno superiore al 30%;*
- *Temperatura ottimale per lo sviluppo delle ife compresa tra i 22° e 25°.*

DURABILITA' EFFETTIVA: Trattamenti preservanti:
- *Impregnazione in profondità, in caso di utilizzo specie legnose impregnabili (classe di trattabilità 1-2);*
- *Impregnazione superficiale a pennello per specie non impregnabili (classe di trattabilità 3-4).*

TRATTAMENTI CURATIVI:
- *Rimozione della causa dell'umidità;*
- *Pulizia dello strato superficiale interessato;*

Decay by Soft-rot fungi

Attacco Biotico: Funghi Ascomiceti

AGENTE: *Funghi della carie bianca*

DESCRIZIONE ANOMALIA:
Colore: *colore bianco-giallastro, perché degradano principalmente la lignina.*
Aspetto superficiale: *fessurazioni e disgregazione di un sottile strato superficiale.*
Consistenza: *molle e soffice al tatto, rottura senza essere friabile.*

ESTENSIONE ANOMALIA: *Localizzato a tutte le zone ad elevate umidità.*

SPECIE LEGNOSE PIU' VULNERABILI: *Attaccano principalmente legni di latifoglie più ricche di lignina*

DECADIMENTO PRESTAZIONALE: *Perdita di prestazioni meccaniche, alterazione dello stato superficiale.*

DURABILITA' NATURALE: *Creare un ambiente sfavorevole alla proliferazione di questi funghi, mantenendo il legno ad una umidità inferiore al 20%, come:*
- *Umidità dell'aria inferiore al 90%;*
- *Evitare ristagni e contatti diretti con l'acqua;*
- *Utilizzare specie legnose più durabili oppure di conifera, perché più ricche di cellulosa e povere di lignina.*

CAUSE INDIVIDUABILI:
- *Umidità del legno superiore al 20%; (causa principale)*
- *Risalita di acqua per capillarità;*
- *Contatto diretto con l'acqua;*
- *Ambienti poco o non ventilati.*

DURABILITA' EFFETTIVA: Trattamenti preservanti:
- *Impregnazione in profondità, in caso di utilizzo specie legnose impregnabili (classe di trattabilità 1-2);*
- *Impregnazione superficiale a pennello per specie non impregnabili (classe di trattabilità 3-4).*

TRATTAMENTI CURATIVI:
- *Rimozione della causa dell'umidità;*
- *Rimosse le cause, intervenire con interventi di consolidamenti tramite asportazione e sostituzione del materiale degradato.*

Decay by White-rot fungi

Attacco Biotico: Insetti xilofagi - Coleotteri

AGENTE: *Cerambicidi - Hylotrupes bajulus, anche detto il capricorno delle case*

DESCRIZIONE ANOMALIA: *Tali insetti possono raggiungere un centimetro di diametro e sono i più pericolosi e presentano:*
- *fori sulla superficie del legno, da 6 a 10 mm, di forma ovale;*
- *gallerie che si estendono verso la periferia del manufatto, protette da una pellicola sottile di legno, pareti striate;*
- *escrementi di colore beige molto chiaro, a forma di piccole botti da 0,8 mm di lunghezza;*
- *lieve rumore di "rosicchiamento"*

ESTENSIONE ANOMALIA: *Su tutti gli elementi.*

DECADIMENTO PRESTAZIONALE: *Perdita di prestazioni meccaniche.*

CAUSE INDIVIDUABILI:
- *strutture lignee in particolare in legno di conifera;*
- *temperatura dell'ambiente ideale per il suo sviluppo durante lo stato di larva compreso tra 28°C e 30°C;*
- *legno «recente», meno di novanta anni, perché ricco di sostanze azotate.*

RIMEDI: *Creare un ambiente sfavorevole alla proliferazione di questi insetti, come:*
- *Temperature elevate che causano la morte delle larve;*
- *Trattamenti preservanti per impregnazione;*
- *Trattamenti preservanti superficiali contenenti Permetrina o Sali di boro;*
- *Trattamenti con gas tossici, fumigazione.*

NOTE: Preferire legno privo di fessure se trattato solo superficialmente.

Decay by insect: *Cerambycidae*

Attacco Biotico: Insetti xilofagi - Anobidi

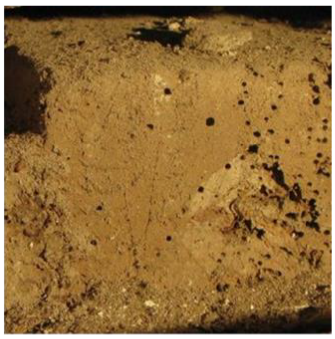

AGENTE: *Anobidi, Xestobium rufovillosum.*

DESCRIZIONE ANOMALIA: *Tali insetti possono raggiungere un diametro dai 2,5 ai 9 cm:*
- *fori sulla superficie del legno, da 1,5 a 3,5 mm, di forma circolare;*
- *Temperatura ottimale 20°C, range 10°-32°C;*
- *Umidità del legno ideale intorno ai 13%;*
- *Rosure prodotto assume una consistenza di polvere fine, costituita da minuscole pallottoline ellittiche;*
- *Attaccano in profondità, sotto un soitile strato integro.*

ESTENSIONE ANOMALIA: Esteso a tutto l'elemento.

SPECIE LEGNOSE PIU' VULNERABILI: Sono specie non molto frequenti in Italia, preferiscono legname di latifoglia, ma attaccano anche conifere se a stretto contatto con latifoglie infestate. Prevalentemente è sempre associato ad un attacco da Funghi

DECADIMENTO PRESTAZIONALE: *Perdita di prestazioni meccaniche.*

CAUSE INDIVIDUABILI:
- *strutture lignee in particolare in legno di latifoglia;*
- *temperatura dell'ambiente ideale per il suo sviluppo durante lo stato di larva compreso tra 10°C e 32°C;*
- *Vicinanza a elementi già infestati;*

RIMEDI: *Creare un ambiente sfavorevole alla proliferazione di questi insetti, come:*
- *Temperature elevate che causano la morte delle larve;*
- *Trattamenti preservanti per impregnazione;*
- *Trattamenti preservanti superficiali contenenti Permetrina o Sali di boro;*
- *Trattamenti con gas tossici, fumigazione.*

NOTE: Preferire legno privo di fessure se trattato solo superficialmente.

Decay by insect: *Anobium*

Attacco Biotico: Insetti xilofagi - Lictidi

AGENTE: *Licidi, Lyctus brunneus e Lyctus linearis.*

DESCRIZIONE ANOMALIA: *Tali insetti possono raggiungere un diametro dai 1 ai 2 mm:*
- *fori sulla superficie del legno, da 1 a 1,5 mm, di forma circolare;*
- *Temperatura ottimale 27°C*
- *Umidità del legno ideale nel range di vaori 8% _ 32%*

ESTENSIONE ANOMALIA: Esteso a tutto l'elemento.

SPECIE LEGNOSE PIU' VULNERABILI: Alburno di latifoglie, legni con un contenuto di amido superiore al 1,5%.

DECADIMENTO PRESTAZIONALE: *Perdita di prestazioni meccaniche.*

CAUSE INDIVIDUABILI:
- *strutture lignee in particolare in legno di latifoglia;*
- *temperatura dell'ambiente ideale per il suo sviluppo durante lo stato di larva compreso tra 26°C e 30°C;*
- *legno «recente», meno di novanta anni, perché ricco di sostanze, quali, amido.*

RIMEDI: *Creare un ambiente sfavorevole alla proliferazione di questi insetti, come:*
- *Temperature elevate che causano la morte delle larve;*
- *Trattamenti preservanti per impregnazione;*
- *Trattamenti preservanti superficiali contenenti Permetrina o Sali di boro;*
- *Trattamenti con gas tossici, fumigazione.*

NOTE: Preferire legno privo di fessure se trattato solo superficialmente.

Decay by insect: *Lyctus*

B.3 Application of the SHA-TS form to the case study "a"

Building location

View of the building with evidence of the investigated member

The investigated member (main beam)

SHA-TS form

Structura health assessment - Timber Structures

Section A: Identification of municipality and building

DATE /1/5//0/4//2/0/2/1/

A1) Building location

Region: Campania ISTAT Code 0 6

Province: Caserta ISTAT Code 0 6 1

Municipality: Gioia Sannitica ISTAT Code 0 4 1

A2) Surveyor identification data

Name and surname: Dante Marranzini

Affiliation: University of Naples Federico II

Title: Engineer

Degree: Doctor in Architecture and Building Engineering

Address:

Telephone number:

Mail: dante.marranzini@unina.it

Signature:

A3) Data of the interviewed thecnician (optio

Name and surname:

Affiliation:

Title:

Degree:

Address:

Mail:

Telephone number:

A4) Source of data

☐ Documentation / Drawings

● On-site survey

☐ Interview

☐ Others

A5) Identification data of the buil

Name of the building or name of its owners	C A S E S T U D Y A
Class of use (NTC18)	● I Class ○ II Class ○ III Class ○ IV Class
Code of use (DPC Italy)	S
Building location as respect to the other buildings	● Isolated ○ Internal ○ At the end ○ At the corn

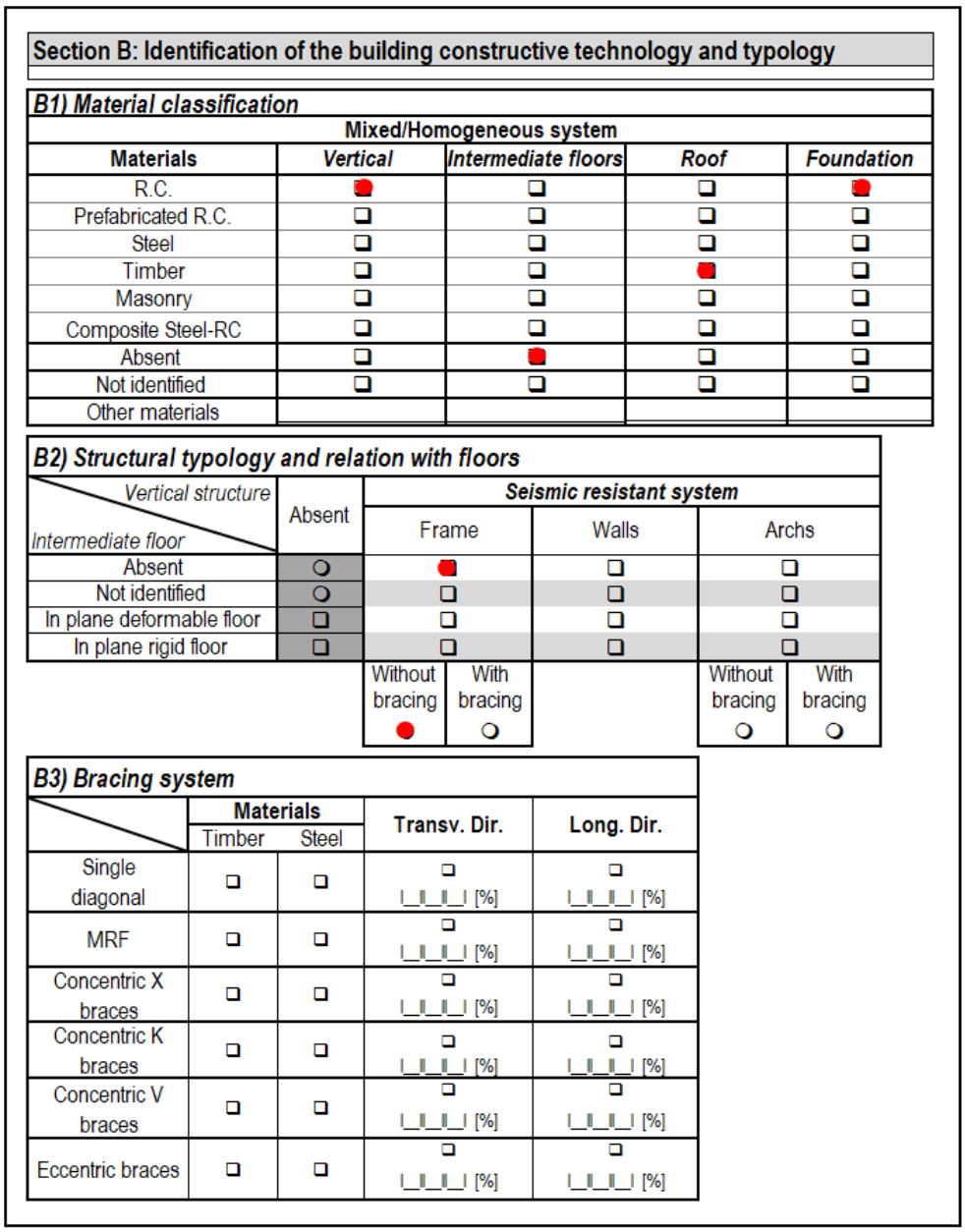

Section B: Identification of the building constructive technology and typology

B1) Material classification

Mixed/Homogeneous system				
Materials	***Vertical***	***Intermediate floors***	***Roof***	***Foundation***
R.C.	●	❑	❑	●
Prefabricated R.C.	❑	❑	❑	❑
Steel	❑	❑	❑	❑
Timber	❑	❑	●	❑
Masonry	❑	❑	❑	❑
Composite Steel-RC	❑	❑	❑	❑
Absent	❑	●	❑	❑
Not identified	❑	❑	❑	❑
Other materials				

B2) Structural typology and relation with floors

Vertical structure / *Intermediate floor*	Absent	***Seismic resistant system***		
		Frame	Walls	Archs
Absent	○	●	❑	❑
Not identified	○	❑	❑	❑
In plane deformable floor	❑	❑	❑	❑
In plane rigid floor	❑	❑	❑	❑
		Without bracing ● / With bracing ○		Without bracing ○ / With bracing ○

B3) Bracing system

	Materials		**Transv. Dir.**	**Long. Dir.**
	Timber	Steel		
Single diagonal	❑	❑	❑ ___ [%]	❑ ___ [%]
MRF	❑	❑	❑ ___ [%]	❑ ___ [%]
Concentric X braces	❑	❑	❑ ___ [%]	❑ ___ [%]
Concentric K braces	❑	❑	❑ ___ [%]	❑ ___ [%]
Concentric V braces	❑	❑	❑ ___ [%]	❑ ___ [%]
Eccentric braces	❑	❑	❑ ___ [%]	❑ ___ [%]

Section B: Identification of the building constructive technology and typology

B4) Roof

B4_A) Deformation characteristics	
Not identified	○
Deformable	●
Rigid	○

B4_B) Number of levels: |__|

Roof bracing system:	YES	NO
	○	●

Simple way system	Double way system	Presence of tie beam	Pushing elements
●	○	YES ○ NO ●	YES ○ NO ●

B4_C) Simple way system		B4_D) Main member typology	Costant section	Variable section	Single section	Composed section
Horizontal ○		Not identified	○	○	○	○
		Solid section	●	❑	●	❑
Sloped	Single ○	Hollow section	❑	❑	❑	❑
	Double ●	Reticular	❑	❑	❑	❑
Curved ○		Other: _____	❑	❑	❑	❑

B4_E) Secondary member typology	Costant section	Variable section	Single section	Composed section
Not identified	○	○	○	○
Solid section	●	❑	●	❑
Hollow section	❑	❑	❑	❑
Reticular	❑	❑	❑	❑
Other: _____	❑	❑	❑	❑

B4_F) Double way system		B4_G) Type of plate / shell	Horizontal		Sloped	
			Cost. sect.	Var. sect.	Cost. sect.	Var. sect.
Horizontal ○		Not identified	○	○	○	○
Sloped ○		Simple layer grid	❑	❑	❑	❑
		Double layer grid	❑	❑	❑	❑
Curved	*Single curvature* ○	Contiunous	❑	❑	❑	❑
	Double curvature ○	Other: _____	❑	❑	❑	❑

B4_G) Closing elements

Not identified	R.C. slab	Skylight	Tiles	Steel sheet	Other
○	❑	❑	●	❑	_____

B5) Foundation

Type of foundation	Not Identified	Presumed	From interview	From drawings	From inspection	Direct / superf. foundation	Indirect / deep foundation
Not identified	○	❑	❑	❑	❑	❑	❑
Isolated plinths	❑	❑	❑	❑	❑	❑	❑
Isolated plinths with connecting beams	❑	❑	❑	❑	❑	❑	❑
Inverse beam grid	❑	❑	❑	●	❑	●	❑
Slabs	❑	❑	❑	❑	❑	❑	❑

Section C: Description of the building

C1) Metrics data

N° total floors with underground ones	Average interstory height (m)	Floor average area (m^2)	
○ 1	○ < 2.50	○ < 200	○ 2500 ÷ 3000
○ 2	○ 2.50 ÷ 3.49	○ 200 ÷ 250	○ 3000 ÷ 3500
○ 3	○ 3.50 ÷ 4.99	○ 250 ÷ 300	○ 3500 ÷ 4000
○ 4	○ 5.00 ÷ 6.99	○ 300 ÷ 400	○ 4000 ÷ 4500
○ 5	○ 7.00 ÷ 9.99	○ 400 ÷ 500	○ 4500 ÷ 5000
○ 6	○ 10 ÷ 14.00	○ 500 ÷ 650	○ 5500 ÷ 6000
Underground floors	○ > 14.00	○ 650 ÷ 900	○ 6000 ÷ 7000
● 0		○ 900 ÷ 1200	○ 7000 ÷ 10000
○ 1		○ 1200 ÷ 1600	○ 10000 ÷ 15000
○ 2		○ 1600 ÷ 2000	○ 15000 ÷ 20000
○ ≥ 3		○ 2000 ÷ 2500	○ > 2000

C2) Age

Construction and renovation age
☐ < 1950
☐ 1950 ÷ 61
☐ 1962 ÷ 71
☐ 1972 ÷ 75
☐ 1976 ÷ 81
☐ 1982 ÷ 86
☐ 1987 ÷ 91
☐ 1992 ÷ 96
☐ 1997 ÷ 01
☐ 2002 ÷ 08
☐ 2009 ÷ 11
● > 2011

C3) Use - Exposure

Use	Use - Exposure
☐ Residential	● > 65%
☐ Productive	○ 30 ÷ 65%
☐ Commercial	○ < 30%
☐ Offices	○ Not used
● Public utility activities	○ In costruction
☐ Storehouses	○ Not finished
☐ Strategic	○ Abandoned
☐ Tourist	**Ownership**
☐ Parking aerea	☐ Public ☐ Private
☐ Exposition space	|_1_|_0_|_0_| % |__|__|__| %
☐ Sport facilities	

C4) Plan and section

Section D: Characterization of the structural members

D1) Typology

❑ Column	❑ Strut
● Primary beam	❑ Diagonal
❑ Secondary beam	❑ King post
❑ Brace	❑ Tie
❑ Plank	❑ Other:_____
❑ Panel	
❑ Other:_____	

D2) Material

- ❑ Massive timber
- ● Glulam timber
- ❑ CLT
- ❑ MDF
- ❑ OSB
- ❑ LVL
- ❑ Other:_____

D3) Timber species

● Softwood — **Norway Spruce *(Picea abies)***

❍ Hardwood _____

❍ Not recognized _____

D4) Year of construction

❑ < 1950	❑ 1972 ÷ 75	❑ 1987 ÷ 91	❑ 2002 ÷ 08	❑ 2015 ÷ 17
❑ 1950 ÷ 61	❑ 1976 ÷ 81	❑ 1992 ÷ 96	❑ 2009 ÷ 11	❑ 2018 ÷ 20
❑ 1962 ÷ 71	❑ 1982 ÷ 86	❑ 1997 ÷ 01	● 2012 ÷ 14	❑ > 2020

D5) Floor

Above ground

- ● 1
- ❍ 2
- ❍ 3
- ❍ 4
- ❍ 5
- ❍ 6

Underground

- ❍ 0
- ❍ 1
- ❍ 2
- ❍ ≥ 3

D6) Hazard class [335-

	Service condition / Exposure to wetting in service	Moisture Content (M.C.)
❍ 1	Indoor, dry	M.C. < 20%
● 2	Indoor or coovered, not exposed to environmental agents	M.C.occasionaly > 20%
❍ 3	Outdoor, not in contact with the ground, exposed to environmental agents	M.C.frequently > 20%
❍ 4	Outdoor, in contact with the ground and or water	M.C.permanently > 20%
❍ 5	Permanently and regularly immersed in salt water	M.C.permanently > 20%

D7) Average environmental temperature

❑ < 10° ● 10° ÷ 20° ❑ 20° ÷ 30° ❑ > 30°

D8) Class of durability [EN 350-1]

❑ 1 - Very durable ❑ 2 - Durable ❑ 3 - Moderately durable ● 4 - Slightly durable ❑ 5 - Not durable

Section E: Decay effects identification

E1) Colour	E2) Aspect to the touch	E3) Superficial aspect
☐ Dark	☐ Dusty ☐ Wet	● Presence of stripes
● White - yellow		☐ Presence of cracks
☐ Ligth blue	☐ Floury ☐ Soft	☐ Presence of exfoliation
☐ No colour alteration		☐ Thin intact layer
☐ Others _____	☐ Buttery ☐ Others_____	☐ Others_____

E4) Cracks	E5) Presence of holes	E6) Presence of galleries
☐ Longitudinal cracks	☐ Circural shap ☐ Oval shape	☐ Visible galleries
☐ Trasnversal cracks	☐ 1 - 2 mm	☐ Not visible galleries
☐ Superficial cracks 1-3 mm	Holes diameter ☐ 3 - 5 mm	Shape of ☐ Circular
☐ Deep cracks >4 mm	☐ > 5 mm	galleries ☐ Oval
☐ Others_____	☐ Others_____	☐ Others_____

E7) Extent of damage

E8_a) Tools for diagnostic

☐ Core extracting tool ☐ Resistance drilling tool ☐ Penetration tool ● Other: Visual

E8_b) Location

● End zone ○ Middle zone ○ Whole member

E8) Other aspects

☐ Presence of beetles ☐ Presence of timber residuals ☐ Presence of excrement

☐ Presence of mold ☐ Mold smell ☐ Gnawing noise

Other: _____

E9) Presence of existing treatments

☐ Not recognizable ● Superficial treatment ☐ Deep treatment

☐ Other: _____

E10 Moisture content (M.C.)

● M.C.< 20% ☐ 20% < M.C.< 30% ☐ M.C.> 30%

Section F: Decay typology

F1) Biological decay

F1_A) Fungi	❑ Basidiomycetes	❑ Brown caries fungi
		❑ Soft caries fungi
	❑ Ascomycetes	❑ White caries fungi
		❑ Chromogen fungi
F1_B) Xylophagous insects	❑Coleoptera	❑ Cerambycidae
		❑ Anobium
		❑ Lyctus
	❑ Isoptera	❑ Rhinotermitidae / Kalotermitidae

F2) Abiotic decay

- ❑ Decay by marine organisms
- ● Decay by UV radiation
- ❑ Other:_____

Section G: Possible interventions and treatments

G1) Criteria of Interventions

- ❑ Reduction of the enviromental humidity RH < 90%
- ❑ Avoid stagnation and direct contact with water
- ❑ Surface cleaning
- ● Avoid direct exposure to UV radiation
- ❑ Avoid rising damp for capillarity
- ❑ Removal and replacement of degraded parts
- ❑ Replacement, if possible, of the whole timber member, using timber with greater durability class
- ❑ Other_____

G2) Treatments

- ❑ Impregnation with fungicidal substances
- ❑ Fumigation treatment
- ❑ Permethrin and Boron treatments
- ❑ Heat treatment
- ● Other **Superficial treatment against UV radiation. Removal of tinsmiths from the end of the beams in order to prevent**

B.4 Application of the SHA-TS form to the case study " b"

Building location

View of the building with evidence of the investigated member

The investigated member (column)

SHA-TS form

Structura health assessment - Timber Structures

Section A: Identification of municipality and building

DATE 15/04/2021

A1) Building location

Region: Campania — ISTAT Code 06

Province: Caserta — ISTAT Code 061

Municipality: Gioia Sannitica — ISTAT Code 041

A2) Surveyor identification data

Name and surname: Dante Marranzini

Affiliation: University of Naples Federico II

Title: Engineer

Degree: Doctor in Architecture and Building Engineering

Address:

Telephone number:

Mail: dante.marranzini@unina.it

Signature:

A3) Data of the interviewed thecnician *(optional)*

Name and surname:

Affiliation:

Title:

Degree:

Address:

Mail:

Telephone number:

A4) Source of data

- ☐ Documentation / Drawings
- ● On-site survey
- ☐ Interview
- ☐ Others

A5) Identification data of the build

Name of the building or name of its owners	CASE STUDY B
Class of use (NTC18)	○ I Class ● II Class ○ III Class ○ IV Class
Code of use (DPC Italy)	S
Building location as respect to the other buildings	● Isolated ○ Internal ○ At the end ○ At the corner

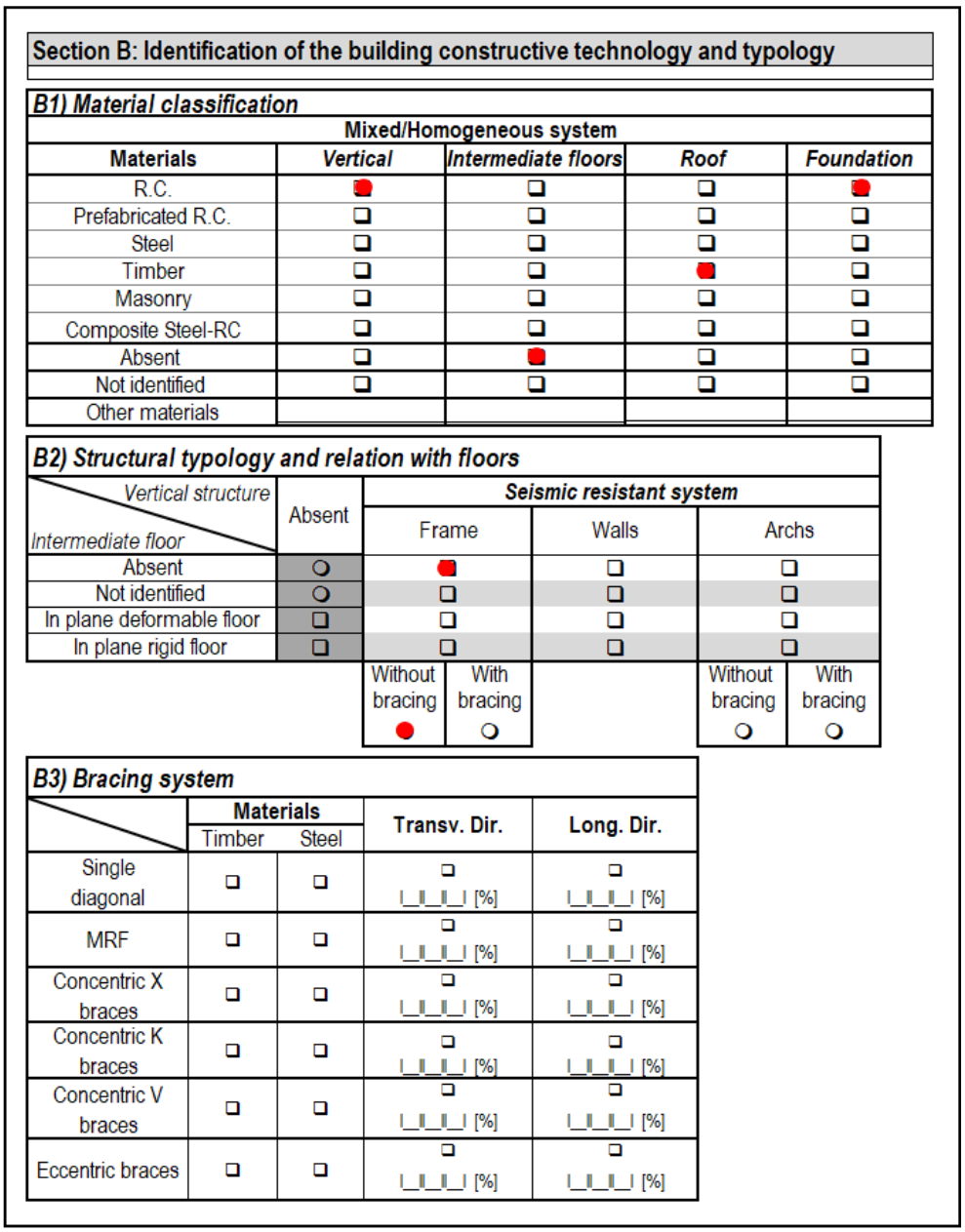

Section B: Identification of the building constructive technology and typology

B1) Material classification

Mixed/Homogeneous system				
Materials	***Vertical***	***Intermediate floors***	***Roof***	***Foundation***
R.C.	●	❑	❑	●
Prefabricated R.C.	❑	❑	❑	❑
Steel	❑	❑	❑	❑
Timber	❑	❑	●	❑
Masonry	❑	❑	❑	❑
Composite Steel-RC	❑	❑	❑	❑
Absent	❑	●	❑	❑
Not identified	❑	❑	❑	❑
Other materials				

B2) Structural typology and relation with floors

Vertical structure / *Intermediate floor*	Absent	***Seismic resistant system***		
		Frame	Walls	Archs
Absent	○	●	❑	❑
Not identified	○	❑	❑	❑
In plane deformable floor	❑	❑	❑	❑
In plane rigid floor	❑	❑	❑	❑
		Without bracing ● / With bracing ○		Without bracing ○ / With bracing ○

B3) Bracing system

	Materials		**Transv. Dir.**	**Long. Dir.**
	Timber	Steel		
Single diagonal	❑	❑	❑ ___ [%]	❑ ___ [%]
MRF	❑	❑	❑ ___ [%]	❑ ___ [%]
Concentric X braces	❑	❑	❑ ___ [%]	❑ ___ [%]
Concentric K braces	❑	❑	❑ ___ [%]	❑ ___ [%]
Concentric V braces	❑	❑	❑ ___ [%]	❑ ___ [%]
Eccentric braces	❑	❑	❑ ___ [%]	❑ ___ [%]

Section B: Identification of the building constructive technology and typology

B4) Roof

B4_A) Deformation characteristics	
Not identified	○
Deformable	●
Rigid	○

B4_B) Number of levels: |__|

Roof bracing system:	YES	NO
	○	●

Simple way system	Double way system	Presence of tie beam	Pushing elements
●	○	YES ○ NO ●	YES ○ NO ●

B4_C) Simple way system		B4_D) Main member typology	Costant section	Variable section	Single section	Composed section
Horizontal ○		Not identified	○	○	○	○
		Solid section	●	❑	●	❑
Sloped	Single ●	Hollow section	❑	❑	❑	❑
	Double ○	Reticular	❑	❑	❑	❑
Curved ○		Other: _____	❑	❑	❑	❑

B4_E) Secondary member typology	Costant section	Variable section	Single section	Composed section
Not identified	○	○	○	○
Solid section	●	❑	●	❑
Hollow section	❑	❑	❑	❑
Reticular	❑	❑	❑	❑
Other: _____	❑	❑	❑	❑

B4_F) Double way system		B4_G) Type of plate / shell	Horizontal		Sloped	
			Cost. sect.	Var. sect.	Cost. sect.	Var. sect.
Horizontal ○		Not identified	○	○	○	○
Sloped ○		Simple layer grid	❑	❑	❑	❑
		Double layer grid	❑	❑	❑	❑
Curved	*Single curvature* ○	Contiunous	❑	❑	❑	❑
	Double curvature ○	Other: _____	❑	❑	❑	❑

B4_G) Closing elements

Not identified	R.C. slab	Skylight	Tiles	Steel sheet	Other
○	❑	❑	●	●	_____

B5) Foundation

Type of foundation	Not Identified	Presumed	From interview	From drawings	From inspection	Direct / superf. foundation	Indirect / deep foundation
Not identified	○	❑	❑	❑	❑	❑	❑
Isolated plinths	❑	❑	❑	❑	❑	❑	❑
Isolated plinths with connecting beams	❑	❑	❑	❑	❑	❑	❑
Inverse beam grid	❑	❑	❑	●	❑	●	❑
Slabs	❑	❑	❑	❑	❑	❑	❑

Section C: Description of the building

C1) Metrics data

N° total floors with underground ones	Average interstory height (m)	Floor average area (m^2)	
○ 1	○ < 2.50	○ < 200	○ 2500 ÷ 3000
○ 2	○ 2.50 ÷ 3.49	○ 200 ÷ 250	○ 3000 ÷ 3500
○ 3	○ 3.50 ÷ 4.99	○ 250 ÷ 300	○ 3500 ÷ 4000
○ 4	○ 5.00 ÷ 6.99	○ 300 ÷ 400	○ 4000 ÷ 4500
○ 5	○ 7.00 ÷ 9.99	○ 400 ÷ 500	○ 4500 ÷ 5000
○ 6	○ 10 ÷ 14.00	○ 500 ÷ 650	○ 5500 ÷ 6000
Underground floors	○ > 14.00	○ 650 ÷ 900	○ 6000 ÷ 7000
○ 0		○ 900 ÷ 1200	○ 7000 ÷ 10000
○ 1		○ 1200 ÷ 1600	○ 10000 ÷ 15000
○ 2		○ 1600 ÷ 2000	○ 15000 ÷ 20000
○ ≥ 3		○ 2000 ÷ 2500	○ > 2000

C2) Age

Construction and renovation age
☐ < 1950
☐ 1950 ÷ 61
☐ 1962 ÷ 71
☐ 1972 ÷ 75
☐ 1976 ÷ 81
☐ 1982 ÷ 86
☐ 1987 ÷ 91
☐ 1992 ÷ 96
☐ 1997 ÷ 01
☐ 2002 ÷ 08
☐ 2009 ÷ 11
● > 2011

C3) Use - Exposure

Use	Use - Exposure
☐ Residential	● > 65%
☐ Productive	○ 30 ÷ 65%
☐ Commercial	○ < 30%
☐ Offices	○ Not used
● Public utility activities	○ In costruction
☐ Storehouses	○ Not finished
☐ Strategic	○ Abandoned
☐ Tourist	**Ownership**
☐ Parking aerea	● Public ☐ Private
☐ Exposition space	|_1_|_0_|_0_| % |__|__|__| %
☐ Sport facilities	

C4) Plan and section

Section D: Characterization of the structural members

D1) Typology

● Column	❑ Strut
❑ Primary beam	❑ Diagonal
❑ Secondary beam	❑ King post
❑ Brace	❑ Tie
❑ Plank	❑ Other:_____
❑ Panel	
❑ Other:_____	

D2) Material

- ❑ Massive timber
- ● Glulam timber
- ❑ CLT
- ❑ MDF
- ❑ OSB
- ❑ LVL
- ❑ Other:_____

D3) Timber species

● Softwood — **Norway Spruce *(Picea abies)***

○ Hardwood _____

○ Not recognized _____

D4) Year of construction

❑ < 1950	❑ 1972 ÷ 75	❑ 1987 ÷ 91	❑ 2002 ÷ 08	❑ 2015 ÷ 17
❑ 1950 ÷ 61	❑ 1976 ÷ 81	❑ 1992 ÷ 96	❑ 2009 ÷ 11	❑ 2018 ÷ 20
❑ 1962 ÷ 71	❑ 1982 ÷ 86	❑ 1997 ÷ 01	● 2012 ÷ 14	❑ > 2020

D5) Floor

Above ground

- ● 1
- ○ 2
- ○ 3
- ○ 4
- ○ 5
- ○ 6

Underground

- ○ 0
- ○ 1
- ○ 2
- ○ ≥ 3

D6) Hazard class [335-

	Service condition / Exposure to wetting in service	Moisture Content (M.C.)
○ 1	Indoor, dry	M.C. < 20%
○ 2	Indoor or coovered, not exposed to environmental agents	M.C.occasionaly > 20%
● 3	Outdoor, not in contact with the ground, exposed to environmental agents	M.C.frequently > 20%
○ 4	Outdoor, in contact with the ground and or water	M.C.permanently > 20%
○ 5	Permanently and regularly immersed in salt water	M.C.permanently > 20%

D7) Average environmental temperature

❑ < 10° ● 10° ÷ 20° ❑ 20° ÷ 30° ❑ > 30°

D8) Class of durability [EN 350-1]

❑ 1 - Very durable ❑ 2 - Durable ❑ 3 - Moderately durable ● 4 - Slightly durable ❑ 5 - Not durable

Section E: Decay effects identification

E1) Colour	E2) Aspect to the touch	E3) Superficial aspect
● Dark	❑ Dusty ● Wet	❑ Presence of stripes
❑ White - yellow		❑ Presence of cracks
❑ Ligth blue	❑ Floury ❑ Soft	● Presence of exfoliation
❑ No colour alteration		❑ Thin intact layer
❑ Others _____	❑ Buttery ❑ Others_____	❑ Others_____

E4) Cracks	E5) Presence of holes	E6) Presence of galleries
❑ Longitudinal cracks	❑ Circural shap ❑ Oval shape	❑ Visible galleries
❑ Trasnversal cracks	❑ 1 - 2 mm	❑ Not visible galleries
❑ Superficial cracks 1-3 mm	Holes diameter ❑ 3 - 5 mm	Shape of ❑ Circular
❑ Deep cracks >4 mm	❑ > 5 mm	galleries ❑ Oval
❑ Others_____	❑ Others_____	❑ Others_____

E7) Extent of damage

E8_a) Tools for diagnostic

❑ Core extracting tool ❑ Resistance drilling tool ❑ Penetration tool ❑ Other: Visual

E8_b) Location

❍ End zone ❍ Middle zone ● Whole member

E8) Other aspects

❑ Presence of beetles ❑ Presence of timber residuals ❑ Presence of excrement

❑ Presence of mold ❑ Mold smell ❑ Gnawing noise

Other: _____

E9) Presence of existing treatments

❑ Not recognizable ● Superficial treatment ❑ Deep treatment

❑ Other: _____

E10 Moisture content (M.C.)

● M.C.< 20% ❑ 20% < M.C.< 30% ❑ M.C.> 30%

Section F: Decay typology

F1) Biological decay

F1_A) Fungi	❑ Basidiomycetes	❑ Brown caries fungi
		❑ Soft caries fungi
	❑ Ascomycetes	❑ White caries fungi
		❑ Chromogen fungi
F1_B) Xylophagous insects	❑ Coleoptera	❑ Cerambycidae
		❑ Anobium
		❑ Lyctus
	❑ Isoptera	❑ Rhinotermitidae / Kalotermitidae

F2) Abiotic decay

- ❑ Decay by marine organisms
- ● Decay by UV radiation
- ❑ Other:_____

Section G: Possible interventions and treatments

G1) Criteria of Interventions	G2) Treatments
❑ Reduction of the enviromental humidity RH < 90%	● Impregnation with fungicidal substances
❑ Avoid stagnation and direct contact with water	❑ Fumigation treatment
❑ Surface cleaning	❑ Permethrin and Boron treatments
● Avoid direct exposure to UV radiation	❑ Heat treatment
❑ Avoid rising damp for capillarity	● Other_**Superficial treatment against UV radiation**
❑ Removal and replacement of degraded parts	
❑ Replacement, if possible, of the whole timber member, using timber with greater durability class	
❑ Other_____	

B.5 Application of the SHA-TS form to the case study " c"

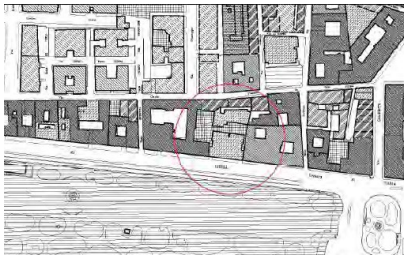

Building location

View of the building with evidence of the investigated member

The investigated member (floor beam)

SHA-TS form

Structura health assessment - Timber Structures

Section A: Identification of municipality and building

DATE | 1 | 5 | / | 0 | 4 | / | 2 | 0 | 2 | 1 |

A1) Building location

Region: Campania — ISTAT Code | 0 | 6 |

Province: Naples — ISTAT Code | 0 | 6 | 3 |

Municipality: Naples — ISTAT Code | 0 | 4 | 9 |

A2) Surveyor identification data

Name and surname: Dante Marranzini

Affiliation: University of Naples Federico II

Title: Engineer

Degree: Doctor in Architecture and Building Engineering

Address: _____

Telephone number: _____

Mail: dante.marranzini@unina.it

Signature: _____

A3) Data of the interviewed thecnician *(optional)*

Name and surname: Prof. Maurizio Nicolella

Affiliation: _____

Title: _____

Degree: _____

Address: _____

Mail: _____

Telephone number: _____

A4) Source of data

❑ Documentation / Drawings

❑ On-site survey

❑ Interview

❑ Others _____

A5) Identification data of the buildi

Name of the building or name of its owners	|C|A|S|E|_|S|T|U|D|Y|_|C|_|_|_|_|_|_|_|
Class of use (NTC18)	❍ I Class ● II Class ❍ III Class ❍ IV Class
Code of use (DPC Italy)	|_S_|_|_|
Building location as respect to the other buildings	● Isolated ❍ Internal ❍ At the end ❍ At the corner

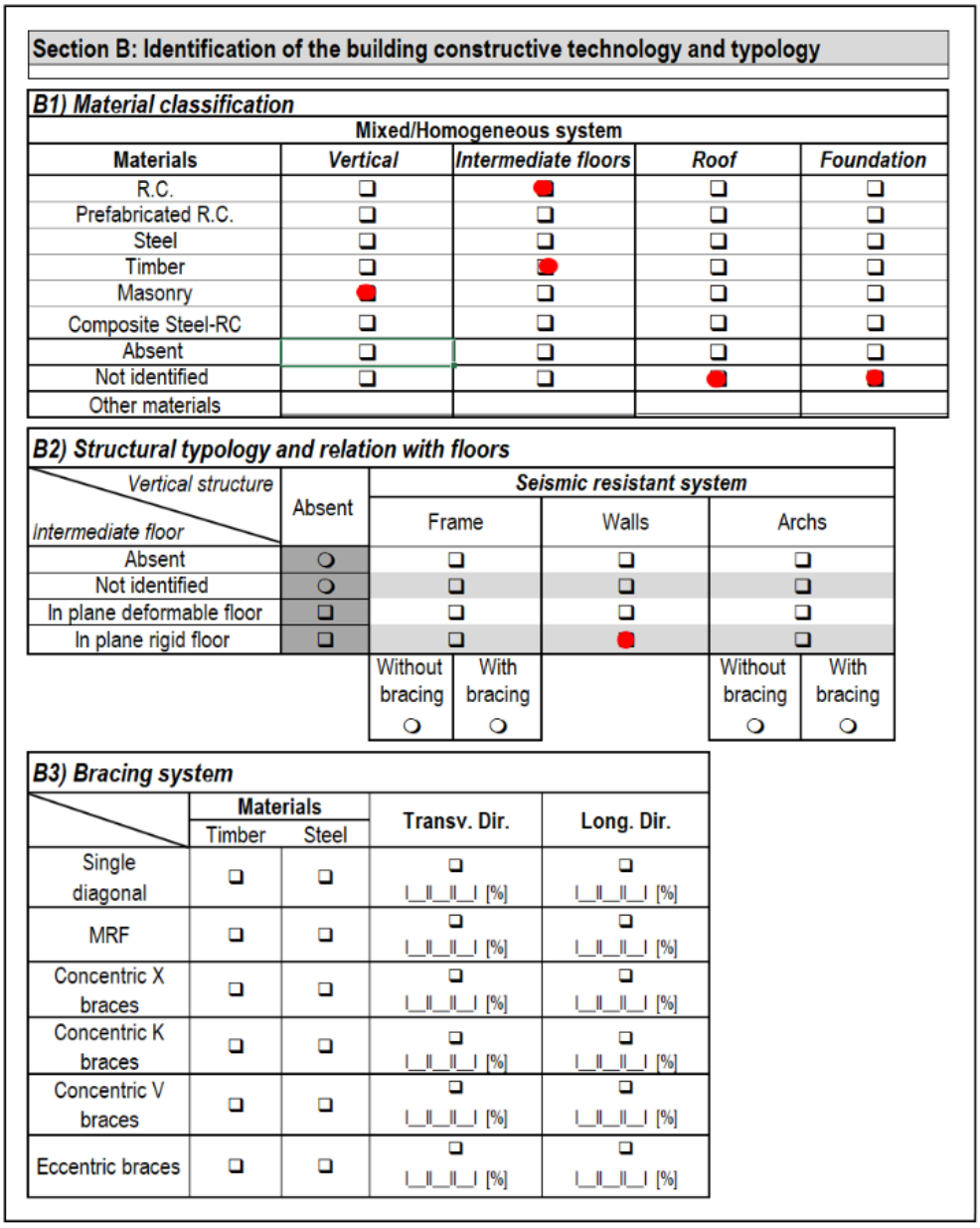

Section B: Identification of the building constructive technology and typology

B1) Material classification

Mixed/Homogeneous system

Materials	*Vertical*	*Intermediate floors*	*Roof*	*Foundation*
R.C.	❑	●	❑	❑
Prefabricated R.C.	❑	❑	❑	❑
Steel	❑	❑	❑	❑
Timber	❑	●	❑	❑
Masonry	●	❑	❑	❑
Composite Steel-RC	❑	❑	❑	❑
Absent	❑	❑	❑	❑
Not identified	❑	❑	●	●
Other materials				

B2) Structural typology and relation with floors

Vertical structure / *Intermediate floor*	Absent	*Seismic resistant system*				
		Frame		Walls	Archs	
Absent	○	❑		❑	❑	
Not identified	○	❑		❑	❑	
In plane deformable floor	❑	❑		❑	❑	
In plane rigid floor	❑	❑		●	❑	
		Without bracing ○	With bracing ○		Without bracing ○	With bracing ○

B3) Bracing system

	Materials		Transv. Dir.	Long. Dir.
	Timber	Steel		
Single diagonal	❑	❑	❑ ___ [%]	❑ ___ [%]
MRF	❑	❑	❑ ___ [%]	❑ ___ [%]
Concentric X braces	❑	❑	❑ ___ [%]	❑ ___ [%]
Concentric K braces	❑	❑	❑ ___ [%]	❑ ___ [%]
Concentric V braces	❑	❑	❑ ___ [%]	❑ ___ [%]
Eccentric braces	❑	❑	❑ ___ [%]	❑ ___ [%]

Section B: Identification of the building constructive technology and typology

B4) Intermediate floor

B4_A) Deformation characteristics		B4_B) Number of levels: |__|		Simple way system	Double way system	Presence of tie beam	Pushing elements
Not identified	○							
Deformable	○	Floor bracing system:	YES ○	NO ●	●	○	YES ○ NO ●	YES ○ NO ●
Rigid	●							

B4_C) Simple way system	B4_D) Main member typology	Costant section	Variable section	Single section	Composed section
Horizontal	Not identified	○	○	○	○
	Solid section	●	❑	●	❑
	Hollow section	❑	❑	❑	❑
	Reticular	❑	❑	❑	❑
	Other: _____	❑	❑	❑	❑

B4_E) Secondary member typology	Costant section	Variable section	Single section	Composed section
Not identified	○	○	○	○
Solid section	●	❑	●	❑
Hollow section	❑	❑	❑	❑
Reticular	❑	❑	❑	❑
Other: _____	❑	❑	❑	❑

B4_F) Double way system		B4_G) Type of plate / shell	Horizontal		Sloped	
			Cost. sect.	Var. sect.	Cost. sect.	Var. sect.
Horizontal ○		Not identified	○	○	○	○
Sloped ○		Simple layer grid	❑	❑	❑	❑
		Double layer grid	❑	❑	❑	❑
Curved	Single curvature ○	Contiunous	❑	❑	❑	❑
	Double curvature ○	Other: _____	❑	❑	❑	❑

B5) Foundation

Type of foundation	Not Identified	Presumed	From interview	From drawings	From inspection	Direct / superf. foundation	Indirect / deep foundation
Not identified	●	❑	❑	❑	❑	❑	❑
Isolated plinths	❑	❑	❑	❑	❑	❑	❑
Isolated plinths with connecting beams	❑	❑	❑	❑	❑	❑	❑
Inverse beam grid	❑	❑	❑	❑	❑	❑	❑
Slabs	❑	❑	❑	❑	❑	❑	❑

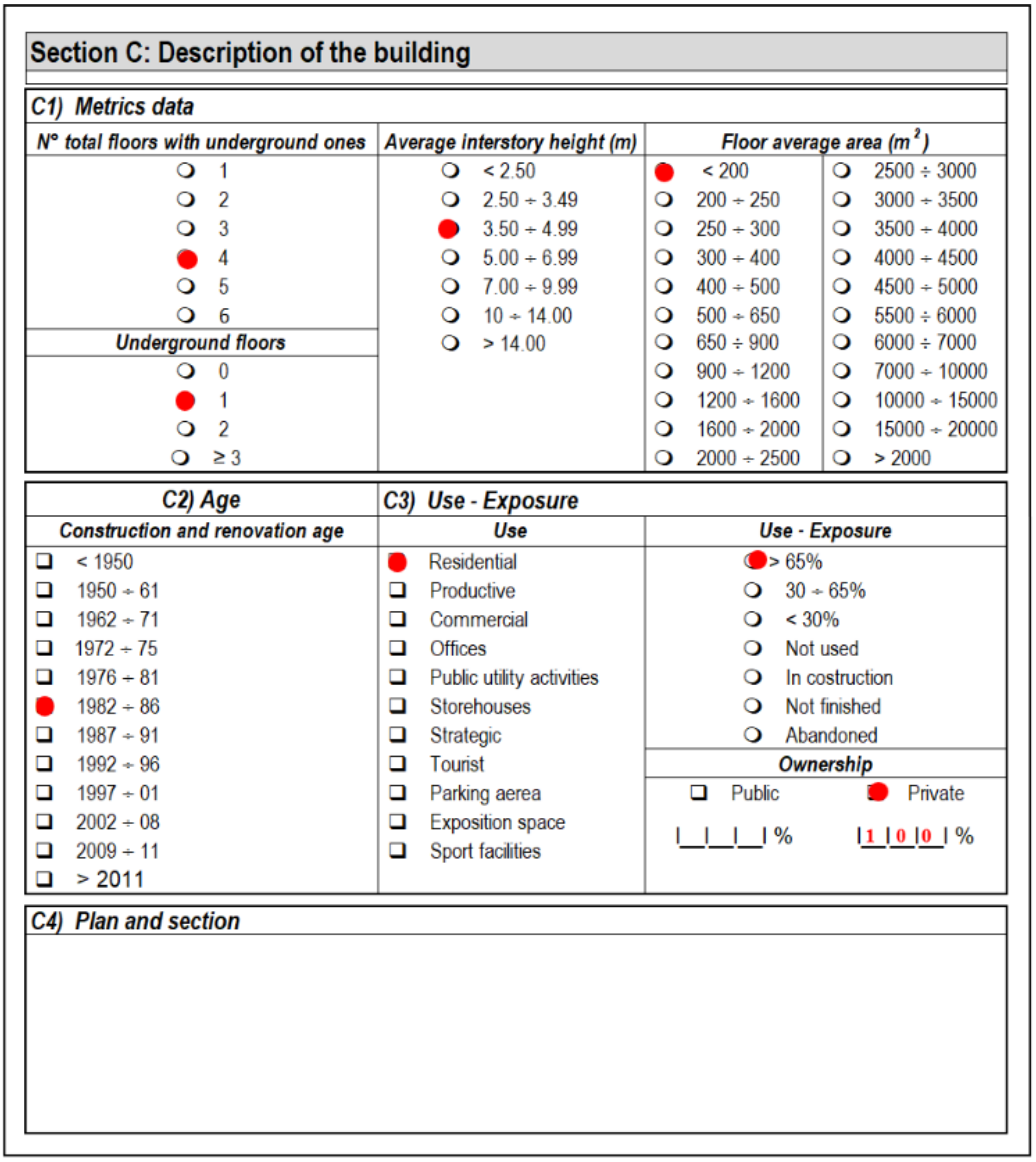

Section C: Description of the building

C1) Metrics data

N° total floors with underground ones	Average interstory height (m)	Floor average area (m^2)	
○ 1	○ < 2.50	● < 200	○ 2500 ÷ 3000
○ 2	○ 2.50 ÷ 3.49	○ 200 ÷ 250	○ 3000 ÷ 3500
○ 3	● 3.50 ÷ 4.99	○ 250 ÷ 300	○ 3500 ÷ 4000
● 4	○ 5.00 ÷ 6.99	○ 300 ÷ 400	○ 4000 ÷ 4500
○ 5	○ 7.00 ÷ 9.99	○ 400 ÷ 500	○ 4500 ÷ 5000
○ 6	○ 10 ÷ 14.00	○ 500 ÷ 650	○ 5500 ÷ 6000
Underground floors	○ > 14.00	○ 650 ÷ 900	○ 6000 ÷ 7000
○ 0		○ 900 ÷ 1200	○ 7000 ÷ 10000
● 1		○ 1200 ÷ 1600	○ 10000 ÷ 15000
○ 2		○ 1600 ÷ 2000	○ 15000 ÷ 20000
○ ≥ 3		○ 2000 ÷ 2500	○ > 2000

C2) Age

Construction and renovation age

- ❑ < 1950
- ❑ 1950 ÷ 61
- ❑ 1962 ÷ 71
- ❑ 1972 ÷ 75
- ❑ 1976 ÷ 81
- ● 1982 ÷ 86
- ❑ 1987 ÷ 91
- ❑ 1992 ÷ 96
- ❑ 1997 ÷ 01
- ❑ 2002 ÷ 08
- ❑ 2009 ÷ 11
- ❑ > 2011

C3) Use - Exposure

Use	Use - Exposure
● Residential	● > 65%
❑ Productive	○ 30 ÷ 65%
❑ Commercial	○ < 30%
❑ Offices	○ Not used
❑ Public utility activities	○ In costruction
❑ Storehouses	○ Not finished
❑ Strategic	○ Abandoned
❑ Tourist	**Ownership**
❑ Parking aerea	❑ Public ● Private
❑ Exposition space	|__|__|__| % |1|0|0| %
❑ Sport facilities	

C4) Plan and section

Section D: Characterization of the structural members

D1) Typology

❑ Column	❑ Strut
● Primary beam	❑ Diagonal
❑ Secondary beam	❑ King post
❑ Brace	❑ Tie
● Plank	❑ Other:_____
❑ Panel	
❑ Other:_____	

D2) Material

- ● Massive timber
- ❑ Glulam timber
- ❑ CLT
- ❑ MDF
- ❑ OSB
- ❑ LVL
- ❑ Other:_____

D3) Timber species

● Softwood — **Silver fir *(Abies alba)***

❍ Hardwood _____

❍ Not recognized _____

D4) Year of construction

❑ < 1950	❑ 1972 ÷ 75	❑ 1987 ÷ 91	❑ 2002 ÷ 08	❑ 2015 ÷ 17
❑ 1950 ÷ 61	❑ 1976 ÷ 81	❑ 1992 ÷ 96	❑ 2009 ÷ 11	❑ 2018 ÷ 20
❑ 1962 ÷ 71	● 1982 ÷ 86	❑ 1997 ÷ 01	❑ 2012 ÷ 14	❑ > 2020

D5) Floor

Above ground

- ● 1
- ❍ 2
- ❍ 3
- ❍ 4
- ❍ 5
- ❍ 6

Underground

- ❍ 0
- ❍ 1
- ❍ 2
- ❍ ≥ 3

D6) Hazard class [335-1]	Service condition / Exposure to wetting in service	Moisture Content (M.C.)
● 1	Indoor, dry	M.C. < 20%
❍ 2	Indoor or coovered, not exposed to environmental agents	M.C.occasionaly > 20%
❍ 3	Outdoor, not in contact with the ground, exposed to environmental agents	M.C.frequently > 20%
❍ 4	Outdoor, in contact with the ground and or water	M.C.permanently > 20%
❍ 5	Permanently and regularly immersed in salt water	M.C.permanently > 20%

D7) Average environmental temperature

❑ < 10° ❑ 10° ÷ 20° ● 20° ÷ 30° ❑ > 30°

D8) Class of durability [EN 350-1]

❑ 1 - Very durable ❑ 2 - Durable ❑ 3 - Moderately durable ● 4 - Slightly durable ❑ 5 - Not durable

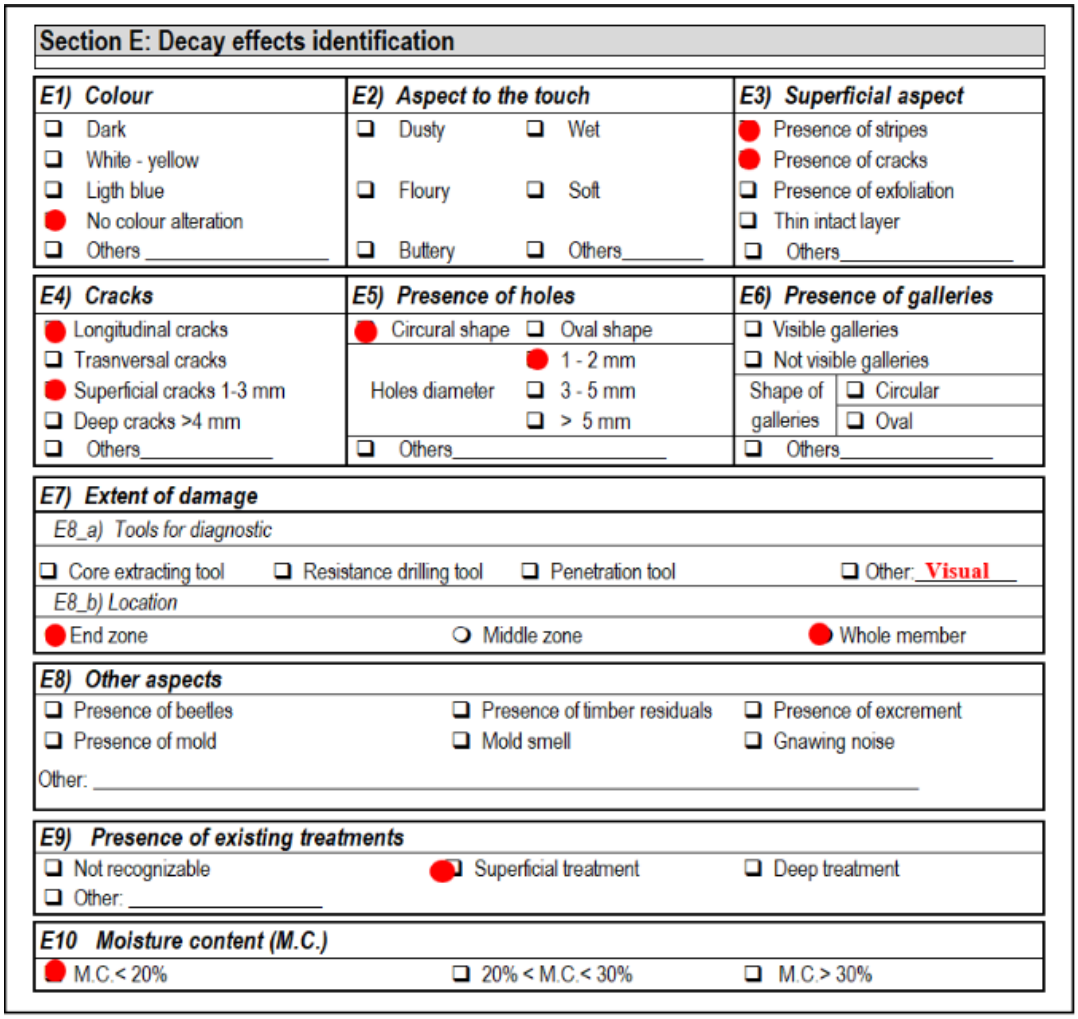

Section E: Decay effects identification

E1) Colour	***E2) Aspect to the touch***	***E3) Superficial aspect***
❑ Dark	❑ Dusty ❑ Wet	● Presence of stripes
❑ White - yellow		● Presence of cracks
❑ Ligth blue	❑ Floury ❑ Soft	❑ Presence of exfoliation
● No colour alteration		❑ Thin intact layer
❑ Others _____	❑ Buttery ❑ Others_____	❑ Others_____

E4) Cracks	***E5) Presence of holes***	***E6) Presence of galleries***
● Longitudinal cracks	● Circural shape ❑ Oval shape	❑ Visible galleries
❑ Trasnversal cracks		❑ Not visible galleries
● Superficial cracks 1-3 mm	Holes diameter ❑ 1 - 2 mm ❑ 3 - 5 mm ❑ > 5 mm	Shape of galleries ❑ Circular ❑ Oval
❑ Deep cracks >4 mm		
❑ Others_____	❑ Others_____	❑ Others_____

E7) Extent of damage

E8_a) Tools for diagnostic

❑ Core extracting tool ❑ Resistance drilling tool ❑ Penetration tool ❑ Other: Visual

E8_b) Location

● End zone ❍ Middle zone ● Whole member

E8) Other aspects

❑ Presence of beetles ❑ Presence of timber residuals ❑ Presence of excrement
❑ Presence of mold ❑ Mold smell ❑ Gnawing noise

Other: _____

E9) Presence of existing treatments

❑ Not recognizable ● Superficial treatment ❑ Deep treatment
❑ Other: _____

E10 Moisture content (M.C.)

● M.C.< 20% ❑ 20% < M.C.< 30% ❑ M.C.> 30%

Section F: Decay typology

F1) Biological decay

F1_A) Fungi	❑ Basidiomycetes	❑ Brown caries fungi
		❑ Soft caries fungi
	❑ Ascomycetes	❑ White caries fungi
		❑ Chromogen fungi
F1_B) Xylophagous insects	❑ Coleoptera	❑ Cerambycidae
		❑ Anobium
		● Lyctus
	❑ Isoptera	❑ Rhinotermitidae / Kalotermitidae

F2) Abiotic decay

- ❑ Decay by marine organisms
- ❑ Decay by UV radiation
- ❑ Other:_____

Section G: Possible interventions and treatments

G1) Criteria of Interventions	***G2) Treatments***
❑ Reduction of the enviromental humidity RH < 90%	❑ Impregnation with fungicidal substances
❑ Avoid stagnation and direct contact with water	❑ Fumigation treatment
● Surface cleaning	● Permethrin and Boron treatments
❑ Avoid direct exposure to UV radiation	❑ Heat treatment
❑ Avoid rising damp for capillarity	❑ Other_____
❑ Removal and replacement of degraded parts	
❑ Replacement, if possible, of the whole timber member, using timber with greater durability class	
❑ Other_____	

B.5 Application of the SHA-TS form to the case study " d"

Building location

View of the building with evidence of the investigated member

The investigated member (floor beam)

SHA-TS form

Structura health assessment - Timber Structures

Section A: Identification of municipality and building

DATE | 1 | 5 | / | 0 | 4 | / | 2 | 0 | 2 | 1 |

A1) Building location

Region: Campania — ISTAT Code | 0 | 6 |

Province: Naples — ISTAT Code | 0 | 6 | 3 |

Municipality: Naples — ISTAT Code | 0 | 4 | 9 |

A2) Surveyor identification data

Name and surname: Dante Marranzini

Affiliation: University of Naples Federico II

Title: Engineer

Degree: Doctor in Architecture and Building Engineering

Address:

Telephone number:

Mail: dante.marranzini@unina.it

Signature:

A3) Data of the interviewed thecnician *(optional)*

Name and surname: Prof. Maurizio Nicolella

Affiliation:

Title:

Degree:

Address:

Mail:

Telephone number:

A4) Source of data

- ☐ Documentation / Drawings
- ☐ On-site survey
- ● Interview
- ☐ Others

A5) Identification data of the buildi

Name of the building or name of its owners	|C|A|S|E|_|S|T|U|D|Y|_|D|_|_|_|_|_|_|_|
Class of use (NTC18)	● I Class ○ II Class ○ III Class ○ IV Class
Code of use (DPC Italy)	|_S_|_|_|
Building location as respect to the other buildings	● Isolated ○ Internal ○ At the end ○ At the corner

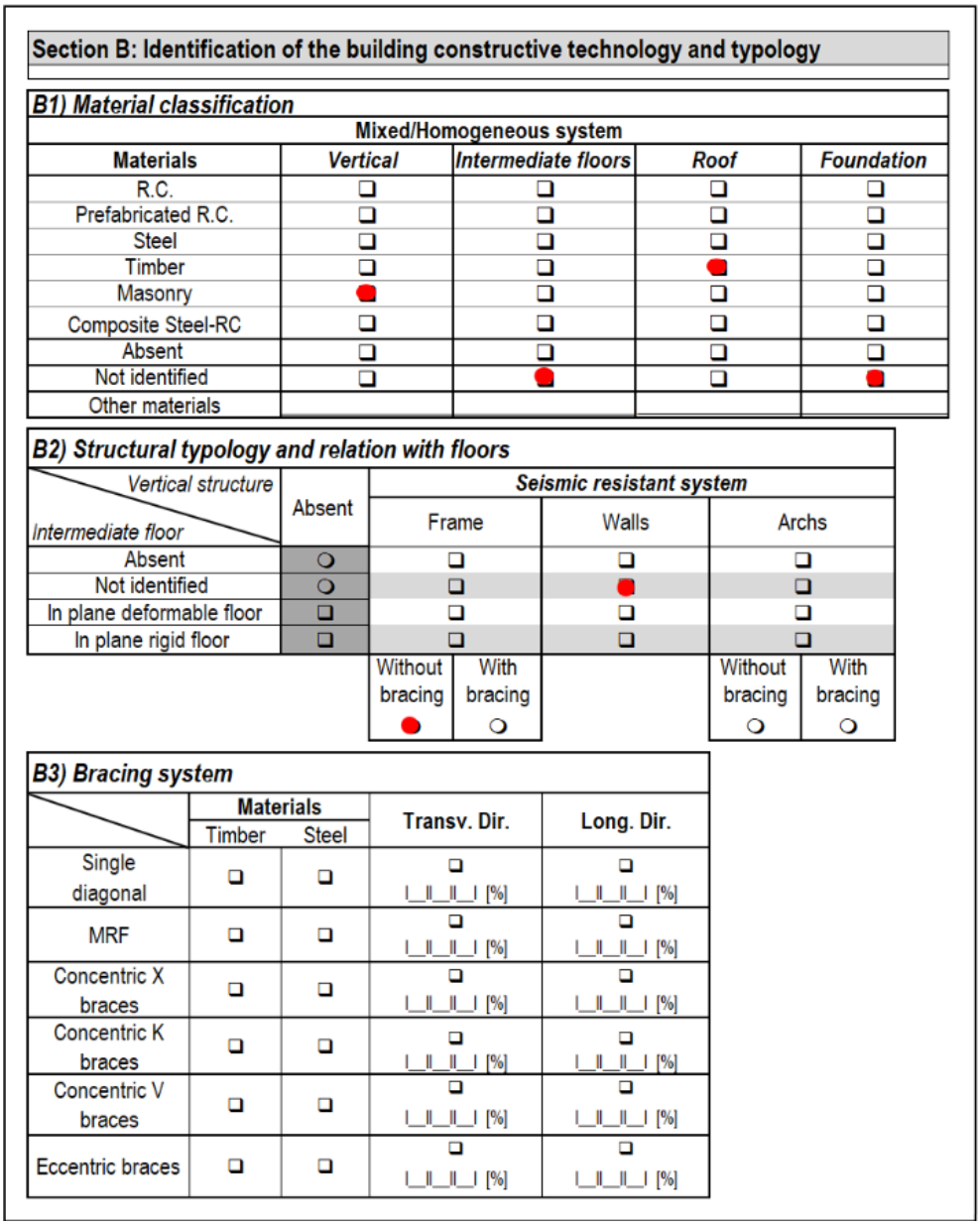

Section B: Identification of the building constructive technology and typology

B1) Material classification

Mixed/Homogeneous system

Materials	*Vertical*	*Intermediate floors*	*Roof*	*Foundation*
R.C.	❑	❑	❑	❑
Prefabricated R.C.	❑	❑	❑	❑
Steel	❑	❑	❑	❑
Timber	❑	❑	●	❑
Masonry	●	❑	❑	❑
Composite Steel-RC	❑	❑	❑	❑
Absent	❑	❑	❑	❑
Not identified	❑	●	❑	●
Other materials				

B2) Structural typology and relation with floors

Vertical structure / *Intermediate floor*	Absent	*Seismic resistant system*		
		Frame	Walls	Archs
Absent	○	❑	❑	❑
Not identified	○	❑	●	❑
In plane deformable floor	❑	❑	❑	❑
In plane rigid floor	❑	❑	❑	❑
		Without bracing ● / With bracing ○		Without bracing ○ / With bracing ○

B3) Bracing system

	Materials		Transv. Dir.	Long. Dir.
	Timber	Steel		
Single diagonal	❑	❑	❑ ___ [%]	❑ ___ [%]
MRF	❑	❑	❑ ___ [%]	❑ ___ [%]
Concentric X braces	❑	❑	❑ ___ [%]	❑ ___ [%]
Concentric K braces	❑	❑	❑ ___ [%]	❑ ___ [%]
Concentric V braces	❑	❑	❑ ___ [%]	❑ ___ [%]
Eccentric braces	❑	❑	❑ ___ [%]	❑ ___ [%]

Section B: Identification of the building constructive technology and typology

B4) Roof

B4_A) Deformation characteristics	
Not identified	○
Deformable	●
Rigid	○

B4_B) Number of levels: I__I

Roof bracing system:	YES	NO
	○	●

	Simple way system	Double way system	Presence of tie beam	Pushing elements
	●	○	YES ● / NO ○	YES ○ / NO ●

B4_C) Simple way system		B4_D) Main member typology	Costant section	Variable section	Single section	Composed section
Horizontal ○		Not identified	○	○	○	○
		Solid section	❑	❑	❑	❑
Sloped	Single ○	Hollow section	❑	❑	❑	❑
	Double ●	Reticular	●	❑	●	❑
Curved ○		Other: _____	❑	❑	❑	❑

B4_E) Secondary member typology	Costant section	Variable section	Single section	Composed section
Not identified	○	○	○	○
Solid section	●	❑	●	❑
Hollow section	❑	❑	❑	❑
Reticular	❑	❑	❑	❑
Other: _____	❑	❑	❑	❑

B4_F) Double way system		B4_G) Type of plate / shell	Horizontal		Sloped	
			Cost. sect.	Var. sect.	Cost. sect.	Var. sect.
Horizontal ○		Not identified	○	○	○	○
Sloped ○		Simple layer grid	❑	❑	❑	❑
		Double layer grid	❑	❑	❑	❑
Curved	*Single curvature* ○	Continuous	❑	❑	❑	❑
	Double curvature ○	Other: _____	❑	❑	❑	❑

B4_G) Closing elements

Not identified	R.C. slab	Skylight	Tiles	Steel sheet	Other
○	❑	❑	●	❑	_____

B5) Foundation

Type of foundation	Not Identified	Presumed	From interview	From drawings	From inspection	Direct / superf. foundation	Indirect / deep foundation
Not identified	●	❑	❑	❑	❑	❑	❑
Isolated plinths	❑	❑	❑	❑	❑	❑	❑
Isolated plinths with connecting beams	❑	❑	❑	❑	❑	❑	❑
Inverse beam grid	❑	❑	❑	❑	❑	❑	❑
Slabs	❑	❑	❑	❑	❑	❑	❑

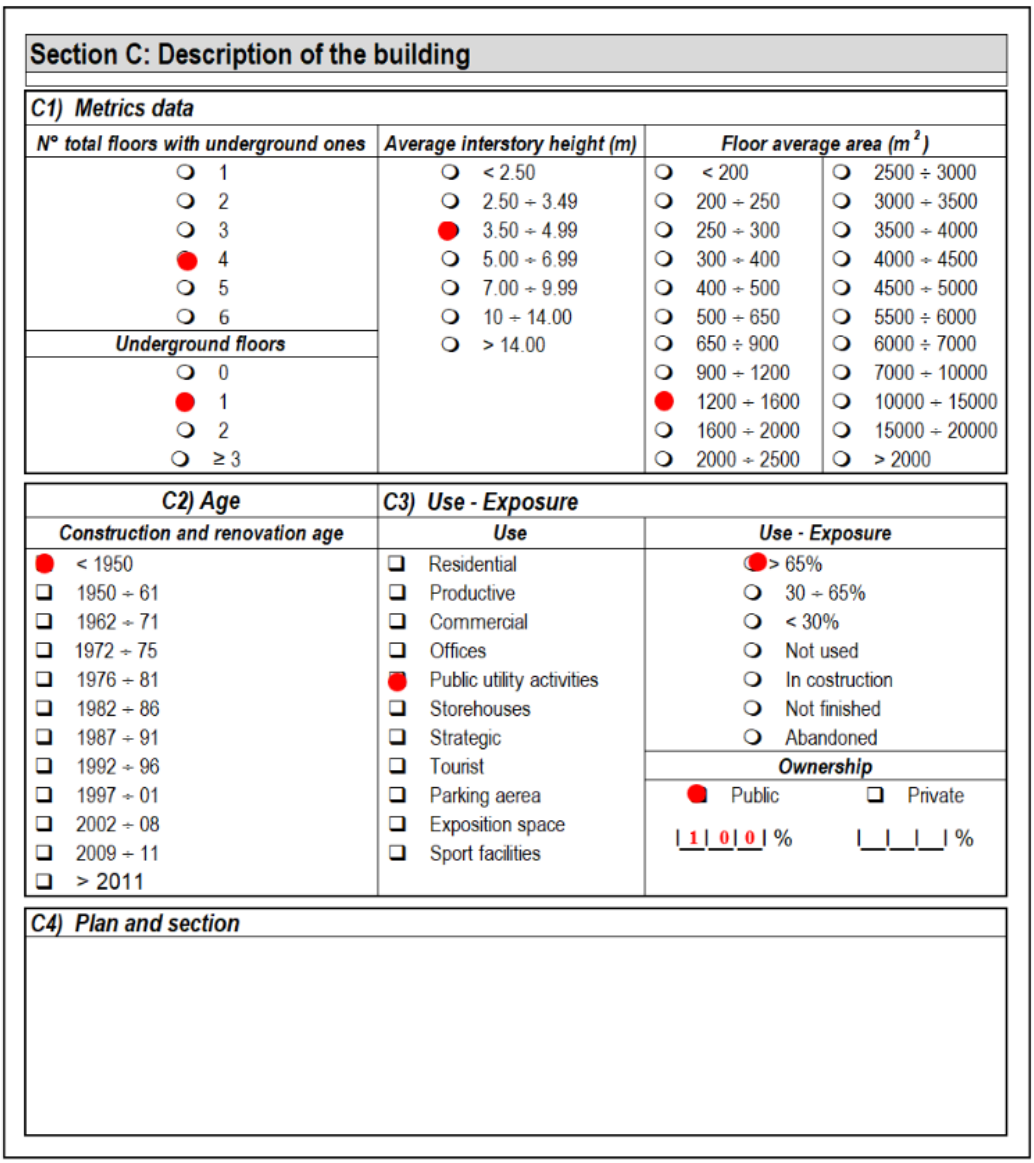

Section C: Description of the building

C1) Metrics data

N° total floors with underground ones

- ○ 1
- ○ 2
- ○ 3
- ● 4
- ○ 5
- ○ 6

Underground floors

- ○ 0
- ● 1
- ○ 2
- ○ ≥ 3

Average interstory height (m)

- ○ < 2.50
- ○ 2.50 ÷ 3.49
- ● 3.50 ÷ 4.99
- ○ 5.00 ÷ 6.99
- ○ 7.00 ÷ 9.99
- ○ 10 ÷ 14.00
- ○ > 14.00

Floor average area (m^2)

○ < 200	○ 2500 ÷ 3000
○ 200 ÷ 250	○ 3000 ÷ 3500
○ 250 ÷ 300	○ 3500 ÷ 4000
○ 300 ÷ 400	○ 4000 ÷ 4500
○ 400 ÷ 500	○ 4500 ÷ 5000
○ 500 ÷ 650	○ 5500 ÷ 6000
○ 650 ÷ 900	○ 6000 ÷ 7000
○ 900 ÷ 1200	○ 7000 ÷ 10000
● 1200 ÷ 1600	○ 10000 ÷ 15000
○ 1600 ÷ 2000	○ 15000 ÷ 20000
○ 2000 ÷ 2500	○ > 2000

C2) Age

Construction and renovation age

- ● < 1950
- ❑ 1950 ÷ 61
- ❑ 1962 ÷ 71
- ❑ 1972 ÷ 75
- ❑ 1976 ÷ 81
- ❑ 1982 ÷ 86
- ❑ 1987 ÷ 91
- ❑ 1992 ÷ 96
- ❑ 1997 ÷ 01
- ❑ 2002 ÷ 08
- ❑ 2009 ÷ 11
- ❑ > 2011

C3) Use - Exposure

Use

- ❑ Residential
- ❑ Productive
- ❑ Commercial
- ❑ Offices
- ● Public utility activities
- ❑ Storehouses
- ❑ Strategic
- ❑ Tourist
- ❑ Parking aerea
- ❑ Exposition space
- ❑ Sport facilities

Use - Exposure

- ● > 65%
- ○ 30 ÷ 65%
- ○ < 30%
- ○ Not used
- ○ In costruction
- ○ Not finished
- ○ Abandoned

Ownership

● Public ❑ Private

1	0	0	%				%

C4) Plan and section

Section D: Characterization of the structural members

D1) Typology		D2) Material
❑ Column	● Strut	● Massive timber
❑ Primary beam	❑ Diagonal	❑ Glulam timber
❑ Secondary beam	❑ King post	❑ CLT
❑ Brace	● Tie	❑ MDF
❑ Plank	❑ Other:_____	❑ OSB
❑ Panel		❑ LVL
❑ Other:_____		❑ Other:_____

D3) Timber species

❍ Softwood ❍ Hardwood ● Not recognized

D4) Year of construction

● < 1950	❑ 1972 ÷ 75	❑ 1987 ÷ 91	❑ 2002 ÷ 08	❑ 2015 ÷ 17
❑ 1950 ÷ 61	❑ 1976 ÷ 81	❑ 1992 ÷ 96	❑ 2009 ÷ 11	❑ 2018 ÷ 20
❑ 1962 ÷ 71	❑ 1982 ÷ 86	❑ 1997 ÷ 01	❑ 2012 ÷ 14	❑ > 2020

D5) Floor

Above ground

❍ 1
❍ 2
❍ 3
● 4
❍ 5
❍ 6

Underground

❍ 0
❍ 1
❍ 2
❍ ≥ 3

D6) Hazard class [335-1]	Service condition / Exposure to wetting in service	Moisture Content (M.C.)
❍ 1	Indoor, dry	M.C. < 20%
● 2	Indoor or coovered, not exposed to environmental agents	M.C.occasionaly > 20%
❍ 3	Outdoor, not in contact with the ground, exposed to environmental agents	M.C.frequently > 20%
❍ 4	Outdoor, in contact with the ground and or water	M.C.permanently > 20%
❍ 5	Permanently and regularly immersed in salt water	M.C.permanently > 20%

D7) Average environmental temperature

❑ < 10° ❑ 10° ÷ 20° ● 20° ÷ 30° ❑ > 30°

D8) Class of durability [EN 350-1]

❑ 1 - Very durable ❑ 2 - Durable ❑ 3 - Moderately durable ❑ 4 - Slightly durable ❑ 5 - Not durable

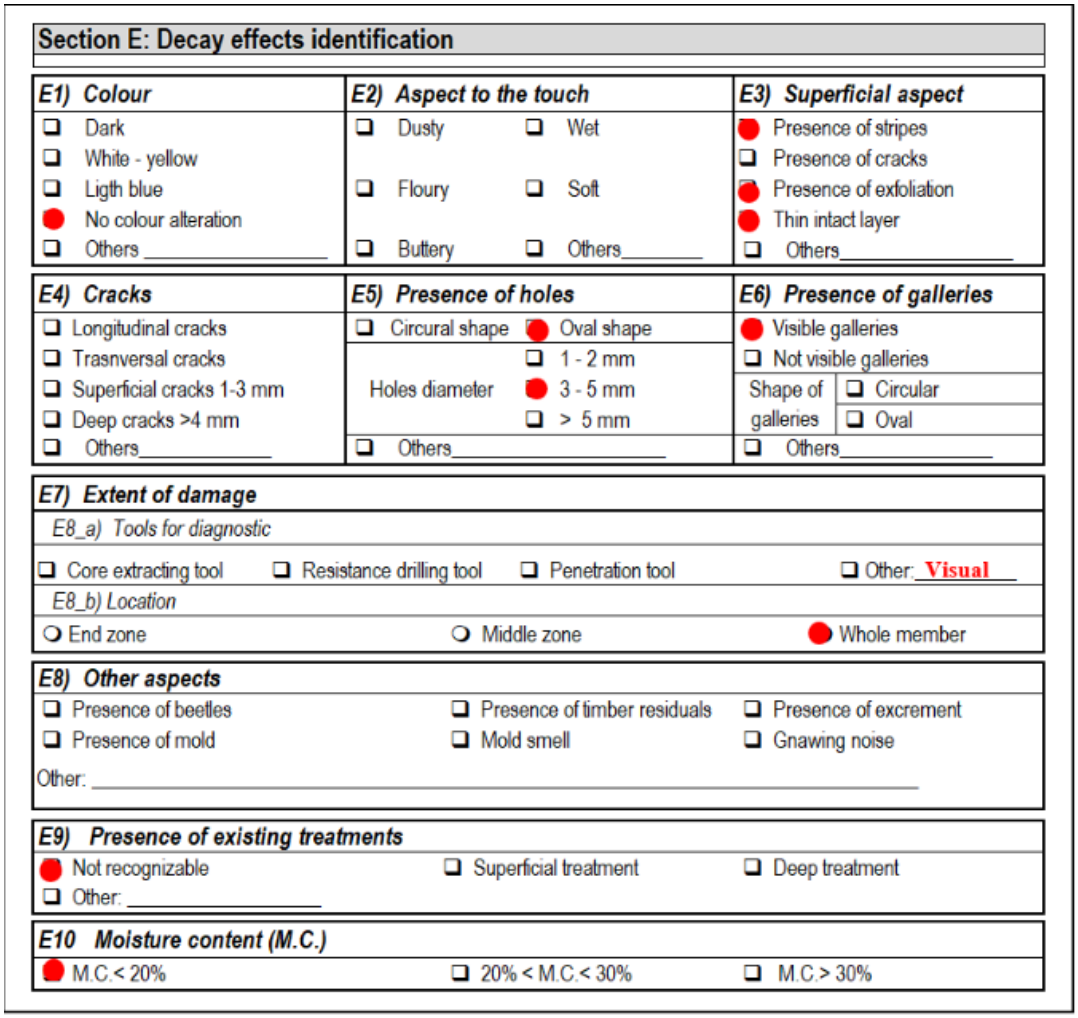

Section E: Decay effects identification

E1) Colour	***E2) Aspect to the touch***	***E3) Superficial aspect***
❑ Dark	❑ Dusty ❑ Wet	● Presence of stripes
❑ White - yellow		❑ Presence of cracks
❑ Ligth blue	❑ Floury ❑ Soft	● Presence of exfoliation
● No colour alteration		● Thin intact layer
❑ Others _____	❑ Buttery ❑ Others_____	❑ Others_____

E4) Cracks	***E5) Presence of holes***	***E6) Presence of galleries***
❑ Longitudinal cracks	❑ Circural shape ● Oval shape	● Visible galleries
❑ Trasnversal cracks	❑ 1 - 2 mm	❑ Not visible galleries
❑ Superficial cracks 1-3 mm	Holes diameter ● 3 - 5 mm	Shape of ❑ Circular
❑ Deep cracks >4 mm	❑ > 5 mm	galleries ❑ Oval
❑ Others_____	❑ Others_____	❑ Others_____

E7) Extent of damage

E8_a) Tools for diagnostic

❑ Core extracting tool ❑ Resistance drilling tool ❑ Penetration tool ❑ Other: Visual

E8_b) Location

○ End zone ○ Middle zone ● Whole member

E8) Other aspects

❑ Presence of beetles ❑ Presence of timber residuals ❑ Presence of excrement
❑ Presence of mold ❑ Mold smell ❑ Gnawing noise

Other: _____

E9) Presence of existing treatments

● Not recognizable ❑ Superficial treatment ❑ Deep treatment
❑ Other: _____

E10 Moisture content (M.C.)

● M.C.< 20% ❑ 20% < M.C.< 30% ❑ M.C.> 30%

Section F: Decay typology

F1) Biological decay

F1_A) Fungi	❑ Basidiomycetes	❑ Brown caries fungi
		❑ Soft caries fungi
	❑ Ascomycetes	❑ White caries fungi
		❑ Chromogen fungi
F1_B) Xylophagous insects	● Coleoptera	● Cerambycidae
		● Anobium
		❑ Lyctus
	❑ Isoptera	❑ Rhinotermitidae / Kalotermitidae

F2) Abiotic decay

- ❑ Decay by marine organisms
- ❑ Decay by UV radiation
- ❑ Other:_____

Section G: Possible interventions and treatments

G1) Criteria of Interventions	G2) Treatments
❑ Reduction of the enviromental humidity RH < 90%	❑ Impregnation with fungicidal substances
❑ Avoid stagnation and direct contact with water	● Fumigation treatment
● Surface cleaning	● Permethrin and Boron treatments
❑ Avoid direct exposure to UV radiation	❑ Heat treatment
❑ Avoid rising damp for capillarity	❑ Other_____
● Removal and replacement of degraded parts	
❑ Replacement, if possible, of the whole timber member, using timber with greater durability class	
❑ Other_____	

APPENDIX C – The IIWC form

C.1 The proposed survey form

Section 1 – Building identification

1. BUILDING IDENTIFICATION		Note
Form number		
Compilation date		
Date of inspection 01		
Date of inspection 02		
Date of inspection 03		

Building localization		Note
Region		
Municipality		
Address		
Address number		
Building name		
Building owner		
Restriction (e.g. historical,...)		
Information about the building history		

Section 2 – Building description

2. BUILDING DESCRIPTION		Note
Construction period		
Total n. of floors		
N. of underground floors		
Average interfloor heigth [m]		
Average floor surface [m^2]		
Use		
Utilization		

Photographic documents	

APPENDIX C – The IIWC form

Section 3 – Identification of the Building Component (BC) and Structural Unit (StU)

3. IDENTIFICATION OF THE BUILDING COMPONENTS (BC) AND STRUCTURAL UNITS (StU)	
Building component	*ID*

ID Building component:	**0**	
Structural unit	*ID*	*Construction technology*
		-
		-
		-
		-
		-
		-
		-
		-
		-
		-
		-
		-
		-
		-
		-
		-

APPENDIX C – The IIWC form

Section 4.1 – Survey of the Structural Unit (StU) (continue)

4.1 SURVEY OF THE STRUCTURAL UNIT		Note
ID Building component		
Structural unit		
ID Structural unit		
General description		
Construction period		
Past work (e.g. structural retrofit,..)		
Description of the past work		

Typological analysy of the StU: Structural Members (StM)			
Type of structural member	*Number of StM*	*ID*	*Note*
-			
-			
-			
-			
-			
-			
-			
-			
-			

Graphical documentation of the StM			

APPENDIX C – The IIWC form

Section 4.1 – Survey of the Structural Unit (StU) (continue)

Typological identification of the StU: Structural Nodes (StN)			
Type of structural node	*Number of StN*	*ID*	*Note*
- - -			
- - -			
- - -			
- - -			
- - -			
- - -			
- - -			
- - -			
- - -			

Technological identification of the StU: Structural nodes (StN)					
Type of structural node	*ID*	*Construction typology*	*Metallic fastners*	*Timber fastners*	*Note*
- - -					
- - -					
- - -					
- - -					
- - -					
- - -					
- - -					
- - -					
- - -					
- - -					
- - -					

Graphical documentation of the StN			

APPENDIX C – The IIWC form

Section 4.2 – Survey of the Structural Member (StM)

4.2 SURVEY OF THE STRUCTURAL MEMBER (StM)	
Structural Member	-
ID	

Identification of the wood species		Note
through Macroscopic recognition		
through Microscopic recognition		
Existing documentation		
Age of the StM		

Geometry and dimension		Note
Type of cross section		
Geometry of the member		
Geometry of the cross-section		
Average dimension of the cross-section [cm]		
Member length [m]		

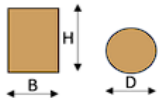

Type of woodworking		Note
Unbarked/Rounded		
Sawn finish	-	
Hewing finish	-	

Type of superficial treatment		Note
Not visible		
Wood oil		
Varnishing		
Painting		
Carving decoration		
Wax		
Other		

Graphical documentation			

APPENDIX C – The IIWC form

Section 4.3 – Survey of the Structural Node (StN)

4.3 SURVEY OF STRUCTURAL NODES (StN)			
ID			
Type	-	-	-
Description			
Construction typology			
Metallic fastners			
Timber fastners			

Graphical documentation		

APPENDIX C – The IIWC form

Section 5.1 – Diagnosis of the Structural Unit (StU)

5.1 DIAGNOSIS OF THE STRUCTURAL UNITS		Note
ID Building Component		
Structural Unit (StU)		
ID StU		

Stability issues: Structural Unit (StU)			
Typology		*ID StM-StN*	*Note*
Traslation			
Out of plane displacement			
Rotation			
Warping			
Disconnection			

Stability issues and mechanical damage: Structural Member (StM)			
Typology		*ID StM*	*Note*
Tension crack			
Delamination			
Distortion			
Compression crack			

Stability issues and mechanical damage: Structural Nodes (StN)			
Typology		*ID StN*	*Note*
Translation			
Rotation			
Compression crack			
Plug shear crack			
Cracks			

Graphical documentation			

APPENDIX C – The IIWC form

Section 5.2 – Diagnosis of the Structural Member (StM) (continue)

5.2 DIAGNOSIS OF THE STRUCTURAL MEMBER (StM)		Note
Structural Member (StM)	-	
ID		

Preliminary assessment: Wood defects			Note
Wanes	-	-	
Ring shakes	-	-	
Knots	-	-	
Group of knots	-	-	
Slope of the grain	-	-	
Shrinkage cracks	-	-	
	-	-	

Visual strength grading		Note
Wood species		
Grade (UNI 11119)	-	
Reference to speficic documents		

Preliminary assessment: Timber decay identification			
Typology	*Effects*	*State of activity*	*Note*
Biotic decay	-	-	
Abiotic decay	-	-	
Mechanical damage	-	-	
Chromatic alteration	-	-	

Diagnostica strumentale: Non-destructive test (NDT)								
Type of test	*Date/Period*	*Hour*	*Testing tool*	*Number of tests*	*Test location*	*Mesaured parameter*	*Note*	*Reference to specific documents*
Envirnomental temperature [°C]								
Environmental relative humidity [%]								
Wood moisture content [%]								
Traditional inspection								
Sclerometric test								
Drilling resistance test								
Acoustic test								
Vibrational test								
Other test:								

APPENDIX C – The IIWC form

Section 5.2 – Diagnosis of the Structural Member (StM) (continue)

Main outcomes

Photographic and graphical documentation		

APPENDIX C – The IIWC form

C.2 Application to the case study of Royal Palace of Naples

Section 1 – Building identification

1. BUILDING IDENTIFICATION		Note
Form number	**1**	
Compilation date	**28/03/2023**	
Date of inspection 01		
Date of inspection 02		
Date of inspection 03		

Building localization		Note
Region	**Campania**	
Municipality	**Naples**	
Address	**Plebiscito square**	
Address number	**1**	
Building name	**Royal Palace of Naples**	
Building owner	**Pubblic**	
Restriction (e.g. historical,...)	**ex L. 1089/1939**	
Information about the building history	***The Royal Palace was built from 1600 onward, reaching its final appearance in 1858. Numerous architects participated in its construction and restoration, including Domenico Fontana. It was the residence of the Spanish and then Austrian viceroys from the mid-17th century to 1734, of the Bourbon dynasty from 1734 to 1860, with the interlude of the French Decade from 1806 to 1815, and finally, following the Unification of Italy in 1861, of the Savoy family. Ceded to the state in 1919 by Victor Emmanuel III of Savoy, it is mainly used as a museum center, in particular the Royal Apartments, and is home to the National Library. (Faggiano et al., 2018)***	

Section 2 – Building description

2. BUILDING DESCRIPTION		Note
Construction period	**1600**	
Total n. of floors	**3**	
N. of underground floors	**0**	
Average interfloor heigth [m]	**4.5**	
Average floor surface [m^2]	**1000**	
Use	**Other**	**Museum - Library - Office**
Utilization	**>65%**	

Photographic documents

Frontal view from Plebiscito square

Diplomatic Hall

Ground floor

Section

APPENDIX C – The IIWC form

Section 3 – Identification of the Building Component (BC) and Structural Unit (StU)

3. IDENTIFICATION OF THE BUILDING COMPONENTS (BC) AND STRUCTURAL UNITS (StU)	
Building component	*ID*
Vertical structures	**EDF.01**
Ground floor	**EDF.02**
First floor	**EDF.03**
Second floor	**EDF.04**
Third floor	**EDF.05**
Roof	**EDF.06**

ID Building component:	**EDF.01**	
Structural unit	*ID*	*Construction technology*
Walls	**USt.01**	**Masonry**

ID Building component:	**EDF.02**	
Structural unit	*ID*	*Construction technology*
Floor slabs	**USt.02**	**R.C.**

ID Building component:	**EDF.03**	
Structural unit	*ID*	*Construction technology*
Floor beams	**USt.03**	**Timber**

ID Building component:	**EDF.04**	
Structural unit	*ID*	*Construction technology*
Floor beams	**USt.04**	**Timber**
Palladian truss	**USt.05**	**Timber**
Cieling vault	**USt.06**	**Timber**

ID Building component:	**EDF.05**	
Structural unit	*ID*	*Construction technology*
Floor beams	**USt.07**	**Timber**

ID Building component:	**EDF.06**	
Structural unit	*ID*	*Construction technology*
Palladian truss	**USt.08**	**Timber**
Palladian truss	**USt.09**	**Steel**
Palladian truss	**USt.10**	**R.C.**

APPENDIX C – The IIWC form

Section 4.1 – Survey of the Structural Unit (StU): The Palladian truss of the Diplomatic Hall (continue)

4.1 SURVEY OF THE STRUCTURAL UNIT		Note
ID Building component	**EDF.04**	
Structural unit	**Palladian truss**	
ID Structural unit	**StU.05**	
General description	***Composite timber beam located inside the Diplomatic Room of the Royal Palace. It serves the function of mid span beam for the floor. It covers a length of 16.70 m.***	
Construction period	**1650-1700**	
Past work (e.g. structural retrofit,..)	**2008**	
Description of the past work	***In 2008, the University of Naples 'Federico II', with the working group coordinated by Prof. F.M. Mazzolani, designed a series of reinforcement and seismic retrofitting works at the Royal Palace. These included the reinforcement of the floor slab in the Diplomatic Hall. The intervention consisted in the execution of a slab in reinforced concrete connected to the floor beams by means of steel collars.***	

Typological analysy of the StU: Structural Members (StM)			
Type of structural member	*Number of StM*	*ID*	*Note*
Rafter	**2**	**StM.1, StM.16**	
Tie-beam	**1**	**StM.17,**	
Secondary tie-beam	**1**	**StM.7**	
Struts	**10**	**StM.2, StM.3, StM.5, StM.6, StM.8, StM.9, StM.11, StM.12, StM.14,**	**There are 2 struts at the 2nd order and 8 struts at the 1st order**
King post	**1**	**StM.4, StM.9, StM.13**	
Queen post	**2**		

APPENDIX C – The IIWC form

Section 4.1 – Survey of the Structural Unit (StU): The Palladian truss of the Diplomatic Hall (continue)

Graphical documentation of the StM

Plan of 2nd floor (Diplomatic Hall)

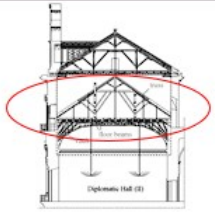

Section (Palladian truss - StU.05)

Frontal view of the StU.05

Frontal view of the StU.05

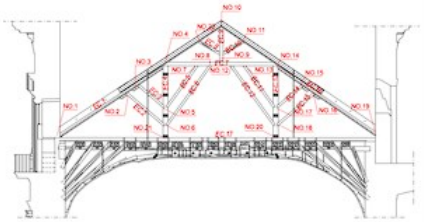

Structural section with evidence of the ID members and nodes

Frontal view of the StU.05

Graphical documentation of the StN

StN1

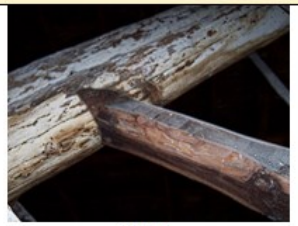

StN22

Frontal view of the 2nd order of the Palladian truss

StN21

StN1

StN1

StN1

StN5, StN6

APPENDIX C – The IIWC form

Section 4.1 – Survey of the Structural Unit (StU): The Palladian truss of the Diplomatic Hall (continue)

Typological identification of the StU: Structural Nodes (StN)					
Type of structural node			*Number of StN*	*ID*	*Note*
Rafter	**King Post**	**Rafter**	**1**	**StN.10**	
Rafter	**Strut**		**6**	**StN.2, StN.3, StN.15, StN.16, StN.11, StN.22**	
Queen Post	**Rafter**	**Secondary tie-beam**	**2**	**StN.4, StN.14**	
Secondary tie-beam	**Strut**		**4**	**StN.7, StN.8, StN.12, StN.13**	
Strut	**Queen Post**		**5**	**StN.5, StN.6, StN.17, StN.18, StN.9**	
Rafter	**Tie-beam**		**2**	**StN.1, StN.19**	
Queen Post	**Tie-beam**		**2**	**StN.20, StN.21**	

Technological identification of the StU: Structural nodes (StN)							
Type of structural node			*ID*	*Construction typology*	*Metallic fastners*	*Timber fastners*	*Note*
Rafter	**King Post**	**Rafter**	**StN.10**	**Single step joint**	**Not present**	**Not present**	
Rafter	**Strut**		**StN.2, StN.3, StN.15,**	**Simple supported**	**Stirrups**	**Not present**	
Rafter	**Strut**		**StN.11, StN.22**	**Single step joint**	**Not present**	**Not present**	
Queen Post	**Rafter**	**Secondary tie-beam**	**StN.4, StN.14**	**Simple notched joint**	**Not present**	**Not present**	
Secondary tie-beam	**Strut**		**StN.7, StN.8, StN.12, StN.13**	**Simple supported**	**Stirrups**	**Other**	**There are timber restraining members fixed to the secondary tie-beam by metal stirrups**
Strut	**Queen Post**		**StN.5, StN.6, StN.17,**	**Notched joint**	**Nails**	**Not present**	
Strut	**Queen Post**		**StN.9**	**Notched joint**	**Not present**	**Not present**	
Rafter	**Tie-beam**		**StN.1, StN.19**	**With timber slices**	**Nails**	**Not present**	
Queen Post	**Tie-beam**		**StN.20, StN.21**	**With timber slices**	**Stirrups**	**Not present**	

APPENDIX C – The IIWC form

Section 4.2 – Survey of the Structural Member (StM): the rafter (StM.1) of the Palladian truss (continue)

4.2 SURVEY OF THE STRUCTURAL MEMBER (StM)	
Structural Member	**Rafter**
ID	**StM.1**

Identification of the wood species		Note
through Macroscopic recognition	**Chestnut (Castanea Sativa Mill.)**	
through Microscopic recognition		
Existing documentation	**Intervention of structural retrofit**	
Age of the StM	**1600-1700**	**reference: Mazzolani et al., 2009**

Geometry and dimension		Note
Type of cross section	**Composed cross-section**	**From the support up to the StN.4 node, the member shows a composed cross section, after which the cross section is single up to the node with the king post. The section consists of a main element with circular geometry and a pair of outer slices with rectangular geometry that connect with the tie-beam located below the floor level**
Geometry of the member	**Costant cross-section**	
Geometry of the cross-section	**Squared**	
Average dimension of the cross-section [cm]	**D=27**	
Member length [m]	**11.00**	

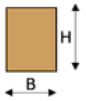

Type of woodworking		Note
Unbarked/Rounded	**YES**	
Sawn finish	**NO**	
Hewing finish	**NO**	

Type of superficial treatment		Note
Not visible	**YES**	
Wood oil	**NO**	
Varnishing	**NO**	
Painting	**NO**	
Carving decoration	**NO**	
Wax	**NO**	
Other	**NO**	

APPENDIX C – The IIWC form

Section 4.2 – Survey of the Structural Member (StM): the rafter (StM.1) of the Palladian truss (continue)

4.2 SURVEY OF THE STRUCTURAL MEMBER (StM)	
Structural Member	**Rafter**
ID	**StM.1**

Identification of the wood species		Note
through Macroscopic recognition	**Chestnut (Castanea Sativa Mill.)**	
through Microscopic recognition		
Existing documentation	**Intervention of structural retrofit**	
Age of the StM	**1600-1700**	**reference: Mazzolani et al., 2009**

Geometry and dimension		Note
Type of cross section	**Composed cross-section**	**From the support up to the StN.4 node, the member shows a composed cross section, after which the cross section is single up to the node with the king post. The section consists of a main element with circular geometry and a pair of outer slices with rectangular geometry that connect with the tie-beam located below the floor level**
Geometry of the member	**Costant cross-section**	
Geometry of the cross-section	**Circular**	
Average dimension of the cross-section [cm]	**D=27**	
Member length [m]	**11.00**	

Type of woodworking		Note
Unbarked/Rounded	**YES**	
Sawn finish	**NO**	
Hewing finish	**NO**	

Type of superficial treatment		Note
Not visible	**YES**	
Wood oil	**NO**	
Varnishing	**NO**	
Painting	**NO**	
Carving decoration	**NO**	
Wax	**NO**	
Other	**NO**	

APPENDIX C – The IIWC form

Section 4.2 – Survey of the Structural Member (StM): the rafter (StM.1) of the Palladian truss

Graphical documentation		
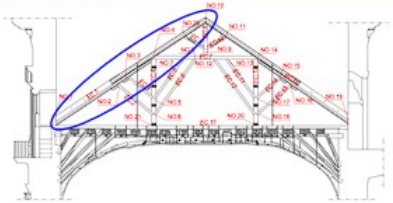 Structural section with evidence of the StM.1	 View of the StM.1 in correspondence of the nodes StN.4	 View of the StM.1 in correspondence of the nodes StN.1

APPENDIX C – The IIWC form

Section 4.2 – Survey of the Structural Member (StM): the queen post (StM.4) of the Palladian truss

4.2 SURVEY OF THE STRUCTURAL MEMBER (StM)	
Structural Member	**Queen Post**
ID	**StM.4**

Identification of the wood species		Note
through Macroscopic recognition	**Chestnut (Castanea Sativa Mill.)**	
through Microscopic recognition		
Existing documentation	**Intervention of structural retrofit**	
Age of the StM	**1600-1700**	**reference: Mazzolani et al., 2009**

Geometry and dimension		Note
Type of cross section	**Composed cross-section**	**At the support point, the section consists of a main element with circular geometry and a pair of outer slices with rectangular geometry**
Geometry of the member	**Costant cross-section**	
Geometry of the cross-section	**Circular**	
Average dimension of the cross-section [cm]	**D=18**	
Member length [m]	**4.00**	

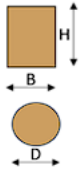

Type of woodworking		Note
Unbarked/Rounded	**YES**	
Sawn finish	**NO**	
Hewing finish	**NO**	

Type of superficial treatment		Note
Not visible	**NO**	
Wood oil	**NO**	
Varnishing	**NO**	
Painting	**NO**	
Carving decoration	**NO**	
Wax	**NO**	
Other	**NO**	

Graphical documentation		
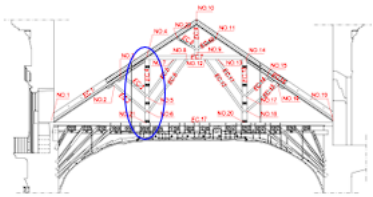 Structural section with evidence of the StM.4	 View of the StM.4 in correspondence of the nodes StN.5, StN. 6	 Frontal view of the StM.4

APPENDIX C – The IIWC form

Section 4.2 – Survey of the Structural Member (StM): the secondary tie-beam (StM.7) of the Palladian truss

4.2 SURVEY OF THE STRUCTURAL MEMBER (StM)	
Structural Member	**Secondary tie-beam**
ID	**StM.7**

Identification of the wood species		Note
through Macroscopic recognition	**Chestnut (Castanea Sativa Mill.)**	
through Microscopic recognition		
Existing documentation	**Intervention of structural retrofit**	
Age of the StM	**1600-1700**	**reference: Mazzolani et al., 2009**

Geometry and dimension		Note
Type of cross section	**Single cross-section**	
Geometry of the member	**Costant cross-section**	**Slightly variable**
Geometry of the cross-section	**Squared**	
Average dimension of the cross-section [cm]	**B=18 H=20**	
Member length [m]	**6.50**	

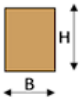

Type of woodworking		Note
Unbarked/Rounded	**NO**	
Sawn finish	**NO**	
Hewing finish	**bevels made with axe**	

Type of superficial treatment		Note
Not visible	**YES**	
Wood oil	**NO**	
Varnishing	**NO**	
Painting	**NO**	
Carving decoration	**NO**	
Wax	**NO**	
Other	**NO**	

Graphical documentation		
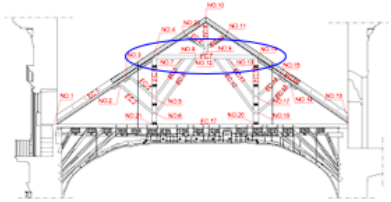	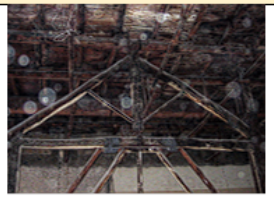	
Structural section with evidence of the StM.7	Frontal view of the StM.7	

APPENDIX C – The IIWC form

Section 4.3 – Survey of the Structural Node StN.01 (rafter-tie beam)

4.3 SURVEY OF STRUCTURAL NODES (StN)			
ID	**StN.01**		
Type	**Rafter**	**Tie-beam**	**-**
Description	**The tie-beam is placed below the slab, therefore it is subjected even to the dead load of the slab. The connection between the rafter and tie-beam is made by means of timber slices. These are placed out of the members and they are constrained to them by forged iron nails. The carpentry joint between the two pairs of slices is the double notches type**		
Construction typology	**With timber slices**		
Metallic fastners	**Nails**		
Timber fastners	**Not present**		

Graphical documentation			
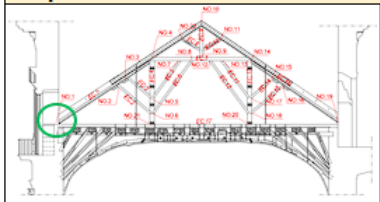 Structural section with evidence of the StN.01	 View of the StN.01		

APPENDIX C – The IIWC form

Section 4.3 – Survey of the Structural Node StN.21 (queen post-tie beam)

4.3 SURVEY OF STRUCTURAL NODES (StN)			
ID	**StN.21**		
Type	**Queen post**	**Tie-beam**	**-**
Description	**The tie-beam is placed below the slab. The connection between the two members is made by means of timber slices. These are fixed to the queen post and tie-beam by forged iron nails. Some metal stirrups are placed for confining the node**		
Construction typology	**With timber slices**		
Metallic fastners	**Nails and metal stirrups**		
Timber fastners	**Not present**		

Graphical documentation			
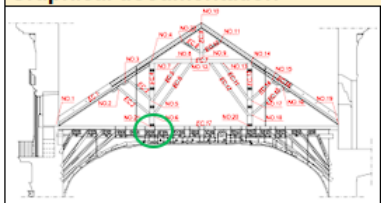 Structural section with evidence of the StN.21	 View of the StN.21		

APPENDIX C – The IIWC form

Section 4.3 – Survey of the Structural Node StN.22 (rafter-strut)

4.3 SURVEY OF STRUCTURAL NODES (StN)			
ID	**StN.22**		
Type	**Rafter**	**Strut**	**-**
Description	**The carpentry joint is of the single step type.**		
Construction typology	**Single step joint**		
Metallic fastners	**Not present**		
Timber fastners	**Not present**		

Graphical documentation			
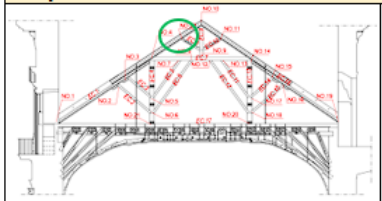 Structural section with evidence of the StN.22	 View of the StN.22		

APPENDIX C – The IIWC form

Section 5.1 – Diagnosis of the Structural Unit (StU)

Stability issues: Structural Unit (StU)			
Typology		*ID StM-StN*	*Note*
Traslation	**Present**		**The whole truss underwent a translation**
Out of plane displacement	**Not present**		
Rotation	**Present**	**StM.04, StM.13**	**The pair of timber slices underwent a rotation**
Warping	**Not present**		
Disconnection	**Present**	**StM.04, StM.13**	**The pair timber slices suffered disconnection that caused rotation**

Stability issues and mechanical damage: Structural Member (StM)			
Typology		*ID StM*	*Note*
Tension crack	**Not present**		
Delamination	**Not present**		
Distortion	**Deflection**	**StM.16**	**Rafter**
Compression crack	**Present**	**StM.01**	**Compression cracks at the rafter-tie beam connection**

Stability issues and mechanical damage: Structural Nodes (StN)			
Typology		*ID StN*	*Note*
Translation	**Present**		**All nodes in the structural unit have suffered a slight translation as a result of the disconnection of queen-posts StM.4 and StM.13**
Rotation	**Not present**		
Compression crack	**Present**	**StN.01**	
Plug shear crack	**Not present**		
Cracks	**Not present**		

APPENDIX C – The IIWC form

Section 5.1 – Diagnosis of the Structural Unit (StU): The Palladian truss of the Diplomatic Hall (continue)

5.1 DIAGNOSIS OF THE STRUCTURAL UNITS		Note
ID Building Component	**BC.04**	
Structural Unit (StU)	**Palladian truss**	
ID StU	**StU.05**	**For illustrative purposes, reference is made to the state of preservation before the 2008 consolidation intervention**

Stability issues: Structural Unit (StU)			
Typology		*ID StM-StN*	*Note*
Traslation	**Present**		**The whole truss underwent a translation**
Out of plane displacement	**Not present**		
Rotation	**Present**	**StM.04, StM.13**	**The pair of timber slices underwent a rotation**
Warping	**Not present**		
Disconnection	**Present**	**StM.04, StM.13**	**The pair timber slices suffered disconnection that caused rotation**

Stability issues and mechanical damage: Structural Member (StM)			
Typology		*ID StM*	*Note*
Tension crack	**Not present**		
Delamination	**Not present**		
Distortion	**Deflection**	**StM.16**	**Rafter**
Compression crack	**Present**	**StM.01**	**Compression cracks at the rafter-tie beam connection**

APPENDIX C – The IIWC form

Section 5.1 – Diagnosis of the Structural Unit (StU): The Palladian truss of the Diplomatic Hall (continue)

Stability issues and mechanical damage: Structural Nodes (StN)			
Typology		*ID StN*	*Note*
Translation	**Present**		**All nodes in the structural unit have suffered a slight translation as a result of the disconnection of queen-posts StM.4 and StM.13**
Rotation	**Not present**		
Compression crack	**Present**	**StN.01**	
Plug shear crack	**Not present**		
Cracks	**Not present**		

Graphical documentation	
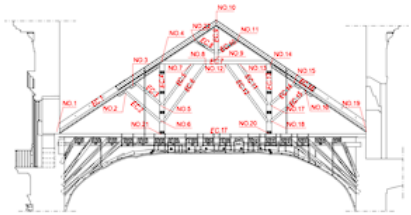 Prospetto frontale dell'incavallatura	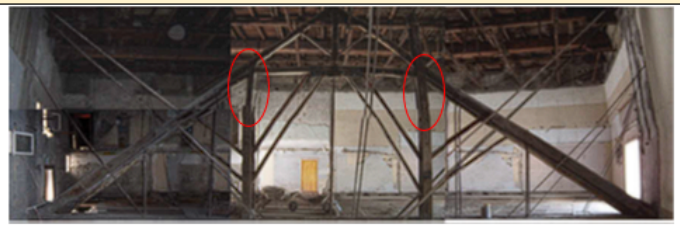 Vista frontale dell'incavallatura con evidenza dei dissesti

APPENDIX C – The IIWC form

Section 5.2 – Diagnosis of the Structural Member (StM): the rafter (StM.1) of the Palladian truss (continue)

5.2 DIAGNOSIS OF THE STRUCTURAL MEMBER (StM)		Note
Structural Member (StM)	**Rafter**	
ID	**StM.1**	

Preliminary assessment: Wood defects			Note
Wanes	**Not present**		**Cross-section is circular in shape**
Ring shakes	**Not present**		
Knots	**Adherent knot**		
Group of knots	**Not present**		
Slope of the grain	**Not present**		
Shrinkage cracks	**Superficial**		

Visual strength grading		Note
Wood species	**Chestnut (Castanea Sativa Mill.)**	
Grade (UNI 11119)	**Not identified**	
Reference to speficic documents		

Preliminary assessment: Timber decay identification			
Typology	*Effects*	*State of activity*	*Note*
Biotic decay	**Flicker hole**	**Active**	**Present flicker holes at rafter-tie beam connection**
Abiotic decay	**Not present**		
Mechanical damage	**Present**		**Compression cracks**
Chromatic alteration	**Present**		**Sign of fungal attack. Restricted to the area of connection with the tie-beam**

APPENDIX C – The IIWC form

Section 5.2 – Diagnosis of the Structural Member (StM): the rafter (StM.1) of the Palladian truss (continue)

Diagnostica strumentale: Non-destructive test (NDT)								
Type of test	*Date/Period*	*Hour*	*Testing tool*	*Number of tests*	*Test location*	*Mesaured parameter*	*Note*	*Reference to specific documents*
Envirnomental temperature [°C]								
Environmental relative humidity [%]								
Wood moisture content [%]								
Traditional inspection			**Other**		**At StN.01 (near the Masonry wall support)**		**Visual inspection performed by plaster removal. Evidence of cross-section reduction due to fungal attack**	**Riggio, 2009**
Sclerometric test								
Drilling resistance test								
Acoustic test								
Vibrational test								
Other test:								

Main outcomes
Visual inspection were carried out at the connection of the strut with the tie beam, near the wall support. A marked reduction in the cross section of the strut was found, with evident signs of biotic degradation caused by xylophagous insects and fungi (Grippa, 2009).

Photographic and graphical documentation		
		
Cross section reduction at StN.01 (frontal view)	Cross section reduction at StN.01 (back view)	

APPENDIX C – The IIWC form

Section 5.2 – Diagnosis of the Structural Member (StM): the queen post (StM.4) of the Palladian truss (continue)

5.2 DIAGNOSIS OF THE STRUCTURAL MEMBER (StM)		Note
Structural Member (StM)	**Queen post**	
ID	**StM.4**	

Preliminary assessment: Wood defects			Note
Wanes	**Not present**		**Cross-section is circular in shape**
Ring shakes	**Not present**		
Knots	**Adherent knot**		
Group of knots	**Not present**		
Slope of the grain	**Not present**		
Shrinkage cracks	**Superficial**		

Visual strength grading		Note
Wood species	**Chestnut (Castanea Sativa Mill.)**	
Grade (UNI 11119)	**Not identified**	
Reference to speficic documents		

Preliminary assessment: Timber decay identification			
Typology	*Effects*	*State of activity*	*Note*
Biotic decay	**Not present**		
Abiotic decay	**Not present**		
Mechanical damage	**Not present**		
Chromatic alteration	**Not present**		

APPENDIX C – The IIWC form

Section 5.2 – Diagnosis of the Structural Member (StM): the queen post (StM.4) of the Palladian truss (continue)

Diagnostica strumentale: Non-destructive test (NDT)								
Type of test	*Date/Period*	*Hour*	*Testing tool*	*Number of tests*	*Test location*	*Mesaured parameter*	*Note*	*Reference to specific documents*
Envirnomental temperature [°C]								
Environmental relative humidity [%]								
Wood moisture content [%]								
Traditional inspection			**Other**		**At StN.21 (queen post-tie beam connection)**		**Visual inspections carried out after removal of the existing slab**	**Riggio, 2009**
Sclerometric test								
Drilling resistance test								
Acoustic test								
Vibrational test								
Other test:								

Main outcomes
The member showed no evident signs of degradation. However, the partial disconnection of the slices from the circular main section is noteworthy. This phenomenon caused a kinematism of rotation and translation of the member (Grippa, 2009)

Photographic and graphical documentation		
		
General view of the StM.4	The StN.21	

APPENDIX C – The IIWC form

Section 5.2 – Diagnosis of the Structural Member (StM): the secondary tie-beam (StM.7) of the Palladian truss (continue)

5.2 DIAGNOSIS OF THE STRUCTURAL MEMBER (StM)		Note
Structural Member (StM)	**Secondary tie beam**	
ID	**StM.7**	

Preliminary assessment: Wood defects			Note
Wanes	**Not present**		
Ring shakes	**Not present**		
Knots	**Adherent knot**		
Group of knots	**Not present**		
Slope of the grain	**Not present**		
Shrinkage cracks	**Superficial**		

Visual strength grading		Note
Wood species	**Chestnut (Castanea Sativa Mill.)**	
Grade (UNI 11119)	**Not identified**	
Reference to speficic documents		

Preliminary assessment: Timber decay identification			
Typology	*Effects*	*State of activity*	*Note*
Biotic decay	**Not present**		
Abiotic decay	**Not present**		
Mechanical damage	**Not present**		
Chromatic alteration	**Not present**		

Diagnostica strumentale: Non-destructive test (NDT)								
Type of test	*Date/Period*	*Hour*	*Testing tool*	*Number of tests*	*Test location*	*Mesaured parameter*	*Note*	*Reference to specific documents*
Envirnomental temperature [°C]								
Environmental relative humidity [%]								
Wood moisture content [%]								
Traditional inspection								
Sclerometric test								
Drilling resistance test								
Acoustic test								
Vibrational test								
Other test:								

Main outcomes
The member did not show any evident signs of degradation

APPENDIX D - Seismic vulnerability assessment of large-span timber buildings through *indicator based approach*

D.1 List of criteria with evidence of the qualitative and quantitative value (continue)

	Criteria	Type of criteria d_{ij}	Qualitativa value d_{ij}	Quantitative value d_{ij}
S1 - S8	Regularity : compact and symmetrical plan Ratio of the largest to the smallest side < 4 Plants that do not exceed 5% of the total area External wall evenly and symmetrically distributed No eccentric core or blocks All the horizontal resistant systems extend over the entire height and without absence of any plane offset External walls evenly distributed in elevation and absence of continuous windows Symmetrical distribution of shear walls both continuous (panels) or reticular (vertical braces)	Binary	No / Yes	0,1
S9	Year of construction and renovation	Range	82-86	1986
			97-01	2001
			02-08	2008
			09-11	2011
S10 - S13	State of conservation: overall State of conservation: vertical structure State of conservation: horizontal structure State of conservation: non-structural elements	Judgment	Good	3
			Medium	2
			Bad	1
S14	Important class of building (0,1,2,3 or4)	Number	0,1,2,3,4	0, 1, 2, 3, 4
S15	Use of building (office, storage, sport …)	Feature	Storage	7.5
			Production	7.5
			Sport	5
			Public service	5
			Market	5
			Strategic	5
			Exhibition space	5
			Touristic	5
			Parking	5
			Office	3
			Residential	2
S16	Buildings position	Feature	Internal	3
			Corner	2
			Extremity	1
			Isolated	0
S17	Braced roof (yes or no)	Binary	No / Si	0.1
S18	Presence of chains (yes or no)	Binary	No / Si	0.1
S19	Pushing elements (yes or no)	Binary	No / Si	0.1
S20	Deformation characteristic	Feature	Deformable	2
			Rigid	1
S21 - S22	Repartition of bracing in transversal direction Repartition of bracing in longitudinal direction	Percentage	Continuos	2
			Discontinuos	1
S23	Way system	Feature	Double way	2
			One way	1
S24	Total number of floors including undergrounds	Number	1.2	1.2

APPENDIX D - Seismic vulnerability assessment of large-span timber buildings through *indicator based approach*

	Criteria	**Type of criteria d_{ij}**	**Qualitativa value d_{ij}**	**Quantitative value d_{ij}**
S25	Column height	Range	<6	3
			6-8	7
			8-10	9
			>10	10
S26	Average interstorey height	Range	<3.50	1.75
			3.50-4.99	4.25
			5.00-6.99	6
			7.00-9.9	8.5
			10.00-14.00	12
			>14	14
S27	Frame span	Range	<10	5
			10-20	15
			20-30	25
			>30	30
S28	Frame spacing	Range	<4	2
			4-6	5
			6-8	7
			>8	8
S29	Number of frames	Number	Da 0 a 5	Da 0 a 5
S30	Number of bays	Number	Da 0 a 9	Da 0 a 9
S31	Average floor area	Range	<200	200
			200-250	250
			250-300	300
			300-400	400
			400-500	500
			500-650	650
			650-900	900
			900-1200	1200
			1200-1600	1600
			1600-2000	2000
			2000-25000	2500
			25000-3000	3000
			3000-3500	3500
S32	Openings in the facade	Percentage	< 10 %	5
			10-19 %	14.5
			20-29 %	24.5
			30-50 %	40
			>50%	50

D.2 – Classification C1: Weights matrix A_{mxn} (part 1; columns S1-S16).

A_{mxn}	S1	S2	S3	S4	S5	S6	S7	S8	S9	S10	S11	S12	S13	S14	S15	S16
S1	**1**	1	1	1	1	1	1	1	2	3	3	3	3	4	4	5
S2	1	**1**	1	1	1	1	1	1	2	3	3	3	3	4	4	5
S3	1	1	**1**	1	1	1	1	1	2	3	3	3	3	4	4	5
S4	1	1	1	**1**	1	1	1	1	2	3	3	3	3	4	4	5
S5	1	1	1	1	**1**	1	1	1	2	3	3	3	3	4	4	5
S6	1	1	1	1	1	**1**	1	1	2	3	3	3	3	4	4	5
S7	1	1	1	1	1	1	**1**	1	2	3	3	3	3	4	4	5
S8	1	1	1	1	1	1	1	**1**	2	3	3	3	3	4	4	5
S9	1/2	1/2	1/2	1/2	1/2	1/2	1/2	1/2	**1**	3	3	3	3	3	3	4
S10	1/3	1/3	1/3	1/3	1/3	1/3	1/3	1/3	1/3	**1**	3	3	3	3	3	3
S11	1/3	1/3	1/3	1/3	1/3	1/3	1/3	1/3	1/3	1/3	**1**	3	3	3	3	3
S12	1/3	1/3	1/3	1/3	1/3	1/3	1/3	1/3	1/3	1/3	1/3	**1**	3	3	3	3
S13	1/3	1/3	1/3	1/3	1/3	1/3	1/3	1/3	1/3	1/3	1/3	1/3	**1**	3	3	3
S14	1/4	1/4	1/4	1/4	1/4	1/4	1/4	1/4	1/3	1/3	1/3	1/3	1/3	**1**	3	3
S15	1/4	1/4	1/4	1/4	1/4	1/4	1/4	1/4	1/3	1/3	1/3	1/3	1/3	1/3	**1**	3
S16	1/5	1/5	1/5	1/5	1/5	1/5	1/5	1/5	1/4	1/3	1/3	1/3	1/3	1/3	1/3	**1**
S17	1/6	1/6	1/6	1/6	1/6	1/6	1/6	1/6	1/5	1/4	1/4	1/4	1/4	1/3	1/3	1/3
S18	1/7	1/7	1/7	1/7	1/7	1/7	1/7	1/7	1/6	1/5	1/5	1/5	1/5	1/4	1/4	1/3
S19	1/7	1/7	1/7	1/7	1/7	1/7	1/7	1/7	1/6	1/5	1/5	1/5	1/5	1/4	1/4	1/3
S20	1/8	1/8	1/8	1/8	1/8	1/8	1/8	1/8	1/7	1/6	1/6	1/6	1/6	1/5	1/5	1/4
S21	1/8	1/8	1/8	1/8	1/8	1/8	1/8	1/8	1/7	1/6	1/6	1/6	1/6	1/5	1/5	1/4
S22	1/8	1/8	1/8	1/8	1/8	1/8	1/8	1/8	1/7	1/6	1/6	1/6	1/6	1/5	1/5	1/4
S23	1/9	1/9	1/9	1/9	1/9	1/9	1/9	1/9	1/8	1/7	1/7	1/7	1/7	1/6	1/6	1/5
S24	1/10	1/10	1/10	1/10	1/10	1/10	1/10	1/10	1/9	1/8	1/8	1/8	1/8	1/7	1/7	1/6
S25	1/11	1/11	1/11	1/11	1/11	1/11	1/11	1/11	1/10	1/9	1/9	1/9	1/9	1/8	1/8	1/7
S26	1/11	1/11	1/11	1/11	1/11	1/11	1/11	1/11	1/10	1/9	1/9	1/9	1/9	1/8	1/8	1/7
S27	1/12	1/12	1/12	1/12	1/12	1/12	1/12	1/12	1/11	1/10	1/10	1/10	1/10	1/9	1/9	1/8
S28	1/12	1/12	1/12	1/12	1/12	1/12	1/12	1/12	1/11	1/10	1/10	1/10	1/10	1/9	1/9	1/8
S29	1/13	1/13	1/13	1/13	1/13	1/13	1/13	1/13	1/12	1/11	1/11	1/11	1/11	1/10	1/10	1/9
S30	1/13	1/13	1/13	1/13	1/13	1/13	1/13	1/13	1/12	1/11	1/11	1/11	1/11	1/10	1/10	1/9
S31	1/13	1/13	1/13	1/13	1/13	1/13	1/13	1/13	1/12	1/11	1/11	1/11	1/11	1/10	1/10	1/9
S32	1/14	1/14	1/14	1/14	1/14	1/14	1/14	1/14	1/13	1/12	1/12	1/12	1/12	1/11	1/11	1/10

D.3 – Classification C1: Weights matrix A_{mxn} (part 2; columns S17-S32).

A_{mxn}	S17	S18	S19	S20	S21	S22	S23	S24	S25	S26	S27	S28	S29	S30	S31	S32	Mgi
S1	6	7	7	8	8	8	9	10	11	11	12	12	13	13	13	14	4.209
S2	6	7	7	8	8	8	9	10	11	11	12	12	13	13	13	14	4.209
S3	6	7	7	8	8	8	9	10	11	11	12	12	13	13	13	14	4.209
S4	6	7	7	8	8	8	9	10	11	11	12	12	13	13	13	14	4.209
S5	6	7	7	8	8	8	9	10	11	11	12	12	13	13	13	14	4.209
S6	6	7	7	8	8	8	9	10	11	11	12	12	13	13	13	14	4.209
S7	6	7	7	8	8	8	9	10	11	11	12	12	13	13	13	14	4.209
S8	6	7	7	8	8	8	9	10	11	11	12	12	13	13	13	14	4.209
S9	5	6	6	7	7	7	8	9	10	10	11	11	12	12	12	13	3.194
S10	4	5	5	6	6	6	7	8	9	9	10	10	11	11	11	12	2.505
S11	4	5	5	6	6	6	7	8	9	9	10	10	11	11	11	12	2,339
S12	4	5	5	6	6	6	7	8	9	9	10	10	11	11	11	12	2.184
S13	4	5	5	6	6	6	7	8	9	9	10	10	11	11	11	12	2.039
S14	3	4	4	5	5	5	6	7	8	8	9	9	10	10	10	11	1.644
S15	3	4	4	5	5	5	6	7	8	8	9	9	10	10	10	11	1.535
S16	3	3	3	4	4	4	5	6	7	7	8	8	9	9	9	10	1.242
S17	**1**	3	3	3	3	3	4	5	6	6	7	7	8	8	8	9	0.988
S18	1/3	**1**	3	3	3	3	3	4	5	5	6	6	7	7	7	8	0.799
S19	1/3	1/3	**1**	3	3	3	3	4	5	5	6	6	7	7	7	8	0.746
S20	1/3	1/3	1/3	**1**	3	3	3	3	4	4	5	5	6	6	6	7	0.608
S21	1/3	1/3	1/3	1/3	**1**	3	3	3	4	4	5	5	6	6	6	7	0.567
S22	1/3	1/3	1/3	1/3	1/3	**1**	3	3	4	4	5	5	6	6	6	7	0.530
S23	1/4	1/3	1/3	1/3	1/3	1/3	**1**	3	3	3	4	4	5	5	5	6	0.432
S24	1/5	1/4	1/4	1/3	1/3	1/3	1/3	**1**	3	3	3	3	4	4	4	5	0.354
S25	1/6	1/5	1/5	1/4	1/4	1/4	1/3	1/3	**1**	3	3	3	3	3	3	4	0.289
S26	1/6	1/5	1/5	1/4	1/4	1/4	1/3	1/3	1/3	**1**	3	3	3	3	3	4	0.269
S27	1/7	1/6	1/6	1/5	1/5	1/5	1/4	1/3	1/3	1/3	**1**	3	3	3	3	3	0.227
S28	1/7	1/6	1/6	1/5	1/5	1/5	1/4	1/3	1/3	1/3	1/3	**1**	3	3	3	3	0.212
S29	1/8	1/7	1/7	1/6	1/6	1/6	1/5	1/4	1/3	1/3	1/3	1/3	**1**	3	3	3	0.180
S30	1/8	1/7	1/7	1/6	1/6	1/6	1/5	1/4	1/3	1/3	1/3	1/3	1/3	**1**	3	3	0.168
S31	1/8	1/7	1/7	1/6	1/6	1/6	1/5	1/4	1/3	1/3	1/3	1/3	1/3	1/3	**1**	3	0.157
S32	1/9	1/8	1/8	1/7	1/7	1/7	1/6	1/5	1/4	1/4	1/3	1/3	1/3	1/3	1/3	**1**	0.133
																∑Mgi	**57.013**

D.4 – Classification C2: Weights matrix A_{mxn} (part 1; columns S1-S16).

A_{mxn}	S1	S2	S3	S4	S5	S6	S7	S8	S9	S10	S11	S12	S13	S14	S15	S16
S1	**1**	2	2	3	3	3	4	5	5	5	5	5	5	5	5	6
S2	1/2	**1**	2	2	2	2	3	4	4	4	4	4	4	4	4	5
S3	1/2	1/2	**1**	2	2	2	3	4	4	4	4	4	4	4	4	5
S4	1/3	1/2	1/2	**1**	2	2	2	3	3	3	3	3	3	3	3	4
S5	1/3	1/2	1/2	1/2	**1**	2	2	3	3	3	3	3	3	3	3	4
S6	1/3	1/2	1/2	1/2	1/2	**1**	2	3	3	3	3	3	3	3	3	4
S7	1/4	1/3	1/3	1/2	1/2	1/2	**1**	3	3	3	3	3	3	3	3	3
S8	1/5	1/4	1/4	1/3	1/3	1/3	1/3	**1**	3	3	3	3	3	3	3	3
S9	1/5	1/4	1/4	1/3	1/3	1/3	1/3	1/3	**1**	3	3	3	3	3	3	3
S10	1/5	1/4	1/4	1/3	1/3	1/3	1/3	1/3	1/3	**1**	3	3	3	3	3	3
S11	1/5	1/4	1/4	1/3	1/3	1/3	1/3	1/3	1/3	1/3	**1**	3	3	3	3	3
S12	1/5	1/4	1/4	1/3	1/3	1/3	1/3	1/3	1/3	1/3	1/3	**1**	3	3	3	3
S13	1/5	1/4	1/4	1/3	1/3	1/3	1/3	1/3	1/3	1/3	1/3	1/3	**1**	3	3	3
S14	1/5	1/4	1/4	1/3	1/3	1/3	1/3	1/3	1/3	1/3	1/3	1/3	1/3	**1**	3	3
S15	1/5	1/4	1/4	1/3	1/3	1/3	1/3	1/3	1/3	1/3	1/3	1/3	1/3	1/3	**1**	3
S16	1/6	1/5	1/5	1/4	1/4	1/4	1/3	1/3	1/3	1/3	1/3	1/3	1/3	1/3	1/3	**1**
S17	1/7	1/6	1/6	1/5	1/5	1/5	1/4	1/3	1/3	1/3	1/3	1/3	1/3	1/3	1/3	1/3
S18	1/7	1/6	1/6	1/5	1/5	1/5	1/4	1/3	1/3	1/3	1/3	1/3	1/3	1/3	1/3	1/3
S19	1/7	1/6	1/6	1/5	1/5	1/5	1/4	1/3	1/3	1/3	1/3	1/3	1/3	1/3	1/3	1/3
S20	1/7	1/6	1/6	1/5	1/5	1/5	1/4	1/3	1/3	1/3	1/3	1/3	1/3	1/3	1/3	1/3
S21	1/8	1/7	1/7	1/6	1/6	1/6	1/5	1/4	1/4	1/4	1/4	1/4	1/4	1/4	1/4	1/3
S22	1/8	1/7	1/7	1/6	1/6	1/6	1/5	1/4	1/4	1/4	1/4	1/4	1/4	1/4	1/4	1/3
S23	1/9	1/8	1/8	1/7	1/7	1/7	1/6	1/5	1/5	1/5	1/5	1/5	1/5	1/5	1/5	1/4
S24	10	1/9	1/9	1/8	1/8	1/8	1/7	1/6	1/6	1/6	1/6	1/6	1/6	1/6	1/6	1/5
S25	1/11	1/10	1/10	1/9	1/9	1/9	1/8	1/7	1/7	1/7	1/7	1/7	1/7	1/7	1/7	1/6
S26	1/11	1/10	1/10	1/9	1/9	1/9	1/8	1/7	1/7	1/7	1/7	1/7	1/7	1/7	1/7	1/6
S27	1/12	1/11	1/11	1/10	1/10	1/10	1/9	1/5	1/5	1/5	1/5	1/5	1/5	1/5	1/5	1/7
S28	1/12	1/11	1/11	1/10	1/10	1/10	1/9	1/5	1/5	1/5	1/5	1/5	1/5	1/5	1/5	1/7
S29	1/13	1/12	1/12	1/11	1/11	1/11	1/10	1/9	1/9	1/9	1/9	1/9	1/9	1/9	1/9	1/8
S30	1/13	1/12	1/12	1/11	1/11	1/11	1/10	1/9	1/9	1/9	1/9	1/9	1/9	1/9	1/9	1/8
S31	1/13	1/12	1/12	1/11	1/11	1/11	1/10	1/9	1/9	1/9	1/9	1/9	1/9	1/9	1/9	1/8
S32	1/14	1/13	1/13	1/12	1/12	1/12	1/11	1/10	1/10	1/10	1/10	1/10	1/10	1/10	1/10	1/9

D.5 – Classification C2: Weights matrix A_{mxn} (part 2; columns S17-S32).

A_{mxn}	S17	S18	S19	S20	S21	S22	S23	S24	S25	S26	S27	S28	S29	S30	S31	S32	Mgi
S1	7	7	7	7	8	8	9	10	11	11	12	12	13	13	13	14	5.989
S2	6	6	6	6	7	7	8	9	10	10	11	11	12	12	12	13	4.866
S3	6	6	6	6	7	7	8	9	10	10	11	11	12	12	12	13	4.660
S4	5	5	5	5	6	6	7	8	9	9	10	10	11	11	11	12	3.773
S5	5	5	5	5	6	6	7	8	9	9	10	10	11	11	11	12	3.613
S6	5	5	5	5	6	6	7	8	9	9	10	10	11	11	11	12	3.460
S7	4	4	4	4	5	5	6	7	8	8	9	9	10	10	10	11	2.947
S8	3	3	3	3	4	4	5	6	7	7	8	8	9	9	9	10	2.364
S9	3	3	3	3	4	4	5	6	7	7	8	8	9	9	9	10	2.207
S10	3	3	3	3	4	4	5	6	7	7	8	8	9	9	9	10	2.060
S11	3	3	3	3	4	4	5	6	7	7	8	8	9	9	9	10	1.924
S12	3	3	3	3	4	4	5	6	7	7	8	8	9	9	9	10	1.796
S13	3	3	3	3	4	4	5	6	7	7	8	8	9	9	9	10	1.677
S14	3	3	3	3	4	4	5	6	7	7	8	8	9	9	9	10	1.565
S15	3	3	3	3	4	4	5	6	7	7	8	8	9	9	9	10	1.462
S16	3	3	3	3	3	3	4	5	6	6	7	7	8	8	8	9	1.223
S17	**1**	3	3	3	3	3	3	4	5	5	6	6	7	7	7	8	1.034
S18	1/3	**1**	3	3	3	3	3	4	5	5	6	6	7	7	7	8	0.965
S19	1/3	1/3	**1**	3	3	3	3	4	5	5	6	6	7	7	7	8	0.901
S20	1/3	1/3	1/3	**1**	3	3	3	4	5	5	6	6	7	7	7	8	0.841
S21	1/3	1/3	1/3	1/3	**1**	3	3	3	4	4	5	5	6	6	6	7	0.668
S22	1/3	1/3	1/3	1/3	1/3	**1**	3	3	4	4	5	5	6	6	6	7	0.623
S23	1/3	1/3	1/3	1/3	1/3	1/3	**1**	3	3	3	4	4	5	5	5	6	0.500
S24	1/4	1/4	1/4	1/4	1/3	1/3	1/3	**1**	3	3	3	3	4	4	4	5	0.398
S25	1/5	1/5	1/5	1/5	1/4	1/4	1/3	1/3	**1**	3	3	3	3	3	3	4	0.320
S26	1/5	1/5	1/5	1/5	1/4	1/4	1/3	1/3	1/3	**1**	3	3	3	3	3	4	0.299
S27	1/6	1/6	1/6	1/6	1/5	1/5	1/4	1/3	1/3	1/3	**1**	3	3	3	3	3	0.280
S28	1/6	1/6	1/6	1/6	1/5	1/5	1/4	1/3	1/3	1/3	1/3	**1**	3	3	3	3	0.261
S29	1/7	1/7	1/7	1/7	1/6	1/6	1/5	1/4	1/3	1/3	1/3	1/3	**1**	3	3	3	0.196
S30	1/7	1/7	1/7	1/7	1/6	1/6	1/5	1/4	1/3	1/3	1/3	1/3	1/3	**1**	3	3	0.183
S31	1/7	1/7	1/7	1/7	1/6	1/6	1/5	1/4	1/3	1/3	1/3	1/3	1/3	1/3	**1**	3	0.171
S32	1/8	1/8	1/8	1/8	1/7	1/7	1/6	1/5	1/4	1/4	1/3	1/3	1/3	1/3	1/3	**1**	0.144
																∑Mgi	**53.369**

D.6 – Classification C3: Weights matrix A_{mxn} (part 1; columns S1-S16).

A_{mxn}	S1	S2	S3	S4	S5	S6	S7	S8	S9	S10	S11	S12	S13	S14	S15	S16
S1	**1**	1	1	1	1	1	1	1	1	1	1	1	1	1	1	1
S2	1	**1**	1	1	1	1	1	1	1	1	1	1	1	1	1	1
S3	1	1	**1**	1	1	1	1	1	1	1	1	1	1	1	1	1
S4	1	1	1	**1**	1	1	1	1	1	1	1	1	1	1	1	1
S5	1	1	1	1	**1**	1	1	1	1	1	1	1	1	1	1	1
S6	1	1	1	1	1	**1**	1	1	1	1	1	1	1	1	1	1
S7	1	1	1	1	1	1	**1**	1	1	1	1	1	1	1	1	1
S8	1	1	1	1	1	1	1	**1**	1	1	1	1	1	1	1	1
S9	1	1	1	1	1	1	1	1	**1**	1	1	1	1	1	1	1
S10	1	1	1	1	1	1	1	1	1	**1**	1	1	1	1	1	1
S11	1	1	1	1	1	1	1	1	1	1	**1**	1	1	1	1	1
S12	1	1	1	1	1	1	1	1	1	1	1	**1**	1	1	1	1
S13	1	1	1	1	1	1	1	1	1	1	1	1	**1**	1	1	1
S14	1	1	1	1	1	1	1	1	1	1	1	1	1	**1**	1	1
S15	1	1	1	1	1	1	1	1	1	1	1	1	1	1	**1**	1
S16	1	1	1	1	1	1	1	1	1	1	1	1	1	1	1	**1**
S17	1	1	1	1	1	1	1	1	1	1	1	1	1	1	1	1
S18	1	1	1	1	1	1	1	1	1	1	1	1	1	1	1	1
S19	1	1	1	1	1	1	1	1	1	1	1	1	1	1	1	1
S20	1	1	1	1	1	1	1	1	1	1	1	1	1	1	1	1
S21	1	1	1	1	1	1	1	1	1	1	1	1	1	1	1	1
S22	1	1	1	1	1	1	1	1	1	1	1	1	1	1	1	1
S23	1	1	1	1	1	1	1	1	1	1	1	1	1	1	1	1
S24	1/2	1/2	1/2	1/2	1/2	1/2	1/2	1/2	1/2	1/2	1/2	1/2	1/2	1/2	1/2	1/2
S25	1/3	1/3	1/3	1/3	1/3	1/3	1/3	1/3	1/3	1/3	1/3	1/3	1/3	1/3	1/3	1/3
S26	1/3	1/3	1/3	1/3	1/3	1/3	1/3	1/3	1/3	1/3	1/3	1/3	1/3	1/3	1/3	1/3
S27	1/4	1/4	1/4	1/4	1/4	1/4	1/4	1/4	1/4	1/4	1/4	1/4	1/4	1/4	1/4	1/4
S28	1/4	1/4	1/4	1/4	1/4	1/4	1/4	1/4	1/4	1/4	1/4	1/4	1/4	1/4	1/4	1/4
S29	1/5	1/5	1/5	1/5	1/5	1/5	1/5	1/5	1/5	1/5	1/5	1/5	1/5	1/5	1/5	1/5
S30	1/5	1/5	1/5	1/5	1/5	1/5	1/5	1/5	1/5	1/5	1/5	1/5	1/5	1/5	1/5	1/5
S31	1/5	1/5	1/5	1/5	1/5	1/5	1/5	1/5	1/5	1/5	1/5	1/5	1/5	1/5	1/5	1/5
S32	1/6	1/6	1/6	1/6	1/6	1/6	1/6	1/6	1/6	1/6	1/6	1/6	1/6	1/6	1/6	1/6

D.7 – Classification C3: Weights matrix A_{mxn} (part 2; columns S17-S32).

A_{mxn}	S17	S18	S19	S20	S21	S22	S23	S24	S25	S26	S27	S28	S29	S30	S31	S32	Mgi
S1	1	1	1	1	1	1	1	2	3	3	4	4	5	5	5	6	1.468
S2	1	1	1	1	1	1	1	2	3	3	4	4	5	5	5	6	1.468
S3	1	1	1	1	1	1	1	2	3	3	4	4	5	5	5	6	1.468
S4	1	1	1	1	1	1	1	2	3	3	4	4	5	5	5	6	1.468
S5	1	1	1	1	1	1	1	2	3	3	4	4	5	5	5	6	1.468
S6	1	1	1	1	1	1	1	2	3	3	4	4	5	5	5	6	1.468
S7	1	1	1	1	1	1	1	2	3	3	4	4	5	5	5	6	1.468
S8	1	1	1	1	1	1	1	2	3	3	4	4	5	5	5	6	1.468
S9	1	1	1	1	1	1	1	2	3	3	4	4	5	5	5	6	1.468
S10	1	1	1	1	1	1	1	2	3	3	4	4	5	5	5	6	1.468
S11	1	1	1	1	1	1	1	2	3	3	4	4	5	5	5	6	1.468
S12	1	1	1	1	1	1	1	2	3	3	4	4	5	5	5	6	1.468
S13	1	1	1	1	1	1	1	2	3	3	4	4	5	5	5	6	1.468
S14	1	1	1	1	1	1	1	2	3	3	4	4	5	5	5	6	1.468
S15	1	1	1	1	1	1	1	2	3	3	4	4	5	5	5	6	1.468
S16	1	1	1	1	1	1	1	2	3	3	4	4	5	5	5	6	1.468
S17	**1**	1	1	1	1	1	1	2	3	3	4	4	5	5	5	6	1.468
S18	1	**1**	1	1	1	1	1	2	3	3	4	4	5	5	5	6	1.468
S19	1	1	**1**	1	1	1	1	2	3	3	4	4	5	5	5	6	1.468
S20	1	1	1	**1**	1	1	1	2	3	3	4	4	5	5	5	6	1.468
S21	1	1	1	1	**1**	1	1	2	3	3	4	4	5	5	5	6	1.468
S22	1	1	1	1	1	**1**	1	2	3	3	4	4	5	5	5	6	1.468
S23	1	1	1	1	1	1	**1**	2	3	3	4	4	5	5	5	6	1.468
S24	1/2	1/2	1/2	1/2	1/2	1/2	1/2	**1**	3	3	3	3	4	4	4	5	0.835
S25	1/3	1/3	1/3	1/3	1/3	1/3	1/3	1/3	**1**	3	3	3	4	4	4	5	0.582
S26	1/3	1/3	1/3	1/3	1/3	1/3	1/3	1/3	1/3	**1**	3	3	4	4	4	5	0.544
S27	1/4	1/4	1/4	1/4	1/4	1/4	1/4	1/3	1/3	1/3	**1**	3	4	4	4	5	0.413
S28	1/4	1/4	1/4	1/4	1/4	1/4	1/4	1/3	1/3	1/3	1/3	**1**	4	4	4	5	0.385
S29	1/5	1/5	1/5	1/5	1/5	1/5	1/5	1/4	1/4	1/4	1/4	1/4	**1**	4	4	5	0.290
S30	1/5	1/5	1/5	1/5	1/5	1/5	1/5	1/4	1/4	1/4	1/4	1/4	1/4	**1**	4	5	0.266
S31	1/5	1/5	1/5	1/5	1/5	1/5	1/5	1/4	1/4	1/4	1/4	1/4	1/4	1/4	**1**	5	0.244
S32	1/6	1/6	1/6	1/6	1/6	1/6	1/6	1/5	1/5	1/5	1/5	1/5	1/5	1/5	1/5	**1**	0.184
																∑Mgi	**37.507**

D.8 – Weights w_j of criteria for the three classification.

	Criteria	C1	C2	C3
S1	Compact and symmetrical plan	0.074	0.044	0.039
S2	Ratio of the largest to the smallest side < 4	0.074	0.041	0.039
S3	Plants that do not exceed 5% of the total area	0.074	0.039	0.039
S4	External wall evenly and symmetrically distributed	0.074	0.036	0.039
S5	No eccentric core or blocks	0.074	0.034	0.039
S6	All the horizontal resistant systems extend over the entire height and without absence of any plane offset	0.074	0.031	0.039
S7	External walls evenly distributed in elevation and absence of continuous windows	0.074	0.029	0.039
S8	Symmetrical distribution of shear walls both continuous (panels) or reticular (vertical braces)	0.074	0.027	0.039
S9	Year of construction and renovation	0.056	0.023	0.039
S10	State of conservation: over all	0.044	0.019	0.039
S11	State of conservation: vertical structures	0.041	0.018	0.039
S12	State of conservation: horizontal structures	0.038	0.017	0.039
S13	State of conservation: non-structural element	0.036	0.016	0.039
S14	Important class of building (0,1,2,3,4)	0.029	0.013	0.039
S15	Use of building	0.027	0.012	0.039
S16	Position of building (isolated, corner …)	0.022	0.009	0.039
S17	Braced roof (yes or no)	0.017	0.112	0.039
S18	Presence of chains (yes or no)	0.014	0.091	0.039
S19	Pushing elements (yes or no)	0.013	0.087	0.039
S20	Deformation characteristic (rigid, deformable)	0.011	0.071	0.039
S21	Repartition of bracing in transversal direction	0.010	0.068	0.039
S22	Repartition of bracing in longitudinal direction	0.009	0.065	0.039
S23	Way system (double or simple)	0.008	0.055	0.039
S24	Total number of floors including undergrounds	0.006	0.007	0.022
S25	Column height	0.005	0.006	0.016
S26	Average interstorey height	0.005	0.006	0.014
S27	Frame span	0.004	0.005	0.011
S28	Frame spacing	0.004	0.005	0.010
S29	Number of span	0.003	0.004	0.008
S30	Number of bay	0.003	0.003	0.007
S31	Average floor area	0.003	0.003	0.007
S32	Openings in the facade	0.002	0.003	0.005
	Summ of weigths	1.000	1.000	1.000

D.9 – Decision matrix (qualitative values)

D_{mxn}	S1	S2	S3	S4	S5	S6	S7	S8	S9	S10	S11	S12	S13	S14	S15	S16	S17
1	S	S	S	S	S	S	S	S	2001	B	B	B	B	1	Storage	Isolated	S
2	S	S	S	S	S	S	N	S	2008	B	B	B	M	3	Market	Isolated	S
3	S	S	S	S	S	S	S	S	2008	B	B	B	B	2	Storage	Isolated	N
4	S	S	S	S	N	N	S	S	2001	B	B	B	B	3	Public service	Extremity	N
5	S	S	S	S	S	S	S	N	2001	B	B	B	B	3	Public service	Isolated	S
6	S	S	N	S	N	N	S	N	2008	B	B	B	B	3	Public service	D'angolo	N
7	S	S	N	S	N	S	S	N	2008	B	B	B	B	3	Market	Interno	S
8	S	S	N	S	S	N	S	N	2011	B	B	B	B	2	Production	Isolated	S
9	S	S	S	S	S	N	S	S	2001	B	B	B	B	3	Public service	Isolated	S
10	S	S	S	S	S	S	S	N	1986	B	B	B	B	3	Sport	Extremity	S

S=Yes; N=No; B=Good; M=Medium; D=Deformable; R=Rigid; C=Continue; NC=Not Continue — No information (the worst value)

D_{mxn}	S18	S19	S20	S21	S22	S23	S24	S25	S26	S27	S28	S29	S30	S31	S32
1	N	N	D	C	NC	Simple	1	<6	3.50-4.99	10-20	4-6	1	9	650-900	10-19
2	N	S	R	C	C	Simple	2	6-8	3.50-4.99	10-20	>8	4	4	1600-2000	10-19
3	N	S	D	NC	NC	Simple	1	<6	5.00-6.99	10-20	4-6	1	4	<200	<10
4	N	N	D	NC	NC	Simple	1	<6	3.50-4.99	10-20	4-6	1	5	250-300	10-19
5	S	S	D	C	NC	Simple	1	6-8	10.00-4.00	>30	4-6	1	6	900-1200	10-19
6	N	N	D	NC	NC	Simple	1	<6	5.00-6.99	10-20	4-6	1	6	300-400	10-19
7	N	N	D	NC	NC	Simple	1	<6	5.00-6.99	10-20	>8	3	4	2500-3000	10-19
8	N	S	D	C	NC	Simple	1	<6	3.50-4.99	10-20	4-6	1	6	650-900	10-19
9	N	N	D	C	NC	Simple	1	6-8	7.00-9.99	20-30	>8	1	3	650-900	10-19
10	N	S	D	C	C	Simple	1	6-8	7.00-9.99	20-30	4-6	1	5	650-900	<10

S=Yes; N=No; B=Good; M=Medium; D=Deformable; R=Rigid; C=Continue; NC=Not Continue — No information (the worst value)

D.10 – Decision matrix (quantitative values)

D_{mxn}	S1	S2	S3	S4	S5	S6	S7	S8	S9	S10	S11	S12	S13	S14	S15	S16	S17
1	1	1	1	1	1	1	1	1	2001	3	3	3	3	1	7.5	0	1
2	1	1	1	1	1	1	0	1	2008	3	3	3	2	3	5	0	1
3	1	1	1	1	1	1	1	1	2008	3	3	3	3	2	7.5	0	0
4	1	1	1	1	0	0	1	1	2001	3	3	3	3	3	5	1	0
5	1	1	0	1	1	1	1	0	2001	3	3	3	3	3	5	0	1
6	1	1	0	1	0	0	1	0	2008	3	3	3	3	3	5	2	0
7	1	1	0	1	0	1	1	0	2008	3	3	3	3	3	5	3	1
8	1	1	0	1	1	0	1	0	2011	3	3	3	3	2	7.5	0	1
9	1	1	1	1	1	0	1	1	2001	3	3	3	3	3	5	0	1
10	1	1	1	1	1	1	1	0	1986	3	3	3	3	3	5	1	1

D_{mxn}	S18	S19	S20	S21	S22	S23	S24	S25	S26	S27	S28	S29	S30	S31	S32
1	0	0	2	2	1	1	1	3	4.25	15	5	1	9	900	14.5
2	0	1	1	2	2	1	2	7	4.25	15	8	4	4	2000	14.5
3	0	1	2	1	1	1	1	3	6	15	5	1	4	200	5
4	0	0	2	1	1	1	1	3	4.25	15	5	1	5	300	14.5
5	1	1	2	2	1	1	1	7	12	30	5	1	6	1200	14.5
6	0	0	2	1	1	1	1	3	6	15	5	1	6	400	14.5
7	0	0	2	1	1	1	1	3	6	15	8	3	4	3000	14.5
8	0	1	2	2	1	1	1	3	4.25	15	5	1	6	900	14.5
9	0	0	2	2	1	1	1	7	8.5	25	8	1	3	900	14.5
10	0	1	2	2	2	1	1	7	8.5	25	5	1	5	900	5

D.11 – Normalized decision matrix

D_{mxn}	S1	S2	S3	S4	S5	S6	S7	S8	S9	S10	S11	S12	S13	S14	S15	S16	S17
1	0.316	0.316	0.408	0.316	0.378	0.408	0.333	0.447	0.316	0.316	0.316	0.316	0.325	0.118	0.405	0.000	0.378
2	0.316	0.316	0.408	0.316	0.378	0.408	0.000	0.447	0.317	0.316	0.316	0.316	0.217	0.354	0.270	0.000	0.378
3	0.316	0.316	0.408	0.316	0.378	0.408	0.333	0.447	0.317	0.316	0.316	0.316	0.325	0.236	0.405	0.000	0.000
4	0.316	0.316	0.408	0.316	0.000	0.000	0.333	0.447	0.316	0.316	0.316	0.316	0.325	0.354	0.270	0.258	0.000
5	0.316	0.316	0.000	0.316	0.378	0.408	0.333	0.000	0.316	0.316	0.316	0.316	0.325	0.354	0.270	0.000	0.378
6	0.316	0.316	0.000	0.316	0.000	0.000	0.333	0.000	0.317	0.316	0.316	0.316	0.325	0.354	0.270	0.516	0.000
7	0.316	0.316	0.000	0.316	0.000	0.408	0.333	0.000	0.317	0.316	0.316	0.316	0.325	0.354	0.270	0.775	0.378
8	0.316	0.316	0.000	0.316	0.378	0.000	0.333	0.000	0.317	0.316	0.316	0.316	0.325	0.236	0.405	0.000	0.378
9	0.316	0.316	0.408	0.316	0.378	0.000	0.333	0.447	0.316	0.316	0.316	0.316	0.325	0.354	0.270	0.000	0.378
10	0.316	0.316	0.408	0.316	0.378	0.408	0.333	0.000	0.313	0.316	0.316	0.316	0.325	0.354	0.270	0.258	0.378

D_{mxn}	S18	S19	S20	S21	S22	S23	S24	S25	S26	S27	S28	S29	S30	S31	S32
1	0.000	0.000	0.329	0.378	0.250	0.316	0.277	0.190	0.196	0.246	0.261	0.174	0.523	0.212	0.348
2	0.000	0.447	0.164	0.378	0.500	0.316	0.555	0.443	0.196	0.246	0.418	0.696	0.232	0.472	0.348
3	0.000	0.447	0.329	0.189	0.250	0.316	0.277	0.190	0.277	0.246	0.261	0.174	0.232	0.047	0.120
4	0.000	0.000	0.329	0.189	0.250	0.316	0.277	0.190	0.196	0.246	0.261	0.174	0.291	0.071	0.348
5	1.000	0.447	0.329	0.378	0.250	0.316	0.277	0.443	0.554	0.492	0.261	0.174	0.349	0.283	0.348
6	0.000	0.000	0.329	0.189	0.250	0.316	0.277	0.190	0.277	0.246	0.261	0.174	0.349	0.094	0.348
7	0.000	0.000	0.329	0.189	0.250	0.316	0.277	0.190	0.277	0.246	0.418	0.522	0.232	0.708	0.348
8	0.000	0.447	0.329	0.378	0.250	0.316	0.277	0.190	0.196	0.246	0.261	0.174	0.349	0.212	0.348
9	0.000	0.000	0.329	0.378	0.250	0.316	0.277	0.443	0.393	0.410	0.418	0.174	0.174	0.212	0.348
10	0.000	0.447	0.329	0.378	0.500	0.316	0.277	0.443	0.393	0.410	0.261	0.174	0.291	0.212	0.120

D.12 – Weighted - normalized decision matrix

Classification C1

V_{mxn}	S1	S2	S3	S4	S5	S6	S7	S8	S9	S10	S11	S12	S13	S14	S15	S16	S17
1	0.023	0.023	0.030	0.023	0.028	0.030	0.025	0.033	0.018	0.014	0.013	0.012	0.012	0.003	0.011	0.000	0.007
2	0.023	0.023	0.030	0.023	0.028	0.030	0.000	0.033	0.018	0.014	0.013	0.012	0.008	0.010	0.007	0.000	0.007
3	0.023	0.023	0.030	0.023	0.028	0.030	0.025	0.033	0.018	0.014	0.013	0.012	0.012	0.007	0.011	0.000	0.000
4	0.023	0.023	0.030	0.023	0.000	0.000	0.025	0.033	0.018	0.014	0.013	0.012	0.012	0.010	0.007	0.006	0.000
5	0.023	0.023	0.000	0.023	0.028	0.030	0.025	0.000	0.018	0.014	0.013	0.012	0.012	0.010	0.007	0.000	0.007
6	0.023	0.023	0.000	0.023	0.000	0.000	0.025	0.000	0.018	0.014	0.013	0.012	0.012	0.010	0.007	0.011	0.000
7	0.023	0.023	0.000	0.023	0.000	0.030	0.025	0.000	0.018	0.014	0.013	0.012	0.012	0.010	0.007	0.017	0.007
8	0.023	0.023	0.000	0.023	0.028	0.000	0.025	0.000	0.018	0.014	0.013	0.012	0.012	0.007	0.011	0.000	0.007
9	0.023	0.023	0.030	0.023	0.028	0.000	0.025	0.033	0.018	0.014	0.013	0.012	0.012	0.010	0.007	0.000	0.007
10	0.023	0.023	0.030	0.023	0.028	0.030	0.025	0.000	0.018	0.014	0.013	0.012	0.012	0.010	0.007	0.006	0.007

V_{mxn}	S18	S19	S20	S21	S22	S23	S24	S25	S26	S27	S28	S29	S30	S31	S32
1	0.000	0.000	0.004	0.004	0.002	0.002	0.002	0.001	0.001	0.001	0.001	0.001	0.002	0.001	0.001
2	0.000	0.006	0.002	0.004	0.005	0.002	0.003	0.002	0.001	0.001	0.002	0.002	0.001	0.001	0.001
3	0.000	0.006	0.004	0.002	0.002	0.002	0.002	0.001	0.001	0.001	0.001	0.001	0.001	0.000	0.000
4	0.000	0.000	0.004	0.002	0.002	0.002	0.002	0.001	0.001	0.001	0.001	0.001	0.001	0.000	0.001
5	0.014	0.006	0.004	0.004	0.002	0.002	0.002	0.002	0.003	0.002	0.001	0.001	0.001	0.001	0.001
6	0.000	0.000	0.004	0.002	0.002	0.002	0.002	0.001	0.001	0.001	0.001	0.001	0.001	0.000	0.001
7	0.000	0.000	0.004	0.002	0.002	0.002	0.002	0.001	0.001	0.001	0.002	0.002	0.001	0.002	0.001
8	0.000	0.006	0.004	0.004	0.002	0.002	0.002	0.001	0.001	0.001	0.001	0.001	0.001	0.001	0.001
9	0.000	0.000	0.004	0.004	0.002	0.002	0.002	0.002	0.002	0.002	0.002	0.001	0.001	0.001	0.001
10	0.000	0.006	0.004	0.004	0.005	0.002	0.002	0.002	0.002	0.002	0.001	0.001	0.001	0.001	0.000

Classification C2

V_{mxn}	S1	S2	S3	S4	S5	S6	S7	S8	S9	S10	S11	S12	S13	S14	S15	S16	S17
1	0.014	0.013	0.016	0.011	0.013	0.013	0.010	0.012	0.007	0.006	0.006	0.005	0.005	0.001	0.005	0.000	0.042
2	0.014	0.013	0.016	0.011	0.013	0.013	0.000	0.012	0.007	0.006	0.006	0.005	0.003	0.004	0.003	0.000	0.042
3	0.014	0.013	0.016	0.011	0.013	0.013	0.010	0.012	0.007	0.006	0.006	0.005	0.005	0.003	0.005	0.000	0.000
4	0.014	0.013	0.016	0.011	0.000	0.000	0.010	0.012	0.007	0.006	0.006	0.005	0.005	0.004	0.003	0.002	0.000
5	0.014	0.013	0.000	0.011	0.013	0.013	0.010	0.000	0.007	0.006	0.006	0.005	0.005	0.004	0.003	0.000	0.042
6	0.014	0.013	0.000	0.011	0.000	0.000	0.010	0.000	0.007	0.006	0.006	0.005	0.005	0.004	0.003	0.005	0.000
7	0.014	0.013	0.000	0.011	0.000	0.013	0.010	0.000	0.007	0.006	0.006	0.005	0.005	0.004	0.003	0.007	0.042
8	0.014	0.013	0.000	0.011	0.013	0.000	0.010	0.000	0.007	0.006	0.006	0.005	0.005	0.003	0.005	0.000	0.042
9	0.014	0.013	0.016	0.011	0.013	0.000	0.010	0.012	0.007	0.006	0.006	0.005	0.005	0.004	0.003	0.000	0.042
10	0.023	0.023	0.030	0.023	0.028	0.030	0.025	0.000	0.007	0.006	0.006	0.005	0.005	0.004	0.003	0.002	0.042

V_{mxn}	S18	S19	S20	S21	S22	S23	S24	S25	S26	S27	S28	S29	S30	S31	S32
1	0.000	0.000	0.023	0.026	0.016	0.017	0.002	0.001	0.001	0.001	0.001	0.001	0.002	0.001	0.001
2	0.000	0.039	0.012	0.026	0.032	0.017	0.004	0.003	0.001	0.001	0.002	0.003	0.001	0.002	0.001
3	0.000	0.039	0.023	0.013	0.016	0.017	0.002	0.001	0.002	0.001	0.001	0.001	0.001	0.000	0.000
4	0.000	0.000	0.023	0.013	0.016	0.017	0.002	0.001	0.001	0.001	0.001	0.001	0.001	0.000	0.001
5	0.091	0.039	0.023	0.026	0.016	0.017	0.002	0.003	0.003	0.003	0.001	0.001	0.001	0.001	0.001
6	0.000	0.000	0.023	0.013	0.016	0.017	0.002	0.001	0.002	0.001	0.001	0.001	0.001	0.000	0.001
7	0.000	0.000	0.023	0.013	0.016	0.017	0.002	0.001	0.002	0.001	0.002	0.002	0.001	0.002	0.001
8	0.000	0.039	0.023	0.026	0.016	0.017	0.002	0.001	0.001	0.001	0.001	0.001	0.001	0.001	0.001
9	0.000	0.000	0.023	0.026	0.016	0.017	0.002	0.003	0.002	0.002	0.002	0.001	0.001	0.001	0.001
10	0.000	0.039	0.023	0.026	0.032	0.017	0.002	0.003	0.002	0.002	0.001	0.001	0.001	0.001	0.000

APPENDIX D - Seismic vulnerability assessment of large-span timber buildings through *indicator based approach*

Classification C3

V_{mxn}	S1	S2	S3	S4	S5	S6	S7	S8	S9	S10	S11	S12	S13	S14	S15	S16	S17
1	0.012	0.012	0.016	0.012	0.015	0.016	0.013	0.018	0.0123	0.012	0.012	0.012	0.013	0.005	0.016	0.000	0.015
2	0.012	0.012	0.016	0.012	0.015	0.016	0.000	0.018	0.0124	0.012	0.012	0.012	0.008	0.014	0.011	0.000	0.015
3	0.012	0.012	0.016	0.012	0.015	0.016	0.013	0.018	0.0124	0.012	0.012	0.012	0.013	0.009	0.016	0.000	0.000
4	0.012	0.012	0.016	0.012	0.000	0.000	0.013	0.018	0.0123	0.012	0.012	0.012	0.013	0.014	0.011	0.010	0.000
5	0.012	0.012	0.000	0.012	0.015	0.016	0.013	0.000	0.0123	0.012	0.012	0.012	0.013	0.014	0.011	0.000	0.015
6	0.012	0.012	0.000	0.012	0.000	0.000	0.013	0.000	0.0124	0.012	0.012	0.012	0.013	0.014	0.011	0.020	0.000
7	0.012	0.012	0.000	0.012	0.000	0.016	0.013	0.000	0.0124	0.012	0.012	0.012	0.013	0.014	0.011	0.030	0.015
8	0.012	0.012	0.000	0.012	0.015	0.000	0.013	0.000	0.0124	0.012	0.012	0.012	0.013	0.009	0.016	0.000	0.015
9	0.012	0.012	0.016	0.012	0.015	0.000	0.013	0.018	0.0123	0.012	0.012	0.012	0.013	0.014	0.011	0.000	0.015
10	0.012	0.012	0.016	0.012	0.015	0.016	0.013	0.000	0.0122	0.012	0.012	0.012	0.013	0.014	0.011	0.010	0.015

V_{mxn}	S18	S19	S20	S21	S22	S23	S24	S25	S26	S27	S28	S29	S30	S31	S32
1	0.000	0.000	0.013	0.015	0.010	0.012	0.006	0.003	0.003	0.003	0.003	0.001	0.004	0.001	0.002
2	0.000	0.018	0.006	0.015	0.020	0.012	0.012	0.007	0.003	0.003	0.004	0.005	0.002	0.003	0.002
3	0.000	0.018	0.013	0.007	0.010	0.012	0.006	0.003	0.004	0.003	0.003	0.001	0.002	0.000	0.001
4	0.000	0.000	0.013	0.007	0.010	0.012	0.006	0.003	0.003	0.003	0.003	0.001	0.002	0.000	0.002
5	0.039	0.018	0.013	0.015	0.010	0.012	0.006	0.007	0.008	0.005	0.003	0.001	0.002	0.002	0.002
6	0.000	0.000	0.013	0.007	0.010	0.012	0.006	0.003	0.004	0.003	0.003	0.001	0.002	0.001	0.002
7	0.000	0.000	0.013	0.007	0.010	0.012	0.006	0.003	0.004	0.003	0.004	0.004	0.002	0.005	0.002
8	0.000	0.018	0.013	0.015	0.010	0.012	0.006	0.003	0.003	0.003	0.003	0.001	0.002	0.001	0.002
9	0.000	0.000	0.013	0.015	0.010	0.012	0.006	0.007	0.006	0.005	0.004	0.001	0.001	0.001	0.002
10	0.000	0.018	0.013	0.015	0.020	0.012	0.006	0.007	0.006	0.005	0.003	0.001	0.002	0.001	0.001

D.13 – Definition of Costs (C) and Benefits (B) for each criterion

	Elementi (criteri)	**Benefit (B) Cost (C)**
S1	Compact and symmetrical plan	B
S2	Ratio of the largest to the smallest side < 4	B
S3	Plants that do not exceed 5% of the total area	B
S4	External wall evenly and symmetrically distributed	B
S5	No eccentric core or blocks	B
S6	All the horizontal resistant systems extend over the entire height and without absence of any plane offset	B
S7	External walls evenly distributed in elevation and absence of continuous windows	B
S8	Symmetrical distribution of shear walls both continuous (panels) or reticular (vertical braces)	B
S9	Year of construction and renovation	B
S10	State of conservation: over all	B
S11	State of conservation: vertical structures	B
S12	State of conservation: horizontal structures	B
S13	State of conservation: non-structural element	B
S14	Important class of building (0,1,2,3,4)	C
S15	Use of building	C
S16	Position of building (isolated, corner …)	C
S17	Braced roof (yes or no)	B
S18	Presence of chains (yes or no)	B
S19	Pushing elements (yes or no)	C
S20	Deformation characteristic (rigid, deformable)	C
S21	Repartition of bracing in transversal direction	B
S22	Repartition of bracing in longitudinal direction	B
S23	Way system (double or simple)	B
S24	Total number of floors including undergrounds	C
S25	Column height	C
S26	Average interstorey height	C
S27	Frame span	C
S28	Frame spacing	C
S29	Number of span	B
S30	Number of bay	B
S31	Average floor area	B
S32	Openings in the facade	C

D.14 – Ideal solution (positive A^+ and negative A^-) and Euclidean distance (positive S^+ and negative S^-)

Classification C1

Ideal positive solution : $A^+ = \{ (\max v_{ij}, j \in JB), (\min vij, j \in JC), j= 1 \dots n \}$																	
A^+	$v_{i,1}$	$v_{i,2}$	$v_{i,3}$	$v_{i,4}$	$v_{i,5}$	$v_{i,6}$	$v_{i,7}$	$v_{i,8}$	$v_{i,9}$	$v_{i,10}$	$v_{i,11}$	$v_{i,12}$	$v_{i,13}$	$v_{i,14}$	$v_{i,15}$	$v_{i,16}$	$v_{i,17}$
	0.023	0.023	0.030	0.023	0.027	0.030	0.024	0.033	0.017	0.0139	0.0130	0.0121	0.0116	0.0034	0.0073	0.0000	0.006
	$v_{i,18}$	$v_{i,19}$	$v_{i,20}$	$v_{i,21}$	$v_{i,22}$	$v_{i,23}$	$v_{i,24}$	$v_{i,25}$	$v_{i,26}$	$v_{i,27}$	$v_{i,28}$	$v_{i,29}$	$v_{i,30}$	$v_{i,31}$	$v_{i,32}$		
	0.014	0.000	0.001	0.003	0.004	0.002	0.001	0.001	0.000	0.001	0.001	0.002	0.001	0.001	0.000		
Euclidean distance (positive) : $S^+ = [\sum_j (v_{ij} - v_j^+)^2]^{1/2}$																	
S_i^+	S_1^+	S_2^+	S_3^+	S_4^+	S_5^+	S_6^+	S_7^+	S_8^+	S_9^+	S_{10}^+							
	0.014	0.030	0.017	0.045	0.045	0.064	0.057	0.056	0.034	0.037							

Ideal negative solution : $A^- = \{ (\min v_{ij}, j \in JB), (\max vij, j \in JC), j= 1 \dots n \}$																	
A^-	$v_{i,1}$	$v_{i,2}$	$v_{i,3}$	$v_{i,4}$	$v_{i,5}$	$v_{i,6}$	$v_{i,7}$	$v_{i,8}$	$v_{i,9}$	$v_{i,10}$	$v_{i,11}$	$v_{i,12}$	$v_{i,13}$	$v_{i,14}$	$v_{i,15}$	$v_{i,16}$	$v_{i,17}$
	0.023	0.023	0.000	0.023	0.000	0.000	0.000	0.000	0.017	0.013	0.013	0.012	0.007	0.010	0.010	0.016	0.000
	$v_{i,18}$	$v_{i,19}$	$v_{i,20}$	$v_{i,21}$	$v_{i,22}$	$v_{i,23}$	$v_{i,24}$	$v_{i,25}$	$v_{i,26}$	$v_{i,27}$	$v_{i,28}$	$v_{i,29}$	$v_{i,30}$	$v_{i,31}$	$v_{i,32}$		
	0.000	0.005	0.003	0.001	0.002	0.002	0.003	0.002	0.002	0.002	0.001	0.000	0.000	0.000	0.000		
Euclidean distance (negative): $S^- = [\sum_j (v_{ij} - v_j^-)^2]^{1/2}$																	
S_i^-	S_1^-	S_2^-	S_3^-	S_4^-	S_5^-	S_6^-	S_7^-	S_8^-	S_9^-	S_{10}^-							
	0.068	0.063	0.067	0.052	0.053	0.026	0.040	0.041	0.061	0.058							

Classification C2

Ideal positive solution : $A^+ = \{ (\max v_{ij}, j \in JB), (\min vij, j \in JC), j= 1 \dots n \}$																	
A^+	$v_{i,1}$	$v_{i,2}$	$v_{i,3}$	$v_{i,4}$	$v_{i,5}$	$v_{i,6}$	$v_{i,7}$	$v_{i,8}$	$v_{i,9}$	$v_{i,10}$	$v_{i,11}$	$v_{i,12}$	$v_{i,13}$	$v_{i,14}$	$v_{i,15}$	$v_{i,16}$	$v_{i,17}$
	0.023	0.023	0.030	0.023	0.027	0.030	0.024	0.012	0.007	0.006	0.005	0.005	0.005	0.001	0.003	0.000	0.042
	$v_{i,18}$	$v_{i,19}$	$v_{i,20}$	$v_{i,21}$	$v_{i,22}$	$v_{i,23}$	$v_{i,24}$	$v_{i,25}$	$v_{i,26}$	$v_{i,27}$	$v_{i,28}$	$v_{i,29}$	$v_{i,30}$	$v_{i,31}$	$v_{i,32}$		
	0.091	0.000	0.011	0.025	0.032	0.017	0.002	0.001	0.001	0.001	0.001	0.002	0.001	0.002	0.091		
Euclidean distance (positive) : $S^+ = [\sum_j (v_{ij} - v_j^+)^2]^{1/2}$																	
S_i^+	S_1^+	S_2^+	S_3^+	S_4^+	S_5^+	S_6^+	S_7^+	S_8^+	S_9^+	S_{10}^+							
	0.100	0.107	0.116	0.114	0.063	0.118	0.107	0.114	0.103	0.100							

Ideal negative solution : $A^- = \{ (\min v_{ij}, j \in JB), (\max vij, j \in JC), j= 1 \dots n \}$																	
A^-	$v_{i,1}$	$v_{i,2}$	$v_{i,3}$	$v_{i,4}$	$v_{i,5}$	$v_{i,6}$	$v_{i,7}$	$v_{i,8}$	$v_{i,9}$	$v_{i,10}$	$v_{i,11}$	$v_{i,12}$	$v_{i,13}$	$v_{i,14}$	$v_{i,15}$	$v_{i,16}$	$v_{i,17}$
	0.014	0.013	0.000	0.011	0.000	0.000	0.000	0.000	0.007	0.006	0.005	0.005	0.003	0.004	0.004	0.007	0.000
	$v_{i,18}$	$v_{i,19}$	$v_{i,20}$	$v_{i,21}$	$v_{i,22}$	$v_{i,23}$	$v_{i,24}$	$v_{i,25}$	$v_{i,26}$	$v_{i,27}$	$v_{i,28}$	$v_{i,29}$	$v_{i,30}$	$v_{i,31}$	$v_{i,32}$		
	0.000	0.039	0.023	0.012	0.016	0.017	0.004	0.002	0.003	0.002	0.002	0.000	0.000	0.000	0.000		
Euclidean distance (negative): $S^- = [\sum_j (v_{ij} - v_j^-)^2]^{1/2}$																	
S_i^-	S_1^-	S_2^-	S_3^-	S_4^-	S_5^-	S_6^-	S_7^-	S_8^-	S_9^-	S_{10}^-							
	0.066	0.056	0.029	0.045	0.103	0.040	0.060	0.047	0.064	0.076							

Classification C3

Ideal positive solution : $A^+ = \{ (\max v_{ij}, j \in JB), (\min vij, j \in JC), j= 1 \dots n \}$																	
A^+	$v_{i,1}$	$v_{i,2}$	$v_{i,3}$	$v_{i,4}$	$v_{i,5}$	$v_{i,6}$	$v_{i,7}$	$v_{i,8}$	$v_{i,9}$	$v_{i,10}$	$v_{i,11}$	$v_{i,12}$	$v_{i,13}$	$v_{i,14}$	$v_{i,15}$	$v_{i,16}$	$v_{i,17}$
	0.012	0.012	0.016	0.012	0.014	0.016	0.013	0.017	0.012	0.012	0.012	0.012	0.012	0.004	0.010	0.000	0.014
	$v_{i,18}$	$v_{i,19}$	$v_{i,20}$	$v_{i,21}$	$v_{i,22}$	$v_{i,23}$	$v_{i,24}$	$v_{i,25}$	$v_{i,26}$	$v_{i,27}$	$v_{i,28}$	$v_{i,29}$	$v_{i,30}$	$v_{i,31}$	$v_{i,32}$		
	0.039	0.000	0.006	0.014	0.019	0.012	0.006	0.002	0.002	0.002	0.002	0.005	0.003	0.004	0.000		
Euclidean distance (positive) : $S^+ = [\sum_j (v_{ij} - v_j^+)^2]^{1/2}$																	
S_i^+	S_1^+	S_2^+	S_3^+	S_4^+	S_5^+	S_6^+	S_7^+	S_8^+	S_9^+	S_{10}^+							
	0.041	0.046	0.048	0.051	0.034	0.059	0.059	0.053	0.045	0.049							

Ideal negative solution : $A^- = \{ (\min v_{ij}, j \in JB), (\max vij, j \in JC), j= 1 \dots n \}$																	
A^-	$v_{i,1}$	$v_{i,2}$	$v_{i,3}$	$v_{i,4}$	$v_{i,5}$	$v_{i,6}$	$v_{i,7}$	$v_{i,8}$	$v_{i,9}$	$v_{i,10}$	$v_{i,11}$	$v_{i,12}$	$v_{i,13}$	$v_{i,14}$	$v_{i,15}$	$v_{i,16}$	$v_{i,17}$
	0.012	0.012	0.000	0.012	0.000	0.000	0.000	0.000	0.012	0.012	0.012	0.012	0.008	0.013	0.015	0.030	0.000
	$v_{i,18}$	$v_{i,19}$	$v_{i,20}$	$v_{i,21}$	$v_{i,22}$	$v_{i,23}$	$v_{i,24}$	$v_{i,25}$	$v_{i,26}$	$v_{i,27}$	$v_{i,28}$	$v_{i,29}$	$v_{i,30}$	$v_{i,31}$	$v_{i,32}$		
	0.000	0.017	0.012	0.007	0.009	0.012	0.012	0.006	0.008	0.005	0.004	0.001	0.001	0.000	0.001		
Euclidean distance (negative): $S^- = [\sum_j (v_{ij} - v_j^-)^2]^{1/2}$																	
S_i^-	S_1^-	S_2^-	S_3^-	S_4^-	S_5^-	S_6^-	S_7^-	S_8^-	S_9^-	S_{10}^-							
	0.053	0.049	0.047	0.039	0.058	0.026	0.033	0.041	0.050	0.042							

APPENDIX E - Durability assessment of typical existing timber structures through *Global durability Factor Method (GDFM)*

E.1 List of criteria with evidence of the qualitative and quantitative value (continue)

	Sub-Factor	Qualitative value	Quantitative value	Best Condition	Worst Condtion	Quantification criteria
A1	Type of timber product	Heavy timber	1	3	1	Saaty
		Timbe-based product	3			
A2	Presence of sapwood	Sapowood	1	5	1	Saaty
		Sapowood in higher percentage	2			
		Not-differiented	3			
		Hardwood in higher percentage	4			
		Hardwood	5			
A3	State of conservation (Crack thickness mm)	Un-cracked	1 mm	1	5	Real value
		Superficial cracks	3 mm			
		Deep cracks	5 mm			
A4	Wood species	Not durable	1	5	1	Numerical Durability class UNI EN 350
		Slightly durable	2			
		Moderately durable	3			
		Durable	4			
		High durable	5			
A5	Quality of storage system at building site	Outdoors, without protection, for a long time	1	9	1	Saaty
		Outdoors, without protection, for a short time	3			
		Outdoors, with protection, for a long time	5			
		Outdoors, with protection, for a short time	7			
		Indoor	9			
A6	Quality of transport system	Outdoors, exposed to the weather	1	3	1	Saaty
		Protected	3			
A7	Presence of quality system ISO 9001	NO	1	3	1	Saaty
		YES	3			
A8	Presence of DoP (CPR 305/2011)	System 4	1	6	1	Saaty
		System 3	2			
		System 2	3			
		System 2+	4			
		System 1	5			
		System 1+	6			

APPENDIX E - Durability assessment of typical existing timber structures through *Global durability Factor Method (GDFM)*

	Sub-Factor	Qualitative value	Quantitative value	Best Condition	Worst Condtion	Quantification criteria
A9	Quality of wood seasoning (Moisture content %)	Worst: U.R. > 20% Good:12% < U.R. ≤ 20% Best: U.R. ≤ 12%	24% 16% 8%	8	24	Real value
B1	Quality of construction details (as designed)	NO YES	1 3	3	1	Saaty
B2	Type of protective treatment	Not identified Superficial Deep	Thickness of treatment [mm]	5	1	Real value
C1	Quality of construction details (as built)	NO YES	1 3	3	1	Saaty
C2	Quality of protection system during construction	NO YES	1 3	3	1	Saaty
D1	Amount of environmental humidity	YES NO	3 1	3	1	Saaty
D2	Water condensation risk	YES NO	3 1	3	1	Saaty
E1	Climatic zone (D.P.R. 412/1993)	A B C D E F	500 GG 750 GG 1150 GG 1750 GG 2550 GG 3500 GG	500	3500	Numerical
E2	Average annual solar irradiance	High (>1200mm/yrs) Mean (500-1200mm/yrs) Low (< 500mm/yrs)	1300 mm/anno 850 mm/anno 400 mm/anno	400	1300	Numerical
E3	Service Class (NTC18)	3.U.R. > 85% 2.65% < U.R. ≤ 85% 1.U.R. ≤ 65%	95% 75% 55%	55	95	Numerical
E4	Annual solar radiance	< 800 800 ÷ 1000 > 1000	700 kWh/m² anno 900 kWh/m² anno 1100 kWh/m² anno	700	1100	Numerical
E5	Use Class (UNI EN 335)	5 4 3 2 1	1 3 5 7 9	9	1	Saaty

APPENDIX E - Durability assessment of typical existing timber structures through *Global durability Factor Method (GDFM)*

	Sub-Factor	Qualitative value	Quantitative value	Best Condition	Worst Condtion	Quantification criteria
F1	Impact class	Class A	6	6	1	Saaty
		Class B	5			
		Class C	4			
		Class D	3			
		Class E	2			
		Class F	1			
G1	Inspectiability conditions	Not inspectable	1	7	1	Saaty
		Low	3			
		Medium	5			
		Good	7			
G2	Quality of maintenance	Preventive	3	3	1	Saaty
		Corrective	1			

E.2 – Weights matrix A_{mxn} (continue)

A_{mx}	E5	E3	A4	A9	A2	E1	B2	G2	A3	A1	D1	D2	E2
E5	1	2	2	2	2	3	3	3	3	4	4	4	5
E3	1/2	1	2	2	2	3	3	3	3	4	4	4	5
A4	1/2	1/2	1	2	2	3	3	3	4	4	4	4	5
A9	1/2	1/2	1/2	1	2	2	2	2	3	3	3	4	4
A2	1/2	1/2	1/2	1/2	1	2	2	2	3	3	3	3	3
E1	1/3	1/3	1/3	1/2	1/2	1	2	2	2	3	3	3	3
B2	1/3	1/3	1/3	1/2	1/2	1/2	1	2	2	2	3	3	3
G2	1/3	1/3	1/3	1/2	1/2	1/2	1/2	1	2	2	3	3	3
A3	1/3	1/3	1/4	1/3	1/3	1/2	1/2	1/2	1	2	2	2	3
A1	1/4	1/4	1/4	1/3	1/3	1/3	1/2	1/2	1/2	1	2	2	3
D1	1/4	1/4	1/4	1/3	1/3	1/3	1/3	1/3	1/2	1/2	1	2	2
D2	1/4	1/4	1/4	1/4	1/3	1/3	1/3	1/3	1/2	1/2	1/2	1	2
E2	1/5	1/5	1/5	1/4	1/3	1/3	1/3	1/3	1/3	1/3	1/2	1/2	1
B1	1/5	1/5	1/5	1/5	1/4	1/3	1/3	1/3	1/3	1/3	1/2	1/2	1/2
C1	1/5	1/5	1/5	1/5	1/4	1/4	1/4	1/4	1/4	1/3	1/3	1/2	1/2
E4	1/6	1/6	1/6	1/5	1/4	1/4	1/4	1/4	1/4	1/4	1/3	1/3	1/3
G1	1/6	1/6	1/6	1/6	1/4	1/4	1/4	1/4	1/5	1/4	1/4	1/3	1/3
A5	1/7	1/7	1/6	1/6	1/5	1/5	1/5	1/5	1/5	1/5	1/4	1/4	1/3
A8	1/7	1/7	1/7	1/6	1/5	1/5	1/5	1/5	1/5	1/5	1/4	1/4	1/4
A7	1/7	1/7	1/7	1/7	1/5	1/5	1/5	1/5	1/5	1/5	1/5	1/5	1/4
C2	1/8	1/8	1/7	1/7	1/6	1/6	1/5	1/5	1/5	1/5	1/5	1/5	1/4
A6	1/9	1/9	1/8	1/7	1/6	1/6	1/6	1/6	1/6	1/5	1/5	1/5	1/5
F1	1/9	1/9	1/8	1/8	1/7	1/7	1/7	1/7	1/7	1/6	1/6	1/6	1/6

APPENDIX E - Durability assessment of typical existing timber structures through *Global durability Factor Method (GDFM)*

A_{mx}	**B1**	**C1**	**E4**	**G1**	**A5**	**A8**	**A7**	**C2**	**A6**	**F1**	**Mgi**
E5	5	5	6	6	7	7	7	8	9	9	4,03
E3	5	5	6	6	7	7	7	8	9	9	3,79
A4	5	5	6	6	6	7	7	7	8	8	3,53
A9	5	5	5	6	6	6	7	7	7	8	2,95
A2	4	4	4	4	5	5	5	6	6	7	2,46
E1	3	4	4	4	5	5	5	6	6	7	2,13
B2	3	4	4	4	5	5	5	5	6	7	1,96
G2	3	4	4	4	5	5	5	5	6	7	1,84
A3	3	4	4	5	5	5	5	5	6	7	1,61
A1	3	3	4	4	5	5	5	5	5	6	1,40
D1	2	3	3	4	4	4	5	5	5	6	1,19
D2	2	2	3	3	4	4	5	5	5	6	1,07
E2	2	2	3	3	3	4	4	4	5	6	0,92
B1	1	2	2	3	3	4	4	4	5	6	0,83
C1	1/2	1	2	2	3	3	3	4	4	5	0,69
E4	1/2	1/2	1	2	3	3	3	3	4	5	0,60
G1	1/3	1/2	1/2	1	2	3	3	3	4	5	0,53
A5	1/3	1/3	1/3	1/2	1	2	3	3	4	4	0,43
A8	1/4	1/3	1/3	1/3	1/2	1	3	3	4	4	0,39
A7	1/4	1/3	1/3	1/3	1/3	1/3	1	2	3	3	0,32
C2	1/4	1/4	1/3	1/3	1/3	1/3	1/2	1	2	3	0,29
A6	1/5	1/4	1/4	1/4	1/4	1/4	1/3	1/2	1	2	0,23
F1	1/6	1/5	1/5	1/5	1/4	1/4	1/3	1/3	1/2	1	0,19
										∑Mgi	33.39

E.3 – Predefined order of criteria and relative weights (w_j).

	Criteria	Order	wj
E5	Use Class (UNI EN 335)	1	0.121
E3	Service Class (NTC18)	2	0.114
A4	Wood species	3	0.106
A9	Quality of wood seasoning	4	0.088
A2	Presence of sapwood	5	0.074
E1	Climatic zone	6	0.064
B2	Type of protective treatment	7	0.059
G2	Quality of maintenance	8	0.055
A3	State of conservation	9	0.048
A1	Type of timber product	10	0.042
D1	Amount of environmental humidity	11	0.036
D2	Water condensation risk	12	0.032
E2	Average annual precipitation	13	0.028
B1	Quality of construction details (as designed)	14	0.025
C1	Quality of construction details (as built)	15	0.021
E4	Average annual solar irradiance	16	0.018
G1	Inspectiability conditions	17	0.016
A5	Quality of storage system at building site	18	0.013
A8	Presence of DoP (CPR 305/2011)	19	0.012
A7	Presence of quality system ISO 9001	20	0.010
C2	Quality of protection system during construction	21	0.009
A6	Quality of transport system	22	0.007
F1	Impact class	23	0.006
		Summ of weights	1.000

E.4 – Decision matrix (quantitative values) for case studies, reference case (Cr) and idal solutions (positive A+ and negative A-)

D_{mxn}	A1	A2	A3	A4	A5	A6	A7	A8	A9	B1	B2
a	3	3	1	2	7	3	1	4	16	3	2
b	1	4	3	4	7	3	1	4	16	3	3
c	1	3	3	4	5	1	1	2	16	1	1
d	1	5	5	4	3	1	1	2	16	1	1
Cr	3	3	1	3	7	3	1	5	16	1	3
A+	3	5	1	5	9	3	1	6	8	3	5
A-	1	1	5	1	1	1	1	1	24	1	1

D_{mxn}	C1	C2	D1	D2	E1	E2	E3	E4	E5	F1	G1
a	3	3	3	3	1150	850	75	700	7	6	5
b	3	1	3	3	1150	850	75	700	5	6	5
c	1	1	3	3	1150	900	55	700	9	6	3
d	1	3	3	3	1150	1080	55	700	9	6	3
Cr	1	1	1	1	1150	850	75	700	7	6	5
A+	3	3	3	3	500	400	55	700	9	6	7
A-	1	1	1	1	3500	1300	95	100	1	1	1

E.5 – Normalized decision matrix (quantitative values) for case studies, reference case (Cr) and idal solutions (positive A+ and negative A-)

D_{mxn}	A1	A2	A3	A4	A5	A6	A7	A8	A9	B1	B2
a	0.0019	0.0019	0.0006	0.0013	0.0044	0.0019	0.0006	0.0025	0.0100	0.0019	0.0013
b	0.0006	0.0025	0.0019	0.0025	0.0044	0.0019	0.0006	0.0025	0.0100	0.0019	0.0019
c	0.0006	0.0019	0.0019	0.0025	0.0031	0.0006	0.0006	0.0012	0.0099	0.0006	0.0006
d	0.0006	0.0029	0.0029	0.0023	0.0017	0.0006	0.0006	0.0012	0.0093	0.0006	0.0006
Cr	0.0019	0.0019	0.0006	0.0019	0.0044	0.0019	0.0006	0.0031	0.0100	0.0006	0.0019
A+	0.0032	0.0053	0.0011	0.0053	0.0095	0.0032	0.0011	0.0063	0.0084	0.0032	0.0053
A-	0.0003	0.0003	0.0013	0.0003	0.0003	0.0003	0.0003	0.0003	0.0064	0.0003	0.0003

D_{mxn}	C1	C2	D1	D2	E1	E2	E3	E4	E5	F1	G1
a	0.0019	0.0019	0.0019	0.0019	0.7214	0.5332	0.0470	0.4391	0.0044	0.0038	0.0031
b	0.0019	0.0006	0.0019	0.0019	0.7214	0.5332	0.0470	0.4391	0.0031	0.0038	0.0031
c	0.0006	0.0006	0.0019	0.0019	0.7097	0.5554	0.0339	0.4320	0.0056	0.0037	0.0019
d	0.0006	0.0017	0.0017	0.0017	0.6659	0.6254	0.0318	0.4053	0.0052	0.0035	0.0017
Cr	0.0006	0.0006	0.0006	0.0006	0.7214	0.5332	0.0470	0.4391	0.0044	0.0038	0.0031
A+	0.0032	0.0032	0.0032	0.0032	0.5260	0.4208	0.0579	0.7364	0.0095	0.0063	0.0074
A-	0.0003	0.0003	0.0003	0.0003	0.9368	0.3479	0.0254	0.0268	0.0003	0.0003	0.0003

E.6 – Weighted - normalized decision matrix (quantitative values) for case studies, reference case (Cr) and idal solutions (positive A+ and negative A-)

V_{mxn}	A1	A2	A3	A4	A5	A6	A7	A8	A9	B1	B2
a	0.00008	0.00014	0.00003	0.00013	0.00006	0.00001	0.00001	0.00003	0.00089	0.00005	0.00007
b	0.00003	0.00018	0.00009	0.00027	0.00006	0.00001	0.00001	0.00003	0.00089	0.00005	0.00011
c	0.00003	0.00014	0.00009	0.00026	0.00004	0.00000	0.00001	0.00001	0.00087	0.00002	0.00004
d	0.00002	0.00021	0.00014	0.00025	0.00002	0.00000	0.00001	0.00001	0.00082	0.00001	0.00003
Cr	0.00008	0.00014	0.00003	0.00020	0.00006	0.00001	0.00001	0.00004	0.00089	0.00002	0.00011
A+	0.00013	0.00039	0.00005	0.00056	0.00012	0.00002	0.00001	0.00007	0.00074	0.00008	0.00031
A-	0.00001	0.00002	0.00006	0.00003	0.00000	0.00000	0.00000	0.00000	0.00057	0.00001	0.00002

V_{mxn}	C1	C2	D1	D2	E1	E2	E3	E4	E5	F1	G1
a	0.00004	0.00002	0.00007	0.00006	0.04605	0.01467	0.00534	0.00784	0.00053	0.00002	0.00005
b	0.00004	0.00001	0.00007	0.00006	0.04605	0.01467	0.00534	0.00784	0.00038	0.00002	0.00005
c	0.00001	0.00001	0.00007	0.00006	0.04530	0.01528	0.00386	0.00771	0.00067	0.00002	0.00003
d	0.00001	0.00001	0.00006	0.00006	0.04251	0.01721	0.00362	0.00724	0.00063	0.00002	0.00003
Cr	0.00001	0.00001	0.00002	0.00002	0.04605	0.01467	0.00534	0.00784	0.00053	0.00002	0.00005
A+	0.00007	0.00003	0.00011	0.00010	0.03358	0.01158	0.00657	0.01315	0.00114	0.00004	0.00012
A-	0.00001	0.00000	0.00001	0.00001	0.05980	0.00957	0.00289	0.00048	0.00003	0.00000	0.00000